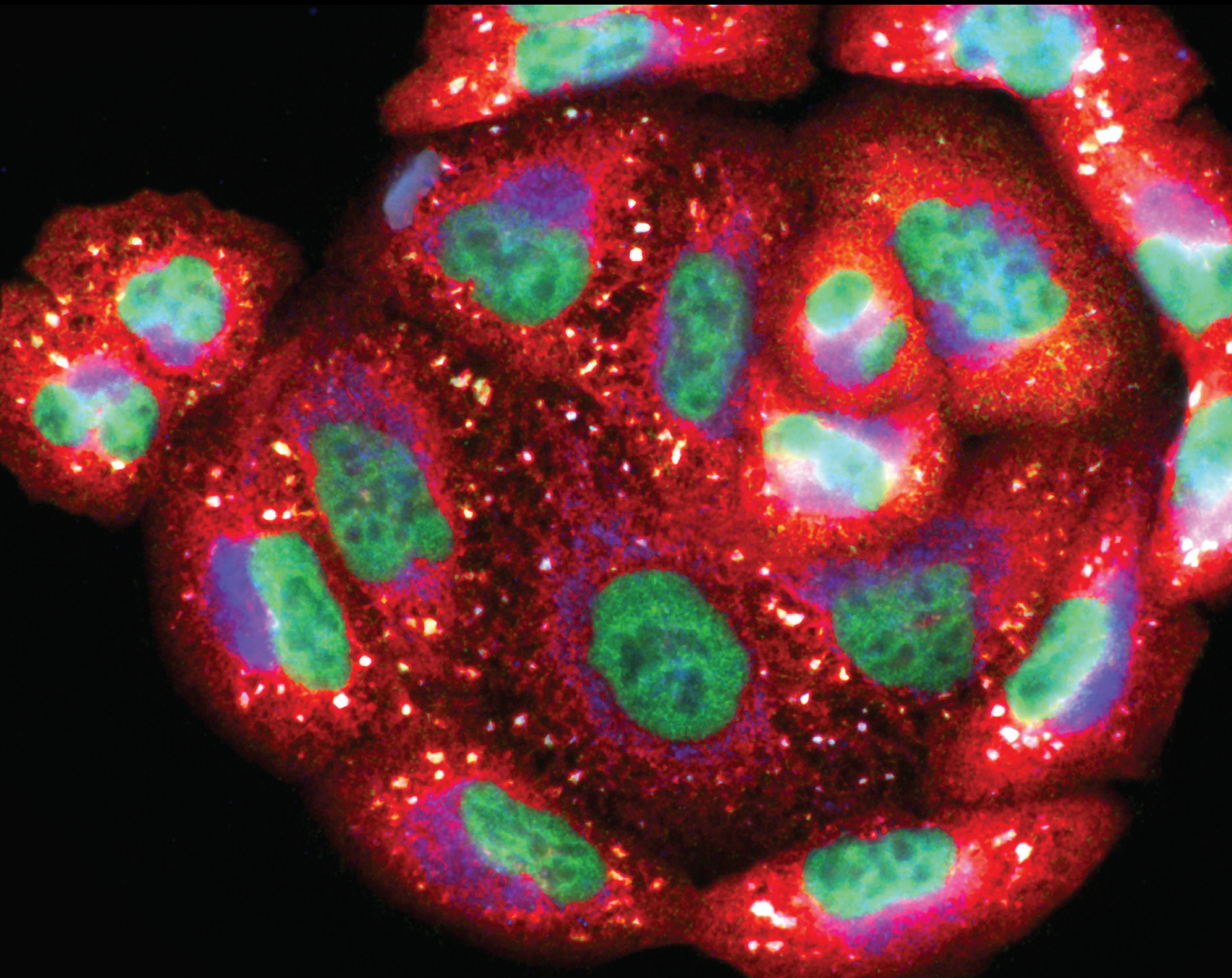# Mitochondrial Quality Control Mechanisms as Molecular Targets in Cardiovascular Disorders

Lead Guest Editor: Hao Zhou
Guest Editors: Sam Toan and Rui Guo

Mitochondrial Quality Control Mechanisms as Molecular Targets in Cardiovascular Disorders

Mitochondrial Quality Control Mechanisms as Molecular Targets in Cardiovascular Disorders

Lead Guest Editor: Hao Zhou
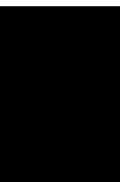Guest Editors: Sam Toan and Rui Guo

Anwen Shao (iD), China
Iman Sherif, Egypt
Salah A Sheweita, Saudi Arabia
Xiaolei Shi, China
Manjari Singh, India
Giulia Sita (iD), Italy
Ramachandran Srinivasan (iD), India
Adrian Sturza (iD), Romania
Kuo-hui Su (iD), United Kingdom
Eisa Tahmasbpour Marzouni (iD), Iran
Hailiang Tang, China
Carla Tatone (iD), Italy
Shane Thomas (iD), Australia
Carlo Gabriele Tocchetti (iD), Italy
Angela Trovato Salinaro, Italy
Rosa Tundis (iD), Italy
Kai Wang (iD), China
Min-qi Wang (iD), China
Natalie Ward (iD), Australia
Grzegorz Wegrzyn, Poland
Philip Wenzel (iD), Germany
Guangzhen Wu (iD), China
Jianbo Xiao (iD), Spain
Qiongming Xu (iD), China
Liang-Jun Yan (iD), USA
Guillermo Zalba (iD), Spain
Jia Zhang (iD), China
Junmin Zhang (iD), China
Junli Zhao (iD), USA
Chen-he Zhou (iD), China
Yong Zhou (iD), China
Mario Zoratti (iD), Italy

Contents

Contents

Hindawi

Retraction

Retracted: Natural Antioxidants Improve the Vulnerability of Cardiomyocytes and Vascular Endothelial Cells under Stress Conditions: A Focus on Mitochondrial Quality Control

Oxidative Medicine and Cellular Longevity

This article has been retracted by Hindawi, as publisher, following an investigation undertaken by the publisher [1]. This investigation has uncovered evidence of systematic manipulation of the publication and peer-review process. We cannot, therefore, vouch for the reliability or integrity of this article.

Please note that this notice is intended solely to alert readers that the peer-review process of this article has been compromised.

Wiley and Hindawi regret that the usual quality checks did not identify these issues before publication and have since put additional measures in place to safeguard research integrity.

We wish to credit our Research Integrity and Research Publishing teams and anonymous and named external researchers and research integrity experts for contributing to this investigation.

The corresponding author, as the representative of all authors, has been given the opportunity to register their agreement or disagreement to this retraction. We have kept a record of any response received.

References

[1] X. Chang, Z. Zhao, W. Zhang et al., "Natural Antioxidants Improve the Vulnerability of Cardiomyocytes and Vascular Endothelial Cells under Stress Conditions: A Focus on Mitochondrial Quality Control," *Oxidative Medicine and Cellular Longevity*, vol. 2021, Article ID 6620677, 27 pages, 2021.

Retraction

Retracted: Alleviation of Inflammation and Oxidative Stress in Pressure Overload-Induced Cardiac Remodeling and Heart Failure via IL-6/STAT3 Inhibition by Raloxifene

Oxidative Medicine and Cellular Longevity

This article has been retracted by Hindawi, as publisher, following an investigation undertaken by the publisher [1]. This investigation has uncovered evidence of systematic manipulation of the publication and peer-review process. We cannot, therefore, vouch for the reliability or integrity of this article.

Please note that this notice is intended solely to alert readers that the peer-review process of this article has been compromised.

Wiley and Hindawi regret that the usual quality checks did not identify these issues before publication and have since put additional measures in place to safeguard research integrity.

We wish to credit our Research Integrity and Research Publishing teams and anonymous and named external researchers and research integrity experts for contributing to this investigation.

The corresponding author, as the representative of all authors, has been given the opportunity to register their agreement or disagreement to this retraction. We have kept a record of any response received.

References

[1] S. Huo, W. Shi, H. Ma et al., "Alleviation of Inflammation and Oxidative Stress in Pressure Overload-Induced Cardiac Remodeling and Heart Failure via IL-6/STAT3 Inhibition by Raloxifene," *Oxidative Medicine and Cellular Longevity*, vol. 2021, Article ID 6699054, 15 pages, 2021.

Retraction

Retracted: Novel Insights into the Molecular Features and Regulatory Mechanisms of Mitochondrial Dynamic Disorder in the Pathogenesis of Cardiovascular Disease

Oxidative Medicine and Cellular Longevity

This article has been retracted by Hindawi following an investigation undertaken by the publisher [1]. This investigation has uncovered evidence of one or more of the following indicators of systematic manipulation of the publication process:

(1) Discrepancies in scope

(2) Discrepancies in the description of the research reported

(3) Discrepancies between the availability of data and the research described

(4) Inappropriate citations

(5) Incoherent, meaningless and/or irrelevant content included in the article

(6) Peer-review manipulation

The presence of these indicators undermines our confidence in the integrity of the article's content and we cannot, therefore, vouch for its reliability. Please note that this notice is intended solely to alert readers that the content of this article is unreliable. We have not investigated whether authors were aware of or involved in the systematic manipulation of the publication process.

Wiley and Hindawi regrets that the usual quality checks did not identify these issues before publication and have since put additional measures in place to safeguard research integrity.

We wish to credit our own Research Integrity and Research Publishing teams and anonymous and named external researchers and research integrity experts for contributing to this investigation.

The corresponding author, as the representative of all authors, has been given the opportunity to register their agreement or disagreement to this retraction. We have kept a record of any response received.

References

[1] Y. Tan, F. Xia, L. Li et al., "Novel Insights into the Molecular Features and Regulatory Mechanisms of Mitochondrial Dynamic Disorder in the Pathogenesis of Cardiovascular Disease," *Oxidative Medicine and Cellular Longevity*, vol. 2021, Article ID 6669075, 11 pages, 2021.

Retraction

Retracted: Modulation of Mitochondrial Quality Control Processes by BGP-15 in Oxidative Stress Scenarios: From Cell Culture to Heart Failure

Oxidative Medicine and Cellular Longevity

This article has been retracted by Hindawi following an investigation undertaken by the publisher [1]. This investigation has uncovered evidence of one or more of the following indicators of systematic manipulation of the publication process:

(1) Discrepancies in scope

(2) Discrepancies in the description of the research reported

(3) Discrepancies between the availability of data and the research described

(4) Inappropriate citations

(5) Incoherent, meaningless and/or irrelevant content included in the article

(6) Peer-review manipulation

The presence of these indicators undermines our confidence in the integrity of the article's content and we cannot, therefore, vouch for its reliability. Please note that this notice is intended solely to alert readers that the content of this article is unreliable. We have not investigated whether authors were aware of or involved in the systematic manipulation of the publication process.

Wiley and Hindawi regrets that the usual quality checks did not identify these issues before publication and have since put additional measures in place to safeguard research integrity.

We wish to credit our own Research Integrity and Research Publishing teams and anonymous and named external researchers and research integrity experts for contributing to this investigation.

The corresponding author, as the representative of all authors, has been given the opportunity to register their agreement or disagreement to this retraction. We have kept a record of any response received.

References

[1] O. Horvath, K. Ordog, K. Bruszt et al., "Modulation of Mitochondrial Quality Control Processes by BGP-15 in Oxidative Stress Scenarios: From Cell Culture to Heart Failure," *Oxidative Medicine and Cellular Longevity*, vol. 2021, Article ID 6643871, 22 pages, 2021.

Retraction

Retracted: Total Glucosides of Peony Protect Cardiomyocytes against Oxidative Stress and Inflammation by Reversing Mitochondrial Dynamics and Bioenergetics

Oxidative Medicine and Cellular Longevity

This article has been retracted by Hindawi following an investigation undertaken by the publisher [1]. This investigation has uncovered evidence of one or more of the following indicators of systematic manipulation of the publication process:

(1) Discrepancies in scope
(2) Discrepancies in the description of the research reported
(3) Discrepancies between the availability of data and the research described
(4) Inappropriate citations
(5) Incoherent, meaningless and/or irrelevant content included in the article
(6) Peer-review manipulation

The presence of these indicators undermines our confidence in the integrity of the article's content and we cannot, therefore, vouch for its reliability. Please note that this notice is intended solely to alert readers that the content of this article is unreliable. We have not investigated whether authors were aware of or involved in the systematic manipulation of the publication process.

Wiley and Hindawi regrets that the usual quality checks did not identify these issues before publication and have since put additional measures in place to safeguard research integrity.

We wish to credit our own Research Integrity and Research Publishing teams and anonymous and named external researchers and research integrity experts for contributing to this investigation.

The corresponding author, as the representative of all authors, has been given the opportunity to register their agreement or disagreement to this retraction. We have kept a record of any response received.

References

[1] M. Wang, Q. Li, Y. Zhang, and H. Liu, "Total Glucosides of Peony Protect Cardiomyocytes against Oxidative Stress and Inflammation by Reversing Mitochondrial Dynamics and Bioenergetics," *Oxidative Medicine and Cellular Longevity*, vol. 2020, Article ID 6632413, 12 pages, 2020.

Retraction

Retracted: The Role of Posttranslational Modification and Mitochondrial Quality Control in Cardiovascular Diseases

Oxidative Medicine and Cellular Longevity

This article has been retracted by Hindawi following an investigation undertaken by the publisher [1]. This investigation has uncovered evidence of one or more of the following indicators of systematic manipulation of the publication process:

(1) Discrepancies in scope

(2) Discrepancies in the description of the research reported

(3) Discrepancies between the availability of data and the research described

(4) Inappropriate citations

(5) Incoherent, meaningless and/or irrelevant content included in the article

(6) Peer-review manipulation

The presence of these indicators undermines our confidence in the integrity of the article's content and we cannot, therefore, vouch for its reliability. Please note that this notice is intended solely to alert readers that the content of this article is unreliable. We have not investigated whether authors were aware of or involved in the systematic manipulation of the publication process.

Wiley and Hindawi regrets that the usual quality checks did not identify these issues before publication and have since put additional measures in place to safeguard research integrity.

We wish to credit our own Research Integrity and Research Publishing teams and anonymous and named external researchers and research integrity experts for contributing to this investigation.

The corresponding author, as the representative of all authors, has been given the opportunity to register their agreement or disagreement to this retraction. We have kept a record of any response received.

References

[1] J. Liu, L. Zhong, and R. Guo, "The Role of Posttranslational Modification and Mitochondrial Quality Control in Cardiovascular Diseases," *Oxidative Medicine and Cellular Longevity*, vol. 2021, Article ID 6635836, 15 pages, 2021.

Hindawi

Retraction

Retracted: S-Nitroso-L-Cysteine Ameliorated Pulmonary Hypertension in the MCT-Induced Rats through Anti-ROS and Anti-Inflammatory Pathways

Oxidative Medicine and Cellular Longevity

This article has been retracted by Hindawi following an investigation undertaken by the publisher [1]. This investigation has uncovered evidence of one or more of the following indicators of systematic manipulation of the publication process:

(1) Discrepancies in scope

(2) Discrepancies in the description of the research reported

(3) Discrepancies between the availability of data and the research described

(4) Inappropriate citations

(5) Incoherent, meaningless and/or irrelevant content included in the article

(6) Peer-review manipulation

The presence of these indicators undermines our confidence in the integrity of the article's content and we cannot, therefore, vouch for its reliability. Please note that this notice is intended solely to alert readers that the content of this article is unreliable. We have not investigated whether authors were aware of or involved in the systematic manipulation of the publication process.

Wiley and Hindawi regrets that the usual quality checks did not identify these issues before publication and have since put additional measures in place to safeguard research integrity.

We wish to credit our own Research Integrity and Research Publishing teams and anonymous and named external researchers and research integrity experts for contributing to this investigation.

The corresponding author, as the representative of all authors, has been given the opportunity to register their agreement or disagreement to this retraction. We have kept a record of any response received.

References

[1] M. Wang, P. Luo, W. Shi et al., "S-Nitroso-L-Cysteine Ameliorated Pulmonary Hypertension in the MCT-Induced Rats through Anti-ROS and Anti-Inflammatory Pathways," *Oxidative Medicine and Cellular Longevity*, vol. 2021, Article ID 6621232, 17 pages, 2021.

Retraction

Retracted: Epicardial Adipose Tissue Volume Is Associated with High Risk Plaque Profiles in Suspect CAD Patients

Oxidative Medicine and Cellular Longevity

This article has been retracted by Hindawi following an investigation undertaken by the publisher [1]. This investigation has uncovered evidence of one or more of the following indicators of systematic manipulation of the publication process:

(1) Discrepancies in scope

(2) Discrepancies in the description of the research reported

(3) Discrepancies between the availability of data and the research described

(4) Inappropriate citations

(5) Incoherent, meaningless and/or irrelevant content included in the article

(6) Peer-review manipulation

The presence of these indicators undermines our confidence in the integrity of the article's content and we cannot, therefore, vouch for its reliability. Please note that this notice is intended solely to alert readers that the content of this article is unreliable. We have not investigated whether authors were aware of or involved in the systematic manipulation of the publication process.

Wiley and Hindawi regrets that the usual quality checks did not identify these issues before publication and have since put additional measures in place to safeguard research integrity.

We wish to credit our own Research Integrity and Research Publishing teams and anonymous and named external researchers and research integrity experts for contributing to this investigation.

The corresponding author, as the representative of all authors, has been given the opportunity to register their agreement or disagreement to this retraction. We have kept a record of any response received.

References

[1] D. Shan, G. Dou, J. Yang et al., "Epicardial Adipose Tissue Volume Is Associated with High Risk Plaque Profiles in Suspect CAD Patients," *Oxidative Medicine and Cellular Longevity*, vol. 2021, Article ID 6663948, 10 pages, 2021.

Retraction

Retracted: Puerarin Attenuates LPS-Induced Inflammatory Responses and Oxidative Stress Injury in Human Umbilical Vein Endothelial Cells through Mitochondrial Quality Control

Oxidative Medicine and Cellular Longevity

This article has been retracted by Hindawi following an investigation undertaken by the publisher [1]. This investigation has uncovered evidence of one or more of the following indicators of systematic manipulation of the publication process:

(1) Discrepancies in scope

(2) Discrepancies in the description of the research reported

(3) Discrepancies between the availability of data and the research described

(4) Inappropriate citations

(5) Incoherent, meaningless and/or irrelevant content included in the article

(6) Peer-review manipulation

The presence of these indicators undermines our confidence in the integrity of the article's content and we cannot, therefore, vouch for its reliability. Please note that this notice is intended solely to alert readers that the content of this article is unreliable. We have not investigated whether authors were aware of or involved in the systematic manipulation of the publication process.

Wiley and Hindawi regrets that the usual quality checks did not identify these issues before publication and have since put additional measures in place to safeguard research integrity.

We wish to credit our own Research Integrity and Research Publishing teams and anonymous and named external researchers and research integrity experts for contributing to this investigation.

The corresponding author, as the representative of all authors, has been given the opportunity to register their agreement or disagreement to this retraction. We have kept a record of any response received.

References

[1] X. Chang, T. Zhang, D. Liu et al., "Puerarin Attenuates LPS-Induced Inflammatory Responses and Oxidative Stress Injury in Human Umbilical Vein Endothelial Cells through Mitochondrial Quality Control," *Oxidative Medicine and Cellular Longevity*, vol. 2021, Article ID 6659240, 14 pages, 2021.

Retraction

Retracted: Oxidized LDL Disrupts Metabolism and Inhibits Macrophage Survival by Activating a miR-9/Drp1/Mitochondrial Fission Signaling Pathway

Oxidative Medicine and Cellular Longevity

This article has been retracted by Hindawi following an investigation undertaken by the publisher [1]. This investigation has uncovered evidence of one or more of the following indicators of systematic manipulation of the publication process:

(1) Discrepancies in scope
(2) Discrepancies in the description of the research reported
(3) Discrepancies between the availability of data and the research described
(4) Inappropriate citations
(5) Incoherent, meaningless and/or irrelevant content included in the article
(6) Peer-review manipulation

The presence of these indicators undermines our confidence in the integrity of the article's content and we cannot, therefore, vouch for its reliability. Please note that this notice is intended solely to alert readers that the content of this article is unreliable. We have not investigated whether authors were aware of or involved in the systematic manipulation of the publication process.

Wiley and Hindawi regrets that the usual quality checks did not identify these issues before publication and have since put additional measures in place to safeguard research integrity.

We wish to credit our own Research Integrity and Research Publishing teams and anonymous and named external researchers and research integrity experts for contributing to this investigation.

The corresponding author, as the representative of all authors, has been given the opportunity to register their agreement or disagreement to this retraction. We have kept a record of any response received.

References

[1] T. Xin, C. Lu, J. Zhang et al., "Oxidized LDL Disrupts Metabolism and Inhibits Macrophage Survival by Activating a miR-9/Drp1/ Mitochondrial Fission Signaling Pathway," *Oxidative Medicine and Cellular Longevity*, vol. 2020, Article ID 8848930, 16 pages, 2020.

Retraction

Retracted: Effects of Xuefu Zhuyu Granules on Patients with Stable Coronary Heart Disease: A Double-Blind, Randomized, and Placebo-Controlled Study

Oxidative Medicine and Cellular Longevity

This article has been retracted by Hindawi following an investigation undertaken by the publisher [1]. This investigation has uncovered evidence of one or more of the following indicators of systematic manipulation of the publication process:

(1) Discrepancies in scope
(2) Discrepancies in the description of the research reported
(3) Discrepancies between the availability of data and the research described
(4) Inappropriate citations
(5) Incoherent, meaningless and/or irrelevant content included in the article
(6) Peer-review manipulation

The presence of these indicators undermines our confidence in the integrity of the article's content and we cannot, therefore, vouch for its reliability. Please note that this notice is intended solely to alert readers that the content of this article is unreliable. We have not investigated whether authors were aware of or involved in the systematic manipulation of the publication process.

Wiley and Hindawi regrets that the usual quality checks did not identify these issues before publication and have since put additional measures in place to safeguard research integrity.

We wish to credit our own Research Integrity and Research Publishing teams and anonymous and named external researchers and research integrity experts for contributing to this investigation.

The corresponding author, as the representative of all authors, has been given the opportunity to register their agreement or disagreement to this retraction. We have kept a record of any response received.

References

[1] Y. Li, T. Tao, D. Song, T. He, and X. Liu, "Effects of Xuefu Zhuyu Granules on Patients with Stable Coronary Heart Disease: A Double-Blind, Randomized, and Placebo-Controlled Study," *Oxidative Medicine and Cellular Longevity*, vol. 2021, Article ID 8877296, 9 pages, 2021.

Retraction

Retracted: Involvement of Mitochondrial Dynamics and Mitophagy in Sevoflurane-Induced Cell Toxicity

Oxidative Medicine and Cellular Longevity

This article has been retracted by Hindawi following an investigation undertaken by the publisher [1]. This investigation has uncovered evidence of one or more of the following indicators of systematic manipulation of the publication process:

(1) Discrepancies in scope

(2) Discrepancies in the description of the research reported

(3) Discrepancies between the availability of data and the research described

(4) Inappropriate citations

(5) Incoherent, meaningless and/or irrelevant content included in the article

(6) Peer-review manipulation

The presence of these indicators undermines our confidence in the integrity of the article's content and we cannot, therefore, vouch for its reliability. Please note that this notice is intended solely to alert readers that the content of this article is unreliable. We have not investigated whether authors were aware of or involved in the systematic manipulation of the publication process.

Wiley and Hindawi regrets that the usual quality checks did not identify these issues before publication and have since put additional measures in place to safeguard research integrity.

We wish to credit our own Research Integrity and Research Publishing teams and anonymous and named external researchers and research integrity experts for contributing to this investigation.

The corresponding author, as the representative of all authors, has been given the opportunity to register their agreement or disagreement to this retraction. We have kept a record of any response received.

References

[1] M. Li, J. Guo, H. Wang, and Y. Li, "Involvement of Mitochondrial Dynamics and Mitophagy in Sevoflurane-Induced Cell Toxicity," *Oxidative Medicine and Cellular Longevity*, vol. 2021, Article ID 6685468, 7 pages, 2021.

Retraction

Retracted: Effects of Xuefu Zhuyu Granules on Patients with Stable Coronary Heart Disease: A Double-Blind, Randomized, and Placebo-Controlled Study

Oxidative Medicine and Cellular Longevity

This article has been retracted by Hindawi following an investigation undertaken by the publisher [1]. This investigation has uncovered evidence of one or more of the following indicators of systematic manipulation of the publication process:

(1) Discrepancies in scope

(2) Discrepancies in the description of the research reported

(3) Discrepancies between the availability of data and the research described

(4) Inappropriate citations

(5) Incoherent, meaningless and/or irrelevant content included in the article

(6) Peer-review manipulation

The presence of these indicators undermines our confidence in the integrity of the article's content and we cannot, therefore, vouch for its reliability. Please note that this notice is intended solely to alert readers that the content of this article is unreliable. We have not investigated whether authors were aware of or involved in the systematic manipulation of the publication process.

Wiley and Hindawi regrets that the usual quality checks did not identify these issues before publication and have since put additional measures in place to safeguard research integrity.

We wish to credit our own Research Integrity and Research Publishing teams and anonymous and named external researchers and research integrity experts for contributing to this investigation.

The corresponding author, as the representative of all authors, has been given the opportunity to register their agreement or disagreement to this retraction. We have kept a record of any response received.

References

[1] Y. Li, T. Tao, D. Song, T. He, and X. Liu, "Effects of Xuefu Zhuyu Granules on Patients with Stable Coronary Heart Disease: A Double-Blind, Randomized, and Placebo-Controlled Study," *Oxidative Medicine and Cellular Longevity*, vol. 2021, Article ID 8877296, 9 pages, 2021.

Research Article

Effects of Xuefu Zhuyu Granules on Patients with Stable Coronary Heart Disease: A Double-Blind, Randomized, and Placebo-Controlled Study

Yuzhen Li❶, Tianqi Tao, Dandan Song, Tao He, and Xiuhua Liu❶

Department of Pathophysiology, Graduate School, PLA General Hospital, 100853 Beijing, China

Correspondence should be addressed to Xiuhua Liu; xiuhualiu98@163.com

Despite advances in the drug treatment strategy for stable coronary heart disease (CHD), the mortality of CHD continues to rise. New or adjuvant treatments would be desirable for CHD. Xuefu Zhuyu granules are derived from the formula of traditional Chinese medicine. To determine whether Xuefu Zhuyu granules might have adjuvant effects on stable CHD, we conducted a controlled clinical trial. Patients with stable CHD were enrolled and randomly assigned to receive Xuefu Zhuyu granules or placebo for 12 weeks in addition to their standard medications for the treatment of CHD. The primary endpoints comprise the Canadian Cardiovascular Society Angina Grading Scale (CCS class), echocardiographic measures, Seattle Angina Questionnaire (SAQ), and coronary artery CT. The secondary endpoints included the parameters of nailfold capillary measurement and cutaneous blood perfusion (CBP). After 12 weeks of follow-up, there was a great improvement of the Canadian Cardiovascular Society Angina Grading Scale (CCS class) in the Xuefu Zhuyu group compared with the placebo group ($p < 0.01$). Also, a decrease was found in the percentage of patients with CCS class II in the Xuefu Zhuyu group between follow-up at 12 weeks and baseline ($p < 0.01$). We observed a significant increase in SAQ scores of physical limitation ($p < 0.01$) and treatment satisfaction ($p < 0.05$) in patients receiving Xuefu Zhuyu treatment at 12 weeks in comparison with those at baseline, but not in placebo treatment ($p > 0.05$). Amelioration in coronary artery stenosis in the Xuefu Zhuyu group was noted ($p < 0.05$). Xuefu Zhuyu granule treatment led to great improvements in cutaneous blood perfusion at follow-up of 12 weeks compared with placebo ($p < 0.05$). These findings suggest that on a background of standard medications, Xuefu Zhuyu granules have the ability to further improve the prognosis of patients with stable CHD.

1. Introduction

With the aging of the world population and the increase in younger patients, coronary heart disease (CHD) is becoming a public health problem. According to the guidelines on the prevention and treatment of CHD, nitrates, β-blocker, calcium channel blocker, anticoagulant, and lipid-lowering medications are standard and first-line treatments for CHD [1, 2]. However, the mortality of CHD resulting from this condition continues to rise all over the world [3, 4]. Thus, new or adjuvant treatments would be desirable for CHD. One such treatment is traditional Chinese medicine (TCM). CHD is a narrowing of the small blood vessels that supply blood and oxygen to the heart [5, 6]. From the viewpoint of

TCM, the major causes of CHD are Qi stagnation and blood stasis [7]. Therefore, regulating Qi and promoting blood circulation might be effective strategies in the management of CHD.

Xuefu Zhuyu granules are derived from the TCM formula of the Qing Dynasty in China. They can modulate Qi and stimulate blood circulation [8]. Xuefu Zhuyu granules are extracted from 11 types of herbs, including radix rehmanniae, angelica, radix paeoniae rubra, rhizoma ligustici wallichii, semen persicae, safflower, Bupleurum, liquorice, Platycodon grandiflorum, fructus aurantii immaturus, and Achyranthes [9, 10]. Radix paeoniae rubra, safflower, and fructus aurantii immaturus are the principal pharmacologically active components [10]. Although some studies suggest

the alleviated effect of Xuefu Zhuyu granules on unstable angina [11, 12], its role in the systemic endpoints of stable CHD is still unknown.

The present study evaluated the effects of Xuefu Zhuyu granules in patients with stable CHD. The primary endpoints consisted of the Canadian Cardiovascular Society Angina Grading Scale (CCS class), echocardiographic measures (chamber dimensions, ejection fraction), Seattle Angina Questionnaire (SAQ), and coronary artery CT. The secondary endpoints included the parameters of nailfold capillary measurement and cutaneous blood perfusion, clotting time, and blood lipids.

2. Materials and Methods

2.1. Study Design. This study was a single-center, placebo-controlled, and randomized double-blinded trial that assessed the effect of Xuefu Zhuyu granules on patients with stable CHD. The principal investigator designed the study. The investigators were blinded to the assigned Xuefu Zhuyu granule treatment. The study was conducted in accordance with the guidelines of the Declaration of Helsinki. And the Ethics Committees of PLA General Hospital and Xiyuan Hospital approved the study protocol. Each patient provided written informed consent.

2.2. Study Patients. A total of 40 patients diagnosed with stable CAD were recruited from the PLA General Hospital and Xiyuan Hospital. The basic parameters of the studied subjects are presented in Table 1. The clinical diagnosis of stable CAD was made according to a clinical evaluation, echocardiography, and coronary artery CT. Patients who satisfied the following inclusion criteria were subsumed in the study: (1) less than or equal to 75 years old, (2) a diameter stenosis of main coronary artery 50% to 75% or a diameter stenosis of coronary collateral branch 50% to 100%, and (3) New York Heart Association (NYHA) functional class of I to II. Exclusion criteria included patients undergoing coronary bypass surgery; patients with other relevant medical comorbidities including malfunction of the liver and kidney, diabetes, poor blood pressure control (>160/100 mmHg), hematopoietic diseases, and cancer; and those participating in other clinical trials.

The participants were randomly assigned to receive Xuefu Zhuyu granules or placebo granules twice daily for 12 weeks in addition to their medications prescribed for CHD by the attending physicians. All examinations including echocardiography, coronary artery CT, capillary observation, and blood sample tests were performed at baseline and after 12 weeks.

2.3. The Primary Endpoints. The primary endpoints were the Canadian Cardiovascular Society Angina Grading Scale (CCS class), echocardiographic measures (chamber dimensions, ejection fraction), Seattle Angina Questionnaire (SAQ), and coronary artery CT.

SAQ is a 19-item questionnaire that includes five perspectives: angina stability, angina frequency, physical limitation, treatment satisfaction, and quality of life. Scores range from 0 to 100, with higher scores indicating fewer symptoms and better health status [13, 14].

2.4. The Secondary Endpoints. The secondary endpoints included the parameters of nailfold capillary measurement and cutaneous blood perfusion.

Nailfold capillary measurement was done by videocapillaroscopy. Patients had a seated rest inside the building for 15 min before nailfold capillary measurement was conducted. The temperature of the examination room was 22–24°C. The nailfold (distal row) of the fourth finger of the left hand was examined in each patient. The two operators were responsible for blindly performing nailfold capillary measurement in each patient by employing an optical videocapillaroscopy equipped with magnification 100x contact lens and connected to image analysis software (Tongren Medical Electronics Technology Co., Ltd., China). The images were analyzed by another investigator in a blind manner.

The mean capillary number for each patient was calculated as the arithmetic mean of visible capillaries in three contiguous microscopic fields per mm^2 [15].

Laser Doppler flowmetry (LDF, Periflux System 5000 equipped with a thermostatic probe, Perimed AB) was employed to detect toe cutaneous blood perfusion (CBP). CBP was evaluated both at basal skin temperature and after probe heating at 44°C (CBP 44°C). And the percentage of CBP 44°C/CBP was calculated.

2.5. The Safety Assessments. The safety assessments included the reports of vital signs, blood, urine, and stool routine examinations, liver function and kidney function, bleeding points, ecchymosis, and adverse events.

Venous blood was drawn between 7 and 10 A.M. after an overnight fast. Blood samples were collected into serum separator tubes. Samples were allowed to clot for 20 min and then centrifuged at 3500 rpm and 4°C for 7 min to obtain serum. Clinical biochemistry parameters were assessed including liver function and kidney function by clinical standard methods.

2.6. Statistical Analysis. All statistical analyses were performed with SPSS software, version 11.0. Continuous variables are presented as the mean ± standard deviation (SD). Categorical data are shown as absolute numbers and percentages. The two-group differences were compared using a 2-sample Student test for continuous variables and a chi-squared test or Wilcoxon test. And the within-group differences were analyzed employing the Wilcoxon paired signed-rank test. A *p* value < 0.05 was considered statistically significant.

3. Results

3.1. Subject Characteristics. A total of 40 cases were included in the present study. The baseline characteristics of the studied subjects are shown in Table 1. The average course of CHD was 60.72 months. The medium age of the total subjects was 58.03 years old. 75% were male, and 25% were female. The distributions of the baseline characteristics between the

TABLE 1: Baseline characteristics of stable CHD patients receiving Xuefu Zhuyu granules or placebo.

	Placebo group ($n = 20$)	Xuefu Zhuyu group ($n = 20$)	All ($n = 40$)
Course of disease (months)	52.13 ± 38.12	69.78 ± 51.69	60.72 ± 45.48
Demographics			
Age (years)	60.00 ± 6.63	56.05 ± 9.86	58.03 ± 8.53
Male, n (%)	15 (75)	15 (75)	30 (75)
Female, n (%)	5 (25)	5 (25)	10 (25)
Race			
Han	19	20	39
Other	1	0	1
Smoking habit, n (%)	6 (30)	5 (25)	11 (27.5)
Alcohol consumption, n (%)	9 (45)	8 (40)	17 (42.5)
Body mass index (kg/m^2)	26.10 ± 3.84	26.79 ± 3.14	26.45 ± 3.47
History of diabetes, n (%)	1 (5)	1 (5)	2 (5)
Family history of CHD	3	5	8
Abnormal blood routine, n (%)	4/19 (21.1)	5/20 (25)	9/39 (23.1)
Abnormal urine routine, n (%)	8/19 (42.1)	7/20 (35)	15/39 (38.5)
Abnormal stool routine, n (%)	1/13 (7.7)	0/16 (0)	1/29 (3.4)
Abnormal liver function, n (%)	2/19 (10.5)	1/20 (5)	3/39 (7.7)
Abnormal kidney functions, n (%)	0/19 (0)	1/20 (5)	1/39 (2.6)
CCS, n (%)			
0	0 (0)	0 (0)	0 (0)
I	10 (50)	12 (60)	22 (55)
II	10 (50)	8 (40)	18 (45)
SAQ			
Physical limitations	63.89 ± 11.58	63.67 ± 13.53	63.78 ± 12.43
Anginal stability	53.75 ± 16.77	50.00 ± 18.14	51.88 ± 17.35
Anginal frequency	82.50 ± 15.52	81.50 ± 10.89	82.00 ± 13.24
Treatment satisfaction	86.18 ± 11.49	80.00 ± 19.59	83.09 ± 16.16
Disease perception	53.75 ± 18.23	55.00 ± 25.99	54.38 ± 22.17
Echocardiography measurements			
LVEF	0.64 ± 0.05	0.63 ± 0.06	0.63 ± 0.06
LVED (mm)	46.06 ± 3.49	48.25 ± 5.30	47.21 ± 4.61
Number of vessel stenosis*			
Coronary 4-vessel stenosis	0 (0)	4 (44.44)	4 (22.22)
Coronary 3-vessel stenosis	2 (22.22)	1 (11.11)	3 (16.67)
Coronary 2-vessel stenosis	3 (33.33)	2 (22.22)	5 (27.78)
Coronary 1-vessel stenosis	4 (44.44)	2 (22.22)	6 (33.33)
Coronary 0-vessel stenosis	0 (0)	0 (0)	0 (0)
Medication			
Aspirin	4 (20)	9 (45)	13 (32.5)
Clopidogrel	0 (0)	0 (0)	0 (0)
Beta-blocker	3 (15)	5 (25)	8 (20)
Calcium-channel blocker	8 (40)	6 (30)	14 (35)
Angiotensin receptor blockers	5 (25)	9 (45)	14 (35)
ACE inhibitor or ARB	2 (10)	4 (20)	6 (15)
Nitrate	3 (15)	4 (20)	7 (17.5)

*$n = 9$.

CCS	Placebo group			Xuefu Zhuyu group			p value
	Baseline	Follow-up at 12 weeks	p value	Baseline	Follow-up at 12 weeks	p value	
0	0 (0%)	0 (0%)		0 (0%)	0 (0%)		
I	10 (50%)	9 (52.94%)	1.000	12 (60%)	20 (100%)	0.005	0.001
II	10 (50%)	8 (47.06%)		8 (40%)	0 (0%)		
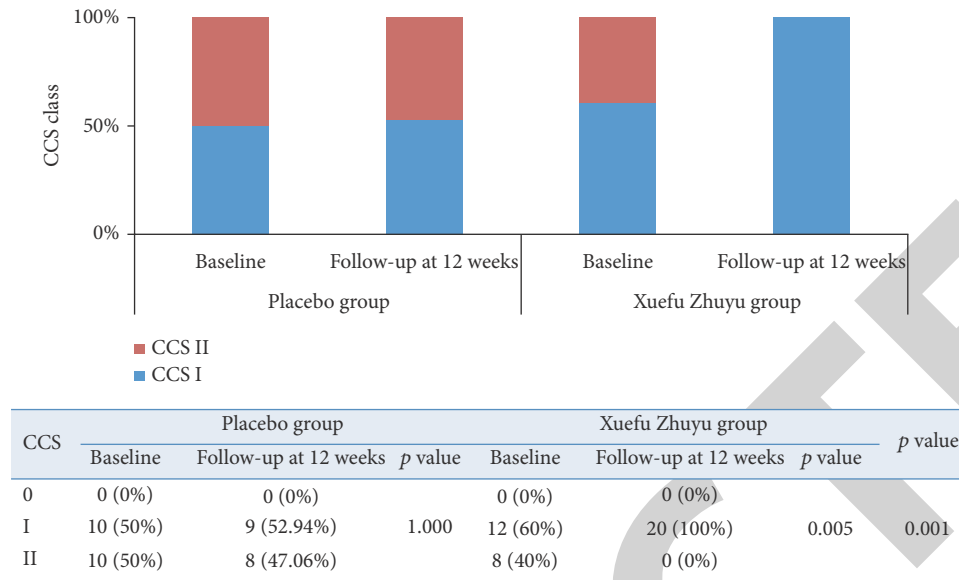
Figure 1: The changes of CCS class in patients receiving Xuefu Zhuyu or placebo granules.

SAQ	Placebo group (n = 20)			Xuefu Zhuyu group (n = 20)			p value
	Baseline	Follow-up at 12 weeks	p value	Baseline	Follow-up at 12 weeks	p value	
Physical limitations	63.89±11.58	66.41±10.85	0.367	63.67±13.53	72.22±8.82	0.001	0.081
Anginal stability	53.75±16.77	77.94±21.44	0.001	50.00±18.14	81.25±24.16	0.000	0.665
Anginal frequency	82.50±15.52	92.35±9.70	0.009	81.50±10.89	93.00±14.55	0.018	0.877
Treatment satisfaction	86.18±11.49	87.89±7.63	0.743	80.00±19.59	90.00±6.36	0.030	0.365
Disease perception	53.75±18.23	70.10±17.19	0.000	55.00±25.99	73.33±20.52	0.007	0.610

Figure 2: The changes of SAQ in patients receiving Xuefu Zhuyu or placebo granules: (a) physical limitations; (b) anginal stability; (c) anginal frequency; (d) treatment satisfaction; (e) disease perception. $^*p < 0.05$, $^{**}p < 0.01$, and $^{***}p < 0.001$. SAQ: Seattle Angina Questionnaire.

Xuefu Zhuyu group and the placebo group were well balanced and homogeneous.

3.2. Effects of Xuefu Zhuyu Granules on CCS Class in Patients with Stable CHD. After 12 weeks of follow-up, in the Xuefu Zhuyu group, 100% of patients showed CCS I. However, in the placebo group, 52.94% and 47.06% of patients showed, respectively, CCS I and CCS II. There was a great improvement of CCS angina classes in the Xuefu Zhuyu group compared with the placebo group ($p < 0.01$) (Figure 1). Also, we observed a significant decrease in the percentage of patients with CCS class II in the Xuefu Zhuyu group (from 40% at baseline to 0% at 12 weeks, $p < 0.01$). No significant change in the percentage of patients with CCS class II was detected in the placebo group (from 50% to 47.06%, $p > 0.05$) (Figure 1).

3.3. Effects of Xuefu Zhuyu Granules on SAQ in Patients with Stable CHD. SAQ is a 19-item questionnaire measuring five domains of health status related to coronary artery disease:

physical limitation, angina stability, angina frequency, treatment satisfaction, and disease perception. After 12 weeks of treatment, there were no significant differences in the SAQ scores of five domains between the Xuefu Zhuyu group and the placebo group (Figure 2). Furthermore, we analyzed the differences in the SAQ scores between follow-up at 12 weeks and baseline (Figure 2). We observed a significant increase in the SAQ scores of all five domains in patients who underwent Xuefu Zhuyu treatment at 12 weeks in comparison with those at baseline (physical limitation: 72.22 ± 8.82 vs. 63.67 ± 13.53, $p \leq 0.001$; angina stability: 81.25 ± 24.16 vs. 50.00 ± 18.14, $p \leq 0.001$; angina frequency: 93.00 ± 14.55 vs. 81.50 ± 10.89, $p < 0.05$; treatment satisfaction: 90.00 ± 6.36 vs. 80.00 ± 19.59, $p < 0.05$; and disease perception: 73.33 ± 20.52 vs. 55.00 ± 25.99, $p < 0.01$). In contrast, in the placebo group, the SAQ scores at 12 weeks were higher only in angina stability (77.94 ± 21.44 vs. 53.75 ± 16.77, $p \leq 0.001$), angina frequency (92.35 ± 9.70 vs. 82.50 ± 15.52, $p < 0.01$), and disease perception (70.10 ± 17.19 vs. 53.75 ± 18.23, $p \leq 0.001$)

TABLE 2: The changes of coronary vessel stenosis in patients receiving Xuefu Zhuyu or placebo granules.

Coronary vessel stenosis (%)	Placebo group ($n = 9$)			Xuefu Zhuyu group ($n = 9$)			p value
	Baseline	12 weeks	p value	Baseline	12 weeks	p value	
4-vessel stenosis	0	11.11		44.44	11.11		
3-vessel stenosis	22.22	44.44		11.11	44.44		
2-vessel stenosis	33.33	11.11	0.317	22.22	11.11	0.025	1.00
1-vessel stenosis	44.44	22.22		22.22	22.22		
0-vessel stenosis	0	11.11		0	11.11		

(a)

(b)

(c)

	Placebo group			Xuefu Zhuyu group			p value
	Baseline	12 weeks	p value	Baseline	12 weeks	p value	
Capillary number (mm^2)	4.84±1.14 ($n = 13$)	5±0.707 ($n = 13$)	0.549	4.93±1.24 ($n = 16$)	5.56±0.81 ($n = 16$)	0.007	0.060
Diameter of input branch (μm)	7.25±1.35 ($n = 12$)	7.5±1.24 ($n = 12$)	0.429	8.35±2.23 ($n = 14$)	8.28±1.64 ($n = 14$)	0.890	0.187
Diameter of output branch (μm)	9.50±1.98 ($n = 12$)	10.58±3.09 ($n = 12$)	0.109	11.14±2.87 ($n = 14$)	11.28±2.49 ($n = 14$)	0.759	0.527
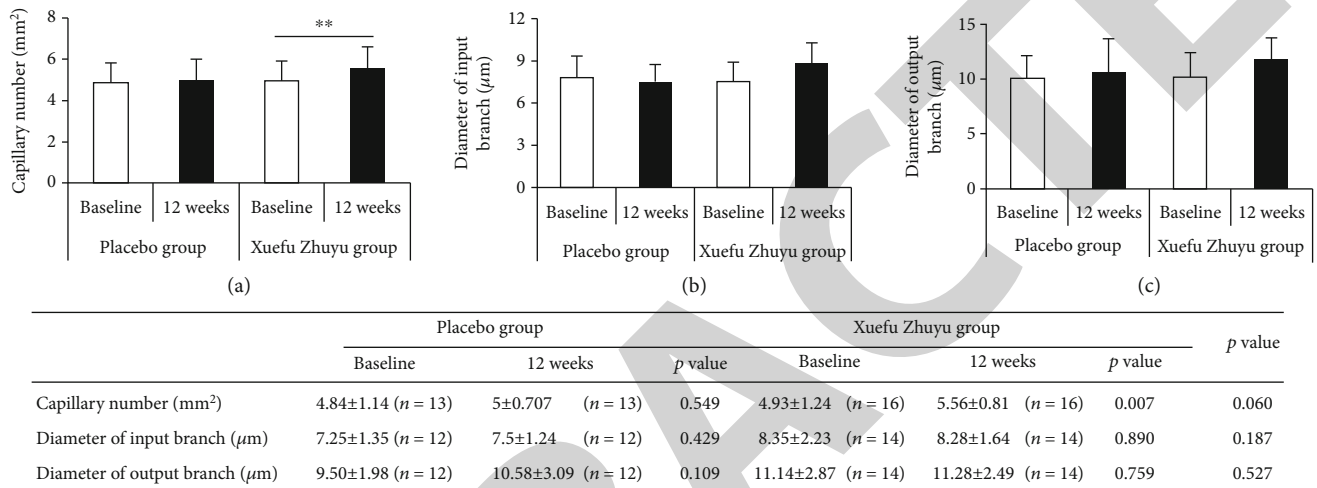
FIGURE 3: The changes of the parameters of nailfold capillaries in patients receiving Xuefu Zhuyu or placebo granules: (a) capillary number; (b) diameter of input branch; (c) diameter of output branch. $^{**}p < 0.01$.

than those at baseline. There were no significant differences between follow-up at 12 weeks and baseline with respect to improvement in physical limitation (66.41 ± 10.85 vs. 63.89 ± 11.58, $p > 0.05$) or treatment satisfaction (87.89 ± 7.63 vs. 86.18 ± 11.49, $p > 0.05$).

3.4. Effects of Xuefu Zhuyu Granules on Echocardiographic Parameters and CTA in Patients with Stable CHD. Echocardiographic analyses showed that no significant improvement in LVEF and LVED was noted in the Xuefu Zhuyu group. The percentage of coronary artery stenosis was not different between the Xuefu Zhuyu group and the placebo group ($p > 0.05$). Further analysis showed that a significant difference in coronary artery stenosis was noted between baseline and follow-up at 12 weeks in the Xuefu Zhuyu group ($p < 0.05$) (Table 2).

3.5. Effects of Xuefu Zhuyu Granules on the Parameters of Nailfold Capillaries in Patients with Stable CHD. The number and diameter of nailfold capillaries were detected using videocapillaroscopy. As shown in Figure 3, there were no significant differences in the number and diameter of nailfold capillaries between the Xuefu Zhuyu group and the placebo group at baseline and 12 weeks. To further analyze the changes of capillary parameters, we compared the number and diameter of nailfold capillaries at baseline with that at 12 weeks. And we found that the number of capillaries at

12 weeks (5.56 ± 0.81) was more than that at baseline (4.93 ± 1.24) ($p < 0.01$) in patients treated with Xuefu Zhuyu granules, but not in the placebo patients ($p > 0.05$).

3.6. Effects of Xuefu Zhuyu Granules on Cutaneous Blood Perfusion in Patients with Stable CHD. Cutaneous blood perfusion is one of the critical indexes reflecting capillary function. As shown in Figure 4, cutaneous blood perfusion did not differ between the two groups at baseline. Xuefu Zhuyu granule treatment led to significant improvements in CBP 44°C and CBP 44°C/CBP at follow-up of 12 weeks compared with placebo (CBP 44°C: 172.60 ± 44.57 vs. 114.00 ± 36.70, $p < 0.01$; CBP 44°C/CBP: 765.50 ± 358.96 vs. 451.10 ± 213.64, $p < 0.05$).

3.7. Safety Endpoints. The safety assessments are shown in Table 3. Vital signs of all patients were recorded at each study visit. There were no statistically significant differences between the placebo and treatment groups ($p > 0.05$). We compared the intergroup and intragroup differences in abnormal percentages of blood routine, urine routine, stool routine, and liver and kidney functions between the placebo and treatment groups. These abnormal percentages did not show great differences. Also, bleeding points, ecchymosis, and serious adverse events did not occur in patients receiving Xuefu Zhuyu or placebo after 12 weeks.
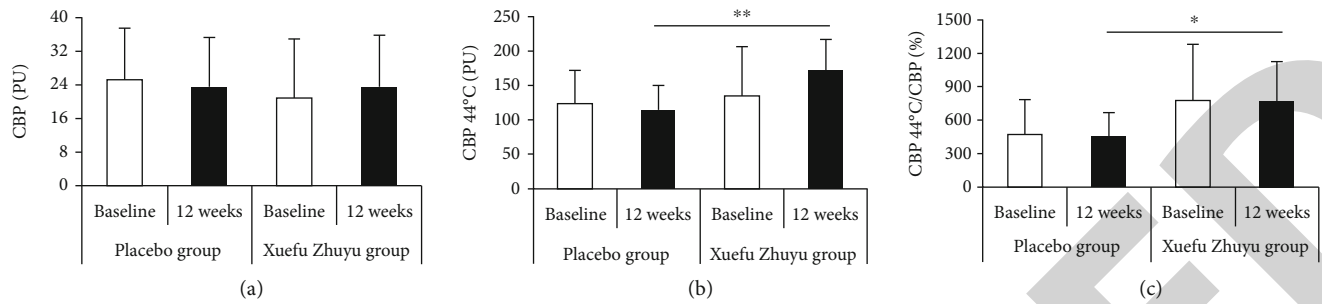
	Placebo group ($n = 10$)			Xuefu Zhuyu group ($n = 10$)			p value
	Baseline	12 weeks	p value	Baseline	12 weeks	p value	
CBP (PU)	25.20±12.39	23.80±11.47	0.796	20.9±13.99	23.50±12.44	0.666	0.956
CBP 44°C (PU)	123±48.94	114.00±36.70	0.647	134.8±70.24	172.60±44.57	0.168	0.005
CBP 44°C/CBP (%)	470.9±306.19	451.10±213.64	0.869	773±504.91	765.50±358.96	0.970	0.029

FIGURE 4: The changes of cutaneous blood perfusion in patients receiving Xuefu Zhuyu or placebo granules: (a) cutaneous blood perfusion (CBP); (b) cutaneous blood perfusion after probe heating at 44°C (CBP 44°C); (c) CBP 44°C/CBP. $^{*}p < 0.05$, $^{**}p < 0.01$.

TABLE 3: The safety endpoints of stable CHD patients receiving Xuefu Zhuyu granules or placebo after 12 weeks.

	Placebo group			Xuefu Zhuyu group			p value
	Baseline ($n = 20$)	12 weeks ($n = 17$)	p value	Baseline ($n = 20$)	12 weeks ($n = 20$)	p value	
Vital signs							
Temperature (°C)	36.60 ± 0.23	36.48 ± 0.26	0.025	36.51 ± 0.21	36.45 ± 0.24	0.323	0.701
Breath	19.20 ± 1.28	18.71 ± 1.21	0.134	18.75 ± 1.33	18.55 ± 1.39	0.530	0.721
Pulse rate	70.70 ± 8.59	68.53 ± 6.37	0.439	74.05 ± 10.99	70.50 ± 9.46	0.274	0.471
Heart rate (bpm)	68.88 ± 9.10	65.64 ± 7.45	0.599	71.50 ± 10.31	68.47 ± 9.72	0.698	0.379
Systolic BP (mmHg)	127.55 ± 16.37	133.76 ± 13.23	0.112	125.90 ± 12.62	131.30 ± 13.51	0.083	0.580
Diastolic BP (mmHg)	80.63 ± 10.03	84.59 ± 10.15	0.021	80.50 ± 7.97	84.80 ± 10.10	0.035	0.950
Abnormal blood routine (%)	10.5	17.6	0.655	25	30	0.705	0.462
Abnormal urine routine (%)	42.1	41.2	1.000	35	44.4	0.414	1.000
Abnormal stool routine (%)	7.1	12.5	1.000	0	0	1.000	0.400
Abnormal liver function (%)	10.5	5.9	0.564	5	10	0.564	1.000
Abnormal kidney function (%)	0	0	1.000	5	10	0.317	0.489
Bleeding point (%)	0	0		0	0		
Ecchymosis (%)	0	0		0	0		
Serious adverse events							
Death	0	0		0	0		
Hospitalization	0	0		0	0		
Worsening CHD	0	0		0	0		
Stroke	0	0		0	0		
Unknown reason	0	0		0	0		

4. Discussion

Stable CHD as a public health problem is still an extremely important focus of clinical cardiology despite the use of medicaments such as β-blocker; calcium channel blocker improves the symptoms of stable CHD patients [1, 2, 16]. High morbidity and mortality all over the world ask for us to seek other novel therapeutic approaches to further improve the prognosis for patients with stable CHD. TCM

has widely been used to effectively treat various heart diseases including chronic heart failure, hypertension, and cardiac hypertrophy [17]. According to the theory of TCM, the occurrence of stable CHD is due to the disturbance of Qi and blood. Therefore, regulation of Qi and blood is critical for patients with stable CHD.

Xuefu Zhuyu has the ability to modulate Qi and blood [8]. And it has been widely applied to stable CHD in the clinic. However, we employ PubMed to search Xuefu Zhuyu

and find that there are 11 publications for the effects of Xuefu Zhuyu on patients with CHD. Among them, only 2 publications focus on stable angina pectoris. One reports that Xuefu Zhuyu could improve the levels of octadecanoic acid, phosphoglycerol, and sphingomyelin [18]. Another is published by our group, which indicates that 2-deoxy-D-glucose and spermine might constitute the partial material foundation of Qi in CHD patients treated with Xuefu Zhuyu [19]. Thus, the efficacy and safety of Xuefu Zhuyu in patients with stable CHD need to be confirmed systematically. In the present study, a double-blind, randomized, and placebo-controlled method is used to detect the effects of Xuefu Zhuyu on the primary endpoints of stable CHD patients. Among the primary endpoints, our study demonstrates that Xuefu Zhuyu granules decrease CCS angina class and increase the SAQ scores of physical limitation and treatment satisfaction. But chamber dimensions and ejection fraction by echocardiographic measures do not show a significant improvement in the Xuefu Zhuyu group compared with the placebo group. A plausible reason is that the chamber dimensions and ejection fraction of enrolled patients are in the normal range. In addition, we find a difference in the percentage of coronary artery stenosis between baseline and 12-week follow-up. Because only 9 patients agree to do the CTA test, the improvement result needs to be further confirmed in a large sample.

Abnormalities in the structure and function of the coronary microcirculation could serve as important markers of risk and contribute to cardiac pathophysiology including CHD [5, 20]. The coronary microvasculature cannot be directly imaged in vivo [21]. Some invasive and noninvasive techniques are employed to assess coronary microvascular function [22]. However, due to the invasiveness, radioactivity, investigational and technical limitations, and costs, it is not easy to observe clinically at all times to accurately monitor the efficacy [20, 21]. It has been demonstrated that peripheral microvascular function reflects coronary vascular function [22]. Nailfold capillary and LDF measurements are noninvasive, continuous, and real-time quantitative methods for peripheral microvascular function [23, 24]. Therefore, we use the two methods to detect the changes of nailfold capillaries and cutaneous blood perfusion as secondary endpoints. The results of our study suggest that Xuefu Zhuyu granules significantly increase the number of nailfold capillaries. It is reported that capillary density may positively affect tissue perfusion [25, 26]. It seems that Xuefu Zhuyu granules can induce an elevation in tissue perfusion. Indeed, our LDF study indicates that Xuefu Zhuyu granules are able to greatly improve cutaneous blood perfusion.

It has been reported that the abnormality of the substrate and energy metabolism is fundamental in the development of CHD [27]. Our previous study analyzed the metabolic profiling of CHD patients undergoing Xuefu Zhuyu granules. We found that 2-deoxy-D-glucose and spermine might constitute the partial material foundation of Qi in CHD patients treated with Xuefu Zhuyu granules [19]. There is evidence that Xuefu Zhuyu decoction decreases the levels of soluble VCAM-1 and soluble ICAM-1 in serum of patients with unstable angina pectoris [28, 29]. Oxidative stress response

has been demonstrated to be an independent risk for the development of CHD. A recent study reports that Xuefu Zhuyu decoction could increase the level of superoxide dismutase and reduce the level of malondialdehyde in patients with CHD [30]. It seems that Xuefu Zhuyu has a potential role in inhibiting oxidative stress response. These findings indicate that Xuefu Zhuyu might exert its treatment effects on CHD patient by regulating metabolic profiling, inhibiting the production of adhesive molecules, and improving oxidative stress response.

Although the present study provides beneficial findings, it has some limitations which have to be acknowledged. First, this study is a single-center trial, which limits generalizability. Second, the sample size of the study is small, which might have decreased the ability to detect a treatment effect. Indeed, significant differences in some outcomes are not observed between the Xuefu Zhuyu group and the placebo group. Therefore, further study with a large sample size needs to be done. Third, only one dosage is employed in the study. Two or more dosages should be used to compare the treatment effects. Fourth, all examinations are performed at 12 weeks. The observation duration is relatively short for safety.

5. Conclusions

The results demonstrate that Xuefu Zhuyu granules are able to further ameliorate the prognosis of patients with stable CHD. The findings support that on a background of standard medications, Xuefu Zhuyu granules could be used in combination therapy for stable CHD.

Data Availability

The data used to support the findings of this study are included within the article.

Conflicts of Interest

The authors report no conflict of interests.

Acknowledgments

References

[1] S. D. Fihn, J. M. Gardin, J. Abrams et al., "2012 ACCF/AHA/ACP/AATS/PCNA/SCAI/STS Guideline for the diagnosis and management of patients with stable ischemic heart disease: a report of the American College of Cardiology Foundation/American Heart Association Task Force on Practice Guidelines, and the American College of Physicians, American Association for Thoracic Surgery, Preventive Cardiovascular Nurses Association, Society for Cardiovascular Angiography and Interventions, and Society of Thoracic Surgeons," *Journal of the American College of Cardiology*, vol. 60, no. 24, pp. e44–e164, 2012.

[2] G. N. Levine, E. R. Bates, J. A. Bittl et al., "2016 ACC/AHA guideline focused update on duration of dual antiplatelet therapy in patients with coronary artery disease: a report of the American College of Cardiology/American Heart Association Task Force on Clinical Practice Guidelines: an update of the 2011 ACCF/AHA/SCAI Guideline for Percutaneous Coronary Intervention, 2011 ACCF/AHA Guideline for Coronary Artery Bypass Graft Surgery, 2012 ACC/AHA/ACP/AATS/PCNA/SCAI/STS Guideline for the Diagnosis and Management of Patients With Stable Ischemic Heart Disease, 2013 ACCF/AHA Guideline for the Management of ST-Elevation Myocardial Infarction, 2014 AHA/ACC Guideline for the Management of Patients With Non-ST-Elevation Acute Coronary Syndromes, and 2014 ACC/AHA Guideline on Perioperative Cardiovascular Evaluation and Management of Patients Undergoing Noncardiac Surgery," *Circulation*, vol. 134, no. 10, pp. e123–e155, 2016.

[3] E. J. Benjamin, M. J. Blaha, S. E. Chiuve et al., "Heart disease and stroke statistics-2017 update: a report from the American Heart Association," *Circulation*, vol. 135, no. 10, pp. e146–e603, 2017.

[4] R. Lozano, M. Naghavi, K. Foreman et al., "Global and regional mortality from 235 causes of death for 20 age groups in 1990 and 2010: a systematic analysis for the Global Burden of Disease Study 2010," *Lancet*, vol. 380, no. 9859, pp. 2095–2128, 2012.

[5] A. R. Pries and B. Reglin, "Coronary microcirculatory pathophysiology: can we afford it to remain a black box?," *European Heart Journal*, vol. 38, no. 7, pp. 478–488, 2017.

[6] G. A. de Waard, S. S. Nijjer, M. A. van Lavieren et al., "Invasive minimal microvascular resistance is a new index to assess microcirculatory function independent of obstructive coronary artery disease," *Journal of the American Heart Association*, vol. 5, no. 12, article e004482, 2016.

[7] J. N. Zhao, Y. Zhang, X. Lan et al., "Efficacy and safety of Xinnaoning capsule in treating chronic stable angina (qi stagnation and blood stasis syndrome): study protocol for a multicenter, randomized, double-blind, placebo-controlled trial," *Medicine (Baltimore)*, vol. 98, no. 31, article e16539, 2019.

[8] H. He, G. Chen, J. Gao et al., "Xue-Fu-Zhu-Yu capsule in the treatment of qi stagnation and blood stasis syndrome: a study protocol for a randomised controlled pilot and feasibility trial," *Trials*, vol. 19, no. 1, p. 515, 2018.

[9] S. Q. Tan, X. Geng, J. H. Liu et al., "Xue-fu-Zhu-Yu decoction protects rats against retinal ischemia by downregulation of HIF-1α and VEGF via inhibition of RBP2 and PKM2," *BMC Complementary and Alternative Medicine*, vol. 17, no. 1, p. 365, 2017.

[10] Y. N. Zhou, M. Y. Sun, Y. P. Mu et al., "Xuefuzhuyu decoction inhibition of angiogenesis attenuates liver fibrosis induced by CCl$_4$ in mice," *Journal of Ethnopharmacology*, vol. 153, no. 3, pp. 659–666, 2014.

[11] J. Wang, X. Yang, F. Chu et al., "The effects of xuefu zhuyu and shengmai on the evolution of syndromes and inflammatory markers in patients with unstable angina pectoris after percutaneous coronary intervention: a randomised controlled clinical trial," *Evidence-based Complementary and Alternative Medicine*, vol. 2013, Article ID 896467, 9 pages, 2013.

[12] F. Y. Chu, J. Wang, K. W. Yao, and Z. Z. Li, "Effect of Xuefu Zhuyu capsule (血府逐瘀胶囊) on the symptoms and signs and health-related quality of life in the unstable angina patients with blood-stasis syndrome after percutaneous coronary intervention: a randomized controlled trial," *Chinese Journal of Integrative Medicine*, vol. 16, no. 5, pp. 399–405, 2010.

[13] S. Verheye, E. M. Jolicœur, M. W. Behan et al., "Efficacy of a device to narrow the coronary sinus in refractory angina," *The New England Journal of Medicine*, vol. 372, no. 6, pp. 519–527, 2015.

[14] J. A. Spertus, J. A. Winder, T. A. Dewhurst et al., "Development and evaluation of the Seattle angina questionnaire: a new functional status measure for coronary artery disease," *Journal of the American College of Cardiology*, vol. 25, no. 2, pp. 333–341, 1995.

[15] R. de Moraes, D. van Bavel, M. B. Gomes, and E. Tibiriçá, "Effects of non-supervised low intensity aerobic excise training on the microvascular endothelial function of patients with type 1 diabetes: a non-pharmacological interventional study," *BMC Cardiovascular Disorders*, vol. 16, no. 1, p. 23, 2016.

[16] J. A. Ladapo, K. S. Goldfeld, and P. S. Douglas, "Projected morbidity and mortality from missed diagnoses of coronary artery disease in the United States," *International Journal of Cardiology*, vol. 195, pp. 250–252, 2015.

[17] X. Li, J. Zhang, J. Huang et al., "A multicenter, randomized, double-blind, parallel-group, placebo-controlled study of the effects of qili qiangxin capsules in patients with chronic heart failure," *Journal of the American College of Cardiology*, vol. 62, no. 12, pp. 1065–1072, 2013.

[18] X. Y. Lu, H. Xu, T. Zhao, and G. Li, "Study of serum metabonomics and formula-pattern correspondence in coronary heart disease patients diagnosed as phlegm or blood stasis pattern based on ultra performance liquid chromatography mass spectrometry," *Chinese Journal of Integrative Medicine*, vol. 24, no. 12, pp. 905–911, 2018.

[19] T. Q. Tao, T. He, X. R. Wang, and X. Liu, "Metabolic profiling analysis of patients with coronary heart disease undergoing xuefu zhuyu decoction treatment," *Frontiers in Pharmacology*, vol. 10, p. 985, 2019.

[20] P. G. Camici, G. d'Amati, and O. Rimoldi, "Coronary microvascular dysfunction: mechanisms and functional assessment," *Nature Reviews. Cardiology*, vol. 12, no. 1, pp. 48–62, 2015.

[21] J. Herrmann, J. C. Kaski, and A. Lerman, "Coronary microvascular dysfunction in the clinical setting: from mystery to reality," *European Heart Journal*, vol. 33, no. 22, pp. 2771–2783, 2012.

[22] A. al-Badri, J. H. Kim, C. Liu, P. K. Mehta, and A. A. Quyyumi, "Peripheral microvascular function reflects coronary vascular function," *Arteriosclerosis, Thrombosis, and Vascular Biology*, vol. 39, no. 7, pp. 1492–1500, 2019.

[23] M. Cutolo, C. Ferrone, C. Pizzorni, S. Soldano, B. Seriolo, and A. Sulli, "Peripheral blood perfusion correlates with microvascular abnormalities in systemic sclerosis: a laser-Doppler and nailfold videocapillaroscopy study," *The Journal of Rheumatology*, vol. 37, no. 6, pp. 1174–1180, 2010.

[24] V. Lambrecht, M. Cutolo, F. de Keyser et al., "Reliability of the quantitative assessment of peripheral blood perfusion by laser speckle contrast analysis in a systemic sclerosis cohort," *Annals of the Rheumatic Diseases*, vol. 75, no. 6, pp. 1263-1264, 2016.

[25] E. H. Serné, R. O. Gans, J. C. ter Maaten, G. J. Tangelder, A. J. M. Donker, and C. D. A. Stehouwer, "Impaired skin capillary recruitment in essential hypertension is caused by both

Retraction

Retracted: Epicardial Adipose Tissue Volume Is Associated with High Risk Plaque Profiles in Suspect CAD Patients

Oxidative Medicine and Cellular Longevity

This article has been retracted by Hindawi following an investigation undertaken by the publisher [1]. This investigation has uncovered evidence of one or more of the following indicators of systematic manipulation of the publication process:

(1) Discrepancies in scope

(2) Discrepancies in the description of the research reported

(3) Discrepancies between the availability of data and the research described

(4) Inappropriate citations

(5) Incoherent, meaningless and/or irrelevant content included in the article

(6) Peer-review manipulation

The presence of these indicators undermines our confidence in the integrity of the article's content and we cannot, therefore, vouch for its reliability. Please note that this notice is intended solely to alert readers that the content of this article is unreliable. We have not investigated whether authors were aware of or involved in the systematic manipulation of the publication process.

Wiley and Hindawi regrets that the usual quality checks did not identify these issues before publication and have since put additional measures in place to safeguard research integrity.

We wish to credit our own Research Integrity and Research Publishing teams and anonymous and named external researchers and research integrity experts for contributing to this investigation.

The corresponding author, as the representative of all authors, has been given the opportunity to register their agreement or disagreement to this retraction. We have kept a record of any response received.

References

[1] D. Shan, G. Dou, J. Yang et al., "Epicardial Adipose Tissue Volume Is Associated with High Risk Plaque Profiles in Suspect CAD Patients," *Oxidative Medicine and Cellular Longevity*, vol. 2021, Article ID 6663948, 10 pages, 2021.

Research Article

Epicardial Adipose Tissue Volume Is Associated with High Risk Plaque Profiles in Suspect CAD Patients

Dongkai Shan,[1] Guanhua Dou,[2] Junjie Yang,[1] Xi Wang,[3] Jingjing Wang,[3] Wei Zhang,[3] Bai He,[3] Yuqi Liu,[1] Yundai Chen ⓘ,[1] and Yang Li ⓘ[1]

[1]*Department of Cardiovascular Medicine, Sixth Medical Center, Chinese PLA General Hospital, Beijing, China*
[2]*Department of Cardiology, Second Medical Center, Chinese PLA General Hospital, Beijing, China*
[3]*Department of Cardiology, First Medical Center, Chinese PLA General Hospital, Beijing, China*

Correspondence should be addressed to Yundai Chen; yundaic@163.com and Yang Li; liyangbsh@163.com

Objective. To explore the association between EAT volume and plaque precise composition and high risk plaque detected by coronary computed tomography angiography (CCTA). *Methods*. 101 patients with suspected coronary artery disease (CAD) underwent CCTA examination from March to July 2019 were enrolled, including 70 cases acute coronary syndrome (ACS) and 31 cases stable angina pectoris (SAP). Based on CCTA image, atherosclerotic plaque precise compositions were analyzed using dedicated quantitative software. High risk plaque was defined as plaque with more than 2 high risk features (spotty calcium, positive remolding, low attenuation plaque, napkin-ring sign) on CCTA image. The association between EAT volume and plaque composition was assessed as well as the different of correlation between ACS and SAP was analyzed. Multivariable logistic regression analysis was used to explore whether EAT volume was independent risk factors of high risk plaque (HRP). *Results*. EAT volume in the ACS group was significantly higher than that of the SAP group ($143.7 \pm 49.8 \, cm^3$ vs. $123.3 \pm 39.2 \, cm^3$, $P = 0.046$). EAT volume demonstrated a significant positive correlation with total plaque burden ($r = 0.298$, $P = 0.003$), noncalcified plaque burden ($r = 0.245$, $P = 0.013$), lipid plaque burden ($r = 0.250$, $P = 0.012$), and homocysteine ($r = 0.413$, $P \leq 0.001$). In ACS, EAT volume was positively correlated with total plaque burden ($r = 0.309$, $P = 0.009$), noncalcified plaque burden ($r = 0.242$, $P = 0.044$), and lipid plaque burden ($r = 0.240$, $P = 0.045$); however, no correlation was observed in SAP. Patients with HRP have larger EAT volume than those without HRP ($169 \pm 6.2 \, cm^3$ vs. $130.6 \pm 5.3 \, cm^3$, $P = 0.002$). After adjustment by traditional risk factors and coronary artery calcium score (CACS), EAT volume was an independent risk predictor of presence of HRP (OR: 1.018 (95% CI: 1.006-1.030), $P = 0.004$). *Conclusions*. With the increasing EAT volume, more dangerous plaque composition burdens increase significantly. EAT volume is a risk predictor of HRP independent of convention cardiovascular risk factors and CACS, which supports the potential impact of EAT on progression of coronary atherosclerotic plaque.

1. Introduction

Epicardial adipose tissue (EAT) was special visceral fat located in the pericardial membrane. As proximity of EAT to coronary artery, several studies have concluded the association between EAT and coronary artery disease (CAD) and revealed that EAT may promote presence and progression of coronary atherosclerotic plaque by releasing proatherogenic cytokines to initiate the development of plaque. In spite of this, the underlying mechanism of EAT atherosclerotic

effect was not clear, and the association between EAT and plaque composition has not been clarified.

Acute coronary syndrome (ACS) is characterized by "vulnerable" feature of atherosclerotic plaque and related to occurrence of adverse cardiovascular events. Anatomically, vulnerable plaque is represented as thin fibrous cap, large lipid core, inflammatory cell infiltration, collagen deposition, neovascularization, and intraplaque hemorrhage [1]. Vulnerable features detected by coronary computed tomography angiography (CCTA) reconstructed image, including spotty

calcium, positive remodeling, low attenuation plaque, and napkin ring sign (NRS), were found associated with further adverse cardiovascular events [2–4]. It is critical to evaluate these vulnerable features in early phase of CAD, for which is strongly related to the patients' prognosis. On the other hand, previous studies have developed precise quantitative software for plaque composition based on CCTA images. By setting attenuation threshold, semiautomatic analysis and processing of target vascular segments were feasible for distinguishing the calcified, noncalcified, lipid, fibrous composition accurately, which was highly in accord with those obtained from high resolution intravascular image.

A few of the studies focused on the proatherogenic effect of EAT found that patients with CAD had increased EAT volume; however, there was no definite conclusion about whether pathological accumulation of EAT lead to plaque vulnerability and acute coronary events [5, 6]. A previous study using integrated backscatter intravascular ultrasound has found EAT volume was an independent risk predictor for the presence of large noncalcified components (plaque burden ≥ 40%) [7]. A virtual histology intravascular ultrasound study has also reported the correlation between plaque instability and EAT thickness [8]. However, these studies failed to clarify the differences role of EAT between ACS and stable angina pectoris (SAP) and limited to the specific study population. The aim of our study was to investigate the relationship between EAT volume and plaque composition measured by a new precise quantitative software. Furthermore, we explored whether the association exists between EAT volume and high risk plaque (HRP) defined according to coronary artery disease reporting and data system (CAD-RADS) 2016 experts consensus [9].

2. Materials and Methods

2.1. Study Population.
This study cohort consisted of patients with suspected CAD underwent CCTA in department of cardiology, Chinese PLA General Hospital. The patients' age ≥ 18 years and successfully complete CCTA examination were enrolled. Exclusion criteria included previous percutaneous coronary intervention and coronary artery bypass graft history, symptom or disease history, or examination results could not meet the ACS or SAP diagnostic criteria, artifacts in CCTA images unable to interpreted, coronary plaques could not be distinguished due to serious calcification, patients with contraindication of CCTA examination, or did not wish to participate in this study. Considering the nature of CCTA examination, all ACS patients recruited in this study were unstable angina pectoris defined according to the ACC/AHA guidelines [10], who was of intermediate pretest likelihood. SAP was diagnosed according to the guidelines for the Diagnosis and Treatment of Chronic Stable Angina Pectoris [11]: the cause of angina pectoris is exercise or other activities that cause abnormal increase of myocardial oxygen demand. From March to July 2019, a total of 101 patients were enrolled, including 70 cases with ACS and 31 cases with SAP. This study complied with the Declaration of Helsinki and was approved by the institutional review board of Chinese PLA General Hospital. Written informed consent was obtained from all patients enrolled.

2.2. Clinical Data Collection.
The basic clinical characteristics including age, gender, height, weight, heart rate, blood pressure (systolic and diastolic blood pressure), family history of CAD, hypertension, diabetes mellitus, hyperlipidemia, smoking history, and other cardiovascular risk factors were collected systematically. Laboratory parameters such as blood lipid levels (total cholesterol, triglyceride, low density lipoprotein cholesterol (LDL-C), and high density lipoprotein cholesterol (HDL-C)), fasting blood glucose levels and left ventricular ejection fraction (EF) measured by echocardiography were recorded. Hypertension was defined as systolic blood pressure ≥ 140 mmHg or diastolic blood pressure ≥ 90 mmHg or being treated with antihypertensive drugs. Diabetes mellitus was defined as fasting blood glucose ≥ 200 mg/dL or being treated with hypoglycemic drugs. Hyperlipidemia was defined as total cholesterol ≥ 220 mg/dL, triglyceride ≥ 150 mg/dL, LDL − C ≥ 160 mg/dL, HDL − C ≤ 40 mg/dL, or being treated with lipid-lowering drugs. Body mass index (BMI) was calculated as weight divided by the square of height.

2.3. CCTA Procedure.
All patients enrolled received 64 multislice dual source spiral CT scan (Somatom Definition Flash, Siemens Medical Solutions, Forchheim, Germany). The CCTA scan protocol consisted of noncontrast scan followed by enhanced contrast scan. To avoid respiratory artifacts, all patients were instructed breath holding training before scan. Continuous electrocardiogram monitoring was performed throughout whole examination process. Unless contraindicated, patients with heart rate (HR) > 70 beats/min were intravenously given 50~100 mg esmolol hydrochloride injection to control heart rate and 0.5 mg nitroglycerin to dilate coronary artery. Nonionic contrast media (Ultravist®, 370 mgI/mL, Schering AG, Guangzhou, China) was intravenously injected via anterior antecubital vein at 5 mL/s. Scanning parameters were as follows: detector collimation, $2 \times 128 \times 0.6$ mm; layer thickness, 0.7 mm; tube current, 290~560 mAs/revolution; tube voltage, 80~120 kV (according to BMI); and gantry rotation time, 0.28 s. The scanning range was from pulmonary artery bifurcation down to 1 cm below the diaphragm, and the region of interest was within the ascending aorta root. According to situation of the heart rate control, prospective or retrospective electrocardiogram gated scan mode was used necessarily and appropriately.

2.4. Postprocessing of Coronary Imaging.
All CCTA image data were transferred to a dedicated workstation (synoMulti-Modality Workplace, syngoMMWP VE40A, Siemens, Germany) for reconstruction. The images were analyzed by two experienced investigators who were blinded to the patients' clinical data. All coronary arteries with diameters ≥ 2 mm were analyzed [12]. Disagreements between two investigators were resolved by consensus reading. The measurement of coronary artery calcium score (CACS) was based on the standard Agatston method [13].

2.5. EAT Volume Quantification.
EAT gross morphology was plotted on CT image by observers in a dedicated software

(Syngo Volume, Siemens Medical Solutions) as described before [14]. EAT was defined as the adipose tissue located between pericardium layer and myocardium. The pericardium contour in the transection slices from bifurcation of pulmonary artery to the diaphragm was traced manually every 10 mm interval, and EAT volume was analyzed automatically by summing of all slices (Figure 1). Manually correction was necessary when mistake occurred with auto measurement. The CT attenuation threshold of adipose tissue was set from -195 to -45 HU. Since paracardial fat was out of visceral pericardium, it was excluded from the analysis.

2.6. Precise Quantification of Atherosclerotic Plaque Composition Based on CCTA Image. Plaque composition analysis was achieved by a precise analyzed software from Siemens (Coronary Plaque Analysis 2.0.3, Siemens, Germany), which could identify lumen boundary in detailed, and calculate maximum lumen diameter stenosis, lesion length, and plaque composition volume [15] (Figure 2). Quantitation of plaque composition included total plaque, calcified plaque, noncalcified plaque, lipid plaque, and fibrous plaque volume/burden. The burden of each composition was defined as the plaque volume normalized by vascular volume of lesion segment (Plaque burden% = $\text{Volume}_{\text{plauqe}}/\text{Volume}_{\text{vascular}} * 100\%$). Total plaque volume was sum of calcified plus noncalcified plaque volume, while noncalcified plaque volume was sum of lipid plus fibrous plaque volume. Specific CT threshold of each plaque composition was used as follows: calcified, 350~1300 HU; fibrous, 30~190 HU; and lipid, -100~30 HU. After identification of vascular and plaque boundary, measurements of plaque composition parameters were completed automatically. If inconsistent with the true lumen, manual correction was needed. Due to the precise quantitation of plaque composition was based on the lesion segment level, the parameters of the most severe lesion segment were used to represent per patient data.

High risk features including spotty calcium, positive remodeling, low attenuation plaque, and NRS were also identified on the reconstruction image. Spotty calcium was defined as punctate calcium with diameter of ≤3 mm. Positive remodeling was defined as remodeling index > 1.1, and remodeling index was the ratio of the maximum lumen diameter of the lesion to the mean diameter of the proximal and distal nonlesion reference vessel; low attenuation plaque defined as noncalcified plaque with internal attenuation less than 30HU; NRS was defined as central low attenuation plaque with a peripheral rim of higher CT attenuation [9]. A plaque could be considered as a HRP if it contained more than two features [9].

2.7. Inter- and Intraobserver Variability. In 30 randomly selected patients, EAT volume and plaque composition were measured by two independent observers. A consensus reading was performed in the final analysis when measurement difference existed. To evaluate intraobserver variability, index analysis was repeated by same observer 4 weeks later. The measurements of EAT volume of inter- and intraobserver agreement were good ($r = 0.96$ and $P < 0.01$ and $r = 0.93$ and $P < 0.01$, respectively). For plaque composition analysis,

inter- and intraobserver agreement were also good for measurement of lipid plaque burden ($r = 0.94$ and $P < 0.01$ and $r = 0.90$ and $P < 0.01$, respectively).

2.8. Statistical Analysis. All data analysis was carried out by SPSS (version 22.0; IBM Corporation, Armonk, NY, USA). Continuous data were represented by mean ± standard deviation. The comparison between two groups was used by Student's t-test if normal distribution or Mann–Whitney U test if nonnormality distribution. One-way ANOVA test was used to analyze the difference of independent simples. Categorical data was represented as the percentages, and chi-square or Fisher's exact test was used appropriately to compare two groups. The correlation between plaque composition and EAT volume was performed by Pearson or Spearman rank correlation. Multivariate logistic regression analysis was performed to reveal association between either clinical parameters or EAT volume and presence of HRP. All statistical tests were two-sides; $P < 0.05$ was regarded as significance.

3. Results

3.1. Basic Clinical Data. The basic clinical data of patients is shown in Table 1. A total of 101 patients were enrolled in the study, with an average age of 61.5 ± 8.6 years, 62.4% male, 16.8% CAD family history, 49.5% hypertension, 31.7% diabetes, 25.7% hyperlipidemia, and 30.7% smoking history. According to clinical symptoms and electrocardiogram results, 70 cases of ACS and 31 cases of SAP were diagnosed. There was no significant difference in age, gender, heart rate, BMI, and blood pressure between ACS group and SAP group. Smoking ratio in ACS was higher than that in SAP (32.9% vs. 16.1%, $P = 0.035$). The serum LDL-C and homocysteine in the ACS group was significantly higher than that in the SAP group. There was no significant difference for CACS and EAT density (attenuation), but coronary diameter stenosis rate in ACS was higher than that in SAP ($59.8 \pm 9.3\%$ vs. $55.8 \pm 10.1\%$, $P = 0.048$). In addition, EAT volume in ACS was significantly higher than the SAP group ($143.7 \pm 49.8\,\text{cm}^3$ vs. $123.3 \pm 39.2\,\text{cm}^3$, $P = 0.046$).

3.2. Correlation Analysis between EAT Volume and Plaque Composition. The total plaque burden ($P = 0.017$), noncalcified plaque burden ($P = 0.050$), and lipid plaque burden ($P = 0.015$) were significantly different among four groups divided according to the EAT volume quartiles. The difference of lipid plaque burden was the most significant, but in the absolute value of plaque composition volume, there was no significant difference among four subgroups whichever composition (Table 2).

Take above into consideration, we conducted correlation analysis between EAT volume and plaque composition burden. EAT volume was positively correlated with total plaque burden ($r = 0.298$, $P = 0.003$), noncalcified plaque burden ($r = 0.245$, $P = 0.013$), and lipid plaque burden ($r = 0.250$, $P = 0.012$) but not with fibrous plaque burden ($r = 0.094$, $P = 0.352$) (Figure 3). Moreover, for serum LDL-C level, no correlation was demonstrated in our
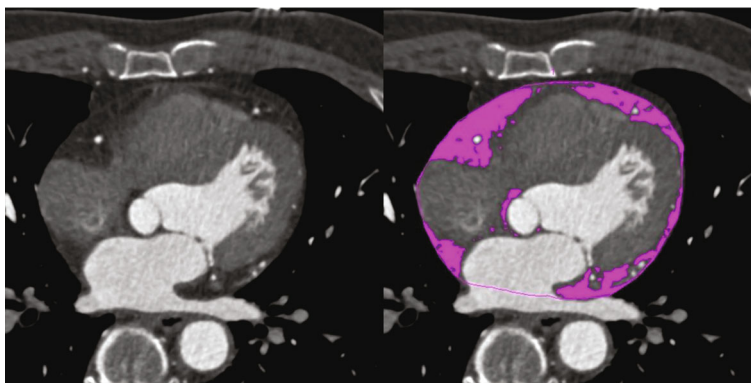
Figure 1: EAT volume quantitative method based on CT scan sequence. EAT volume was measured automatically from pulmonary artery bifurcation to diaphragm after drawing the contour of pericardium. The parts in purple represented the range and distribution of EAT.
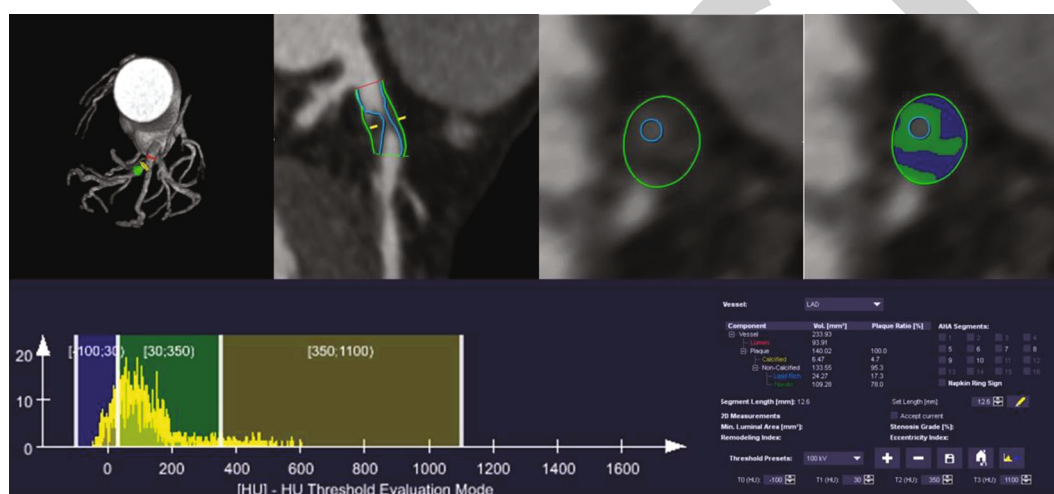
Figure 2: Precise quantitative analysis method for plaque composition based on CCTA images. The vessel and lumen contour were depicted manually. After automatic recognition specific composition CT attenuation, the volume of each composition was calculated. Above case showed a quantitative process of noncalcified plaque located at the proximal segment of left anterior descending branch. The lesion length was 12.6 mm, the lumen volume was 93.91 mm^3, the total plaque volume was 140.02 mm^3, the calcified volume was 6.47 mm^3, the noncalcified volume was 133.55 mm^3, the lipid volume was 24.27 mm^3, and the fibrous volume was 109.28 mm^3.

analysis; however, EAT volume was positively related with homocysteine level.

3.3. Different Correlation of EAT Volume with Plaque Composition in Patients with ACS and SAP.

The plaque composition analysis in patients with ACS and SAP was performed, and results are shown in Table 3. The total plaque burden ($59.3 \pm 11.1\%$ vs. $49.5 \pm 16.7\%$, $P \leq 0.001$), noncalcified plaque burden ($57.1 \pm 12.7\%$ vs. $47.5 \pm 18.3\%$, $P = 0.011$), lipid plaque burden ($19.2 \pm 10.7\%$ vs. $14.6 \pm 10.9\%$, $P = 0.047$), and fibrous plaque burden (37.7% (32.6, 43.1) vs. 32.9% (26.0, 40.1), $P = 0.014$) were significantly higher in patients with ACS than those with SAP.

Moreover, we conducted an intragroup correlation analysis (Table 4). In patients with ACS, EAT volume was positively correlated with total plaque burden ($r = 0.309$, $P = 0.009$), noncalcified plaque burden ($r = 0.242$, $P = 0.044$), and lipid plaque burden ($r = 0.240$, $P = 0.045$); however, in SAP patients, no significant correlation of these plaque compositions with EAT volume was observed.

3.4. EAT Volume Was Associated with HRP.

According to quartiles of EAT volume, the feature distribution of HRP in four groups was demonstrated (Figure 4). With the increase of EAT volume from 1st to 4th, the number of NRS increased from 0 to 1; positive remodeling increased from 14 to 18. No low attenuation plaques was found in 1st and 2nd EAT volume, while 2 and 4 were found in the 3rd and 4th EAT volume, respectively. Spotty calcium increased 4 cases from 1st to 4th group. In patients with SAP, these features were not found with such a trend.

We defined the HRP as plaque with more than two high risk features as previously reported [9]. EAT volume of patients with HRP ($n = 18$) was significantly higher than that without HRP ($n = 83$) (169.0 ± 6.2 cm^3 vs. 130.6 ± 5.3 cm^3, $P = 0.002$) (Figure 5). Univariable logistic regression analysis indicated that EAT volume was significantly associated with HRP. Furthermore, multivariable logistic regression analysis showed that after adjusted smoking history, LDL-C, and CACS, EAT volume remained a significant independent risk factor for HRP (Table 5).

TABLE 1: Clinical data of all patients.

Characteristic	Total ($n = 101$)	ACS ($n = 70$)	SAP ($n = 31$)	P value
Age, year	61.5 ± 8.6	61.5 ± 8.4	61.4 ± 9.2	0.972
Male, %	63 (62.4)	41 (58.6)	22 (71.0)	0.236
HR, beats/min	71.0 (57.2, 81.5)	72.0 (65.0, 83.5)	70.0 (62.0, 76.0)	0.661
BMI, kg/m^2	24.9 ± 3.2	24.6 ± 3.2	25.4 ± 3.2	0.279
Systolic pressure, mmHg	133.0 (122.5, 144.5)	132.0 (121.0, 145.0)	133.0 (127.0, 141.0)	0.439
Diastolic pressure, mmHg	76.0 (69.0, 81.0)	75.0 (68.8, 81.0)	78.0 (69.0, 85.0)	0.560
CAD family history, %	17 (16.8)	12 (17.1)	5 (16.1)	0.900
Hypertension, %	50 (49.5)	33 (47.1)	17 (54.8)	0.476
Diabetes, %	32 (31.7)	23 (32.9)	9 (29.0)	0.703
Hyperlipidemia, %	26 (25.7)	17 (24.3)	9 (29.0)	0.615
Smoking history, %	31 (30.7)	26 (32.9)	5 (16.1)	0.035*
Total cholesterol, mmol/L	4.1 (3.5, 4.6)	4.1 (3.6, 4.6)	3.9 (3.5, 4.7)	0.611
HDL-C, mmol/L	1.1 (0.9, 1.3)	1.1 (1.0, 1.3)	1.0 (0.9, 1.3)	0.124
LDL-C, mmol/L	2.4 ± 0.8	2.6 ± 0.8	2.3 ± 0.8	0.027*
Triglyceride, mmol/L	1.4 (0.9, 1.9)	1.3 (0.9, 1.8)	1.5 (1.0, 1.9)	0.583
Blood glucose, mmol/L	5.4 (4.7, 6.5)	5.4 (4.7, 6.5)	5.3 (4.8, 6.8)	0.941
Homocysteine, μmol/L	16.3 ± 5.4	18.0 ± 5.2	12.5 ± 3.8	≤0.001*
Coronary stenosis rate, %	57.3 ± 9.5	59.8 ± 9.3	55.8 ± 10.1	0.048*
CACS	82.0 (16.3, 333.1)	79.9 (12.6, 325.6)	97.0 (22.2, 342.1)	0.935
EAT volume, cm^3	137.5 ± 47.6	143.7 ± 49.8	123.3 ± 39.2	0.046*
EAT density, HU	-89.5 ± 3.2	-89.7 ± 3.0	-88.9 ± 3.6	0.284

ACS: acute coronary syndrome; SAP: stable angina pectoris; HR: heart rate; BMI: body mass index; CAD: coronary heart disease; HDL-C: high density lipoprotein cholesterol; LDL-C: low density lipoprotein cholesterol; CACS: coronary artery calcium score; EAT: epicardial adipose tissue. *$P < 0.05$ was regarded as significant.

TABLE 2: Coronary plaque composition with EAT volume quartiles.

Plaque composition	EAT 1st ($n = 25$)	EAT 2nd ($n = 25$)	EAT 3rd ($n = 26$)	EAT 4th ($n = 25$)	P value
Total plaque volume, mm^3	217.3 (130.1, 349.2)	237.3 (183.8, 364.7)	236.6 (171.6, 392.5)	280.7 (158.8, 511.7)	0.707
Total plaque burden, %	51.2 ± 13.0	53.0 ± 15.6	59.1 ± 13.2	61.8 ± 10.7	0.017*
Calcified plaque volume, mm^3	5.0 (0.0, 13.1)	3.8 (0.0, 19.4)	2.8 (0.0, 19.3)	5.2 (0.0, 18.0)	0.895
Calcified plaque burden, %	0.9 (0.0, 3.4)	1.0 (0.0, 3.0)	0.6 (0.0, 2.6)	1.7 (0.0, 4.3)	0.864
Noncalcified plaque volume, mm^3	217.3 (126.4, 345.3)	231.0 (123.7, 351.0)	226.3 (165.2, 360.1)	277.4 (157.3, 463.2)	0.603
Noncalcified plaque burden, %	49.2 ± 14.8	50.7 ± 17.6	57.3 ± 14.3	59.1 ± 12.2	0.050*
Lipid plaque volume, mm^3	46.7 (22.5, 96.1)	70.4 (35.4, 104.2)	75.9 (46.9, 132.9)	80.2 (43.8, 189.7)	0.243
Lipid plaque burden, %	13.9 ± 11.6	14.7 ± 7.8	21.5 ± 10.1	20.8 ± 12.0	0.015*
Fibrous plaque volume, mm^3	127.3 (88.3, 241.3)	147.2 (84.5, 279.3)	138.5 (105.4, 212.7)	230.5 (104.4, 307.7)	0.666
Fibrous plaque burden, %	35.2 ± 13.3	36.0 ± 13.0	35.8 ± 8.3	38.3 ± 9.6	0.784

EAT, epicardial adipose tissue. *$P < 0.05$ was regarded as significant.

4. Discussion

This study revealed the association between EAT volume and plaque composition, then evaluated the difference correlation between ACS and SAP. EAT volume was positively correlated with total, noncalcified, and lipid plaque burden in ACS patients but not in SAP. Moreover, multivariable logistic regression analysis showed that EAT volume was a risk factor for HRP, which independent of cardiac risk factors and CACS.

Previous studies have reported that EAT was significantly associated with atherosclerotic plaque size and composition [16]. Adipocyte hypertrophy and proliferation increase proinflammatory cytokines and adipocytokines. Adipocytes can also stimulate macrophages to migrate into media of vessel wall, leading to formation of lipid necrosis core [17].
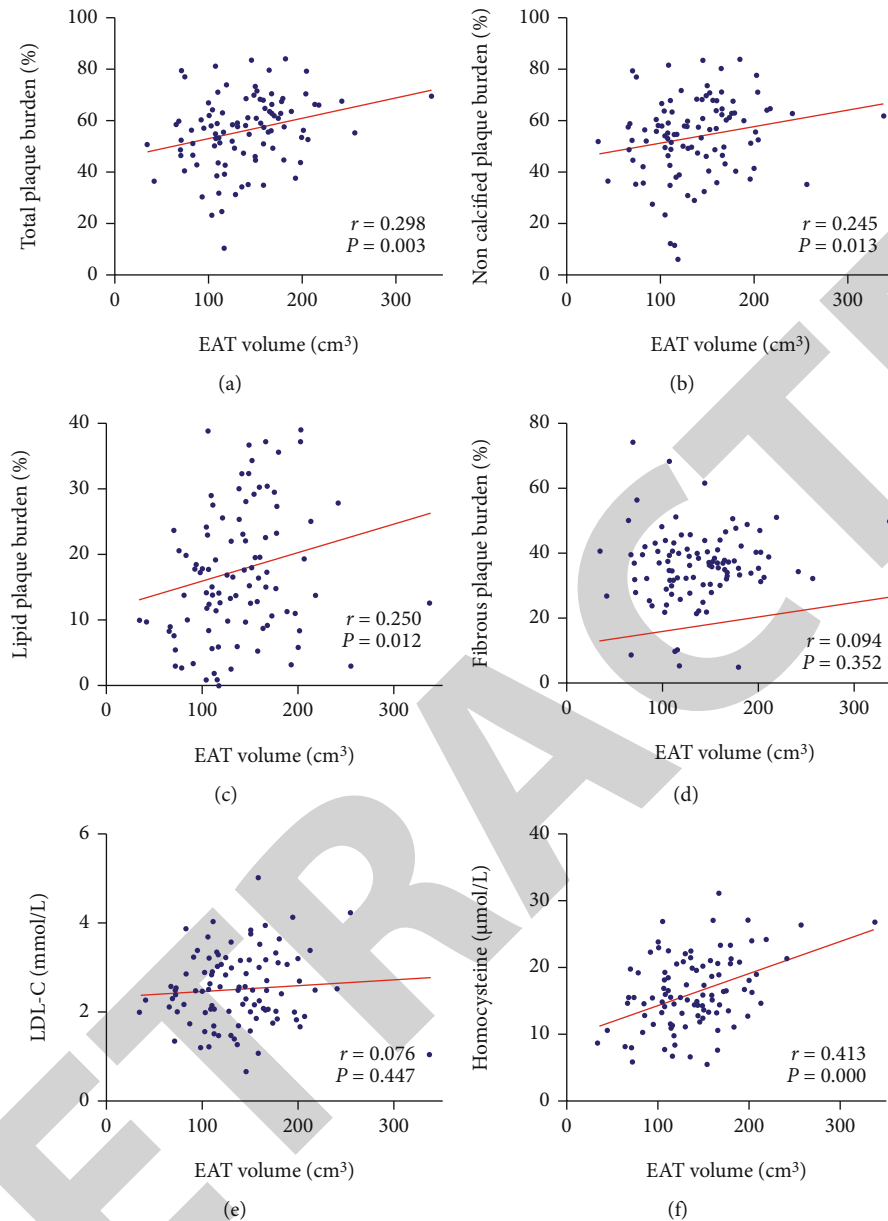
FIGURE 3: Correlation between EAT volume and plaque composition burden, serum LDL-C, and homocysteine. (a–c) EAT volume was positively correlated with total plaque, noncalcified plaque, and lipid plaque burden. (d) EAT volume was not correlation with fibrous plaque burden. (e) EAT volume was not correlation with LDL-C level. (f) EAT volume was positively correlated with homocysteine.

Perivascular adipose tissue outside atherosclerotic plaques with large fat necrosis core had more macrophage distribution than that in either nonatherosclerotic coronary or fibrous plaques [18]. Actually, inflammatory cell infiltration was often observed in the EAT of patients with CAD [19]. EAT, which was highly active in inflammation, may "transfer" inflammatory activity to the arterial media and play a facilitated role in development of atherosclerotic lesions and plaque instability [19]. Several studies have revealed that EAT of tumor-necrosis factor-α, interleukin-6, leptin, and visfatin were significantly higher and adiponectin significant lower in patients with CAD compared to patients without CAD [20, 21]. However, oxidation of adipocytes

and LDL-C was not associated with EAT volume, which may reflect the systemic inflammation factors lack direct relation with local fat depot. Visceral fat adipose including EAT is the main factor leading to local atherosclerosis. On the other hand, we found an association between homocysteine and EAT volume, which has not been confirmed previously. Notably, several studies have found that homocysteine in ACS patients was significantly higher than that in SAP, and it can be used as a predictor of plaque vulnerability [22, 23]. Homocysteine can damage vascular intima, promote infiltration of inflammatory cells, lipid oxidation, vascular inflammation, and platelet activation, then promoting progress of atherosclerosis [24, 25]. Therefore, it

TABLE 3: Comparison of quantitative analysis of plaque composition in ACS and SAP.

Characteristic	Total ($n = 101$)	ACS ($n = 70$)	SAP ($n = 31$)	P value
Total plaque volume, mm^3	237.3 (115.8, 386.4)	254.6 (170.3, 423.1)	213.0 (149.7, 345.0)	0.205
Total plaque burden, %	56.3 ± 13.7	59.3 ± 11.1	49.5 ± 16.7	0.001*
Calcified plaque volume, mm^3	4.5 (0.0, 15.0)	4.8 (0.0, 16.9)	3.8 (0.0, 9.1)	0.804
Calcified plaque burden, %	0.95 (0.0, 3.2)	1.01 (0.0, 3.1)	0.82 (0.0, 3.34)	1.000
Noncalcified plaque volume, mm^3	231.0 (152.1, 369.5)	242.6 (159.4, 377.4)	205.0 (141.4, 336.5)	0.190
Noncalcified plaque burden, %	54.1 ± 15.2	57.1 ± 12.7	47.5 ± 18.3	0.011*
Lipid plaque volume, mm^3	75.9 (36.1, 116.0)	78.1 (46.1, 118.9)	67.1 (21.4, 113.7)	0.190
Lipid plaque burden, %	17.8 ± 10.9	19.2 ± 10.7	14.6 ± 10.9	0.047*
Fibrous plaque volume, mm^3	147.2 (99.7, 280.3)	160.6 (99.5, 288.1)	133.5 (99.0, 224.6)	0.276
Fibrous plaque burden, %	37.3 (31.3, 41.1)	37.7 (32.6, 43.1)	32.9 (26.0, 40.1)	0.014*

ACS: acute coronary syndrome; SAP: stable angina pectoris. *$P < 0.05$ was regarded as significant.

TABLE 4: Correlation between EAT volume and plaque composition burden in ACS and SAP.

Characteristic	ACS ($n = 70$)		SAP ($n = 31$)	
	r	P value	r	P value
Total plaque burden, %	0.309	0.009*	0.145	0.436
Calcified plaque burden, %	0.124	0.305	0.092	0.622
Noncalcified plaque burden, %	0.242	0.044*	0.138	0.461
Lipid plaque burden, %	0.240	0.045*	0.190	0.307
Fibrous plaque burden, %	0.080	0.508	0.082	0.660

ACS: acute coronary syndrome; SAP: stable angina pectoris. *$P < 0.05$ was regarded as significant.

is an important part of systemic risk factors, which is partially consistent with the role of EAT.

In our study, we found that EAT volume was positively correlated with total plaque, noncalcified plaque, and lipid plaque burden, suggesting that larger EAT might be associated with more instable plaque composition, but no correlation was found with calcified and fibrous plaque burden. Especially, the noncalcified plaque and lipid plaque burden increased from 50.7% to 57.3% and 14.7% to 21.5%, respectively, when EAT volume increased from 2nd to 3rd quartile, but the increase was not obvious when EAT volume increased from 1st to 2nd quartile. Therefore, we speculated that there may be a certain threshold, exceeding which accumulation of EAT volume may promote change of plaque composition burden. With increasing of EAT volume, it transforms from normal physiological to morbid pathological state. But the threshold was not confirmed yet. This point contradicted recent study that elevated EAT plays a major role in the early stage of CAD [26]. It is necessary to further explore the association of EAT volume with different phase of CAD, such as initiation of endothelium impair, lipid deposition, or activation of macrophage.

Thin fibrous cap and large lipid core are pathological features of plaque vulnerability. Previous studies have suggested that the thickness of fibrous cap < 65 μm was a sign of plaque rupture [27]. Plaque burden in ACS patient is often higher than that in SAP, and increased plaque burden is prone to rupture that leads to cardiovascular event. The PROSPECT

study found that greater plaque burden was an independent predictor of future cardiovascular events [28]. Invasive coronary image analysis also found that the culprit vessel often had large plaque burden, and culprit lesion size was usually larger than stable lesions [29]. In patients with unstable angina, the volume of ruptured plaques was larger than non-ruptured plaques so was the volume of lipid core [30]. In the subgroup analysis of the PROSPECT study, 32 patients with larger total plaque volume at baseline were more likely to suffer from cardiovascular events during a 39-month follow-up [31]. The results of these studies were consistent with our results, suggesting that unstable plaque composition burden was greater in ACS patients than SAP.

Furthermore, we found an association between EAT volume and HRP. Since the publication of CAD-RADS Coronary Artery Disease Reporting and Data System in 2016 [9], definition of HRP on CCTA imaging has been widely accepted. It has been proved that plaques with positive remodeling, low attenuation plaque, spotty calcium, and NRS have higher risk of rupture, which was easy to lead to ACS [3]. Therefore, the use of indicators to predict the presence of HRP has important clinical significance for early intervention. Oka et al. confirmed that high EAT volume was associated with low attenuation plaque and positive remodeling using 64 row CT examination [32]. Ito et al. used coronary angiography combined with optical coherence tomography (OCT) to reveal that high EAT volume was closely related to plaque stability, and high EAT volume was
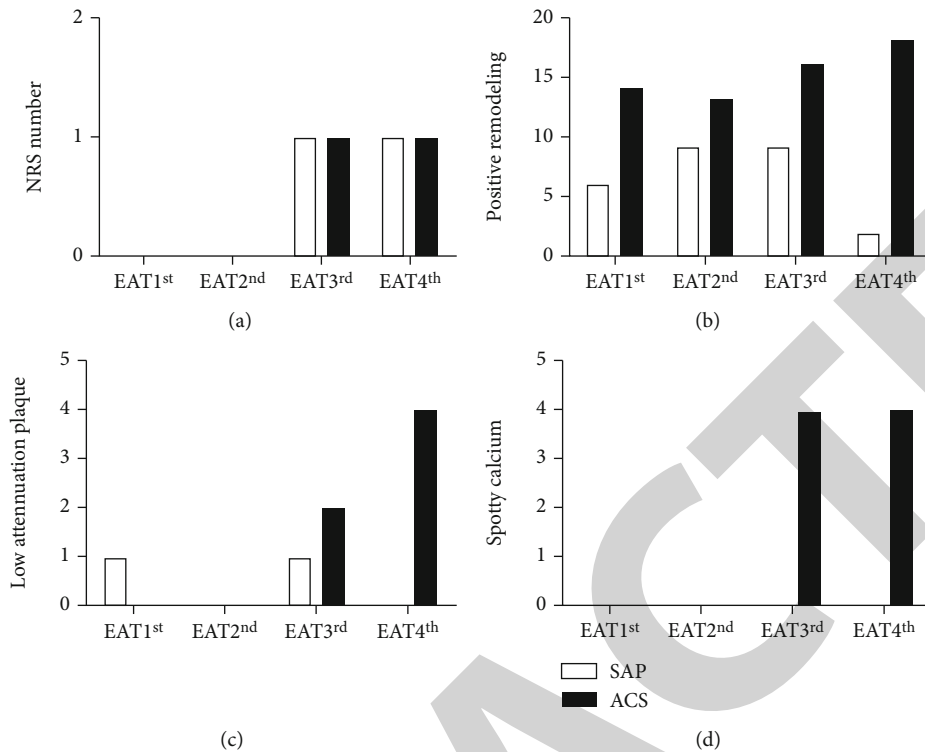
Figure 4: Distribution of HRP features according to quartiles of EAT volume: (a) NRS number; (b) positive remodeling; (c) low attenuation plaque; (d) spotty calcium.
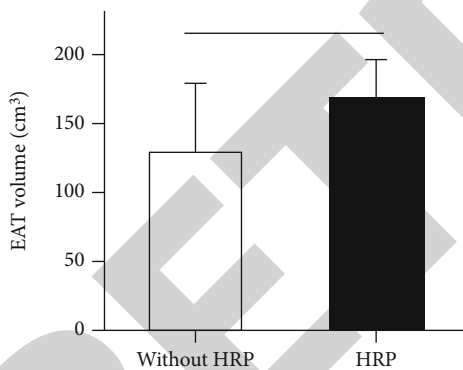
Figure 5: The difference of EAT volume between patients with and without HRP. $^*P < 0.05$ was regarded as significant.

an independent risk factor for ACS [33]. The results of Kazuhiro et al. using intravascular ultrasound (IVUS) also confirmed that EAT volume was associated with lipid enriched plaques. However, there was no report on the relationship between EAT volume and "strictly defined" HRP based on CAD-RADS. The results of our study showed that 18 patients with HRP, including 14 ACS and 4 SAP cases, were associated with EAT volume after adjusting variable, though OR was small relatively (OR = 1.018).

To explore the association between EAT and HRP was not only helpful to understand the mechanism of atherosclerosis but also to optimize the current noninvasive examination flow. For patients underwent CCTA examination, HRP can be directly identified in image reconstruction, and measure-

ment of EAT cannot bring more information for HRP. However, for patients only underwent chest CT plain scan, discovery of increasing EAT volume means more probability of presence of HRP, and next step, contrast enhanced scan was necessary for identifying high risk feature. As the volume was lower than average, we can consider postponing even canceling contrast enhanced scan to avoid further radiation and side effect of contrast agent. Finally, it saved resources of clinical diagnosis and treatment. Overall, it is of great practical significance using noninvasive image indicators for early prediction and warning of HRP.

This study also found that there was not clear relationship between EAT volume and plaque composition in SAP. Despite exist of plaque formation and lumen stenosis, SAP patients have mild inflammation, less macrophage infiltration, and thick fibrous cap on the surface of the plaque, with less erosion, ulcer, or rupture. Studies have shown that normal EAT may play a part in antiatherosclerosis by secreting adipocytokines [34], which include adiponectin and other protective factors [35]. The existence of the physiological and pathological phases of EAT promotes the different "fate" of plaques in ACS and SAP. The reasons for this result may still be complex, even if pathological EAT may still preserve some of its antiatherosclerotic effects. Hirata et al. found that in CAD patients with EAT, even the expression of anti-inflammatory and proinflammatory factors both increased [36]. The effect of EAT on plaque composition may be more than a single mechanism, and the effect of increased EAT volume may not cause significant changes in plaque structure and composition in SAP patients.

TABLE 5: Univariable and multivariable logistic regression of risk factors for HRP.

Variable	Univariable		Multivariable	
	OR (95% CI)	P value	OR (95% CI)	P value
Smoking history	1.476 (0.513-4.250)	0.470	1.202 (0.364-3.969)	0.736
LDL-C	1.278 (0.685-2.383)	0.441	1.287 (0.641-2.585)	0.478
EAT volume	1.017 (1.005-1.029)	0.006*	1.018 (1.006-1.030)	0.004*
CACS	0.997 (0.994-1.000)	0.073*	0.996 (0.993-1.000)	0.044*

LDL-C: low density lipoprotein cholesterol; EAT: epicardial adipose tissue; CACS: coronary artery calcium score. *$P < 0.05$ was regarded as significant.

We must admit the limitations of our study. Firstly, small sample, single center clinical research was not fully persuading. Large-scale, multicenter clinical research is needed to confirm these results. In addition, we did not analysis of the association with HRP in patients with either ACS or SAP, so it is a pity for not clarifying the mechanism of EAT promoting HRP in ACS. Furthermore, although precise composition detection result as reproducible and stable, it is greatly affected by lack of resolution of CCTA image. At last, prospective follow-up was needed to verify whether presence of HRP and increasing EAT have a worsening prognosis.

5. Conclusion

With the increasing EAT volume, more dangerous plaque composition burdens increase significantly. EAT volume is a risk predictor of HRP independent of cardiac risk factors and CACS, which supports the possible of impact of EAT on progression of coronary atherosclerotic plaque.

Data Availability

The datasets used and/or analyzed during the current study are available from the corresponding author upon request.

Conflicts of Interest

The authors declare no conflict of interest.

Authors' Contributions

Dongkai Shan and Guanhua Dou contributed equally to this work.

Acknowledgments

References

[1] M. Seeger, A. Karlas, D. Soliman, J. Pelisek, and V. Ntziachristos, "Multimodal optoacoustic and multiphoton microscopy of human carotid atheroma," *Photoacoustics*, vol. 4, no. 3, pp. 102–111, 2016.

[2] T. Kitagawa, H. Yamamoto, J. Horiguchi et al., "Characterization of noncalcified coronary plaques and identification of culprit lesions in patients with acute coronary syndrome by 64-slice computed tomography," *JACC: Cardiovascular Imaging*, vol. 2, no. 2, pp. 153–160, 2009.

[3] S. Motoyama, M. Sarai, H. Harigaya et al., "Computed tomographic angiography characteristics of atherosclerotic plaques subsequently resulting in acute coronary syndrome," *Journal of the American College of Cardiology*, vol. 54, no. 1, pp. 49–57, 2009.

[4] S. B. Puchner, T. Liu, T. Mayrhofer et al., "High-risk plaque detected on coronary CT angiography predicts acute coronary syndromes independent of significant stenosis in acute chest pain: results from the ROMICAT-II trial," *Journal of the American College of Cardiology*, vol. 64, no. 7, pp. 684–692, 2014.

[5] K. Harada, T. Amano, T. Uetani et al., "Cardiac 64-multislice computed tomography reveals increased epicardial fat volume in patients with acute coronary syndrome," *The American Journal of Cardiology*, vol. 108, no. 8, pp. 1119–1123, 2011.

[6] A. A. Mahabadi, M. H. Berg, N. Lehmann et al., "Association of epicardial fat with cardiovascular risk factors and incident myocardial infarction in the general population: the Heinz Nixdorf Recall Study," *Journal of the American College of Cardiology*, vol. 61, no. 13, pp. 1388–1395, 2013.

[7] N. Alexopoulos, D. S. McLean, M. Janik, C. D. Arepalli, A. E. Stillman, and P. Raggi, "Epicardial adipose tissue and coronary artery plaque characteristics," *Atherosclerosis*, vol. 210, no. 1, pp. 150–154, 2010.

[8] J. S. Park, S. Y. Choi, M. Zheng et al., "Epicardial adipose tissue thickness is a predictor for plaque vulnerability in patients with significant coronary artery disease," *Atherosclerosis*, vol. 226, no. 1, pp. 134–139, 2013.

[9] R. C. Cury, S. Abbara, S. Achenbach et al., "CAD-RADS™ coronary artery disease - reporting and data system. An expert consensus document of the Society of Cardiovascular Computed Tomography (SCCT), the American College of Radiology (ACR) and the North American Society for Cardiovascular Imaging (NASCI). Endorsed by the American College of Cardiology," *Journal of Cardiovascular Computed Tomography*, vol. 10, no. 4, pp. 269–281, 2016.

[10] E. Braunwald, E. M. Antman, J. W. Beasley et al., "ACC/AHA 2002 guideline update for the management of patients with unstable angina and non-ST-segment elevation myocardial infarction–summary article: a report of the American College of Cardiology/American Heart Association task force on practice guidelines (committee on the management of patients

Retraction

Retracted: Alleviation of Inflammation and Oxidative Stress in Pressure Overload-Induced Cardiac Remodeling and Heart Failure via IL-6/STAT3 Inhibition by Raloxifene

Oxidative Medicine and Cellular Longevity

This article has been retracted by Hindawi, as publisher, following an investigation undertaken by the publisher [1]. This investigation has uncovered evidence of systematic manipulation of the publication and peer-review process. We cannot, therefore, vouch for the reliability or integrity of this article.

Please note that this notice is intended solely to alert readers that the peer-review process of this article has been compromised.

Wiley and Hindawi regret that the usual quality checks did not identify these issues before publication and have since put additional measures in place to safeguard research integrity.

We wish to credit our Research Integrity and Research Publishing teams and anonymous and named external researchers and research integrity experts for contributing to this investigation.

The corresponding author, as the representative of all authors, has been given the opportunity to register their agreement or disagreement to this retraction. We have kept a record of any response received.

References

[1] S. Huo, W. Shi, H. Ma et al., "Alleviation of Inflammation and Oxidative Stress in Pressure Overload-Induced Cardiac Remodeling and Heart Failure via IL-6/STAT3 Inhibition by Raloxifene," *Oxidative Medicine and Cellular Longevity*, vol. 2021, Article ID 6699054, 15 pages, 2021.

Research Article

Alleviation of Inflammation and Oxidative Stress in Pressure Overload-Induced Cardiac Remodeling and Heart Failure via IL-6/STAT3 Inhibition by Raloxifene

Shengqi Huo,[1] Wei Shi,[1] Haiyan Ma,[1,2] Dan Yan,[1] Pengcheng Luo,[1] Junyi Guo,[1] Chenglong Li,[3] Jiayuh Lin,[4] Cuntai Zhang,[5] Sheng Li [iD],[1] Jiagao Lv [iD],[1] and Li Lin [iD][1]

[1]*Division of Cardiology, Department of Internal Medicine, Tongji Hospital, Tongji Medical College, Huazhong University of Science and Technology, Wuhan, China*
[2]*Division of Cardiology, Department of Internal Medicine, First People's Hospital of Shangqiu, Shangqiu, China*
[3]*Department of Medicinal Chemistry, College of Pharmacy, University of Florida, Gainesville FL, USA*
[4]*Department of Biochemistry and Molecular Biology, University of Maryland School of Medicine, Baltimore MD, USA*
[5]*Department of Geriatrics, Tongji Hospital, Tongji Medical College, Huazhong University of Science and Technology, Wuhan, China*

Correspondence should be addressed to Jiagao Lv; lujiagao@tjh.tjmu.edu.cn and Li Lin; linlee271227@163.com

Background. Inflammation and oxidative stress are involved in the initiation and progress of heart failure (HF). However, the role of the IL6/STAT3 pathway in the pressure overload-induced HF remains controversial. *Methods and Results.* Transverse aortic constriction (TAC) was used to induce pressure overload-HF in C57BL/6J mice. 18 mice were randomized into three groups (Sham, TAC, and TAC+raloxifene, $n = 6$, respectively). Echocardiographic and histological results showed that cardiac hypertrophy, fibrosis, and left ventricular dysfunction were manifested in mice after TAC treatment of eight weeks, with aggravation of macrophage infiltration and interleukin-6 (IL-6) and tumor necrosis factor-alpha (TNF-α) expression in the myocardium. TAC (four and eight weeks) elevated the phosphorylation of signal transducer and activator of transcription 3 (p-STAT3) and prohibitin2 (PHB2) protein expression. Importantly, IL-6/gp130/STAT3 inhibition by raloxifene alleviated TAC-induced myocardial inflammation, cardiac remodeling, and dysfunction. *In vitro*, we demonstrated cellular hypertrophy with STAT3 activation and oxidative stress exacerbation could be elicited by IL-6 (25 ng/mL, 48 h) in H9c2 myoblasts. Sustained IL-6 stimulation increased intracellular reactive oxygen species, repressed mitochondrial membrane potential (MMP), decreased intracellular content of ATP, and led to decreased SOD activity, an increase in iNOS protein expression, and increased protein expression of Pink1, Parkin, and Bnip3 involving in mitophagy, all of which were reversed by raloxifene. *Conclusion.* Inflammation and IL-6/STAT3 signaling were activated in TAC-induced HF in mice, while sustained IL-6 incubation elicited oxidative stress and mitophagy-related protein increase in H9c2 myoblasts, all of which were inhibited by raloxifene. These indicated IL-6/STAT3 signaling might be involved in the pathogenesis of myocardial hypertrophy and HF.

1. Introduction

Heart failure (HF) is suffered by 26 million people, and the prevalence was approximately 1-2% worldwide as estimated [1]. Hemodynamic overload, caused by aortic coarctation or hypertension, is one of the momentous pathological irritations of HF [2]. HF patients are often associated with cardiac hypertrophy and reduced myocardial compliance. To some

certain people, the current drug-based management is limited or in vain to their remission. Several lines of evidence showed that chronic inflammation plays an important role in adverse cardiac remodeling and the development of HF. In HF patients, the levels of proinflammatory circulatory factors were increased, such as IL-6, TNF-α, CRP, GDF15, and galectin-4 [3]. In patients with chronic persistent systematic inflammation, such as rheumatoid arthritis [4], inflammatory bowel

disease [5], or obesity [6, 7], the risk of cardiovascular disease, including HF, was higher than that in general people. However, the causal relationship between HF and inflammation is still confused.

Although the chimeric monoclonal antibody to TNF-α showed no benefit to patients with moderate-to-severe chronic heart failure [8], other research declared IL-6 exerted an important role in HF and was strongly associated with adverse outcome in HF patients [9, 10]. Interleukin-6, as a typical proinflammatory cytokine, forms a complex with IL-6 receptor (IL-6R) and coreceptor glycoprotein 130 (gp130), which in turn initiates a cascade reaction including Janus kinase (JAK) activation, phosphorylation of STAT3 (p-STAT3), and subsequent dimer formation, nuclear translocation, and gene transcription [11]. However, conflicting consequences of IL-6 deletion in transverse aortic constriction (TAC) mice were reported [12, 13]. The left ventricular remodeling after TAC of IL-6-knockout mice was reduced in the research of Zhao et al. [13], whereas left ventricular hypertrophy and dysfunction by TAC showed no difference between wild-type and IL-6-knockout mice according to Lai et al. [12]. Hence, the role of IL-6 in cardiac hypertrophy and HF is not definite.

Raloxifene is approved by the FDA for the prevention and treatment of postmenopausal osteoporosis [14]. It has been discovered as a novel inhibitor of the IL-6/gp130 interface recently and inhibits the phosphorylation of STAT3 in cancer cells in our previous studies [15, 16]. The protective effect of raloxifene in cardiac remodeling and dysfunction induced by pressure overload is contradictory as previous studies reported [17, 18]; moreover, the potential molecular mechanism and anti-inflammation effect of raloxifene in the cardiovascular system are unclear likewise. In this paper, we provided more evidence about whether IL-6/gp130/STAT3 signaling was activated in TAC mice and the cardioprotective mechanism of raloxifene on pressure overload-induced cardiac hypertrophy and HF.

2. Materials and Methods

All experiments have been approved by the institutional review board of Tongji Hospital, Tongji Medical College, Huazhong University of Science and Technology.

2.1. Transverse Aortic Constriction Mouse Model. Wild-type C57BL/6J mice (male, about 8 weeks and 25 g) purchased from the Jackson Laboratory were randomized into three groups: Sham, TAC, and TAC+raloxifene (raloxifene) groups ($n = 6$). Raloxifene hydrochloride (HY-13738A, MedChemExpress, U.S.) was dissolved with dimethyl sulfoxide (DMSO) firstly and then diluted with phosphate buffer saline (PBS) containing 20% (20μg HPBCD/100μL PBS, 0.2 mg/mL) hydroxypropyl B cyclodextrin (HPBCD). Raloxifene (15 mg/kg) was given daily by intragastric administration to the raloxifene group three days before TAC surgery and continued till mice were sacrificed, while the Sham and TAC groups are supplied by solvent without raloxifene. A practiced single operator performed all surgical procedures of TAC for the experiments as described previously [19]. A

$27^{1/2}$ gauge blunt needle was applied to perform TAC surgery, and the Sham group was conducted with the surgery without tied tightly around the aortic arch against a cannula. After 4 or 8 weeks of TAC, respective 3/3/3 mice of each Sham/TAC/raloxifene group were sacrificed after echocardiography, and heart tissues were harvested which were immediately frozen in liquid nitrogen or embedded in paraffin.

2.2. Transthoracic Echocardiography Measurement. Respective 3/3/3 mice of each Sham/TAC/raloxifene group at 4 or 8 weeks were performed with echocardiography (Vevo 2100, FUJIFILM VisualSonics, Toronto, Canada) in East Hospital, Tongji University School of Medicine, Shanghai, China. Mice were anesthetized with isoflurane (3% for induction and 2% for maintenance) mixed in 1 L/min 100% O_2 via a facemask. Cardiac parameters were measured and averaged from at least 3 separate cardiac cycles. The echocardiography operator was blinded to the grouping of mice.

2.3. Histology and Immunohistochemistry. The paraffin-embedded tissues were sliced and performed with hematoxylin-eosin (HE), Sirius red, or Masson trichrome staining. The interstitial fields and the perivascular fields containing vasculature were imaged. Immunohistochemistry was performed with antibodies of IL-6 (D220828, Sangon, Shanghai, China), TNF-α (bs-2081R, Bioss, Beijing, China), and ANP and MYH7B (ab225844 and ab172967, Abcam, U.S.). The EVOS FL Auto Imaging System (Life Technologies, ThermoFisher Scientific, Waltham, MA, U.S.) was operated to obtain 3-5 random fields of each image.

2.4. Hypertrophic Cell Model and Treatments. H9c2 myoblasts were obtained from the American Type Culture Collection (ATCC, Manassas, U.S.). Cells were cultured in high glucose Dulbecco's modified Eagle's medium (DMEM, KeyGEN BioTECH, Nanjing, Jiangsu, China) supplemented with 10% (v/v) fetal bovine serum (FBS, Gibco, ThermoFisher Scientific, Waltham, MA, U.S.) and 1% (v/v) penicillin/streptomycin (Sangon, Shanghai, China) at 37°C in a 5% CO_2 atmosphere incubator. To induce cellular hypertrophy of H9c2, cells were incubated with IL-6 (No. 200-06, Pepro-Tech, Suzhou, Jiangsu, China, 25 ng/mL), respectively, for 24 h or 48 h, and then, molecular markers were detected by west blotting. To illustrate the effects of raloxifene, H9c2 myoblasts were pretreated with raloxifene (25μM) for 2 hours and then incubated with IL-6 (25 ng/mL) for 24 h, the cycle was repeated once more (a total of 4 hours for raloxifene and 48 hours for IL-6), and then cells were harvested for staining or western blotting.

2.5. Gentian Violet Staining. The cells were treated with IL-6 as above and then were fixed with 4% paraformaldehyde (Sigma-Aldrich) for 20 minutes. The cells were stained with 0.5% (m/v) gentian violet (ThermoFisher Scientific, Waltham, MA, U.S.) solution for 30 minutes at room temperature and washed twice with PBS. Images were obtained by the EVOS FL Auto Imaging System.

2.6. RNA Isolation and Quantitative Real-Time Polymerase Chain Reaction (qRT-PCR). Total RNA was isolated from

frozen heart tissues using the Hipure Total RNA Mini Kit (Magen, Guangzhou, China). The RNA quality and concentration were determined spectrophotometrically (NanoDrop 2000 spectrophotometer, Thermo Scientific, U.S.), and reverse transcription for cDNA synthesis was performed using the ReverTra Ace qPCR RT Kit (TOYOBO Co. Ltd, Osaka, Japan). qPCR was performed with the SYBR green PCR master mix kit (TOYOBO Co. Ltd, Osaka, Japan) on the StepOnePlus real-time PCR system (Applied Biosystems). The mRNA expressions of atrial natriuretic peptide (ANP), B-type natriuretic peptide (BNP), collagen type I alpha 1 (COL1A1), and collagen type III alpha 1 (COL3A1) were normalized to glyceraldehyde-3-phosphate dehydrogenase (GAPDH) by the $\Delta\Delta$Ct method.

The primer sequences are listed as follows (mouse): **ANP** forward: 5′-CCT AAG CCC TTG TGG TGT GT, reverse: 5′-CAG AGT GGG AGA GGC AAG AC; **BNP** forward: 5′-CTG AAG GTG CTG TCC CAG AT, reverse: 5′-CCT TGG TCC TTC AAG AGC TG; **COL1A1** forward: 5′-TGA ACG TGG TGT ACA AGG TC, reverse: 5′-CCA TCT TTA CCA GGA GAA CCA T; **COL3A1** forward: 5′-GCA CAG CAG TCC AAC GTA GA, reverse: 5′-TCT CCA AAT GGG ATC TCT GG; **GAPDH** forward: 5′-AGG TCG GTG TGA ACG GAT TTG, reverse: 5′-TGT AGA CCA TGT AGT TGA GGT CA.

2.7. Measurement of Intracellular Reactive Oxygen Species (ROS).

The fluorescent dye dihydroethidium (DHE; HY-D0079, MedChemExpress, U.S.) was utilized to evaluate superoxide production in cultured cells. H9c2 myoblasts were treated with IL-6 and raloxifene as described above and then were incubated with $10\,\mu$M DHE at 37°C for 30 minutes in the dark and washed twice with PBS. The cells were excited with blue light, and red fluorescence emission images were obtained with the EVOS fluorescence microscope.

2.8. Mitochondrial Membrane Potential Measurement.

The mitochondrial membrane potential (MMP, $\Delta\Psi_m$) was monitored by fluorescent probe JC-1 (PJC-110, Promotor Biological Co. LTD., Wuhan, China). H9c2 myoblasts were treated with IL-6 and raloxifene as described above and then were incubated with JC-1 dye for 20 minutes at 37°C and washed twice with PBS. JC-1 was excited at 488 nm, and the red (aggregate) or green (monomer) emission fluorescence was detected with a standard red or green filter by the MShot fluorescence microscope (Wuhan, China).

2.9. Measurement of the Total SOD Activity.

H9c2 myoblasts were treated with IL-6 and raloxifene as described above and harvested as above. The protein content was measured with the BCA Protein Assay, and then, the activity of total intracellular SOD (superoxide dismutase, units/mg) was analyzed at 450 nm by a microplate reader (TECAN, SUNRISE, Switzerland) using the commercially available kit (Total Superoxide Dismutase Assay Kit, Beyotime, S0101, WST-8) according to the manufacturer's instructions.

2.10. The Intracellular Content of ATP Measurement.

Intracellular ATP content was measured using a commercially available intracellular ATP Assay Kit (S0026, Beyotime, Shanghai, China) according to the manufacturer's instructions. H9c2 myoblasts were treated with IL-6 and raloxifene as described above and harvested as above. $100\,\mu$L ATP detection reagent was added to each well of the 96-well plate and incubated at room temperature for 5 min to minimize the background. $20\,\mu$L supernatant was then mixed up with ATP detection reagent in each well, and luminescence (RLU) was measured by a microplate reader (Synergy 2, Bio-Tek Instruments, U.S.). ATP standard curve was used to transform luminescence (RLU) to ATP concentration.

2.11. Protein Extraction and Western Blotting.

The pulverized cardiac tissues and the collected cultured cells were lysed in RIPA lysis buffer (Sangon, Shanghai, China) containing 1 mM protease inhibitor and 1 mM phosphatase inhibitor for 40 minutes and centrifuged at 12,000 rpm for 20 minutes at 4°C. The supernatant was collected and quantified by the BCA Protein Assay (Sangon, Shanghai, China). Proteins (25-40 μg) were loaded onto 10% Bis-Tris SDS-polyacrylamide gels and underwent electrophoresis at 60 V for 30 minutes and then 120 V for 1 hour. Then, the separated protein was transferred to 0.45 μm PVDF membranes (Bio-Rad) at 230 mA for 100 minutes. After blocking with TBS-T (Tris-buffer saline containing 0.1% Tween 20) containing 5% powdered milk for 90 minutes, then incubated with primary antibodies overnight, including STAT3 (#4904, Cell Signaling Technology, CST), p-STAT3 (Tyr705) (#9145, CST), p-STAT1 (Tyr701) (#7649, CST), p-STAT5 (Tyr694) (D155020, BBI Life Sciences), PHB2 (#14085, CST), SOD2 (#13141, CST), iNOS (#13120, CST), Pink1 (ab23707, Abcam), Parkin (#4211, CST), Bnip3 (ab10433, Abcam), and GAPDH (10494-1-AP, Proteintech), horseradish peroxidase-conjugated secondary antibodies and Immobilon Western Chemiluminescent HRP Substrate (AntGene Co. Ltd, Wuhan, China) were used for protein detection which was operated on the ChemiDoc-It 510 Imager with VisionWorks software (Ultra-Violet Products Ltd., Cambridge, UK).

2.12. Statistical Analysis.

SPSS Statistics 25.0 and GraphPad 5.0 were used for statistical analysis and drawing. Continuous variables were expressed as mean ± SEM. Statistical analysis among multiple groups was tested by the one-way analysis of variance (one-way ANOVA) followed with the Bonferroni posttest, and the Mann-Whitney U test was used for comparison between two groups. Quantitative assessment of western blotting, immunohistochemistry images, and fluorescence intensity was performed by ImageJ 1.45s. For all statistical analyses, $p < 0.05$ indicates statistical significance.

3. Results

3.1. Raloxifene Ameliorated Cardiac Hypertrophy Induced by Pressure Overload in TAC Mice.

TAC enlarged the murine heart size compared with the Sham group morphologically and histologically, and the heart size was decreased by

(a)

(b)

(c)

(d)
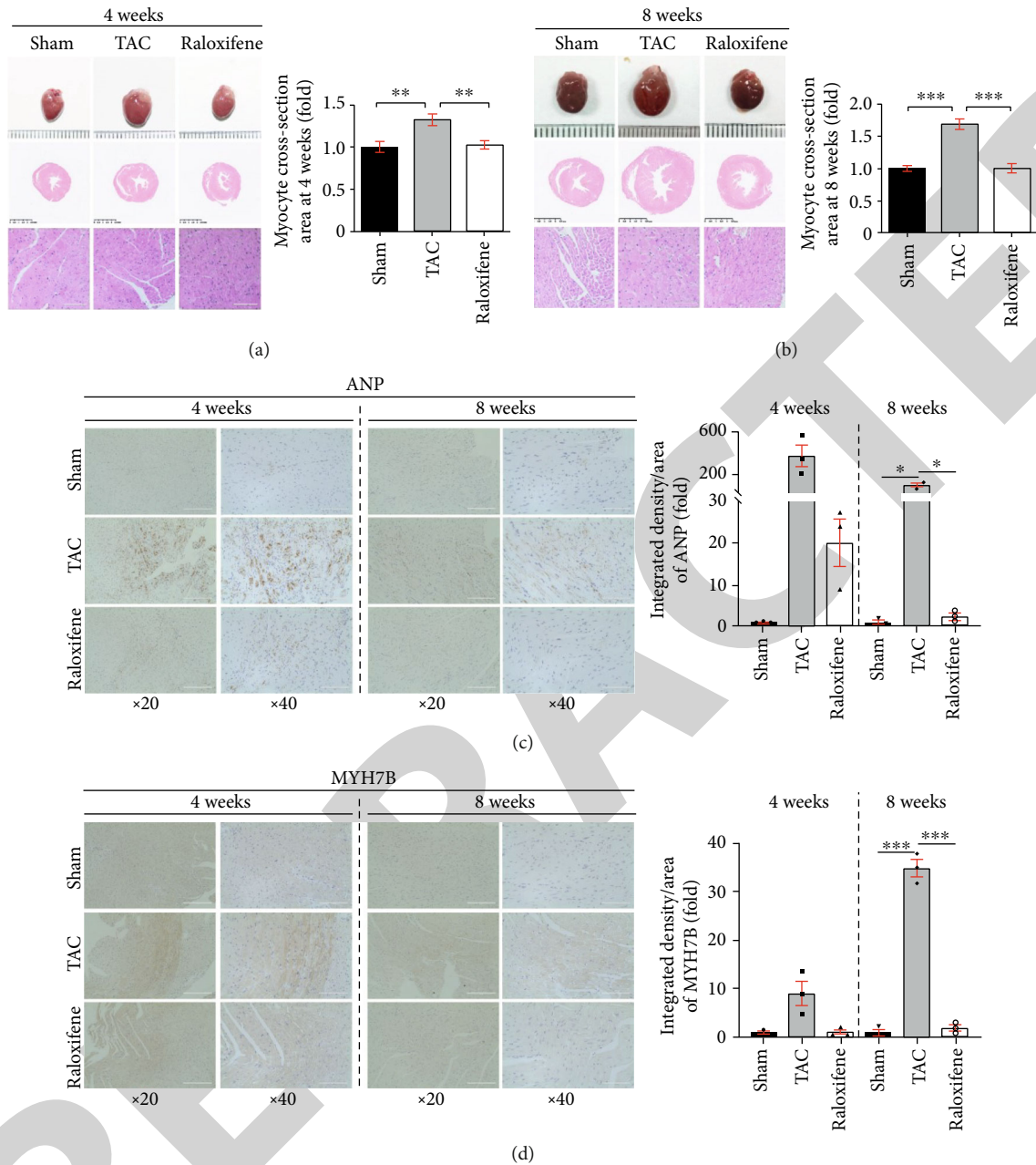
FIGURE 1: Raloxifene mitigated murine cardiac hypertrophy induced by TAC. (a, b) Gross morphology of murine heart, transverse sections, and typical regional enlarged images showed cardiac hypertrophy induced by TAC through HE staining. The respective histogram showed the cross-section area of cardiomyocytes enlarged and raloxifene alleviated the hypertrophic response. (c, d) The increased ANP (c) and MYH7B (d) expression of myocardial tissues after TAC of 4 or 8 weeks detected by immunohistochemistry was mitigated by raloxifene. The minimal interval of scale in the three rows of (a) and (b) is 1 mm, 0.5 mm, and 100 μm, respectively, and 100 μm of (c) and (d). $^*p < 0.05$; ** $p < 0.01$; $^{***}p < 0.001$.

raloxifene treatment (Figures 1(a) and 1(b)). The cross-sectional area of cardiomyocytes was increased on the transverse-axis view after TAC at both time points, and raloxifene mitigated the hypertrophic response (4 weeks, Sham vs. TAC vs. raloxifene = 1 : 1.32 : 1.02 fold, $p < 0.01$; 8 weeks, Sham vs. TAC vs. raloxifene = 1 : 1.69 : 1 fold, $p < 0.001$) (Figures 1(a) and 1(b)).

Table 1 shows other parameters that are identified as cardiac hypertrophic indicators in previous studies [17, 20]. Murine heart weight (HW) after TAC at 4 and 8 weeks was significantly increased compared with the Sham group ($p < 0.05$), and raloxifene reduced heart weight compared with the TAC group at both time points ($p < 0.05$). The ratio of HW/body weight (BW) and HW/tibia length (TL) excludes the bias of body weight and was increased in the TAC group compared with that of the Sham group at both time points ($p < 0.05$). But the ratios of the raloxifene group at 8 weeks were both prominently dropped in comparison with the TAC group ($p < 0.05$), whereas the decrease of the HW/BW ratio at 4 weeks showed no difference ($p = 0.089$)

TABLE 1: LV hypertrophy and dysfunction in murine hearts of four and eight weeks after TAC.

| | 4 weeks | | | 8 weeks | | |
	Sham	TAC	TAC+raloxifene	Sham	TAC	TAC+raloxifene
N	3	3	3	3	3	3
HW (mg)	101.59 ± 1.24	$176.93 \pm 5.82^*$	$124.27 \pm 6.20^†$	136.83 ± 4.99	$237.13 \pm 14.66^{\#,@}$	$147.30 \pm 6.51^\$$
HW/BW (mg/g)	4.17 ± 0.06	$7.28 \pm 0.46^*$	5.62 ± 0.39	5.03 ± 0.16	$8.66 \pm 0.51^\#$	$5.63 \pm 0.56^\$$
HW/TL (mg/mm)	4.57 ± 0.02	$7.80 \pm 0.11^*$	$5.49 \pm 0.28^†$	6.42 ± 0.24	$11.08 \pm 0.37^{\#,@}$	$6.85 \pm 0.54^\$$
LVEF (%)	78.36 ± 2.18	$63.07 \pm 2.52^*$	61.50 ± 3.41	77.14 ± 3.20	$37.09 \pm 2.80^{\#,@}$	$68.91 \pm 6.58^\$$
LVFS (%)	45.65 ± 2.23	$33.55 \pm 1.84^*$	32.20 ± 2.31	44.89 ± 2.87	$16.90 \pm 1.77^\#$	$38.79 \pm 5.58^\$$
LVEDd (mm)	3.21 ± 0.13	3.67 ± 0.16	3.42 ± 0.08	3.19 ± 0.04	$4.39 \pm 0.03^\#$	$3.45 \pm 0.18^\$$
LVEDs (mm)	1.79 ± 0.13	2.44 ± 0.12	2.30 ± 0.14	1.76 ± 0.11	$3.64 \pm 0.08^{\#,@}$	$2.14 \pm 0.29^\$$
LVEVd (μL)	41.72 ± 4.04	57.45 ± 5.97	44.12 ± 5.83	40.72 ± 1.34	$87.04 \pm 1.26^{\#,@}$	$49.70 \pm 6.02^\$$
LVEVs (μL)	14.13 ± 1.18	21.16 ± 2.51	17.53 ± 3.43	12.17 ± 1.17	$56.20 \pm 3.02^{\#,@}$	$16.62 \pm 4.85^\$$

HW = heart weight; BW = body weight; TL = tibia length; LVEF = left ventricular ejection fraction; LVFS = left ventricular fractional shortening; LVEDd/LVEDs = left ventricular end-diastolic/systolic diameter; LVEVd/LVEVs = left ventricular end-diastolic/systolic volume; *4 weeks: TAC group vs. Sham group, $p < 0.05$; †4 weeks: TAC+raloxifene group vs. TAC group, $p < 0.05$; # 8 weeks: TAC group vs. Sham group, $p < 0.05$; $8 weeks: TAC+raloxifene group vs. TAC group, $p < 0.05$; @4 weeks vs. 8 weeks of the indicated group (Sham, TAC, or TAC+raloxifene group), $p < 0.05$.
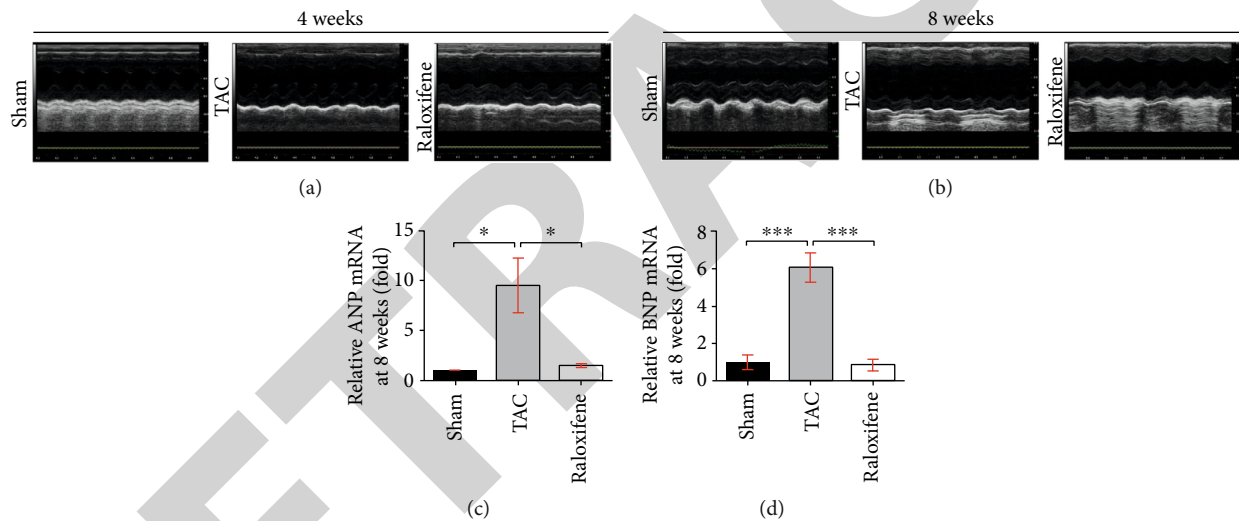
FIGURE 2: Raloxifene reversed the cardiac dysfunction of pressure overload mice. (a, b) M-mode echocardiography images of mice measured at 4 (a) or 8 (b) weeks after TAC. (c, d) The increased mRNA expression of ANP (c) and BNP (d) in the murine hearts at 8 weeks were both reduced by raloxifene treatment. $^*p < 0.05$; $^{***}p < 0.001$.

(Table 1). Meanwhile, the expression of ANP and MYH7B, which are molecular markers of myocardial hypertrophy [21], in myocardial tissue detected by immunohistochemical staining was increased at both time points, while raloxifene moderated this effect (Figures 1(c) and 1(d)).

3.2. Raloxifene Mitigated Pressure Overload-Induced Cardiac Dysfunction in TAC Mice. The left ventricular end-diastolic diameter (LVEDd) and left ventricular end-systolic diameter (LVEDs) of the TAC group at 8 weeks were larger than that of the Sham group or the raloxifene group visually from the images of echocardiography (Figure 2(b)), whereas was not obvious at 4 weeks (Figure 2(a)). The detailed cardiac parameters detected by echocardiography are shown in Table 1. Left ventricular ejection fraction (LVEF) and left ventricular fractional shortening (LVFS) of the TAC group (4 and 8 weeks) were significantly decreased ($p < 0.05$), and raloxifene improved both of them at 8 weeks compared with the TAC group ($p < 0.05$). Other parameters including LVEDd and left ventricular end-diastolic volume (LVEVd), as well as LVEDs and left ventricular end-systolic volume (LVEVs), which reflect systolic function [17], were all significantly increased after TAC operation (8 weeks) compared with the Sham group ($p < 0.05$), but raloxifene ameliorated the deterioration of them compared with the TAC group ($p < 0.05$) (Table 1). However, raloxifene showed no protective effects on cardiac function at 4 weeks because there was no difference between the raloxifene group and the TAC group (Table 1). The ultrasonic parameters,

(a)

(b)

(c)

(d)

(e)

(f)
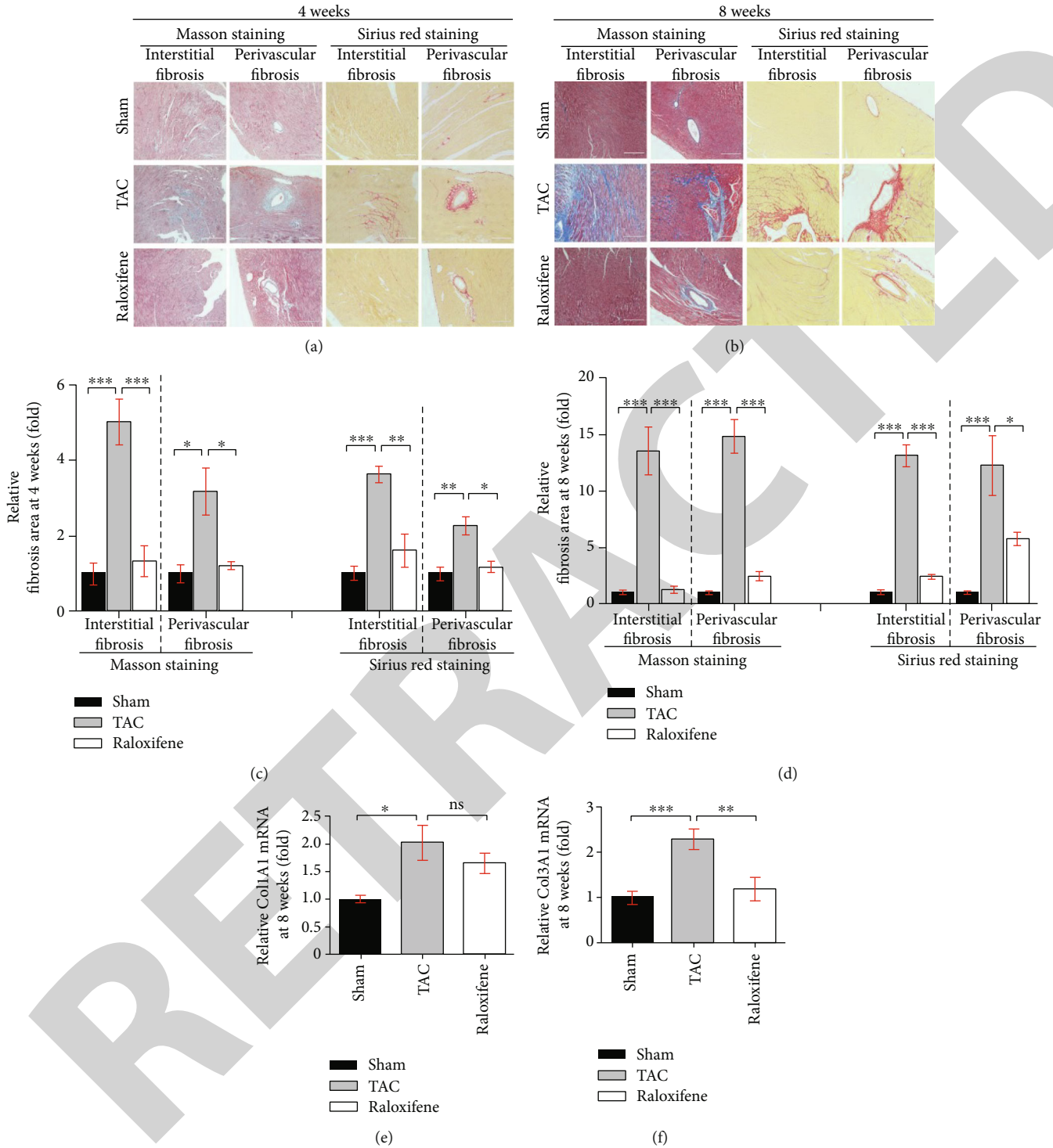
FIGURE 3: Raloxifene alleviated cardiac fibrosis induced by pressure overload. (a, b) The interstitial and perivascular fibrosis of murine hearts increased by Masson staining (left two columns) and Sirius red staining (right two columns) after TAC of 4 (a) or 8 (b) weeks and was alleviated by raloxifene (scale bar, 200 μm). (c, d) The respective histogram exhibited the quantitation for the cardiac fibrosis area of murine hearts at 4 (c) or 8 (d) weeks after TAC. (e, f) Relative Col1A1 (e) and Col3A1 (f) mRNA expression normalized to GAPDH increased in murine hearts after TAC of 8 weeks and was reduced by raloxifene. $^*p < 0.05$; $^{**}p < 0.01$; $^{***}p < 0.001$, "ns" stands for "none significance".

including LVEF, LVEDs, LVEVd, and LVEVs of the 8-week TAC group, also showed that the cardiac function was more severe than that of the 4-week TAC group

(Table 1). However, the parameters indicated that the cardiac function of the Sham group or the raloxifene group showed no difference between the two time points

(a)

(b)

(c)
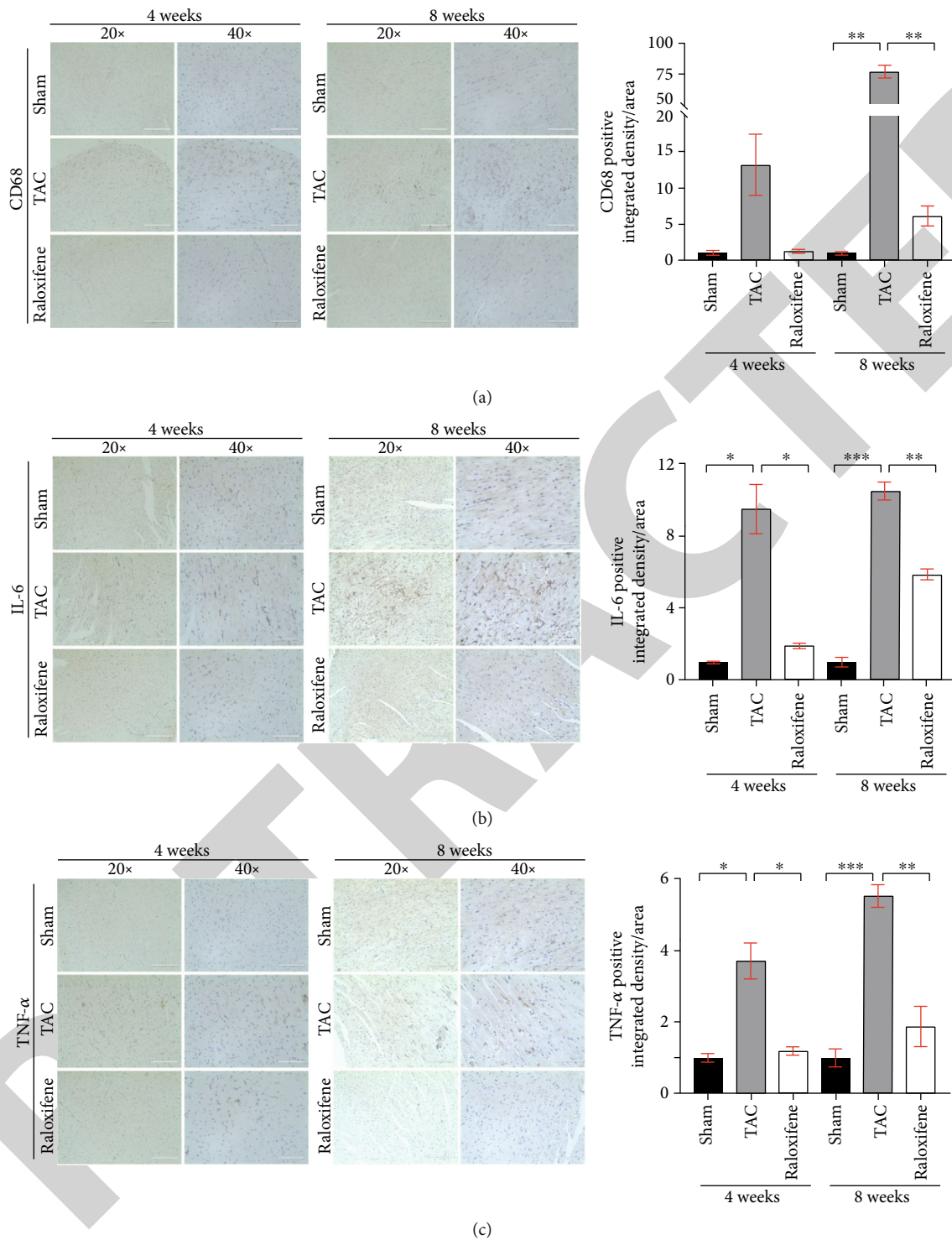
FIGURE 4: Raloxifene alleviated the increase of inflammatory markers in murine myocardial tissues induced by TAC. The local CD68 (a), IL-6 (b), and TNF-α (c) expression of myocardial tissues detected by immunohistochemistry after TAC operation and raloxifene treatment of 4 and 8 weeks (scale bar, 200 μm for 20x, 100 μm for 40x). $^{*}p < 0.05$; $^{**}p < 0.01$; $^{***}p < 0.001$.

(Table 1). The mRNA expressions of BNP and ANP in TAC murine hearts at 8 weeks were abundantly increased compared with the Sham group (ANP, $p < 0.05$; BNP, $p < 0.001$) and were remarkably decreased by raloxifene treatment contrast to the TAC group (ANP, $p < 0.05$; BNP, $p < 0.001$) (Figures 2(c) and 2(d)).

3.3. Raloxifene Prevented Cardiac Fibrosis Induced by Pressure Overload in TAC Mice. Pathological left ventricular remodeling evolved at the late stage of TAC, but cardiac fibrosis has occurred since two weeks after aortic constriction [22]. Cardiac fibrosis detected by Masson staining (left two columns) and Sirius-red staining (right two columns) is

(a)   (b)   (c)

(d)   (e)   (f)
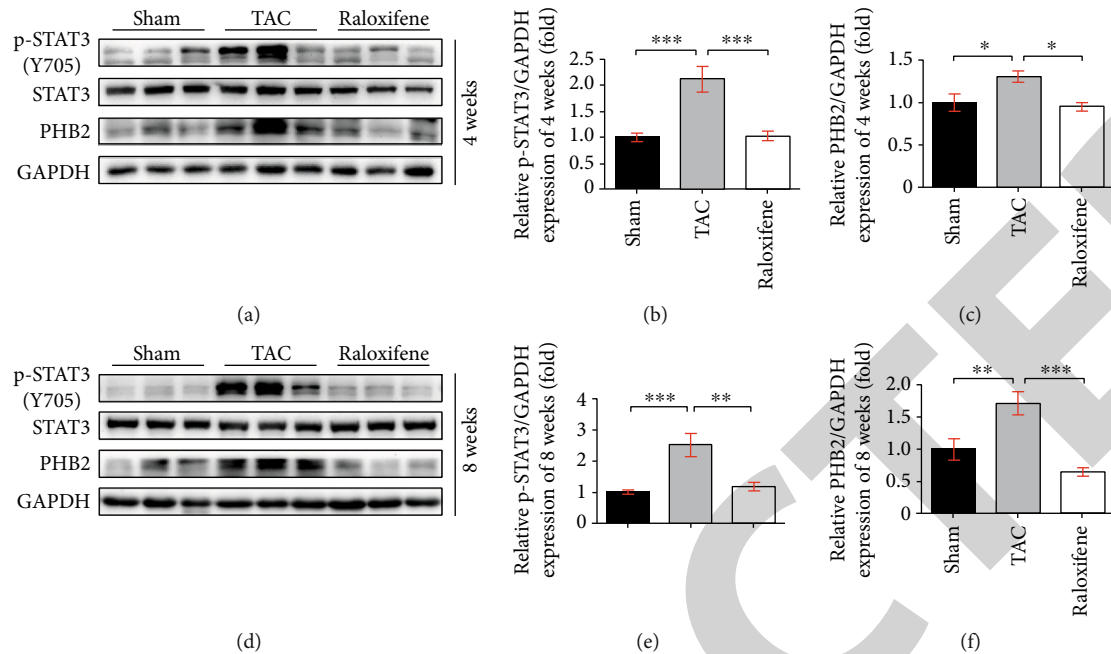
Figure 5: Raloxifene decreased the phosphorylation of STAT3 and the expression of PHB2 in TAC murine heart. The p-STAT3 level, and protein expression of STAT3, PHB2 in murine hearts at 4 (a) and 8 (d) weeks by western blotting, and relative quantitation of p-STAT3 (b, e) and PHB2 (c, f) normalized by GAPDH ($n = 3$ per group). $^*p < 0.05$; $^{**}p < 0.01$; $^{***}p < 0.001$.

shown in Figures 3(a) and 3(b). TAC dramatically exacerbated interstitial and perivascular fibrosis compared with the Sham group at both time points ($p < 0.05$), but raloxifene ameliorated the fibrotic effect of interstitial substance and around the blood vessels at both time points ($p < 0.05$) (Figures 3(c) and 3(d)). Col1A1 and Col3A1 mRNA expressions of murine hearts in the TAC group at 8 weeks were significantly increased compared with the Sham group ($p < 0.05$). Raloxifene downregulated the Col3A1 mRNA expression ($p < 0.05$) while not for Col1A1 ($p = 0.855$) (Figures 3(e) and 3(f)).

3.4. Raloxifene Extenuated the Inflammation including Macrophage Infiltration and IL-6 and TNF-α Expression in TAC Murine Myocardium. We detected the macrophage marker (CD68) and two crucial cytokines of chronic inflammation (IL-6 and TNF-α), in myocardial tissue by immunohistochemical staining. The infiltration of macrophages and the expression of IL-6 and TNF-α in murine heart tissues were increased after TAC at both 4 and 8 weeks, which indicated the myocardial inflammation activation by pressure overload. Raloxifene mitigated the increase of CD68, IL-6, and TNF-α (Figures 4(a)–4(c)).

3.5. Raloxifene Modulated the IL-6/STAT3 Signaling and Inhibited the Phosphorylation of STAT3 in Pressure Overload-Induced Murine Hearts. We detected the protein expression in murine hearts and found that phosphorylation of STAT3 was remarkably increased at both 4 weeks ($p < 0.001$) and 8 weeks ($p < 0.001$) after TAC, and raloxifene decreased the p-STAT3 level significantly at both time points ($p < 0.01$), which indicated the IL-6/STAT3 signaling was activated in TAC murine hearts (Figures 5(a), 5(b), 5(d),

and 5(e)). Meanwhile, the expression of PHB2, a mitochondrial structural protein, in the TAC group was increased notably compared with the Sham group (4 weeks, $p < 0.05$; 8 weeks, $p < 0.01$), which was decreased after raloxifene administration (4 weeks, $p < 0.05$; 8 weeks, $p < 0.001$) (Figures 5(c) and 5(f)).

3.6. Raloxifene Inhibited the Activation of IL-6/STAT3 Signaling and Hypertrophic Response Induced by IL-6 in H9c2 Myoblasts. We treated the H9c2 myoblasts with IL-6 (25 ng/mL) continuously for 24 and 48 hours and found that the cell size was enlarged significantly elicited by IL-6 after 48 hours ($p < 0.001$) (Figures 6(a) and 6(b)). The molecular marker of cellular hypertrophy, such as ANP ($p < 0.05$) and MYH7B ($p < 0.05$), was remarkably upregulated after IL-6 incubation for 48 hours (Figures 6(c)–6(e)). Meanwhile, the level of p-STAT3 (48 h, $p < 0.05$) and the expression of PHB2 (48 h, $p < 0.05$) were also concurrently increased in a time-dependent manner (Figures 6(f) and 6(g)), which illustrated that the hypertrophy of H9c2 myoblasts induced by IL-6 accompanied with activation of inflammatory signaling.

Next, we pretreated H9c2 myoblasts with raloxifene (25 μM) and triggered it with IL-6 (25 ng/mL) for 48 hours. The increase of p-STAT3 level and PHB2 expression in H9c2 myoblasts induced by IL-6 was attenuated by raloxifene (p-STAT3, $p < 0.05$; PHB2, $p < 0.05$) (Figures 6(h)–6(j)). This illustrated that the IL-6/STAT3 signaling was inhibited by raloxifene *in vitro*.

3.7. Raloxifene Inhibited Oxidative Stress Activation and Regulated Mitophagy-Related Protein Expression Induced by IL-6 in H9c2 Myoblasts. We detected the superoxide production of H9c2 myoblasts by DHE staining and found the
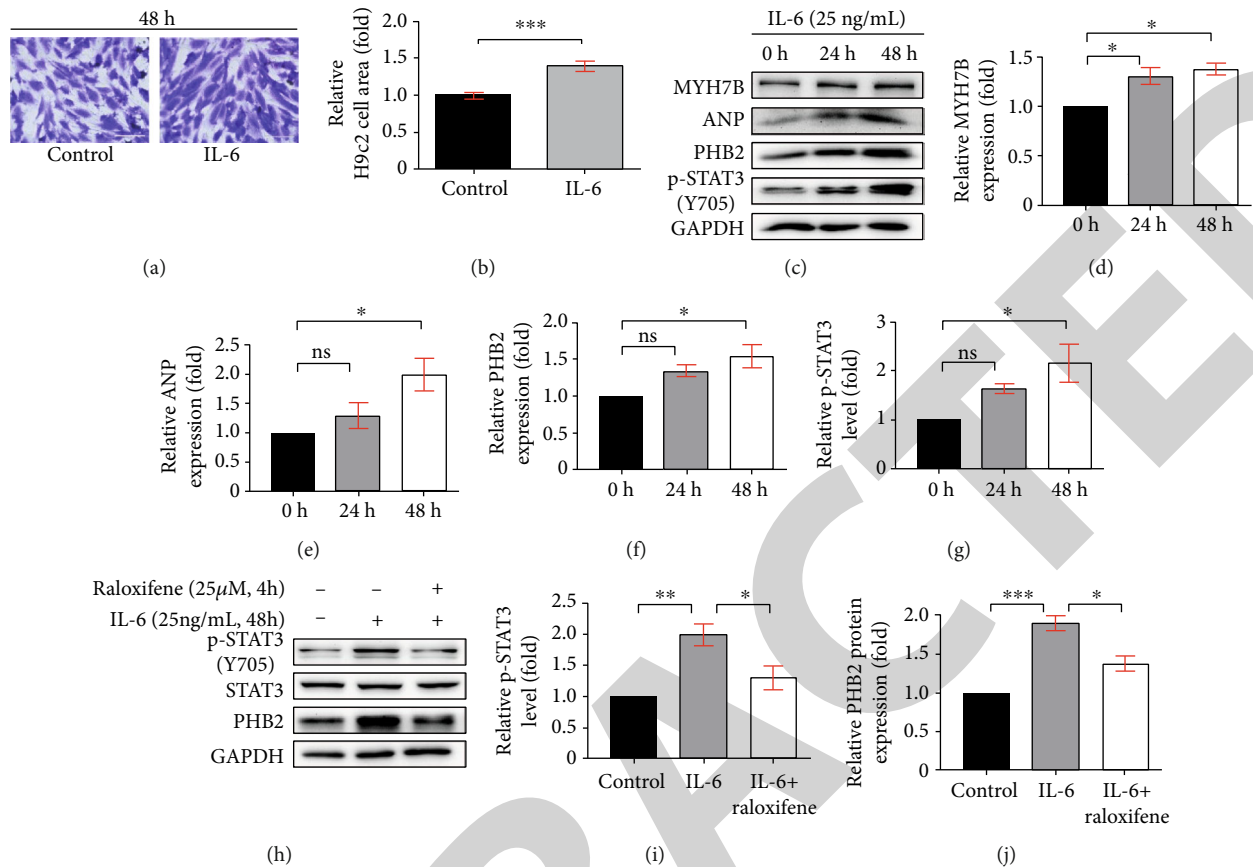
FIGURE 6: Raloxifene repressed the phosphorylation of STAT3 in hypertrophic H9c2 myoblasts. (a, b) The gentian violet staining showed H9c2 myoblasts manifested hypertrophy (a) and the relative cell area was increased (b) after incubation with IL-6 (25 ng/mL) for 48 h. (c–g) The sustained IL-6 incubation increased the protein expression of MYH7B (d), ANP (e), PHB2 (f), and the p-STAT3 level (g) in H9c2 myoblasts analyzed by western blotting (c). (h–j) Raloxifene decreased the level of p-STAT3 (i), and the expression of PHB2 (j) in H9c2 myoblasts induced by IL-6. $^*p < 0.05$; $^{**}p < 0.01$; $^{***}p < 0.001$, "ns" stands for "none significance".

fluorescence intensity which indicated the oxidative stress extent of H9c2 cells was increased by sustained IL-6 stimulation ($p < 0.01$) and raloxifene alleviated the effect ($p < 0.05$) (Figures 7(a) and 7(c)). Excessive oxidative stress caused the dysfunction of mitochondria, which might accompany the decrease of mitochondrial membrane potential. JC-1 staining showed that the JC-1 aggregate/monomer ratio decreased after incubation of IL-6 (25 ng/mL) for 48 h and raloxifene reversed the depolarization of MMP (Figures 7(b) and 7(d)). We further detected the ATP content of H9c2 myoblasts and found that the intracellular ATP content was decreased after the continuous incubation of IL-6 for 48 hours compared with the control group, and the ATP content was maintained after pretreating with raloxifene before IL-6 incubation (Figure 7(e)). Meantime, iNOS expression was increased ($p < 0.001$), but the SOD2 expression showed no difference ($p > 0.99$) after IL-6 irritation, but the total intracellular SOD activity was inhibited by IL-6 ($p < 0.05$). Raloxifene significantly increased SOD2 expression ($p < 0.01$), reduced iNOS expression ($p < 0.001$), and increased the SOD activity ($p < 0.05$) (Figures 7(f)–7(h) and 7(l)). These indicated oxidative stress activation by IL-6 was mitigated by raloxifene in H9c2 myoblasts. The excessive oxidative stress activation usually caused the damage of mitochondria and activated mitophagy. The

mitophagy-related protein including Pink1 ($p < 0.05$), Parkin ($p < 0.001$), and Bnip3 ($p < 0.01$) was increased after IL-6 stimulation, and raloxifene regulated the protein expression to basic status (Figures 7(i)–7(k)).

4. Discussion

Inflammation underlies a wide variety of physiological and pathological processes [23]. The interaction of inflammation and CVD is the hotspot of the cardiovascular field recently. HF is the end-stage of most CVD, more and more clinical and experimental studies indicate that inflammation takes an important part in the initiation and development of CVD, including atherosclerosis [24], hypertension [25], and atrial fibrillation [26]. Therefore, inflammation might contribute to the initiation, maintenance, and progression of HF. Whereupon, we investigated the role of inflammation in the pressure overload-HF mice and IL-6-elicited H9c2 myoblasts, as well as the anti-inflammatory effect of raloxifene.

In response to the pathogenesis of pressure overload after TAC operation, the heart undergoes cardiac hypertrophy and fibrosis at the late stage, evolving into HF finally, while initially benefitting from compensatory elevation of the cardiac wall tension at the early stage to maintain cardiac

(a)

(b)

(c)

(d)

(e)

(f)

(g)

(h)

Figure 7: Continued.

(i) (j) (k) (l)
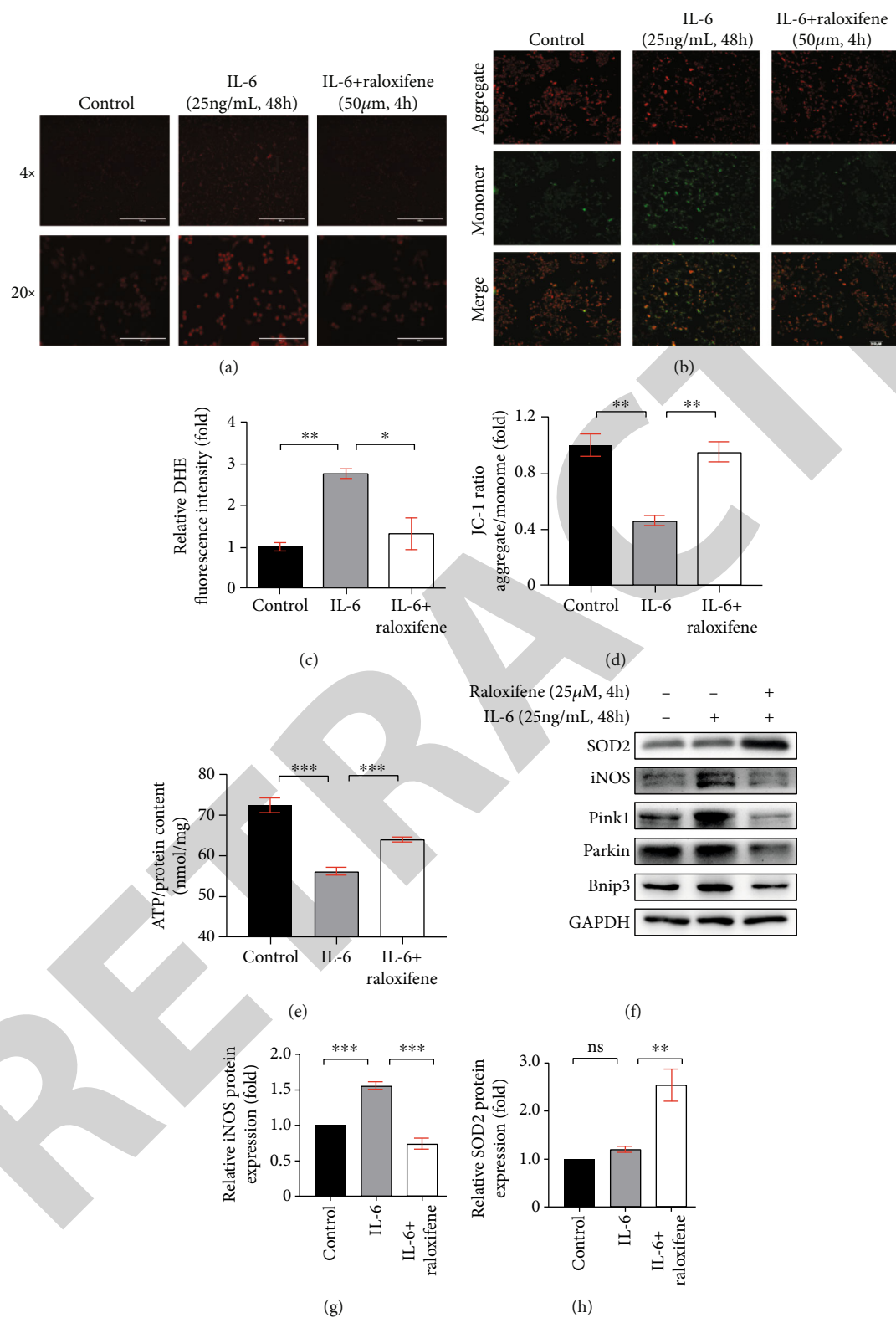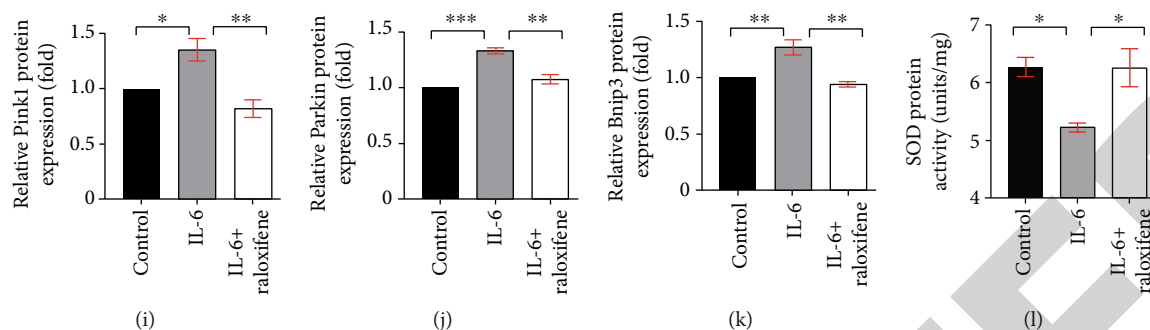
Figure 7: Raloxifene reduced oxidative stress and regulated mitophagy-related protein expression elicited by IL-6 in H9c2 myoblasts. (a, c) The DHE staining (a) showed that raloxifene alleviated reactive oxygen species production induced by IL-6 (scale bar: 1000 μm for 4x; 200 μm for 20x) and the bar graph (c) showing the mean DHE fluorescence intensity of nuclei in H9c2 myoblasts. (b, d) The JC-1 staining (b) showed that raloxifene reversed the decrease of mitochondrial membrane potential elicited by IL-6 (scale bar, 400 μm); red fluorescent (aggregate)/green fluorescent (monomer) ratio (D) was decreased with the IL-6 incubation and was reversed by raloxifene treatment. (e) The intracellular ATP content was decreased after the continuous incubation of IL-6 for 48 hours but was maintained after pretreating with raloxifene before IL-6 incubation. (f–k) Raloxifene increased the antioxidative protein SOD2 expression (h) and decreased the prooxidative protein iNOS expression (g) of H9c2 myoblasts incubated with IL-6. Meanwhile, raloxifene regulated the mitophagy-related protein of Pink1 (i), Parkin (j), and Bnip3 (k) to normal status. (l) The sustained IL-6 stimulation decreased the total intracellular SOD protein activity and was reversed by raloxifene treatment. $^{*}p < 0.05$; $^{**}p < 0.01$; $^{***}p < 0.001$, "ns" stands for "none significance".

function [19, 22]. The heart failure induced by pressure overload through TAC in our study was principally characterized by systolic dysfunction. We compared the difference of tissue features between different stages after TAC. At the early stage (4 weeks), the myocardial hypertrophy and fibrosis have developed but were not conspicuous as compared with that of the late stage (8 weeks). Although the left ventricular dysfunction at 4 weeks was not obvious, inflammation has already been activated at the early stage (4 weeks) and sustained to the late stage (8 weeks), which indicates inflammation might continuously contribute to the HF progression.

Our cooperative group previously found that the N and O of the piperidinyl-ethoxy moiety of raloxifene could form hydrogen bonds with Asn92 and Cys6 residue of gp130 D1 domain, which disrupts the native IL-6 binding interaction with the gp130 [15]. Raloxifene was proved to downregulate the IL-6-induced STAT3 phosphorylation in pancreatic and hepatic cancer cells [15, 16], which indicates that raloxifene is an effective IL-6/gp130 inhibitor. In vitro study, raloxifene was proved to downregulate the STAT3 phosphorylation induced by IL-6 in hepatic cancer cells, but not the induction of STAT1 and STAT6 phosphorylation by IFN-γ, IFN-α, and IL-4 [16]. Supplementary Figure 1 indicated that raloxifene inhibited the STAT3 phosphorylation induced by IL-6 in H9c2 myoblasts but not by the other cytokines of the IL-6 family, such as LIF and OSM. Meanwhile, the induction of STAT1 and STAT5 phosphorylation induced by IL-6, LIF, and OSM was not inhibited by raloxifene. Hence, we thought that raloxifene was a relatively selective inhibitor of IL-6/gp130/STAT3 signaling. We administrated raloxifene to TAC mice and found that the inflammatory IL-6/gp130/STAT3 signaling was suppressed in murine hearts. Myocardial remodeling was ameliorated at both stages, as well as the cardiac function was partly maintained at the late stage (8 weeks). The animal experiments of our study demonstrated the inflammation was activated in TAC mice, which was consistent with previous research [22, 27].

Previous studies also revealed that the IL-6 level of serum in TAC mice was increased [28] and the IL-10/STAT3 signaling was activated in pressure overload-induced cardiac dysfunction [29]. The previous study reported that IL-6 deletion attenuated the left ventricular hypertrophy and dysfunction induced by 6-week TAC in mice and proved that both angiotensin II- and phenylephrine-induced increase in hypertrophy genes were abrogated in IL-6-/- cardiac myocyte [13]. These indicated that IL-6 is critical to cardiac hypertrophy and dysfunction in response to TAC. However, the genome-editing technique used in human cardiovascular disease therapy is still debatable due to the safety concern and ethical issues; hence, the pharmacological intervention on IL-6/gp130/STAT3 signal by raloxifene is more translatable compared with genome manipulation. Raloxifene might modulate multiple mechanisms, and the IL-6/STAT3 signal might be one of the important options. Our results indicated inhibition of the IL-6/gp130/STAT3 pathway accompanied with the alleviation of the pathological remodeling and heart failure induced by pressure overload; therefore, we thought that the intervention of IL-6/STAT3 signal by raloxifene might involve the pivotal mechanism of the remission. We also found that the local inflammation of heart tissues in TAC mice was increased likewise, IL-6/gp130/STAT3 inhibition related to the mitigation of inflammation and the remission of cardiac remodeling and dysfunction in TAC mice, which was not reported by previous research.

When the aorta was constricted, fluctuation and overload of blood pressure activated the renin-angiotensin-aldosterone system (RAAS), which initiates a cascade reaction of neurohormone regulation [22]; in this condition, cardiomyocytes and cardiac fibroblasts would release TNF-α and IL-6 [22, 30]. The proinflammatory cytokines would orchestrate the expression of cytokines and chemokines and thus promotes the injury of resident interstitial cells and the recruitment of immune cells [22, 31, 32]. The accumulation of abundant

inflammatory factors and inflammatory cells provides an inflammatory microenvironment for cardiac remodeling and heart failure. We further found that the phosphorylation of STAT3 in the myocardial tissue of TAC mice was significantly increased and IL-6/gp130/STAT3 inhibition has a cardioprotective effect, all of which indicated that the inflammatory signaling pathway of the IL-6/gp130/STAT3 axis might play a crucial role in the cardiac remodeling and HF. Moreover, inflammation promoted excessive ROS production, which was proved to damage the mitochondrial homeostasis and cause energy metabolism disorder [33].

High energy demand, especially the high ATP consumption, is one of the major features of the heart, and oxidative metabolism in the mitochondria is the predominant derivation of ATP production [34]. The oxidative phosphorylation takes place in the inner mitochondrial membrane; hence, the inner membrane integrity and the mitochondrial membrane potential are critical for mitochondrial function [34]. PHB2 is involved in the electron transport chain and maintains the structure and function of mitochondria [35], and it could translocate to the nucleus and participate in oxidative stress and apoptosis [36]. Theiss et al. reported that STAT3 mediated IL-6-induced PHB transcription and bound to the IL-6 response element in its promoter [37], but the concrete role of PHB2 in myocardial hypertrophy is unsettled [38, 39]. In our study, the PHB2 expression was increased in TAC-induced murine heart and IL-6-elicited H9c2 myoblasts and was decreased by raloxifene treatment. Importantly, the alteration of PHB2 was consistent with the phosphorylation of STAT3. Meantime, the superoxide productions triggered by IL-6 in H9c2 myoblasts were inhibited by raloxifene, the depression of mitochondrial membrane potential induced by IL-6 was reversed by raloxifene, and the ATP content was maintained after pretreating with raloxifene before IL-6 incubation. IL-6 induced the oxidative stress producer (iNOS) increase and scavenger (SOD2) decrease in H9c2 myoblasts, which was reversed by raloxifene. These results indicated that raloxifene could exert the cardioprotective effect via mitigating oxidative stress-induced mitochondrial dysfunction on H9c2 myoblasts induced by continuous IL-6 incubation.

As reported, the damaged mitochondria would release cytochrome C and thereby trigger apoptosis. The appropriate elimination of dysfunctional mitochondria is essential to cellular survival [40]. Mitophagy is an important control mechanism for regulating the adjustments to mitochondrial status with oxidative stress [41], and mitophagy is found to play a protective role in most cardiovascular disease [42]. As our results were shown, two classic mediators of mitophagy, Pink1 and Parkin, were increased by sustained IL-6 incubation. The disturbance of MMP leads to PINK1 accumulation at the surface of the mitochondria, promoting the subsequent recruitment of Parkin, which is the initiation of the classic Pink/Parkin-dependent pathway in mitophagy [43]. Meanwhile, the expression of Bnip3, which plays a critical role in the mitophagy receptor-dependent pathway, was also increased after IL-6 stimulation. Excessive activation of autophagy elicited by pathological stimuli, such as pressure overload, is maladaptive and promotes cell apoptosis, which was reported to aggravate cardiac hypertrophy and speed up the process of HF [44]. Mitophagy, as a selective autophagy, is activated in the early stage of cardiac hypertrophy during HF, which ultimately promotes cell apoptosis [45]. Hence, the proper mitophagy is imperative for cellular survival. We found that raloxifene decreased the expression of Pink1, Parkin, and Bnip3 elicited by IL-6 stimuli, which indicated that the biological effect of raloxifene was involved in the mitochondrial quality control by resuming the increase of mitophagy-related proteins induced by excessive ROS and the loss of MMP. Hence, TAC-induced hemodynamic changes activate inflammation especially the IL-6/STAT3 signaling, as well as the production of reactive oxygen species and subsequent imbalance of mitochondrial homeostasis. In turn, excessive ROS could aggravate the inflammation and HF progress as reported [46, 47], which constitutes to a vicious circle of proinflammatory microenvironment. Raloxifene could block the overactivated IL-6/STAT3 signaling and alleviate the inflammation with decreased oxidative stress and regulation of the mitophagy level.

Previous studies reported the debatable effect of raloxifene. Ogita et al. found that raloxifene prevented cardiac hypertrophy and dysfunction in pressure overload male mice (4 weeks) [18]. However, Westphal et al. reported that raloxifene was not able to reduce the myocardial remodeling and could not maintain EF in female TAC mice at the long-term period (9 weeks) [17]. The severity of cardiac remodeling and heart failure of the TAC model was influenced by multiple factors and depended on the murine strain, sex, and needle size used for TAC operation [20]. The basal line of cardiac function of mice in different studies might be variant, but the main difference between the two studies was the size of a gauge needle used for TAC operation. Ogita et al. adopted the 27-gauge needle, while Westphal et al. used the 26-gauge needle (the outside diameter was larger than that of the 27-gauge needle) for operation. The previous study by Richards et al. explored the influence of gauge (G) of needle used on the TAC severity [21] and found that the 27G TAC group had more severe systolic and diastolic dysfunction, severe cardiac fibrosis, and was more likely to display features of heart failure compared with the 26G TAC group [21]. Therefore, the severity of phenotype was more obvious in the study of Ogita et al., and the cardioprotective effect of raloxifene might be easier to be observed. Intriguingly, although the pathological cardiac remodeling process might progress at different rates or degrees, the cardiac response to various degrees of pressure overload might not be graded or stepwise [21]. Richards et al. observed that several parameters such as fractional shortening, ejection fraction, and perivascular fibrosis were mixed responses, rather than step-wise [21]. The complexity of TAC operation produced unique pathological phenotypes in different studies. In our study, we used the $27^{1/2}$-gauge needle (the outside diameter was smaller than that of the 27-gauge needle) for TAC operation; hence, the pathological remodeling and cardiac dysfunction might be more significant than the previous studies, and we also found that raloxifene decelerated the deterioration of heart dysfunction and mitigated the cardiac remodeling and myocardial inflammation in mice induced by TAC to a certain degree at both four and eight weeks. Moreover, the mechanism of the previous study about the effects of raloxifene on TAC mice focused on

the activity of MAPK signaling [18] but paid less attention to the motivation of inflammation. In this study, we not only provide more evidence about the cardioprotective effect of raloxifene on TAC mice and we newly found that inflammation and IL-6/gp130/STAT3 signaling were activated in TAC murine heart but inhibited by raloxifene accompanied by the improvement of cardiac hypertrophy and heart failure, which is the mechanism of raloxifene differing from that of the others. On the other hand, the possible reason for the divergence in the previous findings is that there was gender difference in the mouse model of pathological hypertrophy and HF, in which male mice showed more eccentric hypertrophy and HF signs than female mice [48]. Meanwhile, the gender difference in the treatment of raloxifene to rat pulmonary arteries and veins was reported by a previous study [49]. The other study also reported that the production of proinflammatory cytokines, such as IL-6, IL-1β, and TNF-α, was more obvious in male mice than that in female mice after lipopolysaccharide (LPS) induction [50]. All evidence above indicated that gender might be involved in the effect of TAC or raloxifene, and the inflammatory response of mice. Hence, male mice might be more sensitive to TAC surgery and show serious inflammation, so the effect of raloxifene on male mice might be more significant. These reported results all suggested that inflammation might play a very important role in the progression of cardiac remodeling and HF. Our data not only showed more evidences but also illustrated that the potential inflammatory pathways might include IL-6/gp130/STAT3 signaling.

Other small molecule STAT3 inhibitor S31-201 [51] was also documented to reduce phosphorylation of STAT3 in Wistar rats induced by renal artery ligation. Meanwhile, the natural product, such as stachydrine [52], celastrol [53], and gallic acid [54], ameliorated isoproterenol- or TAC-induced cardiac hypertrophy, fibrosis, and cardiac dysfunction by inhibiting STAT3 signaling pathways, but the authors did not explore the underlying mechanism. We used raloxifene as an IL-6/STAT3 inhibitor to evaluate its cardioprotective effect on TAC-induced cardiac hypertrophy, heart failure, and myocardial inflammation. Unlike the previous studies, we not only focused on exploring the IL-6/STAT3 signaling pathway but also further evaluated the regulation of raloxifene on the oxidative stress and mitophagy levels induced by continuous inflammatory activation. Raloxifene is also approved by the FDA, and the safety for humans is validated and accepted. The limitation of this research lies in that we did not investigate the further mechanism of how IL-6 regulates mitochondrial homeostasis in the context of TAC-induced HF. To date, the role of IL-6 in the CVD during the acute and chronic phases has been debatable, so the role of IL-6 in the acute phase to heart failure induced by pressure overload is unsettled. Therefore, further studies focused on mitochondrial energy metabolism, mitochondrial quality control, and the relationship between IL-6 were needed to illustrate the detailed mechanism.

5. Conclusions

Overall, during the chronic stage of pressure overload-induced heart failure, the expression of IL-6 was upregulated, which activated gp130/STAT3 signaling and produced excessive ROS. Oxidative stress aggravated depolarization of MMP and the damage of mitochondria, which affected the homeostasis of mitochondrial structure and increased the expression of the mitophagy-related proteins, thus resulting in more ROS production and uncontrolled inflammation. The vicious circle could be suppressed via IL-6/gp130 inhibitor, raloxifene, by prohibiting the binding between IL-6 and gp130, which indicated that the IL-6/gp130/STAT3 axis might be involved in the pathogenesis of myocardial hypertrophy and HF.

Data Availability

All datasets generated for this study are included in the article.

Ethical Approval

The authors declare that all animal experiments have been approved by the institutional review board of Tongji Hospital, Tongji Medical College, Huazhong University of Science and Technology.

Conflicts of Interest

The authors declare that they have no conflict of interest.

Authors' Contributions

Shengqi Huo and Wei Shi have contributed equally to this work.

Acknowledgments

Supplementary Materials

Supplemental Figure 1: raloxifene relative selectively inhibited the phosphorylation of STAT3 induced by IL-6. Raloxifene (25 μm, 4 h) inhibited the STAT3 phosphorylation induced by IL-6 (25 ng/mL, 30 min) in H9c2 myoblasts, but not STAT1 and STAT5 phosphorylation. The phosphorylation of STAT1, STAT3, and STAT5 induced by the other cytokines of the IL-6 family, such as LIF (25 ng/mL, 30 min) and OSM (25 ng/mL, 30 min), was not inhibited by raloxifene. *(Supplementary Materials)*

References

[1] P. Ponikowski, S. D. Anker, K. F. AlHabib et al., "Heart failure: preventing disease and death worldwide," *ESC Heart Failure*, vol. 1, no. 1, pp. 4–25, 2014.

[2] P. Perumareddi, "Prevention of hypertension related to cardiovascular disease," *Primary Care*, vol. 46, no. 1, pp. 27–39, 2019.

[3] E. Rullman, M. Melin, M. Mandic, A. Gonon, R. Fernandez-Gonzalo, and T. Gustafsson, "Circulatory factors associated with function and prognosis in patients with severe heart failure," *Clinical Research in Cardiology*, vol. 109, no. 6, pp. 655–672, 2020.

[4] R. Klingenberg and T. F. Luscher, "Rheumatoid arthritis and coronary atherosclerosis: two cousins engaging in a dangerous liaison," *European Heart Journal*, vol. 36, no. 48, pp. 3423–3425, 2015.

[5] S. Aniwan, D. S. Pardi, W. J. Tremaine, and E. V. Loftus Jr., "Increased risk of acute myocardial infarction and heart failure in patients with inflammatory bowel diseases," *Clinical Gastroenterology and Hepatology*, vol. 16, no. 10, pp. 1607–1615.e1, 2018.

[6] P. Ponikowski, A. A. Voors, S. D. Anker et al., "2016 ESC guidelines for the diagnosis and treatment of acute and chronic heart failure: the task force for the diagnosis and treatment of acute and chronic heart failure of the European Society of Cardiology (ESC). Developed with the special contribution of the Heart Failure Association (HFA) of the ESC," *European Journal of Heart Failure*, vol. 18, no. 8, pp. 891–975, 2016.

[7] S. Kenchaiah, J. C. Evans, D. Levy et al., "Obesity and the risk of heart failure," *The New England Journal of Medicine*, vol. 347, no. 5, pp. 305–313, 2002.

[8] E. S. Chung, M. Packer, K. H. Lo, A. A. Fasanmade, J. T. Willerson, and T. N. F. T. A. C. H. F. I. Anti, "Randomized, double-blind, placebo-controlled, pilot trial of infliximab, a chimeric monoclonal antibody to tumor necrosis factor-alpha, in patients with moderate-to-severe heart failure: results of the anti-TNF therapy against congestive heart failure (ATTACH) trial," *Circulation*, vol. 107, no. 25, pp. 3133–3140, 2003.

[9] J. S. Hanberg, V. S. Rao, T. Ahmad et al., "Inflammation and cardio-renal interactions in heart failure: a potential role for interleukin-6," *European Journal of Heart Failure*, vol. 20, no. 5, pp. 933-934, 2018.

[10] V. Eskandari, A. A. Amirzargar, M. J. Mahmoudi et al., "Gene expression and levels of IL-6 and TNFα in PBMCs correlate with severity and functional class in patients with chronic heart failure," *Irish Journal of Medical Science*, vol. 187, no. 2, pp. 359–368, 2018.

[11] A. Mohr, N. Chatain, T. Domoszlai et al., "Dynamics and non-canonical aspects of JAK/STAT signalling," *European Journal of Cell Biology*, vol. 91, no. 6-7, pp. 524–532, 2012.

[12] N. C. Lai, M. H. Gao, E. Tang et al., "Pressure overload-induced cardiac remodeling and dysfunction in the absence of interleukin 6 in mice," *Laboratory Investigation*, vol. 92, no. 11, pp. 1518–1526, 2012.

[13] L. Zhao, G. Cheng, R. Jin et al., "Deletion of interleukin-6 attenuates pressure overload-induced left ventricular hypertrophy and dysfunction," *Circulation Research*, vol. 118, no. 12, pp. 1918–1929, 2016.

[14] K. R. Snyder, N. Sparano, and J. M. Malinowski, "Raloxifene hydrochloride," *American Journal of Health-System Pharmacy*, vol. 57, no. 18, pp. 1669–1675, 2000, quiz 76-8.

[15] H. Li, H. Xiao, L. Lin et al., "Drug design targeting protein-protein interactions (PPIs) using multiple ligand simultaneous docking (MLSD) and drug repositioning: discovery of raloxifene and bazedoxifene as novel inhibitors of IL-6/GP130 interface," *Journal of Medicinal Chemistry*, vol. 57, no. 3, pp. 632–641, 2014.

[16] Y. Wang, H. Ma, C. Zhao et al., "Growth-suppressive activity of raloxifene on liver cancer cells by targeting IL-6/GP130 signaling," *Oncotarget*, vol. 8, no. 20, pp. 33683–33693, 2017.

[17] C. Westphal, C. Schubert, K. Prelle et al., "Effects of estrogen, an ERα agonist and raloxifene on pressure overload induced cardiac hypertrophy," *PLoS One*, vol. 7, no. 12, 2012.

[18] H. Ogita, K. Node, Y. Liao et al., "Raloxifene prevents cardiac hypertrophy and dysfunction in pressure-overloaded mice," *Hypertension*, vol. 43, no. 2, pp. 237–242, 2004.

[19] A. C. de Almeida, R. J. van Oort, and X. H. Wehrens, "Transverse aortic constriction in mice," *Journal of Visualized Experiments*, vol. 38, 2010.

[20] T. Furihata, S. Kinugawa, S. Takada et al., "The experimental model of transition from compensated cardiac hypertrophy to failure created by transverse aortic constriction in mice," *Int J Cardiol Heart Vasc.*, vol. 11, pp. 24–28, 2016.

[21] D. A. Richards, M. J. Aronovitz, T. D. Calamaras et al., "Distinct phenotypes induced by three degrees of transverse aortic constriction ∗∗in mice∗∗," *Scientific Reports*, vol. 9, no. 1, p. 5844, 2019.

[22] L. Bacmeister, M. Schwarzl, S. Warnke et al., "Inflammation and fibrosis in murine models of heart failure," *Basic Research in Cardiology*, vol. 114, no. 3, p. 19, 2019.

[23] R. Medzhitov, "Origin and physiological roles of inflammation," *Nature*, vol. 454, no. 7203, pp. 428–435, 2008.

[24] P. M. Ridker, B. M. Everett, T. Thuren et al., "Antiinflammatory therapy with canakinumab for atherosclerotic disease," *The New England Journal of Medicine*, vol. 377, no. 12, pp. 1119–1131, 2017.

[25] A. S. Bruno, P. D. D. Lopes, K. C. M. de Oliveira, A. K. de Oliveira, and S. B. de Assis Cau, "Vascular inflammation in hypertension: targeting lipid mediators unbalance and nitrosative stress," *Current Hypertension Reviews*, vol. 16, 2019.

[26] Y. Guo, G. Y. Lip, and S. Apostolakis, "Inflammation in atrial fibrillation," *Journal of the American College of Cardiology*, vol. 60, no. 22, pp. 2263–2270, 2012.

[27] Y. Xia, K. Lee, N. Li, D. Corbett, L. Mendoza, and N. G. Frangogiannis, "Characterization of the inflammatory and fibrotic response in a mouse model of cardiac pressure overload," *Histochemistry and Cell Biology*, vol. 131, no. 4, pp. 471–481, 2009.

[28] Y. Zhang, L. Zhang, X. Fan et al., "Captopril attenuates TAC-induced heart failure via inhibiting Wnt3a/β-catenin and Jak2/Stat3 pathways," *Biomedicine & Pharmacotherapy*, vol. 113, p. 108780, 2019.

[29] S. K. Verma, P. Krishnamurthy, D. Barefield et al., "Interleukin-10 treatment attenuates pressure overload-induced hypertrophic remodeling and improves heart function via signal transducers and activators of transcription 3-dependent inhibition of nuclear factor-κB," *Circulation*, vol. 126, no. 4, pp. 418–429, 2012.

[30] A. Leask, "Getting to the heart of the matter: new insights into cardiac fibrosis," *Circulation Research*, vol. 116, no. 7, pp. 1269–1276, 2015.

[31] D. Lindner, C. Zietsch, J. Tank et al., "Cardiac fibroblasts support cardiac inflammation in heart failure," *Basic Research in Cardiology*, vol. 109, no. 5, p. 428, 2014.

[32] F. J. Carrillo-Salinas, N. Ngwenyama, M. Anastasiou, K. Kaur, and P. Alcaide, "Heart inflammation: immune cell roles and

Retraction

Retracted: Puerarin Attenuates LPS-Induced Inflammatory Responses and Oxidative Stress Injury in Human Umbilical Vein Endothelial Cells through Mitochondrial Quality Control

Oxidative Medicine and Cellular Longevity

This article has been retracted by Hindawi following an investigation undertaken by the publisher [1]. This investigation has uncovered evidence of one or more of the following indicators of systematic manipulation of the publication process:

(1) Discrepancies in scope

(2) Discrepancies in the description of the research reported

(3) Discrepancies between the availability of data and the research described

(4) Inappropriate citations

(5) Incoherent, meaningless and/or irrelevant content included in the article

(6) Peer-review manipulation

The presence of these indicators undermines our confidence in the integrity of the article's content and we cannot, therefore, vouch for its reliability. Please note that this notice is intended solely to alert readers that the content of this article is unreliable. We have not investigated whether authors were aware of or involved in the systematic manipulation of the publication process.

Wiley and Hindawi regrets that the usual quality checks did not identify these issues before publication and have since put additional measures in place to safeguard research integrity.

We wish to credit our own Research Integrity and Research Publishing teams and anonymous and named external researchers and research integrity experts for contributing to this investigation.

The corresponding author, as the representative of all authors, has been given the opportunity to register their agreement or disagreement to this retraction. We have kept a record of any response received.

References

[1] X. Chang, T. Zhang, D. Liu et al., "Puerarin Attenuates LPS-Induced Inflammatory Responses and Oxidative Stress Injury in Human Umbilical Vein Endothelial Cells through Mitochondrial Quality Control," *Oxidative Medicine and Cellular Longevity*, vol. 2021, Article ID 6659240, 14 pages, 2021.

Research Article

Puerarin Attenuates LPS-Induced Inflammatory Responses and Oxidative Stress Injury in Human Umbilical Vein Endothelial Cells through Mitochondrial Quality Control

Xing Chang [iD],[1,2] **Tian Zhang** [iD],[3] **Dong Liu,**[4] **Qingyan Meng,**[3] **Peizheng Yan** [iD],[3] **Duosheng Luo,**[5] **Xue Wang** [iD],[6] **and XiuTeng Zhou** [iD][1,5]

[1]*State Key Laboratory of Dao-di Herbs, National Resource Center for Chinese Materia Medica, China Academy of Chinese Medical Sciences, Beijing, China*
[2]*Guang'anmen Hospital, Chinese Academy of Traditional Chinese Medicine, Beijing, China*
[3]*Shandong University of Traditional Chinese Medicine, Jinan, Shandong, China*
[4]*Institute of the History of Chinese Medicine and Medical Literature, China Academy of Chinese Medical Sciences, Beijing, China*
[5]*Institute of Chinese Medicine, Guangdong Pharmaceutical University, Guangzhou, China*
[6]*School of Business Macau University of Science and Technology, Taipa, Macau, China*

Correspondence should be addressed to Xue Wang; cheer0430@sina.com and XiuTeng Zhou; zxt_0508@163.com

Atherosclerosis is closely associated with the inflammatory reaction of vascular endothelial cells. Puerarin (Pue), the main active component isolated from the rhizome of *Pueraria lobata*, is an isoflavone compound with potent antioxidant properties. Although Pue exhibits promising antiatherosclerotic pharmacological effects, only a few studies have reported its protective effect on endothelial cells. This study found that Pue could partly regulate mitochondrial function in human umbilical vein endothelial cells (HUVECs) and reduce or inhibit lipopolysaccharide-induced inflammatory reactions and oxidative stress injury in HUVECs, likely via mitochondrial quality control. Furthermore, the protective effect of Pue on HUVECs was closely related to the SIRT-1 signaling pathway. Pue increased autophagy and mitochondrial antioxidant potential via increased SIRT-1 expression, reducing excessive production of ROS and inhibiting the expression of inflammatory factors and oxidative stress injury. Therefore, Pue may improve mitochondrial respiratory function and energy metabolism, increasing the vulnerability of HUVECs to an inflammatory state.

1. Introduction

Atherosclerosis (AS) is a protective response to arterial wall endothelium and smooth muscle injury, including the formation of lipid streaks and fiber injury, and is always accompanied by an inflammatory reaction [1, 2]. When the inflammatory response is excessive, it may trigger vascular endothelial cell damage and plaque formation [3, 4]. Endothelial cell structure and function play important roles in maintaining a balance of microcirculation and smooth blood flow, especially in AS development [5, 6]. Endothelial cells are the main cells constituting the intima of the artery wall and are the barrier between blood and external tissues. They function to regulate blood flow, vascular tension, antithrombotic and procoagulant activities, and lipoprotein metabolism [7]. Endothelial cells also produce cytokines and can regulate immune responses through their barrier and secretion functions [8]. Furthermore, endothelial cells can secrete bioactive substances, such as nitric oxide (NO) and endothelin, and affect the function of smooth muscle cells, platelets, and white blood cells [9].

Endothelial cell injury and dysfunction are involved in the early initiation of AS [10]. For instance, during the early stage of AS, endothelial cells can produce a series of inflammatory factors that may further aggravate endothelial cell dysfunction, participate in thrombosis, and promote the

occurrence and development of AS [11]. During the state of inflammatory stress, endothelial cell function and gene expression switch from a resting to an activated state, contributing to various inflammatory reactions [12]. Endothelial cells may be affected by inflammatory factors produced by other cells and can also affect the proliferation and contraction of smooth muscle cells through paracrine signaling [13]. The proliferation of smooth muscle cells is an important feature of late AS development [14].

Most studies to date have focused on the role of endothelial dysfunction in vasculitis and microcirculation diseases. With respect to these types of diseases, endothelial dysfunction caused by inflammation is more likely to lead to AS [15, 16]. During the development of AS, inflammatory reactions are often related to reactive oxygen species- (ROS-) mediated oxidative stress [17]. With the occurrence and development of inflammation, increased activated infiltrating immune cells, and inflammatory resident cells, the demand for mitochondrial energy gradually increases, leading to hypoxia and mitochondrial quality control (MQC) disorder. Furthermore, ROS are overproduced, and endothelial cells exhibit more severe oxidative damage [18, 19].

Mitochondria are the powerhouse of oxidative phosphorylation in eukaryotes [20], wherein carbohydrates, fats, and proteins are oxidized and catabolized to produce energy [21, 22]. Pyruvate is hydrolyzed to form triacyl acid and pyruvic acid in the mitochondria. Ultimately, H_2O and CO_2 are generated, and adenosine triphosphate (ATP) is released to sustain physiological cell functions [23]. Studies have shown that mitochondrial involvement is an important link in AS progression [24]. Mitochondrial energy metabolism disorder is one of the early indications of vascular endothelial cell dysfunction [25]. During AS progression, mitochondrial energy metabolism disorder mainly manifests as respiratory dysfunction and decreased expression of energy metabolism-related genes and proteins [26]. Mitochondria are important mediators in cells, and mitochondrial dysfunction can indirectly activate a variety of inflammatory signal transduction pathways, leading to tissue and cell damage. ROS-mediated oxidative stress may result in MQC disorder through direct cytotoxicity and can promote the occurrence and development of local inflammatory responses [27].

Oxidative stress and inflammation are interdependent, especially in mitochondria. Excessive ROS production at inflammatory sites can lead to oxidative stress-induced damage to mitochondria. Mitochondrial ROS and the accompanying products of oxidative stress can synergistically enhance the response of inflammatory factors. Mitochondria may be the "Trojan horse" of inflammation while maintaining basic cell function [28]. In addition, a study by Chen revealed that damaged mitochondria activate inflammatory bodies of NLR family pyrin domain containing 3 (NLRP3) [29]. Furthermore, activation of NLRP3 is inhibited when mitochondrial autophagy clears abnormal mitochondria and damaged proteins [30]. The oxidative effect of mitochondrial ROS on mitochondrial DNA during activation of NLRP3 leads to a partial inflammatory potential of free circulating mitochondrial DNA. This shows that oxidative stress and the mitochondrial pathway can affect MQC and

endothelial cell inflammatory responses in an interdependent manner.

Puerarin (Pue) is the main active component of *Pueraria lobata*, which is used in traditional Chinese medicine. Pue is a flavonoid glycoside extracted from the dried roots of *P. lobata* [31, 32]. Because of its noticeable estrogen-like effects, Pue helps treat atherosclerotic diseases and protect endothelial cell function [33]. Pue also significantly reduces lipopolysaccharide- (LPS-) induced p-NF-kappa B-p65 and Bax expression and increases the expression levels of Bcl-2. Furthermore, Pue can inhibit the release of inflammatory cytokines and protect umbilical vein endothelial cells [34]. Other studies have shown that Pue can reduce vascular endothelium injury and the expression of IL-1β, IL-8, ICAM-1, and PAI-1 in the supernatant of human umbilical vein endothelial cells (HUVECs) stimulated with LPS. It can also reduce LPS-induced neutrophil adhesion to HUVECs, inhibiting LPS-induced endothelial injury [35].

Although experimental studies have confirmed that Pue has a significant protective effect on endothelial cells, the specific mechanism remains unclear. In the current study, we investigated whether the inhibitory effect of Pue on LPS-induced endothelial cell inflammation and oxidative stress injury was mediated by mitochondria.

2. Results

2.1. Pue Improved HUVEC Activity in LPS-Induced Inflammation.
A HUVEC inflammatory model was established by stimulating HUVECs with LPS to preliminarily confirm the effect of Pue on the function of HUVECs in an LPS-mediated inflammatory state. Different concentrations of Pue (10 mg/L, 20 mg/L, 50 mg/L, 100 mg/L, and 150 mg/L) were then used as intervention treatments. HUVEC activity was determined using CCK-8 assays. CCK-8 analysis showed that LPS decreased the activity of HUVECs compared with that in the control group, as shown in Figure 1(a). Pretreatment with different Pue concentrations improved HUVEC vitality after LPS treatment, with the cell activity being most significant after pretreatment with 100 mg/L Pue (Figure 1(b)). Accordingly, 100 mg/L Pue was chosen as the optimal drug concentration to treat HUVECs in subsequent experiments. The analysis also showed that LPS increased apoptosis levels of HUVECs, but 100 mg/L Pue inhibited the apoptosis (Figures 1(c) and 1(d)). These results indicated that Pue maintained the activity of HUVECs and inhibited cell apoptosis under an LPS-induced inflammatory state.

2.2. Pue Inhibited LPS-Induced Inflammatory Responses and Oxidative Stress Damage in HUVECs.
We found that Pue could also reduce LPS-induced inflammatory injury. Compared with that in the control group, the LPS-induced expression of inflammatory factors, TNF-α, and IL-18 was significantly increased in HUVECs treated with LPS (Figures 2(b) and 2(c)). Furthermore, the expression level of the anti-inflammatory factor IL-10 was significantly reduced (Figure 2(a)). Pretreatment of HUVECs with Pue reversed the LPS-induced increase in TNF-α/IL-18 levels

(a)

(b)

(c)

(d)
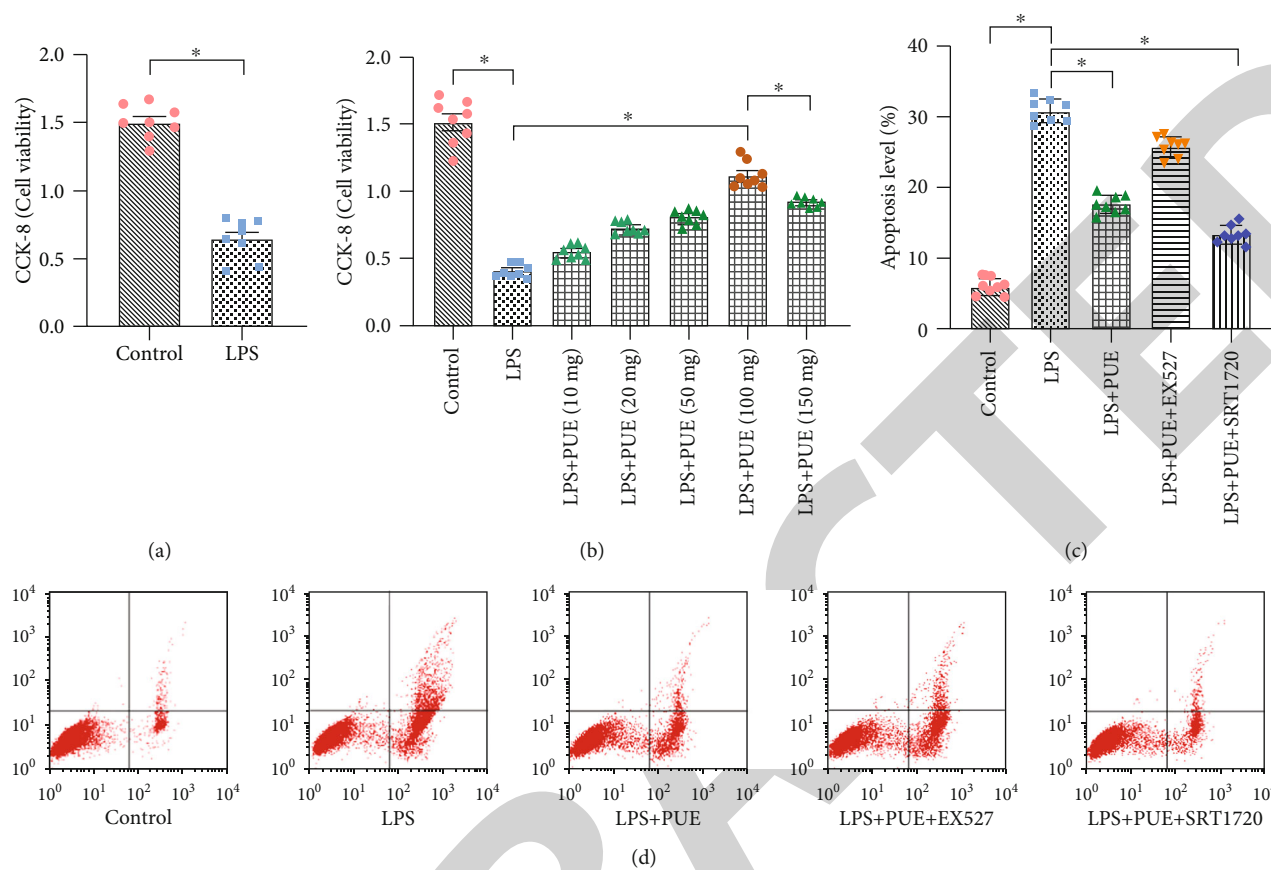
Figure 1: Pue improves the activity of human umbilical vein endothelial cells (HUVECs) under LPS-induced inflammation. (a) Cell viability in an LPS-induced inflammatory state was determined using the CCK-8 method. After LPS stimulation, HUVEC viability was severely reduced. (b) HUVEC treatment with Pue at different concentrations (10, 20, 50, 100, and 150 mg/L). HUVEC viability under different drug concentrations was determined using the CCK-8 method. (c, d) HUVEC apoptosis level was analyzed before and after Pue administration. $^*p < 0.05$.

and downregulation of the IL-10 expression (Figure 2(a)–2(c)). The results confirmed that Pue intervention could improve the HUVEC inflammatory response induced by LPS.

We further investigated the protective mechanism of Pue in improving the vitality and reducing the vulnerability of HUVECs under LPS-induced inflammation. To explore the protective effect of Pue on the redox state of endothelial cells and mitochondrial oxidative stress damage, enzyme-linked immunosorbent assays (ELISAs) were used to evaluate the activity of antioxidant enzymes, such as glutathione (GSH), superoxide dismutase (SOD), and glutathione peroxidase (GPx). We found that the inflammatory state induced by LPS exhibited reduced GSH, SOD, and GPx activity in HUVECs (Figures 3(d)–3(f)). Pretreatment of the cells with Pue resulted in increased GSH, SOD, and GPx activity (Figures 3(d)–3(f)). These results suggested that LPS-induced inflammation could induce oxidative stress damage by inhibiting the activity of antioxidant enzymes, including GSH, SOD, and GPx. However, Pue was able to reverse this phenomenon, which further confirmed the pharmacological activity of Pue against oxidative stress.

2.3. Pue Regulated HUVEC MQC under LPS-Induced Inflammation. Mitochondria are the main sites of ATP production that are required for cellular energy metabolism. Studies have demonstrated that LPS-induced inflammatory responses can cause severe damage to the structure and function of mitochondria [36, 37]. In the current study, we evaluated HUVECs for mitochondrial ROS generation levels and mitochondrial membrane potential (MMP). Compared with those in the control group, the level of mitochondrial ROS generation was increased (Figures 4(a) and 4(f)), and the MMP levels were significantly reduced (Figures 4(d) and 4(e)). Pue treatment of HUVECs resulted in significantly increased MMP levels (Figures 4(d) and 4(e)), while the mitochondrial ROS generation levels were significantly reduced (Figures 4(a) and 4(f)).

Mitochondria are the main sites of oxygen consumption in cells and the main ROS source as well as the main target of ROS attack. Excessive production of mitochondrial ROS results in the release of proinflammatory factors IL-18 and TNF-α and directly affects mitochondrial structure and function [38–40]. LPS-induced HUVEC inflammatory responses and oxidative stress damage changed the structure and function of mitochondria compared with those in the control and
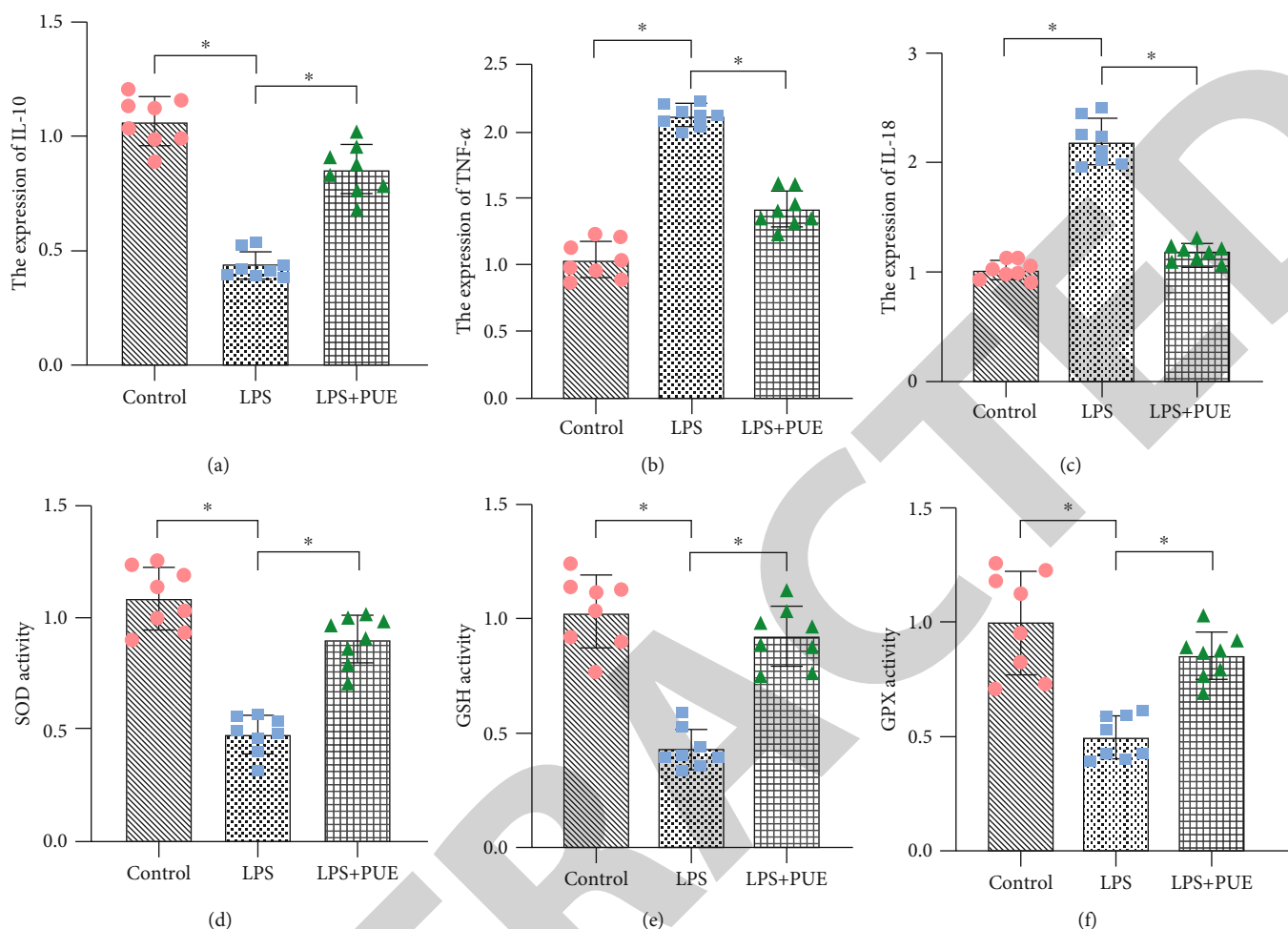
FIGURE 2: Pue inhibits LPS-induced inflammatory responses and oxidative stress damage in human umbilical vein endothelial cells (HUVECs). (a–f) Proinflammatory and anti-inflammatory factors and antioxidant enzymes were evaluated using ELISA. $^*p < 0.05$.

destroyed the MMP. However, Pue intervention significantly increased the activity and number of mitochondria, restored the MMP, and inhibited mitochondrial ROS generation. We also evaluated mitochondrial respiratory complexes I and III activity by ELISA (Figures 4(b) and 4(c)). Mitochondrial respiratory complexes I and III showed reduced expression under LPS-induced inflammatory injury, but their activities were restored with Pue intervention.

2.4. Pue Promoted HUVEC Mitochondrial Energy Metabolism under LPS-Induced Inflammation. Abnormal mitochondrial energy metabolism and respiratory function are closely related to mitochondrial dysfunction [41–43]. In the current study, we investigated whether Pue under inflammatory conditions could improve mitochondrial energy metabolism levels and respiratory function in HUVECs using a mitochondrial energy metabolism test. Compared with those from the control group, HUVECs treated with LPS exhibited significant reduction in mitochondrial respiration levels (Figure 4(a)), maximum respiration capacities (Figure 4(b)), spare respiratory capacities (Figure 4(c)), and ATP production capacities (Figure 4(d)); nonmitochondrial oxygen respiration level (Figure 4(e)) and proton leakage

(Figure 4(f)) increased significantly. However, Pue pretreatment reversed all these reductions, resulting in significant increases in the level of mitochondrial energy metabolism and respiratory function (Figures 4(a)–4(d)), the level of nonmitochondrial oxygen respiration (Figure 4(e)), and proton leakage values (Figure 4(f)) was inhibited.

To investigate how Pue improved the mitochondrial respiratory function of HUVECs in an inflammatory state, EX-527 was used, which is an effective and specific inhibitor of sirtuin-1 (SIRT-1). The results showed that mitochondrial respiratory function of HUVECs was significantly inhibited in the EX-527 + LPS + Pue group compared to that in the LPS + Pue group (Figures 4(a)–4(f)). This demonstrated that the effect of Pue on improving mitochondrial respiratory function was eliminated by the SIRT-1 inhibitor EX-527. Pue was able to improve mitochondrial respiratory function of LPS-treated HUVECs and protect the mitochondria and HUVECs. According to the results, the protective mechanism of Pue may have been mediated through SIRT-1.

2.5. Pue Regulated HUVEC Autophagy in an Inflammatory State through Sirt-1. The protective mechanism of Pue against oxidative stress injury and mitochondrial function

(a) (b) (c) (d)

(e)

(f)
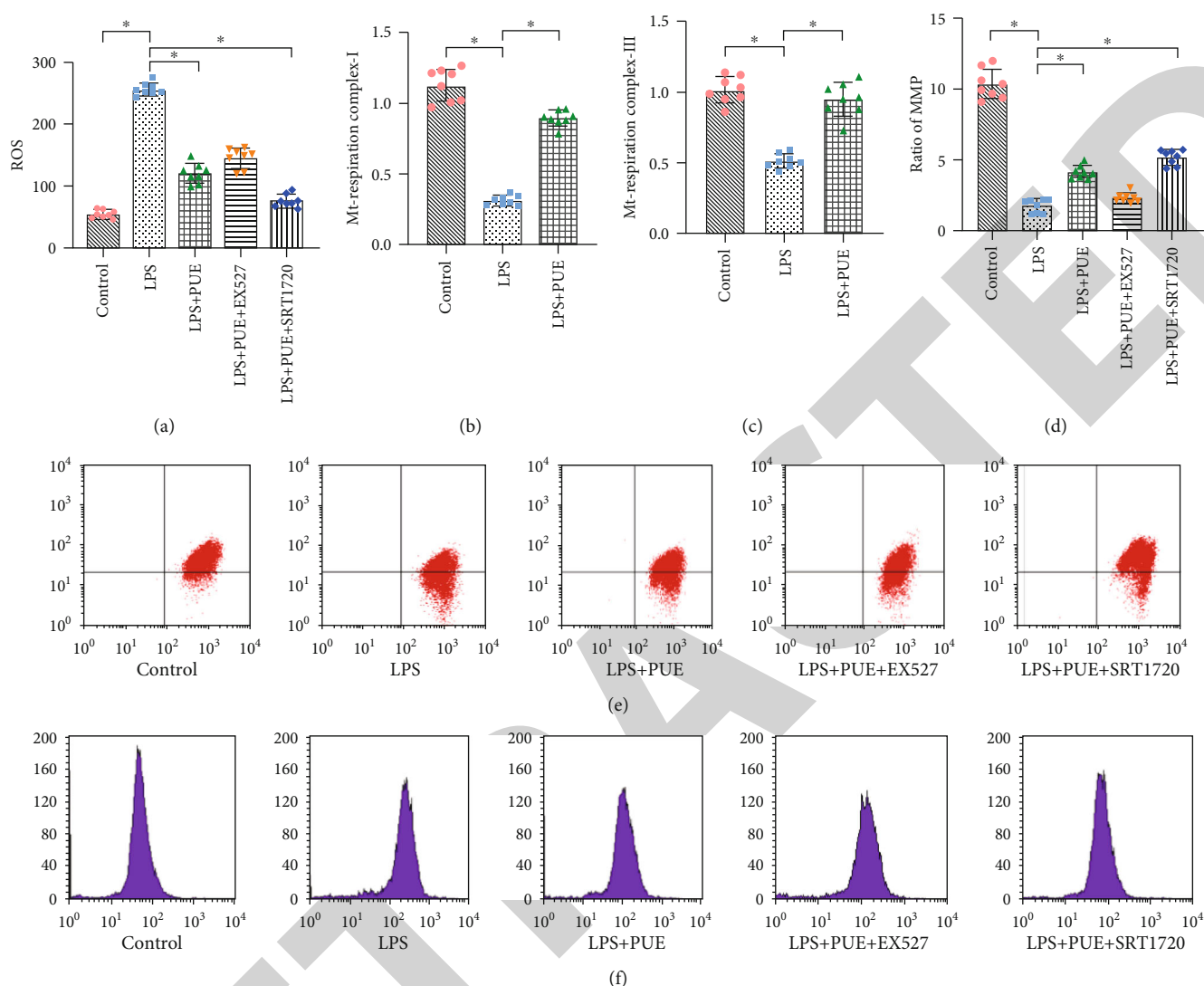
FIGURE 3: Pue improves mitochondrial activity under LPS-induced inflammation and oxidative stress damage. (a, f) HUVEC mitochondrial ROS expression. (d, e) Detection of mitochondrial membrane potential. (b, c) ELISA detection of mitochondrial respiratory complex I and III activity. $^*p < 0.05$.

damage in HUVECs was further explored. Expression levels of select mRNAs were detected by real-time quantitative polymerase chain reaction (qPCR). The qPCR analysis showed that the mRNA levels of atg3, atg7, sirt-1, and PINK1/parkin were significantly lower in the LPS group compared to those in the control group, but they were significantly higher in Pue + LPS-treated HUVECs (Figures 5(a)–5(e)). The mRNA levels of atg5, atg7, sirt-1, and PINK1/parkin in HUVECs treated with EX-527 + Pue + LPS were also significantly reduced. However, the mRNA levels of atg5, atg7, sirt-1, and parkin were significantly increased in HUVECs treated with the SIRT-1 activator SRT1720 (SRT1720 + Pue + LPS). Transmission electron microscopy showed that LPS treatment significantly inhibited mitochondrial autophagy, and Pue increased the level of mitochondrial autophagy (Figure 5(f)). As shown in Figures 5(g) and 5(h), the protein expression of Sirt-1, LC3-I\II, Beclin-1, and Bcl-2 decreased significantly in the LPS group but increased sig-

nificantly in the LPS + Pue group. However, when ex527 was used, the effect of Pue on autophagy was eliminated. However, srt1720 could restore and improve the autophagy regulation ability of Pue. These results suggested that Pue regulated autophagy through the SIRT-1 signaling pathway.

2.6. Inhibition of the SIRT-1 Signaling Pathway Abolished Pue-Mediated Protection.

To further determine whether Pue could induce mitochondrial and HUVEC protection through the SIRT-1 signaling pathway, we used EX-527 and SRT1720 to intervene in Pue + LPS-treated HUVECs. The specific regulatory mechanism of Pue was verified through evaluation of cell viability, apoptosis levels, antioxidant enzyme activity, anti-inflammatory ability, and mitochondrial function in the various HUVEC groups. As shown in Figure 6(a), CCK-8 revealed that EX-527 treatment significantly reduced the activity of HUVECs treated with Pue + LPS. Besides, EX-527 treatment eliminated the
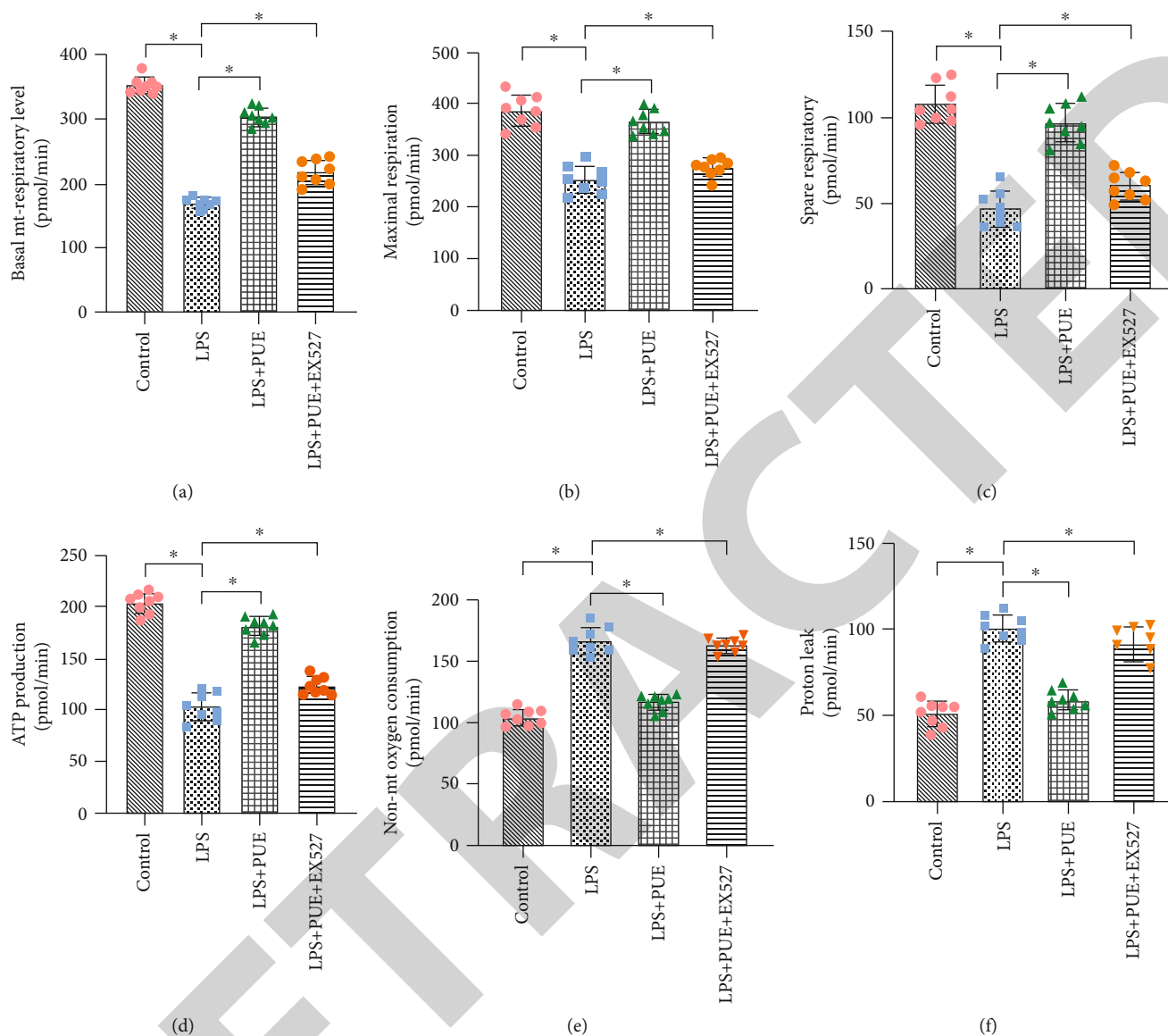
Figure 4: Pue promotes mitochondrial energy metabolism in human umbilical vein endothelial cells (HUVECs) induced with LPS: (a) basic mitochondrial respiratory level; (b) maximum respiratory capacity; (c) spare respiratory capacity; (d) ATP production capacity; (e) nonmitochondrial oxygen respiration; (f) proton leakage level. $^*p < 0.05$.

protective effect of Pue on the mitochondria of HUVECs treated with LPS as well as the inhibitory effect of Pue on the inflammatory response and oxidative stress injury (Figures 6(b)–6(j)). Meanwhile, SRT1720 eliminated the ability of Pue to regulate the inflammatory reaction and oxidative stress injury of HUVECs (Figures 6(b)–6(j)). Laser scanning confocal images of myosin-VI also showed that the expression of myosin-VI was rapidly decreased and increased by LPS and Pue, respectively; EX-527 can eliminate the regulatory effect of Pue, and SRT1720 can further restore the regulatory effect of Pue (Figure 6(k)). These results confirmed that Pue improved the mitochondrial activity of HUVECs and inhibited LPS-induced inflammatory responses and oxidative stress injury through SIRT-1.

3. Discussion

Inflammation and oxidative stress are the main risk factors of cardiovascular damage in patients with AS. Pue, a natural antioxidant, can play a key role in regulating inflammatory responses and oxidative stress injury. However, few studies are aimed at revealing the underlying mechanism by which Pue reduces endothelial cell vulnerability to inflammatory conditions. In the current study, we found that an LPS-induced inflammatory response in HUVECs led to increase ROS production in mitochondria and greater MQC disorder and aggravated the damage caused by oxidative stress. Pue regulates MQC, enhances mitochondrial autophagy, and inhibits LPS-induced inflammation and oxidative stress injury in HUVECs. Pue also increased the MMP and energy

(a)

(b)

(c)

(d)

(e)

(f)

Figure 5: Continued.

(g)

(h)
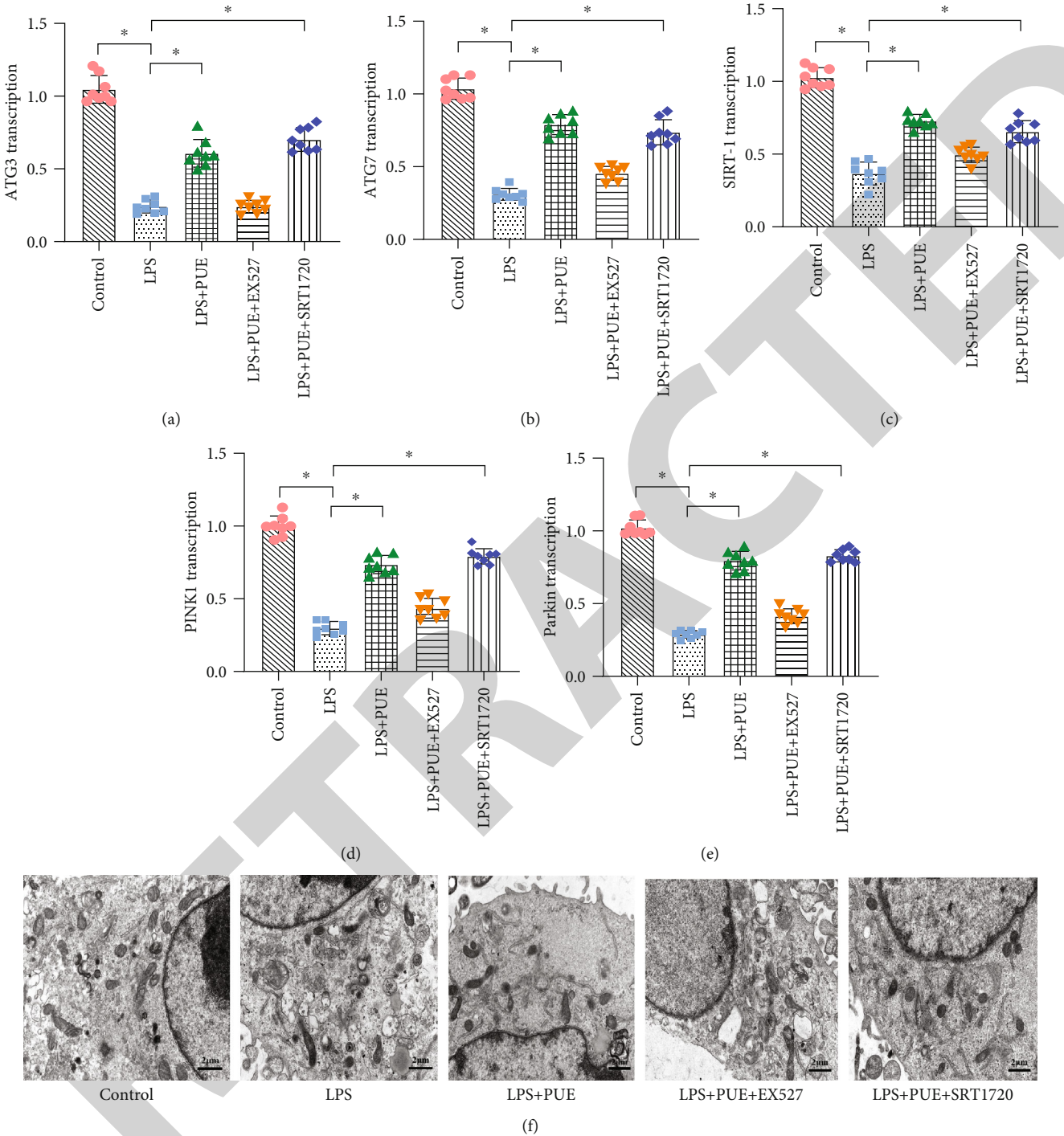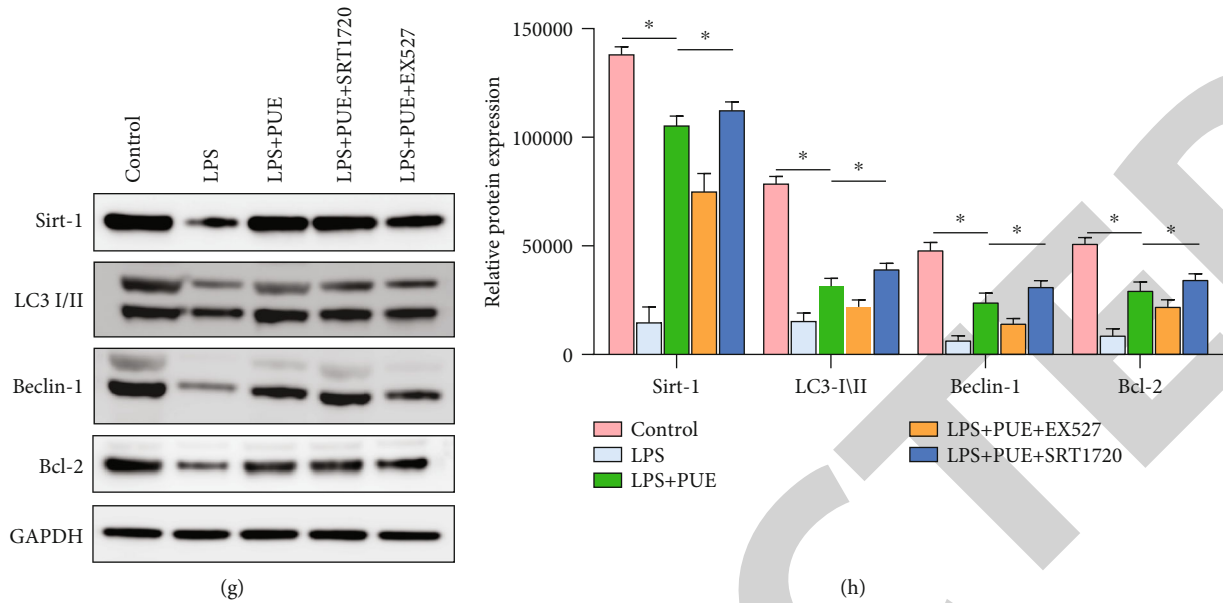
FIGURE 5: Mechanism of Pue in regulating mitochondrial autophagy through SIRT-1. (a–e) Changes in transcription of atg3, atg7, sirt-1, and PINK1/parkin were determined by qPCR. $^*p < 0.05$. (f) Mitochondrial autophagy was observed with transmission electron microscopy. (g, h) Protein expression of Sirt-1, LC3-I\II, Beclin-1, and Bcl-2 was measured using western blotting. $^*p < 0.05$.

metabolism of the HUVECs, increased the activity of SOD and other antioxidant kinases, inhibited the excessive ROS production and inflammation-induced oxidative stress damage, weakened the LPS-induced inflammatory response, and reduced HUVEC vulnerability to the inflammatory state.

Furthermore, it was found that intervention with EX-527, a selective SIRT-1 inhibitor, counteracted Pue regulation of MQC and the protective effect of Pue on HUVECs. However, intervention with the SIRT-1 activator SRT1720 restored the protective effect of Pue to normal or even higher than normal levels. Accordingly, we conclude that Pue protected HUVECs from inflammation through SIRT-1. These results indicate that Pue, as a natural antioxidant, regulated MQC through the SIRT-1 signaling pathway and reduced the vulnerability of HUVECs to the inflammatory state.

Damage to endothelial cells due to changes in membrane structure leads to the production of antiarterial antibodies and the activation of the complement system, which aggravates vascular endothelial damage and promotes AS development [44]. Cytokinins, inflammatory factors, and mitochondrial dysfunction in the environment can all regulate the activity and function of endothelial cells by changing the extracellular concentration of oxidative stress products [45, 46]. A large number of aging vascular endothelial cells are present in advanced arterial plaques. In cell aging, mitochondria dysfunction intensifies, and the level of intracellular ROS significantly increases. The abnormally elevated ROS in the cell further induces vascular damage during cell aging and aggravates lesions [47].

In the current study, we found that markers related to oxidative stress were significantly upregulated in HUVECs treated with LPS, while the expression of mitophagy-related genes and antioxidant stress kinases was significantly downregulated. This indicated that inflammation could increase oxidative stress injury and inhibit mitophagy. Under oxida-

tive stress injury, mitochondrial folding of proteins and useless organelles could not be cleared in a timely manner because mitophagy was inhibited, and the normal level of energy metabolism and respiratory chain function of the mitochondria may have been disrupted, resulting in a rapid decrease of mitochondrial activity and MQC disorder. MQC is an important mechanism for eukaryotes to maintain a relatively stable number and function of mitochondria [48]. MQC ensures the normal operation of the mitochondrial network, further regulates the timely updating of mitochondria, and maintains the relative stability of the quantity and quality of mitochondria in endothelial cells, or it may participate in the occurrence and development of AS [49, 50].

The distribution of mitochondria in endothelial cells can also affect cell signal transduction. Under physiological conditions, endothelial cell mitochondrial dynamics are in a state of stable dynamic equilibrium [51, 52]. Inflammation-induced perinuclear aggregation of mitochondria can lead to mitochondrial ROS accumulation and affect the transcription level of the vascular endothelial growth factor gene [49]. Main functions of mitochondria in endothelial cells are transmitting cell response to environmental signals and participating in the protective mechanism of endothelial cells under oxidative stress and inflammation [53–55].

Many natural products of plants can protect endothelial cells by regulating mitochondrial function and reducing endothelial cell vulnerability under stress [56, 57]. Our study directly confirmed the protective mechanism of natural antioxidants on endothelial cells through MQC. We also found that Pue could regulate the mitophagy of endothelial cells and maintain normal cell activity. Autophagy/mitophagy not only controls the homeostasis of blood vessels but also functions in mitochondria energy metabolism and the mitochondrial antioxidant system to maintain the basic physiological functions of mitochondria [56, 57]. Further research

Figure 6: Continued.

(i)

(j)

(k)
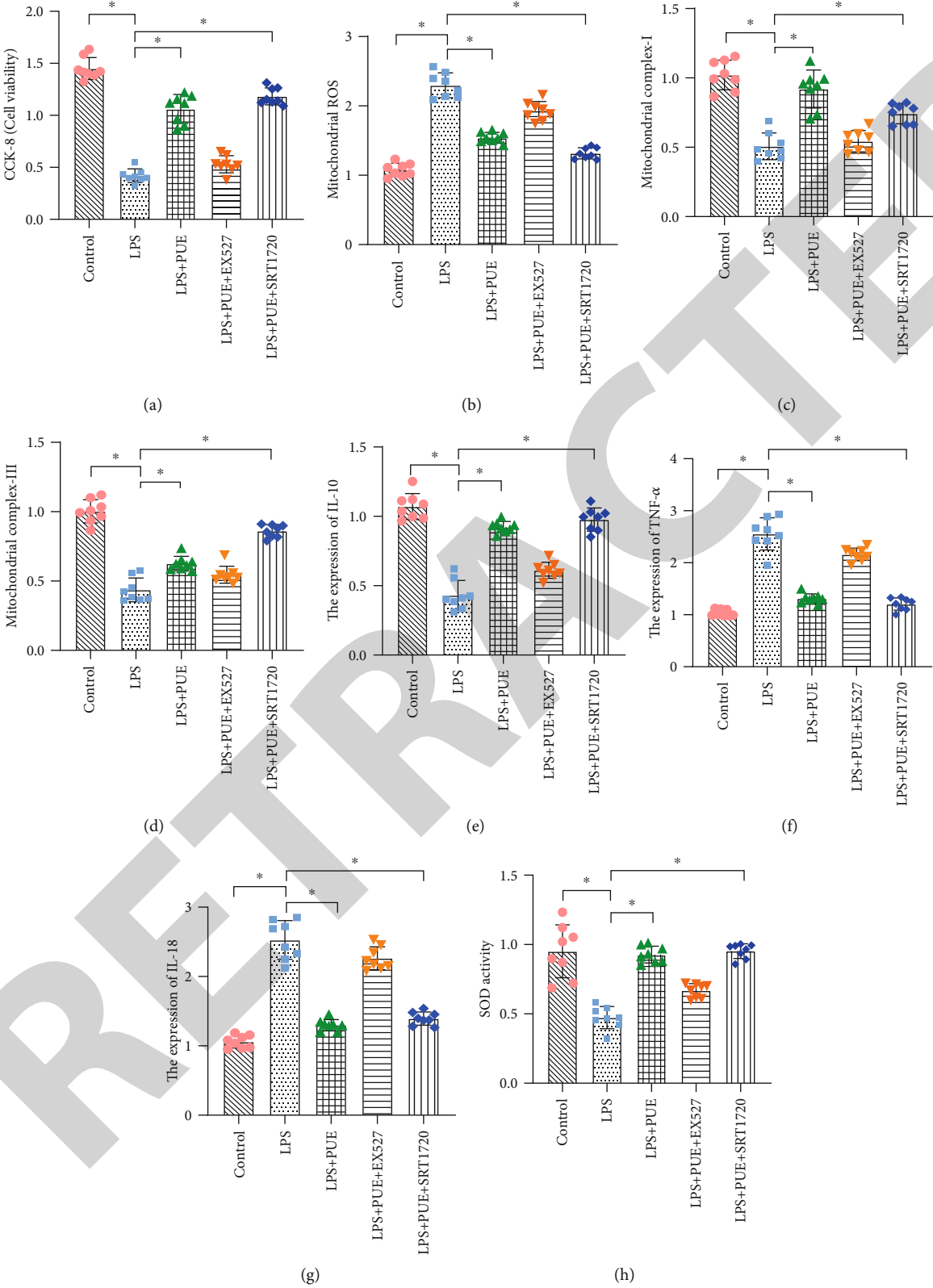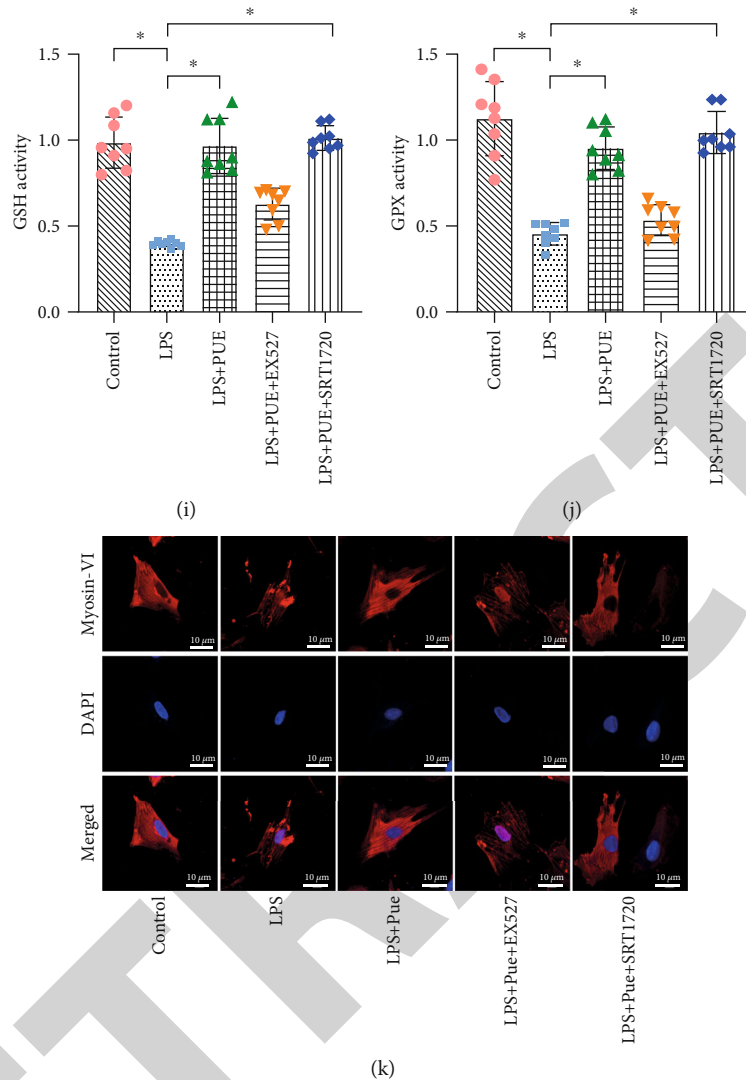
Figure 6: Inhibition of the SIRT-1 signaling pathway abolishes Pue-mediated protection. (a) CCK-8 analysis in different groups of human umbilical vein endothelial cells (HUVECs). (b–j) Enzyme-linked immunosorbent assays (ELISAs) showed antioxidant enzyme activities and anti-inflammatory factors in the different groups. (k) Laser confocal scanning was used to observe the alterations of myosin-VI in endothelial cells under Pue treatment. $^*p < 0.05$.

is needed to determine the mechanistic interaction between autophagy/mitophagy and oxidative stress in the inflammatory state. Furthermore, the mechanism by which Pue affects mitochondrial quality by regulating autophagy levels remains unclear.

SIRT-1 is a highly conserved NAD^+-dependent histone deacetylase. In recent years, SIRT-1 has been shown to play important roles in many biological processes, including cell differentiation, aging, apoptosis, physiological rhythm, metabolic regulation, transcription regulation, signal transduction, and oxidative stress [58, 59]. SIRT-1 exists in the nucleus and is highly expressed in vascular endothelial cells. Moreover, the serum SIRT-1 level in patients with cardiovascular disease is significantly higher than that in healthy individuals [60, 61]. EX-527 is an effective selective inhibitor of SIRT-1 and is often used to block the regulation of SIRT-1. We found in the current study that EX-527 could counteract the protective effect of Pue in HUVECs. However, on inter-

vention with SRT1720, the protective effect of Pue on HUVECs was restored, as along with its regulatory effect on MQC. These results indirectly confirmed that Pue regulated autophagy in HUVECs through SIRT-1 and may further protect HUVECs from inflammatory responses and oxidative stress injury. However, animal studies will be needed to confirm whether Pue directly affects blood flow and AS by regulating MQC and endothelial cells through SIRT-1.

In conclusion, we found that cell viability and MQC of HUVECs were regulated through the SIRT-1 signaling pathway. LPS treatment reduced SIRT-1 signaling and induced oxidative stress injury and apoptosis. Pue was able to regulate MQC by upregulating SIRT-1 signaling, improving the level of autophagy in HUVECs, and further reducing the vulnerability and oxidative stress injury of HUVECs under inflammatory conditions. It should be noted that this study examined only whether Pue improves oxidative stress injury of HUVECs by regulating MQC in an inflammatory state.

The results do not imply Pue can also exert the same protective effect on HUVECs under other stress conditions (such as high glucose and hypoxia).

Notwithstanding this limitation, hypoxia and high glucose stress are related to oxidative stress and MQC disorder. This study characterized Pue as a natural antioxidant; further clinical and basic studies will confirm the regulatory mechanism of Pue on MQC and oxidative stress. In the future, Pue may be developed as a candidate drug for the clinical treatment of AS. We expect Pue to become a treatment strategy potentially widely used to treat a variety of cardiovascular diseases.

4. Materials and Methods

4.1. Cell Culture and Treatment. HUVECs were purchased from the Institute of Basic Medicine, Chinese Academy of Medical Sciences (Beijing, China). LPS was acquired from Sigma-Aldrich (St. Louis, MO, USA). SRT1720 and EX-527 were purchased from MedChemExpress (Princeton, NJ, USA). Pue (purity ≥ 98%) was purchased from the Chinese Medicine Resource Center, Chinese Academy of Traditional Chinese Medicine (Beijing, China).

The cells were cultured in Dulbecco's modified Eagle's medium (DMEM, Gibco, Carlsbad, USA) containing 10% fetal bovine serum (Gibco) and $100 \mu g/mL$ penicillin-streptomycin (Gibco). Cells were passaged using trypsin-EDTA (Gibco). The cells were incubated at 37°C, 95% humidity, and 5% CO_2. The medium was renewed every 2 days. HUVECs were used up to passage five [62]. The HUVECs were activated with $10 \mu g/mL$ LPS for 24 h [63] and pretreated with 10, 20, 50, 100, or 150 mg/L Pue for 24 h before LPS induction. As indicated, HUVECs were incubated with EX-527 (MedChemExpress) for 6 h to inhibit SIRT-1 activity or with SRT1720 (MedChemExpress) for 6 h to activate SIRT-1.

4.2. CCK-8 Assays. HUVECs were determined to be in good condition, with a total cell coverage rate of more than 90%. The cells were washed with phosphate-buffered saline (PBS, Gibco) and then digested with trypsin. The digestion was terminated by adding fresh complete DMEM, and the cells were then counted. The cells were seeded into 12-well plates (50,000 cells/well) and incubated for 12 h. The medium was discarded, the cells were rinsed twice with PBS, and the adherent cells were then observed under an inverted microscope (Olympus, Tokyo, Japan). Cellular metabolic activity as an indicator of cell viability was measured by the CCK-8 essay.

4.3. Mitochondrial Membrane Potential (MMP). MMP of the HUVECs was measured using JC-1 Dye (MedChemExpress). HUVECs were washed three times with PBS and then stained with JC-1 Dye for 30 min in a dark room. The HUVECs were then washed three times with PBS, and the mitochondrial membrane potential images were captured using a Nikon A1 laser confocal microscope (Nikon, Chiyoda, Japan).

4.4. Laser Confocal Microscopy. HUVECs were fixed with 4% paraformaldehyde for 10 min, washed with PBS three times, and blocked on ice with PBS for 30 min. The HUVECs were then incubated with primary antibody (myosin-VI, Abcam, Cambridge, UK) against Tom20 at 4°C overnight. After washing with PBS three times, the cells were stained with Alexa fluor-594-conjugated goat anti-mouse secondary antibody in 1% BSA/PBS at 4°C for 1 h. Nuclei were stained with $4'$,6-diamidino-2-phenylindole (DAPI), and images were captured using a Nikon A1 confocal microscope.

4.5. ELISA Quantitative Analysis. The cells were digested with 0.25% trypsin in PBS according to the manufacturer's instructions. The SOD, GSH, GPx, IL-10, IL-18, and TNF-α contents were detected using a total assay kit.

4.6. Quantitative Real-Time PCR. Total RNA was isolated from HUVECs using a Quick-RNA Microprep Kit (Zymo Research, Irvine, CA, USA). An iScript cDNA Synthesis Kit (Bio-Rad, Hercules, CA, USA) was used to reverse transcribe 150–250 ng total RNA into complementary DNA (cDNA). The cDNA samples were diluted 10-fold with ddH_2O, and real-time quantitative PCR (qPCR) was performed on a LightCycler 480 Instrument using $2 \mu L$ cDNA. Relative gene expression was calculated using the $2^{-\Delta\Delta Ct}$ method [64].

4.7. Cellular Respiration Assays. An XFp Extracellular Flux Analyzer (Seahorse Biosciences, North Billerica, MA, USA) was used according to the manufacturer's instructions to analyze the oxygen consumption rate (OCR) of intact cells in real time. Briefly, HUVECs were inoculated at 5×10^5 cells/well. The results were normalized to the actual cell count determined immediately after obtaining the OCR recording.

4.8. Statistical Analysis. All statistical analyses were performed using the Statistical Product and Service Solutions (SPSS) 22.0 software package (IBM Corp., Armonk, NY, USA) and GraphPad Prism version 7.0 (GraphPad Software, San Diego, CA, USA). All data are expressed as mean ± SEM and were evaluated by analysis of variance; $p < 0.05$ was considered statistically significant. The normal distribution of the data was confirmed by Shapiro–Wilk test.

Data Availability

The data used to support the findings of this study are available from the corresponding author upon request.

Conflicts of Interest

The authors declare that the research was conducted in the absence of any commercial or financial relationships that could be construed as a potential conflict of interest.

Authors' Contributions

CX and WX searched for the related articles. ZT and CX mainly conducted the experimental work. MQY, YPZ, LDZ, and LD collated all the related articles. CX and ZXT wrote the manuscript. All authors commented on the manuscript.

Xingchang and tianzhang is co-first authors, made the same contribution to this article.

Acknowledgments

References

[1] K. Kobiyama and K. Ley, "Atherosclerosis," *Circulation Research*, vol. 123, no. 10, pp. 1118–1120, 2018.

[2] G. Heusch, "Coronary microvascular obstruction: the new frontier in cardioprotection," *Basic Research in Cardiology*, vol. 114, no. 6, p. 45, 2019.

[3] G. K. Hansson, "Inflammation, atherosclerosis, and coronary artery disease," *New England Journal of Medicine*, vol. 352, no. 16, pp. 1685–1695, 2005.

[4] P. Libby, "Inflammation in atherosclerosis," *Nature*, vol. 420, no. 6917, pp. 868–874, 2002.

[5] H. Zhu, Y. Li, M. X. Wang, J. H. Wang, W. X. Du, and F. Zhou, "Analysis of cardiovascular disease-related NF-κB-regulated genes and microRNAs in TNFα-treated primary mouse vascular endothelial cells," *Journal of Zhejiang University-Science B*, vol. 20, no. 10, pp. 803–815, 2019.

[6] H. Haybar, S. Shahrabi, H. Rezaeeyan, R. Shirzad, and N. Saki, "Endothelial cells: from dysfunction mechanism to pharmacological effect in cardiovascular disease," *Cardiovascular Toxicology*, vol. 19, no. 1, pp. 13–22, 2019.

[7] C. Sturtzel, "Endothelial cells," *Advances in Experimental Medicine and Biology*, vol. 1003, pp. 71–91, 2017.

[8] K. D. Falkenberg, K. Rohlenova, Y. Luo, and P. Carmeliet, "The metabolic engine of endothelial cells," *Nature Metabolism*, vol. 1, no. 10, pp. 937–946, 2019.

[9] J. Sabbatinelli, F. Prattichizzo, F. Olivieri, A. D. Procopio, M. R. Rippo, and A. Giuliani, "Where metabolism meets senescence: focus on endothelial cells," *Frontiers in Physiology*, vol. 10, p. 1523, 2019.

[10] D. Wolf and K. Ley, "Immunity and inflammation in atherosclerosis," *Circulation Research*, vol. 124, no. 2, pp. 315–327, 2019.

[11] S. Taleb, "L'inflammation dans l'atherosclerose," *Archives of Cardiovascular Diseases*, vol. 109, no. 12, pp. 708–715, 2016.

[12] J. S. Pober and W. C. Sessa, "Evolving functions of endothelial cells in inflammation," *Nature Reviews Immunology*, vol. 7, no. 10, pp. 803–815, 2007.

[13] W. E. Hughes, A. M. Beyer, and D. D. Gutterman, "Vascular autophagy in health and disease," *Basic Research in Cardiology*, vol. 115, no. 4, p. 41, 2020.

[14] T. Iba and J. H. Levy, "Inflammation and thrombosis: roles of neutrophils, platelets and endothelial cells and their interactions in thrombus formation during sepsis," *Journal of Thrombosis and Haemostasis*, vol. 16, no. 2, pp. 231–241, 2018.

[15] S. Chen, Y. Wang, H. Zhang et al., "The antioxidant MitoQ protects against CSE-induced endothelial barrier injury and inflammation by inhibiting ROS and autophagy in human umbilical vein endothelial cells," *International Journal of Biological Sciences*, vol. 15, no. 7, pp. 1440–1451, 2019.

[16] X. B. Cui, J. N. Luan, K. Dong et al., "Response by Cui et al. to Letter Regarding Article, "RGC-32 (response gene to complement 32) deficiency protects endothelial cells from inflammation and attenuates atherosclerosis"," *Arteriosclerosis, Thrombosis, and Vascular Biology*, vol. 38, no. 6, pp. e97–e98, 2018.

[17] P. Marchio, S. Guerra-Ojeda, J. M. Vila, M. Aldasoro, V. M. Victor, and M. D. Mauricio, "Targeting early atherosclerosis: a focus on oxidative stress and inflammation," *Oxidative Medicine and Cellular Longevity*, vol. 2019, Article ID 8563845, 32 pages, 2019.

[18] T. Yuan, T. Yang, H. Chen et al., "New insights into oxidative stress and inflammation during diabetes mellitus- accelerated atherosclerosis," *Redox Biology*, vol. 20, pp. 247–260, 2019.

[19] V. Lahera, M. Goicoechea, S. G. de Vinuesa et al., "Endothelial dysfunction, oxidative stress and inflammation in atherosclerosis: beneficial effects of statins," *Current Medicinal Chemistry*, vol. 14, no. 2, pp. 243–248, 2007.

[20] M. Manevski, T. Muthumalage, D. Devadoss et al., "Cellular stress responses and dysfunctional mitochondrial-cellular senescence, and therapeutics in chronic respiratory diseases," *Redox Biology*, vol. 33, article 101443, 2020.

[21] A. M. van der Bliek, M. M. Sedensky, and P. G. Morgan, "Cell biology of the mitochondrion," *Genetics*, vol. 207, no. 3, pp. 843–871, 2017.

[22] Y. Qiu, R. Cheng, C. Liang et al., "MicroRNA-20b Promotes Cardiac Hypertrophy by the Inhibition of Mitofusin 2-Mediated Inter-organelle Ca²⁺ Cross-Talk," *Molecular Therapy - Nucleic Acids*, vol. 19, pp. 1343–1356, 2020.

[23] W. Voos, W. Jaworek, A. Wilkening, and M. Bruderek, "Protein quality control at the mitochondrion," *Essays in Biochemistry*, vol. 60, no. 2, pp. 213–225, 2016.

[24] M. Akbari, T. Kirkwood, and V. A. Bohr, "Mitochondria in the signaling pathways that control longevity and health span," *Ageing Research Reviews*, vol. 54, article 100940, 2019.

[25] A. N. Orekhov, A. V. Poznyak, I. A. Sobenin, N. N. Nikifirov, and E. A. Ivanova, "Mitochondrion as a selective target for the treatment of atherosclerosis: role of mitochondrial DNA mutations and defective mitophagy in the pathogenesis of atherosclerosis and chronic inflammation," *Current Neuropharmacology*, vol. 18, no. 11, pp. 1064–1075, 2020.

[26] G. G. Dorighello, B. A. Paim, S. F. Kiihl et al., "Correlation between mitochondrial reactive oxygen and severity of atherosclerosis," *Oxidative Medicine and Cellular Longevity*, vol. 2016, Article ID 7843685, 10 pages, 2016.

[27] P. M. Smith and A. V. Ferguson, "Recent advances in central cardiovascular control: sex, ROS, gas and inflammation," *F1000Research*, vol. 5, 2016.

[28] A. A. Manfredi and P. Rovere-Querini, "The mitochondrion–a Trojan horse that kicks off inflammation?," *New England Journal of Medicine*, vol. 362, no. 22, pp. 2132–2134, 2010.

[29] J. Chen and Z. J. Chen, "PtdIns4P on dispersed _trans_ -Golgi network mediates NLRP3 inflammasome activation," *Nature*, vol. 564, no. 7734, pp. 71–76, 2018.

[30] Z. Zhong, S. Liang, E. Sanchez-Lopez et al., "New mitochondrial DNA synthesis enables NLRP3 inflammasome activation," *Nature*, vol. 560, no. 7717, pp. 198–203, 2018.

[31] L. Zhang, "Pharmacokinetics and drug delivery systems for puerarin, a bioactive flavone from traditional Chinese medicine," *Drug Delivery*, vol. 26, no. 1, pp. 860–869, 2019.

[32] Y. X. Zhou, H. Zhang, and C. Peng, "Puerarin: a review of pharmacological effects," *Phytotherapy Research*, vol. 28, no. 7, pp. 961–975, 2014.

[33] L. Ji, Q. Du, Y. Li, and W. Hu, "Puerarin inhibits the inflammatory response in atherosclerosis _via_ modulation of the NF-κB pathway in a rabbit model," *Pharmacological Reports*, vol. 68, no. 5, pp. 1054–1059, 2016.

[34] Y. Yuan, H. Zhou, Q. Q. Wu et al., "Puerarin attenuates the inflammatory response and apoptosis in LPS-stimulated cardiomyocytes," *Experimental and Therapeutic Medicine*, vol. 11, no. 2, pp. 415–420, 2016.

[35] H. F. Deng, S. Wang, L. Li et al., "Puerarin prevents vascular endothelial injury through suppression of NF-κB activation in LPS-challenged human umbilical vein endothelial cells," *Biomedicine & Pharmacotherapy*, vol. 104, pp. 261–267, 2018.

[36] S. Cao, Q. Zhang, C. Wang et al., "LPS challenge increased intestinal permeability, disrupted mitochondrial function and triggered mitophagy of piglets," *Innate Immunity*, vol. 24, no. 4, pp. 221–230, 2018.

[37] Z. Lv, X. Song, J. Xu et al., "The modulation of Smac/DIABLO on mitochondrial apoptosis induced by LPS in _Crassostrea gigas_," *Fish & Shellfish Immunology*, vol. 84, pp. 587–598, 2019.

[38] D. B. Zorov, M. Juhaszova, and S. J. Sollott, "Mitochondrial reactive oxygen species (ROS) and ROS-induced ROS release," *Physiological Reviews*, vol. 94, no. 3, pp. 909–950, 2014.

[39] Y. M. Kim, S. J. Kim, R. Tatsunami, H. Yamamura, T. Fukai, and M. Ushio-Fukai, "ROS-induced ROS release orchestrated by Nox4, Nox2, and mitochondria in VEGF signaling and angiogenesis," *American Journal of Physiology-Cell Physiology*, vol. 312, no. 6, pp. C749–C764, 2017.

[40] S. I. Zandalinas and R. Mittler, "ROS-induced ROS release in plant and animal cells," *Free Radical Biology and Medicine*, vol. 122, pp. 21–27, 2018.

[41] S. Melser, J. Lavie, and G. Benard, "Mitochondrial degradation and energy metabolism," *Biochimica et Biophysica Acta (BBA)-Molecular Cell Research*, vol. 1853, 10 Pt B, pp. 2812–2821, 2015.

[42] V. W. Dolinsky, L. K. Cole, G. C. Sparagna, and G. M. Hatch, "Cardiac mitochondrial energy metabolism in heart failure: role of cardiolipin and sirtuins," *Biochimica et Biophysica Acta*, vol. 1861, no. 10, pp. 1544–1554, 2016.

[43] Q. G. Karwi, A. R. Jorg, and G. D. Lopaschuk, "Allosteric, transcriptional and post-translational control of mitochondrial energy metabolism," *Biochemical Journal*, vol. 476, no. 12, pp. 1695–1712, 2019.

[44] T. Wang, C. Sun, L. Hu et al., "Sirt6 stabilizes atherosclerosis plaques by promoting macrophage autophagy and reducing contact with endothelial cells," *Biochemistry and Cell Biology*, vol. 98, no. 2, pp. 120–129, 2020.

[45] C. L. Song, J. P. Wang, X. Xue et al., "Effect of circular ANRIL on the inflammatory response of vascular endothelial cells in a rat model of coronary atherosclerosis," *Cellular Physiology and Biochemistry*, vol. 42, no. 3, pp. 1202–1212, 2017.

[46] L. Wang, X. M. Qiu, Q. Hao, and D. J. Li, "Anti-inflammatory effects of a Chinese herbal medicine in atherosclerosis via estrogen receptor _β_ mediating nitric oxide production and NF- _κ_ B suppression in endothelial cells," *Cell Death & Disease*, vol. 4, no. 3, p. e551, 2013.

[47] B. G. Childs, D. J. Baker, T. Wijshake, C. A. Conover, J. Campisi, and J. M. van Deursen, "Senescent intimal foam cells are deleterious at all stages of atherosclerosis," *Science*, vol. 354, no. 6311, pp. 472–477, 2016.

[48] J. Wang, S. Toan, and H. Zhou, "New insights into the role of mitochondria in cardiac microvascular ischemia/reperfusion injury," *Angiogenesis*, vol. 23, no. 3, pp. 299–314, 2020.

[49] H. Zhou and S. Toan, "Pathological roles of mitochondrial oxidative stress and mitochondrial dynamics in cardiac microvascular ischemia/reperfusion injury," *Biomolecules*, vol. 10, no. 1, 2020.

[50] R. Aishwarya, S. Alam, C. S. Abdullah et al., "Pleiotropic effects of mdivi-1 in altering mitochondrial dynamics, respiration, and autophagy in cardiomyocytes," *Redox Biology*, vol. 36, article 101660, 2020.

[51] Q. Wen, T. J. Fan, and C. L. Tian, "Cytotoxicity of atropine to human corneal endothelial cells by inducing mitochondrion-dependent apoptosis," *Experimental Biology and Medicine*, vol. 241, no. 13, pp. 1457–1465, 2016.

[52] W. Zhao, H. Feng, W. Sun, K. Liu, J. J. Lu, and X. Chen, "Tert-butyl hydroperoxide (t-BHP) induced apoptosis and necroptosis in endothelial cells: roles of NOX4 and mitochondrion," *Redox Biology*, vol. 11, pp. 524–534, 2017.

[53] S. M. Davidson, "Endothelial mitochondria and heart disease," *Cardiovascular Research*, vol. 88, no. 1, pp. 58–66, 2010.

[54] X. Tang, Y. X. Luo, H. Z. Chen, and D. P. Liu, "Mitochondria, endothelial cell function, and vascular diseases," *Frontiers in Physiology*, vol. 5, p. 175, 2014.

[55] F. Puhm, T. Afonyushkin, U. Resch et al., "Mitochondria are a subset of extracellular vesicles released by activated monocytes and induce type I IFN and TNF responses in endothelial cells," *Circulation Research*, vol. 125, no. 1, pp. 43–52, 2019.

[56] X. Chang, T. Zhang, W. Zhang, Z. Zhao, and J. Sun, "Natural drugs as a treatment strategy for cardiovascular disease through the regulation of oxidative stress," *Oxidative Medicine and Cellular Longevity*, vol. 2020, Article ID 5430407, 20 pages, 2020.

[57] N. Song, L. Jia, H. Cao et al., "Gypenoside inhibits endothelial cell apoptosis in atherosclerosis by modulating mitochondria through PI3K/Akt/Bad pathway," *Biomed Research International*, vol. 2020, Article ID 2819658, 12 pages, 2020.

[58] M. Savran, H. Asci, O. Ozmen et al., "Melatonin protects the heart and endothelium against high fructose corn syrup consumption-induced cardiovascular toxicity via SIRT-1 signaling," *Human & Experimental Toxicology*, vol. 38, no. 10, pp. 1212–1223, 2019.

[59] A. H. Yamac, M. A. Huyut, E. Yilmaz et al., "MicroRNA 199a is downregulated in patients after coronary artery bypass graft surgery and is associated with increased levels of sirtuin 1 (SIRT 1) protein and major adverse cardiovascular events at 3-year follow-up," *Medical Science Monitor*, vol. 24, pp. 6245–6254, 2018.

[60] B. Sosnowska, M. Mazidi, P. Penson, A. Gluba-Brzozka, J. Rysz, and M. Banach, "The sirtuin family members SIRT1, SIRT3 and SIRT6: their role in vascular biology and atherogenesis," *Atherosclerosis*, vol. 265, pp. 275–282, 2017.

[61] U. Kilic, O. Gok, A. Bacaksiz, M. Izmirli, B. Elibol-Can, and O. Uysal, "SIRT1 gene polymorphisms affect the protein expression in cardiovascular diseases," *PLoS One*, vol. 9, no. 2, article e90428, 2014.

[62] C. Li, Y. Tan, J. Wu et al., "Resveratrol improves Bnip3-related mitophagy and attenuates high-fat-induced endothelial dysfunction," *Frontiers in Cell and Developmental Biology*, vol. 8, p. 796, 2020.

Retraction

Retracted: Involvement of Mitochondrial Dynamics and Mitophagy in Sevoflurane-Induced Cell Toxicity

Oxidative Medicine and Cellular Longevity

This article has been retracted by Hindawi following an investigation undertaken by the publisher [1]. This investigation has uncovered evidence of one or more of the following indicators of systematic manipulation of the publication process:

(1) Discrepancies in scope

(2) Discrepancies in the description of the research reported

(3) Discrepancies between the availability of data and the research described

(4) Inappropriate citations

(5) Incoherent, meaningless and/or irrelevant content included in the article

(6) Peer-review manipulation

The presence of these indicators undermines our confidence in the integrity of the article's content and we cannot, therefore, vouch for its reliability. Please note that this notice is intended solely to alert readers that the content of this article is unreliable. We have not investigated whether authors were aware of or involved in the systematic manipulation of the publication process.

Wiley and Hindawi regrets that the usual quality checks did not identify these issues before publication and have since put additional measures in place to safeguard research integrity.

We wish to credit our own Research Integrity and Research Publishing teams and anonymous and named external researchers and research integrity experts for contributing to this investigation.

The corresponding author, as the representative of all authors, has been given the opportunity to register their agreement or disagreement to this retraction. We have kept a record of any response received.

References

[1] M. Li, J. Guo, H. Wang, and Y. Li, "Involvement of Mitochondrial Dynamics and Mitophagy in Sevoflurane-Induced Cell Toxicity," *Oxidative Medicine and Cellular Longevity*, vol. 2021, Article ID 6685468, 7 pages, 2021.

Review Article

Involvement of Mitochondrial Dynamics and Mitophagy in Sevoflurane-Induced Cell Toxicity

Ming Li [ID],[1] **Jiguang Guo** [ID],[1] **Hongjie Wang** [ID],[1,2] **and Yuzhen Li** [ID][3]

[1]*School of Basic Medical Sciences, Hebei University, Baoding, Hebei Province, China*
[2]*Affiliated Hospital of Hebei University, Baoding, Hebei Province, China*
[3]*Department of Pathophysiology, Graduate School of PLA General Hospital, Beijing, China*

Correspondence should be addressed to Hongjie Wang; hongjiew68@126.com and Yuzhen Li; yuzlif96@163.com

General anesthesia is a powerful and indispensable tool to ensure the accomplishment of surgical procedures or clinical examinations. Sevoflurane as an inhalational anesthetic without unpleasant odor is commonly used in clinical practice, especially for pediatric surgery. However, the toxicity caused by sevoflurane has gained growing attention. Mitochondria play a key role in maintaining cellular metabolism and survival. To maintain the stability of mitochondrial homeostasis, they are constantly going through fusion and fission. Also, damaged mitochondria need to be degraded by autophagy, termed as mitophagy. Accumulating evidence proves that sevoflurane exposure in young age could lead to cell toxicity by triggering the mitochondrial pathway of apoptosis, inducing the abnormalities of mitochondrial dynamics and mitophagy. In the present review, we focus on the current understanding of mitochondrial apoptosis, dynamics and mitophagy in cell function, the implications for cell toxicity in response to sevoflurane, and their underlying potential mechanisms.

1. Introduction

Sevoflurane is one of the most commonly used inhaled anesthetics in clinical practice for nearly 30 years [1]. It has a quick onset of action and short recovery time from anesthesia. And sevoflurane could keep hemodynamics stable. In addition, the inhalation of sevoflurane shows little irritation to the respiratory tract with a special aromatic odor. Its coefficient of blood: gas partition is only 0.69 [2, 3]. Therefore, sevoflurane has been widely administered in pediatric surgeries to maintain the general anesthesia. However, in recent years, the researches based on clinical trials and laboratory experiments have indicated that general anesthesia by inhalation of sevoflurane for children could trigger irreversible neural damage [4–6].

Mitochondria which are semiautonomous and double-membrane organelles provide the most proportion of energy for cell living through citric acid cycle and oxidative phosphorylation. Neural cells are enriched with mitochondria. Neural cells require to consume a lot of energy in order to maintain their normal functions [7]. Therefore, it is no doubt

that mitochondrial abnormality inevitably leads to neural dysfunction. It has been demonstrated that mitochondria are the targets of sevoflurane-induced neural toxicity [8, 9]. Sevoflurane exposure induces neural toxicity by initiating mitochondrial apoptotic pathway, disturbing the balance of mitochondrial dynamics and mitophagy. This review summarizes the recent advances in our understanding of mitochondrial abnormalities in neural injury upon sevoflurane and its molecular mechanism.

2. Apoptosis in Neural Cells by Sevoflurane through Mitochondrial Pathway

2.1. Mitochondrial Pathway of Apoptosis. The mitochondrial pathway of apoptosis, also called the intrinsic apoptotic pathway, is mainly regulated by the B cell lymphoma 2 (Bcl-2) protein family [10]. The Bcl-2 family is divided into three functional groups. Antiapoptotic Bcl-2 proteins include Bcl-2, Bcl-x$_L$, Bcl-w, Mcl-1, and A1/Bfl-1 [11]. They are critical for cell survival [12]. The proapoptotic members are divided into two classes. The effector molecules Bax and Bak are

required for mitochondrial outer membrane permeabilisation (MOMP) [13]. The BH3-only proteins consist of Bim, Bid, Puma, Bmf, Bik, Bad, Noxa, and Hrk [14, 15]. They initiate apoptosis by activation of Bax and Bak, either inhibiting the prosurvival Bcl-2 family proteins [16]. The electron transport chain of the mitochondria having three complexes: complexes I, III, and IV, could function as proton pumps to produce an electrochemical potential of approximately around -150 mV across the inner membrane of mitochondria [17]. This is the formation of mitochondrial membrane potential (MMP) which is treated as the core indicator of the mitochondrial fundamental function [18]. The energy stored in the MMP is used to synthesize ATP and to maintain the different Ca^{2+} concentration across the mitochondrial matrix and the cytosol [17, 19, 20]. Various apoptotic stimuli activate Bak and Bax. The activation of Bak and Bax induces the opening of mitochondrial permeability transition pore (mPTP), subsequently increasing MOMP [21–23]. The increase of MOMP leads to the release of cytochrome c from the mitochondria into the cytoplasm. In the cytosol, cytochrome c interacts with apoptotic protease activation factor 1, which binds to and activates caspase 9 and, in turn, its downstream caspase 3, resulting in apoptosis [10, 24].

2.2. *Sevoflurane Activates Mitochondrial Pathway of Apoptosis to Induce Neural Cell Injury.* It has been demonstrated that sevoflurane could induce neural cell apoptosis by the activation of mitochondrial pathway [25–34]. The sevoflurane treatment downregulates the expression of Bcl-2 and upregulates the expression of Bax, thereby inducing the loss of MMP, stimulating the release of cytochrome c from mitochondria and the activation of caspase 3. Inevitably, neuroapoptosis occurs through the mitochondrial pathway of apoptosis. As early as 2001, Kudo and his colleagues first observed that high concentration of inhaled anesthetic decreased MMP and increased the release of lactate dehydrogenase release (LDH) causing irreversible damage to the cocultured primary neuronal-glial cells [35]. Later, Moe et al. showed that 1 or 2 minimum alveolar concentration (MAC) of sevoflurane similarly with the concentrations used in clinic gradually depolarized the isolated rat presynaptic MMP [36–38]. This depolarization was only partly blocked by the ATP-sensitive potassium channel inhibitor 5-hydroxydecanoate but enhanced when the complex IV of the mitochondrial electron transport chain was inhibited, indicating that the sevoflurane-induced depolarization might be related to ATP synthase reversal [36, 37]. Furthermore, the same results are also obtained in the isolated synaptosomes from human temporal lobe tissue [38]. Exposure of mouse cerebral cortex in the postnatal day (P) P6, P7, and P8 to sevoflurane for 2 hours causes cognitive deficiency, decrease of MMP, and ATP concentration [39]. Sevoflurane inhibits the respiration of mitochondria in human neuroglioma cells [40]. And the mitochondrial respiratory function of neonatal mice is more severely suppressed by sevoflurane to compare with the old one [41].

The increase of reactive oxygen species (ROS) level is observed by most of the experiments as a result of MMP decrease and the inhibition of mitochondrial respiratory

[31–33, 39, 40, 42]. Moe et al. first reported that sevoflurane treatment slowly increased the synaptosomal Ca^{2+} level [36]. Following researchers proved that sevoflurane treatment would induce an increment of cytosolic Ca^{2+} in cultured pheochromocytoma neurosecretory cells and rat hippocampal neurons [33, 40]. Some think that the increased Ca^{2+} is from the endoplasmic reticulum (ER), for the Ca^{2+} level in ER is decreased following the sevoflurane treatment [43]. And the others believe the increased Ca^{2+} is from the membrane Ca^{2+} channel, since nimodipine can block the increase of Ca^{2+} and the dysfunction of mitochondria [33]. The increase of intracellular calcium flux and ROS level could stimulate the opening of mPTP, decrease MMP, and suppress ATP synthesis, subsequently leading to neuroapoptosis by the mitochondrial pathway [33, 44].

3. The Involvement of Mitochondrial Dynamics Imbalance in Neural Injury by Sevoflurane

3.1. *Mitochondrial Dynamics and Neural Cell Function.* Mitochondria are prominently dynamic organelles that are continuously going fusion and fission, known as mitochondrial dynamics [45]. The process of constantly reshaping mitochondria allows them properly in response to the ceaseless change of cellular physiological state [46]. Fused mitochondria are able to promote energy delivery from the cell periphery to the cell core, and fragmented mitochondria can be trafficked to energy-demanding regions of the cell [47, 48]. Proper distribution of fused and fragmented mitochondria is extremely important for the maintenance of synapses and dendritic spines as they are far from the cell body [49]. And according to the energy requirements and metabolic conditions of neural cells, mitochondria can constantly adjust their morphology and distribution through fusion and fission to meet neural functional demands [50]. Thus, the imbalance of mitochondrial fusion and fission inevitably leads to neural dysfunction [50]. It has been proved that mitochondrial fission is mainly regulated by dynamin-related protein 1 (Drp1) and fission, mitochondrial 1 (Fis1) [51, 52]. Drp1 is mainly localized in the cytosol, and Fis1 is anchored in the mitochondrial outer membrane [53, 54]. Upon activation, Drp1 is recruited to mitochondria by Fis1. Then, Drp1 interacts with Fis1 to mediate mitochondrial fission [55]. When endogenous Drp1 is inhibited in the primary cultured neurons, the mitochondria mainly gather in the cell body and fail to locate to the neuritis [56]. The heterozygous de novo mutations of *Drp1* in humans are neonatal lethality or give rise to development delay and refractory epilepsy [57–59].

In mammals, mitochondrial fusion requires the involvement of two 85 kD GTPase isoforms, namely, mitofusin1 (Mfn1) and mitofusin2 (Mfn2), and another dynamin family 100 kD GTPase, optic atrophy 1 (Opa1) [47, 60]. Mfn1 and Mfn2 are located in the outer mitochondrial membrane, which mediate outer membrane fusion [60, 61], while Opa1 is anchored in the inner mitochondrial membrane and facilitates inner membrane fusion [62]. Homozygous mutants of Mfn1 or Mfn2 are embryonic lethality in mouse [63]. Knockout of Mfn2 in mouse Purkinje neurons increases the
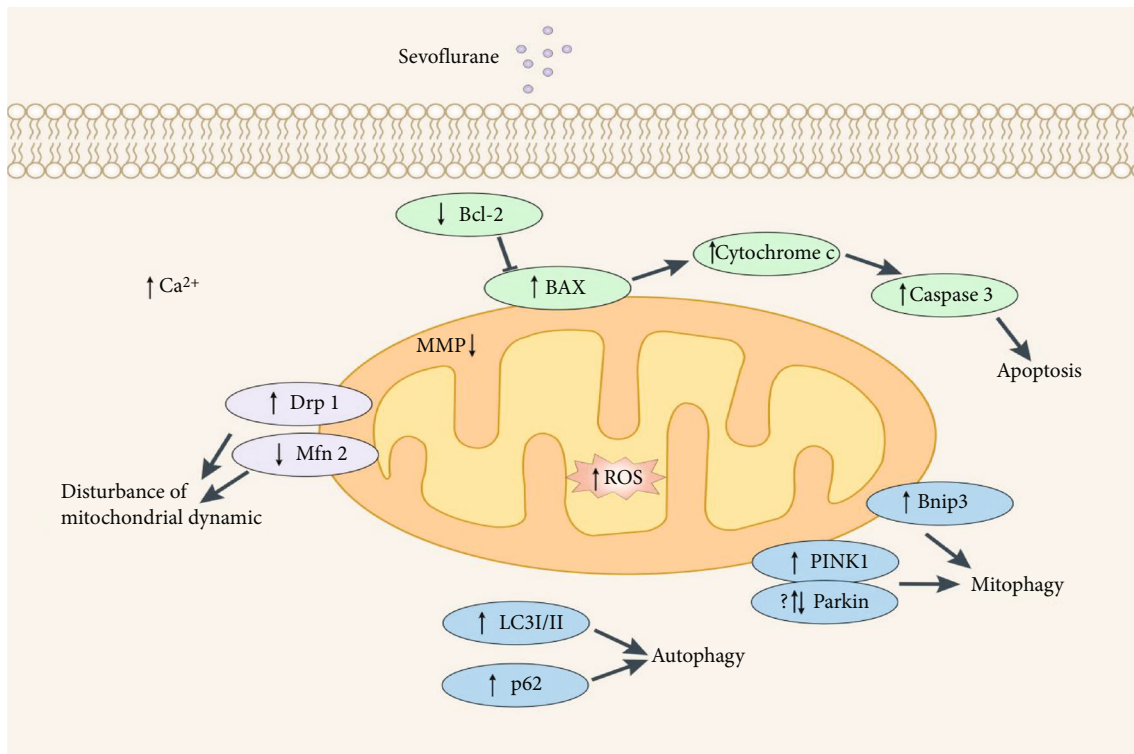
FIGURE 1: Sevoflurane treatment induces the abnormality of mitochondrial pathway of apoptosis, mitochondrial dynamics, and mitophagy. Sevoflurane treatment could induce the reduction of MMP, the decrease of Bcl-2 expression, and the elevation of Bax expression, thereby initiating the mitochondrial pathway of apoptosis. Also, sevoflurane treatment could disturb mitochondrial dynamic by increasing Drp1 expression and reducing Mfn2. And the changes of LC3I/II ratio, p62, PINK1, Parkin, and Bnip3 expression induced by sevoflurane indicate that sevoflurane could disturb mitophagy.

fragmented mitochondria and inhibits the distribution of mitochondria in the dendritic spines [64]. Consequently, the energy supply of the neuritis is reduced, thereby leading to neural degeneration [64]. Also, retinal ganglion cells of $Opa1^{+/-}$ mouse show fragmented mitochondria. And less mitochondria are found in the per micron of dendrite [65]. Human carrying mutations of *Mfn2* display severe peripheral neuropathy, and the mutant Opa1 would lead to vision loss for impaired optic nerve [66–68].

3.2. The Role of Mitochondrial Dynamics in Neural Injury Induced by Sevoflurane. The effect of sevoflurane on mitochondrial dynamics is firstly studied by Amrock et al. [9]. As the neurotoxicity effect of general anesthesia is significantly dominant to young children undergoing rapid synaptogenesis and brain development [69, 70], Amrock et al. chose rat pups between P7 and P13 for studying [9]. The timeframe is considered to be the period of brain growth spurt at birth in humans [71]. Rat pups are exposed to sevoflurane [9]. It is reported that sevoflurane decreases the mitochondrial density in rat hippocampus [9]. And when the primary rat cortical neurons are treated with sevoflurane, fragmental mitochondria show mostly in the cell body of neurons and little is found in the neurites, indicating that sevoflurane could disturb the mitochondrial morphology and distribution [72]. Unfortunately, the authors have not detected the expression changes of the key regulators of

mitochondria dynamic after treating with sevoflurane. Following the study of Amrock et al., some researches focus on the expression changes of mitochondrial fission and fusion proteins. These researches found that sevoflurane induces the upregulation of Drp1 and Fis1 and the downregulation of Mfn2 and Opa1 [26, 27, 40, 73]. It seems that sevoflurane could disturb the balance of mitochondrial dynamics through promoting mitochondrial fission and suppressing mitochondrial fusion, thereby inducing the damage of neural cells.

4. The Effects of Sevoflurane on Mitophagy in Neural Cells

4.1. Mitophagy and Neural Cells. Autophagy is a special kind of physiological process that can degrade unnecessary or damaged cytosolic components through lysosome [74]. Mitophagy refers to the degradation of the dysfunctional or superfluous mitochondria by autophagy mechanism [75]. Therefore, mitophagy plays a key role in maintaining mitochondrial quality control and metabolic balance [76].

Mitophagy is a selective process. Dysfunctional or superfluous mitochondria need to be recognized and engulfed through microtubule-associated protein 1 light chain 3 alpha (LC3) adaptors or LC3 receptors to form mitophagosomes [77]. The PINK1 (PTEN-induced putative kinase 1)/Parkin-dependent pathway is the most well-defined LC3 adaptor

pathway [78]. In the pathway, following MMP collapse due to damage stimuli, PINK1 is stabilized at the outer mitochondrial membrane, which recruits Parkin to the mitochondrial surface [79, 80]. Parkin on the mitochondrial surface polyubiquitinates other outer membrane proteins [81]. Then, polyubiquitin chains are phosphorylated by PINK1. The autophagy adaptor protein p62 discerns the phosphorylated poly-Ub signal and directly binds to LC3 to initiate the formation of mitophagosome and the mitochondrial degradation [82]. BCL2/adenovirus E1B 19 kDa interacting protein 3 (Bnip3) is one of the LC3 receptors [83]. It can interact directly with LC3 through the LC3-interacting region (LIR) to recognize and engulf damaged mitochondria to mitophagosomes [81, 84]. Mutant PINK1 and Parkin account for less than 5% of familial Parkinson's disease [85, 86]. The number of mitochondria is increased as the expression of PINK1 is diminished in the hippocampal neurons of the Alzheimer disease mouse model [87]. Abnormally enlarged mitochondria are observed in the iPSC-derived midbrain neurons from the Parkin mutant patients, which are more vulnerable to mitochondrial stress [88].

4.2. The Effect of Mitophagy on Neural Injury upon Sevoflurane. Accumulating evidence indicates that sevoflurane can interfere mitophagy to induce neural injury. It is reported that treatment of neonatal rat hippocampus with sevoflurane increases the proportion of LC3I/II and the expression level of p62 [26, 40, 42, 89]. The expression of PINK1 and Parkin is upregulated by sevoflurane in the hippocampal neurons of adult female mouse. Xia et al. identified that sevoflurane downregulates the expression of miR145 leading to increased Bnip3 level in neuronal cell lines [29]. The elevated expression of Bnip3 by sevoflurane was further confirmed by Zheng et al. in the mouse hippocampus [73]. These data indicate that sevoflurane could stimulate mitophagy [29, 42, 73]. However, Chen et al. reported that sevoflurane decreases the expression of Parkin in the mitochondria of aged rat hippocampus, and overexpression of Parkin or pretreatment with rapamycin could rescue the impairment of mitophagy induced by sevoflurane, suggesting that sevoflurane treatment blocks the activation of mitophagy [40].

5. Conclusion

In summary, increasing evidence suggests that sevoflurane could induce neural injury by mitochondrial apoptotic pathway. Also, sevoflurane is able to interfere mitochondrial dynamics and mitophagy to promote neural damage (Figure 1). The great progress has significantly improved our understanding of the mechanisms of sevoflurane-induced neural injury. However, the processes of mitochondrial dynamics and mitophagy are very complex. And there is a cross-talk/interplay among the mitochondrial pathway of apoptosis, mitochondrial dynamics, and mitophagy. Therefore, further studies need to be done to explore the regulatory effects of sevoflurane on the complex processes and the cross-talk/interplay. In addition, some studies have suggested that neural injury induced by sevoflurane is due to

insufficient mitophagy. In contrast, some studies have indicated that neural injury triggered by sevoflurane might be the result of excessive mitophagy. Why does mitophagy have inconsistent changes in sevoflurane-treated hippocampus damage? The resolution of these issues will help people deeply understand the mechanisms of sevoflurane-induced neural injury and provide theoretical supports for the therapy of sevoflurane-induced neural injury.

Data Availability

The data used to support the findings of this study are included within the article.

Conflicts of Interest

The authors declare that they have no competing interests.

Authors' Contributions

Ming Li and Jiguang Guo contributed equally to this work.

Acknowledgments

References

[1] N. J. O'Keeffe and T. E. Healy, "The role of new anesthetic agents," *Pharmacology & Therapeutics*, vol. 84, no. 3, pp. 233–248, 1999.

[2] T. Li, Z. Huang, X. Wang, J. Zou, and S. Tan, "Role of the GABAA receptors in the long-term cognitive impairments caused by neonatal sevoflurane exposure," *Reviews in the Neurosciences*, vol. 30, no. 8, pp. 869–879, 2019.

[3] D. P. Strum and E. I. Eger 2nd, "Partition coefficients for sevoflurane in human blood, saline, and olive oil," *Anesthesia and Analgesia*, vol. 66, no. 7, pp. 654–656, 1987.

[4] L. Vutskits and Z. Xie, "Lasting impact of general anaesthesia on the brain: mechanisms and relevance," *Nature Reviews. Neuroscience*, vol. 17, no. 11, pp. 705–717, 2016.

[5] B. A. Rappaport, S. Suresh, S. Hertz, A. S. Evers, and B. A. Orser, "Anesthetic neurotoxicity — clinical implications of animal models," *The New England Journal of Medicine*, vol. 372, no. 9, pp. 796-797, 2015.

[6] K. Servick, "Researchers struggle to gauge risks of childhood anesthesia," *Science*, vol. 346, no. 6214, pp. 1161-1162, 2014.

[7] J. V. Cabral-Costa and A. J. Kowaltowski, "Neurological disorders and mitochondria," *Molecular Aspects of Medicine*, vol. 71, p. 100826, 2020.

[8] Y. Wang, M. Qian, Y. Qu et al., "Genome-wide screen of the hippocampus in aged rats identifies mitochondria, metabolism and aging processes implicated in sevoflurane anesthesia," *Frontiers in Aging Neuroscience*, vol. 12, p. 122, 2020.

[9] L. G. Amrock, M. L. Starner, K. L. Murphy, and M. G. Baxter, "Long-term effects of single or multiple neonatal sevoflurane exposures on rat hippocampal ultrastructure," *Anesthesiology*, vol. 122, no. 1, pp. 87–95, 2015.

[10] F. J. Bock and S. W. G. Tait, "Mitochondria as multifaceted regulators of cell death," *Nature Reviews. Molecular Cell Biology*, vol. 21, no. 2, pp. 85–100, 2020.

[11] E. Ottina, D. Tischner, M. J. Herold, and A. Villunger, "A1/Bfl-1 in leukocyte development and cell death," *Experimental Cell Research*, vol. 318, no. 11, pp. 1291–1303, 2012.

[12] R. J. Youle and A. Strasser, "The BCL-2 protein family: opposing activities that mediate cell death," *Nature Reviews. Molecular Cell Biology*, vol. 9, no. 1, pp. 47–59, 2008.

[13] R. Singh, A. Letai, and K. Sarosiek, "Regulation of apoptosis in health and disease: the balancing act of BCL-2 family proteins," *Nature Reviews. Molecular Cell Biology*, vol. 20, no. 3, pp. 175–193, 2019.

[14] M. Kvansakul and M. G. Hinds, "Structural biology of the Bcl-2 family and its mimicry by viral proteins," *Cell Death & Disease*, vol. 4, no. 11, article e909, 2013.

[15] C. Lanave, M. Santamaria, and C. Saccone, "Comparative genomics: the evolutionary history of the Bcl-2 family," *Gene*, vol. 333, pp. 71–79, 2004.

[16] K. McArthur and B. T. Kile, "Apoptotic caspases: multiple or mistaken identities?," *Trends in Cell Biology*, vol. 28, no. 6, pp. 475–493, 2018.

[17] D. G. Nicholls and S. L. Budd, "Mitochondria and neuronal survival," *Physiological Reviews*, vol. 80, no. 1, pp. 315–360, 2000.

[18] D. G. Nicholls, "Bioenergetics and transmitter release in the isolated nerve terminal," *Neurochemical Research*, vol. 28, no. 10, pp. 1433–1441, 2003.

[19] R. van Belzen, A. B. Kotlyar, N. Moon, W. R. Dunham, and S. P. J. Albracht, "The iron-sulfur clusters 2 and ubisemiquinone radicals of NADH:ubiquinone oxidoreductase are involved in energy coupling in submitochondrial particles†," *Biochemistry*, vol. 36, no. 4, pp. 886–893, 1997.

[20] A. Boveris, N. Oshino, and B. Chance, "The cellular production of hydrogen peroxide," *The Biochemical Journal*, vol. 128, no. 3, pp. 617–630, 1972.

[21] M. Narita, S. Shimizu, T. Ito et al., "Bax interacts with the permeability transition pore to induce permeability transition and cytochrome c release in isolated mitochondria," *Proceedings of the National Academy of Sciences of the United States of America*, vol. 95, no. 25, pp. 14681–14686, 1998.

[22] I. Marzo, C. Brenner, N. Zamzami et al., "Bax and adenine nucleotide translocator cooperate in the mitochondrial control of apoptosis," *Science*, vol. 281, no. 5385, pp. 2027–2031, 1998.

[23] J. Karch, J. Q. Kwong, A. R. Burr et al., "Bax and Bak function as the outer membrane component of the mitochondrial permeability pore in regulating necrotic cell death in mice," *eLife*, vol. 2, article e00772, 2013.

[24] M. C. Wei, W. X. Zong, E. H. Cheng et al., "Proapoptotic BAX and BAK: a requisite gateway to mitochondrial dysfunction and death," *Science*, vol. 292, no. 5517, pp. 727–730, 2001.

[25] M. Xu, J. Feng, M. Tang et al., "Blocking retrograde axonal transport of autophagosomes contributes to sevoflurane-induced neuron apoptosis in APP/PS1 mice," *Acta Neurologica Belgica*, 2020.

[26] Y. Shan, S. Sun, F. Yang, N. Shang, and H. Liu, "Dexmedetomidine protects the developing rat brain against the neurotoxicity wrought by sevoflurane: role of autophagy and Drp1-Bax signaling," *Drug Design, Development and Therapy*, vol. Volume 12, pp. 3617–3624, 2018.

[27] F. Yang, Y. Shan, Z. Tang et al., "The neuroprotective effect of hemin and the related mechanism in sevoflurane exposed neonatal rats," *Frontiers in Neuroscience*, vol. 13, p. 537, 2019.

[28] X. Zhou, D. Xian, J. Xia et al., "MicroRNA-34c is regulated by p53 and is involved in sevoflurane-induced apoptosis in the developing rat brain potentially via the mitochondrial pathway," *Molecular Medicine Reports*, vol. 15, no. 4, pp. 2204–2212, 2017.

[29] H. Xia, Y. Li, G. Zhu, and X. Zhang, "Activation of mitochondria apoptotic pathway is involved in the sevoflurane-induced hippocampal neuronal HT22 cells toxicity through miR-145/Binp3 axis," *International Journal of Clinical and Experimental Pathology*, vol. 10, no. 11, pp. 10873–10882, 2017.

[30] X. Chen, X. Zhou, D. Lu et al., "Aberrantly expressed long noncoding RNAs are involved in sevoflurane-induced developing hippocampal neuronal apoptosis: a microarray related study," *Metabolic Brain Disease*, vol. 31, no. 5, pp. 1031–1040, 2016.

[31] Y. Cheng, Y. Jiang, L. Zhang et al., "Mesenchymal stromal cells attenuate sevoflurane-induced apoptosis in human neuroglioma H4 cells," *BMC Anesthesiol*, vol. 18, no. 1, p. 84, 2018.

[32] Y. Zhang, Y. Li, X. Han, X. Dong, X. Yan, and Q. Xing, "Elevated expression of DJ-1 (encoded by the human PARK7 gene) protects neuronal cells from sevoflurane-induced neurotoxicity," *Cell Stress & Chaperones*, vol. 23, no. 5, pp. 967–974, 2018.

[33] X. Zhu, Y. Yao, M. Guo et al., "Sevoflurane increases intracellular calcium to induce mitochondrial injury and neuroapoptosis," *Toxicology Letters*, vol. 336, pp. 11–20, 2021.

[34] M. Satomoto, Y. Satoh, K. Terui et al., "Neonatal exposure to sevoflurane induces abnormal social behaviors and deficits in fear conditioning in mice," *Anesthesiology*, vol. 110, no. 3, pp. 628–637, 2009.

[35] M. Kudo, M. Aono, Y. Lee, G. Massey, R. D. Pearlstein, and D. S. Warner, "Effects of volatile anesthetics on N-methyl-d-aspartate excitotoxicity in primary rat neuronal-glial cultures," *Anesthesiology*, vol. 95, no. 3, pp. 756–765, 2001.

[36] M. C. Moe, R. Bains, M. L. Vinje, G. A. Larsen, E. B. Kampenhaug, and J. Berg-Johnsen, "Sevoflurane depolarizes presynaptic mitochondria in the central nervous system," *Acta Anaesthesiologica Scandinavica*, vol. 48, no. 5, pp. 562–568, 2004.

[37] R. Bains, M. C. Moe, G. A. Larsen, J. Berg-Johnsen, and M. L. Vinje, "Volatile anaesthetics depolarize neural mitochondria by inhibiton of the electron transport chain," *Acta Anaesthesiologica Scandinavica*, vol. 50, no. 5, pp. 572–579, 2006.

[38] R. Bains, M. C. Moe, M. L. Vinje, and J. Berg-Johnsen, "Sevoflurane and propofol depolarize mitochondria in rat and human cerebrocortical synaptosomes by different mechanisms," *Acta Anaesthesiologica Scandinavica*, vol. 53, no. 10, pp. 1354–1360, 2009.

[39] G. Xu, H. Lu, Y. Dong et al., "Coenzyme Q_{10} reduces sevoflurane-induced cognitive deficiency in young mice," *British Journal of Anaesthesia*, vol. 119, no. 3, pp. 481–491, 2017.

[40] Y. Chen, P. Zhang, X. Lin et al., "Mitophagy impairment is involved in sevoflurane-induced cognitive dysfunction in aged rats," *Aging*, vol. 12, no. 17, pp. 17235–17256, 2020.

[41] Y. Yu, Y. Yang, H. Tan et al., "Tau contributes to sevoflurane-induced neurocognitive impairment in neonatal mice," *Anesthesiology*, vol. 133, no. 3, pp. 595–610, 2020.

[42] J.-S. Ye, L. Chen, Y.-Y. Lu, S.-Q. Lei, M. Peng, and Z.-Y. Xia, "Honokiol-mediated mitophagy ameliorates postoperative

cognitive impairment induced by surgery/sevoflurane via inhibiting the activation of NLRP3 inflammasome in the hippocampus," *Oxidative Medicine and Cellular Longevity*, vol. 2019, Article ID 8639618, 13 pages, 2019.

[43] H. Yang, G. Liang, B. J. Hawkins, M. Madesh, A. Pierwola, and H. Wei, "Inhalational anesthetics induce cell damage by disruption of intracellular calcium homeostasis with different potencies," *Anesthesiology*, vol. 109, no. 2, pp. 243–250, 2008.

[44] Y. Zhang, P. Lu, F. Liang et al., "Cyclophilin D contributes to anesthesia neurotoxicity in the developing brain," *Frontiers in Cell and Development Biology*, vol. 7, p. 396, 2020.

[45] S. A. Detmer and D. C. Chan, "Functions and dysfunctions of mitochondrial dynamics," *Nature Reviews. Molecular Cell Biology*, vol. 8, no. 11, pp. 870–879, 2007.

[46] D. C. Chan, "Mitochondrial dynamics and its involvement in disease," *Annual Review of Pathology*, vol. 15, no. 1, pp. 235–259, 2020.

[47] J. Hom and S. S. Sheu, "Morphological dynamics of mitochondria – A special emphasis on cardiac muscle cells," *Journal of Molecular and Cellular Cardiology*, vol. 46, no. 6, pp. 811–820, 2009.

[48] V. P. Skulachev, "Mitochondrial filaments and clusters as intracellular power-transmitting cables," *Trends in Biochemical Sciences*, vol. 26, no. 1, pp. 23–29, 2001.

[49] A. Boscolo, D. Milanovic, J. A. Starr et al., "Early exposure to general anesthesia disturbs mitochondrial fission and fusion in the developing rat brain," *Anesthesiology*, vol. 118, no. 5, pp. 1086–1097, 2013.

[50] K. Okamoto and J. M. Shaw, "Mitochondrial morphology and dynamics in yeast and multicellular eukaryotes," *Annual Review of Genetics*, vol. 39, no. 1, pp. 503–536, 2005.

[51] Y. Yoon, E. W. Krueger, B. J. Oswald, and M. A. McNiven, "The mitochondrial protein hFis1 regulates mitochondrial fission in mammalian cells through an interaction with the dynamin-like protein DLP1," *Molecular and Cellular Biology*, vol. 23, no. 15, pp. 5409–5420, 2003.

[52] E. Smirnova, L. Griparic, D. L. Shurland, and A. M. van der Bliek, "Dynamin-related protein Drp1 is required for mitochondrial division in mammalian cells," *Molecular Biology of the Cell*, vol. 12, no. 8, pp. 2245–2256, 2001.

[53] D. I. James, P. A. Parone, Y. Mattenberger, and J. C. Martinou, "hFis1, a Novel Component of the Mammalian Mitochondrial Fission Machinery," *The Journal of Biological Chemistry*, vol. 278, no. 38, pp. 36373–36379, 2003.

[54] H. T. Bui and J. M. Shaw, "Dynamin assembly strategies and adaptor proteins in mitochondrial fission," *Current Biology*, vol. 23, no. 19, pp. R891–R899, 2013.

[55] S. B. Ong and A. B. Gustafsson, "New roles for mitochondria in cell death in the reperfused myocardium," *Cardiovascular Research*, vol. 94, no. 2, pp. 190–196, 2012.

[56] N. Ishihara, M. Nomura, A. Jofuku et al., "Mitochondrial fission factor Drp1 is essential for embryonic development and synapse formation in mice," *Nature Cell Biology*, vol. 11, no. 8, pp. 958–966, 2009.

[57] H. R. Waterham, J. Koster, C. W. T. van Roermund, P. A. W. Mooyer, R. J. A. Wanders, and J. V. Leonard, "A lethal defect of mitochondrial and peroxisomal fission," *The New England Journal of Medicine*, vol. 356, no. 17, pp. 1736–1741, 2007.

[58] S. von Spiczak, K. L. Helbig, D. N. Shinde et al., "DNM1encephalopathy," *Neurology*, vol. 89, no. 4, pp. 385–394, 2017.

[59] J. R. Vanstone, A. M. Smith, S. McBride et al., "_DNM1L-_ related mitochondrial fission defect presenting as refractory epilepsy," *European Journal of Human Genetics*, vol. 24, no. 7, pp. 1084–1088, 2016.

[60] A. Santel and M. T. Fuller, "Control of mitochondrial morphology by a human mitofusin," *Journal of Cell Science*, vol. 114, Part 5, pp. 867–874, 2001.

[61] H. Chen, A. Chomyn, and D. C. Chan, "Disruption of Fusion Results in Mitochondrial Heterogeneity and Dysfunction," *The Journal of Biological Chemistry*, vol. 280, no. 28, pp. 26185–26192, 2005.

[62] S. Ehses, I. Raschke, G. Mancuso et al., "Regulation of OPA1 processing and mitochondrial fusion by m-AAA protease isoenzymes and OMA1," *The Journal of Cell Biology*, vol. 187, no. 7, pp. 1023–1036, 2009.

[63] H. Chen, S. A. Detmer, A. J. Ewald, E. E. Griffin, S. E. Fraser, and D. C. Chan, "Mitofusins Mfn1 and Mfn2 coordinately regulate mitochondrial fusion and are essential for embryonic development," *The Journal of Cell Biology*, vol. 160, no. 2, pp. 189–200, 2003.

[64] H. Chen, J. M. McCaffery, and D. C. Chan, "Mitochondrial fusion protects against neurodegeneration in the cerebellum," *Cell*, vol. 130, no. 3, pp. 548–562, 2007.

[65] P. A. Williams, M. Piechota, C. von Ruhland, E. Taylor, J. E. Morgan, and M. Votruba, "Opa1 is essential for retinal ganglion cell synaptic architecture and connectivity," *Brain*, vol. 135, no. 2, pp. 493–505, 2012.

[66] S. L. Sawyer, A. Cheuk-Him Ng, A. M. Innes et al., "Homozygous mutations inMFN2cause multiple symmetric lipomatosis associated with neuropathy," *Human Molecular Genetics*, vol. 24, no. 18, pp. 5109–5114, 2015.

[67] R. D. Bo, M. Moggio, M. Rango et al., "Mutated mitofusin 2 presents with intrafamilial variability and brain mitochondrial dysfunction," *Neurology*, vol. 71, no. 24, pp. 1959–1966, 2008.

[68] C. Alexander, M. Votruba, U. E. A. Pesch et al., "OPA1, encoding a dynamin-related GTPase, is mutated in autosomal dominant optic atrophy linked to chromosome 3q28," *Nature Genetics*, vol. 26, no. 2, pp. 211–215, 2000.

[69] L. Vutskits, "General anesthesia," *Anesthesia and Analgesia*, vol. 115, no. 5, pp. 1174–1182, 2012.

[70] R. T. Wilder, R. P. Flick, J. Sprung et al., "Early exposure to anesthesia and learning disabilities in a population-based birth cohort," *Anesthesiology*, vol. 110, no. 4, pp. 796–804, 2009.

[71] J. Dobbing and J. Sands, "Comparative aspects of the brain growth spurt," *Early Human Development*, vol. 3, no. 1, pp. 79–83, 1979.

[72] F. Xu, R. Armstrong, D. Urrego et al., "The mitochondrial division inhibitor Mdivi-1 rescues mammalian neurons from anesthetic-induced cytotoxicity," *Molecular Brain*, vol. 9, no. 1, p. 35, 2016.

[73] F. Zheng, P. Fang, J. Chang et al., "Methylene blue protects against sevoflurane-induced cognitive dysfunction by suppressing Drp1 deSUMOylation in aged mice," *Neurochemical Research*, vol. 45, no. 4, pp. 956–963, 2020.

[74] M. Russo and G. L. Russo, "Autophagy inducers in cancer," *Biochemical Pharmacology*, vol. 153, pp. 51–61, 2018.

[75] K. Palikaras, E. Lionaki, and N. Tavernarakis, "Mechanisms of mitophagy in cellular homeostasis, physiology and pathology," *Nature Cell Biology*, vol. 20, no. 9, pp. 1013–1022, 2018.

Hindawi

Retraction

Retracted: Modulation of Mitochondrial Quality Control Processes by BGP-15 in Oxidative Stress Scenarios: From Cell Culture to Heart Failure

Oxidative Medicine and Cellular Longevity

This article has been retracted by Hindawi following an investigation undertaken by the publisher [1]. This investigation has uncovered evidence of one or more of the following indicators of systematic manipulation of the publication process:

(1) Discrepancies in scope

(2) Discrepancies in the description of the research reported

(3) Discrepancies between the availability of data and the research described

(4) Inappropriate citations

(5) Incoherent, meaningless and/or irrelevant content included in the article

(6) Peer-review manipulation

The presence of these indicators undermines our confidence in the integrity of the article's content and we cannot, therefore, vouch for its reliability. Please note that this notice is intended solely to alert readers that the content of this article is unreliable. We have not investigated whether authors were aware of or involved in the systematic manipulation of the publication process.

Wiley and Hindawi regrets that the usual quality checks did not identify these issues before publication and have since put additional measures in place to safeguard research integrity.

We wish to credit our own Research Integrity and Research Publishing teams and anonymous and named external researchers and research integrity experts for contributing to this investigation.

The corresponding author, as the representative of all authors, has been given the opportunity to register their agreement or disagreement to this retraction. We have kept a record of any response received.

References

[1] O. Horvath, K. Ordog, K. Bruszt et al., "Modulation of Mitochondrial Quality Control Processes by BGP-15 in Oxidative Stress Scenarios: From Cell Culture to Heart Failure," *Oxidative Medicine and Cellular Longevity*, vol. 2021, Article ID 6643871, 22 pages, 2021.

Research Article

Modulation of Mitochondrial Quality Control Processes by BGP-15 in Oxidative Stress Scenarios: From Cell Culture to Heart Failure

Orsolya Horvath [1,2] **Katalin Ordog** [1,2] **Kitti Bruszt** [1,2] **Nikoletta Kalman** [3]
Dominika Kovacs [3] **Balazs Radnai** [3] **Ferenc Gallyas** [2,3,4] **Kalman Toth** [1,2]
Robert Halmosi [1,2] **and Laszlo Deres** [1,2,4]

[1]*1st Department of Medicine, University of Pecs, Medical School, Pecs, Hungary*
[2]*Szentágothai Research Centre, University of Pecs, Pecs, Hungary*
[3]*Department of Biochemistry and Medical Chemistry, University of Pecs, Medical School, Pecs, Hungary*
[4]*HAS-UP Nuclear-Mitochondrial Interactions Research Group, 1245 Budapest, Hungary*

Correspondence should be addressed to Laszlo Deres; deres.laszlo@pte.hu

Heart failure (HF) is a complex chronic clinical disease characterized by among others the damage of the mitochondrial network. The disruption of the mitochondrial quality control and the imbalance in fusion-fission processes lead to a lack of energy supply and, finally, to cell death. BGP-15 (O-[3-piperidino-2-hydroxy-1-propyl]-nicotinic acid amidoxime dihydrochloride) is an insulin sensitizer molecule and has a cytoprotective effect in a wide variety of experimental models. In our recent work, we aimed to clarify the mitochondrial protective effects of BGP-15 in a hypertension-induced heart failure model and "in vitro." Spontaneously hypertensive rats (SHRs) received BGP-15 or placebo for 18 weeks. BGP-15 treatment preserved the normal mitochondrial ultrastructure and enhanced the mitochondrial fusion. Neonatal rat cardiomyocytes (NRCMs) were stressed by hydrogen-peroxide. BGP-15 treatment inhibited the mitochondrial fission processes, promoted mitochondrial fusion, maintained the integrity of the mitochondrial genome, and moreover enhanced the de novo biogenesis of the mitochondria. As a result of these effects, BGP-15 treatment also supports the maintenance of mitochondrial function through the preservation of the mitochondrial structure during hydrogen peroxide-induced oxidative stress as well as in an "in vivo" heart failure model. It offers the possibility, which pharmacological modulation of mitochondrial quality control under oxidative stress could be a novel therapeutic approach in heart failure.

1. Introduction

Several studies have demonstrated that mitochondria, the powerhouse of cells are damaged in heart failure as well as in hypertension-induced cardiac remodelling [1–3]. The balance of fusion and fission processes that regulate mitochondrial dynamics is essential for maintaining energy production [4, 5]. The most important fusion proteins in the regulation of mitochondrial dynamics are the optic atrophy 1 (OPA1) and the mitofusin 1 and 2 (MFN1, MFN2)

proteins, while the fission processes of mitochondria are controlled by dynamin-related protein 1 (DRP1) [6–8].

In heart failure due to the increased ROS production, fission processes become predominant, resulting in fragmented mitochondrial network, which is unable to perform its function of providing energy to the cell; thereby, mitochondrial fragmentation can induce cell death [2, 4, 9, 10]. The subject of numerous researches is the regulation of mitochondrial dynamics as a new therapeutic target in cardiovascular diseases [6, 11–14].
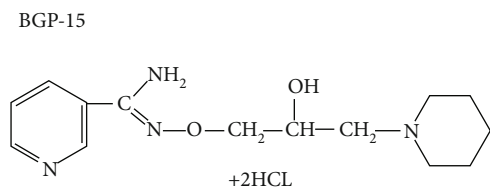
BGP-15

FIGURE 1: Chemical structure of BGP-15 (O-[3-piperidino-2-hydroxy-1-propyl]-nicotinic acid amidoxime dihydrochloride) [24].

BGP-15 (O-[3-piperidino-2-hydroxy-1-propyl]-nicotinic acid amidoxime dihydrochloride) is an insulin sensitizer molecule and has a cytoprotective effect in a wide variety of experimental models (Figure 1). BGP-15 protects against oxidative stress [15–17], promotes mitochondrial fusion [18], inhibits the mitogen-activated protein kinase (MAPK) activation [19–22], and improves cardiac function [21–23], but its specific intracellular target is still unknown.

This study was aimed to further characterize the mitochondrial effects of BGP-15 in a chronic hypertension-induced heart failure animal model and "in vitro" using primer neonatal rat cardiomyocytes (NRCM). We studied the effect of BGP-15 on the processes of mitochondrial quality control, particularly on fusion-fission processes, on mitochondrial biogenesis as well as on mitochondrial function.

2. Materials and Methods

2.1. Ethics Statement. Animals received care according to the Guide for the Care and Use of Laboratory Animals published by the US National Institute of Health and the experiment was approved by the Animal Research Review Committee of the University of Pecs, Medical School (Permit number: BA02/2000-54/2017).

2.2. Animal Model. 15-month-old male Wistar Kyoto (WKY) and spontaneously hypertensive rats (SHR) (Charles River Laboratories, Budapest, Hungary) were used. Two animals were housed per cage under standardized conditions throughout the experiment, with 12 hours of dark-light cycle in solid-bottomed polypropylene cages and received commercial rat chew and water ad libitum. 8 of the 24 animals were sacrificed at the beginning of the experiment, as a baseline (SHR-Baseline). The surviving 16 SHRs were randomly divided into two groups: SHR-B and SHR-C. SHR-B group was treated with the water-soluble BGP-15 (25 mg/b.w. in kg/day, $n = 8$), while SHR-C group received only placebo ($n = 8$, SHR-C) per os for 18 weeks. BGP-15 was a gift from N-Gene Inc. (New York, NY, USA). The dosage of BGP-15 administered in the drinking water was based on preliminary data about the volume of daily water consumption. WKY rats were used as age-matched controls ($n = 8$). At the end of the 18-week long treatment period, animals were sacrificed, and blood was collected to determine the concentration of plasma brain-derived natriuretic peptide (BNP). Hearts were removed, atria and great vessels were trimmed from the ventricles, and the weight of the ventricles was measured; then, it was normalized to the body mass and to the length of the right tibia (indices of cardiac hypertrophy). Hearts were fixed in modified Kranovsky fixative for transmission electron microscopy or freeze-clamped for Western blot analysis. The levels of proteins which are involved in the processes of mitochondrial dynamics and biogenesis were monitored by Western blot analysis. In our research, the following group notations were used according to the applied treatment: WKY: age-matched normotensive Wistar Kyoto rats; SHR-Baseline: 15-month-old spontaneously hypertensive rats; SHR-C: 19-month-old spontaneously hypertensive rats received placebo for 18 weeks; SHR-B: 19-month-old spontaneously hypertensive rats received BGP-15 for 18 weeks.

2.3. Neonatal Rat Cardiomyocyte (NRCM) Cell Culture. Cardiomyocytes were isolated using the Pierce™ Primary Cardiomyocyte Isolation Kit (Life Technologies, Carlsbad, CA, USA #88281) from 1-3-day-old neonatal Wistar rats. The animals were sacrificed, and then, their hearts were removed and minced into 1-3 mm^3 pieces. The pieces were digested with an enzyme complex (Cardiomyocyte Isolation Enzyme 1 (with papain) and Cardiomyocyte Isolation Enzyme 2 (with thermolysin)). After the tissue became primarily a single-cell suspension, the cells had been plated in 6-well plates with a density of 2.5×10^6 cell/well with specific Dulbecco's Modified Eagle Medium (DMEM) for Primary Cell Isolation containing 10% fetal bovine serum (FBS), 100 IU/mL penicillin and 100 μg/mL streptomycin. The medium was replaced 24 hours later with fresh Complete DMEM for Primary Cell Isolation containing Cardiomyocyte Growth Supplement, which inhibited the division of fibroblasts and therefore maintained the cardiomyocyte suspension in high purity during the culture period. NRCMs were cultivated in normal culture conditions, 37°C, saturated humidity atmosphere of 95% air and 5% CO2. Fresh medium was added every 2-3 days.

2.4. Treatments of Neonatal Rat Cardiomyocytes. On the day of the experiments, cells were washed once in PBS and added fresh medium and, then, treated with 150 μM H$_2$O$_2$ with or without 50 μM BGP-15 for 0.5 hours. The following groups were created according to the applied treatment: Control group: cells without any treatment; BGP-15 group: cells with only 50 μM BGP-15 for 0.5 hours; H$_2$O$_2$ group: cells with 150 μM H$_2$O$_2$ for 0.5 hours; H$_2$O$_2$+BGP-15 group: cells with 150 μM H$_2$O$_2$ and 50 μM BGP-15 for 0.5 hours.

2.5. Determination of Plasma B-Type Natriuretic Peptide Level. Blood samples were collected into Vacutainer tubes containing EDTA and aprotinin (0.6 IU/ml) and centrifuged at 1600 g for 15 minutes at 4°C to separate plasma, which was collected and kept at −70°C. Plasma B-type natriuretic peptide-32 levels (BNP-32) were determined by Enzyme-Linked Immunosorbent Assay method (BNP-32, Rat BNP 32 ELISA Kit, Abcam, ab108815CA, USA) as the datasheet recommends.

2.6. Transmission Electron Microscopy. For electron microscopy analysis, hearts were perfused retrogradely through the aortic root with ice-cold PBS to wash out the blood and then with modified Kranovsky fixative (2% paraformaldehyde,

TABLE 1: Effect of BGP-15 administration on gravimetric parameters and on BNP level of SHR animals.

	WKY	SHR-C	SHR-B
BW^{START} (g)	391.51 ± 8.64	$340.66 \pm 6.74^{*}$	$347.4 \pm 10.38^{*}$
BW^{END} (g)	403.22 ± 10.35	$352.13 \pm 6.86^{*}$	$365.29 \pm 6.82^{*}$
HW^{END} (g)	1.11 ± 0.03	$1.41 \pm 0.03^{**}$	$1.28 \pm 0.02^{**,\#}$
VW^{END} (g)	0.98 ± 0.03	$1.27 \pm 0.02^{*}$	$1.12 \pm 0.02^{*}$
VW/BW^{END} (mg/g)	2.43 ± 0.07	$3.60 \pm 0.04^{*}$	$3.07 \pm 0.09^{*,\#}$
VW/TL^{END} (mg/mm)	21.43 ± 0.71	$29.14 \pm 0.39^{*}$	$24.81 \pm 0.53^{*,\#}$
p-BNP (pg/ml)	302.76 ± 13.77	$755.15 \pm 33.34^{*}$	$352.05 \pm 22.50^{\#}$

BW^{START}: body weight at the beginning of the treatment; BW^{END}: body weight at the end of the treatment; HW^{END}: heart weight at the end of the treatment; VW^{END}: ventricles weight at the end of the treatment; TL^{END}: length of right tibia at the end of the treatment; p-BNP: plasma brain-type natriuretic peptide. Values are means + SEM. WKY: age-matched normotensive Wistar-Kyoto rats, $n = 8$, SHR-C: nontreated spontaneously hypertensive rats, $n = 8$, SHR-B: spontaneously hypertensive rats receiving BGP-15 for 18 weeks, $n = 8$. $^{*}p < 0.05$ vs. WKY, $^{**}p < 0.01$ vs. WKY, $^{\#}p < 0.05$ vs. SHR-C.

2.5% glutaraldehyde, 0.1 M Na-cacodylate buffer, pH 7.4, and 3 mM $CaCl_2$). 1 mm thick sections were cut from the free wall of the left ventricle. Dehydrated blocks were embedded in Durcupan resin. From the embedded blocks, semithin sections of 500 nm and ultrathin sections of 50 nm were cut with a Leica ultramicrotome and mounted either on mesh or on Collodion-coated (Parlodion, Electron Microscopy Sciences, Fort Washington, PA) single-slot, copper grids. Additional contrast was provided to these sections with uranyl acetate and lead citrate solutions, and the preparations were examined with a JEOL 1200EX-II electron microscope. 4 animals from each group, 3–5 blocks from each animal were used. The area of the interfibrillar mitochondria (IFM) was measured by freehand polygon selection (n~500/group) using the ImageJ software.

2.7. Western-Blot Analysis

2.7.1. Total Western Blot Sample Preparation from Cardiac Tissue. 50 milligrams of heart samples were homogenized in ice-cold Tris buffer (50 mmol/l, pH 8.0) containing protease inhibitor (1 : 100; Sigma-Aldrich Co., #P8340) and phosphatase inhibitor (1 : 100; Sigma-Aldrich Co., #P5726) and 50 mM sodium vanadate. The supernatants were harvested in 2x concentrated sodium dodecyl sulfate- (SDS-) polyacrylamide gel electrophoresis sample buffer.

2.7.2. Fractionated Western Blot Sample Preparation from Cardiac Tissue. 100 milligrams of heart tissues were minced in ice-cold isolation solution (150 mM NaCl, 50 mM TRIS, and 1 mM EDTA), protease inhibitor (1 : 100; Sigma-Aldrich Co., #P8340), and phosphatase inhibitor (1 : 100; Sigma-Aldrich Co., #P5726)). Samples were disrupted on ice with gently Turrax and, then, processed in a Potter-Elvehjem tissue homogenizer. Samples were centrifuged for 12 minutes at 750 g. Supernatants containing the cytosolic and mitochondrial fractions were aspirated and the precipitated nuclear fractions were harvested in 2x SDS–polyacrylamide gel electrophoresis sample buffer and denatured at 95°C for 5 minutes. Supernatants were then centrifuged for 12 minutes at 11.000 g to gain cytosolic fraction in the supernatant and mitochondrial fraction in the precipitate. Samples were harvested separately in 2x SDS–polyacrylamide gel electrophoresis sample buffer and denatured at 95°C for 5 minutes.

2.7.3. Total Western-Blot Sample Preparation from NRCM Cell Culture. After the appropriate treatment, cells were harvested. The cell pellet was suspended in ice-cold PBS buffer and, then, centrifuged for 5 min at 1,200 rpm at room temperature. The pellets were suspended in 300 μL NP-40 lysis buffer (Amresco, J619) containing protease inhibitor (1 : 100; Sigma-Aldrich Co., #P8340) and phosphatase inhibitor (1 : 100; Sigma-Aldrich Co., #P5726). The samples were shaken for 30 min at 4°C; then, they were centrifuged for 20 min (4°C 12,000 rpm). 4x concentrated SDS-polyacrylamide gel electrophoresis sample buffer was added to each sample.

2.7.4. Fractionated Western Blot Sample Preparation from NRCM Cell Culture. The cell pellet was suspended in an ice-cold isolation solution (0.5 mM TRIS, 1 M EGTA, and 0.4 M sucrose) containing 0.5 mM sodium metavanadate, 0.05 M EDTA, and protease inhibitor (1 : 100; Sigma-Aldrich Co., #P8340). Samples were disrupted on ice by Turrax and, then, processed by a Potter-Elvehjem tissue homogenizer. Centrifugation was carried out for 15 minutes at 750 g. The nuclear fraction in the precipitate was harvested in 72% trichloroacetic acid. Subsequently, supernatants were aspirated and centrifuged for 15 minutes at 10.000 g to gain cytosolic fraction in the supernatant and mitochondrial in the precipitate. Samples were harvested separately in 72% trichloroacetic acid. The precipitated fractions were centrifuged for 10 minutes at 15.000 g. Each precipitate was harvested separately in a 50 mM TRIS and SDS-polyacrylamide gel electrophoresis sample buffer. The samples were shaken for overnight at 4°C and denatured at 95°C for 5 minutes. After that, they were centrifuged for 10 minutes at 15.000 g, and the supernatants were collected as the mitochondrial fraction.

2.7.5. Electrophoresis and Transfer of Proteins. After the preparation, the tissue and cell culture samples were processed in the same manner. Protein levels were measured with

(a)

(b)

(c)
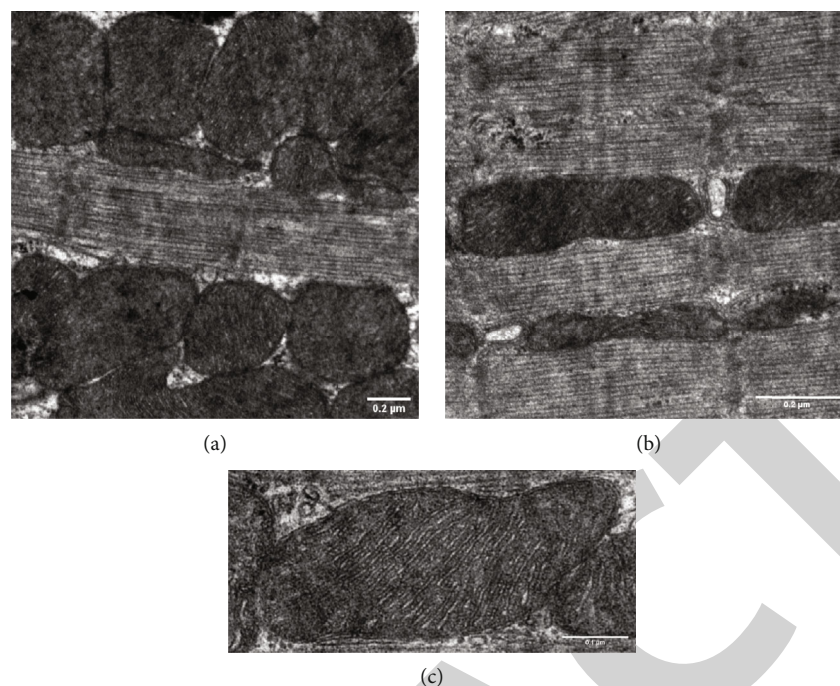
Figure 2: Ultrastructural analysis of interfibrillar mitochondria in the myocardium of WKY animals. Representative electron micrographs of interfibrillar mitochondria in the myocardium of (a, b) WKY animals ((a) magnification: 15 k, scale bar: 0.2 μm; (b) magnification: 20 k, scale bar: 0.2 μm). Ultrastructure of interfibrillar mitochondria in the myocardium of (c) WKY animals (magnification: 40 k, scale bar: 0.1 μm (n = 4 from each group, 3–5 blocks from each animal). WKY: age-matched normotensive Wistar-Kyoto rats.

Nanodrop. Glyceraldehyde 3-phosphate dehydrogenase (GAPDH; 1 : 1000; Cell Signaling #2118) and pyruvate dehydrogenase (PDC; 1 : 1000; Cell Signaling #3205) were used as a representative loading control. Proteins were separated on 12% SDS-polyacrylamide gel and transferred to nitrocellulose membranes. After blocking (2 h with 5% BSA in Tris-buffered saline contained with 1% Tween-20), membranes were probed overnight at 4°C with primary antibodies recognizing the following antigens: optic atrophy 1 (OPA1; 1 : 1000; Cell Signaling #80471), mitofusin-1 (MFN1; 1 : 1000; Abcam ab57602), mitofusin-2 (MFN2; 1 : 1000; Cell Signaling #9482), dynamin-related protein 1 (DRP1; 1 : 1000; Cell Signaling #8570), phosphor-specific DRP1 Ser637 (1 : 500; Cell Signaling #4867), phosphor-specific DRP1 Ser616 (1 : 500; Cell Signaling #3455), voltage-dependent anion channel (VDAC; 1 : 1000; Cell Signaling #4661), mitochondrial fission 1 protein (FIS1; 2 μg/mL, Abcam, ab71498), peroxisome proliferator-activated receptor gamma coactivator 1-alpha (PGC-1α; 1 : 1000; Novus Biologicals, NBP1-04676), cAMP response element-binding protein (CREB; 1 : 1000; Cell Signaling #4820), phosphor-specific cAMP response element-binding protein Ser133 (1 : 1000; Cell Signaling #9198), anti-NADH dehydrogenase Fe-S protein 1 (NDUFs1, Novus Biologicals, NBP1-31142, 1 : 1000), and anti-Ubiquinol-cytochrome c reductase core protein I (UQCRC1, Novus Biologicals, NBP2-03825, 1 : 1000). Membranes were washed six times for 5 min in Tris-buffered saline (pH 7.5) containing 0.2% Tween (TBST) before the addition of horseradish peroxidase-conjugated secondary antibody (goat anti-rabbit IgG, Sigma Aldrich Co. A0545, 1 : 3000 dilution; rabbit anti-mouse IgG, Sigma

Aldrich Co., A9044, 1 : 5000 dilution). Membranes were washed six times for 5 min in TBST, and then, the antibody-antigen complexes were visualized by enhanced chemiluminescence. The results of Western blots were quantified using the NIH ImageJ program.

2.8. Capillary Electrophoresis Immunoassay. Due to the limited availability of primary neonatal cardiomyocytes and the lower protein concentration of the fractionated samples made from it, the more sensitive capillary immunoassay method with less sample requirements and higher throughput is more suitable for measurement. Simple western analysis (Wes) was performed on a Wes system (ProteinSimple, product number 004–600) according to the manufacturer's instructions using a 12-230 kDa Separation Module (ProteinSimple SM-W004) and either the Anti-Rabbit Detection Module (ProteinSimple DM-001) or the Anti-Mouse Detection Module (ProteinSimple DM-002), depending on the primary used antibody. Subcellular NRCM samples were mixed with Fluorescent Master Mix and heated at 95°C for 5 min. The samples, blocking reagent (antibody diluent), primary antibodies (in antibody diluent), HRP-conjugated secondary antibodies, and chemiluminescent substrate, were pipetted into the plate (part of Separation Module). Instrument default settings were used: stacking and separation at 475 V for 30 min; blocking reagent for 5 min, primary and secondary antibody both for 30 min; Luminol/peroxide chemiluminescence detection for ~15 min (exposures of 1-2-4-8-16-32-64-128-512 s). The resulting electropherograms were inspected to check whether automatic peak detection required any manual correction.
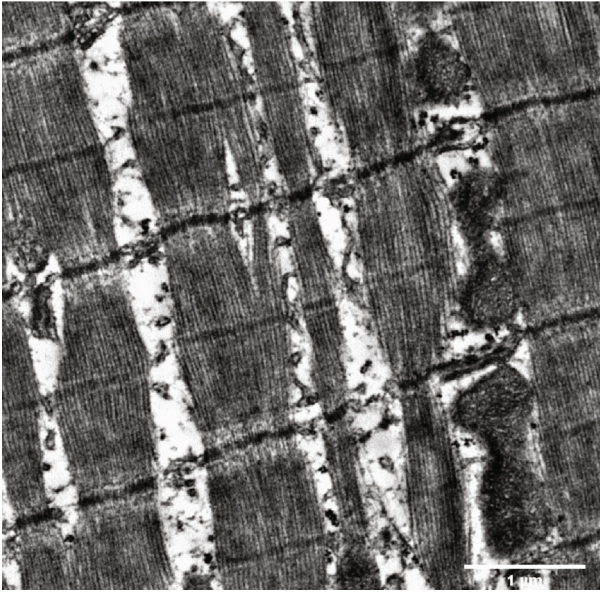
(a)
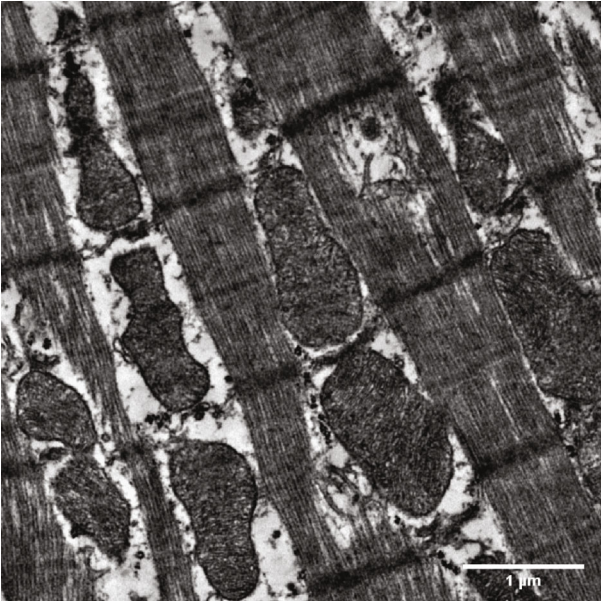
(b)
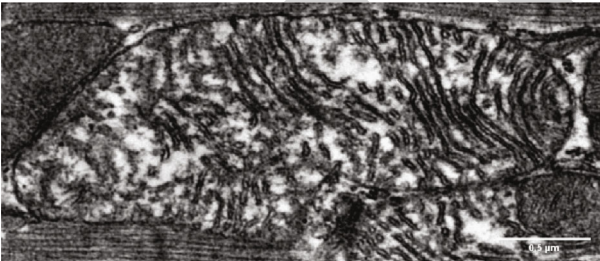
(c)
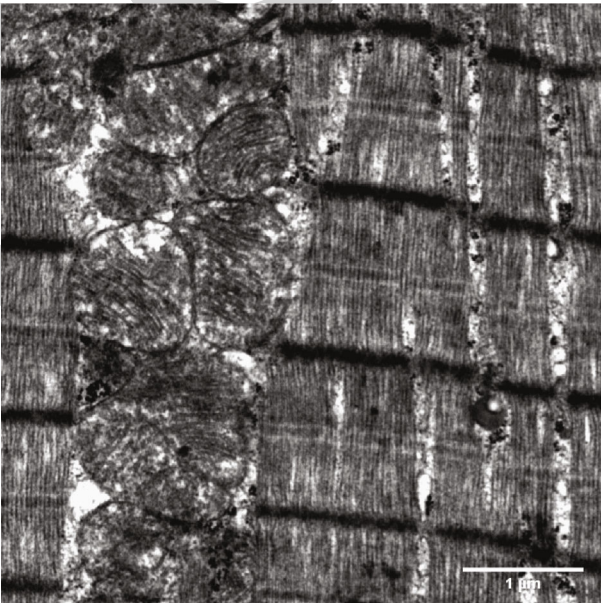
(d)

Figure 3: Continued.

(e)

(f)
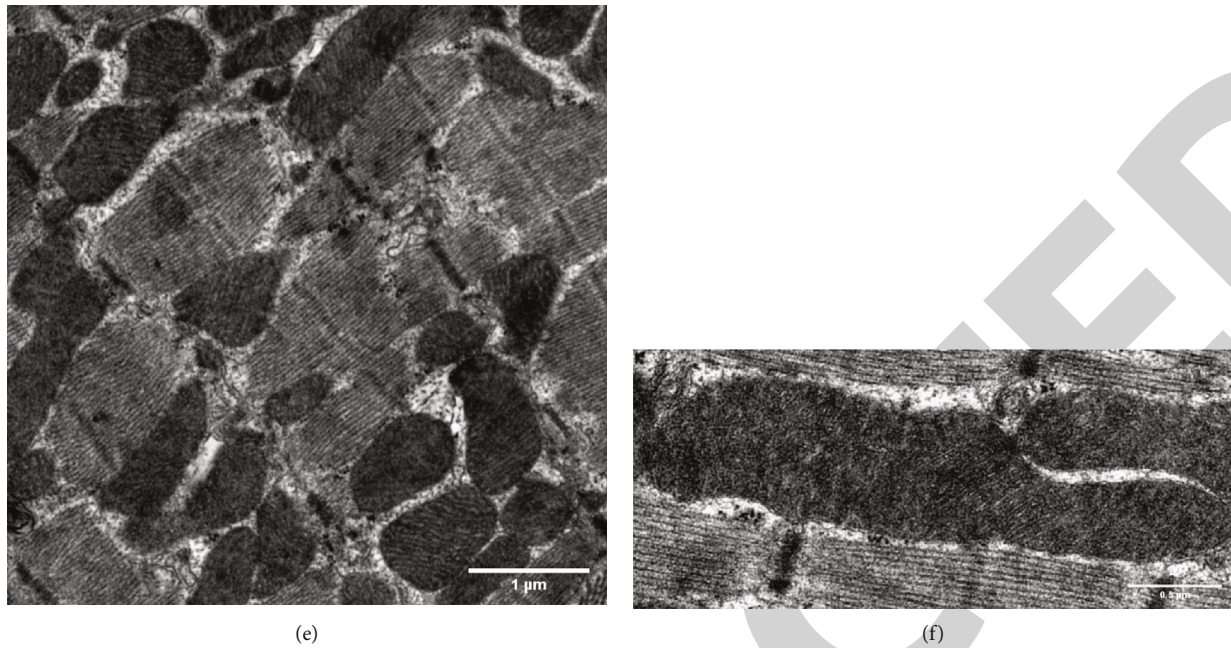
Figure 3: Ultrastructural analysis of interfibrillar mitochondria in the myocardium of SHR animals. Representative electron micrographs of interfibrillar mitochondria in the myocardium of (a, b) SHR-C and (d, e) SHR-B animals (magnification: 10 k, scale bar: 1 μm). Ultrastructure of interfibrillar mitochondria in the myocardium of (c) SHR-C and (f) SHR-B animals (magnification: 25 k, scale bar: 0.5 μm). SHR-C: nontreated spontaneously hypertensive rats; SHR-B: spontaneously hypertensive rats receiving BGP-15 for 18 weeks ($n = 4$ from each group, 3–5 blocks from each animal).

2.9. Evaluation of Mitochondrial Fragmentation with Fluorescent Microscopy.

NRCM cells were seeded at a density of 10^5 cells/well in 6 well plates on glass coverslips with 1% gelatin coating and cultured at least for 2 days before the experiment. On the day of the experiment, cells were washed once in PBS and added fresh medium and, then, treated with H_2O_2 with or without BGP-15. After the appropriate treatment, coverslips were rinsed in PBS and were added 75 nM MitoTracker Red CMXRos dissolved in serum-free DMEM and incubated for 30 min at 37°C. After the incubation, coverslips were rinsed in PBS, and the mitochondrial network was visualized by a Nikon Eclipse Ti-U fluorescent microscope equipped with a Spot RT3 camera using a 60x objective and epifluorescent illumination.

2.10. Quantification of Mitochondrial DNA (mtDNA) Damage by Real-Time PCR.

After the appropriate treatment, cells were harvested, and total DNA was isolated using Gen-Elute™ Mammalian Genomic DNA Miniprep Kits (Sigma-Aldrich # G1N350-1KT). Real-time DNA amplification was performed using a CFX96 Touch Real-Time PCR Detection System (Bio-Rad) as we performed earlier [25]. The following rat primer sequences were used: SRPCR (210 bp) forward: 5′-ATGCACGATAGCTAAGACCCAA-3′; reverse: 5′-CTGAATTAGCGAGAAGGGGTA-3′ and LRPCR (14958 bp) forward: 5′-ATTTTCTCCCAGTTACGAAAG-3′, reverse: 5′-CTTGGTAAGTAAATTTCTTTCTCC-3′. Short fragment, cytochrome c oxidase subunit 1 (COX1), cytochrome c oxidase subunit 3 (COX3), and β-actin were done using a Brilliant II QPCR Master Mix (Agilent Technologies, # 600804).

The final SRPCR, COXI, COXIII, and β-actin cycling parameters followed hot start of 10 min at 95°C, followed by 30 sec at 95°C, 1 min at 60°C, and 30 sec at 72°C for 40 cycles. LRPCR was done using PfuUltra II Hotstart 2x Master Mix (Agilent Technologies, #600852). The final LRPCR cycling parameters followed manufacturer's recommendations: hot start of 2 min at 92°C, followed by 15 sec at 92°C, 30 sec at 50°C, and 8 : 00 min at 68°C for 40 cycles. The relative mitochondrial DNA content was determined by real-time PCR, using COX1 and COX3 primers, normalized to a nuclear-encoded β-actin gene. The following rat primer sequences were used: COX1 (199 bp) forward: 5′-CACAGTAGGGGGCCTAACAG-3′, reverse: 5′-CAAAGTGGGCTTTTGCTCAT-3′; COX3 (244 bp) forward 5′-TCAGGAGTCTCAATTACATG-3′, reverse: 5′-CGTAGTAGACAGACAATTAGG-3′; β-actin (191 bp) forward 5′-GCGGTGACCATAGCCCTCTTT-3′, reverse: 5′-TGCCACTCCCAAAGTAAAGGGTCA-3′. The software automatically generated crossing points and calculation of mtDNA damage was made using the $\Delta 2^{Ct}$ method. EvaGreen dye was used (Biotium # 31000).

2.11. Mitochondrial Membrane Potential Measurement with JC-1 Assay.

The mitochondrial membrane potential ($\Delta\Psi$m) was measured using the mitochondrial membrane potential specific fluorescent probe, JC-1 (Enzo Life Sciences, ENZ-52304) as we performed it earlier [25]. NRCM cells were seeded on glass coverslips coated with gelatin and cultured for at least 2 days before the experiment. After the treatment, cells were washed in PBS and incubated for 15 min at 37°C in

(a)

(b)
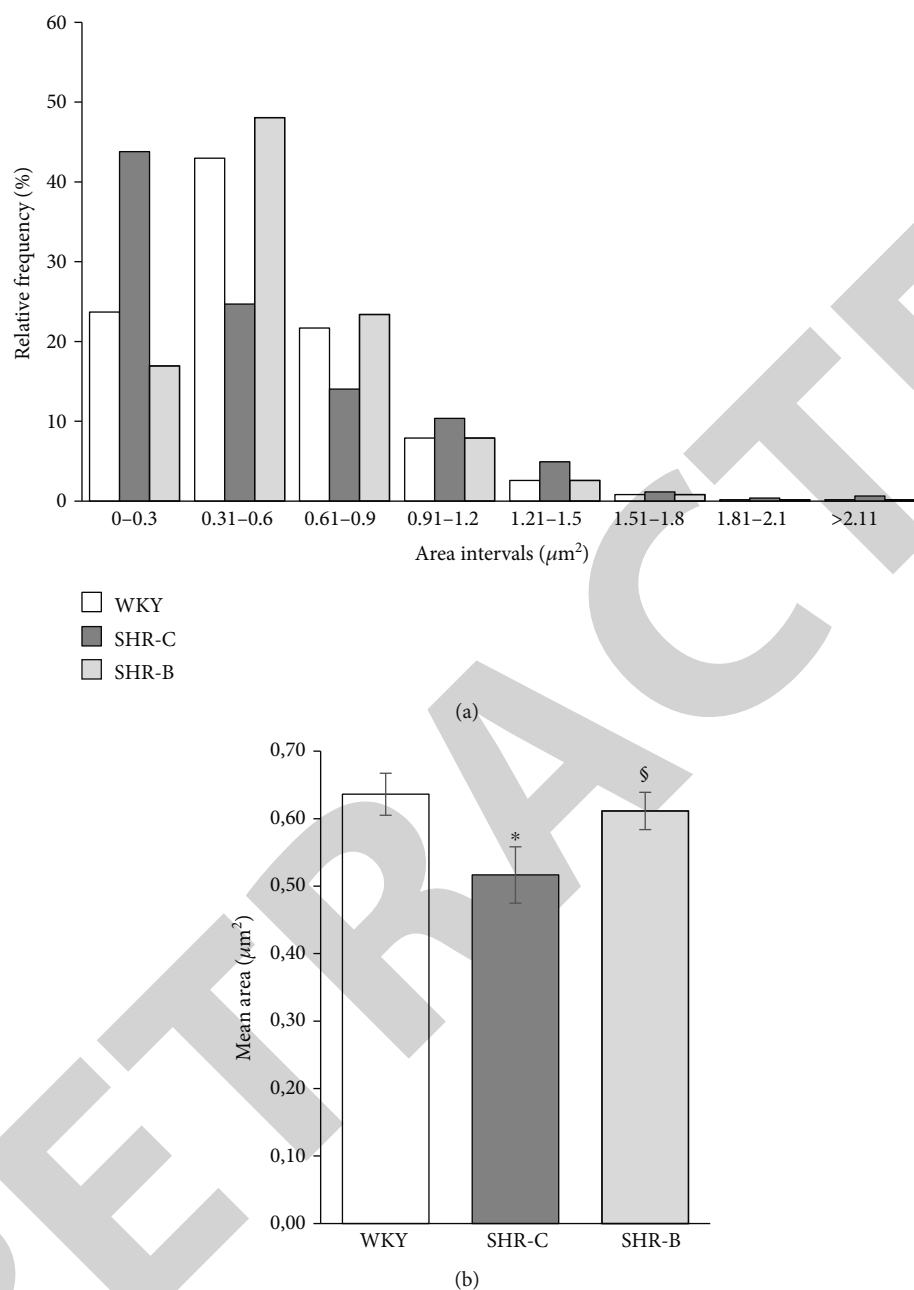
Figure 4: Heart failure-induced fragmentation of interfibrillar mitochondria in the myocardium. (a) Relative frequencies of measured mitochondrial areas in each arbitrary area interval. (b) Means of area values in given groups (~500 mitochondria/group). WKY: age-matched normotensive Wistar-Kyoto rats; SHR-C: nontreated spontaneously hypertensive rats; SHR-B: spontaneously hypertensive rats receiving BGP-15 for 18 weeks. Data are expressed as mean ± SEM. $^*p < 0.05$ vs. WKY, $^\$p < 0.05$ vs. SHR-C.

media containing $5\,\mu$g/mL JC-1. When excited at 488 nm, the dye emits red fluorescence (590 nm) at high $\Delta\Psi$m and green (530 nm) at low $\Delta\Psi$m. Following incubation, the cells were washed once with PBS and then imaged with a Nikon Eclipse Ti-U fluorescent microscope equipped with a Spot RT3 camera using a 60x objective and epifluorescent illumination. All experiments were repeated three times. Fluorescent signals were quantified by using the ImageJ software (NIH, Bethesda, MD, USA).

2.12. Evaluation of the Mitochondrial Energy Metabolism and Function. As we described earlier, Agilent Seahorse Extracellular Flux (XFp) Analyzer (Agilent Technologies, (Santa Clara, CA, USA)) was used to determine the NRCM cells' oxygen consumption rate (OCR) [25]. NRCM cells were seeded in XFp Miniplate at a density of 4×10^4 cells/well in $80\,\mu$L complete growth medium (DMEM for Primary Cell Isolation containing 10% FBS, 100 IU/mL penicillin and $100\,\mu$g/mL streptomycin) and incubated at 37°C, 5% CO_2
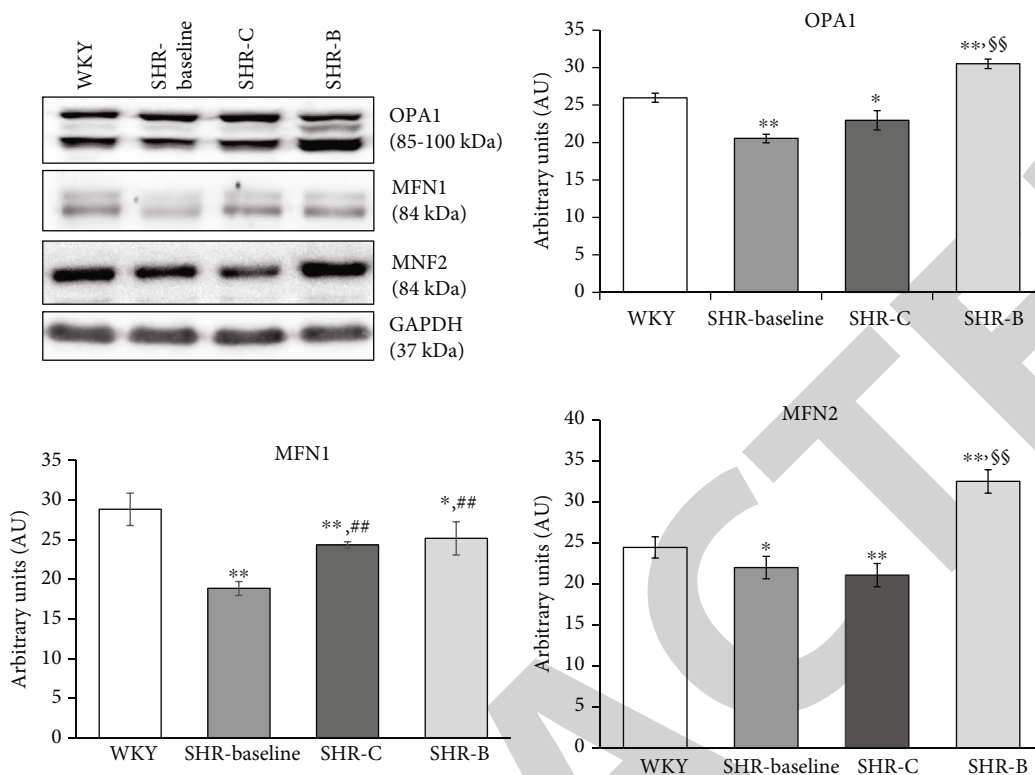
FIGURE 5: Effect of BGP-15 treatment on mitochondrial fusion proteins in a hypertension-induced heart failure model. Western blot analysis of OPA1, MFN1, and MFN2 proteins as well as densitometric evaluations is shown. GAPDH was used as a loading control. WKY: age-matched normotensive Wistar-Kyoto rats; SHR-Baseline: 15-month-old spontaneously hypertensive rats; SHR-C: 19-month-old nontreated spontaneously hypertensive rats; SHR-B: 19-month-old spontaneously hypertensive rats receiving BGP-15 for 18 weeks ($n = 4$). Values are mean ± SEM. $^*p < 0.05$ vs. WKY, $^{**}p < 0.01$ vs. WKY, $^{##}p < 0.01$ vs. SHR-Baseline, $^{§§}p < 0.01$ vs SHR-C.

for 2 days. On the day before the experiment, sensor cartridges were hydrated in XFp calibrant and maintained at 37°C without CO_2 overnight. On the day of the assay, after subjecting cells to the appropriate treatment, DMEM for Primary Cell Isolation medium was replaced by Agilent Seahorse XF Base Medium containing 1 mM pyruvate, 2 mM glutamine, and 10 mM glucose (adjusted pH to 7.4 with 0.1 N NaOH). Before measurement, different compounds were loaded into the appropriate ports of a hydrated sensor cartridge (10 μM oligomycin, 10 μM FCCP, and 5 μM rotenone/antimycin). Three measurements were performed after each injection. OCR was used to determine mitochondrial energy metabolism. The parameter values, including basal respiration, maximal respiration, ATP-associated OCR, and spare respiratory capacity, were determined according to the Seahorse XFp Cell Mito Stress user guide protocol. Data were analyzed using the Seahorse XF test report analysis.

2.13. Analysis of Citrate Synthase Activity in NRCM Cells. NRCM cells were seeded at a density of 10^6 cells/well in 6-well plates and cultured. After the appropriate treatment, cells were harvested; the cell pellet was suspended in ice-cold citrate synthase cell lysis buffer and, then, centrifuged for 5 min at 4°C at 10,000 x g; then, the supernatant was collected for further use. Citrate synthase was measured using a kit from Sigma Aldrich (MAK193) following the manufacturer's instruction. The absorbance was recorded at 412 nm

every 5 minutes for 50 minutes. The colorimetric product (GSH) was proportional to the enzymatic activity of citrate synthase and normalized to the quantity of cells.

2.14. Statistical Analysis. Statistical analysis was performed by analysis of variance, and all of the data were expressed as the mean ± SEM. The homogeneity of the groups was tested by F-test (Levene's test). There were no significant differences among the groups. Comparisons among groups were made by one-way ANOVA with a post hoc correction (SPSS for Windows, version 21.0). The Student's *t*-test was used to compare the mean values of two groups. A value of $p < 0.05$ was considered statistically significant.

3. Results

3.1. In Vivo Results

3.1.1. Effect of BGP-15 Administration on Gravimetric Parameters and on BNP Level. At the beginning of the study, the body weight of WKY rats was significantly higher than the SHR rats (WKY: 391.51 ± 8.64 g, SHR-C: 340.66 ± 6.74 g, SHR-B: 347.4 ± 10.38 g; $p < 0.05$, WKY vs. SHR groups; Table 1). Similar observation can be made at the end of the study (WKY: 403.22 ± 10.35 g, SHR-C: 352.13 ± 6.86 g, SHR-B: 365.29 ± 6.82 g; $p < 0.05$ WKY vs. SHR groups). At the end of the study, heart weights (HW) and ventricles
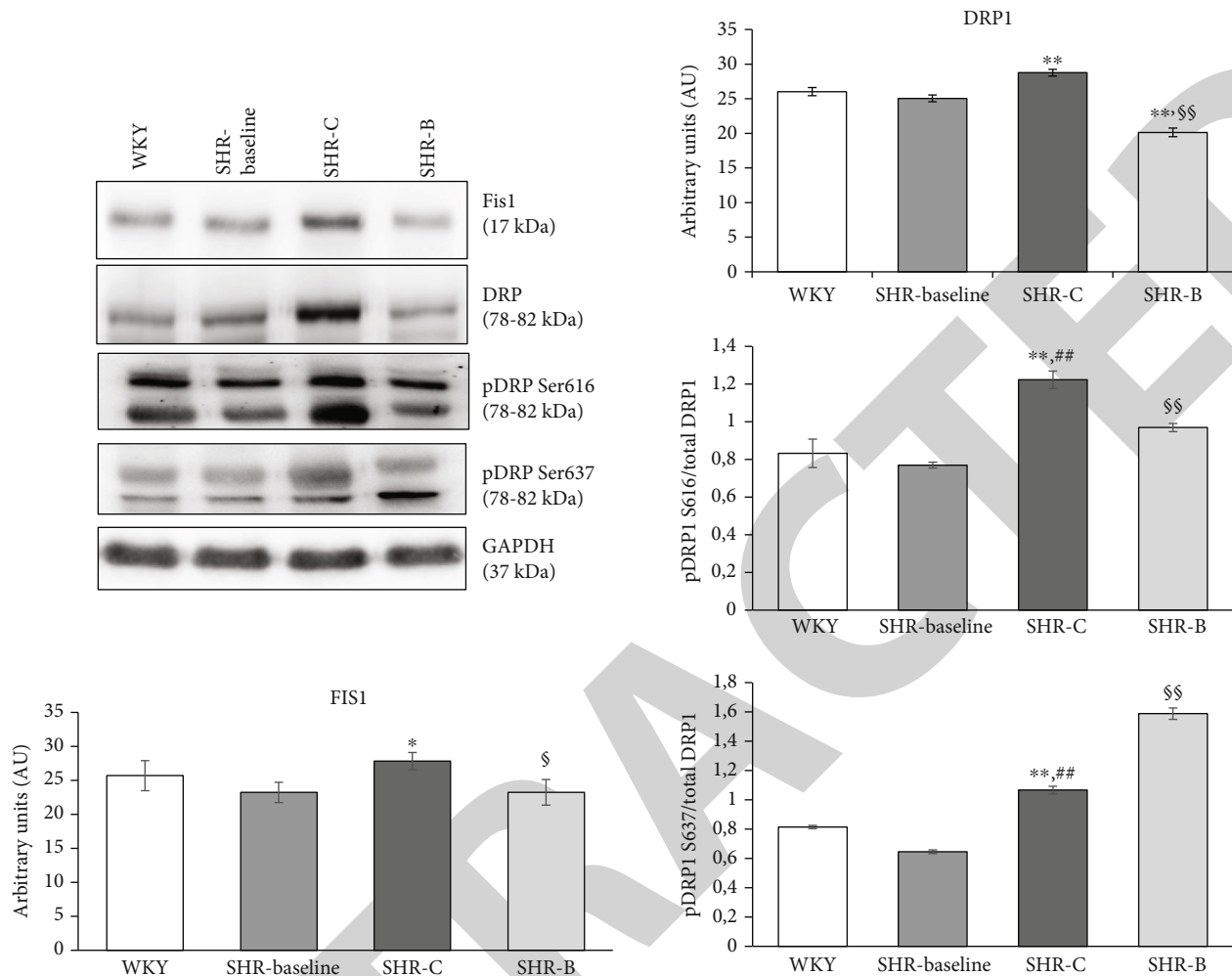
FIGURE 6: Effect of BGP-15 treatment on mitochondrial fission proteins in a hypertension induced-heart failure model. Western blot analysis of Fis1 and DRP1 proteins, as well as densitometric evaluation, is shown. GAPDH was used as a loading control. WKY: age-matched normotensive Wistar-Kyoto rats; SHR-Baseline: 15-month-old spontaneously hypertensive rats; SHR-C: 19-month-old nontreated spontaneously hypertensive rats; SHR-B: 19-month-old spontaneously hypertensive rats receiving BGP-15 for 18 weeks ($n = 4$). Values are mean ± SEM. $^*p < 0.05$ vs. WKY, $^{**}p < 0.01$ vs. WKY, $^{##}p < 0.01$ vs. SHR-Baseline, $^{§}p < 0.05$ vs. SHR-C, $^{§§}p < 0.01$ vs. SHR-C.

weight (VW) were significantly increased in the SHR groups compared to the WKY group (HW: WKY: 1.11 ± 0.03 g, SHR-C: 1.41 ± 0.03 g, SHR-B: 1.28 ± 0.02 g; $p < 0.01$ SHR-B and SHR-C vs.WKY, $p < 0.05$ SHR-B vs. SHR-C; VW: WKY: 0.98 ± 0.03 g, SHR-C: 1.27 ± 0.02 g, SHR-B: 1.12 ± 0.02 g; $p < 0.05$ SHR-groups vs. WKY). The ratio of ventricular weight to body weight (VW/BW) was increased markedly in SHR groups compared to WKY animals (VW/BW (mg/g): WKY: 2.43 ± 0.07, SHR-C: 3.60 ± 0.04, SHR-B: 3.07 ± 0.09; $p < 0.01$ SHR groups vs. WKY, $p < 0.05$ SHR-B vs. SHR-C). Ventricular weight to the length of right tibia ratio (VW/TL) was also significantly increased (VW/TL (mg/mm): WKY: 21.43 ± 0.71, SHR-C: 29.14 ± 0.14, SHR-B: 24.81 ± 0.53; $p < 0.05$ SHR-groups vs. WKY). BGP-15 treatment caused a significant moderation of these ratios ($p < 0.05$ SHR-B vs. SHR-C).

By the end of the treatment, the plasma BNP level increased significantly in the SHR-C group compared to the WKY group (BNP (pg/ml): WKY: 302.76 ± 13.7684; SHR-C: 755.14 ± 33.34; SHR-B: 352.04 ± 22.50; $p < 0.05$ vs.

WKY group; Table 1). However, BGP-15 treatment caused a marked reduction of the BNP level in hypertensive animals ($p < 0.05$, SHR-B vs. SHR-C).

3.1.2. Effect of BGP-15 Administration on Mitochondrial Ultrastructure.
Longitudinal sections of the myocardium were evaluated to assess the status of interfibrillar mitochondria (IFM) by electron microscopy. The mitochondria of SHR-C rats differ from the normal mitochondria of WKY rats (Figures 2(a)–2(c)), because they are morphologically more heterogeneous ($n = 5$ from each group, 3–5 block from each animal). In the nontreated hypertensive animals (SHR-C), mitochondria were loosely arranged between the contractile elements (Figures 3(a) and 3(b)). Moreover, in the SHR-C group, extensive disruption of mitochondrial cristae and enlarged intracristal spaces could be observed (Figure 3(c)). Their shape was often elongated, and the mitochondrial matrix was very light. The mitochondrial ultrastructure in the SHR-B group was
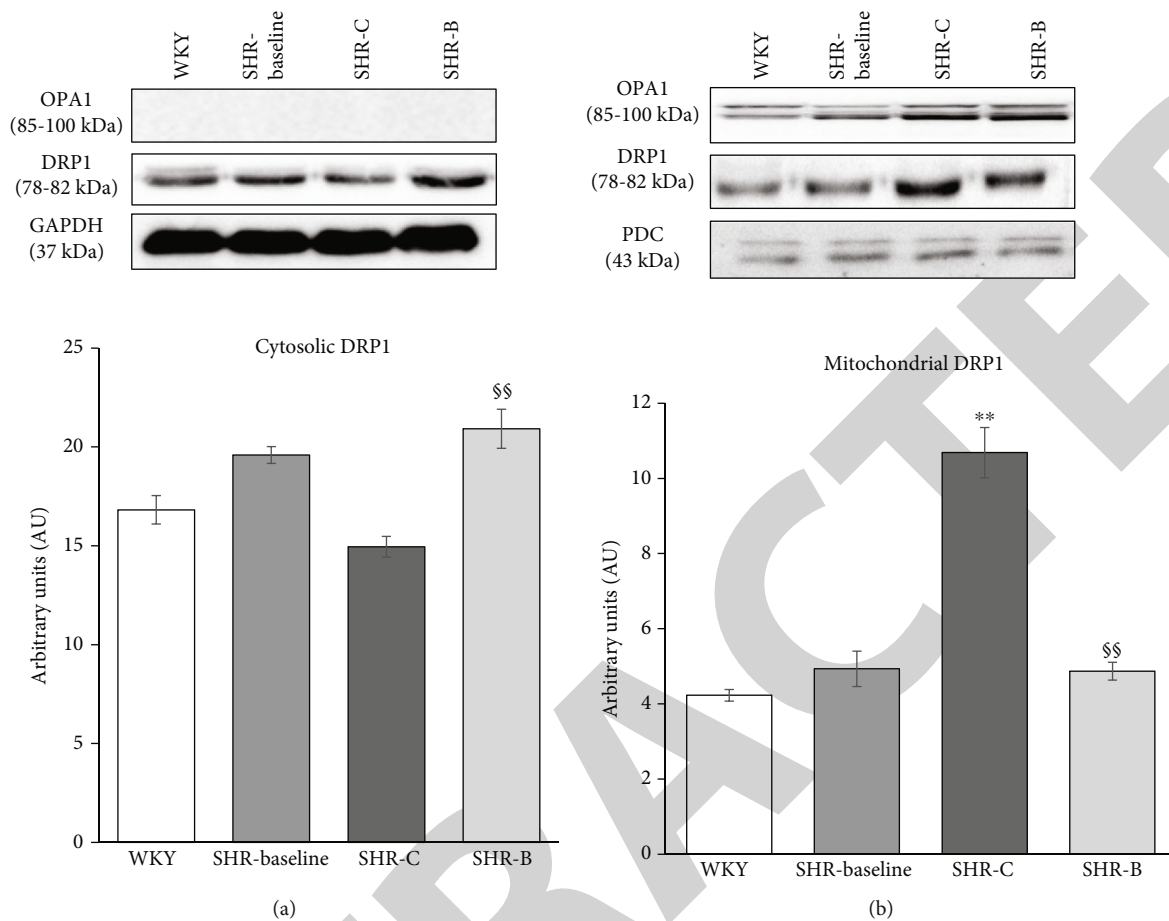
FIGURE 7: Effect of BGP-15 treatment on DRP1 protein intracellular distribution in a hypertension-induced heart failure model. Western blot analysis regarding the intracellular distribution of DRP1 protein and densitometric evaluation are also shown. GAPDH and PDC were used as a loading control. WKY: age-matched normotensive Wistar-Kyoto rats; SHR-Baseline: 15-month-old spontaneously hypertensive rats; SHR-C: 19-month-old nontreated spontaneously hypertensive rats; SHR-B: 19-month-old spontaneously hypertensive rats receiving BGP-15 for 18 weeks ($n = 4$). Values are mean ± SEM. ** $p < 0.01$ vs. WKY, $\S\S p < 0.01$ vs SHR-C.

similar to that of WKY rats (Figures 3(d) and 3(e)). In treated SHR animals (SHR-B), normal, large, and less elongated mitochondria with tightly packed cristae and electron-dense matrix were seen (Figure 3(f)). The area of IFM was assessed on electron micrographs (~500 mitochondria/group were measured; Figure 4(b)). We assessed relative frequencies of the measured mitochondrial areas in arbitrary intervals of $0.3 \mu m^2$ (Figure 4(a)). In all the groups, less than 1% of mitochondrial areas were above the $1.81 \mu m^2$ value. In the SHR-C group, 43.7% of the measured mitochondria belonged to the lowest area range ($<0.3 \mu m^2$). However, in the WKY group, the predominant area range of the measured mitochondria was between 0.3 and $0.6 \mu m^2$. Due to BGP-15 treatment (SHR-B), the distribution of mitochondria was similar to that of the WKY group and the highest number of mitochondria (48%) belonged to the 0.3-$0.6 \mu m^2$ range ($p < 0.05$, SHR-B vs. SHR-C). Our results showed a profound decrease in the mean mitochondrial area of SHR-C group compared to the mitochondria of WKY animals ($p < 0.05$, SHR-C, vs. WKY). The values of BGP-15-treated SHRs differed from that of the SHR-C group ($p < 0.05$), and it was similar to the mitochondria of normotensive animals (WKY).

3.1.3. Effect of BGP-15 Treatment on Mitochondrial Fusion Proteins in SHR Animals.
Regarding the mitochondrial fusion proteins, we determined the levels of OPA1, MFN1, and MFN2 in the myocardium using Western blot analysis (Figure 5). We observed that the level of OPA1 was moderately decreased in the SHR-C group compared to the WKY group ($p < 0.05$, SHR-C vs. WKY). However, BGP-15 treatment caused a significant elevation of OPA1 level in the SHR-B group ($p < 0.01$ SHR-B vs. WKY, $p < 0.05$ SHR-B vs. SHR-C). Considering the amount of MFN1 protein level, there was a significant increase in hypertensive animals by the end of the study compared to the baseline levels ($p < 0.05$, SHR-C and SHR-B vs. SHR-Baseline); however, there was no difference between the SHR groups. The level of MFN2 protein was moderately lower in the SHR-C group than in the WKY group ($p < 0.05$), as observed in the case of OPA1. In the SHR-B group, this parameter increased significantly due to the treatment compared to the other groups ($p < 0.01$ SHR-B vs WKY, SHR-C).

3.1.4. Effect of BGP-15 Administration on Mitochondrial Fission Proteins in SHR Animals.
The levels of fission
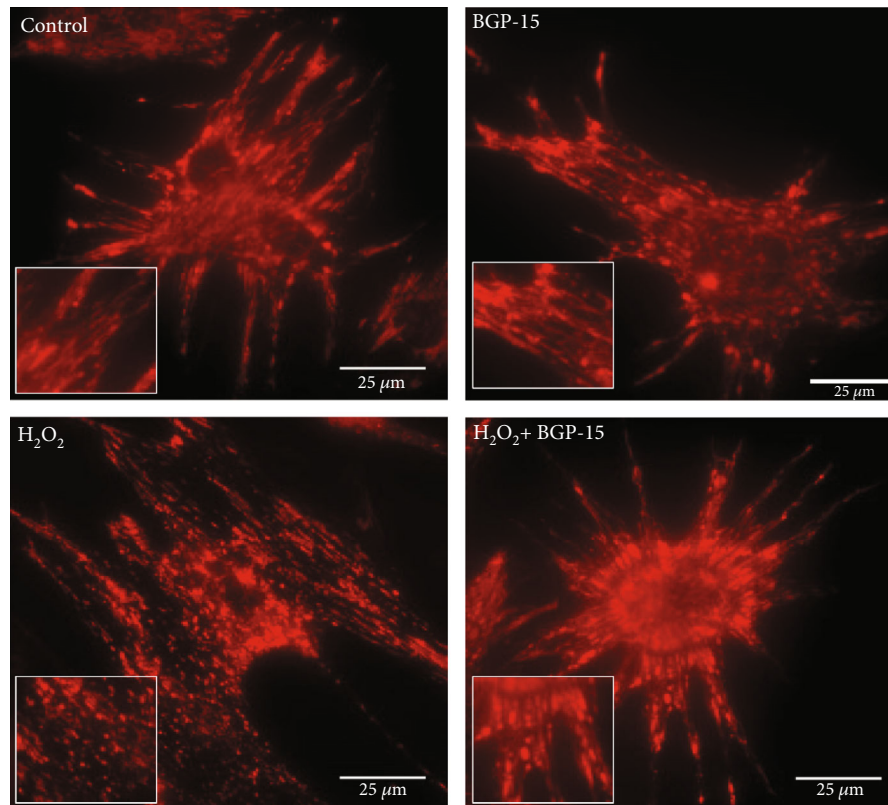
FIGURE 8: Effect of BGP-15 administration on the morphology of mitochondrial network in NRCM cells. For methodical details, see chapter "Materials and Methods." BGP-15 treatment prevented the mitochondrial network from the oxidative stress-induced fragmentation and preserved mitochondria predominantly in the normal filamentous state. The inserts show the filamentous and fragmented states, showing that BGP-15 protected the mitochondrial network. Control group: cells without any treatment; BGP-15 group: cells with only 50 μM BGP-15 for 0.5 hours; H_2O_2 group: cells with 150 μM H_2O_2 for 0.5 hours; H_2O_2+BGP-15 group: cells with 150 μM H_2O_2 and 50 μM BGP-15 for 0.5 hours.

proteins Fis1 and DRP1 were determined in the myocardium in total and in fractionated Western blot samples (Figure 6). The level of Fis1 increased in the SHR-C group compared to the WKY group ($p < 0.05$, SHR-C vs. WKY). This elevation was, however, diminished significantly due to BGP-15 treatment ($p < 0.05$ SHR-B vs. SHR-C). In the case of the fission protein DRP1, the total level was significantly decreased due to BGP-15 treatment compared to other groups ($p < 0.01$ SHR-B vs. WKY, SHR-C). The phosphorylation level of DRP1 at the Ser616 and Ser637 residues was also measured. The phosphorylation of DRP1^{Ser616} and DRP1^{Ser637} was moderate in the WKY group. In the SHR-C group, however, phosphorylation of DRP1^{Ser616} was increased significantly ($p < 0.01$ vs. WKY and SHR-Baseline). BGP-15 treatment decreased DRP1^{Ser616} phosphorylation in SHR-B animals ($p < 0.01$ vs. SHR-C group). Regarding the phosphorylation level of DRP1^{Ser637}, we observed a significant increase in the SHR-C group ($p < 0.01$ vs. WKY, SHR-Baseline). Moreover, BGP-15 treatment caused a further increase in the DRP1^{Ser637} phosphorylation in SHR-B animals ($p < 0.01$ SHR-B vs. SHR-C).

The intracellular distribution of DRP1 was also measured (Figure 7). We observed that the Drp1 accumulated in the mitochondrial fractions of SHR-C animals compared to normotensive animals ($p < 0.01$, SHR-C vs.

WKY). BGP-15 treatment resulted in a significantly reduced translocation of Drp1 into the mitochondria ($p < 0.01$ vs. SHR-C), thereby preserving it in a higher concentration in the cytosolic fraction.

3.2. In Vitro Results

3.2.1. Effect of BGP-15 Administration on Mitochondrial Morphology of NRCM Cells. To examine the changes of the mitochondrial network, we used the MitoTracker Red CMXRos staining method (Figure 8). BGP-15 per se had no effect on the complexity of the mitochondrial network. Filamentous mitochondrial network was observed in the Control group; H_2O_2 treatment, however, caused a marked injury to the mitochondrial network. As a result of the H_2O_2-induced fission processes, degradation of the mitochondrial network could be observed which led to mitochondrial fragmentation. BGP-15 treatment prevented the mitochondrial network from the oxidative stress-induced fragmentation and preserved the normal filamentous network of mitochondria.

3.2.2. Effect of BGP-15 Treatment on Mitochondrial Fusion Proteins in NRCMs. We assessed the levels of OPA1, MFN1 and MFN2 proteins in total Western blot samples of NRCM cells (Figure 9). BGP-15 treatment per se had no effect in the
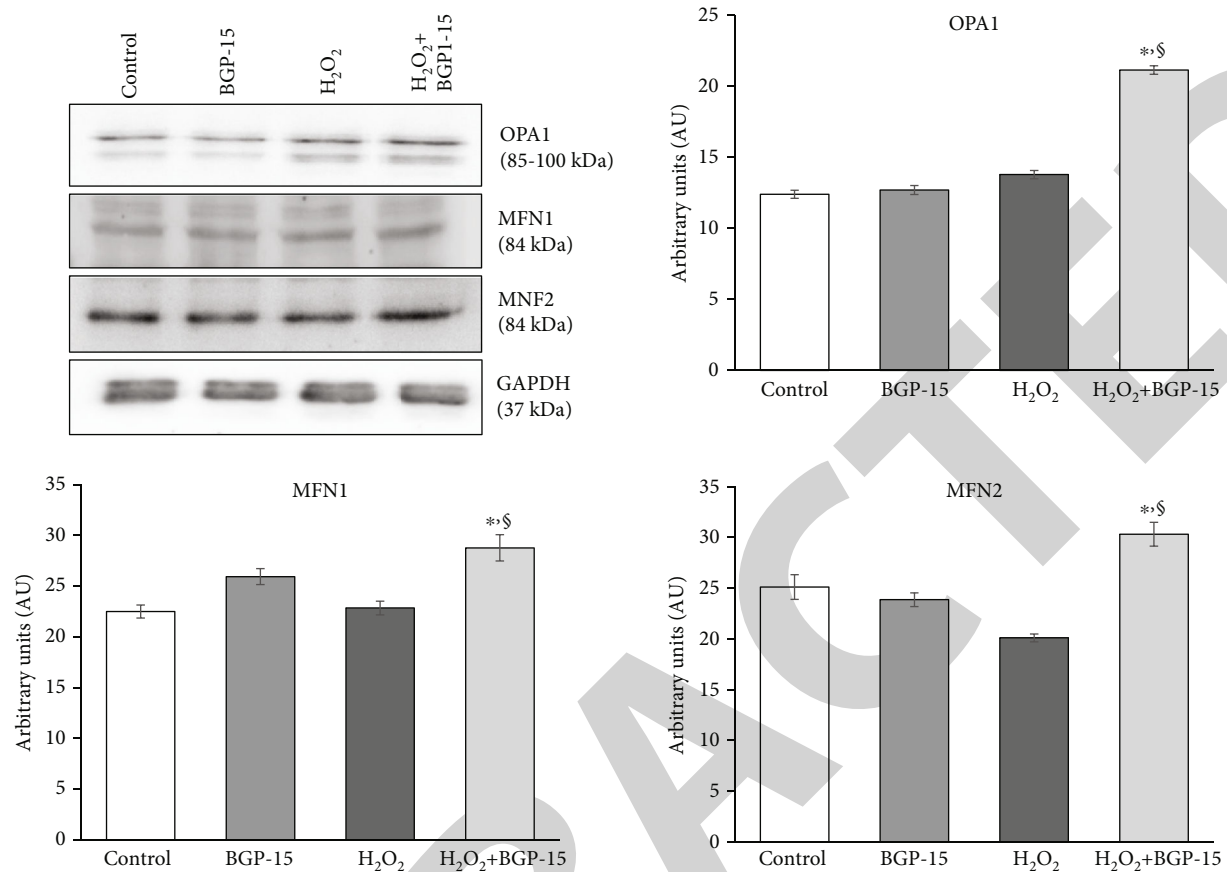
FIGURE 9: Effect of BGP-15 treatment on mitochondrial fusion proteins in NRCM cells. Western blot analysis of OPA1, MFN1, and MFN2 as well as densitometric evaluation is shown. GAPDH was used as a loading control. Control group: cells without any treatment; BGP-15 group: cells with only 50 μM BGP-15 for 0.5 hours; H_2O_2 group: cells with 150 μM H_2O_2 for 0.5 hours; H_2O_2+BGP-15 group: cells with 150 μM H_2O_2 and 50 μM BGP-15 for 0.5 hours. Values are mean ± SEM ($n = 4$). $^*p < 0.05$ vs. Control, $^\S p < 0.05$ vs. H_2O_2 group.

nonstressed cells in comparison to the Control group. H_2O_2 treatment caused a slight decrease in the level of MFN1 and MFN2 proteins and a slight increase in the level of OPA1, but these changes were not significant. BGP-15 treatment caused a significant increase of OPA1, MFN1, and MFN2 proteins in H_2O_2 stressed cells compared to the H_2O_2-stressed group ($p < 0.05$ H_2O_2-BGP15 vs. H_2O_2).

3.2.3. Effect of BGP-15 Administration on Mitochondrial Fission Proteins in NRCMs. We determined the levels of Fis1 and DRP1 in total and in fractionated Western blot samples in NRCM cells (Figure 10). No significant difference was found with BGP-15 treatment in nonstressed cells compared to the Control group. The level of Fis1 increased markedly in the H_2O_2 group compared to the Control group ($p < 0.01$, H_2O_2 vs. Control). Due to BGP-15 treatment, this change was blunted ($p < 0.05$, H_2O_2-BGP15 vs. H_2O_2 group). The case of the fission mediator DRP1 protein total level was a significant elevation in the H_2O_2 group due to oxidative stress ($p < 0.05 H_2O_2$ vs. Control group). However, a control-like value could be seen in the treated group compared to the H_2O_2 group ($p < 0.05$ H_2O_2-BGP15 vs. H_2O_2 group). The phosphorylation of DRP1 on Ser616 and Ser637 residues was also evaluated. The phosphorylation of

both DRP1 phospho-form was moderate in the Control group. Phosphorylation of DRP1[Ser616] increased considerably in the H_2O_2 group ($p < 0.05$ H_2O_2 vs. Control group). However, BGP-15 treatment decreased DRP1[Ser616] phosphorylation compared to nontreated stressed cells ($p < 0.05$ H_2O_2-BGP-15 vs. H_2O_2 group). Measuring the phosphorylation level of DRP1[Ser637], a significant decrease could be observed in the H_2O_2 group compared to the Control group ($p < 0.01$ H_2O_2 vs. Control group). However, BGP-15 treatment enhanced remarkably the DRP1[Ser637] phosphorylation ($p < 0.01$ H_2O_2-BGP15 vs. H_2O_2 group).

Finally, the intracellular distribution of fission mediator DRP1 protein was examined (Figure 11). A significantly higher portion of DRP1 could be found in the mitochondrial fraction of cells in the H_2O_2 group compared to the BGP-15-treated group. The translocation of DRP1 protein from the cytosol to the mitochondria was moderated as a result of the BGP-15 treatment and in this way resulted in higher levels of DRP1 in the cytosolic fraction and lower concentration in the mitochondrial fraction ($p < 0.01$ vs. H_2O_2 group).

3.2.4. Effect of BGP-15 Treatment on the Regulatory Factors of Mitochondrial Biogenesis in NRCMs. We determined the levels of PGC-1α, CREB and VDAC in the total Western blot
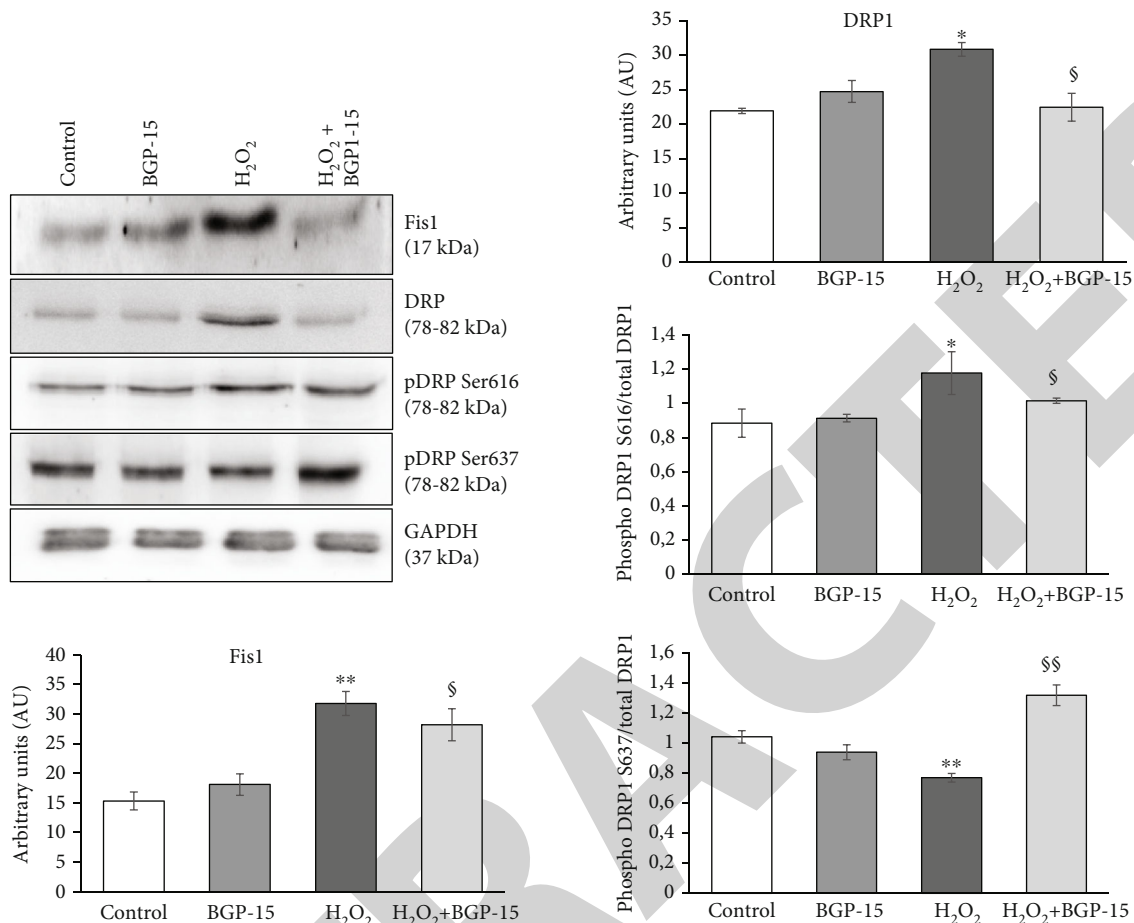
Figure 10: Effect of BGP-15 treatment on mitochondrial fission proteins in NRCM cells. Western blot analysis of Fis1 and DRP1 proteins, as well as densitometric evaluation, is shown. GAPDH was used as a loading control. Control group: cells without any treatment, BGP-15 group: cells with only 50 μM BGP-15 for 0.5 hours; H_2O_2 group: cells with 150 μM H_2O_2 for 0.5 hours; H_2O_2+BGP-15 group: cells with 150 μM H_2O_2 and 50 μM BGP-15 for 0.5 hours. Values are mean ± SEM ($n = 4$). $^*p < 0.05$ vs. Control, $^{**}p < 0.01$ vs. Control, $^§p < 0.05$ vs. H_2O_2 group, $^{§§}p < 0.01$ vs. H_2O_2 group.

samples of NRCMs. BGP-15 treatment had no effect on these factors in nonstressed cells compared to the Control group. The PGC-1α level was increased in the H_2O_2 group compared to the Control group ($p < 0.01$ vs. Control; Figure 12). However, this elevation was much more marked in the treated group ($p < 0.01$ H_2O_2-BGP15 vs. Control and H_2O_2 groups). The phosphorylation level of CREB[Ser133] was low in the Control group. However, a significant increase was seen in the phosphorylation level of CREB-[Ser133] in the H_2O_2 group ($p < 0.01$ H_2O_2 vs. Control) (Figure 12). BGP-15 treatment increased further the phosphorylation level of CREB[Ser133] ($p < 0.01$, H_2O_2-BGP15 vs. H_2O_2 group). The level of VDAC was slightly decreased in the H_2O_2 group compared to the Control group ($p < 0.05$ H_2O_2 vs. Control). The level of the VDAC, however, was significantly elevated in the BGP-15 treated group ($p < 0.01$ H_2O_2-BGP-15 vs. H_2O_2 group).

Moreover, we investigated mitochondrial DNA content compared to the nuclear DNA. The relative mitochondrial DNA content was determined by "real-time" PCR, using COX1 and COX3 primers, normalized to a nuclear-encoded β-actin gene. We found that BGP-15 treatment

increased the relative expression levels of COXI and COXIII genes compared to the H_2O_2 group ($p < 0.05$ H_2O_2-BGP-15 vs. H_2O_2 group; Figure 13).

Furthermore, we also performed a well-accepted method for studying mitochondrial biogenesis by measuring the activity of citrate synthase (Figure 13). Citrate synthase activity was reduced in hydrogen-peroxide stressed group compared to the control group ($p < 0.01$ H_2O_2 vs. Control). The citrate synthase activity was increased significantly due to the treatment ($p < 0.01$ H_2O_2-BGP-15 vs. H_2O_2 group; Figure 13).

Finally, we measured the level of NDUFs1 subunit of NADH-ubiquinone oxidoreductase and UQCRC1 subunit of Ubiquinol Cytochrome c Reductase proteins in order to support our finding regarding the effect of BGP-15 on mitochondrial biogenesis. The expression level of NDUFs1 was significantly decreased in the H2O2 group ($p < 0.01$ H_2O_2 vs. Control; Figure 14). A similar observation was made in the case of UQCRC1 ($p < 0.05$ H_2O_2 vs. Control). However, BGP-15 treatment not only protected against the decrease but also significantly increased the amount of NDUFs1 and UQCRC1 proteins ($p < 0.01$ H_2O_2-BGP-15 vs. H_2O_2 group).
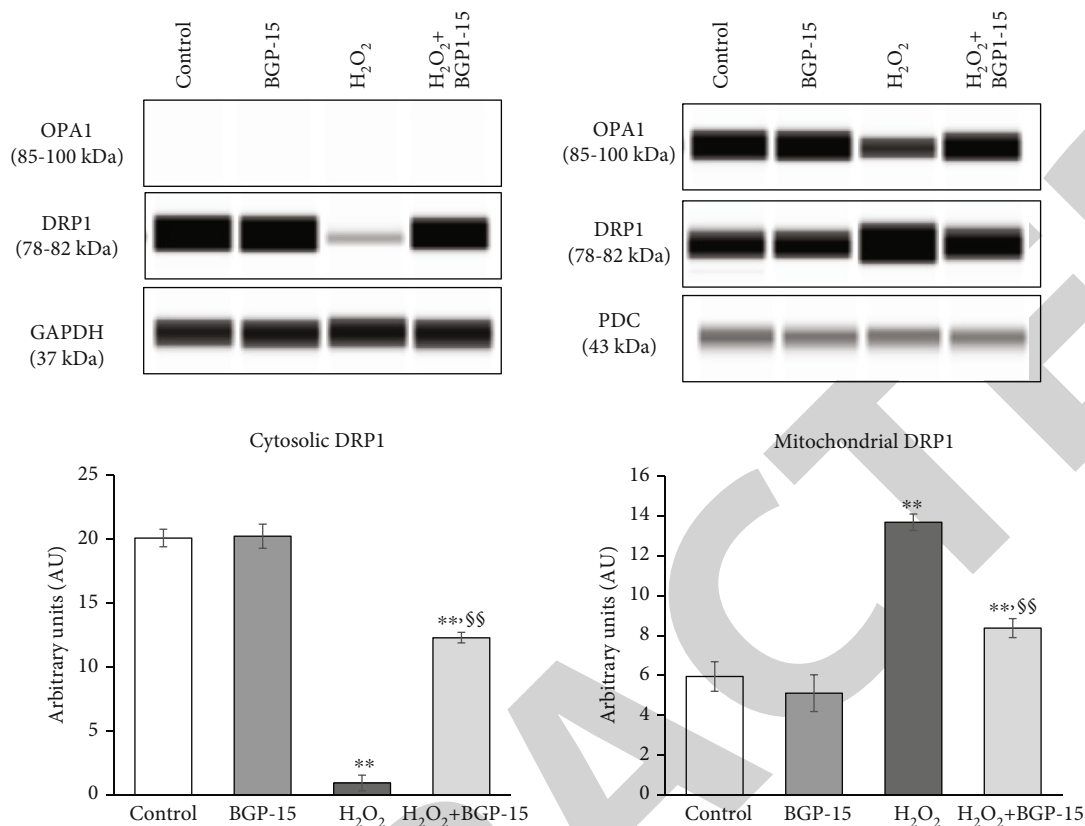
Figure 11: Effect of BGP-15 treatment on intracellular distribution of DRP1 protein in stressed NRCM cells. Western blot analysis of DRP1 protein regarding its intracellular disruption, as well as densitometric evaluation, is shown. GAPDH and PDC were used as a loading control. Control group: cells without any treatment; BGP-15 group: cells with only 50 μM BGP-15 for 0.5 hours; H_2O_2 group: cells with 150 μM H_2O_2 for 0.5 hours; H_2O_2+BGP-15 group: cells with 150 μM H_2O_2 and 50 μM BGP-15 for 0.5 hours. Values are mean ± SEM ($n = 4$). $^{**}p < 0.01$ vs. Control, $^{\S\S}p < 0.01$ vs. H_2O_2 group.

3.2.5. Effect of BGP-15 Administration on Mitochondrial Genome Integrity. Real-time detection of long-range polymerase chain reaction (LRPCR) was used to examine the impact of H_2O_2-induced oxidative injury on mtDNA (Figure 15). No significant difference was found with BGP-15 treatment alone compared to the Control group. H_2O_2 induced a significant damage of the mtDNA ($p < 0.05$, H_2O_2 vs. Control); the amplification rate of the entire mitochondrial genome was markedly diminished. This unfavourable damage was significantly reduced by BGP-15 treatment ($p < 0.01$, H_2O_2-BGP15 vs. H_2O_2).

3.2.6. Effect of BGP-15 on Mitochondrial Membrane Potential ($\Delta\Psi$) in NRCM Cells. We examined the effect of BGP-15 on mitochondrial membrane potential using JC-1, a cell-permeable voltage-sensitive fluorescent mitochondrial dye (Figure 16). JC-1 emits red fluorescence if the mitochondrial membrane potential is high (aggregated dye), while depolarized mitochondria emit green fluorescence (monomer dye). In the control cells, fluorescence microscopy showed strong red fluorescence and weak green fluorescence, which indicates a high $\Delta\Psi$m in mitochondria (Figure 16(a)). BGP-15 per se had no effect on mitochondrial membrane potential. The addition of H_2O_2 to cells facilitates the depolarization of mitochondria, resulting in weaker red fluorescence and

stronger green fluorescence ($p < 0.01$ H_2O_2 vs. Control; Figure 16(b)). If BGP-15 was also administered in peroxide-stressed NRCM cells, red fluorescence increased and green fluorescence decreased compared to the H_2O_2-treated cells ($p < 0.01$, H_2O_2-BGP15 vs. H_2O_2) (Figure 16(b)). Therefore, the quantitative assessment revealed that BGP-15 treatment reduced the H_2O_2-induced depolarization of the mitochondrial membrane; the $\Delta\Psi$m was similar to that of the Control cells.

3.2.7. Effect of BGP-15 on Mitochondrial Oxygen Consumption and Energy Metabolism in NRCM Cells. To determine the mitochondrial energy metabolism and respiratory function, we used the Agilent Seahorse XFp Analyzer system and the Agilent Seahorse XFp Cell Mito Stress Test (Figure 17). BGP-15 itself had no effect on the rate of mitochondrial respiration. The oxygen consumption rate of NRMC cells was decreased in the presence of H_2O_2 to cells compared to Control cells (Figure 17(a)). H_2O_2 treatment decreased the basal respiration although this difference was not significant (Figure 17(b)). However, the maximal respiration, the spare respiratory capacity, and the ATP production were markedly decreased as a result of H_2O_2-induced oxidative damage compared to the Control group ($p < 0.05$, H_2O_2 vs. Control) (Figures 17(c)–17(e)). In the presence of both
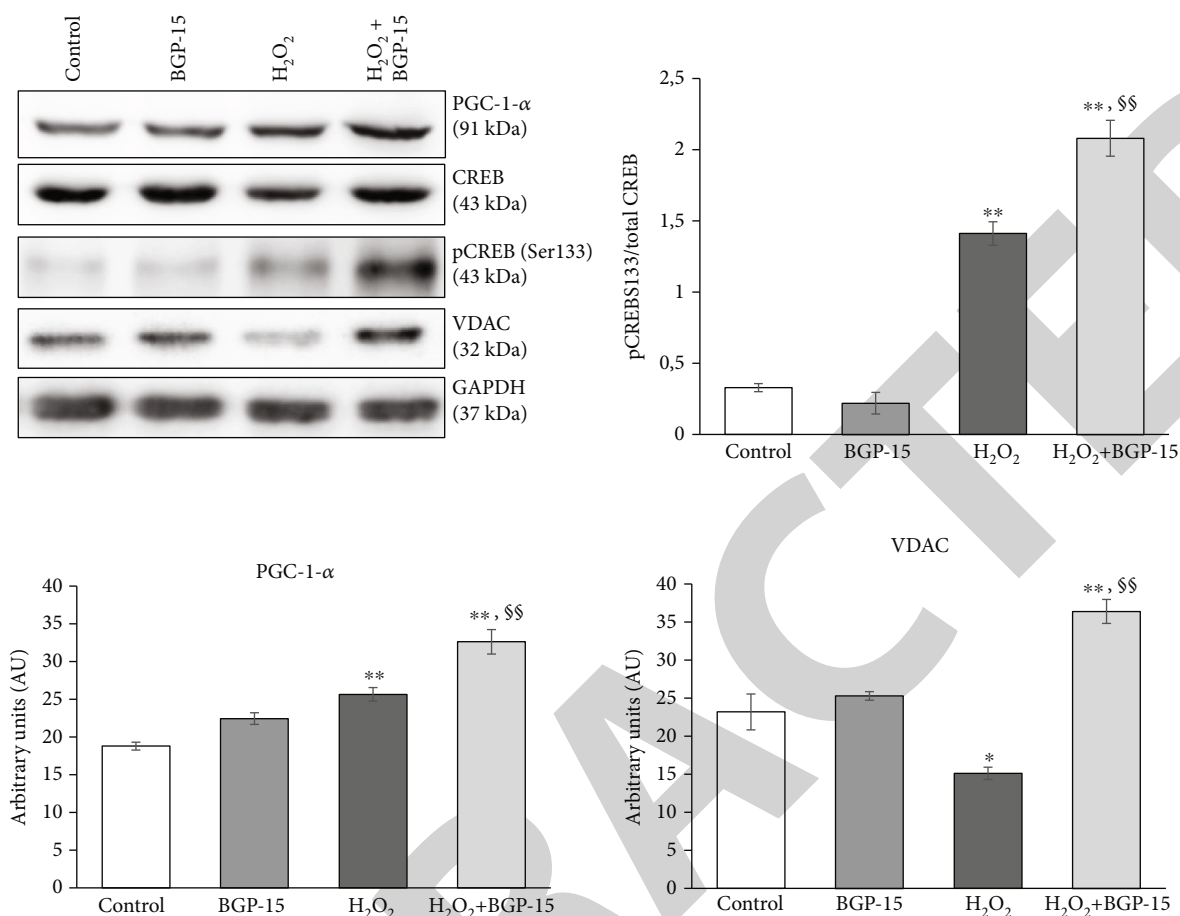
FIGURE 12: Effect of BGP-15 treatment on the regulation of mitochondrial biogenesis in NRCM cells. Western blot analysis of PGC-1-α, CREB, and VDAC proteins as well as densitometric evaluation is shown. GAPDH was used as a loading control. Control group: cells without any treatment; BGP-15 group: cells with only 50 μM BGP-15 for 0.5 hours; H_2O_2 group: cells with 150 μM H_2O_2 for 0.5 hours; H_2O_2+BGP-15 group: cells with 150 μM H_2O_2 and 50 μM BGP-15 for 0.5 hours. Values are mean ± SEM ($n = 4$). $^*p < 0.05$ vs. Control, $^{**}p < 0.01$ vs. Control, $^{\S\S}p < 0.01$ vs H_2O_2 group.

H_2O_2 and BGP-15, the maximal respiration, spare respiratory capacity, and the ATP production were significantly higher compared to the H_2O_2 group ($p < 0.05$, H_2O_2–BGP15 vs. H_2O_2).

4. Discussion

We aimed to study the effect of BGP-15 on various processes of mitochondrial quality control in a hypertension-induced heart failure model and in vitro using hydrogen peroxide-induced oxidative stress. The major findings of this study are that BGP-15, besides its promoting effect on mitochondrial fusion, also inhibits factors playing part in the mitochondrial fission and enhances their de novo biogenesis under stress situations. As a result of these effects, BGP-15 preserves mitochondrial structure and energy production during hydrogen peroxide-induced oxidative stress as well as in an in vivo heart failure model.

In our recent work, spontaneously hypertensive rats (SHR) were used, which is a widely used model in experimental cardiology for the examination of hypertension-induced cardiovascular remodelling and heart failure [26–

28]. 15-month-old SHRs showed already severe left ventricular hypertrophy with mild signs of heart failure. BGP-15 has a positive effect on remodelling processes and cardiac function [29]. In our work, BGP-15 treatment decreased slightly the severity of cardiac hypertrophy, which was proved by gravimetric parameters (weight of ventricles/body weight, weight of ventricles/tibia length) and decreased the severity of heart failure characterized by BNP level (Table 1). In the background of these favourable changes, the mitochondrial structural and functional alterations were assumed.

Mitochondria are dynamic organelles constantly undergoing fusion and fission processes. Hypertension-induced heart failure is characterized by the fragmentation of mitochondria and by compromised energy production leading to decreased contractile force of myofilaments [30, 31]. In our work, mitochondria were structurally damaged in nontreated hypertensive animals (SHR-C). They were loosely arranged between the contractile elements (Figures 3(a)–3(c)). The average size of mitochondria was markedly reduced in the SHR-C group; approximately 40% of mitochondria were smaller than 0.3 μm2 as a result of heart failure-induced mitochondrial fragmentation (Figures 4(a)–
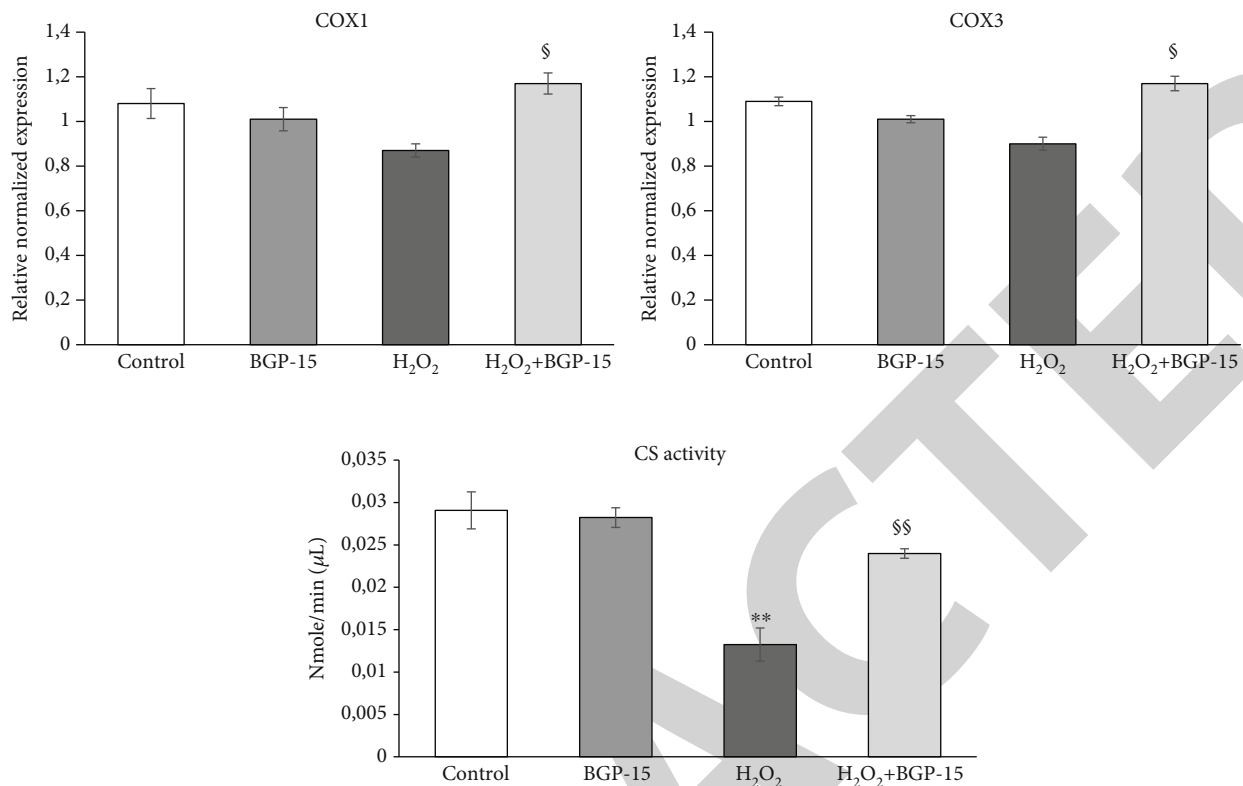
Figure 13: Effect of BGP-15 treatment on the relative DNA content and citrate synthase activity. Relative expression level of electron transport chain complex IV genes (COX1 and COX3 are presented. Comparison of citrate synthase activity in NRCM cells. Control group: cells without any treatment; BGP-15 group: cells with only 50 μM BGP-15 for 0.5 hours, H_2O_2 group: cells with 150 μM H2O2 for 0.5 hours, H2O2+BGP-15 group: cells with 150 μM H_2O_2 and 50 μM BGP-15 for 0.5 hours. Values are mean ± SEM ($n = 4$). **$p < 0.01$ vs. Control, $\S\S p < 0.01$ vs. H_2O_2 group.

4(c)). Ultrastructurally, extensive disruption of mitochondrial cristae and enlarged intracristal spaces was observed. However, BGP-15 treatment resulted in structurally markedly healthier mitochondria that were similar to that of normotensive animals. Mitochondria in the SHR-B group were tightly packed between the myofibrils. Most of mitochondria belonged to the normal size range (0.3-0.6 μm2), which can be—at least partially—the consequence of increased mitochondrial biogenesis. On the ultrastructural level, large mitochondria with tightly packed cristae and electron-dense matrix were seen in the treated group (Figures 3(d)–3(f)).

Oxidative stress induces an imbalance in processes of mitochondrial dynamics, potentially leading to cell death. Proper mitochondrial functions regulated by the quality control processes are fundamental for cardiac work. The deterioration of mitochondrial quality control greatly contributes to the hypertension-induced cardiac remodelling and its progression to heart failure [4, 7, 8]. In our recent study, the expression level of proteins promoting the mitochondrial fusion, particularly OPA1 and MFN2, was increased significantly in the BGP-15-treated animals compared to the SHR-C group (Figure 5). Our results are in accordance with the results of Szabo et al., who published earlier that BGP-15 has promoted mitochondrial fusion in both in vitro and in vivo [18].

Regarding mitochondrial fission, a marked decrease could be seen in the expression levels of DRP1 and Fis1 in hypertensive animals due to BGP-15 treatment (Figure 6). DRP1 is regulated by several posttranslational modifications [32–34]. DRP1^{Ser637} phosphorylation suppresses its translocation to mitochondria and thus inhibits its activity, while DRP1^{Ser616} phosphorylation promotes DRP1 translocation and therefore the mitochondrial fission. BGP-15 treatment increased markedly the DRP1^{Ser637} phosphorylation and decreased the DRP1^{Ser616} phosphorylation in SHR-B animals compared to nontreated hypertensive animals (Figure 6). The subcellular distribution of DRP1 showed changes consistent with the phosphorylation pattern of DRP1. In nontreated hypertensive animals (SHR-C), a high portion of DRP1 could be observed in the mitochondrial fraction (Figure 7). BGP-15 treatment resulted in a significantly reduced translocation to mitochondria of DRP1, retaining it in the cytosolic fraction. This can be a consequence of increased DRP1^{Ser637} phosphorylation in SHR-B animals. Altogether, BGP-15 prevented mitochondria against hypertension-induced fragmentation.

In our in vitro experiments, hydrogen-peroxide was used to induce oxidative injury of NRCM cells. Degradation of the filamentous mitochondrial network by mitochondrial fragmentation could be observed in H_2O_2-stressed NRCM cells. BGP-15 treatment prevented the mitochondrial network
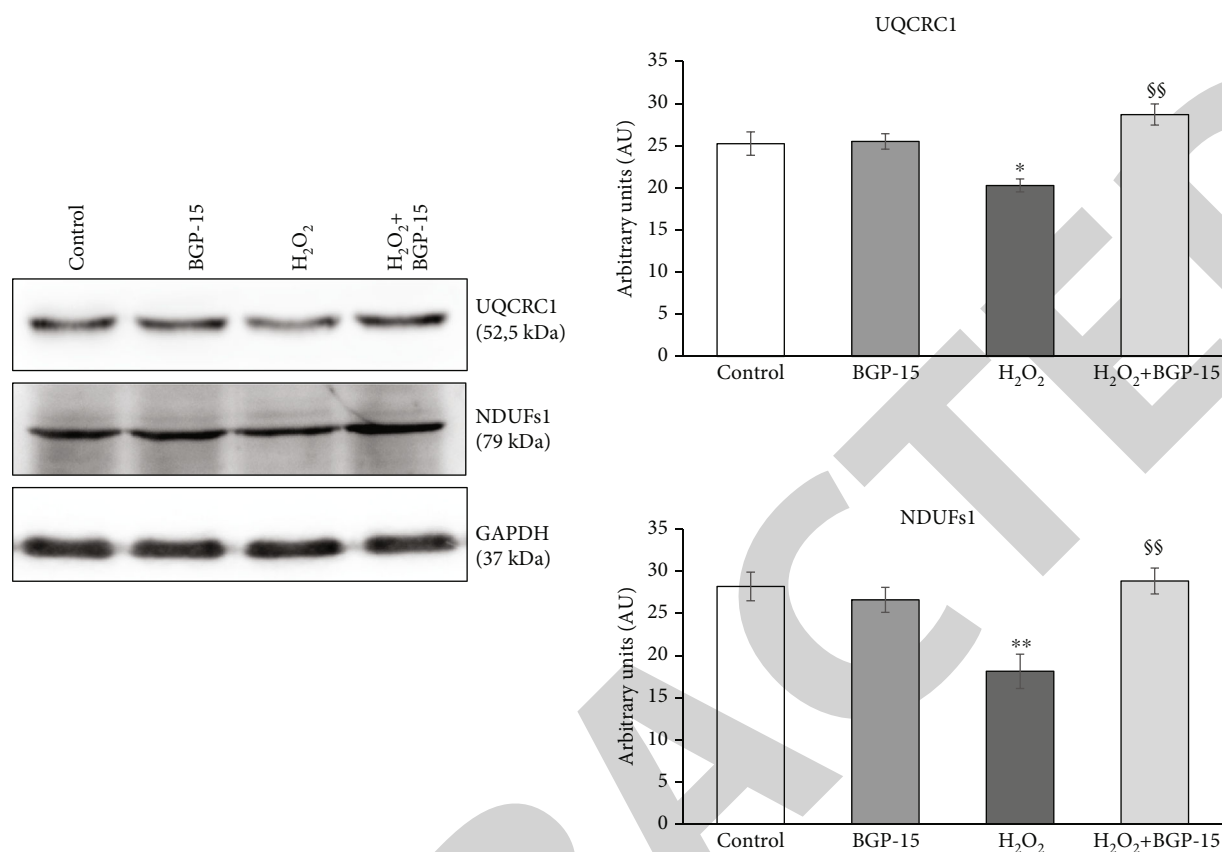
Figure 14: Effect of BGP-15 treatment on the electron transport chain complex I and III proteins in NRCMs. Western blot analysis of UQCRC1 and NDUFs1 proteins as well as densitometric evaluation is shown. GAPDH was used as a loading control. Control group: cells without any treatment; BGP-15 group: cells with only $50 \mu M$ BGP-15 for 0.5 hours; H_2O_2 group: cells with $150 \mu M H_2O_2$ for 0.5 hours; H_2O_2+BGP-15 group: cells with $150 \mu M H_2O_2$ and $50 \mu M$ BGP-15 for 0.5 hours. Values are mean ± SEM ($n = 4$). *$p < 0.05$ vs. Control, ** $p < 0.01$ vs. Control, $^{\S\S}p < 0.01$ vs H_2O_2 group.
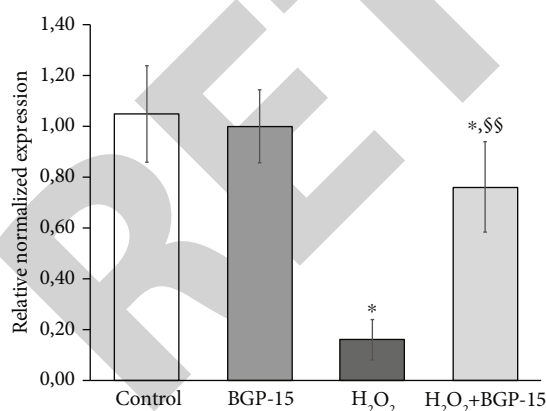
Figure 15: Effect of BGP-15 treatment on oxidative stress-induced mitochondrial DNA damage. Total DNA was isolated for LRPCR and SRPCR analysis. mtDNA damage was calculated using the $\Delta 2^{Ct}$ method. Control group: cells without any treatment; BGP-15 group: cells with only $50 \mu M$ BGP-15 for 0.5 hours; H_2O_2 group: cells with $150 \mu M H_2O_2$ for 0.5 hours; H_2O_2+BGP-15 group: cells with $150 \mu M H_2O_2$ and $50 \mu M$ BGP-15 for 0.5 hours. Values are mean ± SEM ($n = 4$). *$p < 0.05$ vs. Control, $^{\S\S}p < 0.01$ vs H_2O_2 group.

from the oxidative stress-induced fragmentation and preserved mitochondria predominantly in the filamentous state.

Similar changes were seen in the case of fusion and fission processes in NRCM cell culture compared to in vivo model. BGP-15 treatment increased the expression level of fusion proteins (OPA1, MFN1, and MFN2), and thus, it can promote mitochondrial fusion during oxidative stress (Figure 9). On the other hand, the level of fission mediators (DRP1 and Fis1) was decreased due to BGP-15 treatment (Figure 10). BGP-15 also moderated the mitochondrial translocation of DRP1 protein from the cytosol as a result of enhanced DRP1^{Ser637} phosphorylation and decreased phosphorylation of DRP1^{Ser616} (Figure 11). Therefore, BGP-15 treatment has beneficial effects on mitochondrial dynamics by promoting the fusion and blocking the fission processes.

Several studies have demonstrated that mitochondrial biogenesis is compromised in cardiac remodelling and heart failure [35–37]. PGC-1-α is the key regulator of biogenesis, which in turn is regulated by CREB [38–40]. We found that the expression level of PCG-1α increased significantly due to BGP-15 treatment (Figure 12). Moreover, BGP-15 treatment further enhanced the phosphorylation of CREB compared to H_2O_2 group, too (Figure 12). CREB increased the expression level of PGC-1α and therefore

(a)

(b)
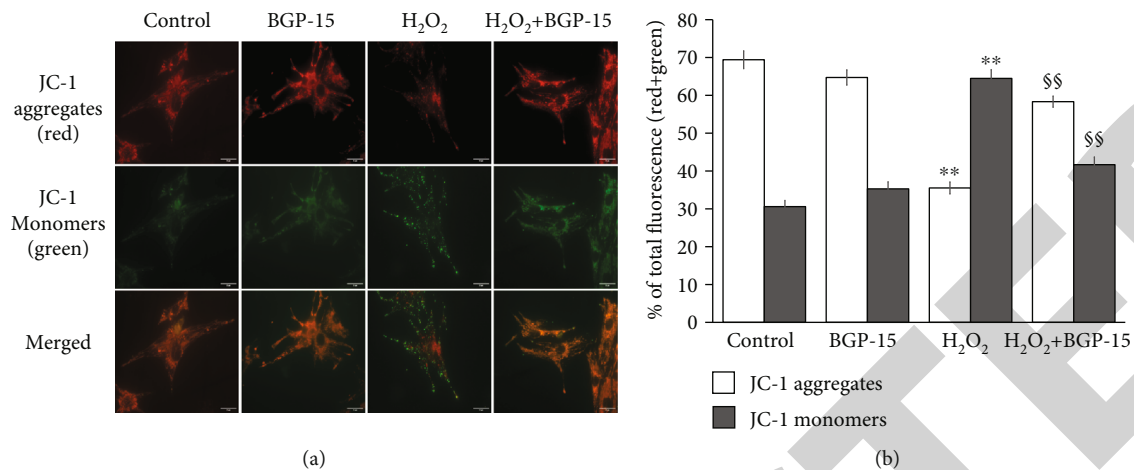
Figure 16: Effect of BGP-15 on the mitochondrial membrane potential in NRCMs, as determined by JC-1. (a) Effect of BGP-15 on H_2O_2-induced mitochondrial membrane depolarization in NRCM cells. Cells were exposed to 150 μm H_2O_2 in the absence or presence of 50 μm BGP-15 for 0.5 hours, after that stained with 100 ng/ml of JC-1. The dye was loaded, and after a 15-minute-long incubation, fluorescent microscopic images were taken using both the red and green channels. Representative merged images are presented. (b) Quantitative analysis of mitochondrial depolarization induced by H_2O_2 (150 μM) and its reduction by BGP-15 (50 μM) in NRCM cells. Control group: cells without any treatment; BGP-15 group: cells with only 50 μM BGP-15 for 0.5 hours; H_2O_2 group: cells with 150 μM H_2O_2 for 0.5 hours; H_2O_2+BGP-15 group: cells with 150 μM H_2O_2 and 50 μM BGP-15 for 0.5 hours. Data are presented as the mean ± SEM. $^{**}p < 0.01$ vs. Control cells; $^{\S\S}p < 0.01$ vs H_2O_2-treated cells.

can enhance mitochondrial biogenesis. VDAC is located in the outer mitochondrial membrane and can be used for mitochondrial loading protein. We found that VDAC was significantly elevated in BGP-15-treated cells that can support our previous results regarding enhanced biogenesis.

Moreover, we examined the level of NDUFs1 subunit of NADH-ubiquinone oxidoreductase and UQCRC1 subunit of Ubiquinol Cytochrome c Reductase proteins. These proteins are part of the mitochondrial electron transport chain (ETC Complex I and III), and in this way, they are essentially important in the maintaining of proper mitochondrial function [41, 42]. The amount of ETC Complex I and Complex III proteins levels was increased significantly due to BGP-15 treatment, which is consistent with our previous results (Figure 14).

In order to support our finding more adequately regarding the effect of BGP-15 on mitochondrial biogenesis, the relative DNA content of ETC Complex IV was determined. We found that BGP-15 treatment increased the relative expression levels of both tested genes (COXI and COXIII; Figure 13). Since both genes are encoded by mitochondrial DNA, this suggests that mitochondrial DNA content was increased in NRCMs cells treated with BGP-15.

Moreover, we also performed a well-accepted and frequently used method for studying mitochondrial biogenesis by measuring the activity of citrate synthase (CS) [43–45]. Citrate synthase is localized within the mitochondrial matrix, and it catalyses the synthesis of citrate from oxaloacetate in the Krebs tricarboxylic acid cycle [44]. Maximal activity of citrate synthase indicates the mitochondrial content of heart muscle. Citrate synthase activity was reduced in hydrogen-peroxide stressed group compared to control group. The citrate synthase activity was increased significantly due to the

treatment (Figure 13). Summarizing these results, we can conclude that mitochondrial biogenesis was increased under oxidative stress in treated NRCMs cells as a result of BGP-15 treatment, and in this way, it was able to enhance the proper mitochondrial function.

Oxidative stress can damage the mtDNA, which is extremely sensitive to it [46, 47]. In our recent work, PCR results showed extensive damage of mtDNA caused by hydrogen peroxide. Thus, the amplification of the entire mitochondrial genome was restrained. BGP-15 treatment, however, preserved mitochondrial genome integrity markedly decreasing the breakage of mtDNA (Figure 15). The protection of mtDNA is extremely important, because the mitochondrial respiratory chain (ETC) complexes are encoded on mtDNA [48, 49]. Complex I-III are critical for ROS production by the respiratory chain [50]. It can generate significant amounts of ROS under several conditions including hypoxia, mitochondrial hyperpolarization, and inhibition of respiratory complexes. BGP-15 is able to reduce the mitochondrial ROS production at complex I [18, 24]. Along these lines, BGP-15 can protect against ROS induced mitochondrial DNA damage and maintain the appropriate mitochondrial function.

The preservation of mitochondrial membrane potential is also important to maintain the metabolic capacity of mitochondria. Well-functioning mitochondrial oxidative phosphorylation and ATP production are essential for the proper function of cardiomyocytes [51, 52]. BGP-15 is able to prevent oxidative stress-induced mitochondrial membrane potential loss and therefore improved mitochondrial function (Figure 16). We observed that oxidative stress leads to mitochondrial respiration damage (Figure 17). However, BGP-15 treatment preserved the mitochondrial function characterized by ATP production
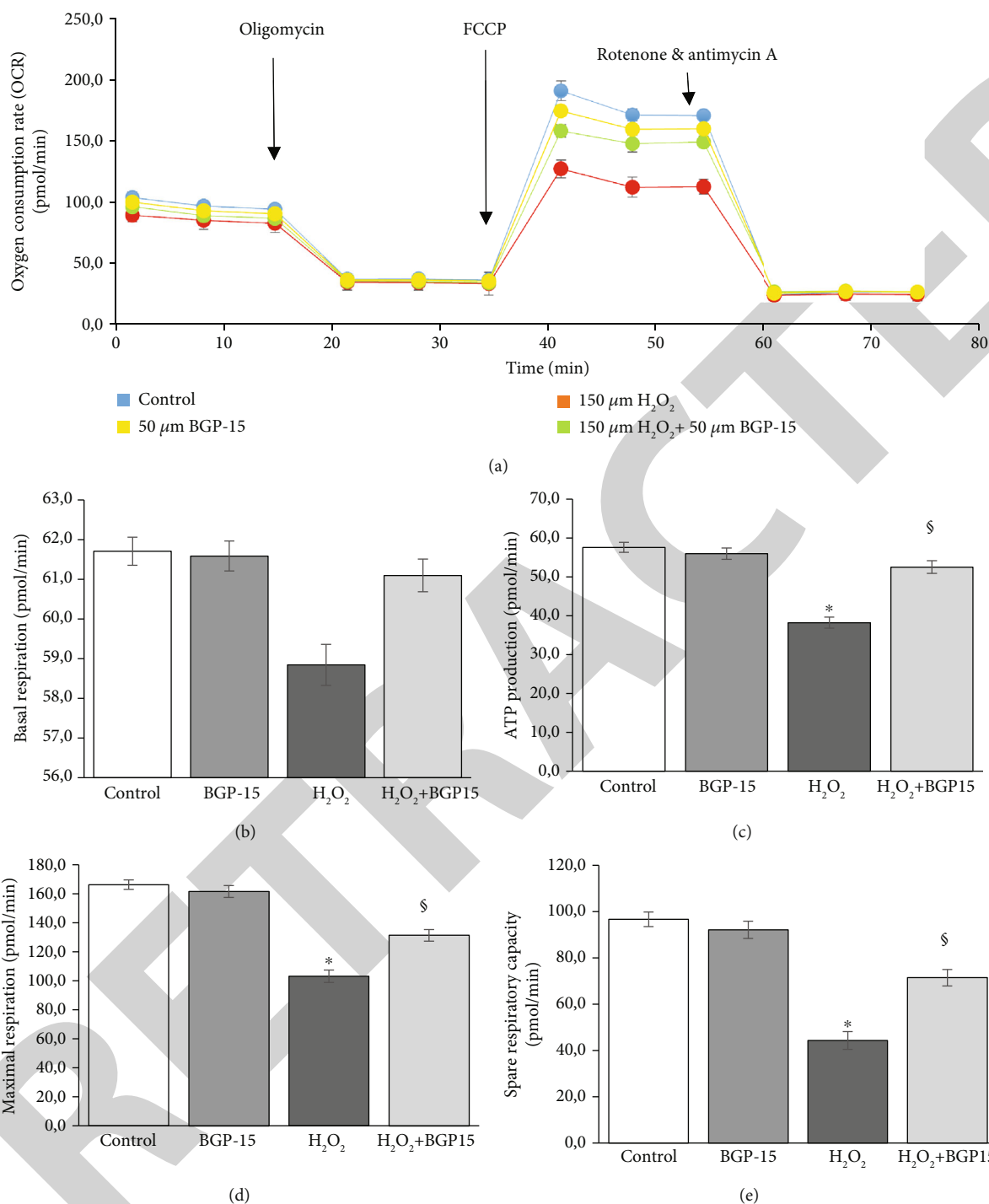
FIGURE 17: Effect of BGP-15 on mitochondrial oxygen consumption and energy metabolism in NRCM cells, as determined by Agilent Seahorse Xfp. Mitochondrial energy metabolism was measured using a Seahorse XFp analyzer. During testing, H9c2 cells were treated with $10 \mu M$ oligomycin, $10 \mu M$ FCCP, and $5 \mu M$ rotenone/antimycin A. Data were automatically calculated according to the Agilent Seahorse XF Cell Mito Stress Test Report Generator. (a) Oxygen consumption rate (OCR). (b) Basal respiration. (c) ATP production. (d) Maximal respiration. (e) Spare respiratory capacity. Control group: cells without any treatment; BGP-15 group: cells with only $50 \mu M$ BGP-15 for 0.5 hours; H_2O_2 group: cells with $150 \mu M$ H_2O_2 for 0.5 hours; H_2O_2+BGP-15 group: cells with $150 \mu M$ H_2O_2 and $50 \mu M$ BGP-15 for 0.5 hours. Values are mean ± SEM ($n = 4$). $^*p < 0.05$ vs. Control, $^§p < 0.05$ vs. H_2O_2 group.

and spare respiratory capacity thereby ensuring the ability of cells to respond to increased energy demand under stress scenario.

BGP-15 also supports the maintenance of mitochondrial function partially via the preservation of the mitochondrial structure.

Our study is the first to demonstrate that BGP-15 preserved the mitochondrial ultrastructure by increased mitochondrial fusion and decreased fission processes as well as positively affected the translocation processes in chronic hypertension-induced heart failure animal model. Furthermore, we can make a similar observation in the case of primer rat cardiomyocytes cell culture experiment during hydrogen-peroxide induced oxidative stress. Comparable changes were seen in the case of fusion and fission processes in NRCM cell culture compared to in vivo model. Moreover, BGP-15 treatment preserved the mitochondrial membrane potential and improved the mitochondrial function. BGP-15 protected the integrity of the mitochondrial genome and enhanced the de novo biogenesis of mitochondria during hydrogen peroxide-induced oxidative stress. Nevertheless, the exact molecular mechanism of the effects is still unknown, but there are clear evidences regarding the specific mechanism of how BGP-15 acts at important integrator points of signal transduction in certain pathological processes. In order to elucidate the potential underlying molecular mechanisms, further targeted studies should be performed in the future.

Our results reveal that pharmacological modulation of the mitochondrial dynamics under cellular stress could be a novel therapeutic approach in various cardiac diseases characterized by oxidative stress-induced mitochondrial damage.

Data Availability

The authors confirm that all data is fully available without restriction. All relevant data is described within the paper.

Ethical Approval

Animals received care according to the Guide for the Care and Use of Laboratory Animals published by the US National Institute of Health and the experiment was approved by the Animal Research Review Committee of the University of Pecs, Medical School (Permit number: BA02/2000-54/2017). The manuscript does not contain clinical studies or patient data.

Conflicts of Interest

On behalf of all authors, the corresponding author states that there is no conflict of interest.

Authors' Contributions

All authors contributed to the study conception and design. Material preparation, data collection, and analysis were performed by Orsolya Horvath, Katalin Ordog, Kitti Bruszt, Nikoletta Kalman, Dominika Kovacs, Balazs Radnai, Ferenc Gallyas, Balazs Sumegi, Kalman Toth, Robert Halmosi, Laszlo Deres. The first draft of the manuscript was written by Orsolya Horvath, and all authors commented on previous versions of the manuscript. All authors read and approved the final manuscript. Prof. Balazs Sumegi has unexpectedly passed away during the course of this study. This paper is dedicated to his memory.

References

[1] M. G. Rosca and C. L. Hoppel, "Mitochondrial dysfunction in heart failure," *Heart Failure Reviews*, vol. 18, no. 5, pp. 607–622, 2013.

[2] B. Zhou and R. Tian, "Mitochondrial dysfunction in pathophysiology of heart failure," *The Journal of Clinical Investigation*, vol. 128, no. 9, pp. 3716–3726, 2018.

[3] A. A. Kumar, D. P. Kelly, and J. A. Chirinos, "Mitochondrial dysfunction in heart failure with preserved ejection fraction," *Circulation*, vol. 139, no. 11, pp. 1435–1450, 2019.

[4] A. A. Knowlton, L. Chen, and Z. A. Malik, "Heart failure and mitochondrial dysfunction: the role of mitochondrial fission/fusion abnormalities and new therapeutic strategies," *Journal of Cardiovascular Pharmacology*, vol. 63, no. 3, pp. 196–206, 2014.

[5] M. T. Breitzig, M. D. Alleyn, R. F. Lockey, and N. Kolliputi, "A mitochondrial delicacy: dynamin-related protein 1 and mitochondrial dynamics," *American Journal of Physiology-Cell Physiology*, vol. 315, pp. C80–C90, 2018.

[6] A. R. Hall, N. Burke, R. K. Dongworth, and D. J. Hausenloy, "Mitochondrial fusion and fission proteins: novel therapeutic targets for combating cardiovascular disease," *British Journal of Pharmacology*, vol. 171, no. 8, pp. 1890–1906, 2014.

[7] J. Nan, W. Zhu, M. S. Rahman et al., "Molecular regulation of mitochondrial dynamics in cardiac disease," *Biochimica et Biophysica Acta (BBA) - Molecular Cell Research*, vol. 1864, pp. 1260–1273, 2017.

[8] C. Vásquez-Trincado, I. García-Carvajal, C. Pennanen et al., "Mitochondrial dynamics, mitophagy and cardiovascular disease," *The Journal of Physiology*, vol. 594, pp. 509–525, 2016.

[9] H. Tsutsui, S. Kinugawa, and S. Matsushima, "Oxidative stress and heart failure," *American Journal of Physiology Heart and Circulatory Physiology*, vol. 301, no. 6, pp. H2181–H2190, 2011.

[10] E. Takimoto and D. A. Kass, "Role of oxidative stress in cardiac hypertrophy and remodeling," *Hypertension*, vol. 49, pp. 241–248, 2007.

[11] D. A. Brown, J. B. Perry, M. E. Allen et al., "Mitochondrial function as a therapeutic target in heart failure," *Nature Reviews Cardiology*, vol. 14, pp. 238–250, 2017.

[12] G. Siasos, V. Tsigkou, M. Kosmopoulos et al., "Mitochondria and cardiovascular diseases—from pathophysiology to treatment," *Annals of Translational Medicine*, vol. 6, 2018.

[13] M. Bonora, M. R. Wieckowski, D. A. Sinclair, G. Kroemer, P. Pinton, and L. Galluzzi, "Targeting mitochondria for cardiovascular disorders: therapeutic potential and obstacles," *Nature Reviews Cardiology*, vol. 16, pp. 33–55, 2019.

[14] J. Kuzmicic, A. del Campo, C. López-Crisosto et al., "Mitochondrial dynamics: a potential new therapeutic target for heart failure," *Revista Española de Cardiología*, vol. 64, pp. 916–923, 2011.

[15] R. Halmosi, Z. Berente, E. Osz, K. Toth, P. Literati-Nagy, and B. Sumegi, "Effect of poly(ADP-ribose) polymerase inhibitors on the ischemia-reperfusion-induced oxidative cell damage and mitochondrial metabolism in Langendorff heart perfusion system," *Molecular Pharmacology*, vol. 59, pp. 1497–1505, 2001.

[16] G. Nagy, A. Szarka, G. Lotz et al., "BGP-15 inhibits caspase-independent programmed cell death in acetaminophen-induced liver injury," *Toxicology and Applied Pharmacology*, vol. 243, pp. 96–103, 2010.

[17] K. Sumegi, K. Fekete, C. Antus et al., "BGP-15 protects against oxidative stress- or lipopolysaccharide-induced mitochondrial destabilization and reduces mitochondrial production of reactive oxygen species," *PLoS One*, vol. 12, article e0169372, 2017.

[18] A. Szabo, K. Sumegi, K. Fekete et al., "Activation of mitochondrial fusion provides a new treatment for mitochondria-related diseases," *Biochemical Pharmacology*, vol. 150, pp. 86–96, 2018.

[19] Z. Sarszegi, E. Bognar, B. Gaszner et al., "BGP-15, a PARP-inhibitor, prevents imatinib-induced cardiotoxicity by activating Akt and suppressing JNK and p38 MAP kinases," *Molecular and Cellular Biochemistry*, vol. 365, pp. 129–137, 2012.

[20] J. Chung, A.-K. Nguyen, D. C. Henstridge et al., "HSP72 protects against obesity-induced insulin resistance," *Proceedings of the National Academy of Sciences of the United States of America*, vol. 105, pp. 1739–1744, 2008.

[21] G. Sapra, Y. K. Tham, N. Cemerlang et al., "The small-molecule BGP-15 protects against heart failure and atrial fibrillation in mice," *Nature Communications*, vol. 5, article 5705, 2014.

[22] O. Horvath, K. Ordog, K. Bruszt et al., "BGP-15 protects against heart failure by enhanced mitochondrial biogenesis and decreased fibrotic remodelling in spontaneously hypertensive rats," *Oxidative Medicine and Cellular Longevity*, vol. 2021, Article ID 1250858, 13 pages, 2021.

[23] M. Bombicz, D. Priksz, R. Gesztelyi et al., "The drug candidate BGP-15 delays the onset of diastolic dysfunction in the Goto-Kakizaki rat model of diabetic cardiomyopathy," *Molecules*, vol. 24, no. 3, p. 586, 2019.

[24] E. Szabados, P. Literati-Nagy, B. Farkas, and B. Sumegi, "BGP-15, a nicsotinic amidoxime derivate protecting heart from ischemia reperfusion injury through modulation of poly(-ADP-ribose) polymerase," *Biochemical Pharmacology*, vol. 59, pp. 937–945, 2000.

[25] K. Ordog, O. Horvath, K. Eros et al., "Mitochondrial protective effects of PARP-inhibition in hypertension-induced myocardial remodeling and in stressed cardiomyocytes," *Life Sciences*, vol. 268, p. 118936, 2021.

[26] G. Itter, W. Jung, and P. Juretschke, "A model of chronic heart failure in spontaneous hypertensive rats (SHR)," *Laboratory Animals*, vol. 38, pp. 138–148, 2016.

[27] M. Kokubo, A. Uemura, T. Matsubara, and T. Murohara, "Noninvasive evaluation of the time course of change in cardiac function in spontaneously hypertensive rats by echocardiography," *Hypertension Research*, vol. 28, pp. 601–609, 2005.

[28] S. A. Doggrell and L. Brown, "Rat models of hypertension, cardiac hypertrophy and failure," *Cardiovascular Research*, vol. 39, pp. 89–105, 1998.

[29] O. Horvath, K. Ordog, K. Bruszt, B. Sumegi, K. Toth, and R. Halmosi, "Role of BGP-15 treatment in hypertensive heart failure progression and mitochondrial protection," *European Heart Journal*, vol. 40, 2019.

[30] S.-B. Ong and D. J. Hausenloy, "Mitochondrial morphology and cardiovascular disease," *Cardiovascular Research*, vol. 88, pp. 16–29, 2010.

[31] D. W. Scheuermann, "The ultrastructure of cardiac muscle in health and disease," *Micron*, vol. 24, pp. 47–73, 1993.

[32] C.-R. Chang and C. Blackstone, "Dynamic regulation of mitochondrial fission through modification of the dynamin-related protein Drp 1," *Annals of the New York Academy of Sciences*, vol. 1201, pp. 34–39, 2010.

[33] Y. Kanamaru, S. Sekine, H. Ichijo, and K. Takeda, "The phosphorylation-dependent regulation of mitochondrial proteins in stress responses," *Journal of Signal Transduction*, vol. 2012, Article ID 931215, 12 pages, 2012.

[34] H. Lee and Y. Yoon, "Mitochondrial fission: regulation and ER connection," *Molecules and Cells*, vol. 37, pp. 89–94, 2014.

[35] A. Pisano, B. Cerbelli, E. Perli et al., "Impaired mitochondrial biogenesis is a common feature to myocardial hypertrophy and end-stage ischemic heart failure," *Cardiovascular Pathology*, vol. 25, no. 2, pp. 103–112, 2016.

[36] A. Garnier, D. Fortin, C. Deloménie, I. Momken, V. Veksler, and R. Ventura-Clapier, "Depressed mitochondrial transcription factors and oxidative capacity in rat failing cardiac and skeletal muscles," *The Journal of Physiology*, vol. 551, no. 2, pp. 491–501, 2003.

[37] C. Riehle and E. D. Abel, "PGC-1 proteins and heart failure," *Trends in Cardiovascular Medicine*, vol. 22, no. 4, pp. 98–105, 2012.

[38] P. J. Fernandez-Marcos and J. Auwerx, "Regulation of PGC-1α, a nodal regulator of mitochondrial biogenesis," *The American Journal of Clinical Nutrition*, vol. 93, no. 4, pp. 884S–890S, 2011.

[39] C. Cantó and J. Auwerx, "PGC-1alpha, SIRT1 and AMPK, an energy sensing network that controls energy expenditure," *Current Opinion in Lipidology*, vol. 20, no. 2, pp. 98–105, 2009.

[40] F. R. Jornayvaz and G. I. Shulman, "Regulation of mitochondrial biogenesis," *Essays in Biochemistry*, vol. 47, pp. 69–84, 2010.

[41] R.-Z. Zhao, S. Jiang, L. Zhang, and Z.-B. Yu, "Mitochondrial electron transport chain, ROS generation and uncoupling (review)," *International Journal of Molecular Medicine*, vol. 44, pp. 3–15, 2019.

[42] D. Nolfi-Donegan, A. Braganza, and S. Shiva, "Mitochondrial electron transport chain: oxidative phosphorylation, oxidant production, and methods of measurement," *Redox Biology*, vol. 37, 2020.

[43] S. Larsen, J. Nielsen, C. N. Hansen et al., "Biomarkers of mitochondrial content in skeletal muscle of healthy young human subjects," *The Journal of Physiology*, vol. 590, no. 14, pp. 3349–3360, 2012.

[44] G. Wiegand and S. J. Remington, "Citrate synthase: structure, control, and mechanism," *Annual Review of Biophysics and Biophysical Chemistry*, vol. 15, pp. 97–117, 1986.

[45] A. J. A. Molina, M. S. Bharadwaj, C. Van Horn et al., "Skeletal muscle mitochondrial content, oxidative capacity, and Mfn2 expression are reduced in older patients with heart failure and preserved ejection fraction and are related to exercise intolerance," *JACC: Heart Failure*, vol. 4, pp. 636–645, 2016.

Retraction

Retracted: Novel Insights into the Molecular Features and Regulatory Mechanisms of Mitochondrial Dynamic Disorder in the Pathogenesis of Cardiovascular Disease

Oxidative Medicine and Cellular Longevity

This article has been retracted by Hindawi following an investigation undertaken by the publisher [1]. This investigation has uncovered evidence of one or more of the following indicators of systematic manipulation of the publication process:

(1) Discrepancies in scope

(2) Discrepancies in the description of the research reported

(3) Discrepancies between the availability of data and the research described

(4) Inappropriate citations

(5) Incoherent, meaningless and/or irrelevant content included in the article

(6) Peer-review manipulation

The presence of these indicators undermines our confidence in the integrity of the article's content and we cannot, therefore, vouch for its reliability. Please note that this notice is intended solely to alert readers that the content of this article is unreliable. We have not investigated whether authors were aware of or involved in the systematic manipulation of the publication process.

Wiley and Hindawi regrets that the usual quality checks did not identify these issues before publication and have since put additional measures in place to safeguard research integrity.

We wish to credit our own Research Integrity and Research Publishing teams and anonymous and named external researchers and research integrity experts for contributing to this investigation.

The corresponding author, as the representative of all authors, has been given the opportunity to register their agreement or disagreement to this retraction. We have kept a record of any response received.

References

[1] Y. Tan, F. Xia, L. Li et al., "Novel Insights into the Molecular Features and Regulatory Mechanisms of Mitochondrial Dynamic Disorder in the Pathogenesis of Cardiovascular Disease," *Oxidative Medicine and Cellular Longevity*, vol. 2021, Article ID 6669075, 11 pages, 2021.

Review Article

Novel Insights into the Molecular Features and Regulatory Mechanisms of Mitochondrial Dynamic Disorder in the Pathogenesis of Cardiovascular Disease

Ying Tan [ID],[1] Fengfan Xia,[2] Lulan Li,[1] Xiaojie Peng,[1] Wenqian Liu,[3] Yaoyuan Zhang,[1] Haihong Fang [ID],[4] Zhenhua Zeng [ID],[1] and Zhongqing Chen [ID][1]

[1]*Department of Critical Care Medicine, Nanfang Hospital, Southern Medical University, Guangzhou 510515, China*

[2]*Department of Cardiology, Shunde Hospital, Southern Medical University (The First People's Hospital of Shunde Foshan), Foshan, 528300 Guangdong, China*

[3]*Department of Critical Care Medicine, Huiqiao Medical Center, Nanfang Hospital, Southern Medical University, Guangzhou 510515, China*

[4]*Department of Anesthesiology, Nanfang Hospital, Southern Medical University, 1838 Guangzhou Ave N, Guangzhou 510515, China*

Correspondence should be addressed to Haihong Fang; f2h1983@163.com, Zhenhua Zeng; zhenhuazeng.2008@163.com, and Zhongqing Chen; zhongqingchen2008@163.com

Mitochondria maintain mitochondrial homeostasis through continuous fusion and fission, that is, mitochondrial dynamics, which is precisely mediated by mitochondrial fission and fusion proteins, including dynamin-related protein 1 (Drp1), mitofusin 1 and 2 (Mfn1/2), and optic atrophy 1 (OPA1). When the mitochondrial fission and fusion of cardiomyocytes are out of balance, they will cause their own morphology and function disorders, which damage the structure and function of the heart, are involved in the occurrence and progression of cardiovascular disease such as ischemia-reperfusion injury (IRI), septic cardiomyopathy, and diabetic cardiomyopathy. In this paper, we focus on the latest findings regarding the molecular features and regulatory mechanisms of mitochondrial dynamic disorder in cardiovascular pathologies. Finally, we will address how these findings can be applied to improve the treatment of cardiovascular disease.

1. Introduction

Mitochondria are highly dynamic organelles that not only by keeping adenosine triphosphate (ATP) levels but also by generating low levels of reactive oxygen species (ROS) for cell signaling and that dysfunction in either of these processes could lead to pathology [1, 2]. In 1914, Lewis M. and Lewis W. [3] first proposed the concept of mitochondrial dynamics, that is, the dynamic change process in which mitochondria constantly divide and fuse in the cell, thus, maintaining its stable morphology and network structure. In recent years, it has been reported that [3–5] factors that maintain cell homeostasis, in addition to mitochondrial fission and fusion, mitochondrial-endoplasmic reticulum structure coupling, mitochondrial biosynthesis, and mitophagy, are all related

to mitochondrial morphology and cell homeostasis. Some scholars [4] included it in the concept of mitochondrial dynamics, while others [5] summarized all the above factors as mitochondrial dynamic-related functions. This review favors the latter, namely, the mitochondrial dynamics for the dynamic process of mitochondrial fission-fusion. Mitochondria are often arranged in parallel in the myocardium along the long axis of the cell, and their size is described by the length/width ratio of the mitochondria. The length/width ratio of fibroblast mitochondria was about 6, and the mitochondria of mature cardiomyocytes were oval (length/width value was about 1.5), smaller, and rounder than the mitochondria of fibroblasts [6]. In the body, mitochondrial structure is continuously reshaped through fission and fusion. Mitochondrial fusion will produce enlarged mitochondria

(longer and larger), and the fission will produce shorter and smaller offspring mitochondria, which are called fragmented mitochondria [7]. Studies [8, 9] have shown that mitochondrial dynamics is involved in mitochondrial maintenance, biological productivity, and cell death. The dynamic balance of mitochondria maintains the homeostasis of cardiomyocytes. Once it is out of balance, which will have a great impact on the pathogenesis of cardiovascular diseases. Moreover, mitochondria are not only the main energy-producing organelles in cells but also critical regulators of cardiomyocytes in response to various stimuli such as hypoxia, oxidative stress, and hyperglycemia [10]. The latest research showed that the imbalance of mitochondrial dynamics is closely associated with the occurrence and development of various cardiovascular diseases, including ischemia-reperfusion injury, atherosclerosis, diabetic cardiomyopathy, septic cardiomyopathy, hypertrophic cardiomyopathy, and heart failure [4] (Figure 1).

2. Mitochondrial Fusion and Fission Machinery

The processes of mitochondrial fusion and fission are highly controlled by the molecular machinery. It was found that the proteins related to mitochondrial dynamics are all important members with the function of Guanosine triphosphatases (GTPase), including (1) mitofusin 1 (Mfn1) and mitofusin 2 (Mfn2) are the proteins that regulate the fusion of mitochondrial outer membrane, which are located in the mitochondrial outer membrane and formed three different molecular compounds, namely, Mfn1 oligomers, Mfn2 oligomers, and Mfn1-Mfn2 oligomers; these compounds can promote mitochondrial fusion process [11]. The Mfn1 and Mfn2 proteins have an N-terminal GTPase domain, and the C-terminal part induces mitochondrial fusion protein oligomerization. Mfn2 is also associated with myocardial cell apoptosis and mitochondrial autophagy. (2) Optic atrophy 1 (OPA1) is the protein that regulates the fusion of mitochondrial intima, which can not only ensure the stability of mitochondrial intima structure but also participate in the remodeling of mitochondrial cristae. OPA1 mainly exists in two forms: long OPA1 (long OPA1 protein structure, L-OPA1) and short OPA1 (short OPA1 protein structure, S-OPA1). Under the action of intestinal peptidase OMA1 and I-AAA proteolytic enzyme YME1L, L-OPA1 can be hydrolyzed into S-OPA1. The former is anchored on the mitochondrial inner membrane to regulate intimal fusion, while the latter is located in the membrane space, promoting mitochondrial fragmentation and fission [12]. (3) The protein regulating mitochondrial fission is Drp1, a member of the GTPase family, which is located in the cytoplasm and participates in the fission of the mitochondrial outer membrane. It is produced by DNM1L gene coding. Drp1 mainly contains four regions from the N-terminal to the C-terminal: GTPase region, intermediate region, polytropic region, and GTPase effector region. Unlike Mfn, Drp1 lacks a lipid-interacting hydrophobic transmembrane domain and must bind to other receptor proteins to be recruited into the mitochondrial outer membrane [13]. Studies [14] showed that Drp1 had dimer or tetramer under basic conditions and further self-assembled

in the fission process to form a larger poly structure. The latter promoted outer membrane fusion and separation through GTP, depending on conformational changes. Mitochondria repair damaged mitochondria through mutual fusion, and self-fission is conducive to the removal of irreparably damaged mitochondria. However, mitochondrial fission first fragments the irreparable mitochondria and then removes the fragmented mitochondria from the cell to maintain the quality of the mitochondria, thereby protecting the normal function of the mitochondrial network [15].

In mammalian cells, mitochondrial fission is regulated by Drp1 and mitochondrial fission 1 protein (Fis1), mitochondrial fission factor (Mff), and mitochondrial dynamic proteins 49 and 51 (MiD49/51) [16]. In the early stage of mitochondrial fission, Drp1 acts as a mechanical enzyme similar to dynein, which plays a role in constricting the mitochondrion physically. Because Drp1 lacks a mitochondrial target sequence, it needs to form a fission complex with Fis1 located on the outer mitochondrial membrane [17]. However, studies in mammalian cells have found that silencing Fis1 has little effect on Drp1 transport to mitochondria [18]. At this point, Mff seems to be a mitochondrial receptor protein for Drp1 [19]. Decreased MFF levels induce mitochondrial elongation and reduce Drp1 transport to mitochondria [19]. Similarly, MiD49 and MiD51 are also involved in the fission mechanism in mammals [20] (Figure 2). At present, it has been widely recognized that multiple receptors can recruit Drp1 to mitochondria to induce mitochondrial fission. Posttranslational modifications can also modify the activity of Drp1. Cdk1/cyclin B kinase [21] and CaMKIα [22] increase Drp1 mitotic activity. On the contrary, phosphorylation of cyclic AMP-dependent protein kinase (PKA) reduces the function of Drp1 [23]. Specifically, Ca^{2+}-calmodulin-dependent phosphatase calcineurin can remove this phosphate residue and promote mitochondrion fission [24].

3. Effects of Mitochondrial Dynamic Imbalance on the Organism

Numerous studies [25] have shown that mitochondrial fusion is beneficial to oxidative phosphorylation. Mitochondrial fusion can prevent mitochondrial DNA loss and protect mitochondrial protein synthesis and thus maintaining normal mitochondrial function. Besides, the mitochondrial fusion event can dilute the damaged mitochondrial proteins and DNA and repair the damaged mitochondria through the process of "functional complementation" [9]. Damage to the mitochondrial fusion mechanism can accelerate mitochondrial fission and then produce mitochondrial fragmentation leading to the loss of oxidative phosphorylation and apoptosis of cardiomyocytes. A study [26] found that inducing Drp1 gene mutation in mice can affect mitochondrial function and induce mitochondrial autophagy, leading to cardiac dilatation and heart failure. Inhibiting Drp1-induced mitochondrial fission with Drp1 inhibitor (Mdivi-1) or other drugs has a protective effect on injured heart and brain after ischemia [27, 28]. At this point, the mitochondrial fission seems to be "harmful." However, many
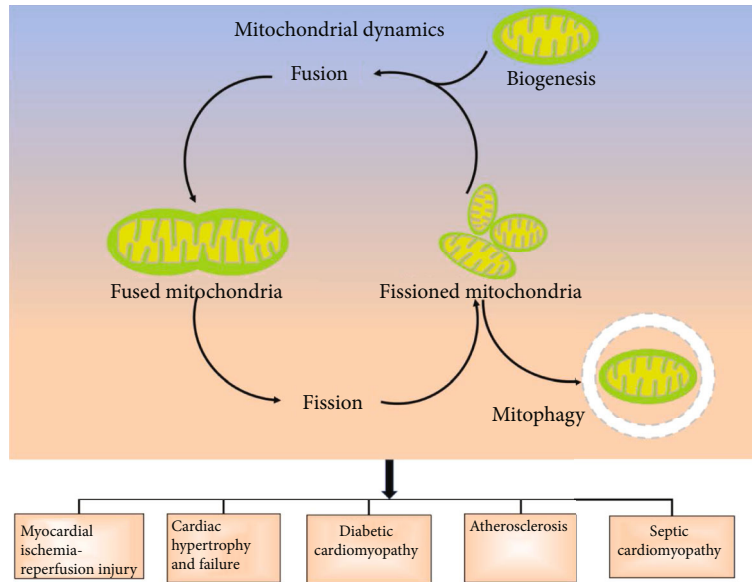
FIGURE 1: Mitochondrial dynamics in cardiovascular disease. Mitochondria dynamic disorder is relevant to various aspects of cardiovascular biology, including cardiac development, responses to ischaemia/reperfusion (I/R) injury, cardiac hypertrophy and failure, type 2 diabetes mellitus (T2DM), atherosclerosis, and sepsis. In addition, mitochondrial fission is required for mitophagy.
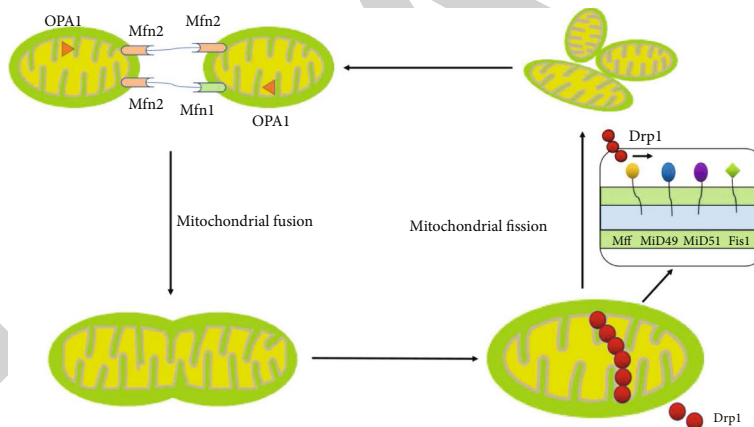
FIGURE 2: The dynamic balance of mitochondrial fission and mitochondrial fusion maintains the proper function of complex organelle. Mitochondrial fusion is mainly regulated by mitofusin (Mfn) 1 and 2 and optical atrophy protein 1 (OPA1). Mitochondrial fission is mainly regulated by Drp1, Drp1, and its adapter proteins Fis1, Mff, and MiD49/51 control mitochondrial fission. This process is required by various cell processes, such as redistribution of mitochondria in mitosis and release of cytochrome c during cell apoptosis.

studies [29, 30] have reported that knockout of myocardial Drpl gene can cause fission disorder, which produces large, long, and dysfunctional mitochondria, and finally leads to heart failure and death. It is obvious that the mitochondrial fission is equally important for the maintenance of cardiac function.

Excessive mitochondrial fragmentation is involved in most heart diseases, thus, enhancing mitochondrial fusion will be a potential therapeutic strategy. The latest research found mitochondrial fusion provoked by fusion promotion and fission inhibition direct the different fate of heart, Mfn2 upregulation other than Drp1 downregulation well maintains heart mitochondrial function is a more safe strategy for correcting excessive mitochondrial fragmentation in

hearts [31]. Maneechote's team intervened rats with ischemia-reperfusion using mitochondrial fusion promoter M1 (2 mg/kg). They found that the administration of M1 before ischemia reduced the infarct size and cardiac apoptosis and exerted the greatest cardioprotective effect. This indicates that myocardial ischemia-reperfusion injury can be reduced by increasing mitochondrial fusion [32]. However, excessive mitochondrial fusion can also lead to disease. Studies have shown that the point mutation of L341P could promote the rapid degradation of SLC25A46. As a mitochondrial carrier protein, the decreased expression of SLC25A46 may promote the stability and oligomerization of Mfn1 and Mfn2 on mitochondria, thereby leading to excessive mitochondrial fusion and ultimately manifested as

a rare disease of cerebellopontine hypoplasia [33]. In addition, increased mitochondrial fusion can lead to increased oxidative stress and abnormal Ca^{2+} homeostasis [34, 35], which can lead to arrhythmias, especially atrial fibrillation [36, 37]. Therefore, the effect of mitochondrial dynamics on the myocardium depends on the proper balance between mitochondrial fusion and fission which cannot be divided. In this process, mitophagy also plays a key role, which can remove the fragmented mitochondria caused by mitochondrial fission. Once the mitochondrial autophagy is impaired or the mitochondria divide excessively, the excessive accumulation of the fragmented mitochondria will cause heart damage.

Mitophagy is the selective sequestration of mitochondria by autophagosomes and is degraded by lysosomes to remove damaged mitochondria [38, 39]. Excessive mitochondrial fission causes increased mitochondrial debris, resulting in abnormal energy metabolism and apoptotic events. In contrast, mitophagy can remove injured mitochondrial fragmentation and thus render the IR-damaged microvasculature less sensitive [40]. A study showed nuclear receptor subfamily 4 group A member 1 (NR4A1) could promote Drp1 activation and inhibit BCL2 interacting protein 3 (Bnip3) transcription, resulting in excessive Drp1-associated fission and defective Bnip3-depended mitophagy [41]. Currently, there are two main opinions on the relationship between mitophagy and mitochondrial fission: "fission-regulated autophagy," that is, mitochondria form small fragments through fission, so that mitophagy can more easily clear the mitochondrial fragments; "autophagy resists fission," mitochondria are fragmented after fission, and the fragmented mitochondria contain incomplete mitochondrial DNA genes and damaged mitochondrial membrane potential. These have become the main removal target of mitophagy [42, 43]. However, the current research results cannot fully explain whether mitochondrial autophagy can remove the mitochondrial debris, thereby preventing cardiovascular damage.

4. Mitochondrial Dynamics and Cardiovascular Disease

4.1. Myocardial Ischemia-Reperfusion Injury(IRI). Most clinical studies using ischemia regulation and related drugs to reduce infarct size have not been successful; therefore, coronary artery microvascular damage as a target of auxiliary cardiac protection has become the focus of attention [44]. During ischemia, myocardial cells are dominated by anaerobic glycolysis, leading to the accumulation of acid products, the depletion of adenosine triphosphate (ATP), calcium overload in the mitochondrial matrix, and the excessive production of ROS. Studies [45] showed that ROS and calcium overload may regulate mitochondrial dynamic changes by mediating the expression of mitochondrial dynamic-related proteins, thus, playing an important role in myocardial ischemia-reperfusion injury. Mitochondrial fission may cause abnormal mitochondrial energy metabolism, promote apoptosis of myocardial cells, and lead to ventricular remodeling after myocardial infarction. Wang et al. confirmed that the regulation of miR-499 level can affect the degree of apo-

ptosis and myocardial infarction and cardiac dysfunction caused by ischemia-reperfusion (I/R) according to targeting calcineurin-mediated Drp1 activation [46]. It has been found that [47] the level of Drp1 protein in the cytoplasm of mouse cardiomyocytes and its phosphorylated protein levels were decreased, while the level of Drp1 protein in the mitochondrial outer membrane was increased, which indicates that the level of miR-499 can affect the degree of apoptosis and myocardial infarction. The decrease in its expression causes the activation of calcineurin, promotes the dephosphorylation of Drp1, and produces fragmented mitochondria. In addition, using mdivi-1 to inhibit Drp1 can increase the proportion of extended mitochondria in cardiomyocytes, delay the opening of mitochondrial permeability transition pore (mPTP), reduce acute IRI-induced cell death, and reduce the area of myocardial infarction caused by IRI, indicating that the inhibition of Drp1 has potential therapeutic effect.

In the reperfused heart, calcium overload is an effective regulator of Drp1 after reperfusion. In the cytoplasm, the accumulation of Ca^{2+} activates calcineurin and dephosphorylates Drp1 (S637), leading to mitochondrial fission and cell apoptosis. mir-499 can offset the effect of calcium overload on Drp1 activity, but the expression of mir-499 is reduced and is more sensitive to IRI [46]. To keep mitochondrial integrity and prevent cardiomyocytes from apoptosis, activation of PIM-1 is used to inhibit Drp1 and prevent mitochondrial fission. In response to IRI, calcium overload mainly targets Drp1, while ROS mainly targets Mfn and OPA1. Mfn1 and Mfn2 are necessary for mitochondrial fusion, but they have opposite effects in IRI, possibly due to the fission effect of Mfn2. Mfn2 upregulates ROS during IRI, which is sufficient to induce cardiomyocyte apoptosis by inhibiting Akt and activating caspase-9. Mfn2 knockout delays mitochondrial membrane permeability and the opening of mPTP to prevent myocardial cells from being affected by IRI. ROS upregulates the level of miR-140, downregulates the Mfn1 expression in the IR heart, disconnects the mitochondrial network, and intensifies myocardial cell apoptosis. ROS activates OMA1, while L-OPA1 is completely sheared into a short soluble S-OPA1, leading to remodeling of mitochondrial cristae and release of cytoplasmic C. There are three Bcl-2 family proteins, namely, Bnip3, Bak, and Bax, which lead to mitochondrial dynamic imbalance and mitochondrial cristal remodeling and further promote mitochondrial dysfunction and cardiomyocytes death, all of which are associated with IRI [48]. In the process of IRI, Mfn2 increases with the rise of ROS. Induction of myocardial apoptosis by inhibiting Akt and activating Caspase-9, as well as increasing Mfn2 levels, is necessary and sufficient.

It has been reported that the level of OPA1 in heart samples from patients with ischemic cardiomyopathy is decreased [49]. However, according to the contradictory and unexpected findings, the role of mitochondrial fusion proteins (Mfn1, Mfn2, and OPA1) as cardiac protective targets is still controversial. In HL-1 cells, the overexpression of Mfn1 or Mfn2 delays the opening of mPTP and reduces I/R-induced cardiomyocyte death [50]. However, in a parallel study, Papanicolaou et al. reported that small interfering RNA (siRNA) knockout of Mfn2 prevented mPTP opening,

thereby making cardiomyocytes more vulnerable to ROS [51]. Similarly, some studies have reported that partial gene ablation of Opa1 can prevent mPTP opening; however, the effect on acute ischemic reperfusion has not been explored [52]. In short, the interaction between mitochondrial fusion proteins and I/R is complicated, which needs further study.

4.2. Cardiac Hypertrophy and Failure. Cardiac hypertrophy is caused by multiple stimuli such as hemodynamic overload, ischemia, and activation of neurohormones. Cardiac hypertrophy was initially considered adaptive, and it involved these changes in the structure, morphology, and function of cardiomyocytes, which ultimately led to an increase in heart mass [53–55]. Initially, as a compensatory process, hypertrophic growth normalizes oxygen demand and wall stress. But long-term exposure to disease-related stimuli ultimately leads to pathological cardiomyocyte growth and heart failure [56].

In cardiomyocytes of adults, mitochondria are tightly packed between myofibrils [57], and it was reported that no mitochondrial dynamic events occurred in this subpopulation of mitochondria [58]. However, significant changes in mitochondrial dynamics can be found in models of cardiac hypertrophy [54] and heart failure. Chen et al. [49] found fragmented mitochondria associated with reduced OPA1 levels in both rat and human models of heart failure. In other studies of neonatal rat cardiomyocytes exposed to phenylephrine to induce cardiomyocyte hypertrophy and in vivo models of cardiac hypertrophy, it was also found that the level of Mfn2 mRNA decreased [59]. A recent study found miR-485-5p regulates mitochondrial fission in a mice model of cardiac hypertrophy induced by phenylephrine through targeting mitochondrial anchored protein ligase [60].

Calcineurin is an important regulator of cardiac hypertrophy and heart failure, and it involves in the regulation of mitochondrial fission through Drp1 dephosphorylation. Wang et al. reported that the A and B subtypes of the calcineurin catalytic subunit are both direct targets of miR-499, promoting the phosphorylation of Drp1 at residue Ser 656, thus inhibiting mitochondrial fission [46]. Interestingly, the miR-499 transgenic mice showed decreased hypertrophy parameters after ischemia-reperfusion (I/R). Conversely, knocking out endogenous miR-499 can intensify maladaptive cardiac remodeling [46]. Recently, a study showed that noradrenaline induces mitochondrial fission by calcineurin-and Drp1-dependent manner. Adenovirus-regulated dominant-negative Drp1 expression inhibits norepinephrine-induced mitochondrial fission and hypertrophic cardiomyocyte growth. In addition, adenoviruses expressing antisense sequences of Mfn2 are enough to promote mitochondrial fission and cause hypertrophic responses in cultured myocardial cells [61]. Consistent with these findings, Papanicolaou et al. confirmed that moderate myocardial hypertrophy with mild functional deterioration appears in Mfn2 knockout mice [51]. In a recent study, heart failure was induced by ascending aorta cerclage in wild-type mice, followed by treatment using Drp1 inhibitor mdivi-1, which showed that mdivi-1 treatment alleviated left ventricular dysfunction, and these effects were considered to be associated with

reduced expression of the autophagy markers LC3 and p62 [62]. These findings reported in this review indicate the major role of mitochondrial fission in pathological cardiac remodeling. In addition, a recent study showed that microRNA-20b intensified cardiac hypertrophy by downregulating Mfn2 and promoting cytoplasmic Ca^{2+} overloading, weakening mitochondrial buffering capacity [63].

Heart failure (HF) is the terminal stage of various cardiovascular diseases, characterized by high morbidity, mortality, and rehospitalization rate. The currently recognized as the pathogenesis of heart failure includes overactivated nervous and humoral system, immune regulation disorder, energy metabolism disorder, oxidative stress damage, among which both energy metabolism and oxidative stress damage mechanisms play a role in mitochondria. According to the analysis of heart tissues of patients with heart failure by electron microscopy, different degrees of mitochondrial damage such as the increased mitochondrial number and decreased volume were found, proving that the normal function of mitochondrial dynamic proteins (MDPs) plays an important role in mitophagy and metabolic regulation, and MDP deficiency can lead to dilated cardiomyopathy and heart failure.

If mitophagy is insufficient, cell homeostasis will be impaired, causing cardiomyopathy and HF. Mfn2 is an important mediator of mitophagy. It regulates mitophagy through the PINK1-Mfn2-Parkin signaling pathway, which plays a significant role in mitochondrial quality control and maturation [7]. Mitochondrial maturation is realized through the elimination of fetal mitochondria after birth. Mfn2-Parkin interaction promotes the widespread elimination of fetal mitochondria in the first 3 weeks after birth, which is considered as a prerequisite for the introduction of mature myocardial mitochondria needed for fatty acid metabolism. Mitochondrial quality control dependent on Mfn2 is achieved by eliminating stress-induced mitochondria, leaving healthy mitochondria to refuse. In addition to Mfn2, Drp1 for mitophagy induction is also essential; this can control the quality of mitochondria and prevent heart failure. Drp1-induced mitochondrial fission can produce a group of tiny mitochondria which can be separated by autophagosomes and then be degraded by lysosomes. It can be seen that mitochondrial fission induced by Drp1 is a prerequisite for mitophagy [64]. Mitophagy was further validated in the TAC model; among them, the deficiency of Drp1 resulted in mitophagy dysfunction and exacerbated the progress of mitochondrial and cardiac dysfunction.

Cardiomyocytes mainly rely on fatty acid metabolism to keep their normal function, and increased glucose utilization is harmful to heart function, resulting in dilated cardiomyopathy [65]. MDPs have been identified as a major regulator of cardiac metabolic state, and active mitochondria may be caused by MDP-mediated metabolic regulation. Compared with adult cardiomyocytes, neonatal cardiomyocyte metabolism requires more glucose to promote heartbeat. During the development of the postpartum heart, it is mainly the conversion of sugar decomposition to fatty acid metabolism. PINK1-Mfn2-Parkin-dependent autophagy helps adult mitochondria replace fetal mitochondria and promote the transformation of metabolism. The latter provides enough

energy to the adult heart for maintaining the normal function; otherwise, it will lead to dilated cardiomyopathy. The end stage of heart failure is characterized by the transition from fatty acid metabolism to glucose metabolism. A recent study [66] found OPA1 dysfunction leads to metabolic abnormality. Specific ablation of YME1L in the mouse heart can activate OMA1, promote the hydrolysis of OPA1 protein, and further induce mitochondrial fragmentation, thus, determining the tendency of the mitochondrial substrate to cell energy demand (fatty acid to glucose). Changes in mitochondrial metabolism and cardiac function can be saved by loss of OMA1, which is promoted by lowering the OPA1 cleavage. The balance of OMA1 and YME1L content is essential for OPA1 to regulate mitochondrial fusion. The specific knockout of the YME1L gene in myocardial tissue can enhance the activity of OMA1, eventually leading to dilated cardiomyopathy and heart failure.

4.3. Diabetic Cardiomyopathy. Mitochondrial fission occurs in diabetic cardiomyopathy, and negative regulation of mitochondrial fusion protein may be caused by reduced PGC-1 expression in diabetic cardiomyopathy. In diabetic cardiomyopathy, decreased OPA1 protein level was detected even though the protein Drp1 and/or Fis1 did not follow this reduced expression pattern [67]. Mitochondria fusion promoter M1 can effectively restore mitochondrial dynamic balance and ameliorate diabetic cardiomyopathy in an Opa1-dependent way [68]. Impaired insulin signaling, such as insufficient insulin production (type 1 diabetes mellitus, T1DM) and/or insulin resistance (type 2 diabetes mellitus, T2DM), can lead to elevated blood sugar levels, often referred to as hyperglycemia. Insulin signaling maintains a normal mitochondrial network, while hyperglycemia leads to mitochondrial fission. Insulin regulates heart metabolism by stimulating glucose uptake and directly regulating mitochondrial function. Insulin treatment improves OPA1 protein level, promotes mitochondrial fusion, increases $\Delta\Psi$m, and raises the level of ATP and oxygen consumption of cardiomyocytes in vivo. Insulin activates the Akt-mTOR-NFκB-OPA1 signaling pathway, leading to mitochondrial fusion and promoting mitochondrial oxidation. Silent OPA1 prevents the insulin-induced all metabolic effects, which phosphorylates Drp1 by activating MAP kinase ERK1/2 and ROCK1 under persistent hyper glucose conditions, leading to mitochondrial fission, ROS production, and cell death. Also, NRCMs grown in medium with high glucose concentration showed low protein levels of OPA1 and more fragmented mitochondria [65], which is similar to the mitochondrial changes observed in heart biopsies of patients with type 2 diabetes.

In contrast, activation and/or elevated Drp1 expression leads to insulin resistance. In addition, the hereditary and pharmacological inhibitory effects of skeletal muscle cells attenuate Drp1-induced mitochondrial fission, membrane potential depolarization, and insulin resistance [69]. Drp1 induces mitochondrial dysfunction and myocardial insulin resistance to mediate mitochondrial fission. Besides, Mfn2 deficiency further leads to insulin resistance, promotes mitochondrial dysfunction, increases H_2O_2 level, and activates JNK, which leads to insulin resistance in skeletal muscles.

Exercise can inhibit mitochondrial fission protein levels and prevent phosphorylation of Drp1 at S616 [70], thus, improving fat oxidation and insulin sensitivity in the heart. The specific role of mitochondrial fission in insulin resistance in the body needs further research.

Mitochondrial dynamics has a direct impact on pancreatic function. In ob/ob mice, the level of OPA1 in islet cells decreased before the onset of diabetes [71]. Silencing the OPA1 gene in islet beta cells could generate similar results [72]. OPA1 deficiency in beta cells maintained normal mtDNA copy numbers; however, there has a significant decrease in complex IV activity and levels of electron transport chain, resulting in reduced insulin secretion and ATP production. Whether mitochondrial fission contributes to diabetic cardiomyopathy-related cardiac dysfunction remains unclear. Similarly, whether mitochondrial fusion acts as a direct mediator of mitochondrial metabolism and heart function remains unclear. However, recent reports indicate that mitochondrial fragments are the "starting point" of many events involved in cardiometabolic diseases [67]. Increased fragmented mitochondria and reduced mitochondrial fusion proteins were observed in atrial tissue from patients with T2DM [73]. In a mouse model of cardiac lipotoxicity, correspondingly, more mitochondrial fragmentation were found, which was attributed to increased mitochondrial fission and decreased fusion [74]. In the early stages of insulin resistance, systolic dysfunction is observed in patients with type 2 diabetes but not in obese patients with metabolic healthy [67]. Thus, it is speculated that the decline in ventricular function during the transition from obesity to diabetes is at least partly caused by the deterioration of cardiomyocyte mitochondrial function. Further researches are needed to prove whether adjustment of mitochondrial dynamics may emerge as an intervention to improve mitochondrial performance and cardiac function.

4.4. Atherosclerosis. Atherosclerosis, a chronic inflammatory disease, is a key risk factor for early death [75]. In this complicated disorder, increased levels of adhesion molecules in arterial endothelium were expressed, promoting the infiltration, differentiation, and transformation of monocytes into highly active lipid foam cells, accompanied by VSMC migration to the intima [75]. Mitochondrial ROS production is a necessary factor for mitochondria to play a role in vascular diseases [76, 77]. In contrast, mitochondrial DNA is likely the most sensitive target of ROS [78, 79]. A recent study suggests that impaired mitochondrial DNA can directly exacerbate atherosclerosis. Ballinger et al. reported that impaired mitochondrial DNA was associated with the degree of atherosclerosis in both mouse models of early atherosclerosis and human aortic specimens [80]. In mice lacking apolipoprotein E, increased mitochondrial DNA damage and intensified atherosclerosis are associated with the deficiency of mitochondrial antioxidant enzyme manganese SOD [80]. Elevated mitochondrial ROS level also leads to endothelial cell dysfunction, accompanied by the proliferation and apoptosis of macrophages and VSMCs, which in turn result in the progression of atherosclerotic lesions and may cause plaque rupture [81]. In direct connection with this, Shenouda

et al. observed increased mitochondrial fragmentation and Fis1 protein levels in venous endothelial cells of T2DM patients, and elevated abundance of Drp1 and Fis1 protein in human aortic endothelial cells pretreated with high glucose [82]. The changes in mitochondrial dynamics are associated with the increase in mtROS production. Silencing the expression of Fis1 or Drp1 with siRNA can prevent alterations in ROS production and mitochondrial network induced by high glucose [82]. Overall, these findings suggest mitochondrial fission plays a significant role in the pathogenesis of vascular diseases.

4.5. Septic Cardiomyopathy. Sepsis refers to systemic inflammatory response syndrome caused by a bacterial infection, and severe sepsis can lead to multiple organ failure [83]. Myocardial damage secondary to sepsis is called septic cardiomyopathy or sepsis-induced myocardial dysfunction [84]. Studies [85] reported that the mortality increased significantly during septic cardiomyopathy. In sepsis, the first manifestation of myocardial mitochondria is increased mitochondrial fission and fragmentation. Oxynitride (peroxynitrite, ONOO⁻) is produced along with the increase of oxynitride during sepsis. Continuous high levels of ROS and reactive nitrogen species (RNS) in mitochondria can directly damage mitochondrial components, including permanent inactivation of mitochondrial semifinished protein and mitochondrial membrane structure damage of mitochondrial DNA (mtDNA) and lipid bimolecular [86], resulting in inhibited function of the mitochondrial respiratory chain and decrease of mtDNA replication number, accelerating the generation of free radicals, which lead to the formation of a vicious cycle of free radical generation, mitochondrial structure destruction, and free radical generation. Studies [87] found that oxidative stress and nitriding stress can lead to increased mitochondrial division and fragmentation. In the early stage, when the body suffers stress factors, the first adaptive change of mitochondrial fission and fusion is triggered, that is, functional compensation is carried out through fusion. When the mitochondrial damage is excessive, mitochondrial fission increases, inducing mitochondrial fragmentation and initiating autophagy mechanism for recycling. Mitochondrial fission is far greater than fusion when mitochondrial injury is excessive, followed by a large number of fragmented mitochondria accumulate in cells and cannot be removed. The activation of cell apoptosis and necrosis signal lead to irreversible damage of the body [88].

Secondly, the influence of sepsis on mitochondrial dynamics is also manifested in the abnormal expression of mitochondrial dynamic regulatory proteins. Studies [89, 90] reported that lipopolysaccharide (LPS) promoted mitochondrial fission in the model of lung injury induced by sepsis, leading to increased Drpl mRNA and protein expression, while Mfn1, Mfn2, and OPAl mRNA and protein expression were decreased. In the model of sepsis-induced myocardial injury, mitochondria underwent morphological changes in the early stage of the disease, which showed the destruction of mitochondrial double-membrane structure, matrix edema, and transparency. Then, mitochondrion fission and fusion were unbalanced, and a large number of fragmented mito-

chondria accumulated in cardiomyocytes. This change was related to the increase of phosphorylated Drpl expression, but not to Mfn2, there was no significant change in Mfn2 expression [91, 92]. Recent research observed that mitochondrial dynamics changed significantly with the progression of sepsis, and this change was parallel to the change of oxygen and nitrogen free radicals [88]. In the model of sepsis-induced liver injury, tubular mitochondria decreased by 45% and globular mitochondria (fragmented mitochondria) increased by 46% in the LPS group at 6 h (NO level reached the maximum). At the same time, the expression of Mfn2 mRNA decreased significantly, while the Drpl mRNA did not change significantly; the percentage of ball and rod-shaped mitochondria recovered in the LPS group at 24 h, with little difference, compared with the control group. At this time, Mfn2 mRNA expression increased compared with 6 h, and there was no difference with the control group [88]. In the cecal ligation and perforation group, the tubular mitochondria decreased by 65%, and the globular mitochondria increased by 100% at 12 h (the maximum value of NO). At this time, the expression of Mfn2 mRNA was significantly decreased while the Drpl mRNA was significantly increased. With the progression of the disease, mitochondrial morphology cannot be restored, the percentage of globular mitochondria was still increased, and the expressions of Mfn2 mRNA and Drp 1mRNA did not change much compared with 12 h [88]. This indicates that changes in mitochondrial dynamics may reflect the degree of progression of the disease to some extent.

At present, there is no specific treatment for sepsis-induced myocardial injury, and the current treatment can only relieve the symptoms of patients, but cannot fundamentally reverse the changes of cardiomyocytes at the molecular level. Studies [93] confirmed that cardiac function can be successfully restored in patients even if the myocardial structure has been changed. A new viewpoint [93] holds that the failing cardiomyocytes as "dysfunctional but alive" tissue, rather than being irreversibly damaged tissue. This perspective can help us break away from traditional therapeutic thinking and design therapies that target cardiomyocytes. Studies [50] showed that the inhibition of the Drpl gene and transfection of Mfn1and Mfn2 gene can prolong mitochondria of cardiomyocytes and delay the opening of mPTP, thereby reducing myocardial injury. Canfield and his team found Mdivi-1 reduced the area of myocardial infarction by using Mdivi-1 to regulate mitochondrial dynamics [94]. Chen and his team first proved that knockout of Mfn1 or Mfn2 reversed myocardial injury caused by homozygous mutation of the Mff gene [8]. These findings show that myocardial injury may be reversed if measures are taken before the mitochondrial dynamic imbalance reaches uncontrollably (cells are on the verge of death). The mechanisms of myocardial injury in sepsis are complex and include almost all aspects of the physiological changes of cardiomyocytes, among which mitochondrial dysfunction is the core. Mitochondrial dynamics are involved in the energy metabolism process of cardiomyocytes, and the imbalance of its fission and fusion will cause insufficiency of cell energy supply and then appear function dysfunction. Sepsis-induced

myocardial injury is related to the imbalance of mitochondrial dynamics, and resetting its fission and fusion balance site is expected to be a new intervention target for the prevention and treatment of septic cardiomyopathy.

5. Concluding Remarks

Mitochondrial dynamics has a crucial effect on the homeostasis of the cardiovascular system, which is related to important cellular functions such as mitochondrial quality control and metabolism. The underlying molecular mechanisms of cardiovascular disease associated with mitochondrial dynamics may be quite different. For example, mitochondrial fission is triggered by the descending effect of hyperglycemia and insulin signaling pathway in diabetic cardiomyopathy; while in IRI, mitochondrial fission is mainly caused by Ca^{2+} overload and increased ROS production; while in HF, insufficient mitochondrial autophagy induced by Mfn2 and abnormal expression of OPA1 will lead to abnormal accumulation of mitochondrial fragment. Therefore, specific treatments for different MDP are necessary in order to improve mitochondrial dynamics and cardiac function. Mitochondrial fusion and fission proteins induce cardiomyopathy independent of mitochondrial dynamics under certain conditions. After treatment of oxidative stress, the increase of Mfn2 protein is associated with mitochondrial fission but not to mitochondrial fusion. Similarly, the OMA1-OPA1 signal causes dilated cardiomyopathy according to independent cell metabolism disorder with mitochondrial fission [67]. Thus, manipulating mitochondrial dynamics is not only a treatment strategy designed to optimize cardiovascular disease.

The mitochondrial fission has been observed in cardiovascular disease, but it is not clear whether restoring mitochondrial fusion alone could reverse cardiac pathogenesis. It is widely recognized that mitochondria undergo asymmetric fission, producing both normal mitochondria and dysfunctional mitochondria; among them, the impaired mitochondria are targeted for clearance through the Parkin/-Pink protein complex [9]. Therefore, the mitochondrial fission is a prerequisite for Parkin/Pink mediated mitophagy, which is crucial for mitochondrial quality control in different cardiovascular diseases. Compared with mitochondrial fission, mitochondrial fusion has a certain beneficial effect, such as inhibiting the release of cytochrome C and improving mitochondrial metabolism, but mitochondrial fusion prevents the selective clearance of damaged mitochondria through mitophagy. It is widely believed that proper mitochondrial fission is protective for cardiomyocytes under stress, while excessive enhancement of fusion result in the accumulation of impaired mitochondria and accelerated progression of cardiomyopathy. It has been suggested that the combination therapy by reducing ROS production and maintaining proper mitochondrial fusion may improve the treatment of cardiovascular disease. Most data have confirmed that some chemical compounds have great potential for the regulation of mitochondrial dynamics. It has been confirmed that using the effective chemical compounds can treat some diseases in animal models [95], such as Mdivi-1, a small molecule inhibitor of Drp1, can relieve myocardial IRI in mice.

Injection of Mdivi-1 into rats in advance can increase the length of mitochondria of cardiomyocytes in mice and reduce the area of myocardial infarction in ischemic mice by more than half [96]. Chemical compounds that inhibit OMA1 have therapeutic values on a variety of diseases, and effective OMA1 inhibitors protect normal mitochondrial networks and inhibit the release of cytochrome C by tightening mitochondrial cristae connections.

In brief, we focus on here evidence for new interventions targeting mitochondrial dynamics with relevance to some cardiovascular diseases. Furthermore, insights into mitochondrial dynamics will reveal new approaches to therapeutic manipulation of cardiomyocyte energetics, mitochondrial quality control, and function.

Conflicts of Interest

The authors have declared that they have no conflicts of interest.

Authors' Contributions

Ying Tan and Fengfan Xia contributed equally to this work.

Acknowledgments

References

[1] M. Akbari, T. B. L. Kirkwood, and V. A. Bohr, "Mitochondria in the signaling pathways that control longevity and health span," *Ageing Research Reviews*, vol. 54, article 100940, 2019.

[2] N.-D. Deirdre, B. Andrea, and S. Sruti, "Mitochondrial electron transport chain: oxidative phosphorylation, oxidant production, and methods of measurement," *Redox Biology*, vol. 37, article 101674, 2020.

[3] M. R. Lewis and W. H. Lewis, "Mitochondria in tissue culture," *Science*, vol. 39, no. 1000, pp. 330–333, 1914.

[4] C. Vásquez-Trincado, I. García-Carvajal, C. Pennanen et al., "Mitochondrial dynamics, mitophagy and cardiovascular disease," *The Journal of Physiology*, vol. 594, no. 3, pp. 509–525, 2016.

[5] L. Archer Stephen, "Mitochondrial dynamics–mitochondrial fission and fusion in human diseases," *The New England Journal of Medicine*, vol. 369, no. 23, pp. 2236–2251, 2013.

[6] M. Song, K. Mihara, Y. Chen, L. Scorrano, and G. W. Dorn II, "Mitochondrial fission and fusion factors reciprocally orchestrate mitophagic culling in mouse hearts and cultured fibroblasts," *Cell Metabolism*, vol. 21, no. 2, pp. 273–286, 2015.

[7] M. Song and G. W. Dorn II, "Mitoconfusion: noncanonical functioning of dynamism factors in static mitochondria of the heart," *Cell Metabolism*, vol. 21, no. 2, pp. 195–205, 2015.

[8] H. Chen, S. Ren, C. Clish et al., "Titration of mitochondrial fusion rescues Mff-deficient cardiomyopathy," *The Journal of Cell Biology*, vol. 211, no. 4, pp. 795–805, 2015.

[9] R. J. Youle and A. M. van der Bliek, "Mitochondrial fission, fusion, and stress," *Science*, vol. 337, no. 6098, pp. 1062–1065, 2012.

[10] J. Neuzil, C. Widén, N. Gellert et al., "Mitochondria transmit apoptosis signalling in cardiomyocyte-like cells and isolated hearts exposed to experimental ischemia-reperfusion injury," *Redox Report*, vol. 12, no. 3, pp. 148–162, 2013.

[11] O. Sang-Bing and J. Hausenloy Derek, "Mitochondrial dynamics as a therapeutic target for treating cardiac diseases," *Handbook of Experimental Pharmacology*, vol. 240, pp. 251–279, 2016.

[12] R. Anand, T. Wai, M. J. Baker et al., "The i-AAA protease YME1L and OMA1 cleave OPA1 to balance mitochondrial fusion and fission," *The Journal of Cell Biology*, vol. 204, no. 6, pp. 919–929, 2014.

[13] O. S. Shirihai, M. Song, and G. W. Dorn II, "How mitochondrial dynamism orchestrates mitophagy," *Circulation Research*, vol. 116, no. 11, pp. 1835–1849, 2015.

[14] B. D. Song and S. L. Schmid, "A molecular motor or a regulator? Dynamin's in a class of its own," *Biochemistry*, vol. 42, no. 6, pp. 1369–1376, 2003.

[15] Y. Ikeda, A. Shirakabe, C. Brady, D. Zablocki, M. Ohishi, and J. Sadoshima, "Molecular mechanisms mediating mitochondrial dynamics and mitophagy and their functional roles in the cardiovascular system," *Journal of Molecular and Cardiology*, vol. 78, pp. 116–122, 2015.

[16] A. R. Hall and D. J. Hausenloy, "The shape of things to come: mitochondrial fusion and fission in the adult heart," *Cardiovascular Research*, vol. 94, no. 3, pp. 391-392, 2012.

[17] E. Bossy-Wetzel, M. J. Barsoum, A. Godzik, R. Schwarzenbacher, and S. A. Lipton, "Mitochondrial fission in apoptosis, neurodegeneration and aging," *Current Opinion in Cell Biology*, vol. 15, no. 6, pp. 706–716, 2003.

[18] Y.-j. Lee, S.-Y. Jeong, M. Karbowski, C. L. Smith, and R. J. Youle, "Roles of the mammalian mitochondrial fission and fusion mediators Fis1, Drp1, and Opa1 in apoptosis," *Molecular Biology of the Cell*, vol. 15, no. 11, pp. 5001–5011, 2004.

[19] S. Gandre-Babbe and A. M. van der Bliek, "The novel tail-anchored membrane protein Mff controls mitochondrial and peroxisomal fission in mammalian cells," *Molecular Biology of the Cell*, vol. 19, no. 6, pp. 2402–2412, 2008.

[20] H. Otera, C. Wang, M. M. Cleland et al., "Mff is an essential factor for mitochondrial recruitment of Drp1 during mitochondrial fission in mammalian cells," *The Journal of Cell Biology*, vol. 191, no. 6, pp. 1141–1158, 2010.

[21] N. Taguchi, N. Ishihara, A. Jofuku, T. Oka, and K. Mihara, "Mitotic Phosphorylation of Dynamin-related GTPase Drp1 Participates in Mitochondrial Fission," *The Journal of Biological Chemistry*, vol. 282, no. 15, pp. 11521–11529, 2007.

[22] X.-J. Han, Y.-F. Lu, S. A. Li et al., "CaM kinase Iα–induced phosphorylation of Drp1 regulates mitochondrial morphology," *The Journal of Cell Biology*, vol. 182, no. 3, pp. 573–585, 2008.

[23] C.-R. Chang and C. Blackstone, "Cyclic AMP-dependent Protein Kinase Phosphorylation of Drp1 Regulates Its GTPase Activity and Mitochondrial Morphology," *The Journal of Biological Chemistry*, vol. 282, no. 30, pp. 21583–21587, 2007.

[24] G. M. Cereghetti, A. Stangherlin, O. M. de Brito et al., "Dephosphorylation by calcineurin regulates translocation of Drp1 to mitochondria," *Proceedings of the National Academy of Sciences of the United States of America*, vol. 105, no. 41, pp. 15803–15808, 2008.

[25] K. Maria, B. Małgorzata, Z. Krzysztof, and B. Zabłocka, "Mitofusin 2 and mitochondrial dynamics in norm and pathology," *Postepy Biochemii*, vol. 62, no. 2, pp. 149–157, 2016.

[26] T. J. Cahill, V. Leo, M. Kelly et al., "Resistance of dynamin-related protein 1 oligomers to disassembly impairs mitophagy, resulting in myocardial inflammation and heart failure.," *The Journal of Biological Chemistry*, vol. 291, no. 49, article 25762, 2016.

[27] W. W. Sharp, Y. H. Fang, M. Han et al., "Dynamin-related protein 1 (Drp1)-mediated diastolic dysfunction in myocardial ischemia-reperfusion injury: therapeutic benefits of Drp1 inhibition to reduce mitochondrial fission," *FASEB Journal*, vol. 28, no. 1, pp. 316–326, 2014.

[28] M.-. H. Disatnik, J. C. B. Ferreira, J. C. Campos et al., "Acute inhibition of excessive mitochondrial fission after myocardial infarction prevents long-term cardiac dysfunction," *Journal of the American Heart Association*, vol. 2, no. 5, article e000461, 2013.

[29] Y. Ikeda, A. Shirakabe, Y. Maejima et al., "Endogenous Drp1 mediates mitochondrial autophagy and protects the heart against energy stress," *Circulation Research*, vol. 116, no. 2, pp. 264–278, 2015.

[30] Y. Kageyama, M. Hoshijima, K. Seo et al., "Parkin-independent mitophagy requires Drp1 and maintains the integrity of mammalian heart and brain," *The EMBO Journal*, vol. 33, no. 23, pp. 2798–2813, 2014.

[31] Y. Qin, A. Li, B. Liu et al., "Mitochondrial fusion mediated by fusion promotion and fission inhibition directs adult mouse heart function toward a different direction," *FASEB Journal*, vol. 34, no. 1, pp. 663–675, 2020.

[32] C. Maneechote, S. Palee, S. Kerdphoo, T. Jaiwongkam, S. C. Chattipakorn, and N. Chattipakorn, "Balancing mitochondrial dynamics via increasing mitochondrial fusion attenuates infarct size and left ventricular dysfunction in rats with cardiac ischemia/reperfusion injury," *Clinical Science*, vol. 133, no. 3, pp. 497–513, 2019.

[33] J. Steffen, A. A. Vashisht, J. Wan et al., "Rapid degradation of mutant SLC25A46 by the ubiquitin-proteasome system results in MFN1/2-mediated hyperfusion of mitochondria," *Molecular Biology of the Cell*, vol. 28, no. 5, pp. 600–612, 2017.

[34] N. C. Denham, C. M. Pearman, J. L. Caldwell et al., "Calcium in the pathophysiology of atrial fibrillation and heart failure," *Frontiers in Physiology*, vol. 9, p. 1380, 2018.

[35] W. Xie, G. Santulli, S. R. Reiken et al., "Mitochondrial oxidative stress promotes atrial fibrillation," *Scientific Reports*, vol. 5, no. 1, article 11427, 2015.

[36] C. J. Redpath, M. Bou Khalil, G. Drozdzal, M. Radisic, and H. M. McBride, "Mitochondrial hyperfusion during oxidative stress is coupled to a dysregulation in calcium handling within a C2C12 cell model," *PloS one*, vol. 8, no. 7, article e69165, 2013.

[37] G. N. Kanaan, D. A. Patten, C. J. Redpath, and M. E. Harper, "Atrial fibrillation is associated with impaired atrial mitochondrial energetics and supercomplex formation in adults with type 2 diabetes," *Canadian Journal of Diabetes*, vol. 43, no. 1, pp. 67–75.e1, 2019.

[38] M. Manevski, T. Muthumalage, D. Devadoss et al., "Cellular stress responses and dysfunctional mitochondrial-cellular senescence, and therapeutics in chronic respiratory diseases," *Redox Biology*, vol. 33, article 101443, 2020.

[39] W. E. Hughes, A. M. Beyer, and D. D. Gutterman, "Vascular autophagy in health and disease," *Basic Research in Cardiology*, vol. 115, no. 4, p. 41, 2020.

[40] E. Yu, J. Mercer, and M. Bennett, "Mitochondria in vascular disease," *Cardiovascular Research*, vol. 95, no. 2, pp. 173–182, 2012.

[41] H. Zhou, J. Wang, P. Zhu et al., "NR4A1 aggravates the cardiac microvascular ischemia reperfusion injury through suppressing FUNDC1-mediated mitophagy and promoting Mff-required mitochondrial fission by CK2α," *Basic Research in Cardiology*, vol. 113, no. 4, p. 63, 2018.

[42] P. Konstantinos, L. Eirini, and T. Nektarios, "Mechanisms of mitophagy in cellular homeostasis, physiology and pathology," *Nature Cell Biology*, vol. 20, no. 9, pp. 1013–1022, 2018.

[43] N. Nadee, M. Michal, and T. Moraes Carlos, "Mechanisms of mitochondrial DNA deletion formation," *Trends in Genetics: TIG*, vol. 35, no. 3, pp. 235–244, 2019.

[44] H. Gerd, "Coronary microvascular obstruction: the new frontier in cardioprotection," *Basic Research in Cardiology*, vol. 114, no. 6, p. 45, 2019.

[45] M. Ding, Q. Dong, Z. Liu et al., "Inhibition of dynamin-related protein 1 protects against myocardial ischemia-reperfusion injury in diabetic mice," *Cardiovascular Diabetology*, vol. 16, no. 1, p. 19, 2017.

[46] J.-X. Wang, J.-Q. Jiao, Q. Li et al., "miR-499 regulates mitochondrial dynamics by targeting calcineurin and dynamin-related protein-1," *Nature Medicine*, vol. 17, no. 1, pp. 71–78, 2011.

[47] S. Din, M. Mason, M. Volkers et al., "Pim-1 preserves mitochondrial morphology by inhibiting dynamin-related protein 1 translocation," *Proceedings of the National Academy of Sciences of the United States of America*, vol. 110, no. 15, pp. 5969–5974, 2013.

[48] M. Karbowski, K. L. Norris, M. M. Cleland, S.-Y. Jeong, and R. J. Youle, "Role of Bax and Bak in mitochondrial morphogenesis," *Nature*, vol. 443, no. 7112, pp. 658–662, 2006.

[49] C. Le, G. Qizhi, P. Stice James, and A. A. Knowlton, "Mitochondrial OPA1, apoptosis, and heart failure," *Cardiovascular Research*, vol. 84, no. 1, pp. 91–99, 2009.

[50] S.-B. Ong, S. Subrayan, S. Y. Lim, D. M. Yellon, S. M. Davidson, and D. J. Hausenloy, "Inhibiting mitochondrial fission protects the heart against ischemia/reperfusion injury," *Circulation*, vol. 121, no. 18, pp. 2012–2022, 2010.

[51] K. N. Papanicolaou, R. J. Khairallah, G. A. Ngoh et al., "Mitofusin-2 maintains mitochondrial structure and contributes to stress-induced permeability transition in cardiac myocytes," *Molecular and Cellular Biology*, vol. 31, no. 6, pp. 1309–1328, 2011.

[52] J. Piquereau, F. Caffin, M. Novotova et al., "Down-regulation of OPA1 alters mouse mitochondrial morphology, PTP function, and cardiac adaptation to pressure overload," *Cardiovascular Research*, vol. 94, no. 3, pp. 408–417, 2012.

[53] N. Frey, H. A. Katus, E. N. Olson, and J. A. Hill, "Hypertrophy of the heart: a new therapeutic target?," *Circulation*, vol. 109, no. 13, pp. 1580–1589, 2004.

[54] S. P. Barry, S. M. Davidson, and P. A. Townsend, "Molecular regulation of cardiac hypertrophy," *The International Journal of Biochemistry and Biology*, vol. 40, no. 10, pp. 2023–2039, 2008.

[55] J. A. Hill and E. N. Olson, "Cardiac plasticity," *The New England Journal of Medicine*, vol. 358, no. 13, pp. 1370–1380, 2008.

[56] J. S. Burchfield, M. Xie, and J. A. Hill, "Pathological ventricular remodeling: mechanisms: part 1 of 2," *Circulation*, vol. 128, no. 4, pp. 388–400, 2013.

[57] M. Vendelin, N. Béraud, K. Guerrero et al., "Mitochondrial regular arrangement in muscle cells: a "crystal-like" pattern," *American Journal of Physiology-Cell Physiology*, vol. 288, no. 3, pp. C757–C767, 2005.

[58] N. Beraud, S. Pelloux, Y. Usson et al., "Mitochondrial dynamics in heart cells: very low amplitude high frequency fluctuations in adult cardiomyocytes and flow motion in non beating Hl-1 cells," *Journal of Bioenergetics and Biomembranes*, vol. 41, no. 2, pp. 195–214, 2009.

[59] L. Fang, X.-L. Moore, X.-M. Gao, A. M. Dart, Y. L. Lim, and X.-J. Du, "Down-regulation of mitofusin-2 expression in cardiac hypertrophy in vitro and in vivo," *Life Sciences*, vol. 80, no. 23, pp. 2154–2160, 2007.

[60] J. Amela, D. Yvan, and EU-Cardio RNA COST Action (CA17129), "Mitochondrial noncoding RNA-regulatory network in cardiovascular disease," *Basic Research in Cardiology*, vol. 115, no. 3, p. 23, 2020.

[61] C. Pennanen, V. Parra, C. Lopez-Crisosto et al., "Mitochondrial fission is required for cardiomyocyte hypertrophy mediated by a Ca2+-calcineurin signaling pathway," *Journal of Cell Science*, vol. 127, pp. 2659–2671, 2014.

[62] S. Givvimani, C. Munjal, N. Tyagi, U. Sen, N. Metreveli, and S. C. Tyagi, "Mitochondrial fission/mitophagy inhibitor (Mdivi) ameliorates pressure overload induced heart failure," *PLoS One*, vol. 7, no. 3, article e32388, 2012.

[63] Y. Qiu, R. Cheng, C. Liang et al., "MicroRNA-20b Promotes Cardiac Hypertrophy by the Inhibition of Mitofusin 2-Mediated Inter-organelle Ca^{2+} Cross-Talk," *Molecular Therapy - Nucleic Acids*, vol. 19, pp. 1343–1356, 2020.

[64] D. P. Narendra, S. M. Jin, A. Tanaka et al., "PINK1 is selectively stabilized on impaired mitochondria to activate Parkin," *PLoS Biology*, vol. 8, no. 1, article e1000298, 2010.

[65] A. Makino, J. Suarez, T. Gawlowski et al., "Regulation of mitochondrial morphology and function by O-Glc NAcylation in neonatal cardiac myocytes," *American Journal of Physiology-Regulatory, Integrative and Comparative Physiology*, vol. 300, no. 6, pp. R1296–R1302, 2011.

[66] T. Wai, J. Garcia-Prieto, M. J. Baker et al., "Imbalanced OPA1 processing and mitochondrial fragmentation cause heart failure in mice," *Science*, vol. 350, no. 6265, article aad0116, 2015.

[67] D. Montaigne, X. Marechal, A. Coisne et al., "Myocardial contractile dysfunction is associated with impaired mitochondrial function and dynamics in type 2 diabetic but not in obese patients," *Circulation*, vol. 130, no. 7, pp. 554–564, 2014.

[68] M. Ding, C. Liu, R. Shi et al., "Mitochondrial fusion promoter restores mitochondrial dynamics balance and ameliorates diabetic cardiomyopathy in an optic atrophy 1-dependent way," *Acta Physiologica*, vol. 229, no. 1, article e13428, 2020.

[69] D. Sebastian, M. I. Hernandez-Alvarez, J. Segales et al., "Mitofusin 2 (Mfn 2) links mitochondrial and endoplasmic reticulum function with insulin signaling and is essential for normal glucose homeostasis," *Proceedings of the National*

Retraction

Retracted: The Role of Posttranslational Modification and Mitochondrial Quality Control in Cardiovascular Diseases

Oxidative Medicine and Cellular Longevity

This article has been retracted by Hindawi following an investigation undertaken by the publisher [1]. This investigation has uncovered evidence of one or more of the following indicators of systematic manipulation of the publication process:

(1) Discrepancies in scope

(2) Discrepancies in the description of the research reported

(3) Discrepancies between the availability of data and the research described

(4) Inappropriate citations

(5) Incoherent, meaningless and/or irrelevant content included in the article

(6) Peer-review manipulation

The presence of these indicators undermines our confidence in the integrity of the article's content and we cannot, therefore, vouch for its reliability. Please note that this notice is intended solely to alert readers that the content of this article is unreliable. We have not investigated whether authors were aware of or involved in the systematic manipulation of the publication process.

Wiley and Hindawi regrets that the usual quality checks did not identify these issues before publication and have since put additional measures in place to safeguard research integrity.

We wish to credit our own Research Integrity and Research Publishing teams and anonymous and named external researchers and research integrity experts for contributing to this investigation.

The corresponding author, as the representative of all authors, has been given the opportunity to register their agreement or disagreement to this retraction. We have kept a record of any response received.

References

[1] J. Liu, L. Zhong, and R. Guo, "The Role of Posttranslational Modification and Mitochondrial Quality Control in Cardiovascular Diseases," *Oxidative Medicine and Cellular Longevity*, vol. 2021, Article ID 6635836, 15 pages, 2021.

Review Article

The Role of Posttranslational Modification and Mitochondrial Quality Control in Cardiovascular Diseases

Jinlin Liu [iD],[1] Li Zhong [iD],[1,2] and Rui Guo [iD][1]

[1]*College of Life Sciences, Institute of Life Science and Green Development, Hebei University, Baoding 071002, China*
[2]*College of Osteopathic Medicine of the Pacific, Western University of Health Sciences, Pomona, California, USA*

Correspondence should be addressed to Rui Guo; rguo@hbu.edu.cn

Cardiovascular disease (CVD) is the leading cause of death in the world. The mechanism behind CVDs has been studied for decades; however, the pathogenesis is still controversial. Mitochondrial homeostasis plays an essential role in maintaining the normal function of the cardiovascular system. The alterations of any protein function in mitochondria may induce abnormal mitochondrial quality control and unexpected mitochondrial dysfunction, leading to CVDs. Posttranslational modifications (PTMs) affect protein function by reversibly changing their conformation. This review summarizes how common and novel PTMs influence the development of CVDs by regulating mitochondrial quality control. It provides not only ideas for future research on the mechanism of some types of CVDs but also ideas for CVD treatments with therapeutic potential.

1. Introduction

Cardiovascular disease (CVD) is currently one of the most perplexing diseases because of its variety and complexity. The mortality rate of CVDs, accounting for 30% of the death toll in the world, has still been increasing every year [1, 2]. CVDs not only affect human life but also cause great socioeconomic burden. Thus, coronary artery disease is considered one of the major CVDs affecting the global human population and has been considered as a major cause of death in both developed and developing countries [3]. Coronary artery disease can cause severe myocardial infarction and contributes to the development of heart failure [4]. However, the pathologic process and risk factors of CVDs are still controversial, especially the molecular mechanisms on modulating mitochondria-associated proteins by posttranslational modifications (PTMs) [5, 6].

The mitochondrion, a membrane-bound organelle, is present in all eukaryotic cells. It is crucial to maintain the normal mitochondrial function to provide energy for cell survival. Therefore, disturbed mitochondrial quality control and homeostasis can result in a variety of CVDs. Mitochondrial biogenesis, fusion, fission, mitophagy, and protein turnover are considered as the main processes for mitochondrial quality control [7–12]. Dysfunctional mitochondria or mitochondrial proteins are degraded and removed by the ubiquitin-proteasome system (UPS) or by autophagy (mitophagy) to maintain a normal mitochondrial homeostasis [13, 14]. PTMs refer to the chemical modifications of specific amino acid residues of proteins, the reactions of which are mostly reversible [15]. A majority of the proteins in cells undergo PTMs by changing their structures and functions by conformational alterations [16]. PTMs of proteins have been shown to affect mitochondrial quality control, thereby exacerbating or alleviating CVDs [17–19]. Therefore, the purpose of this review is to summarize the functional changes of intracellular proteins especially mitochondrial-related proteins by PTMs and their effects on CVDs, particularly myocardial ischemia/reperfusion (I/R) injury, myocardial infarction, and heart failure. The PTMs including acetylation, phosphorylation, SUMOylation, ubiquitination, succinylation, lactylation, and crotonylation are discussed, and they shed light on a theoretical basis of CVD treatment in the future.

2. Mitochondrial Quality Control and Cardiovascular Diseases

Mitochondria are cellular organelles involved in energy production in the form of ATP through the process of oxidative

phosphorylation, citric cycle, and β-oxidation to maintain cardiomyocyte vitality [20]. The mitochondrial environment has thus emerged as a key part in the pathogenesis and progression of CVDs which eventually can lead to heart failure. Mitochondrial fission and fusion, as well as mitophagy, are major processes in maintaining mitochondrial quality control, of which fission and fusion are primarily mediated by the following three particular proteins: (1) optic atrophy 1 (OPA1), localized to the inner membrane of mitochondria (IMM), which can move to the intermembrane space (IMS) and play a unique role in IMM fusion to crest structure adjustment; (2) mitofusins 1 and 2 (Mfn1 and Mfn2), which are located in the outer membrane of mitochondria (OMM) for OMM fusion [21]; and (3) dynamic protein-related protein 1 (Drp1), which is generally located in the cytoplasm and can be transferred to the mitochondria to divide the OMM and mediate the process of mitochondrial fission. Similarly, there are multiple ways to remove damaged mitochondria, such as degradation by proteasomes, combination with mitophagy, and fusion with a lysosome. In a word, the abnormality in mitochondrial quality control that is regulated by a complex network will cause severe mitochondrial disturbance.

There are plenty of mitochondria in cardiac cells for the high energy demand of the heart. ATP synthesis and energy metabolism cannot be performed normally in patients with mitochondrial defects [22]. On the other hand, mitochondrial dysfunction can cause a variety of CVDs or cardiac disorders such as cardiac I/R injury, myocardial infarction, cardiac hypertrophy, and heart failure [23, 24]. Damaged mitochondria are not able to synthesize sufficient ATP, but they increase the reactive oxygen species (ROS) levels. ROS is a major by-product during the process of mitochondrial respiration. Excessive cellular ROS contents not only cause loss of certain DNAs and proteins but also lead to the occurrence of heart failure and other diseases [25–28]. To this end, understanding the mechanisms of mitochondrial quality control and the degradation of unhealthy mitochondria or abnormal mitochondrial proteins plays an important role in maintaining normal cardiac function.

3. The Main Types of Mitochondrial PTMs in Cardiovascular Disease

3.1. SUMOylation. Small ubiquitin-like modifiers (SUMO), with a molecular weight of about 10 kDa, belong to the large family of ubiquitin-like (Ubl) proteins. There are four subtypes of SUMO in mammals, namely, SUMO1, SUMO2, SUMO3, and SUMO4 [29–32], of which SUMO2 and SUMO3 have about 97% similarity [33]. The subtypes SUMO1-SUMO3 are widely expressed, while SUMO4 is only expressed in the kidney, spleen, and lymph nodes [34–36]. SUMOylation is classified as a ubiquitination-like PTM, binding the SUMO protein to the lysine residue of the substrate protein through successive steps of reactions by the SUMO activating enzyme (E1, a heterodimer of SAE1/SAE2 subunits), the SUMO conjugating enzyme (E2, also known as Ubc9), and several E3 ligases with ATP consumption (see Figure 1) [37]. At present, only one type of E1 or E2 has been found whereas there are more than ten types of E3 ligases, which are divided into three categories: protein inhibitor of activated STAT (PIAS) proteins, Ras-related nuclear protein binding protein 2 (RanBP2), and human polycomb 2 (Pc2)/Chromobox 4 (CBX4) [38, 39]. The SUMOylation process is reversible. Importantly, SUMO-specific proteases such as cysteine proteases of the sentrin-specific protease (SENP) family (including SENP1-SENP3 and SENP5-SENP7) are involved not only in the activation of SUMO precursors but also in the separation of SUMO and substrate proteins [33, 37]. Evidence has shown that SUMOylation is involved in mitochondrial quality control, cytochrome C release, and Ca^{2+} homeostasis of cardiomyocytes [40, 41]. As a result, in recent years, more and more attention has been paid to the role of mitochondrial protein SUMOylation in CVDs.

3.1.1. Mitochondrion-Related Protein SUMOylation in Myocardial I/R Injury. Drp1, a GTPase, is not only associated with mitochondrial fission but is also involved in mitochondrial apoptosis [42]. The SUMOylation modification of Drp1 has a great impact on mitochondrial quality control and plays a crucial role in cardiac I/R injury. Previous research indicated that following I/R injury of the heart, the binding capacity of SUMO1 to Drp1 increased and formed a complex. Zinc promoted mitochondrial fission by increasing the acidification of the complex, thereby eliminating damaged mitochondria and maintaining mitochondrial quality stability, further improving cardiac function [43]. Evidence revealed that SENP3, an enzyme of deSUMOylation, was associated with apoptosis induction in response to cardiac I/R by affecting Drp1 localization in the mitochondria. However, mdivi-1, an inhibitor of Drp1, alleviated myocardial damage by inhibiting the expression of SENP3 [44].

3.1.2. Mitochondrion-Related Protein SUMOylation in Heart Failure. In both mouse models and humans, a low level of apoptosis in cardiomyocytes is detrimental to the heart and may contribute to the progression of heart failure [45, 46]. Kim et al. found that SENP5 expression was significantly higher than normal in heart failure [47]. Drp1, a pivotal protein that mediates the apoptosis of cardiomyocytes, was induced by SENP5 which has long been shown to be of great significance for regulating mitochondrial function [48]. Data revealed that SENP5 activity was reduced by apoptotic factors after deletion of Drp1 in cardiomyocytes. On the contrary, upregulation of SENP5 expression elevated mitochondrial apoptosis levels via the connection between Drp1 and SUMO2/3 [47].

3.2. Ubiquitination. The ubiquitin-proteasome system (UPS) is the primary system of protein degradation in eukaryotic cells. Ubiquitin is a polypeptide containing 76 amino acids, and ubiquitination occurs by covalently binding its own COOH group at the glycine end with the free ε-NH2 terminus of a lysine residue in the target protein [49, 50]. Each ubiquitin has multiple binding sites for the combination with other ubiquitin peptides to form ubiquitin chains. The binding of the ubiquitin molecule to the lysine residue of the
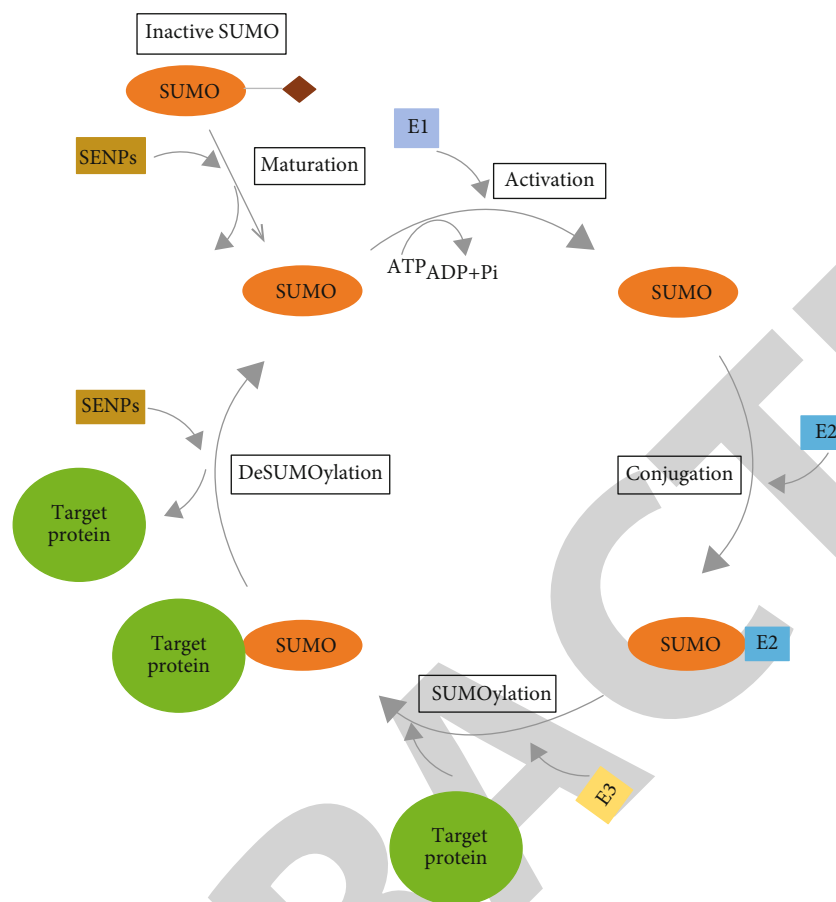
FIGURE 1: The process of protein SUMOylation. First, the inactive SUMO protein is activated by the action of SENPs. By consuming 1 molecule of ATP, a SUMO protein binds to the E1 activating enzyme. The E2 conjugating enzyme replaces E1 to bind to the SUMO protein. Then, E2 presents the SUMO protein to the E3 ligase, which specifically recognizes the target protein and makes SUMO bind to the Lys residue on the target protein to achieve the goal of protein structural and functional changes. SENPs are also required for the deSUMOylation process.

target protein will initiate the degradation of marked proteins [51]. In addition to binding to lysine residues, ubiquitin can also combine with the amino terminus of the substrate [52]. Ubiquitination is a cascade reaction coordinated and catalyzed by E1 (ubiquitin activating enzyme), E2 (ubiquitin conjugating enzyme), and E3 (ubiquitin ligase), and the process is also reversible (see Figure 2) [49, 53]. Similar to SENPs, deubiquitinases (DUBs) are capable of activating ubiquitin precursors by splicing or removing ubiquitin molecules from tagged proteins [54]. Ubiquitination has been widely studied as protein degradation is the major way to maintain mitochondrial quality and intracellular homeostasis.

3.2.1. Mitochondrion-Related Protein Ubiquitination in Myocardial I/R Injury. There are varieties of ubiquitin E3 ligases reported in human cells, which are vital for the ubiquitination process. Parkin, an E3 ligase, can ubiquitinate several mitochondrial outer membrane proteins through its E3 ligase activity to recruit the p62 protein, which interacts with LC3, leading to the process of PINK/Parkin-mediated mitophagy [55]. Evidence has shown that expression of Parkin is beneficial to cardiac function, specifically, by catalyzing CypD ubiquitination in the cell necrosis cascade and inhibit-

ing the opening of the mitochondrial permeability transition pore (mPTP), therefore alleviating myocardial injury [56]. Another study found that Tongxinluo, a medicine for treating coronary heart disease, was involved in activating Parkin and reducing the activity of the ubiquitin system to attenuate myocardial I/R injury [57], although few studies have reported which particular or active ingredients of the Tongxinluo capsule may play a regulatory role in the PINK/Parkin pathway [58, 59]. Phosphatase and tensin homolog (PTEN) is a tumor-suppressor protein located in mitochondria [60]. Li et al. revealed that the terminal end of PTEN can bind to the E3 ligase Parkin and promote the translocation of Parkin within mitochondria. The loss of PTEN was reported to be more susceptible to the I/R injury of the heart, due to its ability to induce structural and functional abnormalities of the mitochondria in mouse cardiomyocytes [54]. In the process of heart remodeling following I/R injury, exogenous ubiquitin treatment significantly reduced Caspase-9 expression in the mitochondrial death pathway, reduced infarct area, increased mitochondrial production, and finally improved heart function. In short, ubiquitination is closely associated with myocardial I/R injury [61].
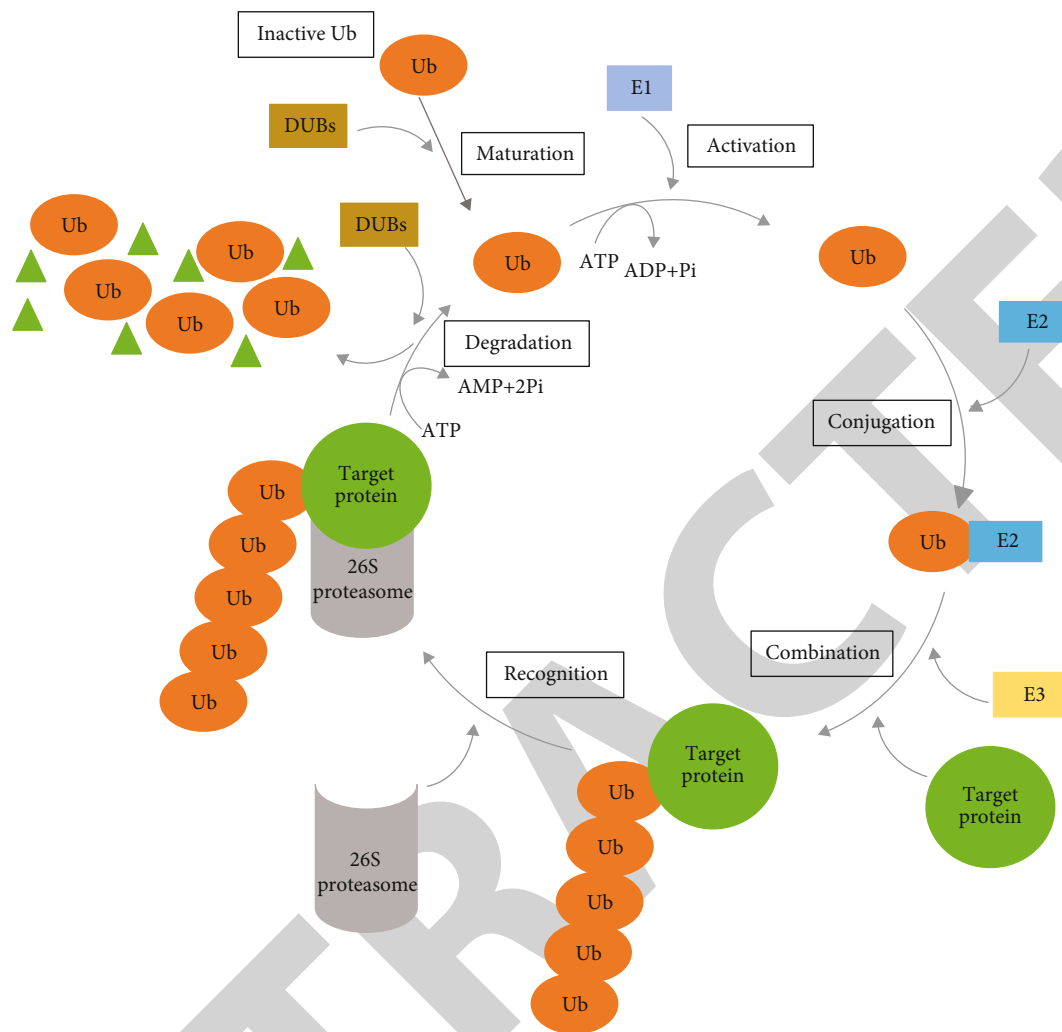
FIGURE 2: The process of protein ubiquitination. First, the inactive ubiquitin (Ub) molecule is activated under the catalysis of DUBs. Under the action of 1 molecule of ATP, Ub binds to an E1 activating enzyme; then, the E2 conjugating enzyme replaces E1 and connects to Ub. Next, E2 presents Ub to the E3 ligase, and the E3 ligase binds specifically to the target protein. The above steps are repeated until the target protein binds more than 4 Ub molecules to form a Ub chain. Then, the 26S proteasome recognizes the Ub chain and places the target protein in its own barrel. Finally, the target protein is degraded into small fragments by ATP consumption, and the Ub molecule is restored for release.

3.2.2. Mitochondrion-Related Protein Ubiquitination in Cardiomyopathy. Mutations in E3 ligases MuRF1 and MuRF2 are critical for the development of hypertrophic cardiomyopathy (HCM). In patients with HCM, increased MuRF1 mutants in adult cardiomyocytes resulted in a reduction of ubiquitination, as well as UPS-mediated degradation of myosin heavy chain 6 (Myh6) and cardiac myosin-binding protein-C (cMyBP-C) [62]. Parkin is necessary for mitochondrial quality control, and its expression is relatively low in a normal heart. It was suggested that the ablation of Drp1 inhibited mitochondrial fission by promoting Parkin expression, which in turn led to cardiomyopathy [63]. In addition, another study found that disturbed mitochondrial redox status induced by lipid toxicity eventually led to mitochondrial dysfunction and cardiomyopathy, the mechanism of which may be due to an enhanced mitochondrial fission through increased AKAP121 (A kinase anchor protein 121) ubiquitination that resulted in a reduction in Drp1 phos-

phorylation at the site of Ser637, as well as the changes in OPA1 protease hydrolysis [64].

3.2.3. Mitochondrion-Related Protein Ubiquitination in Heart Failure. Both coronary artery disease and cardiomyopathy contribute to the development of heart failure. One of the reasons that trigger heart failure is the excessive death of cardiomyocytes. For instance, a certain extent of mitophagy is accompanied with the clearance of damaged mitochondria, the improvement of mitochondrial function, the reduction in ROS production, and the apoptosis of cardiomyocytes. However, excessive mitophagy can cause cardiac injury because of cell death. Evidence has shown that PINK1-associated ubiquitination and phosphorylation enhanced mitochondrial depolarizing by raising Parkin activation and recruitment, causing increased mitophagy via the PINK1-Parkin-SQstm1 (Sequencesome-1) pathway. In addition, alanine mutation of PINK1 at Ser495 partially inhibited

AMPKα2 overexpression-induced mitophagy and improved the mitochondrial function stimulated by phenylephrine in cardiomyocytes. In failing hearts, however, the dominant AMPKα isoform switched from AMPKα2 to AMPKα1, exacerbating the heart failure condition [65]. Moreover, the results obtained by Yang et al. indicated that leptin enhanced OPA1 by inhibiting the activity of OMA1, a mitochondrial protease. In this process, GSK3 phosphorylation was a prerequisite for ubiquitination-dependent degradation of OMA1, thereby attenuating OPA1 cleavage. Additionally, leptin induced mitochondrial fusion and improved mitochondrial respiratory function in hypoxic hMSCs (human mesenchymal stem cells), indicating a protective role of leptin against myocardial infarction by prolonging the hMSCs' survival time for the treatment [66].

3.3. Phosphorylation.
Phosphorylation, one of the earliest known PTMs, plays an extensive role in mediating protein activation or deactivation, and is extremely essential for nearly every aspect of cell life. Protein phosphorylation was first identified by Phoebus Levene in 1906, and phosphorylation as a regulatory physiological mechanism was discovered in 1955. Researchers at the time found that converting phosphorylase B to phosphorylase A required phosphate-containing enzymes to interact with ATP. Phosphorylation or dephosphorylation can be reversibly catalyzed by protein kinases or phosphatases, respectively [67, 68]. Unlike the previous modified binding sites, phosphorylation transfers the phosphorylated group to the protein residues of the serine (Ser), threonine (Thr), and tyrosine (Tyr) in the targeted protein, so the phosphorylated protein is negatively charged [69]. Proteins in mitochondria undergo phosphorylation by the catalysis of related enzymes, which significantly affects the occurrence of CVDs [70].

3.3.1. Mitochondrion-Associated Phosphorylation in Myocardial Infarction and I/R Injury.
Normal mitochondria produce ATP molecules by oxidative phosphorylation. However, mitochondrial dysfunction produces harmful effects on oxidative phosphorylation and facilitates the generation and accumulation of ROS, thus exacerbating myocardial infarction [71]. Metformin, a drug for the treatment of type 2 diabetes, can alleviate myocardial infarction and improve the survival rate of patients. Evidence revealed that metformin significantly increased phosphorylation of Akt (also known as PKB), thereby inhibiting the opening of mPTP, and it activated the downstream kinase of the reperfusion-induced survival kinase (RISK), thereby alleviating myocardial infarction [72, 73]. Phosphorylation of the mitochondrial complex IV (C_{IV}) subunit is essential for maintaining the activity of C_{IV} in myocardial mitochondria. In response to cardiac I/R, protein kinase A-dependent phosphorylation of the IVI1 and VB subunits of C_{IV} were elevated, resulting in a decrease in C_{IV} activity and an increase in ROS production [74, 75]. The signal transducer and activator of transcription 3 (STAT3) plays a key role in regulating mitochondrial metabolism. STAT3 can interact with various mitochondrial proteins and genomes to promote mitochondrial respiration once STAT3 translocated into mitochondria [76]. It has been shown that STAT3 phosphorylation improved mitochondrial function by affecting the mitochondrial complex I (C_I) in the mitochondrial electron transport chain, preventing the opening of mPTP in the outer membrane, and in turn reducing the myocardial infarction area [77–79]. In addition, phosphorylation of proteins in mitochondria is also involved in cell death. For instance, phosphorylation of a voltage-dependent anion channel (VDAC) protein in the OMM can induce apoptosis that affects the cardiovascular heathy condition [80]. To sum up, mitochondrial phosphorylation elicits a pivotal role in myocardial damage by affecting mitochondrial respiration and quality control.

3.3.2. Mitochondrion-Associated Phosphorylation in Heart Failure.
In failing hearts, changes in mitochondrial shape and cristae structure can lead to a reduction in the capacity for energy production [81, 82]. Research by Dey et al. established a nonischemic heart failure model using guinea pigs to mimic human failure. They found that the increase of mitochondrial ROS in heart failure blocked the normal signalling connection between the cytoplasm and the nucleus [83]. Besides, other researchers revealed that the mitochondrial respiratory function of mitochondrial C_I and C_{II}, as well as the ability of oxidative phosphorylation, were repaired in mice with heart failure following a mild linoleic acid feeding [84]. In addition to a decrease in ATP productivity, another characteristic of heart failure is the accumulation of mitochondrial debris. Evidence suggests that Drp1 phosphorylation facilitates the mitochondrial fission process by promoting its recruitment at OMM in chronic heart failure [85].

3.4. Acetylation.
Acetylation is one of the major PTMs in cell biology. Basically, acetylation occurs with the transfer of acetyl groups from acetyl coenzyme A (acetyl CoA) to lysine residues of the target protein by acetyltransferase (HAT), causing a conformational change because of the neutralization of their positive charge. Histone acetylation and deacetylation mediated by histone HAT and histone deacetylase (HDAC) are dynamic processes and are directly involved in the regulation of gene transcription. Acetylation can also occur in nonhistone proteins, such as p53, the first acetylated nonhistone protein discovered in 1997 [86]. There are 18 types of HDACs in eukaryotes, which can be divided into four classes, including I, IIa, IIb, and III. Sirtuins (SIRT) are deacetylases belonging to class III HDACs [87]. At present, there are seven subtypes in mammals, namely, SIRT1-SIRT7. Although they are NAD$^+$ dependent, they play different roles depending on their distributions in the cell. SIRT3 and SIRT5 are only found in mitochondria, SIRT6 and SIRT7 are only found in the nucleus, while SIRT1 and SIRT2 are found in both the cytoplasm and the nucleus [88]. Importantly, studies have shown that more than half of the proteins in mitochondria have acetylation sites and are closely related to energy metabolism [89–92]. Therefore, acetylation and deacetylation have a high regulatory effect on mitochondrial function, and further affect the occurrence of CVDs.

3.4.1. Mitochondrion-Associated Acetylation in Heart Failure.
Lysine acetylation is involved in the regulation of various enzymes related to mitochondrial energy metabolism, in particular, malate dehydrogenase (MDH) and isocitrate dehydrogenase (IDH). Once they are significantly acetylated, however, the expression of SIRT3 and NAD$^+$ is significantly decreased [93]. In addition, it is well known that CypD is a sensor for the opening of mPTP channels on the OMM, and CypD activity has a positive correlation with acetylation of mitochondrial protein [94]. A study showed that the activity of CypD was reduced by SIRT3 deacetylation, finally inhibiting the opening of the mPTP channel [95]. Increasing SIRT3 expression in failing hearts can improve cardiac function. Metformin intake significantly increased SIRT3 expression accompanied with reduced PGC-1 acetylation levels, leading to an attenuation of damaged membrane potential and improvement in mitochondrial respiratory function, thereby improving heart function in mice with myocardial infarction-induced heart failure [96]. Therefore, SIRT3 elicits a significant effect on sustaining normal cardiac function.

3.4.2. Mitochondrion-Associated Acetylation in Myocardial I/R Injury.
SIRT3 is one of the main pathways of deacetylation and I/R regulation. Studies have shown that the absence of one or two SIRT3 alleles (SIRT3$^{-/+}$ or SIRT3$^{-/-}$) in the heart increases susceptibility to I/R injury. After I/R intervention, myocardial cell injury and infarction area increased, along with decreased cardiac recovery [97, 98]. Zhao et al. investigated the effect of HDAC on cardiac I/R injury by establishing models of early and delayed cardiac pharmacologic preconditioning, respectively. The results revealed that HDAC inhibition protected the heart against I/R injury in both pharmacologic pretreatments [99]. Their follow-up experiments further proved that NF-κB, Akt, and MKK3 are important mediators of HDAC-associated cardiac protection in the delayed preconditioning model [100, 101]. Chang et al. found that trans-sodium crocetinate (TSC) reduced cardiac I/R injury by augmenting SIRT3 activity and reducing the phosphorylation and acetylation of FOXO3a protein. The protective effect of SIRT3 can be eliminated by knocking out SIRT3 [102]. In addition, SIRT1 was also found to be involved in cardiac I/R injury. Evidence has shown that the treatment of thymoquinone (TQ) gradually restored left ventricular function by increasing the expression of SIRT1 and the acetylation level of p53 during the construction of myocardial I/R models in rats and suckling mice [103].

3.4.3. Mitochondrion-Associated Acetylation in Cardiac Hypertrophy.
Overexpression of SIRT1 can aggravate cardiac hypertrophy, and when decompensated, can eventually induce heart failure. It was found that the activation or upregulation of SIRT1 induced by phenylephrine was inhibited by downregulating or inhibiting AMPK expression, thus alleviating cardiac hypertrophy [104]. Akt is one of the crucial molecules regulating cardiac hypertrophy. The study by Sundaresan et al. indicated that acetylation of Akt and PDK1 blocked their binding to PIP3. The combination of Akt, PDK1, and PIP3 was intensified and activated via deace-

tylation of Akt by SIRT3, causing cardiac hypertrophy [105]. On the contrary, SIRT3 has the ability of resisting cardiac hypertrophy. Evidence showed that SIRT3 expression was increased in the early stages of cardiac hypertrophy, but it decreased gradually as the disease progressed [106]. Moreover, overexpression of SIRT3 was found to inhibit cardiac hypertrophy, and conversely, knocking out SIRT3 worsened cardiac hypertrophy [107]. Moreover, SIRT6 was reported to reduce the development of cardiac hypertrophy by targeting c-Jun signalling [108]. Since the SIRT family has multiple downstream molecules, the regulation of SIRT on cardiac hypertrophy may vary with different influencing factors.

3.5. Succinylation.
Succinylation is a new reversible PTM proposed by Zhang et al. in 2011 [109]. It is a natural modification, conservative in evolution. Succinylation occurs with the transfer of the succinyl group to the lysine residue of the receptor protein under the action of succinyl transferase. Succinyl coenzyme A and succinate are known as succinyl donors; however, the enzymes involved in the transfer are not clear. Under physiological pH (7.4), the charge of succinylation of lysine residues is changed from +1 to -1. Lysine succinylation triggers more substantial changes to the structure and chemical properties of a substrate protein compared to other lysine modifications as it formed a mass shift of 100.0186 Da at the Lys residue [109]. It has been found that succinylation is more likely to occur in prokaryotes than in eukaryotes, and in eukaryotes, mitochondria are the organelles with the most succinylation [110]. Importantly, SIRT5, as a mitochondrial deacetylase, also shows the activity of deacetylase, which separates the substrate protein from the succinyl group [111, 112]. Many energy metabolic pathways are closely related to SIRT5-mediated succinylation, such as ATP synthesis and TCA [113]. In SIRT5 overexpressed cells, the levels of mitophagic receptor BCL2 interacting protein 3 (BNIP3) and autophagy marker MAPLC3B decreased, while in contrast, knocking down or inhibiting SIRT5 in cells may affect mitochondrial quality control by accelerating mitophagy [114]. With the analysis of succinylation in recognition sites, evidence has shown that succinylation plays an important role in vascular diseases by regulating various metabolic pathways, although the specific pathway remains to be explored [115, 116].

3.5.1. Mitochondrion-Associated Succinylation in Myocardial I/R Injury.
Studies have shown that SIRT5-mediated succinylation plays a protective role in preventing myocardial I/R injury. By comparing different metabonomic methods, succinic acid accumulation has been considered as a common metabolic phenomenon in ischemia tissues due to the effect of succinate dehydrogenase (SDH). However, during reperfusion, the previously existing succinic acid can be oxidized to produce a large amount of ROS, which aggravates myocardial cell damage [117]. When blood flow was restored, injection of dimethyl malonate, a competitive SDH inhibitor, resulted in a significant reduction in myocardial infarct size [117]. Moreover, SIRT5 knockdown in mitochondria of cardiomyocytes increased lysine succinylation and cardiac I/R injury. Succinylated residues on SDH subunit A are the

recognition sites of SIRT5. In a word, their study demonstrated that SIRT5 alleviates heart I/R injury by regulating succinylation modification, whereas deletion of SIRT5 promotes mitochondrial death and cardiac anomalies through the accumulation of mitochondrial ROS, which can be alleviated by SDH inhibition [118].

3.5.2. Mitochondrion-Associated Succinylation in Atrial Fibrillation (AF).
AF has a high mortality and incidence rate. The abnormal energy metabolism of cardiomyocytes not only promotes the risk of AF but also increases the probability of heart failure [119]. Previously, research revealed that in SIRT5-deficient hearts, the occurrence of succinylation leads to a large amount of ROS production [117]. However, the increase in ROS can be detrimental to the heart and can accelerate the development of AF [120]. Recently, it has been found that the succinylation levels involved in energy metabolism were significantly altered in AF patients, suggesting a possible correlation between them [121]. Furthermore, changes in succinic acid expression also affect atrial dysfunction and cardiogenic stroke [122]. However, the mechanism of succinylation in AF is still unclear.

3.5.3. Mitochondrion-Associated Succinylation in Cardiac Hypertrophy.
ECHA, a subunit of mitochondrial functional proteins required for oxidation of long-chain fatty acids, contains abundant sites for succinylation and can be activated by SIRT5 at Lys351 [115]. SIRT5 knockout decreased the ECHA activity, accompanied with a decrease in fatty acid oxidation, and thus inducing fat accumulation in the heart, contributing to the progression of cardiac hypertrophy [115]. Recently, Hershberger et al. investigated the relationship between SIRT5 and stress overload cardiomyopathy caused by converse aortic treatment (TAC). The results showed that after TAC surgery to SIRT5 knockout mice, cardiac fatty acid metabolism and TCA circulation were impaired, resulting in cardiac hypertrophy [123]. However, because of current limited research, the role of the specific pathway of protein succinylation modification in cardiac hypertrophy needs to be further explored in the future.

3.6. Potential Role of Mitochondrion-Related Histone Lactylation in CVDs.
Lactic acid is widely known as a metabolite by-product of glucose metabolism. Even under aerobic conditions, glucose can be incompletely oxidized, resulting in the formation of lactate, through a process known as the Warburg effect [124]. In 2019, Zhang et al. identified a novel PTM, lactylation modification, by using high-performance liquid chromatography- (HPLC-) tandem mass spectrometry (MS/MS), immunoblotting analysis, and isotopic localization [125]. The incomplete oxidation product lactic acid of glucose is further converted to lactic acid coenzyme A which is then transferred to histone lysine residues in the presence of acetyltransferase P300 [125]. Recently, a previously unexplored feedback mechanism was discovered that may regulate glycolytic flux under hyperglycaemic or Warburg-like conditions [126]. It has also been reported that histone lactylation plays an essential role in the phenotypic transformation of macrophages [127].

Inflammation is one of the causes and mechanisms that induce cardiac disorders. In the clearance process of inflammatory infiltration, macrophages express repair genes and reduce inflammatory genes to protect host tissues from impairment. Recently, the study of modulating macrophages upon inflammatory response has become more important, and it has involved multiple inflammatory diseases, such as myocarditis [127, 128], atherosclerosis [129], obesity [130, 131], cancer [132], and colitis [133]. In vivo, macrophages can engulf foreign invasion, abnormal microorganisms, or cellular debris to maintain the normal homeostasis of our body system. Basically, there are two phenotypes of macrophages: the M1 macrophage is mainly implicated in proinflammatory responses, while the M2 macrophage is an anti-inflammatory type. Evidence has shown that inflammatory macrophages undergo aerobic glycolysis to generate lactic acid following toll-like receptor stimulation, and then the lactic acids bind to lysine residues in the histone tails, referred to as histone lactylation, which participates in the transformation process of macrophages from M1 to M2 to restore normal cellular functions [134]. In the pathogenesis of pulmonary fibrosis, lactic acid induced histone lactylation in the promoter of the prefibrotic gene in macrophages, which is mediated by P300 [135]. In addition to binding to histones, lactylation can also occur on the sites of nonhistones. Gao et al. found that lactylated proteins in Botrytis cinerea are mainly distributed in the nucleus, mitochondria, and cytoplasm, and are correlated with their pathogenicity through protein-protein interactions [136].

3.7. Potential Role of Mitochondrion-Related Crotonylation in CVDs.
Another new PTM, lysine crotonylation, was discovered by Tan et al. in 2011. This modification mainly functions in the nucleus and can be detected at multiple histone sites [137]. Lysine crotonylation is enzymatically regulated by the dynamic balance between crotonyl transferases (writer) and decrotonylases (eraser). The crotonyl transferases catalyze the formation, whereas the decrotonylases catalyze the removal of the covalent modification of the crotonylation [138]. Some studies have found that several deacetylases including HDAC1, HDAC2, and HDAC3 also have the activity of decrotonylases, which are regarded as major executors of histone decrotonylation [139–141]. Several proteins that function as crotonyl transferases have also been identified, such as P300, MOF, and CBP [142]. Andrews et al. found that the Taf14 YEATS domain can act as a reader of histone crotonylation [143]. In particular, YEATS domains recognize histone crotonylation by a unique mechanism of aromatic-π stacking, linking crotonylation to transcription, nucleosome remodeling, and other important cellular functions [144]. The histone crotonylation induced by crotonic acid can activate Zscan4 to maintain telomeres and promote CiPSC generation, indicating that the crotonylation facilitates telomere maintenance and enhances chemically induced reprogramming to pluripotency [145]. Nevertheless, the current studies about crotonylation mainly focus on its

TABLE 1: The relationships between PTMs of mitochondrial proteins and cardiovascular diseases.

Mitochondrial proteins	PTMs	Upstream regulators	Impacts on mitochondrial quality control	Mechanism	Cardiovascular diseases	Roles in cardiovascular diseases	References
Drp1	SUMOylation	SUMO1	Positive	Induce autophagy	I/R injury	Weaken myocardial I/R intervention	[43]
Drp1	SUMOylation	SENP5	Positive	Inhibit the activation of apoptosis factor	Heart failure	Relieve heart failure	[47]
CypD	Ubiquitination	Parkin	Positive	Inhibit the opening of mPTP	I/R injury	Alleviate heart I/R injury	[56]
OMA1	Ubiquitination	GSK3	Positive	Increase OPA1 expression	Heart failure	Relieve heart failure	[66]
AKAP121	Ubiquitination	ACSL1	Negative	Increase mitochondrial division	Cardiomyopathy	Promote the formation of lipotoxic cardiomyopathy	[64]
Cytochrome C oxidase	Phosphorylation	PKA	Negative	Increase ROS production		Increase myocardial I/R injury	[74, 75]
STAT3	Phosphorylation	Unclear	Positive	Improve the respiration of C_I, inhibit the opening of MPTP	I/R injury	Relieve myocardial I/R injury	[77–79]
VDAL	Phosphorylation	HK2	Negative	Promote apoptosis		Aggravate heart I/R injury	[80]
Akt	Phosphorylation	PI3K	Positive	Inhibit the opening of mPTP	Myocardial infarction	Alleviate myocardial infarction	[72, 73]
PINK1	Phosphorylation	AMPKα2	Positive	Induce autophagy	Heart failure	Relieve heart failure	[65]
Drp1	Phosphorylation	PKA	Negative	Increase mitochondrial division	Heart failure	Aggravate heart failure	[85]
GSK3β	Acetylation	SIRT3	Positive	Reduce cardiac fibrosis	Heart failure	Relieve heart failure	[93]
CypD	Acetylation	SIRT3	Negative	Induce the opening of mPTP	Heart failure	Aggravate heart failure	[95]
PGC-1α	Acetylation	SIRT3	Negative	Destroy mitochondrial membrane potential	Heart failure	Aggravate heart failure	[96]
FOXO3a	Acetylation	SIRT3	Negative	Oxidative damage to mitochondria	I/R injury	Aggravate myocardial I/R injury	[102]
P53	Acetylation	SIRT1	Negative	Promote ROS production		Accelerate myocardial I/R injury	[103]
Akt/PDK1	Acetylation	SIRT1	Positive	Prevent Akt/PDK1 from combining with PIP3	Myocardial hypertrophy	Reduce myocardial hypertrophy	[105]
SDH	Succinylation	SIRT5	Positive	Decrease ROS production	Atrial fibrillation	Relieve myocardial I/R injury	[118]
Unknown	Succinylation	Unknown	Negative	Increase ROS production		Accelerate myocardial I/R injury	[120]
ECHA	Succinylation	SIRT5	Unknown	Accelerate oxidation of fatty acids	Myocardial hypertrophy	Weaken myocardial hypertrophy	[115]
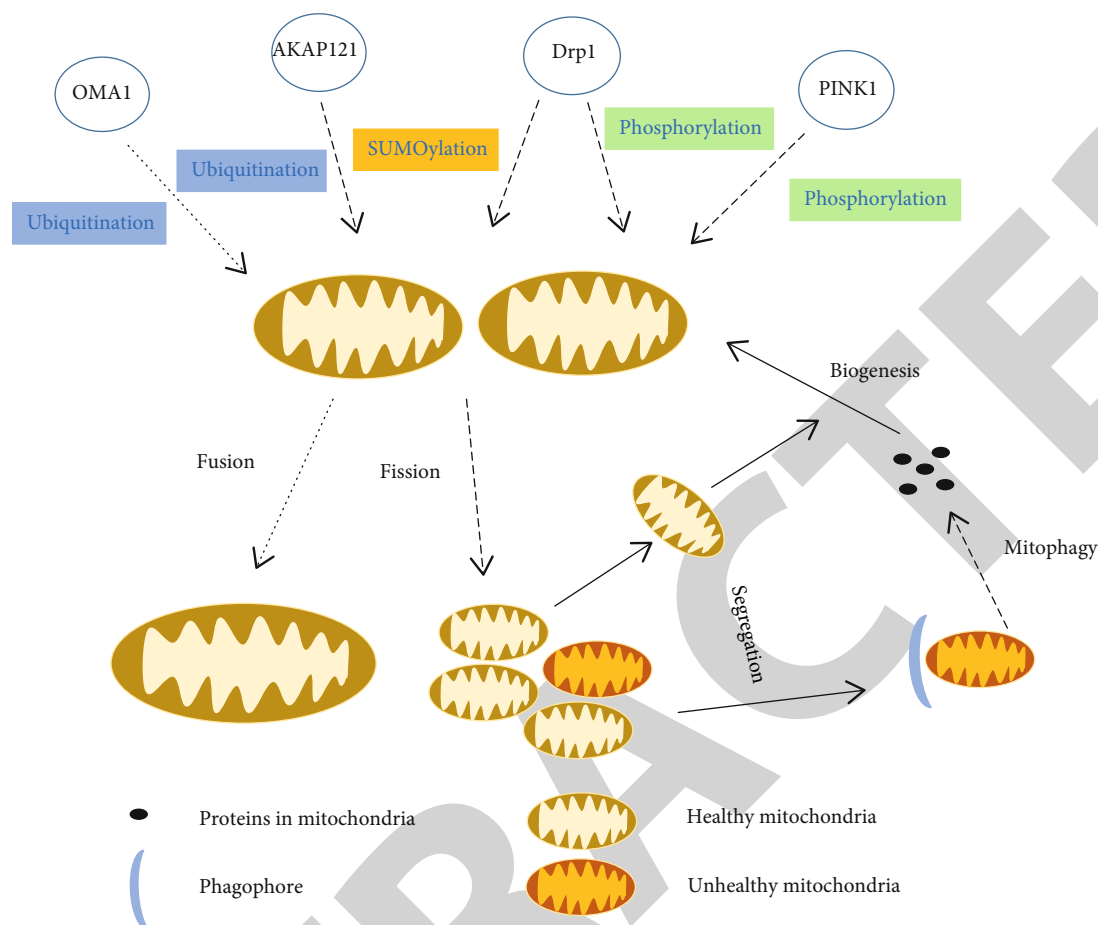
FIGURE 3: The role of posttranscriptional modification of mitochondrial proteins in mitochondrial quality control. The quality control of mitochondria mainly includes fusion, fission, mitophagy, and biogenesis. Ubiquitination of the mitochondrial protein OMA1 promotes the fusion of healthy mitochondria. The ubiquitination of mitochondrial protein AKAP121 and the phosphorylation of Drp1 are conducive to the fission of normal mitochondria. Phosphorylation of mitochondrial protein PINK1 and SUMOylation of Drp1 induces mitophagy in unhealthy mitochondria.

effects on the nucleus and on protein coding; however, the precise role of crotonylation in CVDs has not been well demonstrated, which may be worth exploring in the future.

4. Clinical Perspective and Application of PTMs in CVDs and Other Diseases

With rapid progress in proteomics and mass spectrometry-based technology, a large number of PTMs have been found in human gene products by means of protein profiling techniques [146]. Until 2015, the UniProt database has recorded 469 PTMs including 326 PTMs in eukaryotes and more than 100 different PTMs in *Homo sapiens* [147], suggesting a potential clinical research direction for human diseases. It has been proven that PTMs are closely related to the occurrence of human diseases, such as cancer, diabetes, and CVDs [148–150]. To this end, it is critical for researchers to carry out biomarker discovery through characterization and quantitation of PTMs. PTMs thus exhibit an applicable role in the prediction of CVDs or other diseases by detecting the expression level of circulating PTM proteins or their specific molec-

ular regulators, and may further provide therapeutic approaches by altering the degree of specific protein modifications for disease treatment.

5. Summary and Conclusions

In recent years, with growing numbers of in-depth studies on PTMs, more types of PTMs have gradually been discovered. To make a better understanding of their roles in CVDs, we summarized the current research progress of several major PTMs that affect CVDs by regulating specific mitochondrial proteins which are closely implicated in mitochondrial quality control (see Table 1). The heart is an important organ which requires enough energy supplies provided by mitochondria in cardiomyocytes. Abnormal mitochondrial quality control may contribute to the development of different types of CVDs. Since most PTMs are reversible, it enables us to control the direction of each reaction by regulating different enzymes for the disease intervention based on their particular pathogenesis. Interestingly, lactylation and crotonylation as two novel PTMs that were discovered recently [125, 137], are closely associated with mitochondrial

metabolism, although the precise regulating mechanism and their role participating in CVDs have not been explored yet. In line with this notion, different types of PTMs are not completely independent during the regulation process in CVDs or other disorders. They have complex networks of interactions, especially by modulating several essential mitochondrion-related proteins or enzymes. For instance, the PINK-mediated Parkin pathway exhibits a critical role in regulating not only the mitophagy but also the PTM progress, such as SUMOylation and ubiquitination. Parkin maintains the normal function of mitochondria by inhibiting the opening of mPTP by catalyzing the ubiquitination of CypD in the necrotic cascade, while phosphorylation of PINK1 recruits Parkin to depolarize mitochondria and increase the mitophagy process. The ubiquitin protein itself can also be phosphorylated by PINK, along with the phosphorylation of Parkin at serine-65 (Ser65). This process mediates Parkin activation and recruitment as well as E3 Ub ligase activity [151]. On the other hand, PTMs can also affect proteins that are associated with mitochondrial fusion and fission such as OPA1 (see Figure 3). Acetylation and succinylation normally occur at the lysine residues of the target protein and are closely associated with SIRT activity and energy metabolism. However, although these mitochondrial proteins are mostly involved in the regulation of mitochondrial quality control including mitochondrial fission, fission, mitophagy, and biogenesis, we cannot exclude other proteins modified by different PTMs (some are not described in this review) which may directly or indirectly affect the mitochondrial quality control. Nevertheless, the investigation on the interaction network of PTMs in CVDs by modulating mitochondrial quality control has a promising future en route to exploring novel therapeutic targets.

Conflicts of Interest

The authors declare that there is no conflict of interest regarding the publication of this paper.

Acknowledgments

References

[1] R. Pryor and F. Cabreiro, "Repurposing metformin: an old drug with new tricks in its binding pockets," *The Biochemical Journal*, vol. 471, no. 3, pp. 307–322, 2015.

[2] T. Miki, T. Itoh, D. Sunaga, and T. Miura, "Effects of diabetes on myocardial infarct size and cardioprotection by preconditioning and postconditioning," *Cardiovascular Diabetology*, vol. 11, no. 1, p. 67, 2012.

[3] A. K. Malakar, D. Choudhury, B. Halder, P. Paul, A. Uddin, and S. Chakraborty, "A review on coronary artery disease, its risk factors, and therapeutics," *Journal of Cellular Physiology*, vol. 234, no. 10, pp. 16812–16823, 2019.

[4] A. Mokhtari-Zaer, N. Marefati, S. L. Atkin, A. E. Butler, and A. Sahebkar, "The protective role of curcumin in myocardial ischemia-reperfusion injury," *Journal of Cellular Physiology*, vol. 234, no. 1, pp. 214–222, 2018.

[5] G. Siasos, V. Tsigkou, M. Kosmopoulos et al., "Mitochondria and cardiovascular diseases—from pathophysiology to treatment," *Annals of Translational Medicine*, vol. 6, no. 12, p. 256, 2018.

[6] A. R. Stram and R. M. Payne, "Post-translational modifications in mitochondria: protein signaling in the powerhouse," *Cellular and Molecular Life Sciences*, vol. 73, no. 21, pp. 4063–4073, 2016.

[7] A. M. van der Bliek, Q. Shen, and S. Kawajiri, "Mechanisms of mitochondrial fission and fusion," *Cold Spring Harbor Perspectives in Biology*, vol. 5, no. 6, 2013.

[8] B. M. Baker and C. M. Haynes, "Mitochondrial protein quality control during biogenesis and aging," *Trends in Biochemical Sciences*, vol. 36, no. 5, pp. 254–261, 2011.

[9] Y. Matsushima and L. S. Kaguni, "Matrix proteases in mitochondrial DNA function," *Biochimica et Biophysica Acta*, vol. 1819, no. 9-10, pp. 1080–1087, 2012.

[10] M. Karbowski and R. J. Youle, "Regulating mitochondrial outer membrane proteins by ubiquitination and proteasomal degradation," *Current Opinion in Cell Biology*, vol. 23, no. 4, pp. 476–482, 2011.

[11] V. Soubannier, P. Rippstein, B. A. Kaufman, E. A. Shoubridge, and H. M. McBride, "Reconstitution of mitochondria derived vesicle formation demonstrates selective enrichment of oxidized cargo," *PLoS One*, vol. 7, no. 12, article e52830, 2012.

[12] S. M. Yoo and Y. K. Jung, "A molecular approach to mitophagy and mitochondrial dynamics," *Molecules and Cells*, vol. 41, no. 1, pp. 18–26, 2018.

[13] J. J. Lemasters, "Variants of mitochondrial autophagy: types 1 and 2 mitophagy and micromitophagy (type 3)," *Redox Biology*, vol. 2, pp. 749–754, 2014.

[14] R. J. Youle and D. P. Narendra, "Mechanisms of mitophagy," *Nature Reviews. Molecular Cell Biology*, vol. 12, no. 1, pp. 9–14, 2011.

[15] P. Beltrao, P. Bork, N. J. Krogan, and V. Noort, "Evolution and functional cross-talk of protein post-translational modifications," *Molecular Systems Biology*, vol. 9, no. 1, p. 714, 2013.

[16] H. A. Doyle and M. J. Mamula, "Post-translational protein modifications in antigen recognition and autoimmunity," *Trends in Immunology*, vol. 22, no. 8, pp. 443–449, 2001.

[17] A. Fukushima and G. D. Lopaschuk, "Acetylation control of cardiac fatty acid β-oxidation and energy metabolism in obesity, diabetes, and heart failure," *Biochimica et Biophysica Acta*, vol. 1862, no. 12, pp. 2211–2220, 2016.

[18] T. L. Parry and M. S. Willis, "Cardiac ubiquitin ligases: their role in cardiac metabolism, autophagy, cardioprotection and therapeutic potential," *Biochimica et Biophysica Acta-Molecular Basis of Disease*, vol. 1862, no. 12, pp. 2259–2269, 2016.

[19] J. Nan, W. Zhu, M. S. Rahman et al., "Molecular regulation of mitochondrial dynamics in cardiac disease," *Biochim Biophys Acta Mol Cell Res*, vol. 1864, no. 7, pp. 1260–1273, 2017.

[20] C. J. Hall, L. E. Sanderson, K. E. Crosier, and P. S. Crosier, "Mitochondrial metabolism, reactive oxygen species, and macrophage function-fishing for insights," *Journal of*

Molecular Medicine (Berlin, Germany), vol. 92, no. 11, pp. 1119–1128, 2014.

[21] C. Sauvanet, L. Arnauné-Pelloquin, C. David, P. Belenguer, and M. Rojo, "Mitochondrial morphology and dynamics: actors, mechanisms and functions," *Medical Science (Paris)*, vol. 26, no. 10, pp. 823–829, 2010.

[22] S. Koene and J. Smeitink, "Mitochondrial medicine: entering the era of treatment," *Journal of Internal Medicine*, vol. 265, no. 2, pp. 193–209, 2009.

[23] B. Zhou and R. Tian, "Mitochondrial dysfunction in pathophysiology of heart failure," *The Journal of Clinical Investigation*, vol. 128, no. 9, pp. 3716–3726, 2018.

[24] D. A. Chistiakov, T. P. Shkurat, A. A. Melnichenko, A. V. Grechko, and A. N. Orekhov, "The role of mitochondrial dysfunction in cardiovascular disease: a brief review," *Annals of Medicine*, vol. 50, no. 2, pp. 121–127, 2018.

[25] S. Koene and J. Smeitink, "Metabolic manipulators: a well founded strategy to combat mitochondrial dysfunction," *Journal of Inherited Metabolic Disease*, vol. 34, no. 2, pp. 315–325, 2011.

[26] D. P. Narendra and R. J. Youle, "Targeting mitochondrial dysfunction: role for PINK1 and Parkin in mitochondrial quality control," *Antioxidants & Redox Signaling*, vol. 14, no. 10, pp. 1929–1938, 2011.

[27] F. Billia, L. Hauck, F. Konecny, V. Rao, J. Shen, and T. W. Mak, "PTEN-inducible kinase 1 (PINK1)/Park6 is indispensable for normal heart function," *Proceedings of the National Academy of Sciences of the United States of America*, vol. 108, no. 23, pp. 9572–9577, 2011.

[28] G. R. Drummond, S. Selemidis, K. K. Griendling, and C. G. Sobey, "Combating oxidative stress in vascular disease: NADPH oxidases as therapeutic targets," *Nature Reviews Drug Discovery*, vol. 10, no. 6, pp. 453–471, 2011.

[29] S. Adorisio, A. Fierabracci, I. Muscari et al., "SUMO proteins: guardians of immune system," *Journal of Autoimmunity*, vol. 84, pp. 21–28, 2017.

[30] X. Liu, Q. Wang, W. Chen, and C. Wang, "Dynamic regulation of innate immunity by ubiquitin and ubiquitin-like proteins," *Cytokine & Growth Factor Reviews*, vol. 24, no. 6, pp. 559–570, 2013.

[31] E. Chang and J. I. Abe, "Kinase-SUMO networks in diabetes-mediated cardiovascular disease," *Metabolism*, vol. 65, no. 5, pp. 623–633, 2016.

[32] B. Guo, S. H. Yang, J. Witty, and A. D. Sharrocks, "Signalling pathways and the regulation of SUMO modification," *Biochemical Society Transactions*, vol. 35, no. 6, pp. 1414–1418, 2007.

[33] S. Dehnavi, M. Sadeghi, P. E. Penson, M. Banach, T. Jamialahmadi, and A. Sahebkar, "The role of protein SUMOylation in the pathogenesis of atherosclerosis," *Journal of Clinical Medicine*, vol. 8, no. 11, p. 1856, 2019.

[34] N.-T. Le, J. P. Corsetti, J. L. Dehoff-Sparks, C. E. Sparks, K. Fujiwara, and J.-i. Abe, "Reactive oxygen species, SUMOylation, and endothelial inflammation," *International Journal of Inflammation*, vol. 2012, Article ID 678190, 13 pages, 2012.

[35] G. Gill, "SUMO and ubiquitin in the nucleus: different functions, similar mechanisms?," *Genes & Development*, vol. 18, no. 17, pp. 2046–2059, 2004.

[36] N.-T. Le, U. G. Sandhu, R. A. Quintana-Quezada, N. M. Hoang, K. Fujiwara, and J.-i. Abe, "Flow signaling and atherosclerosis," *Cellular and Molecular Life Sciences*, vol. 74, no. 10, pp. 1835–1858, 2017.

[37] E. T. Yeh, "SUMOylation and De-SUMOylation: Wrestling with Life's Processes∗," *The Journal of Biological Chemistry*, vol. 284, no. 13, pp. 8223–8227, 2009.

[38] J. R. Gareau and C. D. Lima, "The SUMO pathway: emerging mechanisms that shape specificity, conjugation and recognition," *Nature Reviews Molecular Cell Biology*, vol. 11, no. 12, pp. 861–871, 2010.

[39] J. S. Seeler and A. Dejean, "Nuclear and unclear functions of SUMO," *Nature Reviews. Molecular Cell Biology*, vol. 4, no. 9, pp. 690–699, 2003.

[40] F. Paasch, F. den Brave, I. Psakhye, B. Pfander, and S. Jentsch, "Failed mitochondrial import and impaired proteostasis trigger SUMOylation of mitochondrial proteins," *The Journal of Biological Chemistry*, vol. 293, no. 2, pp. 599–609, 2018.

[41] J. Prudent, R. Zunino, A. Sugiura, S. Mattie, G. C. Shore, and H. M. McBride, "MAPL SUMOylation of Drp1 stabilizes an ER/mitochondrial platform required for cell death," *Molecular Cell*, vol. 59, no. 6, pp. 941–955, 2015.

[42] J. X. Wang, J. Q. Jiao, Q. Li et al., "miR-499 regulates mitochondrial dynamics by targeting calcineurin and dynamin-related protein-1," *Nature Medicine*, vol. 17, no. 1, pp. 71–78, 2011.

[43] X. Bian, J. Xu, H. Zhao et al., "Zinc-induced SUMOylation of dynamin-related protein 1 protects the heart against ischemia-reperfusion injury," *Oxidative Medicine and Cellular Longevity*, vol. 2019, Article ID 1232146, 11 pages, 2019.

[44] L. Gao, Y. Zhao, J. He et al., "The desumoylating enzyme sentrin-specific protease 3 contributes to myocardial ischemia reperfusion injury," *Journal of Genetics and Genomics*, vol. 45, no. 3, pp. 125–135, 2018.

[45] J. Han, C. Q. Zhong, and D. W. Zhang, "Programmed necrosis: backup to and competitor with apoptosis in the immune system," *Nature Immunology*, vol. 12, no. 12, pp. 1143–1149, 2011.

[46] G. Olivetti, R. Abbi, F. Quaini et al., "Apoptosis in the failing human heart," *The New England Journal of Medicine*, vol. 336, no. 16, pp. 1131–1141, 1997.

[47] E. Y. Kim, Y. Zhang, I. Beketaev et al., "SENP5, a SUMO isopeptidase, induces apoptosis and cardiomyopathy," *Journal of Molecular and Cellular Cardiology*, vol. 78, pp. 154–164, 2015.

[48] R. Zunino, A. Schauss, P. Rippstein, M. Andrade-Navarro, and H. M. McBride, "The SUMO protease SENP5 is required to maintain mitochondrial morphology and function," *Journal of Cell Science*, vol. 120, no. 7, pp. 1178–1188, 2007.

[49] D. Nandi, P. Tahiliani, A. Kumar, and D. Chandu, "The ubiquitin-proteasome system," *Journal of Biosciences*, vol. 31, no. 1, pp. 137–155, 2006.

[50] M. Schmidt and D. Finley, "Regulation of proteasome activity in health and disease," *Biochimica et Biophysica Acta*, vol. 1843, no. 1, pp. 13–25, 2014.

[51] M. H. Glickman and A. Ciechanover, "The ubiquitin-proteasome proteolytic pathway: destruction for the sake of construction," *Physiological Reviews*, vol. 82, no. 2, pp. 373–428, 2002.

[52] D. Komander and M. Rape, "The ubiquitin code," *Annual Review of Biochemistry*, vol. 81, no. 1, pp. 203–229, 2012.

[53] C. M. Pickart and M. J. Eddins, "Ubiquitin: structures, functions, mechanisms," *Biochimica et Biophysica Acta*, vol. 1695, no. 1-3, pp. 55–72, 2004.

[54] G. Li, J. Yang, C. Yang et al., "PTENα regulates mitophagy and maintains mitochondrial quality control," *Autophagy*, vol. 14, no. 10, pp. 1742–1760, 2018.

[55] N. H. Hideki Shimura, S.-i. Kubo, Y. Mizuno et al., "Familial Parkinson disease gene product, parkin, is a ubiquitin-protein ligase," *Nature Genetics*, vol. 25, no. 3, pp. 302–305, 2000.

[56] T. Sun, W. Ding, T. Xu et al., "Parkin regulates programmed necrosis and myocardial ischemia/reperfusion injury by targeting Cyclophilin-D," *Antioxidants & Redox Signaling*, vol. 31, no. 16, pp. 1177–1193, 2019.

[57] H. X. Yang, P. Wang, N. N. Wang, S. D. Li, and M. H. Yang, "Tongxinluo ameliorates myocardial ischemia-reperfusion injury mainly via activating Parkin-mediated mitophagy and downregulating ubiquitin-proteasome system," *Chinese Journal of Integrative Medicine*, 2019.

[58] T. Wu, R. A. Harrison, X. Y. Chen et al., "Tongxinluo (Tong xin luo or Tong-xin-luo) capsule for unstable angina pectoris," *Cochrane Database of Systematic Reviews*, vol. 18, no. 4, 2006.

[59] J. Ru, P. Li, J. Wang et al., "TCMSP: a database of systems pharmacology for drug discovery from herbal medicines," *Journal of Cheminformatics*, vol. 6, no. 1, 2014.

[60] L. C. Cantley and B. G. Neel, "New insights into tumor suppression: PTEN suppresses tumor formation by restraining the phosphoinositide 3-kinase/AKT pathway," *Proc. Natl. Acad. Sci. USA*, vol. 96, no. 8, pp. 4240–4245, 1999.

[61] S. Dalal, C. R. Daniels, Y. Li, G. L. Wright, M. Singh, and K. Singh, "Exogenous ubiquitin attenuates hypoxia reoxygenation-induced cardiac myocyte apoptosis via the involvement of CXCR4 and modulation of mitochondrial homeostasis," *Biochemistry and Cell Biology*, vol. 98, no. 4, pp. 492–501, 2020.

[62] M. Su, J. Wang, L. Kang et al., "Rare variants in genes encoding MuRF1 and MuRF2 are modifiers of hypertrophic cardiomyopathy," *International Journal of Molecular Sciences*, vol. 15, no. 6, pp. 9302–9313, 2014.

[63] M. Song, G. Gong, Y. Burelle et al., "Interdependence of Parkin-mediated mitophagy and mitochondrial fission in adult mouse hearts," *Circulation Research*, vol. 117, no. 4, pp. 346–351, 2015.

[64] K. Tsushima, H. Bugger, A. R. Wende et al., "Mitochondrial reactive oxygen species in lipotoxic hearts induce post-translational modifications of AKAP121, DRP1, and OPA1 that promote mitochondrial fission," *Circulation Research*, vol. 122, no. 1, pp. 58–73, 2018.

[65] B. Wang, J. Nie, L. Wu et al., "AMPKα2 protects against the development of heart failure by enhancing mitophagy via PINK1 phosphorylation," *Circulation Research*, vol. 122, no. 5, pp. 712–729, 2018.

[66] F. Yang, R. Wu, Z. Jiang et al., "Leptin increases mitochondrial OPA1 via GSK3-mediated OMA1 ubiquitination to enhance therapeutic effects of mesenchymal stem cell transplantation," *Cell Death & Disease*, vol. 9, no. 5, p. 556, 2018.

[67] E. H. Fischer and E. G. Krebs, "Conversion of phosphorylase b to phosphorylase a in muscle extracts," *The Journal of Biological Chemistry*, vol. 216, no. 1, pp. 121–132, 1955.

[68] L. N. Johnson, "The regulation of protein phosphorylation," *Biochemical Society Transactions*, vol. 37, no. 4, pp. 627–641, 2009.

[69] D. Barford, "Protein phosphatases," *Current Biology*, vol. 5, no. 6, pp. 728–734, 1995.

[70] A. Hofer and T. Wenz, "Post-translational modification of mitochondria as a novel mode of regulation," *Experimental Gerontology*, vol. 56, pp. 202–220, 2014.

[71] F. G. Tahrir, D. Langford, S. Amini, T. Mohseni Ahooyi, and K. Khalili, "Mitochondrial quality control in cardiac cells: mechanisms and role in cardiac cell injury and disease," *Journal of Cellular Physiology*, vol. 234, no. 6, pp. 8122–8133, 2018.

[72] S. El Messaoudi, G. A. Rongen, and N. P. Riksen, "Metformin therapy in diabetes: the role of cardioprotection," *Current Atherosclerosis Reports*, vol. 15, no. 4, p. 314, 2013.

[73] G. S. Bhamra, D. J. Hausenloy, S. M. Davidson et al., "Metformin protects the ischemic heart by the Akt-mediated inhibition of mitochondrial permeability transition pore opening," *Basic Research in Cardiology*, vol. 103, no. 3, pp. 274–284, 2008.

[74] J. K. Fang, S. K. Prabu, N. B. Sepuri et al., "Site specific phosphorylation of cytochrome c oxidase subunits I, IVi1 and Vb in rabbit hearts subjected to ischemia/reperfusion," *FEBS Letters*, vol. 581, no. 7, pp. 1302–1310, 2007.

[75] S. K. Prabu, H. K. Anandatheerthavarada, H. Raza, S. Srinivasan, J. F. Spear, and N. G. Avadhani, "Protein Kinase A-mediated Phosphorylation Modulates Cytochrome _c_ Oxidase Function and Augments Hypoxia and Myocardial Ischemia-related Injury∗," *The Journal of Biological Chemistry*, vol. 281, no. 4, pp. 2061–2070, 2006.

[76] Y. Su, X. Huang, Z. Huang, T. Huang, Y. Xu, and C. Yi, "STAT3 localizes in mitochondria-associated ER membranes instead of in mitochondria," *Frontiers in Cell and Development Biology*, vol. 8, p. 274, 2020.

[77] J. Wegrzyn, R. Potla, Y. J. Chwae et al., "Function of mitochondrial Stat3 in cellular respiration," *Science*, vol. 323, no. 5915, pp. 793–797, 2009.

[78] G. Heusch, J. Musiolik, N. Gedik, and A. Skyschally, "Mitochondrial STAT3 activation and cardioprotection by ischemic postconditioning in pigs with regional myocardial ischemia/reperfusion," *Circulation Research*, vol. 109, no. 11, pp. 1302–1308, 2011.

[79] K. Boengler, D. Hilfiker-Kleiner, H. Drexler, G. Heusch, and R. Schulz, "The myocardial JAK/STAT pathway: from protection to failure," *Pharmacology & Therapeutics*, vol. 120, no. 2, pp. 172–185, 2008.

[80] S. Yuan, Y. Fu, X. Wang et al., "Voltage-dependent anion channel 1 is involved in endostatin-induced endothelial cell apoptosis," *The FASEB Journal*, vol. 22, no. 8, pp. 2809–2820, 2008.

[81] H. Bugger, M. Schwarzer, D. Chen et al., "Proteomic remodelling of mitochondrial oxidative pathways in pressure overload-induced heart failure," *Cardiovascular Research*, vol. 85, no. 2, pp. 376–384, 2010.

[82] L. Chen, Q. Gong, J. P. Stice, and A. A. Knowlton, "Mitochondrial OPA1, apoptosis, and heart failure," *Cardiovascular Research*, vol. 84, no. 1, pp. 91–99, 2009.

[83] S. Dey, D. DeMazumder, A. Sidor, D. B. Foster, and B. O'Rourke, "Mitochondrial ROS drive sudden cardiac death and chronic proteome remodeling in heart failure," *Circulation Research*, vol. 123, no. 3, pp. 356–371, 2018.

[84] S. Maekawa, S. Takada, H. Nambu et al., "Linoleic acid improves assembly of the CII subunit and CIII2/CIV complex of the mitochondrial oxidative phosphorylation system in heart failure," *Cell Communication and Signaling: CCS*, vol. 17, no. 1, p. 128, 2019.

[85] J. T. Cribbs and S. Strack, "Reversible phosphorylation of Drp1 by cyclic AMP-dependent protein kinase and calcineurin regulates mitochondrial fission and cell death," *EMBO Reports*, vol. 8, no. 10, pp. 939–944, 2007.

[86] W. Gu and R. G. Roeder, "Activation of p53 sequence-specific DNA binding by acetylation of the p53 C-terminal domain," *Cell*, vol. 90, no. 4, pp. 595–606, 1997.

[87] S. G. Gray and T. J. Ekstrom, "The human histone deacetylase family," *Experimental Cell Research*, vol. 262, no. 2, pp. 75–83, 2001.

[88] O. Augereau, S. Claverol, N. Boudes et al., "Identification of tyrosine-phosphorylated proteins of the mitochondrial oxidative phosphorylation machinery," *Cellular and Molecular Life Sciences*, vol. 62, no. 13, pp. 1478–1488, 2005.

[89] K. L. Guan and Y. Xiong, "Regulation of intermediary metabolism by protein acetylation," *Trends in Biochemical Sciences*, vol. 36, no. 2, pp. 108–116, 2011.

[90] D. B. Foster, T. Liu, J. Rucker et al., "The cardiac acetyl-lysine proteome," *PLoS One*, vol. 8, no. 7, article e67513, 2013.

[91] J. Baeza, M. J. Smallegan, and J. M. Denu, "Mechanisms and dynamics of protein acetylation in mitochondria," *Trends in Biochemical Sciences*, vol. 41, no. 3, pp. 231–244, 2016.

[92] A. S. Hebert, K. E. Dittenhafer-Reed, W. Yu et al., "Calorie restriction and SIRT3 trigger global reprogramming of the mitochondrial protein acetylome," *Molecular Cell*, vol. 49, no. 1, pp. 186–199, 2013.

[93] N. R. Sundaresan, S. Bindu, V. B. Pillai et al., "SIRT3 blocks aging-associated tissue fibrosis in mice by deacetylating and activating glycogen synthase kinase 3β," *Molecular and Cellular Biology*, vol. 36, no. 5, pp. 678–692, 2016.

[94] A. P. Halestrap, "Mitochondrial permeability: dual role for the ADP/ATP translocator?," *Nature*, vol. 430, no. 7003, pp. 1–983, 2004.

[95] A. V. Hafner, J. Dai, A. P. Gomes et al., "Regulation of the mPTP by SIRT3-mediated deacetylation of CypD at lysine 166 suppresses age-related cardiac hypertrophy," *Aging (Albany NY)*, vol. 2, no. 12, pp. 914–923, 2010.

[96] D. Sun and F. Yang, "Metformin improves cardiac function in mice with heart failure after myocardial infarction by regulating mitochondrial energy metabolism," *Biochemical and Biophysical Research Communications*, vol. 486, no. 2, pp. 329–335, 2017.

[97] R. M. Parodi-Rullán, X. Chapa-Dubocq, P. J. Rullán, S. Jang, and S. Javadov, "High sensitivity of SIRT3 deficient hearts to ischemia-reperfusion is associated with mitochondrial abnormalities," *Frontiers in Pharmacology*, vol. 8, p. 275, 2017.

[98] G. A. Porter, W. R. Urciuoli, P. S. Brookes, and S. M. Nadtochiy, "SIRT3 deficiency exacerbates ischemia-reperfusion injury: implication for aged hearts," *American Journal of Physiology. Heart and Circulatory Physiology*, vol. 306, no. 12, pp. H1602–H1609, 2014.

[99] T. C. Zhao, G. Cheng, L. X. Zhang, Y. T. Tseng, and J. F. Padbury, "Inhibition of histone deacetylases triggers pharmacologic preconditioning effects against myocardial ischemic injury," *Cardiovascular Research*, vol. 76, no. 3, pp. 473–481, 2007.

[100] L. X. Zhang, Y. Zhao, G. Cheng et al., "Targeted deletion of NF-kappa B p50 diminishes the cardioprotection of histone deacetylase inhibition," *American Journal of Physiology-Heart and Circulatory Physiology*, vol. 298, no. 6, pp. H2154–H2163, 2010.

[101] T. C. Zhao, J. du, S. Zhuang, P. Liu, and L. X. Zhang, "HDAC inhibition elicits myocardial protective effect through modulation of MKK3/Akt-1," *PLoS One*, vol. 8, no. 6, article e65474, 2013.

[102] G. Chang, Y. Chen, H. Zhang, and W. Zhou, "Trans sodium crocetinate alleviates ischemia/reperfusion-induced myocardial oxidative stress and apoptosis _via_ the SIRT3/FOXO3a/SOD2 signaling pathway," *International Immunopharmacology*, vol. 71, pp. 361–371, 2019.

[103] Y. Lu, Y. Feng, D. Liu et al., "Thymoquinone attenuates myocardial ischemia/reperfusion injury through activation of SIRT1 signaling," *Cellular Physiology and Biochemistry*, vol. 47, no. 3, pp. 1193–1206, 2018.

[104] S. Oka, R. Alcendor, P. Zhai et al., "PPARα-Sirt1 complex mediates cardiac hypertrophy and failure through suppression of the ERR transcriptional pathway," *Cell Metabolism*, vol. 14, no. 5, pp. 598–611, 2011.

[105] N. R. Sundaresan, V. B. Pillai, D. Wolfgeher et al., "The deacetylase SIRT1 promotes membrane localization and activation of Akt and PDK1 during tumorigenesis and cardiac hypertrophy," *Science Signaling*, vol. 4, no. 182, p. ra46, 2011.

[106] N. R. Sundaresan, S. A. Samant, V. B. Pillai, S. B. Rajamohan, and M. P. Gupta, "SIRT3 is a stress-responsive deacetylase in cardiomyocytes that protects cells from stress-mediated cell death by deacetylation of Ku70," *Molecular and Cellular Biology*, vol. 28, no. 20, pp. 6384–6401, 2008.

[107] S. Matsushima and J. Sadoshima, "The role of sirtuins in cardiac disease," *American Journal of Physiology-Heart and Circulatory Physiology*, vol. 309, no. 9, pp. H1375–H1389, 2015.

[108] N. R. Sundaresan, P. Vasudevan, L. Zhong et al., "The sirtuin SIRT6 blocks IGF-Akt signaling and development of cardiac hypertrophy by targeting c-Jun," *Nature Medicine*, vol. 18, no. 11, pp. 1643–1650, 2012.

[109] Z. Zhang, M. Tan, Z. Xie, L. Dai, Y. Chen, and Y. Zhao, "Identification of lysine succinylation as a new post-translational modification," *Nature Chemical Biology*, vol. 7, no. 1, pp. 58–63, 2011.

[110] B. T. Weinert, C. Schölz, S. A. Wagner et al., "Lysine succinylation is a frequently occurring modification in prokaryotes and eukaryotes and extensively overlaps with acetylation," *Cell Reports*, vol. 4, no. 4, pp. 842–851, 2013.

[111] J. Du, Y. Zhou, X. Su et al., "Sirt5 is a NAD-dependent protein lysine demalonylase and desuccinylase," *Science*, vol. 334, no. 6057, pp. 806–809, 2011.

[112] M. Tan, C. Peng, K. A. Anderson et al., "Lysine glutarylation is a protein posttranslational modification regulated by SIRT5," *Cell Metabolism*, vol. 19, no. 4, pp. 605–617, 2014.

[113] M. J. Rardin, W. He, Y. Nishida et al., "SIRT5 regulates the mitochondrial lysine succinylome and metabolic networks," *Cell Metabolism*, vol. 18, no. 6, pp. 920–933, 2013.

[114] L. Polletta, E. Vernucci, I. Carnevale et al., "SIRT5 regulation of ammonia-induced autophagy and mitophagy," *Autophagy*, vol. 11, no. 2, pp. 253–270, 2015.

[115] S. Sadhukhan, X. Liu, D. Ryu et al., "Metabolomics-assisted proteomics identifies succinylation and SIRT5 as important regulators of cardiac function," *Proceedings of the National Academy of Sciences of the United States of America*, vol. 113, no. 16, pp. 4320–4325, 2016.

[116] J. Park, Y. Chen, D. X. Tishkoff et al., "SIRT5-mediated lysine desuccinylation impacts diverse metabolic pathways," *Molecular Cell*, vol. 50, no. 6, pp. 919–930, 2013.

[117] E. T. Chouchani, V. R. Pell, E. Gaude et al., "Ischaemic accumulation of succinate controls reperfusion injury through mitochondrial ROS," *Nature*, vol. 515, no. 7527, pp. 431–435, 2014.

[118] J. A. Boylston, J. Sun, Y. Chen, M. Gucek, M. N. Sack, and E. Murphy, "Characterization of the cardiac succinylome and its role in ischemia- reperfusion injury," *Journal of Molecular and Cellular Cardiology*, vol. 88, pp. 73–81, 2015.

[119] T. Tu, S. Zhou, Z. Liu, X. Li, and Q. Liu, "Quantitative proteomics of changes in energy metabolism-related proteins in atrial tissue from valvular disease patients with permanent atrial fibrillation," *Circulation Journal*, vol. 78, no. 4, pp. 993–1001, 2014.

[120] W. Xie, G. Santulli, S. R. Reiken et al., "Mitochondrial oxidative stress promotes atrial fibrillation," *Scientific Reports*, vol. 5, no. 1, p. 11427, 2015.

[121] F. Bai, T. Tu, F. Qin et al., "Quantitative proteomics of changes in succinylated proteins expression profiling in left appendages tissue from valvular heart disease patients with atrial fibrillation," *Clinica Chimica Acta*, vol. 495, pp. 345–354, 2019.

[122] S. E. Nelson, Z. Ament, Z. Wolcott, R. E. Gerszten, and W. T. Kimberly, "Succinate links atrial dysfunction and cardioembolic stroke," *Neurology*, vol. 92, no. 8, pp. e802–e810, 2019.

[123] K. A. Hershberger, D. M. Abraham, J. Liu, J. W. Locasale, P. A. Grimsrud, and M. D. Hirschey, "Ablation of Sirtuin5 in the postnatal mouse heart results in protein succinylation and normal survival in response to chronic pressure overload," *Journal of Biological Chemistry*, vol. 293, no. 27, pp. 10630–10645, 2018.

[124] M. V. Liberti and J. W. Locasale, "Histone lactylation: a new role for glucose metabolism," *Trends in Biochemical Sciences*, vol. 45, no. 3, pp. 179–182, 2020.

[125] D. Zhang, Z. Tang, H. Huang et al., "Metabolic regulation of gene expression by histone lactylation," *Nature*, vol. 574, no. 7779, pp. 575–580, 2019.

[126] D. O. Gaffney, E. Q. Jennings, C. C. Anderson et al., "Nonenzymatic lysine lactoylation of glycolytic enzymes," *Cell Chemical Biology*, vol. 27, no. 2, pp. 206–213.e6, 2020, e6.

[127] L. T. Izzo and K. E. Wellen, "Histone lactylation links metabolism and gene regulation," *Nature*, vol. 574, no. 7779, pp. 492-493, 2019.

[128] X. Yang, Y. Yue, and S. Xiong, "Dpep2 emerging as a modulator of macrophage inflammation confers protection against CVB3-induced viral myocarditis," *Frontiers in Cellular and Infection Microbiology*, vol. 9, p. 57, 2019.

[129] J. Khallou-Laschet, A. Varthaman, G. Fornasa et al., "Macrophage plasticity in experimental atherosclerosis," *PLoS One*, vol. 5, no. 1, article e8852, 2010.

[130] X. A. M. H. van Dierendonck, T. Sancerni, M. C. Alves-Guerra, and R. Stienstra, "The role of uncoupling protein 2 in macrophages and its impact on obesity- induced adipose tissue inflammation and insulin resistance," *The Journal of Biological Chemistry*, vol. 295, no. 51, pp. 17535–17548, 2020.

[131] W. Ying, W. Fu, Y. S. Lee, and J. M. Olefsky, "The role of macrophages in obesity-associated islet inflammation and β-cell abnormalities," *Nature Reviews. Endocrinology*, vol. 16, no. 2, pp. 81–90, 2020.

[132] O. R. Colegio, N. Q. Chu, A. L. Szabo et al., "Functional polarization of tumour-associated macrophages by tumour-derived lactic acid," *Nature*, vol. 513, no. 7519, pp. 559–563, 2014.

[133] Y. A. Shim, A. Weliwitigoda, T. Campbell, M. Dosanjh, and P. Johnson, "Splenic erythroid progenitors decrease TNF-α production by macrophages and reduce systemic inflammation in a mouse model of T cell-induced colitis," *European Journal of Immunology*, 2020.

[134] R. A. Irizarry-Caro, M. M. McDaniel, G. R. Overcast, V. G. Jain, T. D. Troutman, and C. Pasare, "TLR signaling adapter BCAP regulates inflammatory to reparatory macrophage transition by promoting histone lactylation," *Proceedings of the National Academy of Sciences of the United States of America*, vol. 117, no. 48, pp. 30628–30638, 2020.

[135] H. Cui, N. Xie, S. Banerjee et al., "Lung myofibroblast promote macrophage pro-fibrotic activity through lactate-induced histone lactylation," *American Journal of Respiratory Cell and Molecular Biology*, vol. 64, no. 1, pp. 115–125, 2020.

[136] M. Gao, N. Zhang, and W. Liang, "Systematic analysis of lysine lactylation in the plant fungal pathogen Botrytis cinerea," *Frontiers in Microbiology*, vol. 11, p. 594743, 2020.

[137] M. Tan, H. Luo, S. Lee et al., "Identification of 67 histone marks and histone lysine crotonylation as a new type of histone modification," *Cell*, vol. 146, no. 6, pp. 1015–1027, 2011.

[138] J. Wan, H. Liu, J. Chu, and H. Zhang, "Functions and mechanisms of lysine crotonylation," *Journal of Cellular and Molecular Medicine*, vol. 23, no. 11, pp. 7163–7169, 2019.

[139] R. Fellows, J. Denizot, C. Stellato et al., "Microbiota derived short chain fatty acids promote histone crotonylation in the colon through histone deacetylases," *Nature Communications*, vol. 9, no. 1, p. 105, 2018.

[140] K. RDW, A. Chandru, P. J. Watson et al., "Histone deacetylase (HDAC) 1 and 2 complexes regulate both histone acetylation and crotonylation in vivo," *Scientific Reports*, vol. 8, no. 1, article 14690, 2018.

[141] W. Wei, X. Liu, J. Chen et al., "Class I histone deacetylases are major histone decrotonylases: evidence for critical and broad function of histone crotonylation in transcription," *Cell Research*, vol. 27, no. 7, pp. 898–915, 2017.

[142] X. Liu, W. Wei, Y. Liu et al., "MOF as an evolutionarily conserved histone crotonyltransferase and transcriptional activation by histone acetyltransferase-deficient and crotonyltransferase-competent CBP/p300," *Cell Discovery*, vol. 3, no. 1, p. 17016, 2017.

[143] F. H. Andrews, S. A. Shinsky, E. K. Shanle et al., "The Taf14 YEATS domain is a reader of histone crotonylation," *Nature Chemical Biology*, vol. 12, no. 6, pp. 396–398, 2016.

[144] Y. Li, D. Zhao, Z. Chen, and H. Li, "YEATS domain: linking histone crotonylation to gene regulation," *Transcription-Austin*, vol. 8, no. 1, pp. 9–14, 2016.

[145] H. Fu, C. L. Tian, X. Ye et al., "Dynamics of telomere rejuvenation during chemical induction to pluripotent stem cells," *Stem Cell Reports*, vol. 11, no. 1, pp. 70–87, 2018.

Retraction

Retracted: S-Nitroso-L-Cysteine Ameliorated Pulmonary Hypertension in the MCT-Induced Rats through Anti-ROS and Anti-Inflammatory Pathways

Oxidative Medicine and Cellular Longevity

This article has been retracted by Hindawi following an investigation undertaken by the publisher [1]. This investigation has uncovered evidence of one or more of the following indicators of systematic manipulation of the publication process:

(1) Discrepancies in scope

(2) Discrepancies in the description of the research reported

(3) Discrepancies between the availability of data and the research described

(4) Inappropriate citations

(5) Incoherent, meaningless and/or irrelevant content included in the article

(6) Peer-review manipulation

The presence of these indicators undermines our confidence in the integrity of the article's content and we cannot, therefore, vouch for its reliability. Please note that this notice is intended solely to alert readers that the content of this article is unreliable. We have not investigated whether authors were aware of or involved in the systematic manipulation of the publication process.

Wiley and Hindawi regrets that the usual quality checks did not identify these issues before publication and have since put additional measures in place to safeguard research integrity.

We wish to credit our own Research Integrity and Research Publishing teams and anonymous and named external researchers and research integrity experts for contributing to this investigation.

The corresponding author, as the representative of all authors, has been given the opportunity to register their agreement or disagreement to this retraction. We have kept a record of any response received.

References

[1] M. Wang, P. Luo, W. Shi et al., "S-Nitroso-L-Cysteine Ameliorated Pulmonary Hypertension in the MCT-Induced Rats through Anti-ROS and Anti-Inflammatory Pathways," *Oxidative Medicine and Cellular Longevity*, vol. 2021, Article ID 6621232, 17 pages, 2021.

Research Article

S-Nitroso-L-Cysteine Ameliorated Pulmonary Hypertension in the MCT-Induced Rats through Anti-ROS and Anti-Inflammatory Pathways

Moran Wang,[1] Pengcheng Luo,[1,2] Wei Shi,[1] Junyi Guo,[1] Shengqi Huo,[1] Dan Yan,[1,2] Lulu Peng,[1] Cuntai Zhang,[2] Jiagao Lv,[1] Li Lin,[1] and Sheng Li [1]

[1]*Division of Cardiology, Department of Internal Medicine, Tongji Hospital, Tongji Medical College, Huazhong University of Science and Technology, Wuhan, China*
[2]*Department of Geriatrics, Tongji Hospital, Tongji Medical College, Huazhong University of Science and Technology, Wuhan, China*

Correspondence should be addressed to Sheng Li; shengli410@126.com

Pulmonary hypertension (PH) is a progressive and life-threatening chronic disease in which increased pulmonary artery pressure (PAP) and pulmonary vasculature remodeling are prevalent. Inhaled nitric oxide (NO) has been used in newborns to decrease PAP in the clinic; however, the effects of NO endogenous derivatives, S-nitrosothiols (SNO), on PH are still unknown. We have reported that S-nitroso-L-cysteine (CSNO), one of the endogenous derivatives of NO, inhibited RhoA activity through oxidative nitrosation of its C16/20 residues, which may be beneficial for both vasodilation and remodeling. In this study, we presented data to show that inhaled CSNO attenuated PAP in the monocrotaline- (MCT-) induced PH rats and, moreover, improved right ventricular (RV) hypertrophy and fibrosis induced by RV overloaded pressure. In addition, aerosolized CSNO significantly inhibited the hyperactivation of signal transducers and activators of transduction 3 (STAT3) and extracellular regulated protein kinases (ERK) pathways in the lung of MCT-induced rats. CSNO also regulated the expression of smooth muscle contractile protein and improved aberrant endoplasmic reticulum (ER) stress and mitophagy in lung tissues following MCT induction. On the other hand, CSNO inhibited reactive oxygen species (ROS) production in vitro, which is induced by angiotensin II (AngII) as well as interleukin 6 (IL-6). In addition, CSNO inhibited excessive ER stress and mitophagy induced by AngII and IL-6 in vitro; finally, STAT3 and ERK phosphorylation was inhibited by CSNO in a concentration-dependent manner. Taken together, CSNO led to pulmonary artery relaxation and regulated pulmonary circulation remodeling through anti-ROS and anti-inflammatory pathways and may be used as a therapeutic option for PH treatment.

1. Introduction

Pulmonary hypertension (PH) is a life-threatening cardiopulmonary disease characterized by pulmonary artery vascular contraction and remodeling, possibly due to pulmonary vascular endothelial cell dysfunction, smooth muscle cell proliferation, and perivascular inflammation [1, 2]. Pulmonary artery vascular remodeling results in a continuous increase in pulmonary vascular resistance, eventually leading to right ventricular failure and even death. So far, the strategy which can improve PH vascular remodeling and survival is limited and needs to be explored. Therefore, it is urgent to hunt for novel treatments for PH.

The nitric oxide (NO) signaling pathway is widely studied in PH. An expanding body of knowledge has related deficient NO signaling to PH pathogenesis. Endothelial cell injury is regarded as the initiating trigger of pulmonary hypertension, while continuous contraction, proliferation, and migration of smooth muscle cells mainly contribute to pulmonary hypertension progression. In addition, endothelial dysfunction may lead to a decreased output of NO and its endogenous derivatives, S-nitrosothiols (SNO). SNO not

only leads to vasodilation as NO does but also is able to modify protein-free thiol groups by S-nitrosylation, which may further regulate cell bioactivities and functions, including reactive oxygen species (ROS) production, proliferation, and inflammation. Previously, we reported that CSNO can transport NO equivalents into intact vascular cells and regulate constriction of vascular smooth muscle cells by S-nitrosylation [3, 4], suggesting a role of SNO in the pathogenesis of pulmonary hypertension and its treatment. So far, NO nebulizer therapy is only implemented in the pulmonary hypertension crisis in neonates. Whether aerosolized CSNO can effectively improve the development and progression of PH still remains uncertain.

Pulmonary vascular remodeling is a characteristic of PH development. Perivascular inflammation is now recognized to contribute greatly to PH development in patients and experimental animals. Abundant evidence implicates that IL-6 plays an important role in pulmonary vascular remodeling. IL-6 recognizes IL-6R and gp130, further leads to phosphorylation modification of STAT3, and eventually regulates downstream genes. The overactivated STAT3 pathway contributes to PH development; moreover, binding of p-STAT3 to the eNOS promoter impairs eNOS activity, leading to decreased eNOS protein levels and NO production [5]. It was reported that the activation of the ERK signaling pathway contributes to arterial wall remodeling in rats with hypertension. In addition, p-STAT3 and p-ERK both contribute to the smooth muscle cell (SMC) phenotype switch, which was associated with the progression of experimental occlusive pulmonary vascular disease [6].

In recent decades, evidence indicating endoplasmic reticulum stress in pulmonary arterial hypertension has been accumulated, but targeted clinical treatment is still lacking [7]. Endoplasmic reticulum (ER) stress participates in many known PAH-triggering and PAH-facilitating processes. For example, both inflammation and hypoxia are closely associated with ER stress. Moreover, the loss-of-function mutations in BMPRII lead to ER stress as well [8]. It was reported that the inhibition of ER stress signaling prevented and reversed vascular remodeling in PH [7]. The unfolded protein response (UPR) triggered by ER stress serves as an adaptive mechanism to protect the cell from stress and restore ER homeostasis in the initial stages [9]; however, excessive ER stress would trigger UPR termination, cell death, and mitochondrial collapse, involving disturbance of mitochondria-associated endoplasmic reticulum membrane (MAM) and resultant mitochondrial dysfunction [10]. ER structural remodeling leads to decreased influx of Ca^{2+} from the ER to mitochondria and resultant decreasing mitochondrial Ca^{2+} (Ca^{2+}m), contributing to mitochondrial suppression, as many Ca^{2+}-dependent mitochondrial enzymes are inhibited.

Emerging evidence from clinical and basic medical research has suggested mitophagy serves as a double-edged sword in pulmonary diseases. As a highly conserved process mediated under various cellular stress conditions, mitophagy leads to beneficial or detrimental consequences in different diseases. Mitophagy plays an essential role in cell survival through the maintenance of energy homeostasis, while excessive mitophagy promotes cell death [11]. It was reported that cigarette smoke would induce mitophagy through stabilization of the mitophagy regulator PINK1 and increasing the expression of BNIP3L in chronic obstructive pulmonary disease (COPD) development, which leads to mitochondrial dysfunction and cell injury. Moreover, it was reported that Parkin translocates to mitochondria upon dissipation of the mitochondrial membrane potential ($\Delta\Psi$m) by the uncoupler carbonyl cyanide m-chlorophenylhydrazone (CCCP) or in response to ROS. The precise role of mitophagy in PH is still uncertain and needs further study.

Previously, we reported that CSNO regulated constriction of vascular smooth muscle cells by oxidative nitrosation of RhoA, and CSNO caused Keap1 thiol modification, which activated the antioxidant response element (ARE), leading to transcriptional upregulation of cytoprotective and antioxidant genes. In this study, we investigated the effect of CSNO on pulmonary vessel constriction and remodeling and explored the underlying mechanisms through which CSNO attenuated mPAP, alternated pulmonary vascular remodeling, and improved RV hypertrophy and PH development.

2. Materials and Methods

2.1. Ethics Statement. All studies using Sprague-Dawley rats were approved by the institutional animal care and use committee of Tongji Medical College, Huazhong University of Science and Technology, and performed in accordance with the National Institutes of Health Guide for the Care and Use of Laboratory Animals.

2.2. Animals and Treatment. Male Sprague-Dawley rats (age: 8-10 weeks; weight: 220-250 g) were allowed to acclimate to the experimental environment for 1 week. Then, they received 1 intraperitoneal injection of MCT at 60 mg/kg to produce the pulmonary hypertension model. According to previous studies, stable pulmonary hypertension was established in rats after two weeks after the injection of MCT.

Rats were randomly divided into four groups ($n = 6$ per group) as described below. (1) In the negative control (NC) group, a single dose of solvent but without MCT was given intraperitoneally on day 1 of the experiment. (2) In the diseased nontreatment (NT) group, a single dose of MCT (60 mg/kg) was given intraperitoneally on day 1 of the experiment. (3) In the diseased early treatment (ET) group, a single dose of MCT (60 mg/kg) was given intraperitoneally on day 1, and aerosol inhalation of CSNO was administrated from day 1 to day 28 (88 ppm for 20 minutes per day). (4) In the diseased late treatment (LT) group, a single dose of MCT (60 mg/kg) was given intraperitoneally on day 1, and aerosol inhalation of CSNO was administrated from day 14 to day 28 (88 ppm for 20 minutes per day).

Sodium nitrite was obtained from Sigma-Aldrich, and L-cysteine was obtained from Tokyo Chemical Industry. CSNO was synthesized as previously described. Monocrotaline, obtaining from MCE, was dissolved in solvent (ethanol and 0.9% NaCl at 1 : 4).

2.3. Hemodynamic Measurements. Pulmonary hemodynamic studies were conducted on day 28; all animals were anesthetized by isoflurane inhalation (1.5-2%) and then euthanized by cervical dislocation. A PE-50 tube, with specific angles, was carefully inserted into the right jugular vein, through the right ventricle, eventually to the pulmonary artery to continuously monitor the hemodynamic parameters. Cardiac output (CO) was measured using the thermodilution method with the CO pod (ML313C, ADInstruments) and the PowerLab/4SP data acquisition system [12]. Pulmonary vascular resistance is calculated by the ratio of mPAP and CO: PVR = mPAP/CO.

2.4. HE and EVG Staining. Animals were sacrificed after hemodynamic measurements on day 28. Middle and lower portions of the left lungs were embedded in paraffin, followed by staining with both hematoxylin and eosin (HE) staining and Elastic van Gieson (EVG) staining in a standard manner. Medial wall thickness was determined in distal pulmonary arteries with diameters between 50 and 150 μm. Image capture was performed using the EVOS FL Auto Imaging System (Life Technologies, Thermo Fisher Scientific).

Two indexes reflecting the vessel thickness were calculated: the ratio of vascular wall thickness (WT%) = 100% × (outer diameter of the pulmonary arterioles − inner diameter of the pulmonary arterioles)/(outer diameter of the pulmonary arterioles); the ratio of vascular wall area (WA%) = 100% × (transection area of the walls of pulmonary arterioles)/(cross − sectional area of pulmonary arterioles).

2.5. Masson's Trichrome Staining. Paraffin-embedded lung tissues and frozen right ventricle sections were stained with Masson's trichrome staining in a standard manner.

Two indexes reflecting the collagen deposition level were calculated: tissue collagen volume fraction (CVF) (%) = collagen area/entire area × 100%; perivascular collagen area versus vascular lumen area (PVCA/VA) (%) = collagen area surrounding the vessel/vascular lumen area × 100%.

2.6. Immunohistochemistry Staining. Monoclonal antibodies against α-smooth muscle actin (α-SMA) (Denmark, 1:200 dilution) were used to perform immunohistochemical studies in paraffin-embedded lung tissues. The categorization of pulmonary arteries is based on the degree of muscularization. The vessels were categorized as fully muscularized, partially muscularized, or nonmuscularized vessels, according to previous studies. Immunohistochemistry photomicrographs were captured with EVOS FL Auto Imaging System (Life Technologies, Thermo Fisher Scientific).

2.7. Measurement of RVHI. The hearts without residuary blood were quickly separated, and each chamber was weighed to determine the grade of the right ventricular hypertrophy index (RVHI). The index of RVH was expressed as the weight ratio of RV to LV plus the septum (RV/(LV + S)).

2.8. Western Blot Analysis. Lung tissue homogenates and collected cultured cells were lysed in the RIPA lysis buffer. Equal amounts of proteins were loaded for gel electrophoresis using 10% Bis-Tris SDS-PAGE, transferred to a PVDF membrane, and probed with antibodies. Prestained Protein Ladder (Thermo Fisher Scientific), p-JAK2 (Tyr1007/1008, CST, #3776, 1:1000 dilution), p-STAT3 (Tyrosine 705, CST, #9145, 1:1000 dilution), p-MEK1/2 (Ser217/221, CST, #9154, 1:1000 dilution), p-ERK1/2 (Thr202/Tyr204, CST, #4370, 1:1000 dilution), SMMHC (Proteintech, #21404-1-AP, 1:1000 dilution), SM22α (Proteintech, #55135-1-AP, 1:1000 dilution), MMP2 (Santa Cruz Biotechnology, sc-10736, 1:1000 dilution), MMP9 (Abcam, ab38898, 1:1000 dilution), iNOS (Abcam, ab49999, 1:1000 dilution), Bip (CST, #3183, 1:1000 dilution), CHOP (CST, #2895, 1:1000 dilution), p-EIF2α (Ser51, CST, #3398P, 1:1000 dilution), p-PERK(Thr982, Affinity, DF7576, 1:1000 dilution), PINK1 (Abcam, ab23707, 1:1000 dilution), Parkin (CST, #4211, 1:1000 dilution), BNIP3 (Abcam, ab10433, 1:1000 dilution), BNIP3L (CST, #12396, 1:1000 dilution), FUNDC1 (CST, #49240, 1:1000 dilution), LC3B (CST, #3868, 1:1000 dilution), P62 (CST, #23214, 1:1000 dilution), β-actin (Santa Cruz Biotechnology, sc-47778, 1:2000 dilution), and GAPDH (CST, #2118 L, 1:2000 dilution) antibodies and HRP-conjugated secondary antibodies were used.

2.9. Quantitative PCR. Quantitative PCR studies were performed as we recently delineated. Primer sequences are listed as follows: Rat Fibronectin Forward 5$'$-AGGCACAAGGT CCGAGAAGAGG-3$'$, Reverse 5$'$-CATGAGTCATCCGT AGGCTGGTTC-3$'$; Rat COL1A1 Forward 5$'$-TGTTGG TCCTGCTGGCAAGAATG-3$'$, Reverse 5$'$-GTCACCTTG TTCGCCTGTCTCAC-3$'$; Rat COL3A1 Forward 5$'$-GACA CGCTGGTGCTCAAGGAC-3$'$, Reverse 5$'$-GTTCGCCTG AAGGACCTCGTTG-3$'$; Rat iNOS Forward 5$'$-GTGTTC CACCAGGAGATGTTG-3$'$, Reverse 5$'$-GAAGGCGTAGC TGAACAAGG-3$'$; Rat NOX4 Forward 5$'$-TGCATGGTG GTGGTATTGTTCCTC-3$'$, Reverse 5$'$-AGCAGCAGCAG CATGTAGAAGAC-3$'$; Rat IL-1β Forward 5$'$-TCCATG AGCTTTGTACAAGG-3$'$, Reverse 5$'$-GGTGCTGATGT ACCAGTTGG-3$'$; Rat IL-6 Forward 5$'$-TGTTCTCAGGG AGATCTTGG-3$'$, Reverse 5$'$-TCCAGGTAGAAACGGA ACTC-3$'$; Rat TNFα Forward 5$'$-GATCGGTCCCAACAAG GAGG-3$'$, Reverse 5$'$-TTTGCTACGACGTGGGCTAC-3$'$; and Rat GAPDH Forward 5$'$-GACATGCCGCCTGGAG AAAC-3$'$, Reverse 5$'$-AGCCCAGGATGCCCTTTAGT-3$'$.

2.10. Cell Culture. The A7R5 cell line was purchased from the American Type Culture Collection and cultured in DMEM (Dulbecco's modified Eagle's medium) containing 10% FBS (fetal bovine serum, HyClone) and 1% penicillin/streptomycin in a humidified 37°C incubator with 95% air and 5% CO_2. N-Acetyl-cysteine (NAC) was purchased from Sigma-Aldrich (St. Louis, MO, USA). Dihydroethidium (DHE) was purchased from MCE.

2.11. Wound Healing Assay. The wound healing assay was performed as previously described. A7R5 cells were seeded in 6-well plates (1.5×10^5/well) and were grown to confluence. A 10 μL pipette tip was used to scratch the monolayer cells, followed by PBS rinsing to remove floating cells.

2.12. Statistical Analysis. Data was represented as mean ± SEM performed in quadruplicate. Statistical analysis was performed with SPSS software (version 21.0). One-way ANOVA and two-way ANOVA followed by Bonferroni's post hoc test were used to test for significant differences among test groups. Statistical significance was defined as $P < 0.05$. Quantitative assessments were performed by ImageJ and Image-Pro Plus (6.0).

3. Results

3.1. CSNO Attenuated Pulmonary Hemodynamic Changes and Right Ventricular Hypertrophy Induced by MCT In Vivo. To assess the effect of CSNO on PH development, a catheter with specific angles was inserted into the pulmonary artery through the right ventricle to directly measure pulmonary artery pressure (PAP). As shown in Figure 1(a), MCT administration significantly elevated mean pulmonary artery pressure (mPAP), indicating that the PH model was established successfully as expected. When diseased animals were treated with CSNO, the mPAP decreased significantly compared to the nontreatment group, with the trend being more effective in the early treatment group (Figures 1(a) and 1(b)). To further confirm the effect of CSNO on hemodynamic changes in pulmonary arteries and avoid potential bias resulting from a different baseline, we calculated pulmonary vascular resistance (PVR) in different groups (Figure 1(c)). In agreement with mPAP changes, the PVR index was elevated in the diseased nontreatment group and, importantly, decreased in both CSNO treatment groups significantly, with the trend being more effective in the early treatment group (Figure 1(c)).

RVHI, the index of RV hypertrophy, was also increased in the NT group than in the NC group. When diseased animals were treated with CSNO, RVHI was significantly decreased in both the ET and LT groups (Figure 1(d)), indicating that CSNO treatment improved right ventricular hypertrophy. In addition, MCT-induced PH animals exhibited a significantly increased RV/BW ratio; again, CSNO treatment significantly reduced this ratio, with the trend being more effective in the early treatment group (Figure 1(e)). These data indicate that CSNO treatment can effectively improve hemodynamic alterations in the process of PH in MCT-induced rats.

3.2. CSNO Ameliorated Vascular Remodeling and Regulated Smooth Muscle Contractile Protein Expression and MMP Expression. Pulmonary vascular remodeling, characterized by proliferation and migration of vascular smooth muscle cells, leading to continuous progress and deterioration of PH, is the key process in the pathophysiology development of PH. As shown in Figures 2(a) and 2(b), pulmonary artery wall thickness, the main manifestation of vascular remodeling, was significantly increased in the NT group, but when treated with CSNO, the remodeling in these rats was markedly ameliorated. CSNO treatment obtained therapeutic effects in both the ratio of vascular wall thickness (WT%) (Figure 2(c)) and ratio of vascular wall area (WA%) (Figure 2(d)) indexes, which are both critical indexes to eval-

uate pulmonary vascular remodeling. The above effects were further confirmed by hematoxylin and eosin (HE) staining (Figure 2(a)) and Elastic van Gieson (EVG) staining (Figure 2(b)). In addition, the fracture of the pulmonary artery vascular wall external elastic layer was also improved in rats following CSNO treatment (Figure 2(b)).

To further investigate the role of smooth muscle in vascular remodeling, we explored smooth muscle contractile protein expression by Western blot. As shown in Figure 2(e), CSNO treatment significantly increased the expression of SMMHC and SM22α, which are both contractile markers for the smooth muscle phenotype switch. In addition, CSNO treatment significantly inhibited PH animals' lung tissue MMP2 and MMP9 expression, where levels are closely related to the ability of vascular smooth muscle cells to migrate (Figures 2(e)–2(i)). These data further confirm the effect of CSNO on pulmonary vascular remodeling in PH animals.

3.3. CSNO Ameliorated Pulmonary Vascular Muscularization and Collagen Deposition. Lung vascular muscularization and pulmonary and right ventricular collagen deposition are all the key features of pulmonary vascular remodeling. Compared to the NC group, MCT-induced animals showed an increased pulmonary muscularization degree, vascular partial muscularization and full muscularization distribution (Figures 3(a) and 3(d)). Notably, both the early and late CSNO interventions significantly improved the muscularization degree, which may be due to the increased percentage of nonmuscularization and decreased percentage of full muscularization (Figure 3(d)). CSNO treatment also inhibited collagen volume fraction (CVF) (Figure 3(e)) and the ratio of perivascular collagen area versus vascular lumen area (PVCA/VA) in the pulmonary perivascular area (Figures 3(b) and 3(f)) and, in addition, CVF in the right ventricle (Figures 3(c) and 3(g)).

To further explore the inhibition of CSNO on collagen deposition in lung tissues, we determined the mRNA levels of COL1A1, COL3A1, and Fibronectin in each group. As shown in Figures 3(h)–3(j), both the early and late CSNO treatments attenuated the elevated mRNA levels of COL1A1, COL3A1, and Fibronectin in lung tissues of rats with PH. The amelioration of CSNO on the pulmonary vascular muscularization, collagen deposition, and right ventricular collagen deposition may contribute to the improvement of CSNO on PH development.

3.4. CSNO Treatment Ameliorated Oxidative Stress and Inflammatory Pathways in Lung Tissues. Oxidative stress plays an important role in PH development and pathophysiological processes in PH. We first investigated the transcription levels of NOX4 and iNOS in lung tissues by RT-PCR and found that they were both elevated in MCT-induced PH groups (Figures 4(g) and 4(h)). Notably, CSNO intervention decreased the transcription of these proteins in both the early treatment group and the late treatment group (Figures 4(g) and 4(h)). Next, we explored the protein expression of iNOS in lung tissues and found that, in agreement with the mRNA change, CSNO treatment decreased the expression of iNOS
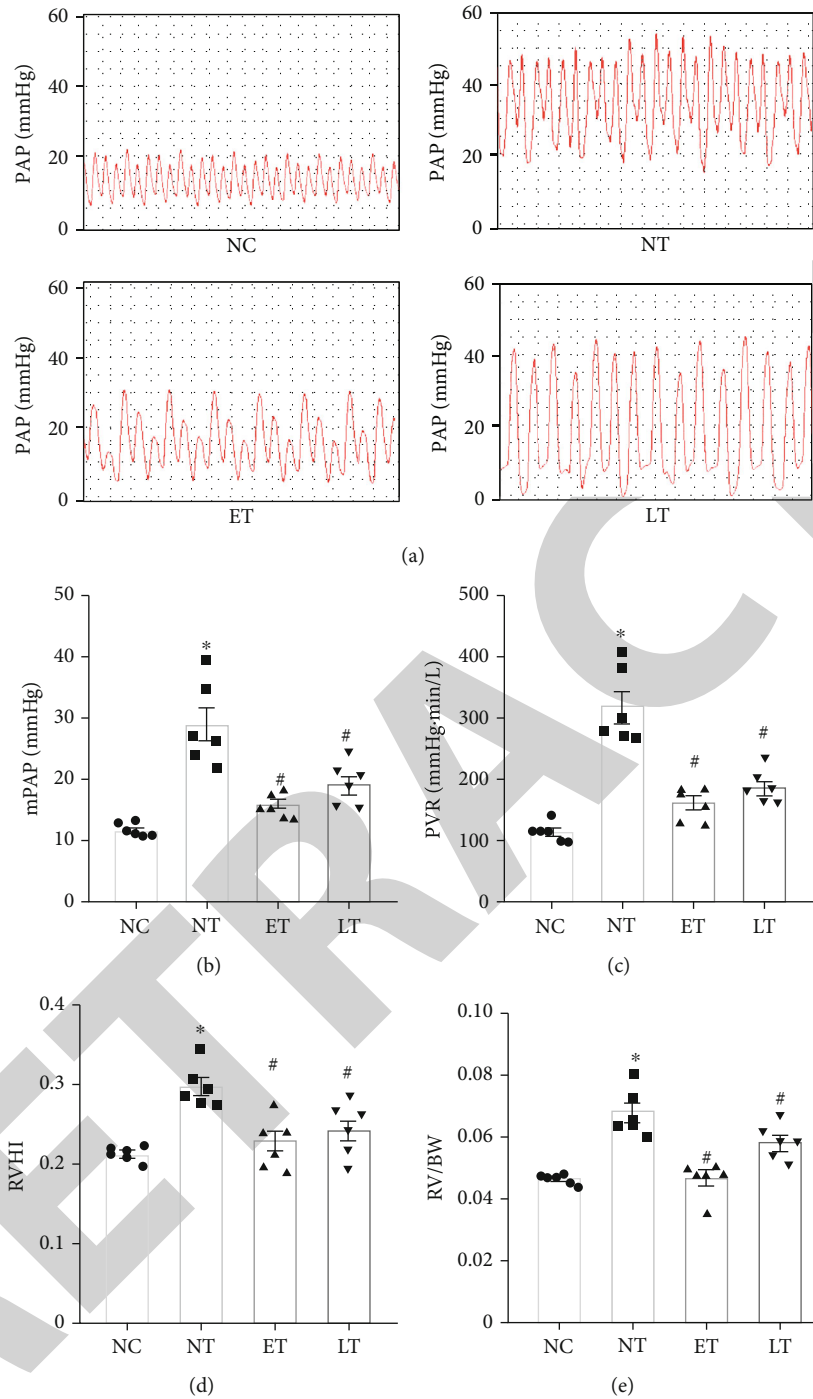
Figure 1: Effect of CSNO on pulmonary hemodynamic parameters in MCT-induced PH animals. Representative images of pulmonary artery pressure (PAP) measurement interface from rats on day 28 by the PowerLab/4SP data acquisition system (a). Comparison of mean pulmonary artery pressure (mPAP) (b), pulmonary vascular resistance (PVR) (c), RVHI (d), and the ratio of RV/BW (e) in each group. Data are presented as mean ± SEM. $n = 6$ rats. $^*P < 0.05$ vs. the NC group, $^\#P < 0.05$ vs. the NT group.

when compared with the nontreatment group (Figures 4(a) and 4(b)). Further, we investigated the levels of IL-1β, IL-6, and TNFα in lung tissues to evaluate local inflammation. As shown in Figures 4(i)–4(k), IL-1β, IL-6, and TNFα were all elevated in the MCT-induced PH groups and significantly decreased in both the ET and LT groups, indicating that

CSNO treatment ameliorated lung tissue inflammation in PH.

To elucidate the underlying mechanisms of the phenomena observed above, we explored the alternations of JAK2/-STAT3 and MEK/ERK pathways in the lung tissues of these animals. CSNO inhibited the phosphorylation of JAK2 and
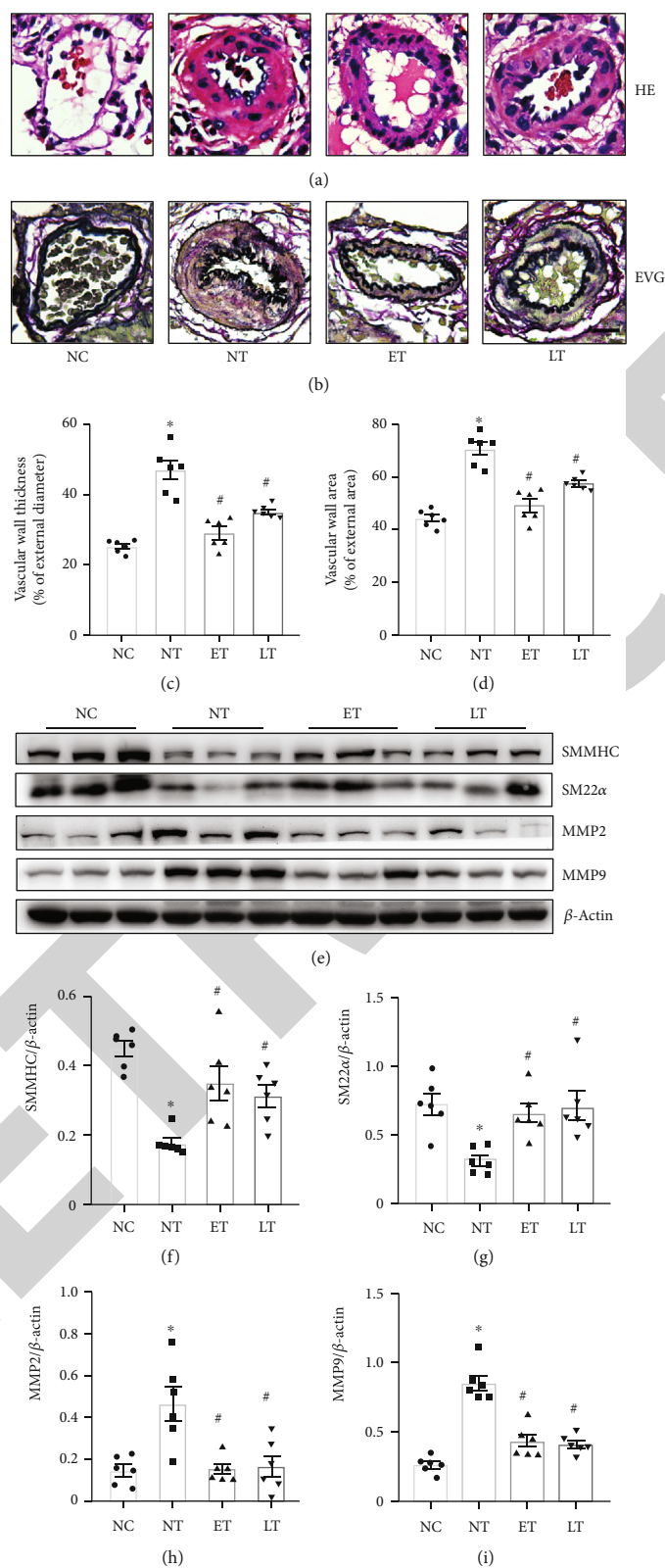
Figure 2: Effect of CSNO on pulmonary vascular remodeling in MCT-induced PH animals. (a) Hematoxylin and eosin (HE) staining for rat pulmonary arterioles. Scale bar: 20 μm. (b) Elastic van Gieson (EVG) staining of the elastic fiber of rat pulmonary arterioles. Scale bar: 20 μm. Comparison of (c) vascular wall thickness and (d) vascular wall area in each group as indicated. (e) Lung tissue SMMHC, SM22α, MMP2, and MMP9 expression in each group as indicated. (f–i) Schematic representation of the quantitative expression of indicated proteins. Data are presented as mean ± SEM. $n = 6$ rats. $^*P < 0.05$ vs. the NC group, $^#P < 0.05$ vs. the NT group.
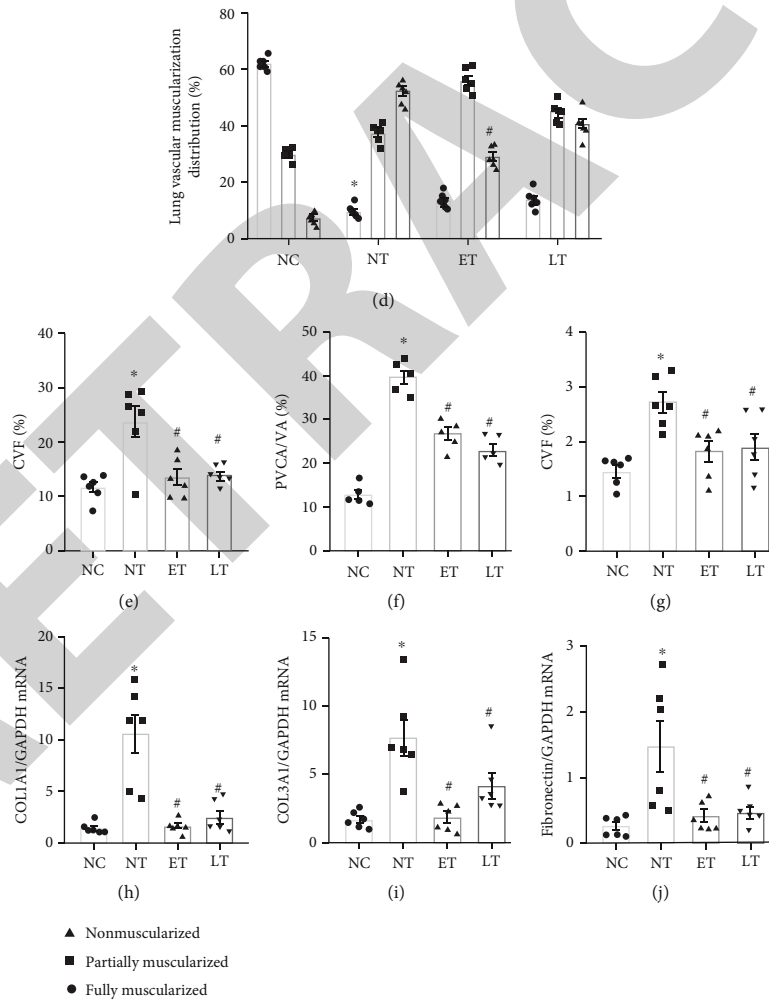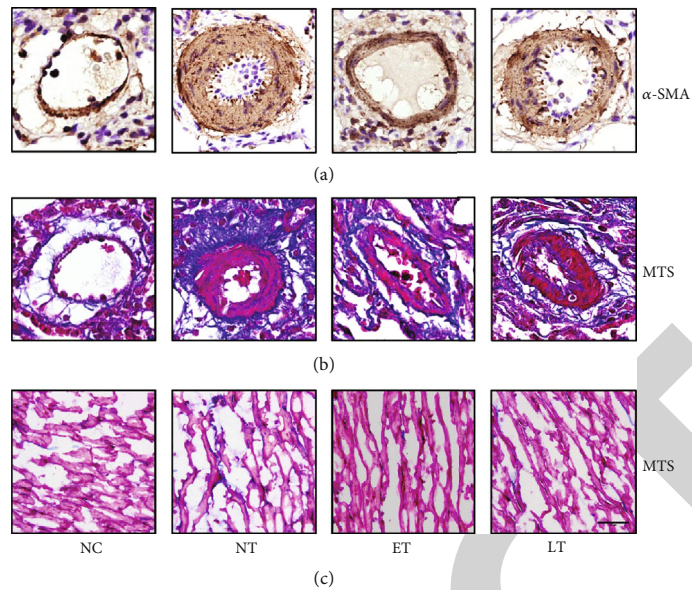
Figure 3: Effect of CSNO on muscularization and collagen deposition. (a) Immunohistochemical staining of α-SMA in lung tissues. Scale bar: 20 μm. (b) Masson's trichrome staining of lung tissues. (c) Masson's trichrome staining of RV tissues. (d) Categorization of pulmonary arteries based on the degree of muscularization, as fully muscularized, partially muscularized, or nonmuscularized vessels. (e, f) Indexes to evaluate collagen deposition in the lung tissues and pulmonary perivascular area. (g) Index to evaluate collagen deposition in RV. (h–j) A comparison of mRNA levels of COL1A1, COL3A1, and Fibronectin by RT-qPCR analysis in lung tissues. Magnification = 400x. Bar = 20 μm. Data are displayed as mean ± SEM. n = 6 rats. $^*P < 0.05$ vs. the NC group, $^\#P < 0.05$ vs. the NT group.
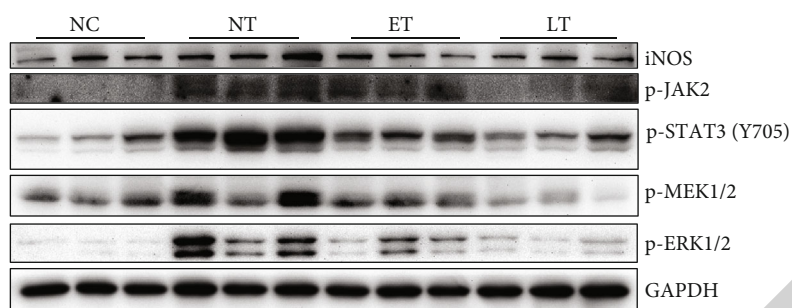
(a)
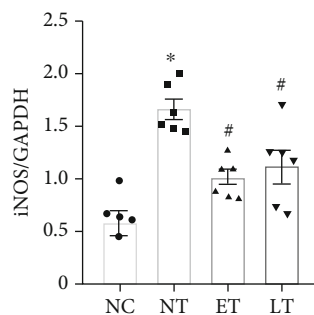
(b)
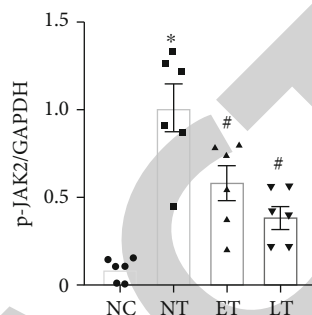
(c)
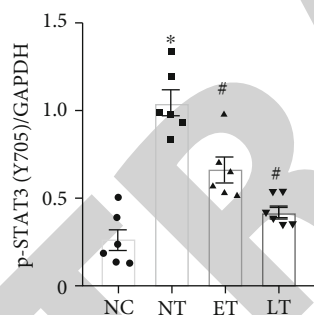
(d)
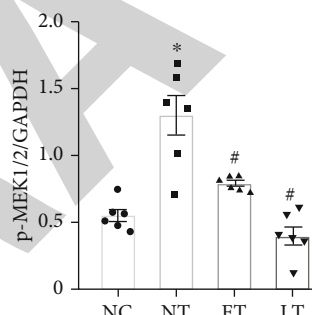
(e)
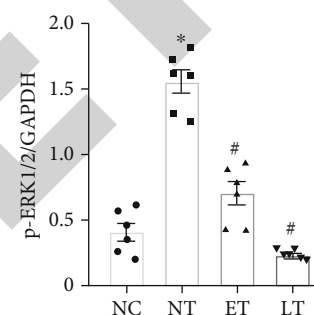
(f)
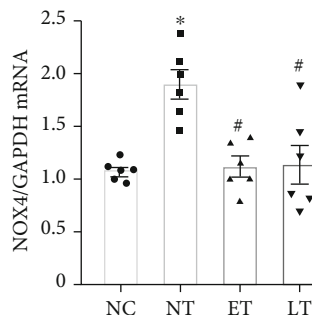
(g)

FIGURE 4: Continued.
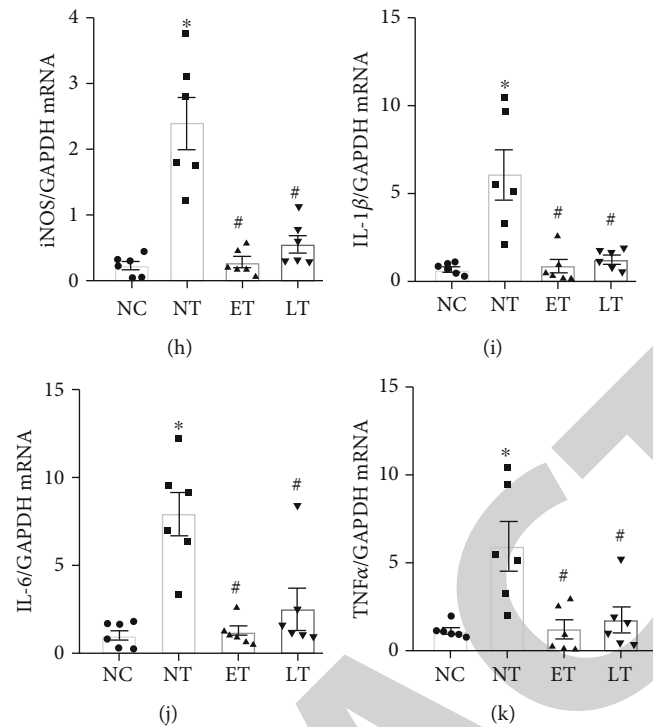
Figure 4: CSNO inhibited ROS and cytokine production and mediated STAT3 and ERK signaling pathways. (a–f) iNOS, p-JAK2, p-STAT3 (Y705), p-MEK1/2, p-ERK1/2, and GAPDH protein expressions were determined by immunoblotting. (g–k) NOX4, iNOS, IL-1β, IL-6, and TNFα mRNA levels were determined by RT-qPCR. Data are presented as mean ± SEM. $n = 6$ rats. $^*P < 0.05$ vs. the NC group, $^#P < 0.05$ vs. the NT group.

STAT3 in lung tissues induced by MCT induction (Figures 4(a), 4(c), and 4(d)). In addition, p-MEK1/2 and p-ERK1/2 in lung tissues were remarkably enhanced in the MCT-induced groups and suppressed in both the ET and LT groups (Figures 4(a), 4(e), and 4(f)), suggesting CSNO may achieve its effects through multiple signaling pathways.

3.5. CSNO Treatment Improved Aberrant ER Stress and Mitophagy in Lung Tissues of MCT-Induced PH Rats. ER stress has been reported as an important cellular response in PH development. Figure 5(a) shows that the expression of Bip, p-PERK, p-EIF2α, and CHOP remarkably elevated in MCT-induced PH rat lung tissues. Notably, their expression was significantly decreased in rats with CSNO inhalation, which indicated that CSNO improved ER stress occurring in lung tissues of MCT-induced PH rats (Figures 5(a)–5(e)).

ER stress and mitophagy are closely related and interact with each other. We further investigated the changes of mitophagy in PH. As shown in Figure 5(f), mitophagy-related proteins including PINK1, Parkin, BNIP3, BNIP3L, FUNDC1, and LC3B were elevated in the NT group. In the lung tissues of PH rats treated with CSNO inhalation, their expression was decreased, suggesting CSNO improved mitophagy in MCT-induced rat lung tissues (Figures 5(f)–5(l)).

3.6. CSNO Inhibited Aberrant ROS Production, Wound Healing, ER Stress, and Mitophagy In Vitro. To confirm the beneficial effects of CSNO observed in vivo, we further investigated its effects in vitro using cultured smooth muscle cells.

We first evaluated ROS production induced by AngII and IL-6 in A7R5 cells. As shown in Figures 6(a)–6(d), CSNO treatment significantly inhibited ROS production in these cells. Next, we investigated the effect of CSNO on A7R5 cell migration by the wound healing assay. As shown in Figures 6(e) and 6(f), CSNO suppressed A7R5 cell migration in a dose-dependent manner. Furthermore, we determined the STAT3 and ERK phosphorylation and found that CSNO intervention significantly decreased the elevated phosphorylation of ERK1/2 and STAT3 induced by either AngII or IL-6 (Figures 6(g)–6(j)).

Finally, we explored the effects of CSNO on ER stress and mitophagy in A7R5 cells. As shown in Figure 7, AngII and IL-6 were effective stimuli leading to ER stress and mitophagy in A7R5 cells; however, when cells were treated with CSNO, the excessively expressed ER stress-related proteins and mitophagy-related proteins were significantly inhibited (Figures 7(a)–7(l)). Further, the transcription levels of Bip, CHOP, and XBP1 in A7R5 cells were elevated following AngII and IL-6 induction; when cells were treated with CSNO, the transcription of these proteins was inhibited (Figures 7(m)–7(r)).

4. Discussion

Pulmonary hypertension, known as a "malignant tumor of the cardiovascular system" [13], is a chronic disorder accompanied by poor prognosis. So far, the strategies are mainly aimed at relieving symptoms and improving prognosis, neglecting characteristic lesions that are closely associated

(a)

(b)

(c)

(d)

(e)

(f)
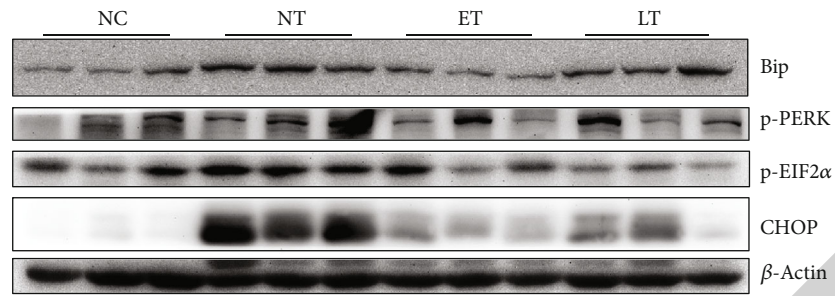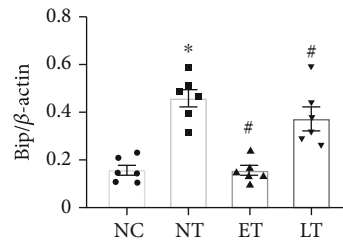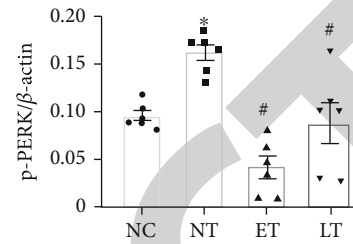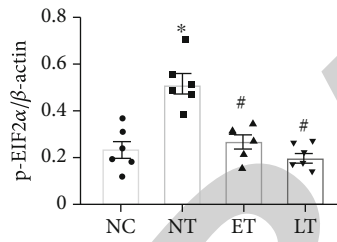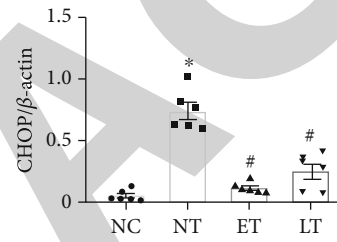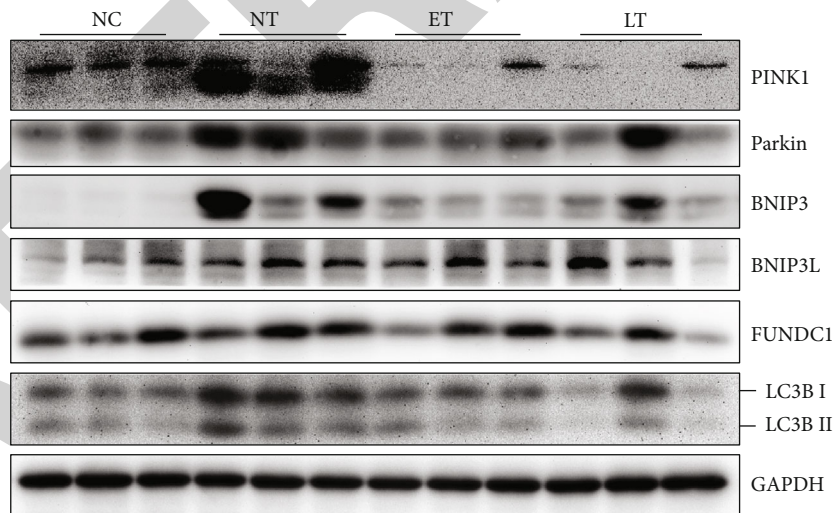
Figure 5: Continued.
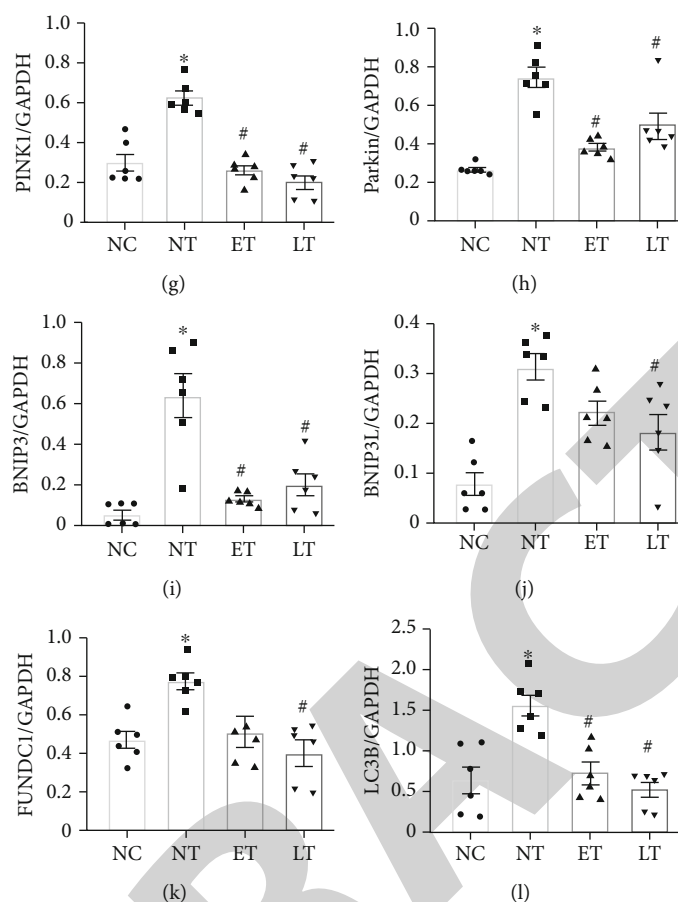
FIGURE 5: CSNO attenuated ER stress and mitophagy in MCT-induced rats. (a) Representative images of Bip, p-PERK, p-EIF2α, and CHOP expression in MCT-induced rat lung tissues. (b–e) Quantification of corresponding images. (f) Representative images of PINK1, Parkin, BNIP3, BNIP3L, FUNDC1, and LC3B expression in MCT-induced rat lung tissues. (g–l) Quantification of corresponding images. Data were presented as mean ± SEM. $n = 6$ rats. $^{*}P < 0.05$ vs. the NC group, $^{#}P < 0.05$ vs. the NT group.

with the overall survival [14]. Therefore, new therapies are needed for PH based on its pathogenesis.

NO has been suggested to exert vasodilation and antiproliferation effects. It has been reported that inhaled NO can selectively dilate pulmonary vessels in both patients with PH and animal models of PH [15]. However, the oxygen-rich environment of the airway and lung may predispose it toward toxicity by forming reactive nitrogen/oxygen species; thus, so far, NO is mainly utilized in pulmonary hypertension crises in neonates. SNO including CSNO are endogenous NO derivatives that are relatively resistant to toxic reactions with oxygen. In addition, besides leading to vasodilation through the cGMP-dependent pathway as NO does, CSNO also regulates protein function by S-nitrosylation of thiols, an effect through protein posttranslational modification which NO gas lacks, so it may mimic the whole function of the endogenous nitric oxide species and restore the endothelial dysfunction which has been reported in PH. Previously, we have reported that CSNO inhibited RhoA activity through oxidative nitrosylation of C16/20 residues, which may be beneficial for both vasodilation and remodeling [4]. We also observed CSNO could induce upregulation of cytoprotective and antioxidant genes by thiol modification of Keap1 [16]. Whether

CSNO could regulate aberrant redox and ameliorate PH progression is unknown.

Inflammation can be exacerbated by endothelial dysfunction and NO deficiency. Notably, endothelial dysfunction in PH leads to the decrease of SNO production, while the expression and activity of GSNOR (S-nitrosoglutathione reductase), which can degrade SNO as an enzyme, increased [17], suggesting that SNO insufficiency may be involved in the progression of PH. In this study, we found that CSNO exogenous supplement improved pulmonary hemodynamics and vascular remodeling in the PH animals and further demonstrated the importance of SNO in maintaining vasculature resistant balance in PH pathogenesis.

Torok et al. [18] reported that L-Leu, a LAT inhibitor that blocks CSNO transmembrane movement, inhibited pulmonary vasodilation in L-cysteine-exposed lungs following NO inhalation. Moreover, Jankov et al. [19] reported that NaNO$_2$, a CSNO precursor, reversed chronic hypoxic PH partly via upregulated SNO-LTA4H. Another SNO precursor such as O-nitrosoethanol has been explored to maintain the lung function in PH [20]. We previously reported that CSNO inhibited RhoA activity through SNO-RhoA modification in vitro, which suggested CSNO

(a)

(b)

(c)

(d)

(e)

(f)

(g)

(h)
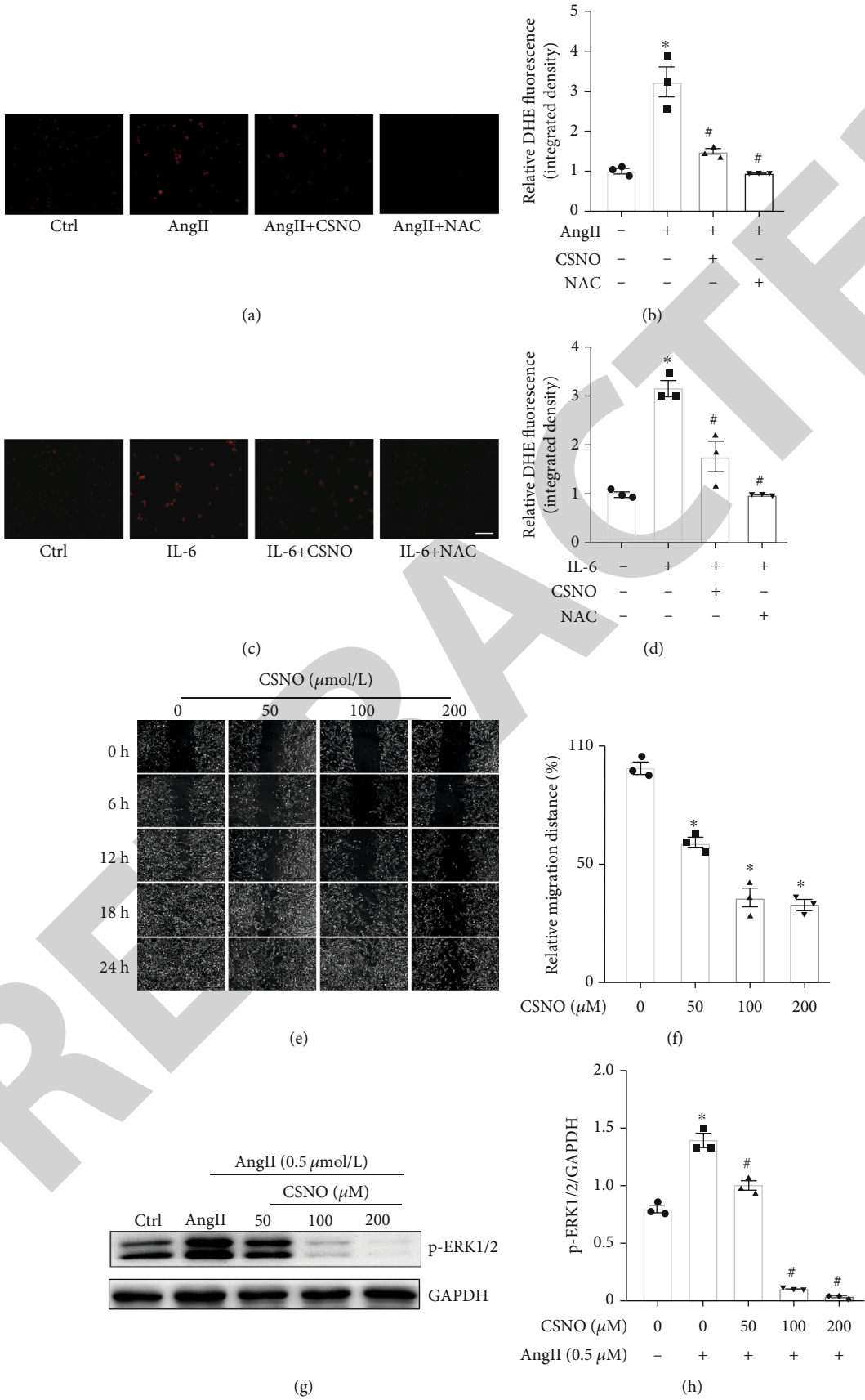
FIGURE 6: Continued.
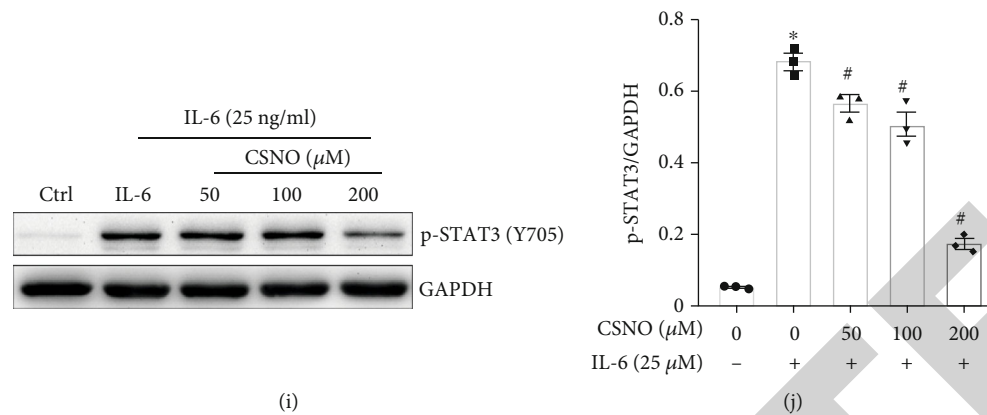
FIGURE 6: CSNO suppressed ROS generation, cell migration, and phosphorylation of STAT3 and ERK in vitro. (a, c) A7R5 cells were pretreated with CSNO (50 μmol/L) or NAC (5 mmol/L) for 1 hour, then stimulated with 0.5 μmol/L AngII or 25 ng/mL IL-6 for an additional 24 hours. Cytosolic ROS production was detected using the DHE fluorescence probe. (b, d) Quantification of DHE fluorescence in A7R5 cells. (e) A7R5 cells were treated with different concentrations of CSNO as indicated, and cell migration was determined by the wound healing assay. (f) Quantitative analysis of corresponding images. (g) A7R5 cells were pretreated with CSNO (50 μmol/L) for 1 hour and incubated with 0.5 μmol/L AngII for an additional 5 minutes; then, ERK1/2 phosphorylation was determined by immunoblotting. (h) Quantification of corresponding images. (i) A7R5 cells were pretreated with CSNO (50 μmol/L) for 1 hour and incubated with 25 ng/mL IL-6 for an additional 30 minutes; then, STAT3 phosphorylation was determined by immunoblotting. (j) Quantification of corresponding images. These data are calculated from three independent experiments and are displayed as mean ± SEM. $^*P < 0.05$ vs. controls, $^#P < 0.05$ vs. AngII or IL-6 treatment.

may contribute to reversing vascular remodeling. In this study, we presented direct data to show that CSNO improved pulmonary vasoconstriction and remodeling in PH. To our knowledge, our study is the first one showing that inhaled CSNO could alleviate the development of PH.

In decades, greater attention has been focused on inflammation in patients and experimental animals with PH. Inflammation precedes vascular remodeling and elevated pulmonary artery pressures in experimental PH [21, 11]. An expanding body of knowledge has related inflammatory factors to worse clinical outcomes, quality of life-related symptoms, and death in PH patients. IL-6 was reported to trigger smooth muscle cell proliferation [22] and vascular remodeling [23]. Moreover, IL-6 overexpression induced PH in rodents [22]. Consistent with other studies, our data showed that IL-6 expression was significantly elevated in lung tissues of PH rats, accompanied by increased IL-1β and TNFα. And importantly, the expressions of these inflammatory proteins were significantly decreased following CSNO treatment.

Abundant studies have reported STAT3 and ERK abnormal activation in PH, and inhibition of their activities contributed to the reversal of PH [24, 25]. Consistent with previous studies, our data showed excessive phosphorylation of STAT3 and ERK in lung tissues of MCT-induced rats, and we further found that overactivation can be reversed by CSNO intervention. Our results suggested that CSNO improved PH development by regulating STAT3 and ERK activity in the lungs. In addition, CSNO showed inhibition of hyperactivated STAT3 and ERK in A7R5 cells, which is consistent with the data from our study in vivo. Interestingly, both STAT3 [26] and ERK [27] could be modified by S-nitrosylation, leading to the reduction of phosphorylation on Tyr705 and Thr202/Tyr204 modification, respectively.

Moreover, STAT3 and ERK S-nitrosylation modification was accompanied by cell growth inhibition [28, 26], suggesting that CSNO may regulate STAT3 and ERK1/2 S-nitrosylation modification to improve PH.

The inhibition of ER stress improving PH progression suggests its contribution to PH development. Consistent with previous studies, excessive ER stress was observed in lung tissues following MCT injection. In this study, we found that ER stress-related proteins significantly increased in lung tissues in MCT-induced PH animals. It is reported that the PERK pathway plays an important role in the pathogenesis of chronic hypoxia-induced PH [29]. Inflammation is regarded as a trigger factor of ER stress. Interestingly, ER stress and inflammatory markers were largely mimicked by chronic stimulation of PDGF, which is a stimulus used to induce the smooth muscle phenotype switch.

Moderate ER stress is an adaptive strategy for the accumulation of UPR in the ER. Excessive ER stress injures mitochondrial function and contributes to pulmonary vascular remodeling in PH [7]. Moreover, severe ER stress leads to mitochondrial dysfunction by abnormal Ca$^+$ influx from ER to mitochondrial and aberrant ROS regulation. Mitochondrial dysfunction has been theorized as a crucial player in PH development, which leads to the increasing production of ROS [30].

The increasing evidence suggested mitochondrial dysfunction contributes to the development and progression of pulmonary hypertension. Reactive oxygen species generated by mitochondria was increased in the vascular smooth muscle cells isolated from the pulmonary vessels of rats with PH [31]. Hsu et al. [32] reported that transplantation of viable mitochondria improved right ventricular performance and pulmonary artery remodeling in rats with established PH. Interestingly, it was reported that S-nitrosylation of PINK1

(a)

(b)

(c)

(d)

(e)

(f)

(g)

(h)

(i)

(j)
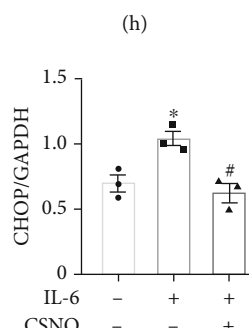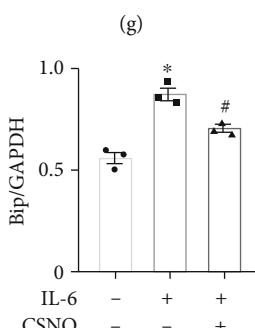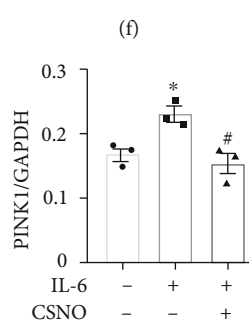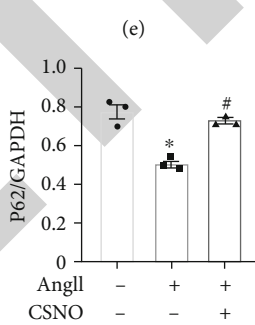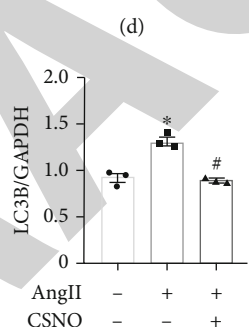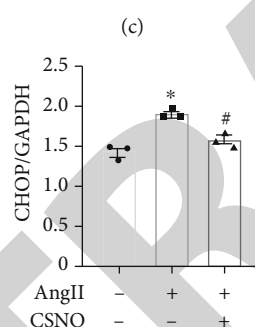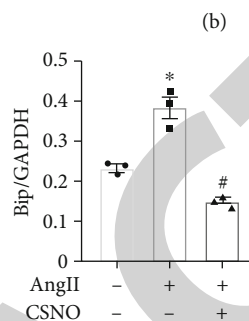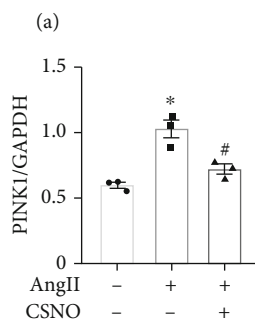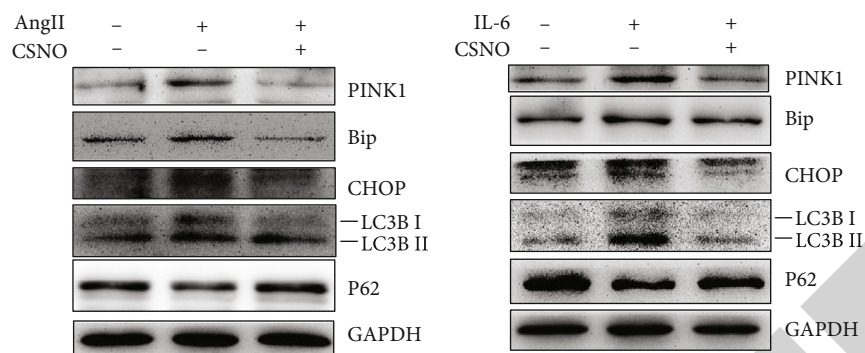
Figure 7: Continued.
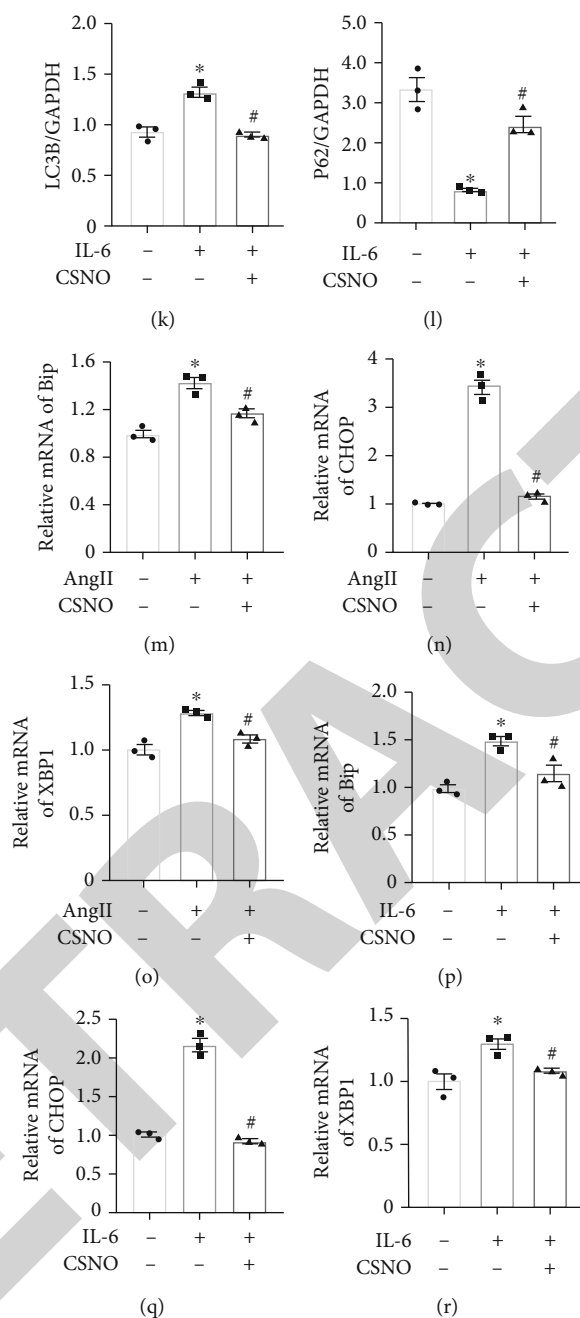
FIGURE 7: CSNO inhibited mitophagy and ER stress in vitro. (a) A7R5 cells were pretreated with CSNO (50 μmol/L) for 1 hour and incubated with 0.5 μmol/L AngII for an additional 24 hours. Protein expression was determined by immunoblotting using specific antibodies as indicated. Representative images of PINK1, Bip, CHOP, LC3B, and P62 expression. (c–g) Quantification of corresponding images. (b) A7R5 cells were pretreated with CSNO (50 μmol/L) for 1 hour and incubated with 25 ng/mL IL-6 for an additional 24 hours. Protein expression was determined by immunoblotting using specific antibodies as indicated. (h–l) Quantification of corresponding images. (m–r) Bip, CHOP, and XBP1 mRNA levels were determined by RT-qPCR. These data are calculated from three independent experiments and are displayed as mean ± SEM. $^*P < 0.05$ vs. controls, $^\#P < 0.05$ vs. AngII or IL-6 treatment.

led to activity inhibition and further reduced Parkin translocation to mitochondria [33]. In our study, we also observed that CSNO inhibited the excessive elevation of mitophagy-related proteins including PINK1, Parkin, BNIP3, BNIP3L, FUNDC1, and LC3B in the lung tissues of PH rats. These data suggested a role of SNO in regulating mitochondrial function.

Accumulating evidence indicated that mitophagy, including PINK1/Parkin- and BNIP3L-dependent mitophagy, was involved in the pathogenesis of COPD and other cigarette smoke-associated pulmonary diseases [34, 35]. PINK1 and Parkin were increased in the lungs of smokers, patients with COPD, and chronic cigarette smoke-exposed mouse lungs [36]. PINK1/Parkin-mediated mitophagy was

reported to participate in proliferation and atherosclerotic lesion deterioration [37]. In the present study, data showed that the expression of mitophagy-related proteins was increased following MCT induction, and CSNO application partly reversed their excessively increased expression in vivo. Moreover, amelioration on AngII-induced proliferation of vascular smooth muscle cells was accompanied by downregulation of the expression of PINK1, Parkin, and LC3B. AngII could induce the contractile-synthetic phenotypic switch and proliferation of VSMC in vitro [38]. Previous studies have documented that the possible mechanisms for AngII-mediated autophagy may be associated with the activation of NADPH oxidase, further inducing ROS generation [39]. The mRNA transcription of NOX4 and iNOS decreased in lung tissues when rats were treated with inhaled CSNO, indicating that CSNO treatment improved oxidative stress and may further contribute to the amelioration of PH development. We also presented data on ROS production detected by the DHE probe, which was induced by AngII and IL-6 in vitro. Notably, CSNO treatment alleviated ROS production in A7R5 cells, in accordance with our data from the study in vivo. Moreover, our data showed increased expression of PINK1 and Parkin in A7R5 cells induced by AngII and IL-6, indicating that aberrant ROS relates to excessive mitophagy. Furthermore, we presented data that CSNO treatment improved excessive ROS production and aberrant mitophagy in vivo and in vitro. The precise mechanisms of the interaction of oxidative stress and mitophagy need further investigation.

Some limitations of this article are as follows. First, we only chose one of the PH animal models, MCT-induced PH in rats, to test whether CSNO could improve PH. So far, no model has been able to fully simulate PH in humans. Different PH models mimic distinct characteristics occurring in human PH. Among these models, the MCT-induced model simulates relatively high PAP and severe PH development to a great extent. Second, in this study, we did not compare the difference of improvements in CSNO, sodium nitrite, and L-cysteine treatment in MCT-induced rats, respectively. Sodium nitrite and L-cysteine are the precursors of CSNO, and they were reported to improve PH by S-nitrosylation of the target protein. However, CSNO is a functional SNO and may directly modify related proteins by S-nitrosylation, which might be more effective than NaNO$_2$/L-cysteine.

5. Conclusions

In conclusion, we presented data showing that CSNO attenuated pulmonary artery blood pressure and pulmonary vascular wall remodeling as well as RV hypertrophy; we also showed that the beneficial effects of CSNO on PH may occur through inhibition of oxidative stress, inflammation, and mitophagy.

Data Availability

All data generated or analyzed during this study are included in this article.

Conflicts of Interest

The authors declare that there is no conflict of interest.

Acknowledgments

References

[1] K. Satoh, T. Satoh, N. Kikuchi et al., "Basigin mediates pulmonary hypertension by promoting inflammation and vascular smooth muscle cell proliferation," *Circulation Research*, vol. 8, pp. 738–750, 2014.

[2] C. Xue, M. Sowden, and B. C. Berk, "Extracellular cyclophilin A, especially acetylated, causes pulmonary hypertension by stimulating endothelial apoptosis, redox stress, and inflammation," *Arteriosclerosis, Thrombosis, and Vascular Biology*, vol. 6, pp. 1138–1146, 2017.

[3] S. Li and A. R. Whorton, "Functional characterization of two S-nitroso-L-cysteine transporters, which mediate movement of NO equivalents into vascular cells," *American Journal of Physiology. Cell Physiology*, vol. 4, pp. C1263–C1271, 2007.

[4] L. Lin, C. Xu, M. S. Carraway, C. A. Piantadosi, A. R. Whorton, and S. Li, "RhoA inactivation by S-nitrosylation regulates vascular smooth muscle contractile signaling," *Nitric Oxide-Biology and Chemistry*, vol. 74, pp. 56–64, 2018.

[5] N. Sud and S. M. Black, "Endothelin-1 impairs nitric oxide signaling in endothelial cells through a protein kinase Cdelta-dependent activation of STAT3 and decreased endothelial nitric oxide synthase expression," *DNA and Cell Biology*, vol. 11, pp. 543–553, 2009.

[6] S. Otsuki, H. Sawada, N. Yodoya et al., "Potential contribution of phenotypically modulated smooth muscle cells and related inflammation in the development of experimental obstructive pulmonary vasculopathy in rats," *PLoS One*, vol. 2, article e0118655, 2015.

[7] P. Dromparis, R. Paulin, T. H. Stenson, A. Haromy, G. Sutendra, and E. D. Michelakis, "Attenuating endoplasmic reticulum stress as a novel therapeutic strategy in pulmonary hypertension," *Circulation*, vol. 1, pp. 115–125, 2013.

[8] A. Sobolewski, N. Rudarakanchana, P. D. Upton et al., "Failure of bone morphogenetic protein receptor trafficking in pulmonary arterial hypertension: potential for rescue," *Human Molecular Genetics*, vol. 20, pp. 3180–3190, 2008.

[9] P. Walter and D. Ron, "The unfolded protein response: from stress pathway to homeostatic regulation," *Science*, vol. 334, no. 6059, pp. 1081–1086, 2011.

[10] G. C. Shore, F. R. Papa, and S. A. Oakes, "Signaling cell death from the endoplasmic reticulum stress response," *Current Opinion in Cell Biology*, vol. 23, no. 2, pp. 143–149, 2011.

Retraction

Retracted: Natural Antioxidants Improve the Vulnerability of Cardiomyocytes and Vascular Endothelial Cells under Stress Conditions: A Focus on Mitochondrial Quality Control

Oxidative Medicine and Cellular Longevity

This article has been retracted by Hindawi, as publisher, following an investigation undertaken by the publisher [1]. This investigation has uncovered evidence of systematic manipulation of the publication and peer-review process. We cannot, therefore, vouch for the reliability or integrity of this article.

Please note that this notice is intended solely to alert readers that the peer-review process of this article has been compromised.

Wiley and Hindawi regret that the usual quality checks did not identify these issues before publication and have since put additional measures in place to safeguard research integrity.

We wish to credit our Research Integrity and Research Publishing teams and anonymous and named external researchers and research integrity experts for contributing to this investigation.

The corresponding author, as the representative of all authors, has been given the opportunity to register their agreement or disagreement to this retraction. We have kept a record of any response received.

References

[1] X. Chang, Z. Zhao, W. Zhang et al., "Natural Antioxidants Improve the Vulnerability of Cardiomyocytes and Vascular Endothelial Cells under Stress Conditions: A Focus on Mitochondrial Quality Control," *Oxidative Medicine and Cellular Longevity*, vol. 2021, Article ID 6620677, 27 pages, 2021.

Review Article

Natural Antioxidants Improve the Vulnerability of Cardiomyocytes and Vascular Endothelial Cells under Stress Conditions: A Focus on Mitochondrial Quality Control

Xing Chang [iD],[1,2] Zhenyu Zhao [iD],[1] Wenjin Zhang [iD],[1,3] Dong Liu,[4] Chunxia Ma,[5] Tian Zhang [iD],[6] Qingyan Meng,[3] Peizheng Yan,[3] Longqiong Zou,[7] and Ming Zhang [iD][1]

[1]*Wangjing Hospital, China Academy of Chinese Medical Sciences, China*
[2]*Guang'anmen Hospital, Chinese Academy of Traditional Chinese Medicine, Beijing, China*
[3]*College of Pharmacy, Ningxia Medical University, Ningxia, China*
[4]*China Academy of Chinese Medical Sciences, Institute of the History of Chinese Medicine and Medical Literature, Beijing, China*
[5]*Shandong Analysis and Test Centre, Qilu University of Technology, Jinan, China*
[6]*Shandong University of Traditional Chinese Medicine, Jinan, Shandong, China*
[7]*Chongqing Sanxia Yunhai Pharmaceutical Co., Ltd., Chongqing, China*

Correspondence should be addressed to Tian Zhang; tianna0819@163.com and Ming Zhang; zyyzhangming@163.com

Cardiovascular disease has become one of the main causes of human death. In addition, many cardiovascular diseases are accompanied by a series of irreversible damages that lead to organ and vascular complications. In recent years, the potential therapeutic strategy of natural antioxidants in the treatment of cardiovascular diseases through mitochondrial quality control has received extensive attention. Mitochondria are the main site of energy metabolism in eukaryotic cells, including myocardial and vascular endothelial cells. Mitochondrial quality control processes ensure normal activities of mitochondria and cells by maintaining stable mitochondrial quantity and quality, thus protecting myocardial and endothelial cells against stress. Various stresses can affect mitochondrial morphology and function. Natural antioxidants extracted from plants and natural medicines are becoming increasingly common in the clinical treatment of diseases, especially in the treatment of cardiovascular diseases. Natural antioxidants can effectively protect myocardial and endothelial cells from stress-induced injury by regulating mitochondrial quality control, and their safety and effectiveness have been preliminarily verified. This review summarises the damage mechanisms of various stresses in cardiomyocytes and vascular endothelial cells and the mechanisms of natural antioxidants in improving the vulnerability of these cell types to stress by regulating mitochondrial quality control. This review is aimed at paving the way for novel treatments for cardiovascular diseases and the development of natural antioxidant drugs.

1. Introduction

Mitochondria are double-membrane-bound organelles that play an important role in the energy homeostasis of eukaryotic cells, including cardiomyocytes and endothelial cells [1]. According to the physiological needs in different living environments, mitochondria regulate their quantity and morphology [2]. With changes in the physiological environment, mitochondria can perform specific physiologi-

cal processes related to quantity, morphology, and quality to maintain their structure and function. This process, termed "mitochondrial homeostasis," is an important prerequisite for mitochondrial quality control (MQC) [3, 4].

Under oxidative stress, ischaemia, hypoxia, inflammation, and other stress conditions, mitochondrial homeostasis is disrupted [5]. This results in a disbalance of MQC, which affects mitochondrial quality and quantity, which can further lead to mitochondrial dysfunction and enhanced vulnerability,

and induce apoptosis in cells [6, 7]. In the process of MQC, mitochondria can regulate their accumulation by decreasing enzyme activity and through mitochondrial fusion/fission and mitophagy to ensure normal physiological functionality [8, 9]. MQC plays an important role in maintaining the physiological functions of myocardial and endothelial cells and has attracted extensive attention in the treatment of cardiovascular diseases (CVDs) in recent years. MQC can be regulated by natural antioxidants in the treatment of CVDs and can further maintain the normal function of mitochondria.

Antioxidants are substances that prevent the harmful effects of oxygen. Antioxidants capture and neutralise free radicals to reduce damage to the body and organs. Antioxidants are made by the body but can also be supplied by plants or drugs. Natural antioxidants have long been used by humans [10]. They are found in many Chinese herbal and natural medicines and can effectively remove reactive oxygen species (ROS) and maintain the oxidation/antioxidation balance in cells and mitochondria. They can rapidly reach lesion sites and react with free radicals and have the characteristics of high safety, strong antioxidant capacity, and limited side effects [11]. Thus, natural antioxidants can significantly delay or inhibit ROS-induced oxidative damage. They can reduce excessive ROS production and improve the ability of cellular and mitochondrial antioxidant systems to scavenge free radicals, quench $^1O_2$, and break down H_2O_2 [12]. They can regulate the redox state of cells and terminate oxidation processes by inhibiting the initiation and extension of redox reactions [13].

Recent studies have revealed that natural antioxidants can protect myocardial cells and endothelial cells via MQC under various stress conditions. In this review, the latest findings on the regulation of MQC based on *in vivo* and *in vitro* studies are discussed. In addition, the mechanisms of natural antioxidants of different types and sources in improving the vulnerability sensitivity of cardiomyocytes and endothelial cells under stress by regulating MQC are explored.

2. Method and Strategy

The literature on the advantages and mechanisms of natural antioxidants in improving cardiomyocyte and endothelial cell vulnerability through MQC published before November 2020 was searched in the Web of Science, MEDLINE, PubMed, Scopus, Google Scholar, and China National Knowledge Infrastructure databases. Keywords included "natural plants and mitochondrial quality control," "natural antioxidants and oxidative stress," "natural antioxidants and cardiomyocytes/endothelial cells," "active ingredients of natural drugs and oxidative stress," "natural plants," and "cardiomyocytes/endothelial cells." Original research articles related to natural antioxidants, MQC, and cardiomyocytes and endothelial cells were selected.

3. MQC

In 2019, a study published in *Nature* revealed that MQC defects can lead to CVDs and emphasised the importance of MQC [14]. MQC comprises mitochondrial autophagy, mitochondrial biosynthesis, mitochondrial fusion/fission, the mitochondrial respiratory chain, and the mitochondrial antioxidant system. MQC ensures the normal operation of the mitochondrial network and regulates timely mitochondrial turnover to maintain a stable quantity and quality of mitochondria in cardiomyocytes and endothelial cells [15]. Via MQC, mitochondria can regulate their numbers through mitochondrial fusion/fission, deliver damaged mitochondria or incorrectly folded proteins to lysosomes for degradation through mitophagy, and produce new mitochondria through biosynthesis. All MQC processes function independently as well as interact with each other to meet the energy demands of myocardial cells and endothelial cells under various conditions.

3.1. Regulatory Mechanism of MQC in Cardiomyocytes. Mitochondria comprise 25–30% of the myocardial cell volume and are widely distributed in the cell body and around the nucleus. The mammalian mitochondrial genome has 37 genes, 13 of which encode polypeptide subunits of enzyme complexes of the oxidative phosphorylation system, which provides more than 95% of the myocardial energy requirement for adenosine triphosphate (ATP) production [16, 17]. Mitochondria are the main organelles that mediate the energy production and apoptosis of cardiomyocytes [18, 19]. Because of the high energy requirement of myocardial cells, MQC is very important in these cells.

In a clinical study of 156 myocardial biopsy specimens, a single cardiomyocyte with obvious mitochondrial malformations was found in four samples [20]. The mitochondrial malformations in these four cardiomyocytes were accompanied by nuclear hypertrophy and/or sparse myofibrils. The malformations induced various disorders, including myocarditis, dilated cardiomyopathy, amyloidosis, and heart failure, all of which were accompanied by left ventricular systolic dysfunction [20].

Changes in mitochondrial quality and quantity directly affect the viability of cardiomyocytes and indirectly affect the pathological changes in myocardial diseases. As dynamic organelles, mitochondria can reshape their morphology under stress in myocardial infarction [21]. This reshaping of mitochondrial morphology (mitochondrion fission and fusion) is closely related to the expression of dynamin-related protein 1 (Drp-1) and mitofusin 1(Mfn1). Overexpression of Drp-1 and a decrease in Mfn1 expression in cardiomyocytes can destroy the mitochondrial fission/fusion balance and directly affect the contractility and function of cardiomyocytes [19]. Therefore, MQC plays an important role in myocardial cells.

3.2. Regulatory Mechanism of MQC in Endothelial Cells. In contrast to cardiomyocytes with their high energy demand, endothelial cells require less energy, and accordingly, their mitochondria account for only 2–6% of the cytoplasmic volume. The mitochondrial content of endothelial cells varies by the vascular bed and is higher in active endothelial cells. For example, endothelial cells at the blood-brain barrier are relatively active, and their mitochondrial content is as high as 8–11% [22].

The mitochondrial distribution in endothelial cells influences cell signal transduction. Under physiological conditions, mitochondria of endothelial cells are in a stable dynamic equilibrium state. Hypoxia-induced perinuclear aggregation of mitochondria can lead to the accumulation of mitochondrial (mt) ROS and induce transcription of the vascular endothelial growth factor gene [23]. Mitofusin-1 (Mfn1) is a mediator of mitochondrial fusion. When endothelial cells are injured by oxidative stress, the *Mfn1* mRNA expression is inhibited, resulting in the disbalance of mitochondrial fusion/fission in endothelial cells, reducing the quality of mitochondria and the function of endothelial cells [24, 25].

Peroxisome proliferator-activated receptor-gamma coactivator 1 alpha (PGC-1α) is abundant in endothelial cells and participates in the formation of mitochondria. In addition, it plays roles in antiapoptosis and anti-inflammation, improving the bioavailability of nitric oxide in endothelial cells. PGC-1α can increase the expression of uncoupling protein 2 and mitochondrial antioxidant enzymes, which is crucial for MQC and repair of oxidative damage in endothelial cells [26, 27].

Numerous studies have revealed that natural antioxidants can protect myocardial cells and endothelial cells under stress through the regulation of MQC. MQC is involved in cell protection against oxidative stress, inflammation, ischaemia/reperfusion (I/R), hypoxia/reoxygenation (H/R), high glucose, and lipid toxicity, and improves the vulnerability of myocardial cells and endothelial cells under stress.

4. Oxidative Stress

Oxidative stress is a state of imbalance between oxidation and antioxidation *in vivo* mediated by ROS [28]. Oxidative stress is considered an important cause of human ageing and various diseases and is a major factor leading to the apoptosis and death of myocardial cells and vascular endothelial cells [29]. Under oxidative stress, the efficiency of mitochondrial ATP synthesis strongly decreases and while ROS excessively accumulate, leading to the destruction of the interaction between mitochondria and the endoplasmic reticulum, thus accelerating apoptosis [30]. MQC can regulate the contractility, necrosis, and apoptosis of cardiomyocytes and endothelial cells under oxidative stress.

4.1. Effect of mtROS on MQC. Mitochondria are the main oxygen- (O$_2$-) consuming sites in cells and the main source of ROS [31]. The mitochondrial respiratory chain, also known as the electron transport chain, is the core of mitochondrial energy production. Electron transport between respiratory chain complexes is coupled to proton transport through the mitochondrial membrane, resulting in the electrochemical gradient required for ATP synthesis [32, 33]. In addition, the respiratory chain is the main source of mitochondrial ROS production. ROS are a by-product of electron transfer in the respiratory chain. They are mainly produced by NADH: ubiquinone oxidoreductase and cytochrome C (cytC) oxidoreductase in the respiratory chain [34].

While mitochondria are the main source of ROS production, they are also the primary target of ROS attack. Proinflammatory factors released in response to excessive ROS production can directly damage mitochondrial respiratory chain function, reduce mitochondrial energy metabolism, and damage the mitochondrial antioxidant system, leading to further aggravation of oxidative stress damage [35, 36]. Excessive ROS production can also cause an abnormal opening of the mitochondrial membrane permeability transition pore (mPTP), which leads to an imbalance in mitochondrial membrane permeability transition and ion concentrations inside and outside the mitochondria. In addition, ROS activate various factors, including cytC, Bax, and caspase, to induce apoptosis of cardiomyocytes and endothelial cells [31, 37]. ROS-mediated oxidative stress can change mitochondrial structure and function, leading to excessive mitochondrial fission [38]. The qualitative and morphological damage of mitochondria caused by the imbalance of mitochondrial dynamics leads to apoptosis induction [39].

Endothelial cells isolated from a hypoxia-induced pulmonary hypertension rat model (such as microvascular endothelial cells) reportedly show excessive mtROS production, an imbalance in intracellular calcium (Ca^{2+}) levels, and an increase in abnormal mitochondrial fission [40]. Inhibition of mtROS suppresses abnormal mitochondrial division in endothelial cells, whereas mtROS production is induced in microvascular endothelial cells of normoxic rats, which increases the level of abnormal mitochondria [40]. It has been suggested that oxidative stress-mediated by mtROS may lead to an imbalance in mitochondrial Ca^{2+}, division, and respiratory function. Natural antioxidants, which can scavenge free radicals and inhibit excessive ROS production, highlight the advantages and potential of regulating MQC.

4.2. Role of the Mitochondrial Antioxidant System in MQC. Myocardial cells and endothelial cells are vulnerable to oxidative stress [41]. To suppress ROS-mediated oxidative stress and mitochondrial damage, mitochondria have a complete antioxidant system and an ROS-scavenging system [42]. The mitochondrial antioxidant system comprises superoxide dismutase (SOD), glutathione peroxidase (GSH-Px), and peroxiredoxin (PRX) [43]. They can directly scavenge free radicals or convert highly reactive superoxide radicals into hydrogen peroxide, which can be further eliminated by catalase and the GSH-Px and peroxiredoxin/thioredoxin systems [44].

SOD is the most important antioxidant in mitochondria and is located in the mitochondrial matrix. It reduces oxidative free radicals to H$_2$O$_2$, eliminates large amounts of O$_2^-$, and prevents superoxide-induced damage to mitochondrial (mt) DNA and proteins [45]. GSH is the most abundant nonprotein sulfhydryl and has a wide range of antioxidant effects. It mainly reduces lipid peroxides induced by ROS and hydroxyl groups [46] and reduces H$_2$O$_2$ to H$_2$O [47]. Together, these antioxidants constitute the mitochondrial antioxidant system. As shown in Figure 1 and Table 1, H/R, I/R, lipid toxicity, inflammation, high glucose, and other stress conditions are accompanied by the massive release free radicals, such as H$_2$O$_2$, NO, OH, and ONOO$^-$, which also
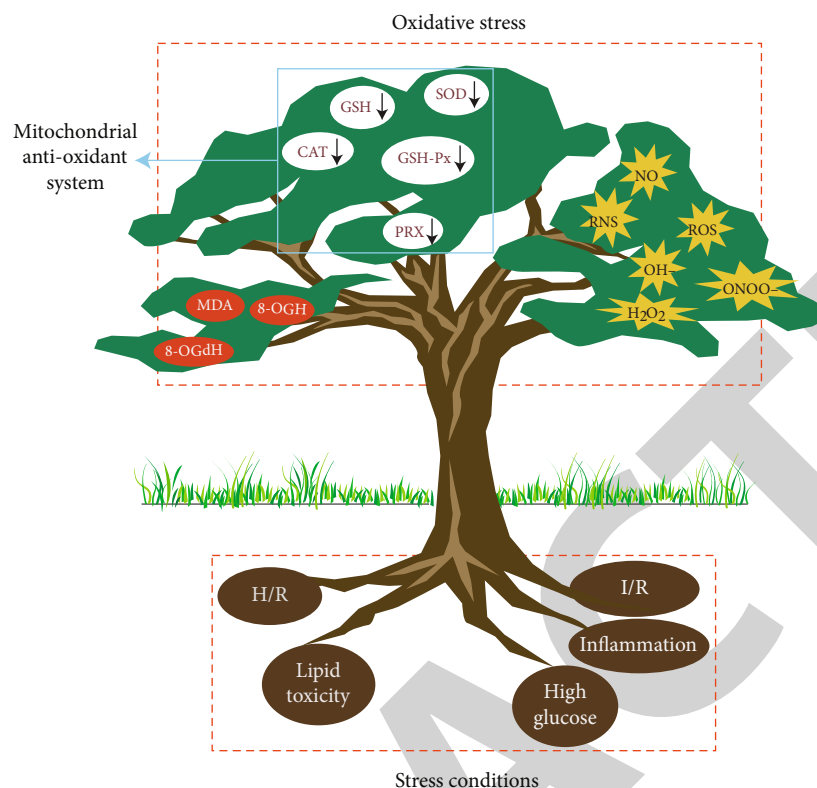
Figure 1: Mechanism of oxidative stress-mediated by different stress conditions. Under stress conditions (small red rectangle), cells release free radicals (H_2O_2, NO, OH, and $ONOO^-$), leading to the production of reactive oxygen species (ROS) and reactive nitrogen species (RNS). Excessive ROS and RNS production reduce the activity of antioxidant enzymes in the mitochondrial antioxidant system, causing ROS-mediated stress damage and the subsequent appearance of oxidative stress markers (red circles). H/R: hypoxia/reoxygenation; I/R: ischaemia/reperfusion; SOD: superoxide dismutase; GSH-Px: glutathione peroxidase; PRX: peroxiredoxin; CAT: catalase; MDA: malondialdehyde; 8-OHG: 8-hydroxyguanosine; 8-OHdG: 8-2′-hydroxydeoxyguanosine.

leads to the excessive production of ROS and reactive nitrogen species (RNS). The excessive production of ROS and RNS further reduces the activity of antioxidant enzymes, including SOD, GSH, CAT, GSH-Px, and PRX. The mitochondrial antioxidant system cannot control ROS-mediated oxidative stress damage, leading to the appearance of oxidative stress markers, such as malondialdehyde (MDA), 8-hydroxyguanosine, and 8-2′-hydroxydeoxyguanosine. This may be the main pathological mechanism of cardiomyocyte and vascular endothelial cell damage caused by different stress conditions.

Natural antioxidants have become key candidate drugs for MQC regulation to repair mitochondrial oxidative damage and improve the vulnerability of cardiomyocytes and endothelial cells after the destruction of the mitochondrial antioxidant system.

4.3. Natural Antioxidants That Protect Myocardial and Endothelial Cells through MQC under Oxidative Stress Conditions

4.3.1. Panax notoginseng Saponins. P. notoginseng saponins are active components in *P. notoginseng*, which is used as a natural medicinal herb, with strong antioxidant effects [48]. *P. notoginseng* saponins significantly reverse the downregula-

tion of forkhead box O3a and Mn-SOD, upregulate PGC-1α, LC3-II, and Beclin-1, regulate PGC-1α expression and mitophagy, reduce ROS-mediated oxidative damage, improve mitochondrial dysfunction caused by ageing and morphological changes in rat myocardium, and inhibit the apoptosis of cardiomyocytes [49].

4.3.2. Astragaloside IV. Astragaloside IV (AS-IV) is a natural antioxidant found in rhizomes of *Astragalus membranaceus*. It has various pharmacological activities, including antioxidation, anti-inflammation, and antitumour activities [50]. AS-IV significantly inhibits doxorubicin-induced ROS overproduction and release of lactate dehydrogenase (LDH), creatine kinase MB isoenzyme, and cytC, increases the activities of succinate dehydrogenase and ATP synthase, and restores ATP synthesis [51]. Further, AS-IV significantly inhibits mitochondrial apoptosis pathway activation by inducing phosphorylation of phosphatidylinositol 3-kinase (PI3K)/Akt, and the PI3K inhibitor LY294002 significantly inhibits the antiapoptotic effect of AS-IV. [51].

4.3.3. Cabbage Extract. Extract of *Brassica oleracea* L., a member of the cabbage family (Brassicaceae), has various pharmacological effects, and its antioxidant effect is exploited in the treatment of various CVDs [52]. Recent *in vitro*

TABLE 1: Effects of different stress conditions on MQC.

Stress condition	Impact on ROS	Effects on MQC of cardiomyocytes/endothelial cells	Natural antioxidants
Oxidative stress	Mitochondrial respiratory chain dysfunction leads to excessive ROS production	(1) Excessive mitochondrial fission (2) Mitochondrial Ca^{2+} homeostasis imbalance (3) Abnormal opening of mPTP (4) Mitochondrial respiratory dysfunction	(1) *P. notoginseng* saponins (2) Astragaloside IV (3) Cabbage extract (4) Mistletoe extracts (5) Tanshinone IIA (6) Ligustrazine (7) Resveratrol (8) Luteolin (9) Grape seed procyanidins
Hypoxia	Mitochondrial oxidative phosphorylation dysfunction leads to excessive ROS production	(1) Excessive mitochondrial fission (2) Mitochondrial Ca^{2+} homeostasis imbalance (3) Mitochondrial biosynthesis decreases (4) Loss of mitochondrial membrane potential	(1) Ginseng polysaccharide (2) Isoquercetin (3) Vitex flavonoids (4) Schisandrin/schisandrin B (5) Picroside (6) Anthocyanin
Ischaemia/reperfusion	Decoupling of the mitochondrial respiratory chain leading to excessive ROS production	(1) Mitochondrial Ca^{2+} homeostasis imbalance (2) Mitochondrial respiratory dysfunction (3) The level of mitochondrial ATP synthesis decreases	(1) *Panax quinquefolium* saponin (2) Ginsenoside RG5 (3) Lycopene (4) Cynomorium songaricum extract (5) Quercetin
High glucose	High levels of insulin interfere with NOX4 lead to excessive ROS production	(1) Excessive mitochondrial fission (2) Interference with the mitochondrial electron transport chain (3) Loss of mitochondrial membrane potential	(1) Naringin (2) Berberine (3) Cinnamaldehyde (4) Rosmarinic acid (5) Resveratrol (6) Pleurotus nebrodensis extract (7) Obtusin (8) Polydatin
Inflammation	Activated infiltrating immune cells and inflammatory resident cells lead to excessive ROS production	(1) mtDNA damage (2) Excessive mitochondrial fission	(1) Apigenin (2) Ilexonin A (3) Allicin (4) Melatonin
Lipid toxicity	Lipotoxicity increases the oxidation of fatty acids and leads to excessive ROS production	(1) Mitochondrial autophagy is inhibited (2) Loss of mitochondrial membrane potential (3) mtDNA damage	(1) Chlorogenic acid (2) Mangiferin (3) Anthocyanin (4) Melatonin

research has revealed that cabbage extract inhibits ROS production and increases SOD-1, catalase (CAT), and GPX activities. It inhibits the overactivation of MAPK proteins (ERK1/2, JNK, and P-38) and apoptosis of H9C2 cardiomyocytes without any cytotoxicity [53]. This suggests that cabbage extract can regulate MQC to reduce H_2O_2-induced oxidative stress injury in H9C2 cardiomyocytes and can be used in dietary replacement therapy to protect cardiomyocytes.

4.3.4. Homoeriodictyol. Homoeriodictyol is an effective active component of mistletoe that has many pharmacological effects, including improvement of microcirculation, antioxidation, and antiplatelet aggregation [54, 55]. Nuclear factor erythroid 2-related factor 2 (Nrf2) plays an important role in cytoprotection from ROS-induced oxidative damage. An *in vitro* study found that homoeriodictyol can upregulate the expression of Nrf2. It further corrects mitochondrial membrane potential (MMP) loss, inhibits the release of cytC and apoptosis-inducing factor, inhibits the overexpression of caspase-3/9 induced by H_2O_2, increases the expression of Bcl-2 and Bcl-xL, and suppresses apoptosis of endothelial cells under oxidative stress [56].

4.3.5. Tanshinone IIA. Tanshinone IIA is a lipid-soluble phenanthrenequinone compound in *Salvia miltiorrhiza* that has antibacterial, anti-inflammatory, antioxidant, and other pharmacological effects [57]. Tanshinone IIA protects bovine retinal endothelial cells from oxidative stress induced by methylglyoxal [22]. In endothelial cells, it significantly reduces abnormal mitochondria, increases the mRNA expression of *Mfn1* and *OPA1*, inhibits mitochondrial fusion, repairs oxidative stress injury, and increases cellular activity. siRNA-mediated silencing of *GLO1* inhibits the induction of mitochondrial fusion by tanshinone IIA. Thus, it was concluded that tanshinone IIA treatment regulates MQC by increasing the level of GLO1 and improves the vulnerability of endothelial cells under oxidative stress [22, 58].

4.3.6. Ligustrazine. Ligustrazine is an alkaloid in *Ligusticum chuanxiong*, Hort. It has strong antioxidant, antiplatelet aggregation, and microcirculation improvement effects [59]. Ligustrazine improves oxidative stress injury induced by high homocysteine, restores the MMP, inhibits the release of cytC from the mitochondria into the cytoplasm, reduces the level of LDH, inhibits apoptosis, and improves the cellular activity in human umbilical vein endothelial cells (HUVECs) [60].

4.3.7. Resveratrol. Resveratrol is a polyphenol compound abundant in peanut, *Polygonum cuspidatum*, and mulberry. It has strong antioxidant activity and is commonly used in the treatment of CVDs [61, 62]. Resveratrol protects against oxidative damage of MQC in endothelial cells. It activates TyrRS-PARP1 signalling and increases the expression of Mfn1, Mfn2, and OPA1. Moreover, it inhibits excessive mitochondrial fission, restores the MMP, and inhibits apoptosis in HUVECs. The regulatory effect of resveratrol on mitochondrial fission/fusion and its protective effect on endothelial cells were affected by siRNA interference of *TyrRS* and *PARP1*, indicating that resveratrol regulates mitochondrial fission/fusion through TyrRS-PARP1 signalling [63].

Resveratrol increases the enzyme activities of isocitrate dehydrogenase 2 (IDH2), GSH-Px, and manganese SOD (SOD2) via SIRT3 signalling, and upregulates the expression of *Atp6*, *CO1*, *ND2*, and *ND5* mediated by forkhead box O3a. It inhibits ROS production in mitochondria, enhances the activities of electron chain complex I and ATP synthesis, restores the MMP, and inhibits apoptosis in HUVECs. In addition, it enhances the phosphorylation of adenosine monophosphate-activated protein kinase (p-AMPK) and the expression of PGC-1α and SIRT3. MQC regulation and the protective effect of resveratrol on endothelial cells were inhibited by treatment with an AMPK inhibitor or siRNAs against *AMPK*, *PGC-1α*, and *SIRT3*. This suggests that resveratrol can reduce the oxidative damage of endothelial cells by regulating MQC, which may be mediated by the AMPK-PGC-1α-SIRT3 pathway [64].

4.3.8. Luteolin. Luteolin is a flavonoid compound widely found in pepper, chrysanthemum, and other plants, and has a strong antioxidant effect [65]. Luteolin protects endothelial cells from oxidative stress injury induced by H_2O_2 by regulating ROS-mediated p38MAPK/NF-κB and Ca^{2+}-induced mitochondrial apoptosis signalling. It strongly suppresses increases in intracellular Ca^{2+}, restores the MMP, regulates p53 phosphorylation and the Bcl-2/Bax ratio, and inhibits cytC release, caspase-3 overexpression, and apoptosis in endothelial cells [66].

4.3.9. Grape Seed Proanthocyanidins. Grape seed proanthocyanidins are extracted from the seeds of grapes (*Vitis vinifera*). As natural polyphenol compounds and natural antioxidants, grape seed proanthocyanidins scavenge free radicals and have antioxidant and anti-inflammatory effects [67, 68]. Grape seed proanthocyanidins inhibit excessive ROS production, restore the MMP, improve the respiratory function of mitochondria, reduce the level of 8-hydroxydeoxyguanosine (8-OHdG), enhance endothelial nitric oxide synthase (eNOS) and VE-cadherin expression, and inhibit apoptosis in endothelial cells. In HUVECs, they improve oxidative stress injury induced by indole sulphate [69].

5. Hypoxia

Hypoxia is a pathological process comprising abnormal changes in tissue metabolism, function, and morphology due to insufficient O_2 supply or respiratory dysfunction [70]. Hypoxia is a common mechanism in the development of various diseases. Hypoxia in the brain and heart is also the primary cause of death. O_2 plays an important role in the regulation of metabolism, energy production, and internal homeostasis [71]. If tissues, organs, and cells cannot adapt to the lack of O_2 supply, excessive ROS production and oxidative stress damage may occur under hypoxia, which leads to MQC imbalance, cell apoptosis, and tissue necrosis [72].

5.1. Effects of Hypoxia on ROS. Mitochondria are very sensitive to the O_2 concentration in the living environment. The balance between O_2 supply and consumption in the body is the physiological basis for maintaining normal mitochondrial respiratory chain function. In mitochondria, long-term insufficient O_2 supply will directly affect O_2 exchange, transport, and release in tissues, resulting in intracellular hypoxia [73].

Under hypoxia, there is insufficient O_2 to serve as an electron acceptor in oxidative phosphorylation, and thus, free electrons increase and excessive ROS are generated. ROS accumulation can lead to oxidative damage of macromolecules and abnormal mPTP opening [74]. Oxidative phosphorylation dysfunction under hypoxia can also lead to mitochondrial respiratory chain damage [75, 76]. Excessive mtROS production due to respiratory chain injury can induce cell signal transduction pathways and cause lipid peroxidation of the cell membrane, resulting in apoptosis and homeostasis imbalance [77]. Myocardial myofibrillar protein oxidation by ROS suppresses cardiac systolic and diastolic function, resulting in the decline of cardiac function [78, 79].

5.2. Effect of Hypoxia on MQC. Hypoxia affects not only mitochondrial respiratory chain function but also the morphology and quality of mitochondria, and induces functional and morphological changes in the peripheral mitochondria. It also causes damage to lipids, proteins, and DNA, resulting

in MMP loss, cytC release, and caspase-3/9 activation, thus increasing the vulnerability of cardiomyocytes and endothelial cells [80].

ROS directly affect mitochondrial Ca^{2+} homeostasis, lead to dysfunction of the mitochondrial Ca^{2+} uniporter, and induce mitochondrial Ca^{2+} overload [81]. Mitochondrial Ca^{2+} transport, mPTP opening, and caspase-3/7/8/9 activity were significantly decreased after siRNA treatment. The imbalance of MQC caused by H/R is mainly related to the dysregulation of the mitochondrial Ca^{2+} uniporter [82].

MQC is determined by mitochondrial fission/fusion balance, mitophagy, mitochondrial respiratory function, and mitochondrial biosynthesis. These processes are enhanced by OPA1 knockout and attenuated by OPA1 overexpression [83]. The antiapoptotic effect of hypoxic postconditioning cannot be attenuated only by SOD and CAT in the mitochondrial antioxidant system [83]. Therefore, it is necessary to find natural antioxidants that can regulate MQC to improve cell vulnerability under hypoxia.

5.3. Natural Antioxidants That Protect Myocardial and Endothelial Cells through MQC under Hypoxia

5.3.1. Ginseng Polysaccharide. Ginseng polysaccharide is an acidic polysaccharide present in *Panax ginseng*. As a natural antioxidant, ginseng polysaccharide has good anti-inflammatory, antitumour, and antithrombotic effects [84, 85]. It is effective in protecting myocardial cells from H/R injury. It restores mitochondrial energy metabolism and the MMP, blocks mitochondrial cytC release, increases ATP production, and regulates the O_2 consumption rate. It also induces glucocorticoid receptor and oestrogen receptor expression activates the reperfusion injury salvage kinase (RISK) pathway, increases the production of nitric oxide by increasing eNOS and iNOS expression, and protects endothelial cells [85].

5.3.2. Isoquercetin. Isoquercetin is a flavonoid isolated from the seed pod of *Cercis canadensis* and exists in plants such as *Eucommia ulmoides* Oliv. and mulberry leaf. The pharmacological activities of many plants are related to isoquercetin [86, 87]. Isoquercetin has a strong antioxidant effect through which it inhibits ROS production in mitochondria, improves energy metabolism in mitochondria, inhibits cytC release and apoptosis, and protects myocardial cells from damage induced by hypoxia-induced oxidative stress [88].

5.3.3. Bauhinia championii Flavone. *Bauhinia championii* flavone scavenges free radicals and has an antiarrhythmic effect [89, 90]. It improves mitochondrial dysfunction, alleviates H9C2 cardiomyocyte apoptosis induced by H/R, significantly inhibits ROS production, increases ATP synthesis, and inhibits abnormal mPTP opening. In addition, it inhibits the mitochondrial translocation of Bax, cytC release, and caspase-3 expression, increases PI3K and Akt phosphorylation, regulates the Bcl-2/Bax ratio, and inhibits H/R-induced apoptosis in cardiomyocytes. LY294002, a specific inhibitor of PI3K, partially reversed the regulatory effects of *B. championii* flavone on cardiomyocytes and MQC, suggesting that the flavone improves mitochondrial function through PI3K/Akt signalling, thus reducing H/R-induced cardiomyocyte apoptosis [91].

5.3.4. Schisandrin/Schisandrin B. Schisandrin and schisandrin B are active lignoid substances extracted from *Schisandra chinensis*. They have anti-inflammatory, antioxidation, antitumour, and immune-regulatory effects [92, 93]. Both schisandrin and schisandrin B protect H9C2 cardiomyocytes from apoptosis induced by H/R by inhibiting abnormal mPTP opening and cytC release, increasing the cleavage of caspase-3 and poly ADP ribose polymerase, and enhancing GSH expression [94].

5.3.5. Picroside. Picroside is an active component in *Picrorhiza* sp. that has strong anti-inflammatory and antioxidant effects [95, 96]. Picroside significantly inhibits ROS production in mitochondria, inhibits mPTP opening, increases the MMP, inhibits cytC release from the mitochondria downregulates caspase-3, and suppresses cardiomyocyte apoptosis induced by H/R in cardiomyocytes, suggesting that picroside improves cardiomyocyte activity by reducing ROS production [97].

5.3.6. Anthocyanins. Anthocyanins are water-soluble pigments that are widely present in plant vacuoles and belong to the flavonoid compounds. They are derived from chlorophyll and have anti-inflammatory, antioxidant, and antiallergic effects [98, 99]. As natural antioxidants, anthocyanins improve oxidative stress injury induced by peroxynitrite, restore the MMP, inhibit caspase-3/9 expression and Bax transport to the nucleus, and improve the function of endothelial cells [100].

6. Ischaemia/Reperfusion

Ischaemia-induced myocardial, vascular, or other organ tissue damage is the main cause of cardiovascular and cerebrovascular diseases, such as coronary atherosclerosis, myocardial infarction, and stroke [101]. In the process of I/R, the main factor of tissue damage is not ischaemia itself, but the ROS-induced oxidative stress damage in cells (such as myocardial cells and vascular endothelial cells) after the recovery of blood supply, leading to tissue damage or necrosis [102]. During I/R, ROS-induced mitochondrial Ca^{2+} imbalance, mitochondrial respiratory chain dysfunction, and energy metabolism disorders are the main causes of increased vulnerability of myocardial cells and endothelial cells [103].

6.1. Effect of I/R on mtROS. As highly dynamic organelles, mitochondria constantly undergo fusion and fission, and the balance between these processes plays an important role in cell homeostasis [104]. The fusion and fission of mitochondria are mediated by fusion and cleavage proteins. During I/R, ROS-mediated oxidative stress leads to imbalances in mitochondrial fusion/mitogen protein expression and post-translational modification regulation, resulting in abnormal mitochondrial fusion/fission and MQC imbalance [105].

When mitochondrial dysfunction occurs, the defence mechanism of the mitochondrial antioxidant system is also affected. ROS production exceeds the scavenging capacity

of the mitochondrial antioxidant system, which results in oxidative stress damage [106]. The explosive increase in ROS may be caused by respiratory chain decoupling. I/R induces the activities of nicotinamide adenine dinucleotide phosphate oxidase (NOX), xanthine oxidase, and NOS, enhancing ROS production [107]. Excessive ROS trigger cell apoptosis and aggravate tissue damage by inducing mPTP opening, activating various enzymes and transcription factors, and stimulating inflammatory reactions and mtDNA damage [108]. Therefore, the imbalance of MQC caused by ROS plays an important role in the tissue damage caused by I/R.

6.2. Effects of I/R on MQC. I/R affects MQC in various ways. In the ischaemic state, aerobic oxidation is inhibited, which leads to a serious shortage of ATP synthesis. Consequently, energy metabolism in the heart is dominated by anaerobic glycolysis [109]. Anaerobic glycolysis produces a large amount of lactic acid, resulting in a decrease in Na^+/K^+-ATPase activity and an increase in intracellular Na^+. The Na^+/Ca^{2+} pump is then activated and the Ca^{2+} concentration in the cytoplasm increases rapidly. To maintain intracellular Ca^{2+} homeostasis, mitochondria import excess Ca^{2+} from the cytoplasm, which results in an overload of mitochondrial Ca^{2+} and changes in membrane permeability, leading to mitochondrial swelling and irreversible damage [110, 111]. A high concentration of Ca^{2+} also enhances the ATP hydrolysis activity of F0F1 ATPase and inhibits the synthesis of mitochondrial ATP through Ca^{2+} binding to ATPase inhibitor protein [112].

Under the condition of reperfusion, cells reabsorb O_2 from the blood, which leads to explosive ROS formation and serious protein and lipid peroxidation, resulting in a decline in mitochondrial cytC oxidase and ATP synthase activities, thus affecting respiratory chain function [113]. ROS also activate phospholipase, degrade membrane phospholipids, and damage the mitochondrial structure and respiratory chain function [114]. In conclusion, early correction of MQC imbalance and inhibition of ROS-mediated oxidative stress injury are important ways to improve the vulnerability of myocardial cells and endothelial cells under I/R.

6.3. Natural Antioxidants That Protect Myocardial and Endothelial Cells through MQC during I/R

6.3.1. Panax quinquefolium Saponin. Abnormal mPTP opening is an important mechanism of myocardial injury induced by I/R [114]. *P. quinquefolium* saponin is the most abundant compound in *P. quinquefolium*. It reduces blood lipids, blood pressure, and lipid peroxidation, and is an effective natural antioxidant [115]. *P. quinquefolium* saponin improves the vulnerability of cardiomyocytes in the I/R state by regulating MQC. It effectively inhibits mPTP opening, regulates MMP depolarisation, increases the Bcl-2/Bax ratio, inhibits the translocation of mitochondrial cytC to the cytoplasm, protects mitochondrial structure, inhibits ROS production and caspase-9/3 expression, and suppresses apoptosis in cardiomyocytes under I/R injury [116].

6.3.2. Ginsenoside Rg5. Ginsenoside Rg5 is a sterol present in ginseng with antioxidant activity [117]. Rg5 inhibits fatty acid oxidation, improves pyruvate dehydrogenase activity, and prevents cell acidification. Rg5 activates Akt signalling to regulate Drp-1, promotes mitochondrial hexokinase- (HK-) II binding, increases the permeability of cardiomyocytes to ATP/5, improves mitochondrial respiratory function and hypoxia tolerance, and improves the vulnerability of myocardial cells to ischaemia [118].

6.3.3. Lycopene. Lycopene is an antioxidant that exists mainly in mature fruits of tomato (*Solanum lycopersicum*). It is one of the strongest natural antioxidants found in plants. Lycopene is far more effective in scavenging free radicals than other carotenoids and vitamin E [119, 120]. I/R injury increases the 8-OHdG content in cardiomyocytes, decreases mtDNA transcription, and results in mitochondrial energy metabolism disorder. Lycopene suppresses mtROS production, restores the protein expression of a key activator of mtDNA transcription (TFAM), and inhibits 8-OHdG expression, thus protecting cardiomyocytes from oxidative stress induced by I/R [121].

6.3.4. Cynomorium songaricum Extract. C. songaricum Rupr. is a perennial fleshy parasitic herb. It contains flavonoids, triterpenoids, tannins, steroids, and organic acids. *C. songaricum* extract has free radical-scavenging, antihypoxia, and immunoregulatory effects [122, 123]. *In vivo* and *in vitro* studies have shown that *C. songaricum* extract protects H9C2 cells and rat myocardium by enhancing mitochondrial ATP production and the glutathione redox cycle, regulating MQC, and inhibiting LDH and caspase-3 expression [124].

6.3.5. Quercetin. Quercetin is an antioxidant that exists in Berberidaceae and *Hypericum andraeanum* and has anti-inflammatory and immunomodulatory effects. It reduces blood pressure and improves capillary elasticity [125, 126]. Ang-II decreases the activity of HUVECs in a concentration-dependent manner. Quercetin inhibits Ang-II-induced damage to HUVECs in a concentration- and time-dependent manner. Quercetin restores the MMP, inhibits the translocation of cytC, and upregulates Bax and Bcl-2 and inhibits caspase-3/9 activation, thus inhibiting apoptosis in HUVECs [127].

7. High Glucose

With the increase in energy consumption per capita, lipid metabolism disorders caused by high glucose and CVD caused by oxidative stress are on the rise and have been widely studied [128]. These disorders are mainly due to MQC imbalance caused by hyperglycaemia and cardiomyocyte and vascular endothelial cell dysfunctions, including oxidative stress, increased glycation end products, coagulation, and fibrinolysis system dysfunction, which cause the accumulation of vascular substances, vascular stenosis, and atherosclerosis [129, 130]. Therefore, CVDs associated with diabetes mellitus are a major cause of death, which is closely related to high glucose-mediated MQC imbalance and cell dysfunction [131].

7.1. High Glucose- and ROS-Mediated Oxidative Stress.

High glucose-induced vascular injury involves the polyol pathway, changes in redox status, an increase in diacylglycerol formation, and the accumulation of nonenzymatic glycation end products [132]. High glucose levels regulate multiple signalling pathways to induce apoptosis in cardiomyocytes and endothelial cells, mainly via ROS-mediated oxidative stress [133].

When blood glucose levels rise, insulin secretion from β cells in the pancreatic islets into the blood increases. Under normal physiological conditions, the surrounding tissues respond to insulin by increasing the expression of glucose transporters on the plasma membrane. However, consistent high glucose levels and consequent long-term high insulin levels will lead to insulin resistance [134]. High levels of insulin interfere with NOX4 signal transduction and enhance ROS production [135]. Thus, insulin resistance induced by high glucose indirectly leads to excessive ROS production and oxidative stress damage, which may be why high glucose levels can lead to type 2 diabetes mellitus complicated by CVD.

7.2. Effects of High Glucose on MQC in Cardiomyocytes and Endothelial Cells.

Enhanced ROS in response to high glucose interferes with the mitochondrial electron transport chain, which increases the oxidation of coenzyme Q, thus forming peroxides. These peroxides react with nitrous oxide to form peroxynitrite ($ONOO^-$), which leads to mitochondrial protein dysfunction, lipid oxidation, and DNA modification, eventually leading to cell apoptosis [136].

As the centre of glucose metabolism, mitochondria are likely to be affected by diabetes-related metabolic damage. Although the reasons for the increased risk of heart failure are multifactorial, high glucose-induced mitochondrial dysfunction in cardiomyocytes and endothelial cells plays a key role [137, 138]. Mitochondrial energy metabolism and dynamics defects, oxidative stress, Ca^{2+} homeostasis, and mitochondrion-induced cell death have been observed in diabetic myocardial mitochondria. Mitochondrial dysfunction seems to be the main cause of arrhythmia in diabetes mellitus [139].

In HUVECs treated with high glucose, the expression of Tom22 and OXPHOS was impaired and mitochondrial fusion was decreased, and deletion of Tom22 resulted in a decrease in mitochondrial fusion and ATP production and an increase in apoptosis in HUVECs [24]. Rotenone, an inhibitor of mitochondrial electron transport, suppresses excess ROS production in streptozotocin-induced diabetic rats that exhibited mitochondrial damage, loss of MMP, as well as increased caspase-3/9 activities and apoptosis [140]. High glucose levels induce apoptosis and MMP loss in HUVECs by enhancing Bax expression and suppressing Bcl-2 expression. Cells exposed to high levels of sugar release cytC in excess [141]. Therefore, regulation of the MQC imbalance induced by high glucose is a key target to improve the vulnerability of cardiomyocytes and endothelial cells in a high-glucose environment.

7.3. Natural Antioxidants That Protect Myocardial and Endothelial Cells through MQC under High-Glucose Conditions

7.3.1. Naringin.

Naringin is a dihydroflavonoid extracted from the dried outer peel of *Citrus grandis* (L.) Osbeck and *Citrus paradisi* Macfad. [142]. It has anti-inflammatory, antiviral, and antithrombotic effects [143]. Naringin significantly inhibits p38 and p53 phosphorylation induced by high glucose, restores the MMP, regulates Bax and Bak expression, prevents mitochondrial cytC release, increases Bcl-2 expression, and inhibits caspase-3/8/9 activation and apoptosis in H9C2 cells [144].

7.3.2. Berberine.

Berberine is a quaternary ammonium alkaloid in *Coptis chinensis*. It has various pharmacological activities, including antioxidative, hypoglycaemic, blood lipid-regulatory, blood pressure-lowering, and antiarrhythmia effects [145, 146]. Cardiomyocyte hypertrophy induced by type 2 diabetes mellitus is closely related to mitochondrial dysfunction. Berberine significantly improves mitochondrial fusion/fission imbalance and mitochondrial energy metabolism in H9C2 cells. It increases the level of mitophagy induced by high glucose levels by activating AMPK signalling, and promotes mitochondrial biosynthesis in H9C2 cells and improves the vulnerability of cardiomyocytes to high glucose [147].

7.3.3. Cinnamaldehyde.

Cinnamaldehyde is an organic aldehyde found in *Cinnamomum cassia*. It has antioxidant, vasodilatory, and blood pressure-lowering effects [148]. Transient receptor potential cation channel subfamily A member 1 (TRPA1) has an antioxidant effect. Cinnamaldehyde significantly reduces high glucose-induced ROS production, upregulation of nitrotyrosine, P22, and P47, and apoptosis in H9C2 cardiomyocytes. It upregulates Nrf2 and its target genes, heme oxygenase-1 (*HO-1*), *GPX-1*, and quinone oxidoreductase-1 (*NQO-1*). Hc030031, a TRPA1 inhibitor, abolishes the protective effect of cinnamaldehyde on cardiomyocytes. Cinnamaldehyde significantly reduces the levels of nitrotyrosine, fibrosis, and cardiomyocyte hypertrophy in rats and increased the expression of HO-1, GPX-1, NQO-1, and CAT in the myocardium of diabetic mice. Thus, it seems to protect cardiomyocytes against oxidative stress injury induced by high glucose through the TRPA1/Nrf2 pathway [149].

7.3.4. Rosmarinic Acid.

Rosmarinic acid is a water-soluble natural phenolic acid isolated from rosemary (*Rosmarinus officinalis*). It mainly exists in Labiatae, Arnebiaceae, and Cucurbitaceae. It is a natural antioxidant [150, 151]. Rosmarinic acid inhibits ROS production and abnormal mPTP activation induced by high glucose, as well as cytC release and caspase-3 activation. It protects H9C2 cells against apoptosis induced by high glucose. It increases STAT3 phosphorylation. siRNA-mediated knockdown of STAT3 inhibits the protective effect of rosmarinic acid on high glucose-induced apoptosis, indicating that rosmarinic acid improves mitochondrial function and inhibits cardiomyocyte apoptosis induced by high glucose through the STAT3 pathway [152].

7.3.5. Resveratrol.

Resveratrol inhibits high glucose-induced mtROS production in human coronary artery endothelial cells via the intracellular target protein deacetylase silent information regulator (SIRT)2/SIRT1 [153]. In endothelial cells, SIRT1 overexpression attenuates mtROS production and overexpression of RSV and SIRT1 significantly reduces

the level of H_2O_2 and increased Mn-SOD and GSH expression in a concentration-dependent manner. Thus, resveratrol reduces mtROS production by activating SIRT1 and restoring the antioxidant defence mechanism of mitochondria, which implies the potential of new therapeutic methods targeting endothelial mitochondria in metabolic diseases [154].

7.3.6. Pleurotus nebrodensis Extract.

The fungus *P. nebrodensis* contains polysaccharides, vitamins, and other physiologically active substances that can regulate the physiological balance and enhance immune function in the human body [155]. *P. nebrodensis* extract improves high glucose-induced mitochondrial dysfunction in EA.hy926 endothelial cells. It inhibits the increase in electron transport chain complex I activity and decrease in ROS production induced by hyperglycaemia. It suppresses the oxidative damage of lipids and proteins, regulates imbalanced SOD and CAT activities, reduces the level of nitric oxide, restores mitochondrial function, and improves the vulnerability of endothelial cells to hyperglycaemia [153].

7.3.7. Obtusin.

Obtusin is an anthraquinone compound with antioxidant activity extracted from *Cassia obtusifolia* [156]. Obtusin inhibits high glucose-induced mitochondrial apoptosis in HUVECs and high glucose-induced ROS production. It decreases the MDA content and restores the activities of mitochondrial complexes I/III, CAT, and SOD. Obtusin restores the MMP and prevents the release of Omi/HtrA2 into the cytoplasm, thus protecting endothelial cells from apoptosis [157].

7.3.8. Polydatin.

Polydatin is a small-molecule compound in *Polygonum cuspidatum*, which is used as a medicinal herb. It has many biological functions, including antioxidation, anti-inflammation, and renal protection [158]. Methylglyoxal, an active metabolite of glucose, induces apoptosis of vascular cells in diabetic complications. Polydatin significantly inhibits ROS production induced by methylglyoxal, restores the MMP and mitochondrial morphological changes, and increases Akt phosphorylation, and it inhibits methylglyoxal-induced apoptosis of HUVECs. Polydatin improves the vulnerability of methylglyoxal-induced HUVECs at least in part by inhibiting oxidative stress, maintaining the mitochondrial function, and activating Akt signalling [159].

8. Inflammation

Inflammation is a defence response of tissues, including blood vessels, to injury and a physiological homeostatic response [160]. Normal inflammation can eliminate invasive organisms and foreign stimuli; however, excessive inflammation can damage cardiomyocytes and endothelial cells, leading to the occurrence of CVDs, such as myocarditis, atherosclerosis, acute myocardial infarction, vasculitis, and heart failure [161]. Different types of inflammatory reactions are involved in the development of CVDs. These inflammatory reactions are often related to ROS-mediated oxidative stress. Moreover, with the onset and development of inflammation, activated infiltrating immune cells and inflammatory resident cells will gradually increase the demand for mito-chondrial energy, which will lead to hypoxia, mitochondrial energy metabolism dysfunction, and ROS production [162]. Furthermore, MQC imbalance and increased ROS levels lead to serious oxidative damage and promote the onset of inflammation.

8.1. Effect of Inflammation on ROS.

As important intracellular messengers, ROS can activate various inflammatory signal transduction pathways. Oxidative stress can lead to MQC imbalance through direct cytotoxicity and promote the onset and development of local inflammatory responses [163]. Oxidative stress and inflammation are interdependent, especially in mitochondria. Excessive ROS production at inflammatory sites can lead to oxidative stress damage to mitochondria. Oxidative stress products can enhance inflammatory factor responses, and there are interactions between them. Mitochondria may be the "Trojan horse" of inflammation while maintaining the basic cellular functions [164].

Abnormal mitochondrial fission in endothelial cells can also lead to inflammation and oxidative stress. Inflammation may be inhibited via the regulation of the mitochondrial fission/fusion balance. In normal physiology, Drp-1 plays a beneficial role in maintaining the fission/fusion balance in endothelial cells. However, under inflammation, Drp-1 increases, resulting in excessive mitochondrial fission, which leads to chronic inflammation. When mitochondria are damaged by stress or bacterial toxins, NLRP3 is also activated, leading to an inflammatory state [165, 166]. Zhong et al. found that damaged mitochondria activate NLRP3 and NLRP3 activation which was inhibited when mitochondrial autophagy cleared abnormal mitochondria and damaged proteins [167]. mtROS can also induce NLRP3 activation. The oxidative effect of ROS on mtDNA during NLRP3 activation leads to a partial inflammatory potential of free, circulating mtDNA. Thus, MQC imbalance plays an important regulatory role in cell injury in the inflammatory state.

8.2. Effect of Inflammation on MQC.

mtDNA is indispensable for energy metabolism and the regulation of cell death. ROS can damage mtDNA [168]. In the process of inflammation, ROS affect the mitochondrial structure, dynamics, and genomic stability, resulting in mtDNA mutation and mitochondrial dysfunction, and increasing the release of proinflammatory factors [169, 170]. Tumour necrosis factor- (TNF-) α affects the stability of mtDNA and mitochondrial function [171]. Damaged mitochondria release mtDNA into the cytoplasm, which causes inflammation, and mtDNA is released into the circulation after tissue inflammation. As an important factor of inflammation and the immune response, the increase in circulating mtDNA and the upregulation of TLR9 expression participate in experimental autoimmune myocarditis and TLR4 activation-mediated myocarditis [171].

Treatments with interleukin-6 (IL-6) and TNF-α lead to Drp-1 phosphorylation and mitochondrial translocation, resulting in abnormal mitochondrial fission in H9C2 cardiomyocytes [172]. Therefore, mitochondrial dysfunction is usually associated with GTPase Drp-1-mediated mitochondrial mitosis. Interestingly, inhibition of NF-κB inflammatory signalling indirectly inhibits endothelial mitochondrial

fission; thus, NF-κB seems to be a signal of inflammatory mitochondrial fission in endothelial cells. In addition, salicylate seems to maintain the mitochondrion fission/fusion balance against TNF-α by inhibiting NF-κB [172]. Thus, the NF-κB cascade and mitochondrion fission pathway regulate MQC and endothelial cell inflammatory responses in an interdependent manner and effective MQC-regulatory drugs with anti-inflammatory and antioxidant actions are urgently needed to protect myocardial cells and endothelial cells.

8.3. Natural Antioxidants That Protect Myocardial and Endothelial Cells through MQC in the Inflammatory State

8.3.1. Apigenin. Apigenin is a flavonoid antioxidant that exists mainly in plants of the families Verbenaceae and Selaginellaceae. It has antiviral and anti-inflammatory effects and is used for treating an HIV infection. Compared with other flavonoids, apigenin has low toxicity [173].

Inflammation is characterised by increased ROS production, dysfunction of mitochondrial energy metabolism, and abnormal immune function, which can lead to the occurrence of diseases. Apigenin can inhibit ROS production, restore the activity of mitochondrial complex I, stabilise mitochondrial function during inflammation, and reduce caspase-3 activity to suppress lipopolysaccharide- (LPS-) induced apoptosis in endothelial cells [174]. Apigenin protects mice against myocardial infarction. It regulates mitophagy via mir-103-1-5p and parkin, suppresses apoptosis in myocardial cells, and effectively reduces the myocardial infarction area [175].

8.3.2. Ilexonin A. Ilexonin A is a pentacyclic triterpenoid isolated from the dried leaf of *Ilex latifolia* that has strong antioxidant and anti-inflammatory activities [172]. Ilexonin A activates Nrf2, increases the expression of proteosome 20S subunit beta 5 (PSMB5) and NO production, inhibits ROS production and the production of inflammatory cytokines induced by palmitate, inhibits Drp-1 expression and mitochondrial overfission, and protects endothelial cells. *Nrf2* knockout inhibits the induction of PSMB5 expression and eliminates the inhibition of ROS production and mitochondrial fission by ilexonin A. Thus, ilexonin A promotes PSMB5 expression in an Nrf2-dependent manner, thus inhibiting mitochondrial overfission to protect endothelial cell function in the inflammatory state [176].

8.3.3. Allicin. Allicin is an organic sulphur-containing compound that mainly exists in the bulbs of onion and other Alliaceae plants. To date, two types of organic sulphur compounds have been isolated from garlic, which have shown antioxidative effects, plasma cholesterol-lowering, blood pressure-lowering, and platelet activity-inhibiting effects [177, 178]. As a vascular protective agent, allicin can protect endothelial cells by regulating MQC.

Allicin can significantly inhibit LPS-induced oxidative stress injury and inflammatory reactions in HUVECs. Allicin inhibits ROS and LDH overproduction, reduces lipid peroxidation, and improves antioxidant enzyme activities in the mitochondria. It restores the MMP, inhibits cytC release, and promotes ATP synthesis. It inhibits the expression of

TNF-α and IL-8 and the adhesion of endothelial cells and increases the apoptosis of HUVECs induced by LPS. Allicin increases the expression of LXR-α and Nrf2 signalling in a dose-dependent manner. The effects of allicin on MQC regulation and endothelial cell protection are inhibited by siRNA-mediated knockdown of LXR-α [179], suggesting that the protective mechanism of allicin on endothelial cells is mediated by LXR-α.

In vivo, allicin suppresses the accumulation of interstitial collagen and type I/III collagens, ROS levels, protein carbonylation, and thiobarbituric acid-reactive substances, and increases GPX activity. In addition, allicin significantly increases the mRNA and protein levels of Nrf2, NQO-1, and γ-GCS, and prevents the occurrence of myocardial remodelling and the development of myocardial hypertrophy [180].

8.3.4. Melatonin. Melatonin is an amine hormone mainly produced in the pineal gland of mammals and humans, and it also exists in many plants. Melatonin regulates the sleep-wake cycle and has strong antioxidant activity [181]. Melatonin has different effects on inflammation and mitochondrial function in endothelial cells. It inhibits abnormal NF-κB activation, restores the MMP, and increases the expression of mitochondrial glutathione. It inhibits the expression of IL-6 and IL-8 and LPS-induced inflammatory injury in endothelial cells [182].

9. Lipid Toxicity

Lipid toxicity occurs when lipids accumulate in cells and tissues, and the cells and tissues cannot fully metabolise or store them. Lipid toxicity is closely related to diabetes, atherosclerosis, coronary heart disease, and heart failure [183]. In normal cells, fatty acid synthesis, transportation, and utilisation are in dynamic equilibrium. Free fatty acids (FFAs) can be produced by biochemical synthesis or hydrolysis of triglycerides and phospholipids. FFAs are important components of the cell membrane that can produce energy or signalling molecules through the process of β-oxidation, and participate in the mechanism of posttranslational protein modification and posttranscriptional protein regulation [184]. When the demand for FFAs increases, FFAs can enter cells via protein or nonprotein carrier pathways. Excess FFAs can be converted into triglycerides [185]. Adipocytes can store a large number of triglycerides, whereas nonadipocytes, such as myocardial cells and endothelial cells, can store only a limited amount. If triglycerides are overloaded, they will be dysfunctional, and apoptosis and necrosis will occur [186]. Lipid toxicity damages cardiomyocytes and endothelial cells mainly via oxidative stress.

9.1. Lipid Toxicity and OS. Lipid toxicity is closely related to oxidative stress. For example, α/β-polyunsaturated fatty aldehydes produced by oxidative stress participate in the modification of proteins, DNA, and RNA and important pathways of oxidative stress damage, including the unfolded protein response, endoplasmic reticulum stress, and DNA damage. In addition, although cellular and mitochondrial antioxidant systems can limit the production of some lipids,

α/β-polyunsaturated fatty aldehydes cause serious mitochondrial energy metabolism dysfunction, eventually leading to MQC imbalance and apoptosis [187, 188].

Lipid peroxidation is the result of a hydroxyl radical attack of phospholipids and triglycerides. Mitochondria are considered the main source of H_2O_2. Superoxide anions are produced by complexes I and III and can be converted by SOD to H_2O_2, which can give rise to hydroxyl radicals. Triglycerides are the main target of hydroxyl radical-mediated attack and lipid-free radical formation. Lipid-free radicals are rapidly oxidised, resulting in lipid peroxidation of the acyl chain, which eventually leads to mitochondrial metabolic dysfunction and increases cell vulnerability [189, 190].

Lipid toxicity and high glucose often cooccur in diabetes mellitus complicated with CVD. FFAs can escape from adipocytes into the blood and accumulate heterotopically in nonadipocytes, causing lipid toxicity [191, 192]. Triglycerides can reduce the biological effects of insulin in muscle and liver, and cause insulin resistance. Triglyceride accumulation in pancreatic islets can lead to functional damage of β cells and dysfunction of insulin secretion stimulated by glucose. Thus, lipid toxicity may reduce glucose oxidation by increasing fatty acid oxidation, which leads to ROS overproduction and increased vulnerability of cardiomyocytes and endothelial cells [191]. Long-term mitochondrial or cellular metabolic disorders eventually lead to type 2 diabetes. Constitutive hyperglycaemia can also lead to increased FFA metabolism, and FFAs reduce endothelium-derived myocardial vasodilation, leading to a series of CVDs [193, 194].

9.2. Lipid Toxicity and MQC.
The regulation of lipid metabolism is closely related to MQC in cardiomyocytes and endothelial cells [195]. In response to LPS, TNF-α and TFAM levels, nuclear accumulation of Nrf1, and PGC-1 expression are increased, mitophagy is stimulated, and the expression of withering markers is increased in adult rat cardiomyocytes [196]. Neonatal rat cardiomyocytes cultured in high-fat condition produce excessive ROS, including H_2O_2, causing abnormal MMP, resulting in myocardial cell damage. Hyperlipidaemia affects the MMP and ROS production of H9C2 cardiomyocytes [197].

Low-density lipoprotein (LDL), a lipoprotein particle that carries cholesterol into peripheral tissue cells, can be oxidised into oxidised low-density lipoprotein (ox-LDL). When ox-LDL is in excess, the cholesterol it carries accumulates on the arterial wall, which is the main cause of atherosclerosis [198]. Ox-LDL stimulates inflammatory activation and MQC imbalance in human artery endothelial cells [199]. It induces high mRNA expression of *TNF-α*, *IL-6*, and *IL-1β*, increases mtROS production, and destroys mtDNA and the MMP in these cells. In addition, it mediates TLR9/NF-κB and NLRP3/caspase-1 activation, which leads to an increase in apoptosis in endothelial cells [200]. Therefore, it is necessary to find effective natural drugs to regulate oxidative stress and MQC.

9.3. Natural Antioxidants That Protect Myocardial and Endothelial Cells through MQC in Lipid Toxicity

9.3.1. Chlorogenic Acid.
Chlorogenic acid is a phenolic component in *Flos lonicerae* that has higher antioxidant capacity than caffeic acid. It has anti-inflammatory, hypolipidemic, and free radical-scavenging effects [201–203]. Chlorogenic acid increases SIRT1 deacetylase activity and AMPK/PGC-1 expression and alleviates oxidative stress injury and mitochondrial dysfunction induced by ox-LDL. Silencing of *SIRT1*, *AMPK*, and *PGC-1* reduces the protective effect of chlorogenic acid on endothelial cells, indicating that chlorogenic acid alleviates ox-LDL-induced mitochondrial dysfunction and improves the vulnerability of endothelial cells by activating SIRT1 and regulating PGC-1 signalling [204].

9.3.2. Mangiferin.
Mangiferin is a polyphenol compound with a xanthone skeleton that is mainly found in the seeds, leaves, flowers, and fruits of plants of the family Lacqueraceae [205]. Mangiferin has antioxidant, anti-inflammatory, and immunomodulatory effects [206, 207]. It has a certain protective effect on mitochondrial HK-II in vascular endothelial cells. HK-II also has an anticell death effect. In vascular endothelial cells, stimulation with the saturated fatty acid palmitate causes HK-II release from the mitochondria due to cell acidification. Mangiferin increases the activity of pyruvate dehydrogenase, reduces the accumulation of lactic acid, promotes Akt phosphorylation of HK-II, and prevents HK-II shedding from the mitochondria. Mangiferin also prevents mPTP opening, restores the MMP, and suppresses apoptosis, thus protecting vascular endothelial cells [208].

9.3.3. Delphinidin-3-Glucoside.
Delphinidin-3-glucoside inhibits LDL oxidation and platelet aggregation [209]. It reduces the ROS and superoxide anion production and mitochondrial dysfunction induced by ox-LDL, restores the MMP, and inhibits abnormal mPTP opening and the proliferation and apoptosis of primary HUVECs induced by ox-LDL. *In vitro* and *in vivo* studies have shown that delphinidin-3-glucoside can enter endothelial cells in a temperature-, concentration-, and time-dependent manner through sodium-dependent glucose transporter (SGLT1). It decreases apoptosis-related caspase-3 and Bax expression and increases Bcl-2 expression. siRNA-mediated knockdown of *SGLT1* or phloridzin treatment (an SGLT1 inhibitor) affects the protective action of delphinidin-3-glucoside on endothelial cells, indicating that delphinidin-3-glucoside regulates MQC through the SGLT1 pathway to protect endothelial cells [209].

9.3.4. Melatonin.
Melatonin protects endothelial cells from LPS-induced apoptosis, especially in the regulation of mitochondrial fission [210]. LPS-induced cytosolic Ca^{2+} overload can lead to the upregulation of Ca^{2+}-dependent xanthine oxidase. High levels of xanthine oxidase expression and excessive ROS production can lead to Drp-1 phosphorylation at serine 616 and migration to the mitochondrial surface. Phosphorylated Drp-1 initiates mitochondrial fission, resulting in abnormal MMP, cytC leakage, and high caspase-9 expression. Melatonin can stimulate the AMPK pathway and SERCA2a expression, inhibit ROS overproduction and Ca^{2+} overload induced by xanthine oxidase, and regulate Drp-1 phosphorylation and mitochondrial fission/fusion balance, thus protecting HUVECs [210].

10. Future Research Directions

CVDs and microvascular diseases have high incidence and mortality rates. Although their pathological mechanisms are complex, they are closely related to the biological activities of cardiac myocytes and endothelial cells. New therapeutic and regulatory targets to improve the biological activities of myocardial cells and endothelial cells and restore their physiological functions under various stresses and in diseases are urgently needed. As shown in Figure 2, natural antioxidants can regulate MQC through different signalling pathways. As the main source of intracellular energy and an important participant in various signalling pathways, mitochondria play indispensable roles in cell survival and death and are important targets for the protection of myocardial cells and endothelial cells.

As shown in Figure 2, Figure 3, and Table 2, natural antioxidants can improve the vulnerability of myocardial and endothelial cells under stress, and provide a good reference for the treatment of CVDs and other vascular diseases. Although new natural antioxidants are being explored and experimental research on natural antioxidants for the treatment of various diseases by regulating MQC is ongoing, there remain many urgent problems to be solved.

10.1. Clinical Value of Natural Antioxidants. Compared with synthetic antioxidants, natural antioxidants are safer and more efficient. Their antioxidant and protective effects on cardiomyocytes and endothelial cells have been demonstrated in numerous *in vivo* and *in vitro* studies. In addition, natural antioxidants have many other pharmacological effects, such as cardiovascular protection, anti-inflammatory, antiviral, antitumour, and antiageing effects. They exhibit certain beneficial effects in improving mitochondrial function and energy metabolism, stabilising the MMP, regulating mitochondrial antioxidant enzyme activities, regulating mPTP, and protecting cardiomyocytes and endothelial cells. Accordingly, natural antioxidants are gaining increasing attention in research on CVDs, skin diseases, and ageing.

Currently, the large-scale application of natural antioxidants in clinical practice is still limited and most drugs are still in the experimental stage. In the future, efforts should be made to discover new raw material sources and monomers with antioxidant activity, and more genetic and clinical studies of natural antioxidants regulating MQC are needed to promote their clinical value. With the development of mitochondrial research, we may discover that MQC disorder is involved in more pathological mechanisms in human diseases. Although there are still controversies in clinical practice, the mutation and deletion of mitochondrial DNA may be an important reason for human ageing and disease development. In the future, how to use natural antioxidants in the clinic, to maintain the integrity of the mitochondrial genome, and to avoid inflammatory reaction caused by MQC disorder under oxidative stress will have profound guiding significance to reveal the aetiology of human diseases and improve clinical treatment.

10.2. Synergy of Natural Antioxidants. Numerous diseases present similar manifestations of mitochondrial dysfunction.
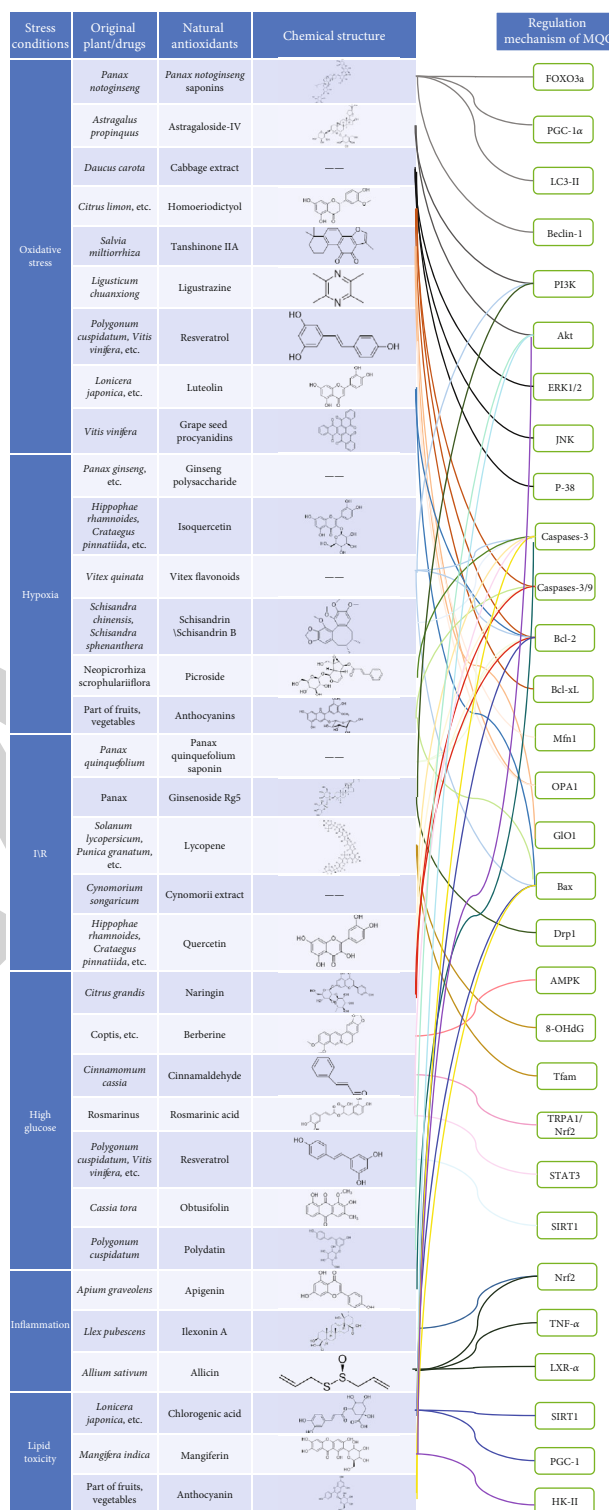
Figure 2: Mechanism of natural antioxidants that regulate MQC through different signalling pathways.

Whether different pathologies share a common mechanism remains to be elucidated. Most natural antioxidants regulate MQC via similar mechanisms. It is currently unknown whether there are effective natural antioxidants that can simultaneously treat multiple diseases, with different targets.
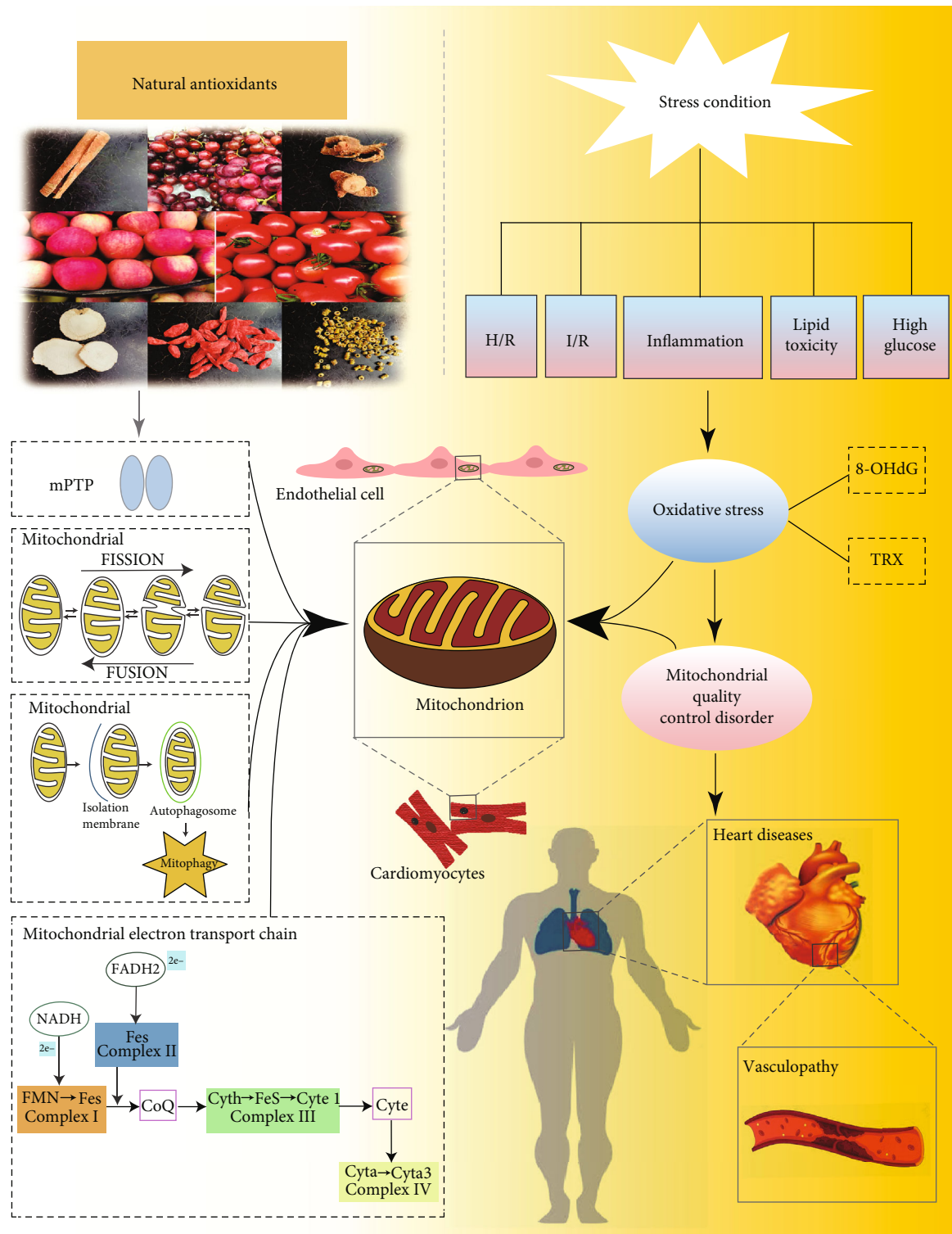
FIGURE 3: Mechanism of natural antioxidants in improving the vulnerability of cardiomyocytes/endothelial cells under stress by regulating mitochondrial quality control (MQC). (1) Different stress conditions can mediate severe oxidative stress damage and lead to MQC disorder, which further leads to increased vulnerability and apoptosis of cardiomyocytes and endothelial cells. This mechanism is reflected in many cardiovascular and microcirculation diseases. (2) Natural antioxidants can improve the quality and quantity of mitochondria by inhibiting the abnormal opening of the mitochondrial membrane permeability transition pore (mPTP), regulating the balance of mitochondrial lysis/fusion, regulating mitochondrial autophagy, and improving the function of the mitochondrial respiratory chain. It can also improve the vulnerability of myocardial cells and endothelial cells under stress, and provide a good reference for the treatment of cardiovascular diseases (CVDs) and other vascular diseases. H/R: hypoxia/reoxygenation; I/R: ischaemia/reperfusion; 8-OHdG: 8-2′-hydroxydeoxyguanosine.

TABLE 2: Mechanisms of various natural antioxidants in protecting myocardial cells and endothelial cells under stress.

Natural antioxidant	Source	Chemical formula	Regulation mechanism of MQC	Stress condition	Targeted cells
Panax notoginseng saponins	*Panax notoginseng*	—	(1) Inhibits ROS overproduction (2) Upregulates forkhead box O3a and Mn-SOD expression (3) Upregulates expression of PGC-1α, LC3-II, and Beclin-1	Oxidative stress	Cardiomyocytes
Astragaloside IV	*Astragalus propinquus*	$C_{41}H_{68}O_{14}$	(1) Inhibits ROS overproduction (2) Inhibits LDH/creatine kinase MB isoenzyme/CytC release (3) Increases succinate dehydrogenase and ATPase activities (4) Induces phosphorylation of PI3K and Akt	Oxidative stress	Cardiomyocytes
Cabbage extract	*Daucus carota*	—	(1) Inhibits ROS overproduction (2) Enhances SOD-1, cat, and GPX activities (3) Inhibits MAPK (ERK1/2, JNK, and P-38) activation	Oxidative stress	Cardiomyocytes
Homoeriodictyol	*Citrus limon* etc.	$C_{16}H_{14}O_6$	(1) Activates Nrf2 signalling (2) Restores MMP level (3) Inhibits CytC/apoptosis-inducing factor release (4) Inhibits caspase 3/9 overexpression (5) Increases the expression of Bcl-2 and Bcl-xL	Oxidative stress	HUVECs
Tanshinone IIA	*Salvia miltiorrhiza*	$C_{19}H_{18}O_3$	(1) Increases mRNA levels of Mfn1 and OPA1 (2) Regulates the mitochondrial fission/fusion balance (3) Enhances GlO1 expression	Oxidative stress	Bovine retinal endothelial cells
Ligustrazine	*Ligusticum chuanxiong*	$C_8H_{12}N_2$	(1) Inhibits CytC release (2) Restores the MMP level (3) Inhibits LDH	Oxidative stress	HUVECs
Resveratrol	*Polygonum cuspidatum, Vitis vinifera,* etc.	$C_{14}H_{12}O_3$	(1) Inhibits ROS overproduction (2) Activates TyrRs-PARP1 and AMPK\PCG-α\Sirt3 signalling (3) Increases protein expression of Mfn1, Mfn2, and Opa1 (4) Regulates the mitochondrial fission/fusion balance (5) Increases IDH2, GSH-Px, and SOD2 activities	Oxidative stress	HUVECs
Luteolin	*Lonicera japonica* etc.	$C_{15}H_{10}O_6$	(1) Restores MMP level (2) Regulates Ca^+ homeostasis (3) Regulates p53 phosphorylation (4) Adjusts the Bcl-2/Bax ratio (5) Inhibits CytC release	Oxidative stress	Endothelial cells
Grape seed procyanidins	*Vitis vinifera*	$C_{30}H_{12}O_6$	(1) Inhibits ROS overproduction (2) Restores the MMP level (3) Inhibits 8-OHdG expression (4) Enhances eNOS and VE-cadherin expression	Oxidative stress	HUVECs

TABLE 2: Continued.

Natural antioxidant	Source	Chemical formula	Regulation mechanism of MQC	Stress condition	Targeted cells
Ginseng polysaccharide	*Panax ginseng* etc.	—	(1) Maintains the level of MMP (2) Inhibits CytC release (3) Improves mitochondrial respiratory function and ATP production (4) Activates risk signalling (5) Induces glucocorticoid and oestrogen receptor expression and enhances eNOS and iNOS expression	Hypoxia	Endothelial cells
Isoquercetin	*Hippophae rhamnoides, Crataegus pinnatifida*, etc.	$C_{21}H_{20}O_{12}$	(1) Inhibits ROS overproduction (2) Improves the level of mitochondrial energy metabolism (3) Inhibits CytC release	Hypoxia	Cardiomyocytes
Vitex flavonoids	*Vitex quinata*	—	(1) Inhibits ROS overproduction (2) Inhibition of abnormal opening of MPTP (3) Inhibits CytC release and caspase-3 expression (4) Activates PI3K/Akt signalling (5) Adjusts the Bcl-2/Bax ratio	Hypoxia	Cardiomyocytes
Schisandrin/schisandrin B	*Schisandra chinensis, Schisandra sphenanthera*	$C_{24}H_{32}O_6$/$C_{23}H_{28}O_6$	(1) Inhibits abnormal opening of MPTP (2) Inhibits CytC release (3) Enhances GSH activity (4) Increases the cleavage of caspase-3 and poly ADP ribose polymerase	Hypoxia	Cardiomyocytes
Picroside	*Neopicrorhiza scrophulariiflora*	—	(1) Inhibits ROS overproduction (2) Inhibits abnormal opening of MPTP (3) Restores the MMP level (4) Inhibits CytC release (5) Downregulates caspase-3 expression	Hypoxia	Cardiomyocytes
Anthocyanins	Fruits, vegetables	—	(1) Restores the MMP level (2) Inhibits Bax transport to the nucleus (3) Inhibits the expression of caspases 3/9	Hypoxia	Endothelial cells
Panax quinquefolium saponin	*Panax quinquefolium*	—	(1) Inhibits abnormal MPTP opening (2) Regulates the mitochondrial Bcl-2/Bax ratio (3) Inhibits CytC release (4) Downregulates caspases 3/9 (5) Inhibits ROS overproduction	I\R	Cardiomyocytes
Ginsenoside Rg5	*Panax*	$C_{41}H_{68}O_{12}$	(1) Inhibits fatty acid oxidation (2) Activates Akt signalling (3) Regulates Drp1 expression (4) Promotes HK-II mitochondrial binding	I/R	Cardiomyocytes
Lycopene	*Solanum lycopersicum, Punica granatum*, etc.	$C_{40}H_{56}$	(1) Inhibits 8-OHdG expression (2) Inhibits ROS overproduction (3) Recovers TFAM protein expression	I/R	Cardiomyocytes

TABLE 2: Continued.

Natural antioxidant	Source	Chemical formula	Regulation mechanism of MQC	Stress condition	Targeted cells
Cynomorii extract	*Cynomorium songaricum*	—	(1) Increases mitochondrial ATP production (2) Enhances the redox cycle of glutathione (3) Inhibits expression of LDH and caspase-3	I/R	Cardiomyocytes
Quercetin	*Hippophae rhamnoides, Crataegus pinnatifida*, etc.	$C_{15}H_{10}O_7$	(1) Restores the MMP level (2) Inhibits CytC release (3) Adjusts the Bcl-2/Bax ratio (4) Inhibits activation of caspases 3/9	I\R	HUVECs
Naringin	*Citrus grandis*	$C_{27}H_{32}O_{14}$	(1) Inhibits p38 and p53 phosphorylation (2) Restores the MMP level (3) Inhibits CytC release (4) Adjusts theBcl-2/Bax ratio (5) Inhibits activation of caspases 3/8/9	High glucose	Cardiomyocytes
Berberine	*Coptis* etc.	$C_{20}H_{18}NO_4$	(1) Regulates the mitochondrial fission/fusion balance (2) Activates AMPK signalling (3) Restores mitochondrial autophagy flux (4) Promotes mitochondrial biosynthesis	High glucose	Cardiomyocytes
Cinnamaldehyde	*Cinnamomum cassia*	C_9H_8O	(1) Inhibits ROS overproduction (2) Activates TRPA1/Nrf2 signalling (3) Enhances HO-1, GPx-1, and NQO-1 expression (4) Upregulates nitrotyrosine, P22, and P47 expression	High glucose	Cardiomyocytes
Rosmarinic acid	*Rosmarinus*	$C_{18}H_{16}O_8$	(1) Inhibits ROS overproduction (2) Inhibits abnormal mPTP opening (3) Inhibits CytC release and caspase-3 activation (4) Increases STAT3 phosphorylation	High glucose	Cardiomyocytes
Resveratrol	*Polygonum cuspidatum, Vitis vinifera*, etc.	$C_{14}H_{12}O_3$	(1) Inhibits ROS overproduction (2) Activates SIRT1 signalling (3) Upregulates Mn-SOD expression and GSH activity	High glucose	Human coronary artery endothelial cells
Obtusifolin	*Cassia tora*	$C_{16}H_{12}O_5$	(1) Inhibits ROS overproduction (2) Inhibits electronic transport chain complex I activity (3) Regulates SOD and CAT activities	High glucose	HUVECs
Polydatin	*Polygonum cuspidatum*	$C_{20}H_{22}O_8$	(1) Inhibits ROS overproduction (2) Restores the MMP level and morphological changes of mitochondria (3) Increases Akt phosphorylation	High glucose	Endothelial cells

TABLE 2: Continued.

Natural antioxidant	Source	Chemical formula	Regulation mechanism of MQC	Stress condition	Targeted cells
Apigenin	*Apium graveolens*	$C_{15}H_{10}O_5$	(1) Inhibits ROS overproduction (2) Recovers mitochondrial complex I activity (3) Decreases caspase-3 expression (4) Adjusts miR-103-1-5p and parkin (5) Regulates mitochondrial autophagy	Inflammation	Cardiomyocytes
Ilexonin A	*Ilex pubescens*	$C_{36}H_{56}O_{11}$	(1) Activates Nrf2 signalling (2) Enhances PSMB5 expression (3) Inhibits ROS overproduction (4) Inhibits abnormal mitochondrial fission	Inflammation	Endothelial cells
Allicin	*Allium sativum*	$C_6H_{10}OS_2$	(1) Inhibits ROS/LDH/thiobarbituric acid-reactive substance overproduction (2) Restores the MMP level (3) Inhibits CytC release (4) Inhibits TNF-α and IL-8 expression (5) Activates LXR-α and Nrf2 signalling	Inflammation	Endothelial cells
Melatonin	—	$C_{13}H_{16}N_2O_2$	(1) Inhibits abnormal NF-κB activation (2) Restores the MMP level (3) Increases glutathione expression in mitochondria (4) Inhibits IL-6 and IL-8 expression	Inflammation	Endothelial cells
Chlorogenic acid	*Lonicera japonica* etc.	$C_{16}H_{18}O_9$	(1) Increases SIRT1/AMPK/PGC-1 expression (2) Inhibits ROS overproduction (3) Decreases caspase-3 expression (4) Adjusts the Bcl-2/Bax ratio	Lipid toxicity	Endothelial cells
Mangiferin	*Mangifera indica*	$C_{19}H_{18}O_{11}$	(1) Increases pyruvate dehydrogenase activity (2) Promotes translocation of Akt to HK-II (3) Inhibits abnormal mPTP opening (4) Restores the MMP level	Lipid toxicity	Endothelial cells
Anthocyanin	Fruits, vegetables	—	(1) Restores the MMP level (2) Inhibits abnormal mPTP opening (3) Inhibits CytC release (4) Decreases caspase-3 and Bax expression	Lipid toxicity	HUVECs
Melatonin		—	(1) Activates AMPK/SERCA2a signalling (2) Inhibits ROS overproduction and Ca^+ overload (3) Regulates Drp1 phosphorylation (4) Regulates the mitochondrial fission/fusion balance	Lipid toxicity	HUVECs

At present, various types of natural antioxidants are often used together in the clinic, and medicinal herbs contain various types of active ingredients, which makes it difficult to understand and utilise the synergistic effects of different active components on MQC regulation and simultaneously avoid antagonistic interactions. These are relevant issues that need to be addressed in future.

The combined effect of multiple antioxidants is often greater than that of a single drug at the same dose. Natural antioxidant components often have synergistic antioxidant effects, which are influenced by the drug concentration and reaction system. Therefore, future research should focus on synergistic effects between antioxidants, looking for efficient, low-toxicity compounds to meet clinical needs. At present, natural plants or herbs are usually used to extract antioxidants in the pharmaceutical industry. There are serious problems, such as lack of resources, backward extraction technology, and low content of active ingredients, which limit the popularisation and application of natural antioxidants. Therefore, in the future, we should explore more new sources of natural antioxidant raw materials, constantly improve the extraction of effective ingredients, the planting of natural antioxidant raw materials, and further clarify the synergistic effect of natural antioxidants, to improve their clinical value.

10.3. Targeting Experimental Research on Mitochondria. The effects of natural antioxidants on MQC have been studied mainly in animal and cell models, but few studies revealed the biological activity of natural antioxidants *in vitro* or by direct administration. It is difficult to judge whether natural antioxidants exert their effects by directly acting on mitochondria based only on animal and cell experiments. Therefore, the functions of natural drugs should be further investigated in isolated mitochondria to better understand their effect on MQC and their protective mechanism in myocardial cells.

Further, more in-depth studies should be conducted on the intake of natural antioxidants, dosing, bioavailability to the mitochondria, and tolerance of the intracellular environment. Interaction mechanisms among various stress conditions, such as high glucose, lipid toxicity, hypoxia, and ischaemia, remain to be elucidated. Causes and mechanisms of MQC disorders under stress conditions should be further explored to develop more effective natural antioxidants specifically targeting the MQC-regulatory effect and to provide more experimental evidence of and theoretical support for the mechanisms of natural antioxidants in protecting cardiomyocytes and endothelial cells.

10.4. Clinical Application of Mitochondrion-Targeted Therapy. The adverse consequences of oxidative stress and mitochondrial dysfunction mediated by various stresses seriously threaten the lives of patients with CVDs and bring great pressure to clinical treatment. Therefore, it is very important to analyse and summarise the targets and signalling pathways that regulate mitochondrial quality control and explore effective targeted therapies for MQC. In addition to natural antioxidants, mitochondrial transplantation, lifestyle intervention, and drug intervention can play effective roles in mitochondrial protection and restore or improve mitochondrial respiratory function and energy metabolism.

Mitochondrial transplantation is a new treatment for CVDs. It refers to the isolation of mitochondria from normal tissues and transportation of functional mitochondria to damaged tissues and organs to replace the damaged mitochondria and restore the normal mitochondria. This method can restore the normal structure and function of mitochondria in the clinic. In addition to natural antioxidants, some mitochondrion-targeted regulatory drugs, such as Mdivi1, P110, and Dynasore, can also reduce mitochondrial oxidative stress and improve mitochondrial function. Coenzyme Q10, which exists in the inner membrane of mitochondria, can also play an important role in ATP production and has certain antioxidant properties. Whether the combination of the above drugs and natural antioxidants can be effective needs more in-depth clinical research. In clinical practice, early effective MQC, reduction of mitochondrial dysfunction, and oxidative stress in CVDs are expected to become new targets in treatment strategy.

11. Conclusions

This review discussed the major effects of oxidative stress, hypoxia, I/R, inflammation, high glucose, and lipid toxicity on the MQC in cardiomyocytes and endothelial cells. These and other stress conditions induce excessive ROS production in these cell types, leading to MQC disorder and serious oxidative stress damage, which form an important mechanism in the development of CVDs and microvascular diseases. This review further explored the mechanism of 34 natural antioxidants in improving the vulnerability of cardiomyocytes and endothelial cells under stress by regulating MQC. Different types of natural antioxidants can maintain or restore the physiological function of mitochondria under stress by regulating MQC and improving cell viability and vulnerability. In conclusion, natural antioxidants have certain advantages in the regulation of MQC and the improvement of cardiomyocyte and endothelial cell activity and show promise as candidate drugs for clinical treatment of CVDs in future.

Data Availability

The data used to support the findings of this study are included within the article.

Conflicts of Interest

The authors declare that the research was conducted in the absence of any commercial or financial relationships that could be construed as a potential conflict of interest.

Authors' Contributions

Xing Chang and Zhenyu Zhao contributed to this work equally.

Acknowledgments

References

[1] K. C. Yang, M. G. Bonini, and S. J. Dudley, "Mitochondria and arrhythmias," *Free Radical Biology and Medicine*, vol. 71, pp. 351–361, 2014.

[2] M. R. Savona and J. C. Rathmell, "Mitochondrial homeostasis in AML and gasping for response in resistance to BCL2 blockade," *Cancer Discovery*, vol. 9, no. 7, pp. 831–833, 2019.

[3] J. A. Nicolás-Ávila, A. V. Lechuga-Vieco, L. Esteban-Martínez et al., "A network of macrophages supports mitochondrial homeostasis in the heart," *Cell*, vol. 183, no. 1, pp. 94–109.e23, 2020.

[4] K. Ma, G. Chen, W. Li, O. Kepp, Y. Zhu, and Q. Chen, "Mitophagy, mitochondrial homeostasis, and cell fate," *Frontiers in Cell and Developmental Biology*, vol. 8, p. 467, 2020.

[5] Y. Meng, M. Tian, S. Yin et al., "Downregulation of TSPO expression inhibits oxidative stress and maintains mitochondrial homeostasis in cardiomyocytes subjected to anoxia/reoxygenation injury," *Biomedicine & Pharmacotherapy*, vol. 121, p. 109588, 2020.

[6] A. Diokmetzidou, E. Soumaka, I. Kloukina et al., "Desmin and αB-crystallin interplay in the maintenance of mitochondrial homeostasis and cardiomyocyte survival," *Journal of Cell Science*, vol. 129, no. 20, pp. 3705–3720, 2016.

[7] L. H. Wu, H. C. Chang, P. C. Ting, and D. L. Wang, "Laminar shear stress promotes mitochondrial homeostasis in endothelial cells," *Journal of Cellular Physiology*, vol. 233, no. 6, pp. 5058–5069, 2018.

[8] J. Wang, S. Toan, and H. Zhou, "Mitochondrial quality control in cardiac microvascular ischemia-reperfusion injury: new insights into the mechanisms and therapeutic potentials," *Pharmacological Research*, vol. 156, p. 104771, 2020.

[9] H. M. Ni, J. A. Williams, and W. X. Ding, "Mitochondrial dynamics and mitochondrial quality control," *Redox Biology*, vol. 4, pp. 6–13, 2015.

[10] A. Vaiserman, A. Koliada, A. Zayachkivska, and O. Lushchak, "Nanodelivery of natural antioxidants: an anti-aging perspective," *Frontiers in Bioengineering and Biotechnology*, vol. 7, 2019.

[11] V. Unsal and E. Belge-Kurutas, "Experimental hepatic carcinogenesis: oxidative stress and natural antioxidants," *Open Access Macedonian Journal of Medical Sciences*, vol. 5, no. 5, pp. 686–691, 2017.

[12] A. Serrano, G. Ros, and G. Nieto, "Regulation of inflammatory response and the production of reactive oxygen species by a functional cooked ham reformulated with natural antioxidants in a macrophage immunity model," *Antioxidants (Basel)*, vol. 8, no. 8, p. 286, 2019.

[13] K. V. Ramana, A. Reddy, N. Majeti, and S. S. Singhal, "Therapeutic potential of natural antioxidants," *Oxidative Medicine and Cellular Longevity*, vol. 2018, Article ID 9471051, 3 pages, 2018.

[14] A. Hoshino, W.-j. Wang, S. Wada et al., "The ADP/ATP translocase drives mitophagy independent of nucleotide exchange," *Nature*, vol. 575, no. 7782, pp. 375–379, 2019.

[15] R. Shi, M. Guberman, and L. A. Kirshenbaum, "Mitochondrial quality control: the role of mitophagy in aging," *Trends in Cardiovascular Medicine*, vol. 28, no. 4, pp. 246–260, 2018.

[16] F. G. Tahrir, D. Langford, S. Amini, T. M. Ahooyi, and K. Khalili, "Mitochondrial quality control in cardiac cells: mechanisms and role in cardiac cell injury and disease," *Journal of Cellular Physiology*, vol. 234, no. 6, pp. 8122–8133, 2018.

[17] J. C. Campos, L. H. M. Bozi, L. R. G. Bechara, V. M. Lima, and J. C. B. Ferreira, "Mitochondrial quality control in cardiac diseases," *Frontiers in Physiology*, vol. 7, p. 479, 2016.

[18] J. Gao, L. Zhao, J. Wang et al., "C-phycocyanin ameliorates mitochondrial fission and fusion dynamics in ischemic cardiomyocyte damage," *Frontiers in Pharmacology*, vol. 10, p. 733, 2019.

[19] S. Givvimani, S. B. Pushpakumar, N. Metreveli, S. Veeranki, S. Kundu, and S. C. Tyagi, "Role of mitochondrial fission and fusion in cardiomyocyte contractility," *International Journal of Cardiology*, vol. 187, pp. 325–333, 2015.

[20] G. Takemura, H. Kanamori, H. Okada et al., "Mitochondrial deformity confined to a single cardiomyocyte in human endomyocardial biopsy specimens: report of 4 cases," *Journal of Cardiology Cases*, vol. 16, no. 5, pp. 178–182, 2017.

[21] M. A. Sazonova, A. I. Ryzhkova, V. V. Sinyov et al., "Mitochondrial genome mutations associated with myocardial infarction," *Disease Markers*, vol. 2018, Article ID 9749457, 6 pages, 2018.

[22] J. W. Shin, S. H. Park, Y. G. Kang, Y. Wu, H. J. Choi, and J. W. Shin, "Changes, and the relevance thereof, in mitochondrial morphology during differentiation into endothelial Cells," *PLoS One*, vol. 11, no. 8, p. e161015, 2016.

[23] A.-B. Al-Mehdi, V. M. Pastukh, B. M. Swiger et al., "Perinuclear mitochondrial clustering creates an oxidant-rich nuclear domain required for hypoxia-induced transcription," *Science Signaling*, vol. 5, no. 231, p. a47, 2012.

[24] Y. Zeng, Q. Pan, X. Wang et al., "Impaired mitochondrial fusion and oxidative phosphorylation triggered by high glucose is mediated by Tom22 in endothelial cells," *Oxidative Medicine and Cellular Longevity*, vol. 2019, Article ID 4508762, 23 pages, 2019.

[25] S. Zhang, Y. Gao, and J. Wang, "Advanced glycation end products influence mitochondrial fusion-fission dynamics through RAGE in human aortic endothelial cells," *International Journal of Clinical and Experimental Pathology*, vol. 10, no. 7, pp. 8010–8022, 2017.

[26] L. Zuo, Q. Li, B. Sun, Z. Xu, and Z. Ge, "Cilostazol promotes mitochondrial biogenesis in human umbilical vein endothelial cells through activating the expression of PGC-1α," *Biochemical and Biophysical Research Communications*, vol. 433, no. 1, pp. 52–57, 2013.

[27] I. Valle, A. Alvarez-Barrientos, E. Arza, S. Lamas, and M. Monsalve, "PGC-1alpha regulates the mitochondrial antioxidant defense system in vascular endothelial cells," *Cardiovascular Research*, vol. 66, no. 3, pp. 562–573, 2005.

[28] U. Krengel and S. Tornroth-Horsefield, "Coping with oxidative stress," *Science*, vol. 347, no. 6218, pp. 125-126, 2015.

[29] S. I. Hashem, C. N. Perry, M. Bauer et al., "Brief report: oxidative stress mediates cardiomyocyte apoptosis in a human model of Danon disease and heart failure," *Stem Cells*, vol. 33, no. 7, pp. 2343–2350, 2015.

[30] Y. Mikhed, A. Daiber, and S. Steven, "Mitochondrial oxidative stress, mitochondrial DNA damage and their role in age-related vascular dysfunction," *International Journal of Molecular Sciences*, vol. 16, no. 7, pp. 15918–15953, 2015.

[31] D. B. Zorov, M. Juhaszova, and S. J. Sollott, "Mitochondrial reactive oxygen species (ROS) and ROS-induced ROS release," *Physiological Reviews*, vol. 94, no. 3, pp. 909–950, 2014.

[32] R. Guo, J. Gu, S. Zong, M. Wu, and M. Yang, "Structure and mechanism of mitochondrial electron transport chain," *Biomedical Journal*, vol. 41, no. 1, pp. 9–20, 2018.

[33] R. Hardeland, "Melatonin and the electron transport chain," *Cellular and Molecular Life Sciences*, vol. 74, no. 21, pp. 3883–3896, 2017.

[34] R. Z. Zhao, S. Jiang, L. Zhang, and Z. B. Yu, "Mitochondrial electron transport chain, ROS generation and uncoupling (review)," *International Journal of Molecular Medicine*, vol. 44, no. 1, pp. 3–15, 2019.

[35] S. Deshwal, S. Antonucci, N. Kaludercic, and F. Di Lisa, "Measurement of mitochondrial ROS formation," *Methods in Molecular Biology*, vol. 1782, pp. 403–418, 2018.

[36] S. Cadenas, "Mitochondrial uncoupling, ROS generation and cardioprotection," *Biochimica et Biophysica Acta - Bioenergetics*, vol. 1859, no. 9, pp. 940–950, 2018.

[37] L. Formentini, F. Santacatterina, C. N. de Arenas et al., "Mitochondrial ROS production protects the intestine from inflammation through functional M2 macrophage polarization," *Cell Reports*, vol. 19, no. 6, pp. 1202–1213, 2017.

[38] J. Gatliff, D. East, J. Crosby et al., "TSPO interacts with VDAC1 and triggers a ROS-mediated inhibition of mitochondrial quality control," *Autophagy*, vol. 10, no. 12, pp. 2279–2296, 2015.

[39] T. Xin, W. Lv, D. Liu, Y. Jing, and F. Hu, "Opa1 reduces hypoxia-induced cardiomyocyte death by improving mitochondrial quality control," *Frontiers in Cell and Developmental Biology*, vol. 8, p. 853, 2020.

[40] K. Suresh, L. Servinsky, H. Jiang et al., "Regulation of mitochondrial fragmentation in microvascular endothelial cells isolated from the SU5416/hypoxia model of pulmonary arterial hypertension," *American Journal of Physiology-Lung Cellular and Molecular Physiology*, vol. 317, no. 5, pp. L639–L652, 2019.

[41] N. Zheng, H. Li, X. Wang, Z. Zhao, and D. Shan, "Oxidative stress-induced cardiomyocyte apoptosis is associated with dysregulated Akt/p53 signaling pathway," *Journal of Receptors and Signal Transduction*, vol. 40, no. 6, pp. 599–604, 2020.

[42] M. C. Martí, I. Florez-Sarasa, D. Camejo et al., "Response of mitochondrial antioxidant system and respiratory pathways to reactive nitrogen species in pea leaves," *Physiologia Plantarum*, vol. 147, no. 2, pp. 194–206, 2013.

[43] F. Xia, X. Wang, M. Li, and P. Mao, "Mitochondrial structural and antioxidant system responses to aging in oat (_Avena sativa_ L.) seeds with different moisture contents," *Plant Physiology and Biochemistry*, vol. 94, pp. 122–129, 2015.

[44] J. Li, X. Zhou, B. Wei, S. Cheng, Q. Zhou, and S. Ji, "GABA application improves the mitochondrial antioxidant system and reduces peel browning in 'Nanguo' pears after removal from cold storage," *Food Chemistry*, vol. 297, p. 124903, 2019.

[45] R. Bonetta, "Potential therapeutic applications of MnSODs and SOD-mimetics," *Chemistry*, vol. 24, no. 20, pp. 5032–5041, 2018.

[46] S. C. Lu, "Glutathione synthesis," *Biochimica et Biophysica Acta*, vol. 1830, no. 5, pp. 3143–3153, 2013.

[47] J.-H. Shao, Q.-W. Fu, L.-X. Li et al., "Prx II reduces oxidative stress and cell senescence in chondrocytes by activating the p16-CDK4/6-pRb-E2F signaling pathway," *European Review for Medical and Pharmacological Sciences*, vol. 24, no. 7, pp. 3448–3458, 2020.

[48] C. Xu, W. Wang, B. Wang et al., "Analytical methods and biological activities of *Panax notoginseng* saponins: Recent trends," *Journal of Ethnopharmacology*, vol. 236, pp. 443–465, 2019.

[49] Z. Zhou, J. Wang, Y. Song et al., "Panax notoginseng saponins attenuate cardiomyocyte apoptosis through mitochondrial pathway in natural aging rats," *Phytotherapy Research*, vol. 32, no. 2, pp. 243–250, 2018.

[50] L. Li, X. Hou, R. Xu, C. Liu, and M. Tu, "Research review on the pharmacological effects of astragaloside IV," *Fundamental & Clinical Pharmacology*, vol. 31, no. 1, pp. 17–36, 2017.

[51] Y. Jia, D. Zuo, Z. Li et al., "Astragaloside IV inhibits doxorubicin-induced cardiomyocyte apoptosis mediated by mitochondrial apoptotic pathway via activating the PI3K/Akt pathway," *Chemical and Pharmaceutical Bulletin*, vol. 62, no. 1, pp. 45–53, 2014.

[52] X. Qing, X. Zhao, C. Hu et al., "Selenium alleviates chromium toxicity by preventing oxidative stress in cabbage (_Brassica campestris_ L. ssp. _Pekinensis_) leaves," *Ecotoxicology and Environmental Safety*, vol. 114, pp. 179–189, 2015.

[53] D. K. Yang, "Cabbage (Brassica oleracea var. capitata) protects against H_2O_2-induced oxidative stress by preventing mitochondrial dysfunction in H9c2 cardiomyoblasts," *Evidence-Based Complementary and Alternative Medicine*, vol. 2018, Article ID 2179021, 10 pages, 2018.

[54] M. Freuding, C. Keinki, O. Micke, J. Buentzel, and J. Huebner, "Mistletoe in oncological treatment: a systematic review," *Journal of Cancer Research and Clinical Oncology*, vol. 145, no. 3, pp. 695–707, 2019.

[55] P. Yang, Y. Jiang, Y. Pan et al., "Mistletoe extract Fraxini inhibits the proliferation of liver cancer by down-regulating c-Myc expression," *Scientific Reports*, vol. 9, no. 1, p. 6428, 2019.

[56] T. Shen, H. Z. Li, A. L. Li, Y. R. Li, X. N. Wang, and D. M. Ren, "Homoeriodictyol protects human endothelial cells against oxidative insults through activation of Nrf2 and inhibition of mitochondrial dysfunction," *Vascular Pharmacology*, vol. 109, pp. 72–82, 2018.

[57] F. Feng, N. Li, P. Cheng et al., "Tanshinone IIA attenuates silica-induced pulmonary fibrosis via inhibition of TGF-β1-Smad signaling pathway," *Biomedicine & Pharmacotherapy*, vol. 121, p. 109586, 2020.

[58] S. Qian, Y. Qian, D. Huo, S. Wang, and Q. Qian, "Tanshinone IIa protects retinal endothelial cells against mitochondrial fission induced by methylglyoxal through glyoxalase 1," *European Journal of Pharmacology*, vol. 857, p. 172419, 2019.

[59] J. Zou, P. Gao, X. Hao, H. Xu, P. Zhan, and X. Liu, "Recent progress in the structural modification and pharmacological activities of ligustrazine derivatives," *European Journal of Medicinal Chemistry*, vol. 147, pp. 150–162, 2018.

[60] X. Fan, E. Wang, J. He et al., "Ligustrazine protects homocysteine-induced apoptosis in human umbilical vein endothelial cells by modulating mitochondrial dysfunction," *Journal of Cardiovascular Translational Research*, vol. 12, no. 6, pp. 591–599, 2019.

[61] J. Breuss, A. Atanasov, and P. Uhrin, "Resveratrol and its effects on the vascular system," *International Journal of Molecular Sciences*, vol. 20, no. 7, p. 1523, 2019.

[62] S. Galiniak, D. Aebisher, and D. Bartusik-Aebisher, "Health benefits of resveratrol administration," *Acta Biochimica Polonica*, vol. 66, no. 1, pp. 13–21, 2019.

[63] J. Yang, X. Zhou, X. Zeng, O. Hu, L. Yi, and M. Mi, "Resveratrol attenuates oxidative injury in human umbilical vein endothelial cells through regulating mitochondrial fusion via TyrRS-PARP1 pathway," *Nutrition & Metabolism*, vol. 16, 2019.

[64] X. Zhou, M. Chen, X. Zeng et al., "Resveratrol regulates mitochondrial reactive oxygen species homeostasis through Sirt3 signaling pathway in human vascular endothelial cells," *Cell Death & Disease*, vol. 5, no. 12, p. e1576, 2014.

[65] H. Xu, W. Yu, S. Sun, C. Li, Y. Zhang, and J. Ren, "Luteolin attenuates doxorubicin-induced cardiotoxicity through promoting mitochondrial autophagy," *Frontiers in Physiology*, vol. 11, p. 113, 2020.

[66] H.-I. Chen, W.-S. Hu, M.-Y. Hung et al., "Protective effects of luteolin against oxidative stress and mitochondrial dysfunction in endothelial cells," *Nutrition, Metabolism and Cardiovascular Diseases*, vol. 30, no. 6, pp. 1032–1043, 2020.

[67] Q. H. Li, H. S. Yan, H. Q. Li, J. J. Gao, and R. R. Hao, "Effects of dietary supplementation with grape seed procyanidins on nutrient utilisation and gut function in weaned piglets," *Animal*, vol. 14, no. 3, pp. 491–498, 2020.

[68] H. Han, H. Wang, Y. Du, and L. Gao, "Grape seed procyanidins attenuates cisplatin-induced human embryonic renal cell cytotoxicity by modulating heme oxygenase-1 in vitro," *Cell Biochemistry and Biophysics*, vol. 77, no. 4, pp. 367–377, 2019.

[69] Z. Lu, F. Lu, Y. Zheng, Y. Zeng, C. Zou, and X. Liu, "Grape seed proanthocyanidin extract protects human umbilical vein endothelial cells from indoxyl sulfate-induced injury via ameliorating mitochondrial dysfunction," *Renal Failure*, vol. 38, no. 1, pp. 100–108, 2015.

[70] S. Shu, Y. Wang, M. Zheng et al., "Hypoxia and hypoxia-inducible factors in kidney injury and repair," *Cells*, vol. 8, no. 3, 2019.

[71] E.-J. Yeo, "Hypoxia and aging," *Experimental and Molecular Medicine*, vol. 51, no. 6, pp. 1–15, 2019.

[72] M.-H. Wu, K.-Y. Hsiao, and S.-J. Tsai, "Hypoxia: The force of endometriosis," *Journal of Obstetrics and Gynaecology Research*, vol. 45, no. 3, pp. 532–541, 2019.

[73] R. Scherz-Shouval and Z. Elazar, "Regulation of autophagy by ROS: physiology and pathology," *Trends in Biochemical Sciences*, vol. 36, no. 1, pp. 30–38, 2011.

[74] P. Venditti and S. Di Meo, "The role of reactive oxygen species in the life cycle of the mitochondrion," *International Journal of Molecular Sciences*, vol. 21, no. 6, p. 2173, 2020.

[75] R. B. Hamanaka, S. E. Weinberg, C. R. Reczek, and N. S. Chandel, "The mitochondrial respiratory chain is required for organismal adaptation to hypoxia," *Cell Reports*, vol. 15, no. 3, pp. 451–459, 2016.

[76] J. Li and F. Chen, "Effect of iron supplementation on function of mitochondrial respiratory chain of liver in hypoxia training rats," *Zhongguo Ying Yong Sheng Li Xue Za Zhi*, vol. 31, no. 3, pp. 263–265, 2015.

[77] E. E. Farmer and M. J. Mueller, "ROS-mediated lipid peroxidation and RES-activated signaling," *Annual Review of Plant Biology*, vol. 64, no. 1, pp. 429–450, 2013.

[78] S. Lu, Y. Zhang, S. Zhong et al., "N-n-butyl Haloperidol Iodide Protects against Hypoxia/Reoxygenation Injury in Cardiac Microvascular Endothelial Cells by Regulating the ROS/MAPK/Egr-1 Pathway," *Frontiers in Pharmacology*, vol. 7, 2017.

[79] Y. Zhang, H. Zhou, W. Wu et al., "Liraglutide protects cardiac microvascular endothelial cells against hypoxia/reoxygenation injury through the suppression of the SR- Ca^{2+}-XO-ROS axis via activation of the GLP-1R/PI3K/Akt/survivin pathways," *Free Radical Biology and Medicine*, vol. 95, pp. 278–292, 2016.

[80] M. Dhar-Mascareño, J. M. Cárcamo, and D. W. Golde, "Hypoxia-reoxygenation-induced mitochondrial damage and apoptosis in human endothelial cells are inhibited by vitamin C," *Free Radical Biology and Medicine*, vol. 38, no. 10, pp. 1311–1322, 2005.

[81] C.-Y. Kuo, Y.-C. Chiu, A. Y.-L. Lee, and T.-L. Hwang, "Mitochondrial Lon protease controls ROS-dependent apoptosis in cardiomyocyte under hypoxia," *Mitochondrion*, vol. 23, pp. 7–16, 2015.

[82] Y. Oropeza-Almazán, E. Vázquez-Garza, H. Chapoy-Villanueva, G. Torre-Amione, and G. García-Rivas, "Small interfering RNA targeting mitochondrial calcium uniporter improves cardiomyocyte cell viability in hypoxia/reoxygenation injury by reducing calcium overload," *Oxidative Medicine and Cellular Longevity*, vol. 2017, Article ID 5750897, 13 pages, 2017.

[83] R.-h. Tu, L. Chen, G.-q. Zhong et al., "The effect of mitochondrial oxidative stress and the expression of Bcl-2 and Bax proteins on cardiomyocyte apoptosis during hypoxia post-conditioning," *Zhonghua Xin Xue Guan Bing Za Zhi*, vol. 40, no. 6, pp. 516–521, 2012.

[84] K. F. Akhter, M. A. Mumin, E. M. K. Lui, and P. A. Charpentier, "Fabrication of fluorescent labeled ginseng polysaccharide nanoparticles for bioimaging and their immunomodulatory activity on macrophage cell lines," *International Journal of Biological Macromolecules*, vol. 109, pp. 254–262, 2018.

[85] Y.-H. Zuo, Q.-B. Han, G.-T. Dong et al., "Panax ginseng polysaccharide protected H9c2 cardiomyocyte from hypoxia/reoxygenation injury through regulating mitochondrial metabolism and RISK pathway," *Frontiers in Physiology*, vol. 9, 2018.

[86] Y. Dai, H. Zhang, J. Zhang, and M. Yan, "Isoquercetin attenuates oxidative stress and neuronal apoptosis after ischemia/reperfusion injury via Nrf2-mediated inhibition of the NOX4/ROS/NF-κB pathway," *Chem Biol Interact*, vol. 284, pp. 32–40, 2018.

[87] M. Chen, L. H. Dai, A. Fei, S. M. Pan, and H. R. Wang, "Isoquercetin activates the ERK1/2-Nrf2 pathway and protects against cerebral ischemia-reperfusion injury in vivo and in vitro," *Experimental and Therapeutic Medicine*, vol. 13, no. 4, pp. 1353–1359, 2017.

[88] H. Cao, H. Xu, G. Zhu, and S. Liu, "Isoquercetin ameliorated hypoxia/reoxygenation-induced H9C2 cardiomyocyte apoptosis _via_ a mitochondrial-dependent pathway," *Biomedicine & Pharmacotherapy*, vol. 95, pp. 938–943, 2017.

[89] O. M. Bello, A. B. Ogbesejana, C. O. Adetunji, and S. O. Oguntoye, "Flavonoids isolated from <i>Vitex grandifolia</i>, an underutilized vegetable, exert monoamine A & B inhibitory and anti-inflammatory effects and their structure-activity relationship," *Turk J Pharm Sci*, vol. 16, no. 4, pp. 437–443, 2019.

[90] Y. A. Kim, H. Kim, and Y. Seo, "Antiproliferative effect of flavonoids from the halophyte Vitex rotundifolia on human cancer cells," *Natural Product Communications*, vol. 8, no. 10, pp. 1405–1408, 2013.

[91] P. Liao, G. Sun, C. Zhang et al., "Bauhinia championii flavone attenuates hypoxia-reoxygenation induced apoptosis in H9c2 cardiomyocytes by improving mitochondrial dysfunction," *Molecules*, vol. 21, no. 11, p. 1469, 2016.

[92] Z. Mou, Z. Feng, Z. Xu et al., "Schisandrin B alleviates diabetic nephropathy through suppressing excessive inflammation and oxidative stress," *Biochemical and Biophysical Research Communications*, vol. 508, no. 1, pp. 243–249, 2019.

[93] Y. H. Choi, "Schisandrin A prevents oxidative stress-induced DNA damage and apoptosis by attenuating ROS generation in C2C12 cells," *Biomedicine & Pharmacotherapy*, vol. 106, pp. 902–909, 2018.

[94] P. Y. Chiu, K. F. Luk, H. Y. Leung, K. M. Ng, and K. M. Ko, "Schisandrin B stereoisomers protect against hypoxia/reoxygenation-induced apoptosis and inhibit associated changes in Ca^{2+}-induced mitochondrial permeability transition and mitochondrial membrane potential in H9c2 cardiomyocytes," *Life Sciences*, vol. 82, no. 21-22, pp. 1092–1101, 2008.

[95] H. Han, Z. Q. Li, Z. L. Gao et al., "Synthesis and biological evaluation of picroside derivatives as hepatoprotective agents," *Natural Product Research*, vol. 33, no. 19, pp. 2845–2850, 2019.

[96] Y. Li, L. Wang, Z. Chen, and X. Liu, "Picroside II attenuates ischemia/reperfusion testicular injury by alleviating oxidative stress and apoptosis through reducing nitric oxide synthesis," *Acta Cirurgica Brasileira*, vol. 34, no. 11, p. e201901102, 2019.

[97] J. Z. Li, S. Y. Yu, D. Mo, X. N. Tang, and Q. R. Shao, "Picroside inhibits hypoxia/reoxygenation-induced cardiomyocyte apoptosis by ameliorating mitochondrial function through a mechanism involving a decrease in reactive oxygen species production," *International Journal of Molecular Medicine*, vol. 35, no. 2, pp. 446–452, 2015.

[98] M. Jezek, C. Zörb, N. Merkt, and C.-M. Geilfus, "Anthocyanin Management in Fruits by Fertilization," *Journal of Agricultural and Food Chemistry*, vol. 66, no. 4, pp. 753–764, 2018.

[99] S. Silva, E. M. Costa, C. Calhau, R. M. Morais, and M. E. Pintado, "Anthocyanin extraction from plant tissues: A review," *Critical Reviews in Food Science and Nutrition*, vol. 57, no. 14, pp. 3072–3083, 2015.

[100] J. Paixao, T. C. Dinis, and L. M. Almeida, "Dietary anthocyanins protect endothelial cells against peroxynitrite-induced mitochondrial apoptosis pathway and Bax nuclear translocation: an in vitro approach," *Apoptosis*, vol. 16, no. 10, pp. 976–989, 2011.

[101] T. Mazo, V. D'Annunzio, M. Donato, V. Perez, T. Zaobornyj, and R. J. Gelpi, "Dyslipidemia in ischemia/reperfusion injury," *Advances in Experimental Medicine and Biology*, vol. 1127, pp. 117–130, 2019.

[102] T. Kalogeris, C. P. Baines, M. Krenz, and R. J. Korthuis, "Ischemia/reperfusion," *Comprehensive Physiology*, vol. 7, no. 1, pp. 113–170, 2016.

[103] J. Cai, Y. Jiang, M. Zhang et al., "Protective effects of mitochondrion-targeted peptide SS-31 against hind limb ischemia-reperfusion injury," *Journal of Physiology and Biochemistry*, vol. 74, no. 2, pp. 335–343, 2018.

[104] A. M. Bertholet, T. Delerue, A. M. Millet et al., "Mitochondrial fusion/fission dynamics in neurodegeneration and neuronal plasticity," *Neurobiology of Disease*, vol. 90, pp. 3–19, 2016.

[105] Y. Li and X. Liu, "Novel insights into the role of mitochondrial fusion and fission in cardiomyocyte apoptosis induced by ischemia/reperfusion," *Journal of Cellular Physiology*, vol. 233, no. 8, pp. 5589–5597, 2018.

[106] W. Chen and D. Li, "Reactive oxygen species (ROS)-responsive nanomedicine for solving ischemia-reperfusion injury," *Frontiers in Chemistry*, vol. 8, 2020.

[107] S. Cadenas, "ROS and redox signaling in myocardial ischemia-reperfusion injury and cardioprotection," *Free Radical Biology and Medicine*, vol. 117, pp. 76–89, 2018.

[108] H. Bugger and K. Pfeil, "Mitochondrial ROS in myocardial ischemia reperfusion and remodeling," *Biochimica et Biophysica Acta (BBA) - Molecular Basis of Disease*, vol. 1866, no. 7, p. 165768, 2020.

[109] S. B. Ong, P. Samangouei, S. B. Kalkhoran, and D. J. Hausenloy, "The mitochondrial permeability transition pore and its role in myocardial ischemia reperfusion injury," *Journal of Molecular and Cellular Cardiology*, vol. 78, pp. 23–34, 2015.

[110] M. I. Ragone and A. E. Consolini, "CARDIAC role of the mitochondrial Ca2+ transporters in the high-[K+](o) cardioprotection of rat hearts under ischemia and reperfusion: a mechano-energetic study," *Journal of Cardiovascular Pharmacology*, vol. 54, no. 3, pp. 213–222, 2009.

[111] Q. Chen, A. K. S. Camara, D. F. Stowe, C. L. Hoppel, and E. J. Lesnefsky, "Modulation of electron transport protects cardiac mitochondria and decreases myocardial injury during ischemia and reperfusion," *American Journal of Physiology-Cell Physiology*, vol. 292, no. 1, pp. C137–C147, 2007.

[112] M.-Y. Wu, G.-T. Yiang, W.-T. Liao et al., "Current mechanistic concepts in ischemia and reperfusion injury," *Cellular Physiology and Biochemistry*, vol. 46, no. 4, pp. 1650–1667, 2018.

[113] A. R. Anzell, R. Maizy, K. Przyklenk, and T. H. Sanderson, "Mitochondrial quality control and disease: insights into ischemia-reperfusion injury," *Molecular Neurobiology*, vol. 55, no. 3, pp. 2547–2564, 2018.

[114] M. Yang, B. S. Linn, Y. Zhang, and J. Ren, "Mitophagy and mitochondrial integrity in cardiac ischemia-reperfusion injury," *Biochimica et Biophysica Acta (BBA) - Molecular Basis of Disease*, vol. 1865, no. 9, pp. 2293–2302, 2019.

[115] H. Sun, S. Ling, D. Zhao et al., "Panax quinquefolium saponin attenuates cardiac remodeling induced by simulated microgravity," *Phytomedicine*, vol. 56, pp. 83–93, 2019.

[116] D. Li, M. Liu, T. Q. Tao, D. D. Song, X. H. Liu, and D. Z. Shi, "Panax quinquefolium saponin attenuates cardiomyocyte apoptosis and opening of the mitochondrial permeability transition pore in a rat model of ischemia/reperfusion," *Cellular Physiology and Biochemistry*, vol. 34, no. 4, pp. 1413–1426, 2014.

[117] S.-L. Feng, H.-B. Luo, L. Cai et al., "Ginsenoside Rg5 overcomes chemotherapeutic multidrug resistance mediated by ABCB1 transporter: _in vitro_ and _in vivo_ study," *Journal of Ginseng Research*, vol. 44, no. 2, pp. 247–257, 2020.

[118] Y.-L. Yang, J. Li, K. Liu et al., "Ginsenoside Rg5 increases cardiomyocyte resistance to ischemic injury through regulation of mitochondrial hexokinase-II and dynamin-related protein 1," *Cell Death & Disease*, vol. 8, no. 2, p. e2625, 2017.

[119] M. Bacanli, N. Basaran, and A. A. Basaran, "Lycopene: Is it Beneficial to Human Health as an Antioxidant?," *The Turkish Journal of Pharmaceutical Sciences*, vol. 14, no. 3, pp. 311–318, 2017.

[120] I. Mozos, D. Stoian, A. Caraba, C. Malainer, J. O. Horbańczuk, and A. G. Atanasov, "Lycopene and Vascular Health," *Frontiers in Pharmacology*, vol. 9, 2018.

[121] R. Yue, X. Xia, J. Jiang et al., "Mitochondrial DNA oxidative damage contributes to cardiomyocyte ischemia/reperfusion-injury in rats: cardioprotective role of lycopene," *Journal of Cellular Physiology*, vol. 230, no. 9, pp. 2128–2141, 2015.

[122] L. Zhang, D. Pei, Y.-r. Huang et al., "Chemical Constituents from Cynomorium songaricum," *Zhong Yao Cai*, vol. 39, no. 1, pp. 74–77, 2016.

[123] S.-A. Xie, G.-Y. Li, J. Huang et al., "A new flavanol from Cynomorium songaricum," *Journal of Asian Natural Products Research*, vol. 15, no. 4, pp. 413–416, 2013.

[124] J. Chen and K. M. Ko, "Ursolic-Acid-Enriched Herba Cynomorii Extract Protects against Oxidant Injury in H9c2 Cells and Rat Myocardium by Increasing Mitochondrial ATP Generation Capacity and Enhancing Cellular Glutathione Redox Cycling, Possibly through Mitochondrial Uncoupling," *Evidence-Based Complementary and Alternative Medicine*, vol. 2013, Article ID 924128, 14 pages, 2013.

[125] Y. Marunaka, R. Marunaka, H. Sun et al., "Actions of Quercetin, a Polyphenol, on Blood Pressure," *Molecules*, vol. 22, no. 2, p. 209, 2017.

[126] D. Xu, M.-J. Hu, Y.-Q. Wang, and Y.-L. Cui, "Antioxidant Activities of Quercetin and Its Complexes for Medicinal Application," *Molecules*, vol. 24, no. 6, p. 1123, 2019.

[127] Y. Lu, R. H. Wang, B. B. Guo, and Y. P. Jia, "Quercetin inhibits angiotensin II induced apoptosis via mitochondrial pathway in human umbilical vein endothelial cells," *European Review for Medical and Pharmacological Sciences*, vol. 20, no. 8, pp. 1609–1616, 2016.

[128] Y. Wen, Q. Guo, X. Yang et al., "High glucose concentrations in peritoneal dialysate are associated with all-cause and cardiovascular disease mortality in continuous ambulatory peritoneal dialysis patients," *Peritoneal Dialysis International: Journal of the International Society for Peritoneal Dialysis*, vol. 35, no. 1, pp. 70–77, 2015.

[129] R. P. Da, L. Meira, D. O. Souza, L. D. Bobermin, A. Quincozes-Santos, and M. C. Leite, "High-glucose medium induces cellular differentiation and changes in metabolic functionality of oligodendroglia," *Molecular Biology Reports*, vol. 46, no. 5, pp. 4817–4826, 2019.

[130] H. Kang, X. Ma, J. Liu, Y. Fan, and X. Deng, "High glucose-induced endothelial progenitor cell dysfunction," *Diabetes and Vascular Disease Research*, vol. 14, no. 5, pp. 381–394, 2017.

[131] A. V. Haas and M. E. McDonnell, "Pathogenesis of cardiovascular disease in diabetes," *Endocrinology and Metabolism Clinics of North America*, vol. 47, no. 1, pp. 51–63, 2018.

[132] N. Abuarab, T. S. Munsey, L. H. Jiang, J. Li, and A. Sivaprasadarao, "High glucose-induced ROS activates TRPM2 to trigger lysosomal membrane permeabilization and Zn2+-mediated mitochondrial fission," *Science Signaling*, vol. 10, no. 490, p. eaal4161, 2017.

[133] X. Wang, F. Yu, and W. Q. Zheng, "Aldose reductase inhibitor Epalrestat alleviates high glucose-induced cardiomyocyte apoptosis via ROS," *European Review for Medical and Pharmacological Sciences*, vol. 23, 3 Supplement, pp. 294–303, 2019.

[134] T. Rharass and S. Lucas, "High glucose level impairs human mature bone marrow adipocyte function through increased ROS production," *Frontiers in Endocrinology (Lausanne)*, vol. 10, p. 607, 2019.

[135] G. C. Parker, "Retraction of "High glucose via NOX-dependent ROS generation and AKT activity promotes adipose-derived stem cell de-differentiation"," *Stem Cells and Development*, vol. 21, no. 6, p. 995, 2012.

[136] J. Alcántar-Fernández, A. González-Maciel, R. Reynoso-Robles et al., "High-glucose diets induce mitochondrial dysfunction in Caenorhabditis elegans," *PLoS One*, vol. 14, no. 12, p. e226652, 2019.

[137] J. Zhang, Y. Guo, W. Ge, X. Zhou, and M. Pan, "High glucose induces the apoptosis of HUVECs in mitochondria dependent manner by enhancing VDAC1 expression," *Pharmazie*, vol. 73, no. 12, pp. 725–728, 2018.

[138] H. Mollazadeh, M. T. Boroushaki, M. Soukhtanloo, A. R. Afshari, and M. M. Vahedi, "Effects of pomegranate seed oil on oxidant/antioxidant balance in heart and kidney homogenates and mitochondria of diabetic rats and high glucose-treated H9c2 cell line," *Avicenna Journal of Phytomedicine*, vol. 7, no. 4, pp. 317–333, 2017.

[139] H. H. El, R. Vettor, and M. Rossato, "Cardiomyocyte mitochondrial dysfunction in diabetes and its contribution in cardiac arrhythmogenesis," *Mitochondrion*, vol. 46, pp. 6–14, 2019.

[140] S. Ghosh, T. Pulinilkunnil, G. Yuen et al., "Cardiomyocyte apoptosis induced by short-term diabetes requires mitochondrial GSH depletion," *American Journal of Physiology-Heart and Circulatory Physiology*, vol. 289, no. 2, pp. H768–H776, 2005.

[141] H. Liu, H. Peng, S. Chen et al., "S1PR2 antagonist protects endothelial cells against high glucose-induced mitochondrial apoptosis through the Akt/GSK-3β signaling pathway," *Biochemical and Biophysical Research Communications*, vol. 490, no. 3, pp. 1119–1124, 2017.

[142] S. O. Rotimi, I. B. Adelani, G. E. Bankole, and O. A. Rotimi, "Naringin enhances reverse cholesterol transport in high fat/low streptozocin induced diabetic rats," *Biomedicine & Pharmacotherapy*, vol. 101, pp. 430–437, 2018.

[143] R. Chen, Q. L. Qi, M. T. Wang, and Q. Y. Li, "Therapeutic potential of naringin: an overview," *Pharmaceutical Biology*, vol. 54, no. 12, pp. 3203–3210, 2016.

[144] H. Huang, K. Wu, Q. You, R. Huang, S. Li, and K. Wu, "Naringin inhibits high glucose-induced cardiomyocyte apoptosis by attenuating mitochondrial dysfunction and modulating the activation of the p38 signaling pathway," *International Journal of Molecular Medicine*, vol. 32, no. 2, pp. 396–402, 2013.

[145] K. Wang, X. Feng, L. Chai, S. Cao, and F. Qiu, "The metabolism of berberine and its contribution to the pharmacological effects," *Drug Metabolism Reviews*, vol. 49, no. 2, pp. 139–157, 2017.

[146] Q. Hou, W. J. He, Y. S. Wu, H. J. Hao, X. Y. Xie, and X. B. Fu, "Berberine: a traditional natural product with novel biological activities," *Alternative Therapies in Health and Medicine*, vol. 26, no. S2, pp. 20–27, 2020.

[147] W. Hang, B. He, J. Chen et al., "Berberine ameliorates high glucose-induced cardiomyocyte injury via AMPK signaling activation to stimulate mitochondrial biogenesis and restore autophagic flux," *Frontiers in Pharmacology*, vol. 9, p. 1121, 2018.

[148] R. Zhu, H. Liu, C. Liu et al., "Cinnamaldehyde in diabetes: a review of pharmacology, pharmacokinetics and safety," *Pharmacological Research*, vol. 122, pp. 78–89, 2017.

[149] D. Wang, J. Hou, Y. Yang et al., "Cinnamaldehyde ameliorates high-glucose-induced oxidative stress and cardiomyocyte injury through transient receptor potential ankyrin 1," *Journal of Cardiovascular Pharmacology*, vol. 74, no. 1, pp. 30–37, 2019.

[150] C. Colica, L. Di Renzo, V. Aiello, A. De Lorenzo, and L. Abenavoli, "Rosmarinic acid as potential anti-inflammatory agent," *Reviews on Recent Clinical Trials*, vol. 13, no. 4, pp. 240–242, 2018.

[151] M. Alagawany, M. E. A. El-Hack, M. R. Farag et al., "Rosmarinic acid: modes of action, medicinal values and health benefits," *Animal Health Research Reviews*, vol. 18, no. 2, pp. 167–176, 2017.

[152] J. Diao, J. Wei, R. Yan et al., "Rosmarinic Acid suppressed high glucose-induced apoptosis in H9c2 cells by ameliorating the mitochondrial function and activating STAT3," *Biochemical and Biophysical Research Communications*, vol. 477, no. 4, pp. 1024–1030, 2016.

[153] G. Gambato, E. M. Pavao, G. Chilanti, R. C. Fontana, M. Salvador, and M. Camassola, "Pleurotus albidus modulates mitochondrial metabolism disrupted by hyperglycaemia in EA.hy926 endothelial cells," *Biomed Research International*, vol. 2018, Article ID 2859787, 10 pages, 2018.

[154] Z. Ungvari, A. Labinskyy, P. Mukhopadhyay et al., "Resveratrol attenuates mitochondrial oxidative stress in coronary arterial endothelial cells," *American Journal of Physiology-Heart and Circulatory Physiology*, vol. 297, no. 5, pp. H1876–H1881, 2009.

[155] J. Wang and B. Yan, "A polysaccharide (PNPA) from _Pleurotus nebrodensis_ ameliorates hepatic ischemic/reperfusion (I/R) injury in rats," *International Journal of Biological Macromolecules*, vol. 105, Part 1, pp. 447–451, 2017.

[156] K. S. Kwon, J. H. Lee, K. S. So et al., "Aurantio-obtusin, an anthraquinone from cassiae semen, ameliorates lung inflammatory responses," *Phytotherapy Research*, vol. 32, no. 8, pp. 1537–1545, 2018.

[157] Y. Tang, Z. Y. Zhong, Y. F. Liu, and G. T. Sheng, "Obtusifolin inhibits high glucose-induced mitochondrial apoptosis in human umbilical vein endothelial cells," *Molecular Medicine Reports*, vol. 18, no. 3, pp. 3011–3019, 2018.

[158] K. S. Tang and J. S. Tan, "The protective mechanisms of polydatin in cerebral ischemia," *European Journal of Pharmacology*, vol. 842, pp. 133–138, 2019.

[159] N. Pang, T. Chen, X. Deng et al., "Polydatin prevents methylglyoxal-induced apoptosis through reducing oxidative stress and improving mitochondrial function in human umbilical vein endothelial cells*Oxidative Medicine and Cellular Longevity*," vol. 2017, Article ID 7180943, 9 pages, 2017.

[160] G. S. Hotamisligil, "Inflammation, metaflammation and immunometabolic disorders," *Nature*, vol. 542, no. 7640, pp. 177–185, 2017.

[161] L. Ferrucci and E. Fabbri, "Inflammageing: chronic inflammation in ageing, cardiovascular disease, and frailty," *Nature Reviews Cardiology*, vol. 15, no. 9, pp. 505–522, 2018.

[162] A. N. Orekhov, A. V. Poznyak, I. A. Sobenin, N. N. Nikifirov, and E. A. Ivanova, "Mitochondrion as a selective target for treatment of atherosclerosis: role of mitochondrial DNA mutations and defective mitophagy in the pathogenesis of atherosclerosis and chronic inflammation," *Current Neuropharmacology*, vol. 18, pp. 1064–1075, 2019.

[163] P. M. Smith and A. V. Ferguson, "Recent advances in central cardiovascular control: sex, ROS, gas and inflammation," *F1000Research*, vol. 5, p. 420, 2016.

[164] A. A. Manfredi and P. Rovere-Querini, "The mitochondrion–a Trojan horse that kicks off inflammation?," *New England Journal of Medicine*, vol. 362, no. 22, pp. 2132–2134, 2010.

[165] X. Wang, Z. Chen, X. Fan et al., "Inhibition of DNM1L and mitochondrial fission attenuates inflammatory response in fibroblast-like synoviocytes of rheumatoid arthritis," *Journal of Cellular and Molecular Medicine*, vol. 24, no. 2, pp. 1516–1528, 2019.

[166] H. A. Cooper, S. Cicalese, K. J. Preston et al., "Targeting mitochondrial fission as a potential therapeutic for abdominal aortic aneurysm," *Cardiovascular Research*, vol. 8, p. cvaa133, 2020.

[167] Z. Zhong, S. Liang, E. Sanchez-Lopez et al., "New mitochondrial DNA synthesis enables NLRP3 inflammasome activation," *Nature*, vol. 560, no. 7717, pp. 198–203, 2018.

[168] C. A. Piantadosi, "Mitochondrial DNA, oxidants, and innate immunity," *Free Radical Biology and Medicine*, vol. 152, pp. 455–461, 2020.

[169] D. Sun and F. Yang, "Metformin improves cardiac function in mice with heart failure after myocardial infarction by regulating mitochondrial energy metabolism," *Biochemical and Biophysical Research Communications*, vol. 486, no. 2, pp. 329–335, 2017.

[170] J. S. Riley and S. W. Tait, "Mitochondrial DNA in inflammation and immunity," *EMBO Reports*, vol. 21, no. 4, p. e49799, 2020.

[171] B. Wu, H. Ni, J. Li et al., "The impact of circulating mitochondrial DNA on cardiomyocyte apoptosis and myocardial injury after TLR4 activation in experimental autoimmune myocarditis," *Cellular Physiology and Biochemistry*, vol. 42, no. 2, pp. 713–728, 2017.

[172] B. Q. Zhang, G. Y. Zheng, Y. Han, X. D. Chen, and Q. Jiang, "Ilexonin A promotes neuronal proliferation and regeneration via activation of the canonical Wnt signaling pathway after cerebral ischemia reperfusion in rats," *Evidence-Based Complementary and Alternative Medicine*, vol. 2016, Article ID 9753189, 11 pages, 2016.

[173] B. Salehi, A. Venditti, M. Sharifi-Rad et al., "The therapeutic potential of apigenin," *International Journal of Molecular Sciences*, vol. 20, no. 6, p. 1305, 2019.

[174] S. Duarte, D. Arango, A. Parihar, P. Hamel, R. Yasmeen, and A. I. Doseff, "Apigenin protects endothelial cells from lipopolysaccharide (LPS)-induced inflammation by decreasing caspase-3 activation and modulating mitochondrial function," *International Journal of Molecular Sciences*, vol. 14, no. 9, pp. 17664–17679, 2013.

[175] Z. Wang, H. Zhang, Z. Liu, Z. Ma, D. An, and D. Xu, "Apigenin attenuates myocardial infarction-induced cardiomyocyte injury by modulating Parkin-mediated mitochondrial autophagy," *Journal of Biosciences*, vol. 45, 2020.

[176] Y. Zhu, M. Li, Y. Lu, J. Li, Y. Ke, and J. Yang, "Ilexgenin A inhibits mitochondrial fission and promote Drp1 degradation

by Nrf2-induced PSMB5 in endothelial cells," *Drug Development Research*, vol. 80, no. 4, pp. 481–489, 2019.

[177] J. Reiter, A. M. Hubbers, F. Albrecht, L. Leichert, and A. J. Slusarenko, "Allicin, a natural antimicrobial defence substance from garlic, inhibits DNA gyrase activity in bacteria," *International Journal of Medical Microbiology*, vol. 310, no. 1, p. 151359, 2020.

[178] P. Shi, Y. Cao, J. Gao et al., "Allicin improves the function of cardiac microvascular endothelial cells by increasing PECAM-1 in rats with cardiac hypertrophy," *Phytomedicine*, vol. 51, pp. 241–254, 2018.

[179] M. Zhang, H. Pan, Y. Xu, X. Wang, Z. Qiu, and L. Jiang, "Allicin decreases lipopolysaccharide-induced oxidative stress and inflammation in human umbilical vein endothelial cells through suppression of mitochondrial dysfunction and activation of Nrf2," *Cellular Physiology and Biochemistry*, vol. 41, no. 6, pp. 2255–2267, 2017.

[180] X. H. Li, C. Y. Li, Z. G. Xiang et al., "Allicin ameliorates cardiac hypertrophy and fibrosis through enhancing of Nrf2 antioxidant signaling pathways," *Cardiovascular Drugs and Therapy*, vol. 26, no. 6, pp. 457–465, 2012.

[181] O. C. Baltatu, F. G. Amaral, L. A. Campos, and J. Cipolla-Neto, "Melatonin, mitochondria and hypertension," *Cellular and Molecular Life Sciences*, vol. 74, no. 21, pp. 3955–3964, 2017.

[182] D. A. Lowes, A. M. Almawash, N. R. Webster, V. L. Reid, and H. F. Galley, "Melatonin and structurally similar compounds have differing effects on inflammation and mitochondrial function in endothelial cells under conditions mimicking sepsis," *British Journal of Anaesthesia*, vol. 107, no. 2, pp. 193–201, 2011.

[183] L. Lieben, "Lipid toxicity drives renal disease," *Nature Reviews Nephrology*, vol. 13, no. 4, p. 194, 2017.

[184] A. Ghosh, L. Gao, A. Thakur, P. M. Siu, and C. Lai, "Role of free fatty acids in endothelial dysfunction," *Journal of Biomedical Science*, vol. 24, no. 1, p. 50, 2017.

[185] S. Bo, M. Seletto, A. Choc et al., "The acute impact of the intake of four types of bread on satiety and blood concentrations of glucose, insulin, free fatty acids, triglyceride and acylated ghrelin. A randomized controlled cross-over trial," *Food Research International*, vol. 92, pp. 40–47, 2017.

[186] J. E. Schaffer, "Lipotoxicity: when tissues overeat," *Current Opinion in Lipidology*, vol. 14, no. 3, pp. 281–287, 2003.

[187] J. A. Mayr, "Lipid metabolism in mitochondrial membranes," *Journal of Inherited Metabolic Disease*, vol. 38, no. 1, pp. 137–144, 2015.

[188] J. Vamecq, A. F. Dessein, M. Fontaine et al., "Mitochondrial dysfunction and lipid homeostasis," *Current Drug Metabolism*, vol. 13, no. 10, pp. 1388–1400, 2012.

[189] R. Abeti, M. H. Parkinson, I. P. Hargreaves et al., "Mitochondrial energy imbalance and lipid peroxidation cause cell death in Friedreich's ataxia," *Cell Death & Disease*, vol. 7, no. 5, p. e2237, 2016.

[190] O. V. Ketsa, I. O. Shmarakov, and M. M. Marchenko, "Lipid peroxidation in cardiac mitochondrial fraction of rats exposed to different supplementation with polyunsaturated fatty acids," *Biomed Khim*, vol. 62, no. 1, pp. 50–55, 2016.

[191] I. Cavallari, A. Delli Veneri, E. Maddaloni et al., "Comparison of lipid-lowering medications and risk for cardiovascular disease in diabetes," *Current Diabetes Reports*, vol. 18, no. 12, p. ???, 2018.

[192] J. White, D. I. Swerdlow, D. Preiss et al., "Association of lipid fractions with risks for coronary artery disease and diabetes," *JAMA Cardiology*, vol. 1, no. 6, pp. 692–699, 2016.

[193] M. Chakraborty, P. Singh, J. Dsouza, K. Pethusamy, and P. V. Thatkar, "Fasting and postprandial lipid parameters: A comparative evaluation of cardiovascular risk assessment in pre-diabetes and diabetes," *Journal of Family Medicine and Primary Care*, vol. 9, no. 1, pp. 287–292, 2020.

[194] A. M. Chamberlain, S. S. Cohen, J. M. Killian, K. L. Monda, S. A. Weston, and T. Okerson, "Lipid-lowering prescription patterns in patients with diabetes mellitus or cardiovascular disease," *American Journal of Cardiology*, vol. 124, no. 7, pp. 995–1001, 2019.

[195] H. E. Kim, A. R. Grant, M. S. Simic et al., "Lipid biosynthesis coordinates a mitochondrial-to-cytosolic stress response," *Cell*, vol. 166, no. 6, pp. 1539–1552.e16, 2016.

[196] D. L. Hickson-Bick, C. Jones, and L. M. Buja, "Stimulation of mitochondrial biogenesis and autophagy by lipopolysaccharide in the neonatal rat cardiomyocyte protects against programmed cell death," *Journal of Molecular and Cellular Cardiology*, vol. 44, no. 2, pp. 411–418, 2008.

[197] A. Xu, J. Liu, P. Liu, M. Jia, H. Wang, and L. Tao, "Mitochondrial translocation of Nur77 induced by ROS contributed to cardiomyocyte apoptosis in metabolic syndrome," *Biochem Biophys Res Commun*, vol. 446, no. 4, pp. 1184–1189, 2014.

[198] K. Tsilingiri, H. de la Fuente, M. Relaño et al., "Oxidized low-density lipoprotein receptor in lymphocytes prevents atherosclerosis and predicts subclinical disease," *Circulation*, vol. 139, no. 2, pp. 243–255, 2019.

[199] W. Y. Chen, Y. F. Chen, H. C. Chan et al., "Role of apolipoprotein E in electronegative low-density lipoprotein-induced mitochondrial dysfunction in cardiomyocytes," *Metabolism-Clinical and Experimental*, vol. 107, p. 154227, 2020.

[200] Y. Zeng, J. Xu, Y. Q. Hua, Y. Peng, and X. L. Xu, "MDM2 contributes to oxidized low-density lipoprotein-induced inflammation through modulation of mitochondrial damage in endothelial cells," *Atherosclerosis*, vol. 305, pp. 1–9, 2020.

[201] N. Stefanello, R. M. Spanevello, S. Passamonti et al., "Coffee, caffeine, chlorogenic acid, and the purinergic system," *Food and Chemical Toxicology*, vol. 123, pp. 298–313, 2019.

[202] M. Naveed, V. Hejazi, M. Abbas et al., "Chlorogenic acid (CGA): A pharmacological review and call for further research," *Biomedicine & Pharmacotherapy*, vol. 97, pp. 67–74, 2018.

[203] J. Tosovic, S. Markovic, M. J. Dimitric, M. Mojovic, and D. Milenkovic, "Antioxidative mechanisms in chlorogenic acid," *Food Chemistry*, vol. 237, pp. 390–398, 2017.

[204] K. L. Tsai, C. H. Hung, S. H. Chan et al., "Chlorogenic acid protects against oxLDL-induced oxidative damage and mitochondrial dysfunction by modulating SIRT1 in endothelial cells," *Molecular Nutrition & Food Research*, vol. 62, no. 11, p. ???, 2018.

[205] S. du, H. Liu, T. Lei et al., "Mangiferin: An effective therapeutic agent against several disorders (Review)," *Molecular Medicine Reports*, vol. 18, no. 6, pp. 4775–4786, 2018.

[206] T. Jiang, F. Han, G. Gao, and M. Liu, "Mangiferin exert cardioprotective and anti-apoptotic effects in heart failure induced rats," *Life Sciences*, vol. 249, p. 117476, 2020.

[207] L. Z. Ding, X. Teng, Z. B. Zhang, C. J. Zheng, and S. H. Chen, "Mangiferin inhibits apoptosis and oxidative stress via

Retraction

Retracted: Total Glucosides of Peony Protect Cardiomyocytes against Oxidative Stress and Inflammation by Reversing Mitochondrial Dynamics and Bioenergetics

Oxidative Medicine and Cellular Longevity

This article has been retracted by Hindawi following an investigation undertaken by the publisher [1]. This investigation has uncovered evidence of one or more of the following indicators of systematic manipulation of the publication process:

(1) Discrepancies in scope
(2) Discrepancies in the description of the research reported
(3) Discrepancies between the availability of data and the research described
(4) Inappropriate citations
(5) Incoherent, meaningless and/or irrelevant content included in the article
(6) Peer-review manipulation

The presence of these indicators undermines our confidence in the integrity of the article's content and we cannot, therefore, vouch for its reliability. Please note that this notice is intended solely to alert readers that the content of this article is unreliable. We have not investigated whether authors were aware of or involved in the systematic manipulation of the publication process.

Wiley and Hindawi regrets that the usual quality checks did not identify these issues before publication and have since put additional measures in place to safeguard research integrity.

We wish to credit our own Research Integrity and Research Publishing teams and anonymous and named external researchers and research integrity experts for contributing to this investigation.

The corresponding author, as the representative of all authors, has been given the opportunity to register their agreement or disagreement to this retraction. We have kept a record of any response received.

References

[1] M. Wang, Q. Li, Y. Zhang, and H. Liu, "Total Glucosides of Peony Protect Cardiomyocytes against Oxidative Stress and Inflammation by Reversing Mitochondrial Dynamics and Bioenergetics," *Oxidative Medicine and Cellular Longevity*, vol. 2020, Article ID 6632413, 12 pages, 2020.

Research Article

Total Glucosides of Peony Protect Cardiomyocytes against Oxidative Stress and Inflammation by Reversing Mitochondrial Dynamics and Bioenergetics

Mengmeng Wang [ID],[1] Qiang Li,[2] Ying Zhang,[3] and Hao Liu[4]

[1]*Department of Rheumatism and Immunology, Tianjin First Central hospital, Tianjin, China*
[2]*Department of Pharmacy, Tianjin Union Medical Center, Tianjin, China*
[3]*Department of Cardiology, Chinese PLA General Hospital, Beijing, China*
[4]*Department of Pharmacy, Nankai University, Tianjin, China*

Correspondence should be addressed to Mengmeng Wang; doublemeng373@sina.com

Total glucosides of peony (TGP) are used to treat rheumatoid arthritis and systemic lupus erythematosus. We explored the protective effects of TGP on cardiomyocyte oxidative stress and inflammation in the presence of hydrogen peroxide by focusing on mitochondrial dynamics and bioenergetics. Our study demonstrated that hydrogen peroxide significantly repressed cardiomyocyte viability and promoted cell apoptosis through induction of the mitochondrial death pathway. TGP treatment sustained cardiomyocyte viability, reduced cardiomyocyte apoptosis, and decreased inflammation and oxidative stress. Molecular investigation indicated that hydrogen peroxide caused mitochondrial dynamics disruption and bioenergetics reduction in cardiomyocytes, but this alteration could be normalized by TGP. We found that disruption of mitochondrial dynamics abolished the regulatory effects of TGP on mitochondrial bioenergetics; TGP modulated mitochondrial dynamics through the AMP-activated protein kinase (AMPK) pathway; and inhibition of AMPK alleviated the protective effects of TGP on mitochondria. Our results showed that TGP treatment reduces cardiomyocyte oxidative stress and inflammation in the presence of hydrogen peroxide by correcting mitochondrial dynamics and enhancing mitochondrial bioenergetics. Additionally, the regulatory effects of TGP on mitochondrial function seem to be mediated through the AMPK pathway. These findings are promising for myocardial injury in patients with rheumatoid arthritis and systemic lupus erythematosus.

1. Introduction

Total glucosides of peony (TGP) are used to treat rheumatoid arthritis and systemic lupus erythematosus [1] as well as hepatitis, dysmenorrhea, muscle cramps, and spasms. The active components of TGP include monoterpene glycosides, galloyl glucoses, and phenolic compounds [2]. In long-term clinical use, TGP have therapeutic effects and no severe side effects [3–5]. Anti-inflammatory activity has been identified as the primary molecular mechanism underlying TGP [6]. In animal studies, TGP administration has been shown to impair inflammation cell activation and recruitment [4]. Inflammation-related signaling pathways such as NF-κB

[7] and home oxygenase-1 are also regulated by TGP [8]. TGP has also been used as an antioxidant to decrease reactive oxygen species (ROS) production and oxidative stress [9, 10]. TGP treatment activates the Nrf2 signaling pathway, contributing to the transcriptional upregulation of antioxidative factors such as superoxide dismutase (SOD) and glutathione (GSH) [11, 12]. The anti-inflammatory and anti-oxidative properties of TGP make it a promising option for the treatment of diabetic nephropathy [13], kidney injury [14], fatty liver disease [15], and pulmonary arterial hypertension [16]. However, the regulatory effects of TGP on cardiomyocyte (patho)physiological responses have not been fully explored.

Cardiomyocyte oxidative stress and inflammation are risk factors for the development of cardiovascular diseases such as ischemic heart disorder, myocardial ischemia-reperfusion injury, diabetic cardiomyopathy, myocardial fibrosis, and hypertension [17–20]. At the molecular level, cardiomyocytes contain abundant mitochondria, which generate adenosine triphosphate (ATP) to mediate cardiomyocyte contractility [21, 22]. However, damaged mitochondria cannot transfer electrons, which subsequently convert into ROS [23]. Excessive ROS production is associated with cardiomyocyte oxidative stress [24, 25] resulting in cardiomyocyte dysfunction or death. Oxidative stress is also followed by increased inflammation, which is used to repair damaged myocardium or remove dead cardiomyocytes [26–28]. However, uncontrolled inflammation promotes myocardial edema, induces the accumulation of inflammation cells, and augments cytokine release, a process that attends cardiac fibroblast proliferation and collagen deposition [29, 30]. These pathological alterations have been observed in postinfarction cardiac injury, heart failure, and diabetic cardiomyopathy [31, 32]. In this study, we verified whether TGP can attenuate mitochondrial damage and thus repress oxidative stress and inflammation in cardiomyocytes.

Mitochondria regulate cardiomyocyte oxidative stress and inflammation [33, 34]. Impaired mitochondrial metabolism is followed by ROS production and inflammation. Several mechanisms have been proposed to explain impaired mitochondrial metabolism, such as mitochondrial complex inactivation and mitochondrial metabolism switch from oxidative phosphorylation to glycolysis [35, 36]. It is necessary to explore whether TGP has the ability to normalize mitochondrial metabolism in cardiomyocytes. Recent studies have reported that disruption of mitochondrial dynamics, an alteration of mitochondrial morphology, functions upstream of mitochondrial metabolism switching [37, 38]. However, it is unclear whether TGP affects cardiomyocyte function and viability by affecting mitochondrial dynamics and bioenergetics. This study explored the protective effect of TGP on cardiomyocyte oxidative stress and inflammation by focusing on mitochondrial dynamics and bioenergetics.

2. Materials and Methods

2.1. Cell Cultures.
The H9C2 cardiomyocyte cell line was purchased from the Beijing Union Cell Resource Center. H9C2 cells were cultivated in DMEM (Gibco, USA) medium supplemented with 15% fetal bovine serum (FBS) (modified, Gibco, USA), 100 IU/mL penicillin, and 100 μg/mL streptomycin in a 5% CO_2 incubator at 37°C. Hydrogen peroxide (0.3 mM) was added to the medium to induce oxidative stress. TGP purchased from Sigma was added to the medium at a final concentration of 300 mol/L for 24 hours before hydrogen peroxide treatment [39].

2.2. Mitochondrial Membrane Potential and Mitochondrial ROS Detection.
To observe mitochondrial membrane potential, we added 5 mg/L JC-1 staining buffer to the cardiomyocyte medium for 30 min in the dark. Cells were then washed with PBS to remove free JC-1. Using a multifunctional

microplate reader, we set the excitation light to 490 nm and the emission light to 530 nm to detect JC-1 monomers, and we set the excitation light to 525 nm and the emission light to 590 nm to detect JC-1 polymers [40]. We used the ratio of red to green fluorescence to measure the degree of mitochondrial membrane potential depolarization.

2.3. Determination of the Opening Level of Mitochondrial Permeability Transition Pore (mPTP).
After cells were collected, we turned on the multifunctional microplate reader in advanced mode and set the temperature to 25°C and the wavelength to 540 nm (reading starting at 10 min and every 30 sec until 30 min); before initiating the program, we set it to zero. Next, we pipetted 20 μL of cell suspension concentrated at 10 μg/μL into the corresponding wells of a 96-well plate. We then added 170 μL of buffer Reagent A, mixed it well, and immediately placed it into the microplate reader (wavelength, 540 nm) to read the absorbance value at A540 [41]. After the samples stood at room temperature for 1 min, we reread the absorbance value at A540. At that point, the recorded initial A540 value was 0 min. Next, we added 10 μL of Reagent B and mixed it well [42]. We immediately put the plate into the multifunctional microplate reader (wavelength, 540 nm) and dynamically recorded the change values of the actual absorbance value for 10 min. Finally, we calculated the ratio of absorbance (A540/initial A540).

2.4. Detection of Mitochondrial Morphology.
Mitochondrial morphology was evaluated in H9c2 cells that were incubated with a 100 nM MitoTracker Green probe (Thermo Fisher Scientific, Waltham, MA, USA) for 30 min at 37°C. Images were acquired using a confocal laser scanning microscope (FV 1000, Olympus, Tokyo, Japan) [43]. The percentage of cells with fragmented mitochondria (small and round) was determined.

2.5. Immunofluorescence.
After fixation with 4% paraformaldehyde, the cells were permeated with 0.5% Triton X-100 for 15 min, blocked with 10% donkey serum for 30 min, and stained with a TdT-mediated dUTP Nick-End Labeling (TUNEL) Kit (C1086, Beyotime, Shanghai, China) according to the manufacturer's instructions. The slides or cells were incubated with the TUNEL cocktail for 1 h. After washing with PBS 3 times, the slides or cells were incubated with sarcomeric α actinin and LC3B antibodies overnight at 4°C [44]. The next day, the slides or cells were incubated with secondary antibodies, wheat germ agglutinin (WGA), and 4',6-diamidino-2-phenylindole (DAPI) for 30 min. Three researchers who were blind to the sample identified quantified TUNEL by either manual counting or digital thresholding. This included image segmentation and the creation of a binary image from grayscale [45]. We analyzed the converted binary images using the ImageJ software (NIH, Bethesda, MA, USA; Laboratory for Optical and Computational Instrumentation, University of Wisconsin-Madison, WI, USA).

2.6. Mitochondrial ROS Assay.
The production of mitochondrial ROS in the H9C2 cells was detected using a MitoSOX red mitochondrial superoxide indicator (Molecular Probes, USA). After various treatments, H9C2 cells were incubated

with MitoSOX ($10 \mu M$) and stained in the dark at 37°C for 30 min. The fluorescent image was then captured by a fluorescence microscope, and the fluorescence intensity was calculated using the ImageJ software [46].

2.7. Measurement of Caspase-3 Activity. Caspase-3 activity was determined by measuring the generation of the fluorogenic cleavage product methylcoumarylamide using a Caspase-3 Activity Assay Kit (Beyotime, Shanghai, China) according to the manufacturer's instructions [47]. H9C2 cells were briefly homogenized in an ice-cold buffer and then centrifuged at 1000 *g* for 5 min. After centrifugation, the supernatant was transferred to a new tube for caspase-3 activity testing. Fluorescence from a $100 \mu L$ sample was assayed in fluorescent spectrophotometry with $100 \mu L$ of detection buffer and then normalized by protein concentration [48].

2.8. siRNA Knockdown. Drp1 siRNAs were purchased from Dharmacon (OnTarget-Plus Smart Pool). Cells were washed and incubated with 20 nM siRNA in OptiMEM media (Life Technologies #31985070) supplemented with 1 : 50 Oligofectamine (Life Technologies #12252011) for 5 hours. Cells were then washed with 1X PBS and incubated overnight with DMEM supplemented with 30% FBS and no antibiotics [49]. The next day, the cells were washed with 1X PBS and used for the experiments.

2.9. Measurement of Inflammation Factors Levels. The levels of MCP1 and TNFα were measured using ELISA kits following the protocols provided by the manufacturer (R&D Systems, Inc. MN) [50].

2.10. SDS/PAGE and Immunoblotting. Samples were briefly heated to 50°C for 5 min in beta-mercaptoethanol 4x loading buffer and then run on 4-20% Criterion precast gels (Bio-Rad, CA) in 0.1% SDS Tris glycine running buffer. The SDS-PAGE-resolved proteins were transferred to iBlot stacks with regular PVDF membranes using the Life Technologies iBlot 2 system. Nonspecific binding sites were blocked with 5% nonfat dry milk in PBS-T ($3 mM KH_2PO_4$, 10 mM Na_2HPO_4, 150 mM NaCl, 0.1% Tween 20, and pH 7.2-7.4) for 30 min at room temperature. Membranes were then incubated with specific primary antibodies diluted in 5% nonfat dry milk in PBS-T overnight at 4°C. After washing 3 times for 10 min, membranes were incubated with horseradish peroxidase conjugated secondary antibodies diluted in 5% nonfat dry milk in PBS-T for 1 h. After washing 3 times for 10 min, protein-antibody reactions were detected by SuperSignal chemiluminescence (Pierce Biotechnology Inc., Rockford, IL) and imaged using the Image Lab software 5 (Bio-Rad). Protein densities were measured using the Image Lab software 5 [51]. For Western blot tests of total cell extraction, a classic Bradford protein concentration assay was used for protein quantification; 30-50 μg of protein was suspended in 4x Laemmli buffer to load a final volume of 30 μL. Samples were not reduced for Western blot tests of biotinylation. Western blots against the NaV 1.5 protein were performed, and then the membranes were stripped and reblotted with conjugated streptavidin HRP [52].

2.11. Measurement of Lactate Product and Adenosine Triphosphate (ATP) Level. The L-Lactate Assay Kit and the ATP Assay Kit (both from Sigma-Aldrich, Taufkirchen, Germany) were used according to the manufacturer's instructions to determine the levels of lactate product and ATP [53].

2.12. Real-Time Polymerase Chain Reaction (PCR). Total RNA was extracted from samples using TRIzol Reagent (Thermo Fisher) and digested with DNase I (Invitrogen) to eliminate genomic DNA. cDNA was synthetized using the SuperScript III First-Strand Synthesis System for RT-PCR (Invitrogen) according to the manufacturer's instructions [54]. Real-time PCR was performed using the QuantiFast SYBR Green PCR Kit (Qiagen) and the StepOnePlus Real-Time PCR System (Applied Biosystems). Ct values were normalized with respect to β-actin. Fold change was calculated with respect to sham vehicle [55].

2.13. Statistics. All data are expressed as mean ± SEM. Statistical differences were measured using a paired or unpaired two-sided Student's *t*-test and one-way ANOVA with Bonferroni or Dunnett corrections for multiple comparisons when appropriate. A value of $P < 0.05$ was considered statistically significant. Data analysis was performed using the GraphPad Prism software, version 7 (GraphPad Software, San Diego, CA).

3. Results

3.1. TGP Administration Significantly Reduces Cardiomyocyte Apoptosis and Inflammation in the Presence of Hydrogen Peroxide. In this study, cardiomyocytes were pretreated with TGP and then cultured with hydrogen peroxide to induce oxidative stress and inflammation. Cardiomyocyte viability was then determined using a CCK-8 assay. Compared to the control group, hydrogen peroxide administration significantly reduced cell viability, but this alteration could be attenuated by the TGP treatment (Figure 1(a)). Western blots were used to analyze the alteration of apoptosis-related proteins. As shown in Figures 1(b)–1(e), compared to the control group, the expression of caspase-9, Bax, and Bad was elevated by hydrogen peroxide, but this trend could be inhibited by TGP pretreatment. This data indicates that cardiomyocyte viability can be reversed by TGP in the presence of hydrogen peroxide.

Next, we analyzed the alteration of inflammation factors in response to TGP treatment. The levels of proinflammatory factors such as TNFα and MCP1 were upregulated in response to hydrogen peroxide treatment (Figures 1(f) and 1(g)). However, TGP exerts anti-inflammatory action to prevent the activation of proinflammatory factors (Figures 1(f) and 1(g)). These results indicate that TGP administration reduces cardiomyocyte apoptosis and inflammation in the presence of hydrogen peroxide.

3.2. Cardiomyocyte Oxidative Stress Is Attenuated by TGP. To understand the alteration of oxidative stress in TGP-treated cardiomyocytes, a mitochondrial ROS probe was used. As shown in Figures 2(a) and 2(b), compared to the control group, the levels of mitochondrial ROS were upregulated in

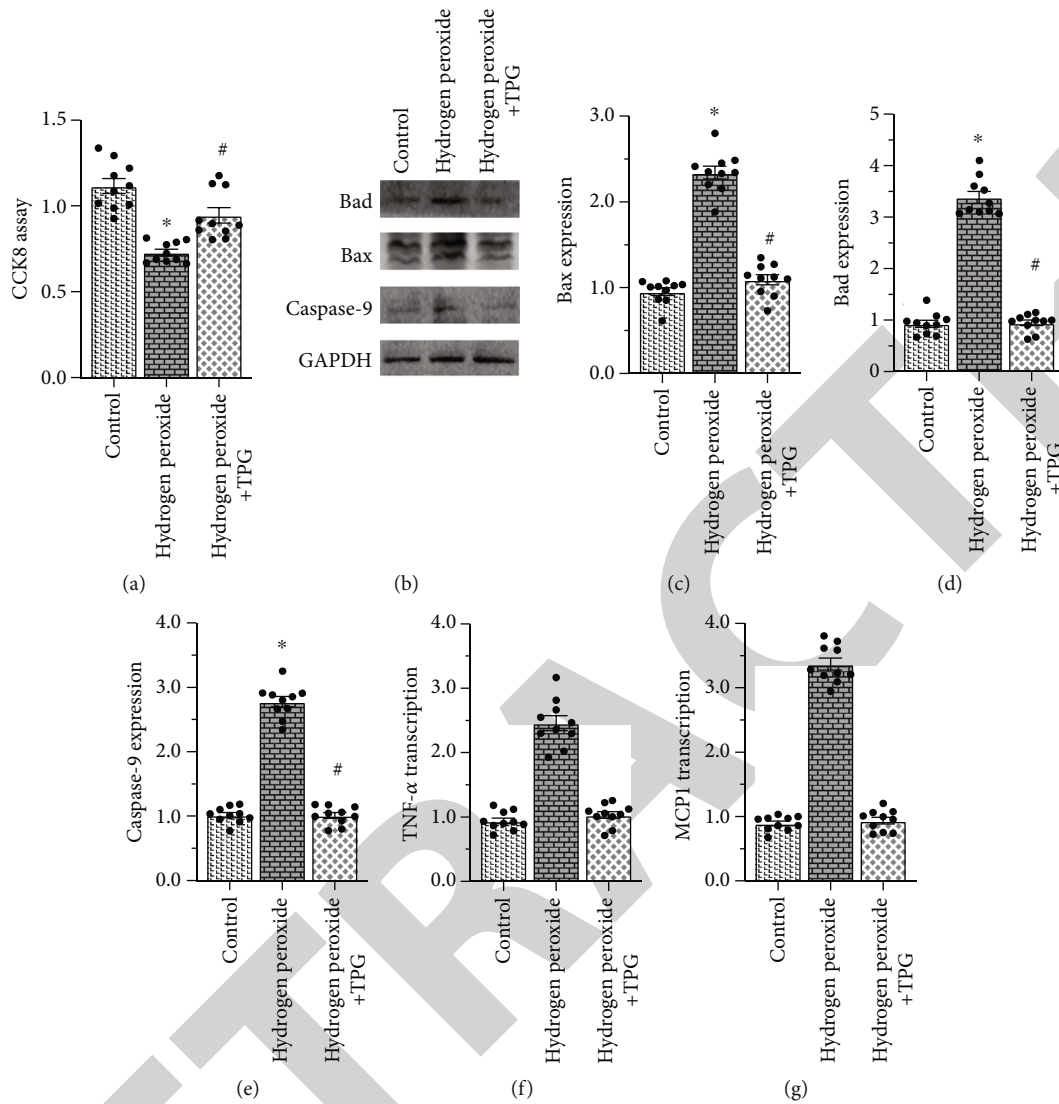(a)   (b)   (c)   (d)

(e)   (f)   (g)

Figure 1: TGP treatment attenuates cardiomyocyte apoptosis and inflammation induced by hydrogen peroxide. (a) Cardiomyocyte cell viability was determined using a CCK-8 assay. (b–e) Western blots were used to observe the alterations of caspase-9, Bax, and Bad in cardiomyocytes treated with TGP in the presence of hydrogen peroxide. (f, g) RNA was isolated from cardiomyocytes, then the transcription of MCP1α and MCP1 was analyzed using qPCR. $*p < 0.05$.

response to hydrogen peroxide treatment. TGP treatment repressed the production of mitochondrial ROS in cardiomyocytes (Figures 2(a) and 2(b)), supporting the antioxidative effects of TGP on hydrogen peroxide-treated cardiomyocytes. Decreased ROS production results from two molecular mechanisms; one is driven by the enhanced antioxidative action of TGP, and the other is involved in decreased ROS production in mitochondria. Therefore, we analyzed the alteration of antioxidative factors in response to TGP treatment. As shown in Figures 2(c)–2(e), compared to the control group, the activity of antioxidative enzymes such as SOD, GSH, and glutathione peroxidase (GPX) was reduced by hydrogen peroxide, but this alteration could be reversed by TGP, suggesting that TGP treatment enhanced the anti-oxidative defense system in hydrogen peroxide-treated cardiomyocytes. We also analyzed the regulatory effect of TGP on mitochondrial complexes I and III, which

are the primary sites for ROS production. As shown in Figures 2(f) and 2(g), compared to the control group, the activity of complex I/III was downregulated by hydrogen peroxide in cardiomyocytes. Decreased complex I/III cannot capture electrons, resulting in ROS production [28]. In comparison, TGP treatment drastically improved the activities of complex I/III in hydrogen peroxide-treated cardiomyocytes (Figures 2(f) and 2(g)). These results indicate that TGP-afforded antioxidative action is mediated by increased antioxidative stress and decreased mitochondrial ROS production.

3.3. Mitochondrial Dynamics and Bioenergetics Are Normalized by TGP. Mitochondrial dynamics and bioenergetics are closely associated with cardiomyocyte damage, especially oxidative stress and inflammation [37]. Thus, we analyzed the regulatory effects of TGP on mitochondrial
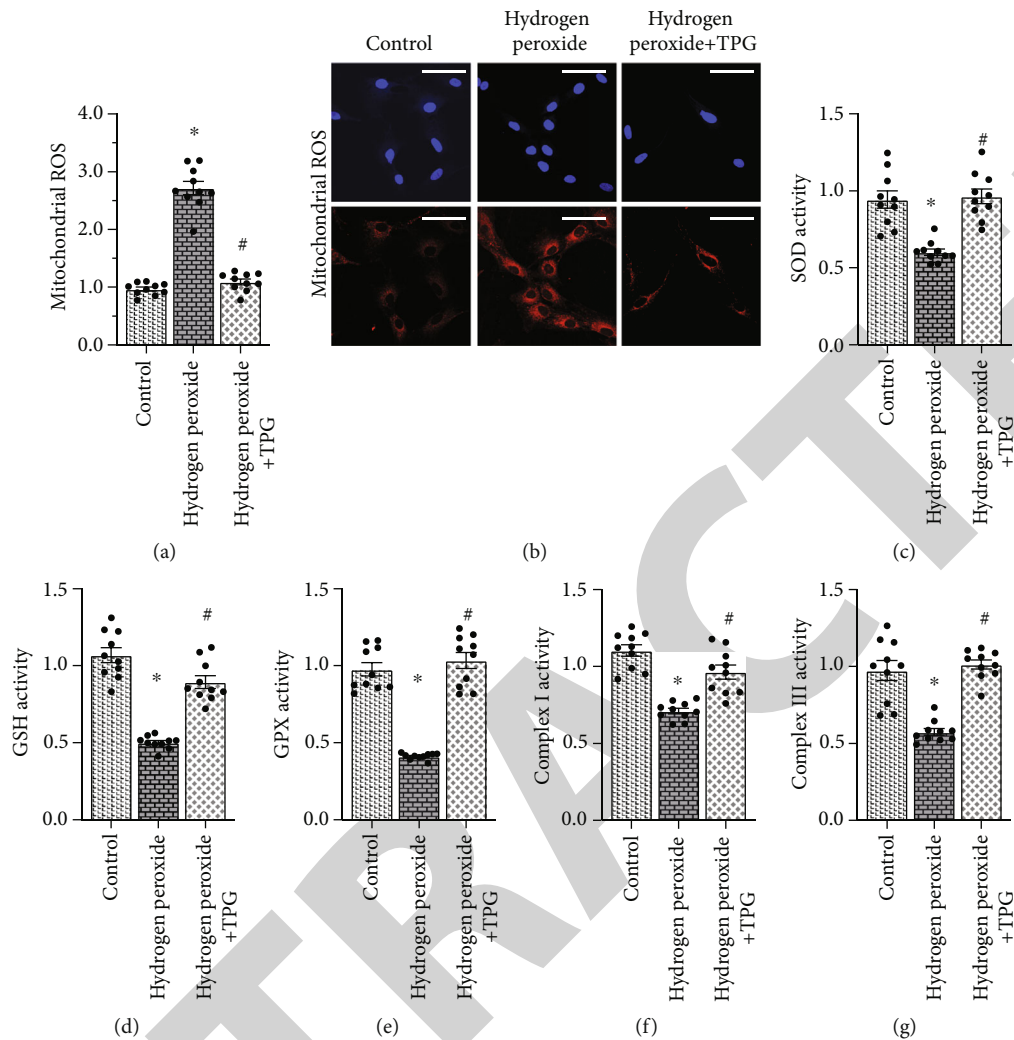
Figure 2: Cardiomyocyte oxidative stress is attenuated by TGP. (a, b) Mitochondrial ROS was determined through immunofluorescence in response to TGP treatment. (c–e) The levels of antioxidative stress, including SOD, GSH, and GXP, were measured by ELISA. (f, g) The activity of mitochondrial complexes I and III was determined by ELISA. $*p < 0.05$.

dynamics and bioenergetics. First, mitochondrial membrane potential, the marker of mitochondrial bioenergetics, was stained by JC-1. Hydrogen peroxide treatment significantly reduced mitochondrial membrane potential (Figures 3(a) and 3(b)), represented by decreased red fluorescence and increased green fluorescence. TGP treatment stabilized mitochondrial membrane potential in the presence of hydrogen peroxide. Cellular ATP production was also derived from mitochondrial bioenergetics. As shown in Figure 3(c), compared to the control group, hydrogen peroxide reduced the ATP content, whereas TGP favored ATP synthesis in cardiomyocytes. These results indicate that mitochondrial bioenergetics can be stabilized by TGP in hydrogen peroxide-treated cardiomyocytes.

Immunofluorescence also demonstrated a fragmented mitochondrial network in hydrogen peroxide-treated cardiomyocytes (Figures 3(d)–3(f)), suggesting a disruption in mitochondrial dynamics. RNA analysis demonstrated that mitochondrial fission genes were upregulated, whereas the transcription of mitochondrial fusion genes was drastically

repressed in hydrogen peroxide-treated cardiomyocytes (Figures 3(g) and 3(h)). In TGP-treated cardiomyocytes, the normal mitochondrial network was sustained, and the ratio of fragmented mitochondria was reduced, followed by normalization of mitochondrial dynamics. To understand whether mitochondrial dynamics function upstream of bioenergetics, an adenovirus-mediated Drp1 overexpression assay was conducted. In Drp1-overexpressed cardiomyocytes, TGP failed to sustain ATP production (Figure 3(i)), suggesting that TGP regulated bioenergetics by normalizing mitochondrial dynamics.

3.4. Induction of Mitochondrial Fission Abolishes the Beneficial Effects of TGP on Mitochondrial Function and Cardiomyocyte Viability. To understand whether mitochondrial dynamics are required for TGP-sustained mitochondrial function and cardiomyocyte viability, Drp1-mediated mitochondrial fission was induced in TGP-treated cardiomyocytes. Mitochondrial function and cardiomyocyte viability were then remeasured. As shown in Figures 4(a) and 4(b),

(a)

(b)

(c)

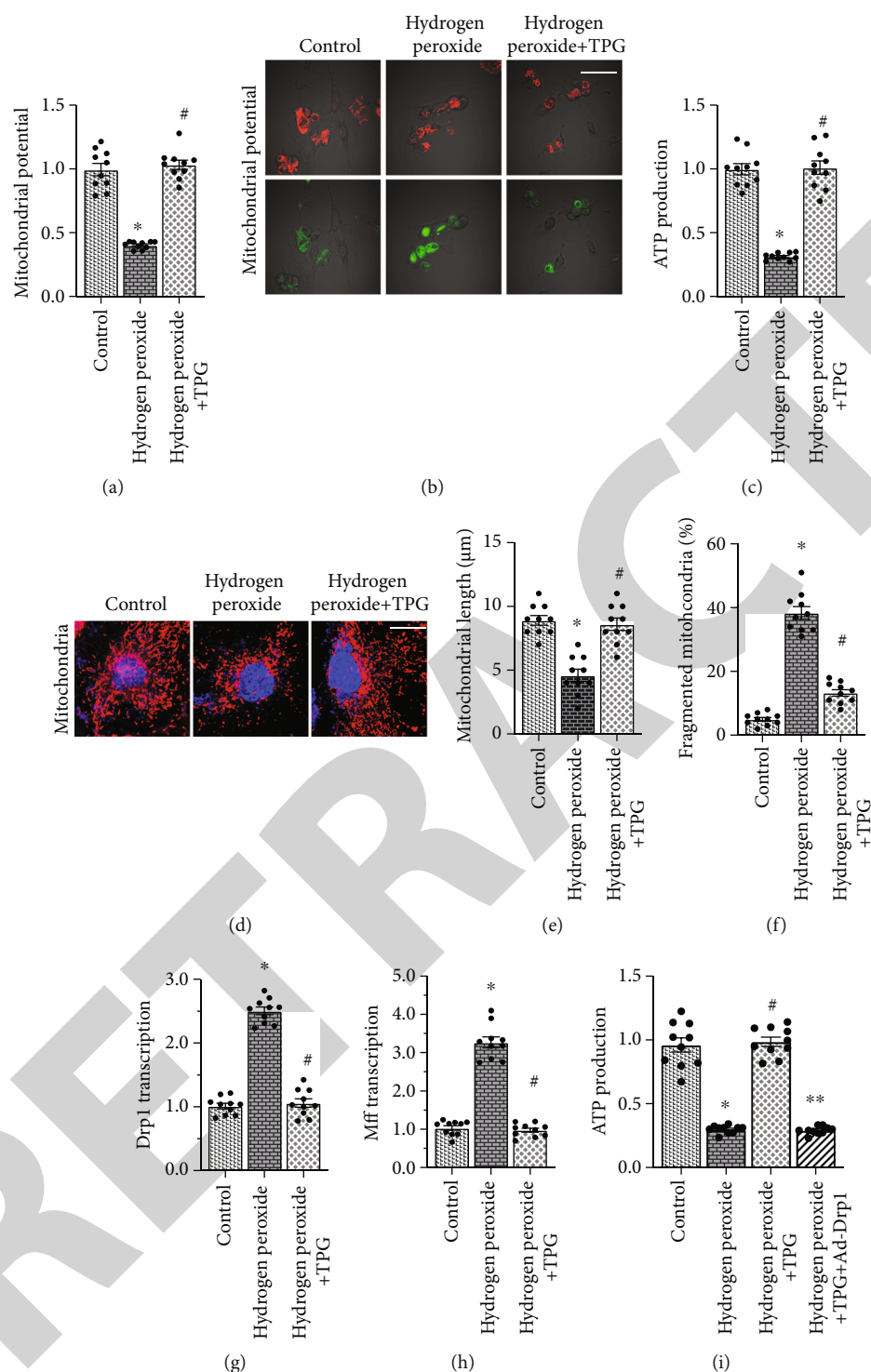(d)

(e)

(f)

(g)

(h)

(i)

Figure 3: Mitochondrial dynamics and bioenergetics are normalized by TGP. (a, b) Mitochondrial membrane potential was observed using a JC-1 probe. (c) ATP production was measured by ELISA in cardiomyocytes treated with TGP. (d–f) Mitochondrial morphology was observed through immunofluorescence. (g, h) RNA was isolated from cardiomyocytes, then the transcription of MCP1α and MCP1 was analyzed using qPCR. (i) ATP production was determined by ELISA in cardiomyocytes transfected with Drp1 adenovirus. $*p < 0.05$.

compared to the control group, although TGP repressed mitochondrial ROS production, this effect was abolished by Drp1 overexpression. In Drp1-overexpressed cardiomyocytes, TGP failed to sustain mitochondrial potential in the presence of hydrogen peroxide (Figures 4(c) and 4(d)). These

results indicate that TGP controlled mitochondrial function by correcting disrupted mitochondrial dynamics.

In addition, hydrogen peroxide-mediated cardiomyocyte viability reduction could be reversed by TGP, but this protective effect was undetectable in Drp1-overexpressed cardiomyocytes.
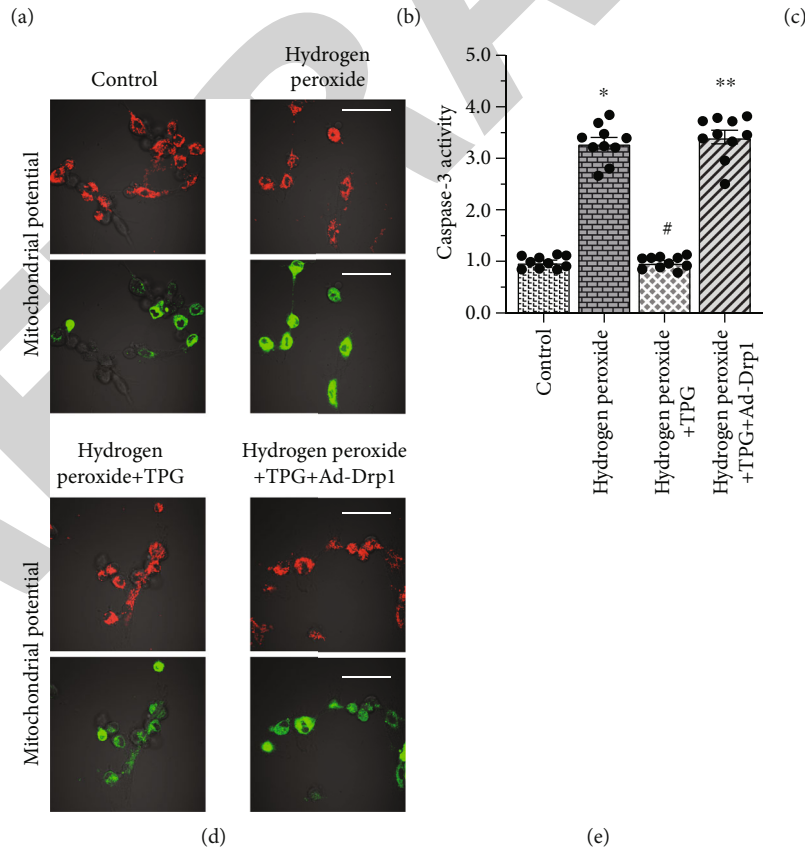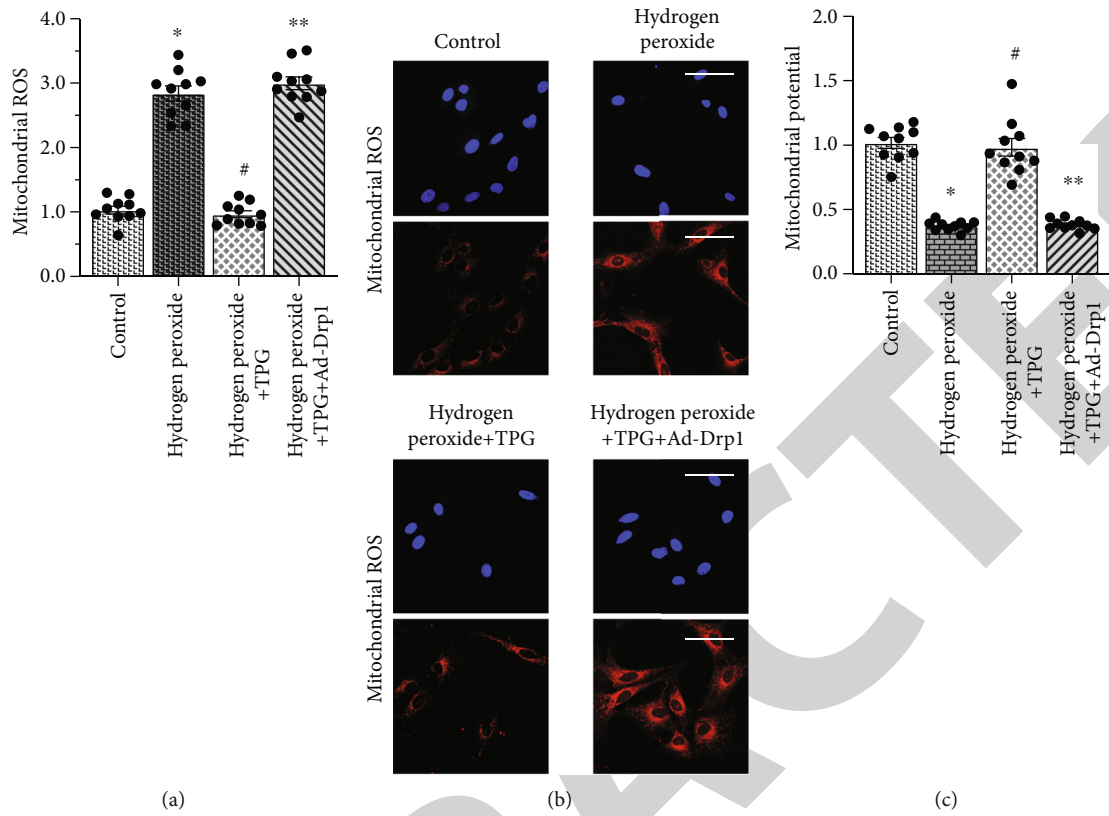
(a)

(b)

(c)

(d)

(e)

Figure 4: Induction of mitochondrial fission abolishes the beneficial effects of TGP on mitochondrial function and cardiomyocyte viability. (a, b) Mitochondrial ROS was determined by immunofluorescence in response to TGP treatment. Drp1 adenovirus was transfected into cardiomyocytes to overexpress Drp1. (c, d) Mitochondrial membrane potential was observed using a JC-1 probe. (e) ELISA was used to observe the alteration of caspase-3. $*p < 0.05$.
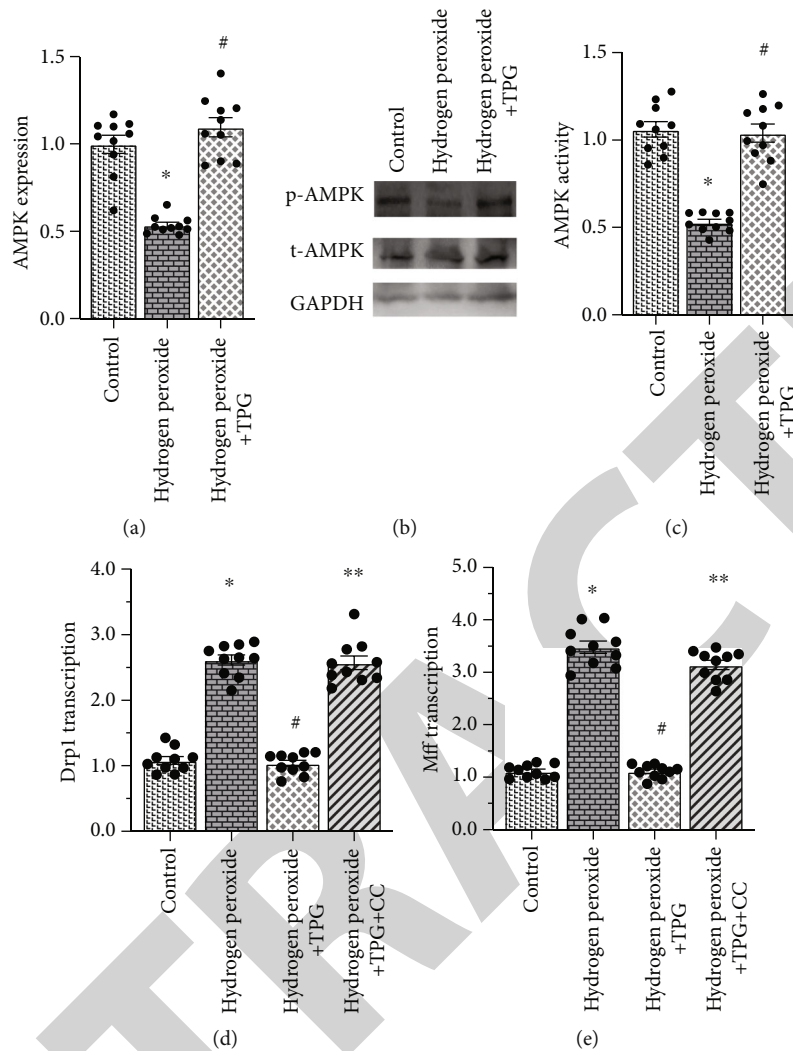
Figure 5: TGP maintains mitochondrial dynamics through the AMPK pathway. (a, b) Western blots were used to observe the alteration of AMPK in cardiomyocytes treated with TGP in the presence of hydrogen peroxide. Drp1 adenovirus was transfected into cardiomyocytes to overexpress Drp1. (c) ELISA was used to evaluate the activity of AMPK. (d, e) RNA was isolated from cardiomyocytes, then the transcription of MCP1α and MCP1 was analyzed using qPCR. Compound C was used to inhibit the activity of AMPK. $*p < 0.05$.

In accordance with this finding, hydrogen peroxide elevated the activity of caspase-3, but this alteration could be repressed by TGP (Figure 4(e)). The antiapoptotic action of TGP was blocked by Drp1 overexpression, suggesting that TGP protects cardiomyocyte viability and mitochondrial fusion by preserving mitochondrial dynamics.

3.5. TGP Maintains Mitochondrial Dynamics through the AMPK Pathway. Previous studies have reported a link between the AMP-activated protein kinase (AMPK) pathway and mitochondrial dynamics [56]. In diabetic cardiomyopathy, AMPK activation is followed by decreased mitochondrial fission and increased mitochondrial fusion through the inhibition of Drp1 activation. Ample evidence indicates the promotive role of TGP in inducing AMPK activation. Therefore, we investigated whether TGP modulated mitochondrial dynamics through the AMPK pathway. First, Western blots were used to observe the alteration of AMPK in response to hydrogen peroxide or TGP treatment. As

shown in Figures 5(a) and 5(b), compared to the control group, AMPK expression was significantly reduced, followed by a decline in AMPK activity (Figure 5(c)). TGP treatment elevated AMPK expression (Figures 5(a) and 5(b)) and improved AMPK activity (Figure 5(c)), suggesting that TGP can correct hydrogen peroxide-mediated AMPK inhibition. To understand whether TGP modulates mitochondrial dynamics through AMPK, compound C, an AMPK pathway inhibitor, was added to TGP-treated cardiomyocytes. Mitochondrial dynamics were then reanalyzed. As shown in Figures 5(d) and 5(e), hydrogen peroxide upregulated the transcription of mitochondrial fission-related genes, but this phenotypic alteration could be attenuated by TGP. Inhibition of the AMPK pathway abolished the regulatory effect of TGP on mitochondrial fission (Figures 5(d) and 5(e)). Similarly, mitochondrial fusion-related genes were drastically upregulated by TGP in the presence of hydrogen peroxide, but this effect was not seen in cardiomyocytes treated with compound C (Figures 5(d) and 5(e)). These

results indicate that the AMPK pathway is involved in TGP-regulated mitochondrial dynamics.

4. Discussion

In this study, we explored the cardioprotective effects of TGP on cardiomyocyte oxidative stress and inflammation by focusing on mitochondrial dynamics and bioenergetics. After exposure to hydrogen peroxide, cardiomyocyte viability was reduced, but the apoptosis rate was increased. Mitochondria-mediated apoptosis has been regarded as the primary reason for the initiation of cardiomyocyte death. TGP treatment significantly reduced cardiomyocyte death by blocking mitochondrial apoptosis. We also observed the antioxidative and anti-inflammatory actions of TGP on hydrogen peroxide-treated cardiomyocytes. At the molecular level, TGP upregulated the activities of antioxidative factors and inhibited the formation of mitochondrial ROS, resulting in inhibition of oxidative stress in cardiomyocytes. Additionally, TGP administration was associated with a drop in the transcription of proinflammatory genes. Molecular investigation demonstrated that TGP modulated mitochondrial function by correcting mitochondrial dynamics and improving mitochondrial bioenergetics. Disruption of mitochondrial dynamics abolished the protective effects of TGP on mitochondrial bioenergetics, suggesting that mitochondrial dynamics function upstream of bioenergetics. Finally, we observed that TGP modulated mitochondrial dynamics and bioenergetics through the AMPK pathway. Our results showed that TGP played a cardioprotective role in cardiomyocyte oxidative stress and inflammation by normalizing mitochondrial dynamics and improving mitochondrial bioenergetics. This finding supports the use of TGP in regulating cardiomyocyte viability, especially in rheumatoid arthritis.

Several studies have reported the antioxidative, anti-inflammatory, and antiproliferative properties of TGP. For example, in a mice model of constipation and intestinal inflammation, TGP significantly reduced the symptoms and improved the prognosis [57]. TGP also alleviates cerebral ischemia-reperfusion injury by modulating the inflammation response [58]. At the molecular level, Toll-like receptor-2 [59], TNF receptor-associated factor [59], NF-κB [59], microphthalmia-associated transcription factor (MITF) [60], and tyrosinase-related protein 1 (TRP-1) [60] have been regarded as the downstream targets of TGP. In this study, we found that TNFα and MCP1 could be reduced by TGP in hydrogen peroxide-treated cardiomyocytes, confirming the anti-inflammatory action of TGP. Additionally, we found that the levels of cellular antioxidative factors were significantly elevated by TGP. Mitochondrial complex activity was also normalized by TGP, resulting in a decline in the production of mitochondrial ROS in cardiomyocytes. These findings suggest that TGP regulates oxidative stress by affecting ROS-related signaling pathways, such as the Nrf2/ARE axis [61] or the PKCδ/NF-κB pathway [62].

Mitochondrial dynamics are alterations of mitochondrial shape and size and include mitochondrial fission and fusion [63–66]. Increased mitochondrial fission and decreased mitochondrial fusion are apoptotic signals for cardiomyocytes under stressful conditions, including but not limited to cardiac ischemia-reperfusion injury, diabetic cardiomyopathy, heart failure, and sepsis-related myocardial damage [21, 27]. Disruption of mitochondrial dynamics is followed by mitochondrial fragmentation with low mitochondrial membrane potential and increased mitochondrial ROS production [67–69]. In this study, we observed that disruption of mitochondrial dynamics is followed by mitochondrial damage and cardiomyocyte death. TGP treatment has the ability to reverse mitochondrial dynamics and thus promote mitochondrial bioenergetics, leading to increased cellular ATP production. Previous studies have reported the regulatory effects of TGP on mitochondria. In retinal pigment epithelial cells, TGP attenuates oxidative stress-related mitochondrial dynamics by activating the CaMKII/AMPK pathway [9]. In streptozotocin-induced cognitive impairment in mice, TGP treatment sustains mitochondrial membrane potential, promotes ATP synthesis, and blocks mitochondrial apoptosis [70]. These results suggest that the molecular mechanism underlying TGP-mediated cardioprotection and mitochondria may be the potential targets of TGP.

Our results showed that TGP treatment improves cardiomyocyte oxidative stress and inflammation in the presence of hydrogen peroxide by correcting mitochondrial dynamics and enhancing mitochondrial bioenergetics. Additionally, the regulatory effects of TGP on mitochondrial function seem to be mediated through the AMPK pathway. These findings are promising for the treatment of myocardial injury in patients with rheumatoid arthritis and systemic lupus erythematosus.

Data Availability

All data generated or analyzed during this study are included in this article.

Conflicts of Interest

The authors declare no conflicts of interest.

References

[1] H. Jiang, J. Li, L. Wang et al., "Total glucosides of paeony: a review of its phytochemistry, role in autoimmune diseases, and mechanisms of action," *Journal of Ethnopharmacology*, vol. 258, p. 112913, 2020.

[2] E. Tkachenko, J. P. Okhovat, P. Manjaly, K. P. Huang, M. M. Senna, and A. Mostaghimi, "Complementary & alternative medicine for alopecia areata: a systematic review," *Journal of the American Academy of Dermatology*, 2019.

[3] L. Zhang and W. Wei, "Anti-inflammatory and immunoregulatory effects of paeoniflorin and total glucosides of paeony," *Pharmacology & Therapeutics*, vol. 207, p. 107452, 2020.

[4] H. Li, X. Y. Cao, W. Z. Dang, B. Jiang, J. Zou, and X. Y. Shen, "Total glucosides of paeony protects against collagen-induced mouse arthritis via inhibiting follicular helper T cell differentiation," *Phytomedicine*, vol. 65, p. 153091, 2019.

[5] T. Ngo, K. Kim, Y. Bian et al., "Antithrombotic effects of paeoniflorin from paeonia suffruticosa by selective inhibition on

shear stress-induced platelet aggregation," *International Journal of Molecular Sciences*, vol. 20, no. 20, p. 5040, 2019.

[6] Q. Xin, R. Yuan, W. Shi, Z. Zhu, Y. Wang, and W. Cong, "A review for the anti-inflammatory effects of paeoniflorin in inflammatory disorders," *Life Sciences*, vol. 237, p. 116925, 2019.

[7] H. H. Tang, H. L. Li, Y. X. Li et al., "Protective effects of a traditional Chinese herbal formula Jiang-Xian HuGan on Concanavalin A-induced mouse hepatitis via NF-kappaB and Nrf2 signaling pathways," *Journal of Ethnopharmacology*, vol. 217, pp. 118–125, 2018.

[8] D. S. Lee, W. Ko, B. K. Song et al., "The herbal extract KCHO-1 exerts a neuroprotective effect by ameliorating oxidative stress via heme oxygenase-1 upregulation," *Molecular Medicine Reports*, vol. 13, no. 6, pp. 4911–4919, 2016.

[9] X. Zhu, K. Wang, F. Zhou, and L. Zhu, "Paeoniflorin attenuates atRAL-induced oxidative stress, mitochondrial dysfunction and endoplasmic reticulum stress in retinal pigment epithelial cells via triggering Ca(2+)/CaMKII-dependent activation of AMPK," *Archives of Pharmacal Research*, vol. 41, no. 10, pp. 1009–1018, 2018.

[10] I. C. Chen, T. H. Lin, Y. H. Hsieh et al., "Formulated Chinese medicine Shaoyao Gancao Tang reduces tau aggregation and exerts neuroprotection through anti-oxidation and anti-inflammation," *Oxidative Medicine and Cellular Longevity*, vol. 2018, Article ID 9595741, 16 pages, 2018.

[11] Y. S. Lu, Y. Jiang, J. P. Yuan et al., "UVA induced oxidative stress was inhibited by paeoniflorin/Nrf2 signaling or PLIN2," *Frontiers in Pharmacology*, vol. 11, p. 736, 2020.

[12] Z. Wen, W. Hou, W. Wu et al., "6′-O-Galloylpaeoniflorin attenuates cerebral ischemia reperfusion-induced neuroinflammation and oxidative stress via PI3K/Akt/Nrf2 activation," *Oxidative Medicine and Cellular Longevity*, vol. 2018, Article ID 8678267, 14 pages, 2018.

[13] L. Kishore, N. Kaur, and R. Singh, "Nephroprotective effect of paeonia emodi via inhibition of advanced glycation end products and oxidative stress in streptozotocin-nicotinamide induced diabetic nephropathy," *Journal of Food and Drug Analysis*, vol. 25, no. 3, pp. 576–588, 2017.

[14] C. M. Liu, H. X. Yang, J. Q. Ma et al., "Role of AMPK pathway in lead-induced endoplasmic reticulum stress in kidney and in paeonol-induced protection in mice," *Food and Chemical Toxicology*, vol. 122, pp. 87–94, 2018.

[15] M. H. Jang, K. Y. Kim, P. H. Song et al., "Moutan cortex protects hepatocytes against oxidative injury through AMP-activated protein kinase pathway," *Biological & Pharmaceutical Bulletin*, vol. 40, no. 6, pp. 797–806, 2017.

[16] M. H. Liu, A. H. Lin, H. K. Ko, D. W. Perng, T. S. Lee, and Y. R. Kou, "Prevention of bleomycin-induced pulmonary inflammation and fibrosis in mice by paeonol," *Frontiers in Physiology*, vol. 8, 2017.

[17] L. Bacmeister, M. Schwarzl, S. Warnke et al., "Inflammation and fibrosis in murine models of heart failure," *Basic Research in Cardiology*, vol. 114, no. 3, 2019.

[18] J. A. Silverblatt, O. J. Ziff, L. Dancy et al., "Therapies to limit myocardial injury in animal models of myocarditis: a systematic review and meta-analysis," *Basic Research in Cardiology*, vol. 114, no. 6, p. 48, 2019.

[19] L. Kraft, T. Erdenesukh, M. Sauter, C. Tschope, and K. Klingel, "Blocking the IL-1β signalling pathway prevents chronic viral myocarditis and cardiac remodeling," *Basic Research in Cardiology*, vol. 114, no. 2, 2019.

[20] M. Kohlhauer, V. R. Pell, N. Burger et al., "Protection against cardiac ischemia-reperfusion injury by hypothermia and by inhibition of succinate accumulation and oxidation is additive," *Basic Research in Cardiology*, vol. 114, no. 3, p. 18, 2019.

[21] J. Wang, S. Toan, and H. Zhou, "Mitochondrial quality control in cardiac microvascular ischemia-reperfusion injury: new insights into the mechanisms and therapeutic potentials," *Pharmacological Research*, vol. 156, p. 104771, 2020.

[22] H. Zhou, P. Zhu, J. Guo et al., "Ripk3 induces mitochondrial apoptosis via inhibition of FUNDC1 mitophagy in cardiac IR injury," *Redox Biology*, vol. 13, pp. 498–507, 2017.

[23] B. W. L. Lee, P. Ghode, and D. S. T. Ong, "Redox regulation of cell state and fate," *Redox Biology*, vol. 25, p. 101056, 2019.

[24] A. J. Kowaltowski, "Strategies to detect mitochondrial oxidants," *Redox Biology*, vol. 21, p. 101065, 2019.

[25] Y. R. Kim, J. I. Baek, S. H. Kim et al., "Therapeutic potential of the mitochondria-targeted antioxidant MitoQ in mitochondrial-ROS induced sensorineural hearing loss caused by Idh2 deficiency," *Redox Biology*, vol. 20, pp. 544–555, 2019.

[26] D. Pozzer, E. Varone, A. Chernorudskiy et al., "A maladaptive ER stress response triggers dysfunction in highly active muscles of mice with SELENON loss," *Redox Biology*, vol. 20, pp. 354–366, 2019.

[27] J. Wang, S. Toan, and H. Zhou, "New insights into the role of mitochondria in cardiac microvascular ischemia/reperfusion injury," *Angiogenesis*, vol. 23, no. 3, pp. 299–314, 2020.

[28] H. Zhou and S. Toan, "Pathological roles of mitochondrial oxidative stress and mitochondrial dynamics in cardiac microvascular ischemia/reperfusion injury," *Biomolecules*, vol. 10, no. 1, p. 85, 2020.

[29] S. Dassanayaka, K. R. Brittian, A. Jurkovic et al., "E2f1 deletion attenuates infarct-induced ventricular remodeling without affecting O-GlcNAcylation," *Basic Research in Cardiology*, vol. 114, no. 4, p. 28, 2019.

[30] D. Curley, B. Lavin Plaza, A. M. Shah, and R. M. Botnar, "Molecular imaging of cardiac remodelling after myocardial infarction," *Basic Research in Cardiology*, vol. 113, no. 2, p. 10, 2018.

[31] S. M. Davidson, S. Arjun, M. V. Basalay et al., "The 10th biennial hatter cardiovascular institute workshop: cellular protection-evaluating new directions in the setting of myocardial infarction, ischaemic stroke, and cardio-oncology," *Basic Research in Cardiology*, vol. 113, no. 6, p. 43, 2018.

[32] H. Zhou, S. Hu, Q. Jin et al., "Mff-dependent mitochondrial fission contributes to the pathogenesis of cardiac microvasculature ischemia/reperfusion injury via induction of mROS-mediated cardiolipin oxidation and HK2/VDAC1 disassociation-involved mPTP opening," *Journal of the American Heart Association*, vol. 6, no. 3, 2017.

[33] H. M. Schmidt, E. E. Kelley, and A. C. Straub, "The impact of xanthine oxidase (XO) on hemolytic diseases," *Redox Biology*, vol. 21, p. 101072, 2019.

[34] G. Farber, M. M. Parks, N. Lustgarten Guahmich et al., "ADAM10 controls the differentiation of the coronary arterial endothelium," *Angiogenesis*, vol. 22, no. 2, pp. 237–250, 2019.

[35] S. C. Kelly, N. N. Patel, A. M. Eccardt, and J. S. Fisher, "Glucose-dependent trans-plasma membrane electron transport and p70(S6k) phosphorylation in skeletal muscle cells," *Redox Biology*, vol. 27, p. 101075, 2019.

[36] A. Guidarelli, M. Fiorani, L. Cerioni, and O. Cantoni, "Calcium signals between the ryanodine receptor- and

mitochondria critically regulate the effects of arsenite on mitochondrial superoxide formation and on the ensuing survival vs apoptotic signaling," *Redox Biology*, vol. 20, pp. 285–295, 2019.

[37] J. Wang, P. Zhu, S. Toan, R. Li, J. Ren, and H. Zhou, "Pum2-Mff axis fine-tunes mitochondrial quality control in acute ischemic kidney injury," *Cell Biology and Toxicology*, vol. 36, no. 4, pp. 365–378, 2020.

[38] R. B. Li, S. Toan, and H. Zhou, "Role of mitochondrial quality control in the pathogenesis of nonalcoholic fatty liver disease," *Aging*, vol. 12, no. 7, pp. 6467–6485, 2020.

[39] C. Luo, H. Wang, X. Chen et al., "Protection of H9c2 rat cardiomyoblasts against oxidative insults by total paeony glucosides from Radix Paeoniae Rubrae," *Phytomedicine*, vol. 21, no. 1, pp. 20–24, 2013.

[40] M. Zarfati, I. Avivi, B. Brenner, T. Katz, and A. Aharon, "Extracellular vesicles of multiple myeloma cells utilize the proteasome inhibitor mechanism to moderate endothelial angiogenesis," *Angiogenesis*, vol. 22, no. 1, pp. 185–196, 2019.

[41] J. Herzog, F. P. Schmidt, O. Hahad et al., "Acute exposure to nocturnal train noise induces endothelial dysfunction and pro-thromboinflammatory changes of the plasma proteome in healthy subjects," *Basic Research in Cardiology*, vol. 114, no. 6, p. 46, 2019.

[42] J. Guo, S. Shen, X. Liu et al., "Role of linc00174/miR-138-5p (miR-150-5p)/FOSL2 feedback loop on regulating the blood-tumor barrier permeability," *Mol Ther Nucleic Acids.*, vol. 18, pp. 1072–1090, 2019.

[43] J. Mo, B. Enkhjargal, Z. D. Travis et al., "AVE 0991 attenuates oxidative stress and neuronal apoptosis via Mas/PKA/CREB/UCP-2 pathway after subarachnoid hemorrhage in rats," *Redox Biology*, vol. 20, pp. 75–86, 2019.

[44] M. S. Narzt, I. M. Nagelreiter, O. Oskolkova et al., "A novel role for NUPR1 in the keratinocyte stress response to UV oxidized phospholipids," *Redox Biology*, vol. 20, pp. 467–482, 2019.

[45] J. Darden, L. B. Payne, H. Zhao, and J. C. Chappell, "Excess vascular endothelial growth factor-A disrupts pericyte recruitment during blood vessel formation," *Angiogenesis*, vol. 22, no. 1, pp. 167–183, 2019.

[46] H. Zhou, P. Zhu, J. Wang, S. Toan, and J. Ren, "DNA-PKcs promotes alcohol-related liver disease by activating Drp1-related mitochondrial fission and repressing FUNDC1-required mitophagy," *Signal Transduction and Targeted Therapy*, vol. 4, no. 1, 2019.

[47] A. Linkermann, "Death and fire-the concept of necroinflammation," *Cell Death and Differentiation*, vol. 26, no. 1, pp. 1–3, 2019.

[48] E. H. Kim, S. W. Wong, and J. Martinez, "Programmed necrosis and disease: we interrupt your regular programming to bring you necroinflammation," *Cell Death and Differentiation*, vol. 26, no. 1, pp. 25–40, 2019.

[49] S. L. Hernandez, M. Nelson, G. R. Sampedro et al., "Staphylococcus aureus alpha toxin activates notch in vascular cells," *Angiogenesis*, vol. 22, no. 1, pp. 197–209, 2019.

[50] S. Guo, J. Lu, Y. Zhuo et al., "Endogenous cholesterol ester hydroperoxides modulate cholesterol levels and inhibit cholesterol uptake in hepatocytes and macrophages," *Redox Biology*, vol. 21, p. 101069, 2019.

[51] J. Eiringhaus, J. Herting, F. Schatter et al., "Protein kinase/phosphatase balance mediates the effects of increased late sodium current on ventricular calcium cycling," *Basic Research in Cardiology*, vol. 114, no. 2, 2019.

[52] D. J. Mallick, A. Korotkov, H. Li, J. Wu, and A. Eastman, "Nuphar alkaloids induce very rapid apoptosis through a novel caspase-dependent but BAX/BAK-independent pathway," *Cell Biology and Toxicology*, vol. 35, no. 5, pp. 435–443, 2019.

[53] M. Imber, A. J. Pietrzyk-Brzezinska, and H. Antelmann, "Redox regulation by reversible protein S-thiolation in Gram-positive bacteria," *Redox Biology*, vol. 20, pp. 130–145, 2019.

[54] H. Dong, C. Weng, R. Bai et al., "The regulatory network of miR-141 in the inhibition of angiogenesis," *Angiogenesis*, vol. 22, no. 2, pp. 251–262, 2019.

[55] D. Aluja, J. Inserte, P. Penela et al., "Calpains mediate isoproterenol-induced hypertrophy through modulation of GRK2," *Basic Research in Cardiology*, vol. 114, no. 3, 2019.

[56] H. Zhou, S. Wang, P. Zhu, S. Hu, Y. Chen, and J. Ren, "Empagliflozin rescues diabetic myocardial microvascular injury via AMPK-mediated inhibition of mitochondrial fission," *Redox Biology*, vol. 15, pp. 335–346, 2018.

[57] G. Liu, Z. Wang, Z. Li et al., "Total glucosides of paeony (TGP) alleviates constipation and intestinal inflammation in mice induced by Sjogren's syndrome," *Journal of Ethnopharmacology*, vol. 260, p. 113056, 2020.

[58] L. Y. Li, L. Ma, and W. L. Dong, "Total glucosides of paeony (*Paeonia lactiflora*) alleviates blood-brain barrier disruption and cerebral ischemia/reperfusion injury in rats *via* suppressing inflammation and apoptosis," *Die Pharmazie*, vol. 75, no. 5, pp. 208–212, 2020.

[59] H. Chen, Y. Wen, T. Pan, and S. Xu, "Total glucosides of paeony improve complete Freund's adjuvant-induced rheumatoid arthritis in rats by inhibiting toll-like receptor 2-mediated tumor necrosis factor receptor-associated factor 6/ nuclear factor-kappa B pathway activation," *Journal of Traditional Chinese Medicine*, vol. 39, no. 4, pp. 566–574, 2019.

[60] M. Hu, C. Chen, J. Liu et al., "The melanogenic effects and underlying mechanism of paeoniflorin in human melanocytes and vitiligo mice," *Fitoterapia*, vol. 140, p. 104416, 2020.

[61] X. Yang, W. Yao, H. Shi et al., "Paeoniflorin protects Schwann cells against high glucose induced oxidative injury by activating Nrf2/ARE pathway and inhibiting apoptosis," *Journal of Ethnopharmacology*, vol. 185, pp. 361–369, 2016.

[62] H. Dong, R. Li, C. Yu, T. Xu, X. Zhang, and M. Dong, "Paeoniflorin inhibition of 6-hydroxydopamine-induced apoptosis in PC12 cells via suppressing reactive oxygen species-mediated PKCdelta/NF-kappaB pathway," *Neuroscience*, vol. 285, pp. 70–80, 2015.

[63] H. H. Wang, Y. J. Wu, Y. M. Tseng, C. H. Su, C. L. Hsieh, and H. I. Yeh, "Mitochondrial fission protein 1 up-regulation ameliorates senescence-related endothelial dysfunction of human endothelial progenitor cells," *Angiogenesis*, vol. 22, no. 4, pp. 569–582, 2019.

[64] S. Gumeni, Z. Evangelakou, E. N. Tsakiri, L. Scorrano, and I. P. Trougakos, "Functional wiring of proteostatic and mitostatic modules ensures transient organismal survival during imbalanced mitochondrial dynamics," *Redox Biology*, vol. 24, p. 101219, 2019.

[65] A. Mukwaya, P. Mirabelli, A. Lennikov et al., "Revascularization after angiogenesis inhibition favors new sprouting over abandoned vessel reuse," *Angiogenesis*, vol. 22, no. 4, pp. 553–567, 2019.

Retraction

Retracted: Oxidized LDL Disrupts Metabolism and Inhibits Macrophage Survival by Activating a miR-9/Drp1/Mitochondrial Fission Signaling Pathway

Oxidative Medicine and Cellular Longevity

This article has been retracted by Hindawi following an investigation undertaken by the publisher [1]. This investigation has uncovered evidence of one or more of the following indicators of systematic manipulation of the publication process:

(1) Discrepancies in scope

(2) Discrepancies in the description of the research reported

(3) Discrepancies between the availability of data and the research described

(4) Inappropriate citations

(5) Incoherent, meaningless and/or irrelevant content included in the article

(6) Peer-review manipulation

The presence of these indicators undermines our confidence in the integrity of the article's content and we cannot, therefore, vouch for its reliability. Please note that this notice is intended solely to alert readers that the content of this article is unreliable. We have not investigated whether authors were aware of or involved in the systematic manipulation of the publication process.

Wiley and Hindawi regrets that the usual quality checks did not identify these issues before publication and have since put additional measures in place to safeguard research integrity.

We wish to credit our own Research Integrity and Research Publishing teams and anonymous and named external researchers and research integrity experts for contributing to this investigation.

The corresponding author, as the representative of all authors, has been given the opportunity to register their agreement or disagreement to this retraction. We have kept a record of any response received.

References

[1] T. Xin, C. Lu, J. Zhang et al., "Oxidized LDL Disrupts Metabolism and Inhibits Macrophage Survival by Activating a miR-9/Drp1/ Mitochondrial Fission Signaling Pathway," *Oxidative Medicine and Cellular Longevity*, vol. 2020, Article ID 8848930, 16 pages, 2020.

Research Article

Oxidized LDL Disrupts Metabolism and Inhibits Macrophage Survival by Activating a miR-9/Drp1/Mitochondrial Fission Signaling Pathway

Ting Xin ⓘ, Chengzhi Lu, Jing Zhang, Jiaxin Wen, Shuangbin Yan, Chao Li, Feng Zhang, and Jin Zhang

Department of Cardiology, Tianjin First Center Hospital, Tianjin, China

Correspondence should be addressed to Ting Xin; 820826393@qq.com

Mitochondrial dysfunction is associated with macrophage damage, but the role of mitochondrial fission in macrophage cholesterol metabolism is not fully understood. In this study, we explored the influences of miR-9 and mitochondrial fission on macrophage viability and cholesterol metabolism. Macrophages were incubated with oxidized low-density lipoprotein (ox-LDL) *in vitro*, after which mitochondrial fission, cell viability, and cholesterol metabolism were examined using qPCR, ELISAs, and immunofluorescence. ox-LDL treatment significantly increased Drp1-associated mitochondrial fission. Transfection of Drp1 siRNA significantly reduced cell death, attenuated oxidative stress, and inhibited inflammatory responses in ox-LDL-treated macrophages. Interestingly, inhibition of Drp1-related mitochondrial fission also improved cholesterol metabolism by balancing the transcription of cholesterol influx/efflux enzymes. We also found that miR-9 was downregulated in ox-LDL-treated macrophages, and administration of a miR-9 mimic decreased Drp1 transcription and mitochondrial fission, as well as its effects. These results indicate that signaling via the novel miR-9/Drp1/mitochondrial fission axis is a key determinant of macrophage viability and cholesterol metabolism.

1. Introduction

Atherosclerosis (AS) is a leading cause of ischemic heart disease. Among the molecular mechanisms underlying AS, inflammation response and lipid metabolism disorder have been identified as particularly important [1, 2]. At the molecular level, chronic hyperlipidemia induces endothelial dysfunction and thus promotes deposition of cholesterol on the vascular wall [3]. Smooth muscle cells and macrophages uptake excess cholesterol then migrate into the middle layer of vessel wall, contributing to the formation of plaques [4]. Therefore, increased intake and decreased efflux of cholesterol from macrophages have been identified as a key contributor to macrophage dysfunction, which is associated with the development of AS [5, 6]. However, cholesterol metabolism homeostasis in macrophages under hyperlipidemia stress conditions has not been well studied [7, 8].

Mitochondria serve as the primary energy source for cells by producing ATP through oxidative phosphorylation [9–12]. Properly functioning mitochondria consume glucose and cholesterol to generate ATP that supports macrophage metabolism. Predictably, mitochondrial dysfunction impairs cholesterol decomposition and leads to accumulation of cholesterol in macrophages, ultimately promoting formation of plaques [13, 14]. Mitochondria are therefore a potential target for therapies aiming to regulate cholesterol metabolism in macrophages [15, 16]. Many recent studies have reported that events that alter mitochondrial morphology, such as fission, fusion, and autophagy, have important effects on mitochondrial function [17–20]. Under normal conditions, mitochondrial fission increases the number of mitochondria in a cell and thus enhances mitochondria-dependent energy output [21]. Mitochondrial fusion enhances communication among mitochondria by allowing them to exchange DNA

and metabolic substrates [22], which is vital for maintaining mitochondrial homeostasis. Mitochondrial autophagy, which is termed mitophagy [23], is a process by which damaged mitochondria are removed through lysosomes. Moderate mitophagy attenuates the number of dysfunctional mitochondria and promotes mitochondrial biogenesis [20, 24]. Together, these three mitochondrial morphology alterations act as upstream mediators of mitochondrial function. However, whether abnormalities in mitochondrial morphology are associated with cholesterol metabolism disorders in macrophages remains unknown.

Biogenesis of endogenous microRNAs begins with the synthesis of primary microRNAs, or pri-miRNAs, in the nucleus [25]. pri-miRNAs are cut into hairpin RNAs called pre-miRNAs. pre-miRNAs are further cut into shorter double-stranded micro-RNAs, and RNA helicase then generates one or two mature single-stranded microRNAs [26]. MicroRNAs regulate gene expression by silencing translation of messenger mRNAs [26]. Mature single-stranded microRNAs bind to members of the Argonaute protein family to form an RNA-induced silencing complex (RISC) [27]. The target mRNA then binds to complementary bases in the $3'$ noncoding region of the RISC [28]. The resulting destabilization or cleavage of the sigma region ultimately suppresses translation of the target mRNA. Recent studies have shown that microRNA can directly bind to an A/U- (adenine/uracil-) rich conserved element in the $3'$ noncoding region of mRNA after the cell cycle stops to activate mRNA translation [29]. Through these mechanisms, microRNAs can regulate various cellular processes, including metabolism, division, differentiation, apoptosis, and autophagy [30]. Our previous studies demonstrated that macrophage functions and inflammatory response are regulated by miR-9. In addition, recent research has identified new roles for miR-9 in regulating mitochondrial function [31]. In this study, we explored the influence of miR-9 on macrophage viability and cholesterol metabolism with a focus on mitochondrial fission.

2. Results

2.1. ox-LDL Activates Mitochondrial Fission and Inhibits Mitochondrial Fusion in Macrophages.
To understand changes in mitochondrial dynamics in response to ox-LDL treatment, an immunofluorescence assay was used to examine mitochondrial morphology. As shown in Figures 1(a)–1(c), normal mitochondria were rod shaped and evenly dispersed throughout the cytoplasm of macrophages. After exposure to ox-LDL, numbers of fragmented mitochondria increased, indicating disturbances in mitochondrial dynamics. RNA analysis demonstrated that the Mff, Fis1, and Drp1 genes, which are related to mitochondrial fission, were significantly upregulated in response to ox-LDL (Figures 1(d)–1(i)). Interestingly, levels of the mitochondrial fusion-related genes Mfn2, Mfn1, and Opa1 decreased markedly after exposure to ox-LDL (Figures 1(d)–1(i)). Together, our data indicate that ox-LDL activates mitochondrial fission and inhibits mitochondrial fusion in macrophages.

2.2. Inhibition of Drp1-Related Mitochondrial Fission Attenuates ox-LDL-Induced Macrophage Death.
To determine whether increased mitochondrial fission is required for ox-LDL-mediated macrophage damage, macrophages were transfected with siRNA against Drp1 and cell viability was then measured in a CCK-8 assay. As illustrated in Figure 2(a), compared to the control group, ox-LDL significantly decreased cell viability, and this effect was attenuated by Drp1 siRNA (siRNA/Drp1). The protective effect exerted by siRNA/Drp1 on macrophage viability was further examined in an LDH release assay. As shown in Figure 2(b), compared to the control group, ox-LDL promoted LDH release from macrophages into the medium. Loss of Drp1 through transfection of siRNA/Drp1 significantly reduced LDH release. Taken together, these results indicate that inhibition of Drp1 sustained macrophage viability. To further examine whether Drp1 knockdown was associated with increased cell viability, numbers of apoptotic cells were measured in a TUNEL assay. As shown in Figures 2(c) and 2(d), compared to the control group, numbers of TUNEL-positive cells increased after ox-LDL treatment. However, siRNA/Drp1 transfection inhibited ox-LDL-induced macrophage death, as evidenced by decreased TUNEL-positive cell numbers. Cell viability was also examined by analyzing the expression of caspase-3, a critical proapoptotic enzyme that induces DNA breakage. As shown in Figures 2(e) and 2(f), caspase-3 expression was undetectable in macrophages under normal conditions; ox-LDL treatment significantly increased caspase-3 levels in macrophages, and siRNA/Drp1 inhibited this effect. Taken together, these results demonstrated that inhibition of Drp1-related mitochondrial fission significantly reduces ox-LDL-induced macrophage death.

2.3. Inhibition of Drp1-Related Mitochondrial Fission Improves Cholesterol Metabolism in Macrophages.
At the molecular level, excessive cholesterol accumulation has been identified as an early inducer of macrophage dysfunction that contributes to the progression of atherosclerosis [32, 33]. Thus, we examined cholesterol metabolism in macrophages transfected with siRNA/Drp1. CD36 and LOX-1 are involved in ox-LDL uptake, while ABCA1 and ABCG1 are involved in cholesterol efflux [34, 35]. A qPCR assay demonstrated that transcription of CD36 and LOX-1 increased significantly in response to ox-LDL (Figures 3(a) and 3(b)). In contrast, transcription of ABCA1 and ABCG1 was markedly reduced after exposure to ox-LDL (Figures 3(c) and 3(d)). Conversely, after transfection of siRNA/Drp1, CD31 and LOX-1 transcription was downregulated and ABCA1 and ABCG1 transcription was upregulated (Figures 3(a)–3(d)). This indicates that inhibition of mitochondrial fission reduces cholesterol uptake and promotes cholesterol efflux. This finding was confirmed through immunofluorescence. As shown in Figures 3(e)–3(g), compared to the control group, CD36 was upregulated and ABCA1 was downregulated after ox-LDL treatment. After transfection of siRNA/Drp1, CD36 expression decreased and ABCA1 expression increased (Figures 3(e)–3(g)). These data confirmed that inhibition of mitochondrial fission improved cholesterol metabolism.
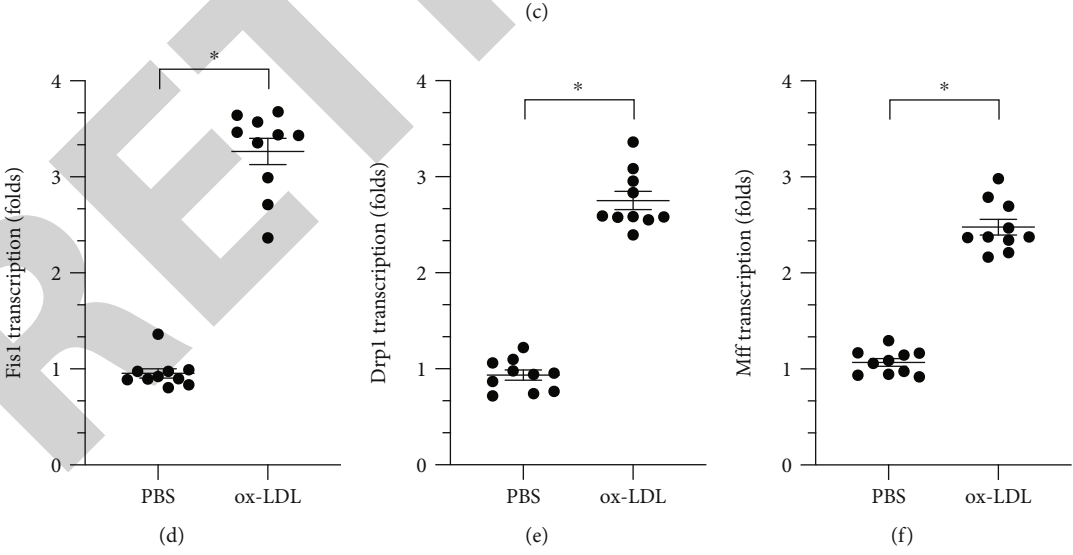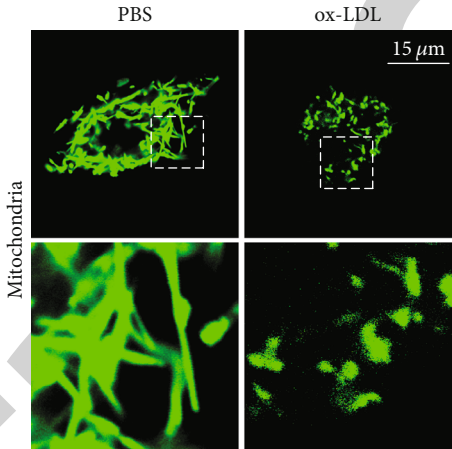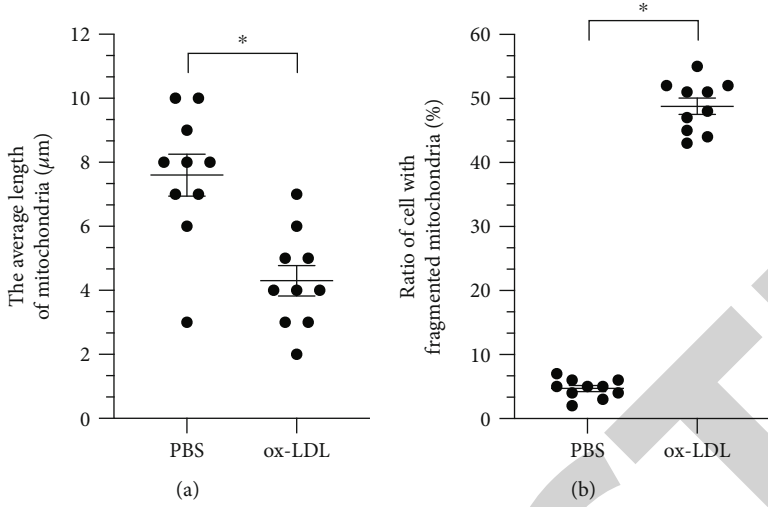
(a)

(b)

(c)

(d)

(e)

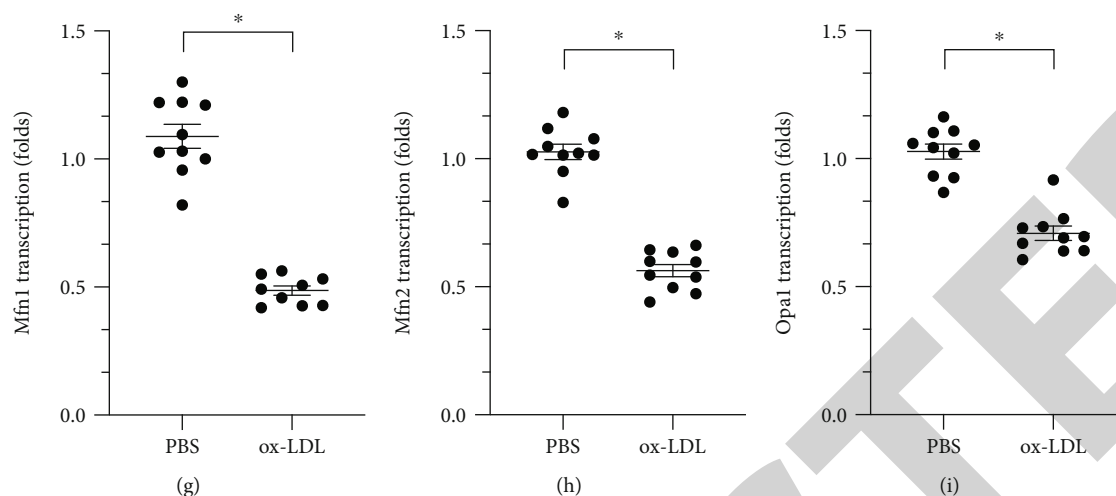
(f)

Figure 1: Continued.

(g) (h) (i)

Figure 1: ox-LDL activates mitochondrial fission and inhibits mitochondrial fusion in macrophages. (a–c) Immunofluorescence assay of mitochondrial morphology. Average mitochondrial length and ratio of fragmented mitochondria were measured in response to ox-LDL treatment. (d–i) RNA was collected from cells, and Mff, Fis1, Drp1, Mfn1, Mfn2, and Opa1 transcription was measured. $^*p < 0.05$.

2.4. ox-LDL Triggers Oxidative Stress in Macrophages through Drp1-Related Mitochondrial Fission.
Oxidative stress and inflammation response are associated with macrophage dysfunction [36–38]. We therefore examined whether mitochondrial fission also regulated oxidative stress in ox-LDL-treated macrophages. Intracellular ROS levels were measured through immunofluorescence. As shown in Figures 4(a) and 4(b), compared to the control group, ox-LDL treatment significantly increased ROS levels, and inhibition of mitochondrial fission inhibited ROS production. We also measured mitochondrial ROS levels. As shown in Figures 4(c) and 4(d), compared to control group, mitochondrial ROS levels increased dramatically after ox-LDL treatment, and this effect was reversed by siRNA/Drp1. Finally, we measured changes in the activity of antioxidative enzymes. As shown in Figures 4(e)–4(g), compared to the control group, GSH, GPX, and SOD activity was significantly downregulated after exposure to ox-LDL. However, inhibition of mitochondrial fission through transfection of siRNA/Drp1 significantly reversed this reduction in GSH, SOD, and GPX activity. Overall, our data illustrated that ox-LDL-induced oxidative stress was attenuated by inhibition of Drp1-related mitochondrial fission.

2.5. ox-LDL Induces Inflammatory Response Dependent on Drp1-Related Mitochondrial Fission in Macrophages.
To understand the role of Drp1-related mitochondrial fission in macrophage inflammatory responses, ELISA was used to measure levels of proinflammatory factors in macrophages. As shown in Figures 5(a)–5(d), compared to the control group, ox-LDL upregulated IL-6, IL-12, MCP1, and TNFα levels, and siRNA/Drp1 transfection decreased levels of these proinflammatory factors. Consistent with these findings, IL-6, IL-12, MCP1, and TNFα transcription was increased by ox-LDL and inhibited by siRNA/Drp1 (Figures 5(e)–5(h)). These data suggest that siRNA/Drp1 attenuated the ox-LDL-induced inflammatory response in macrophages.

2.6. ox-LDL Regulates Drp1-Related Mitochondrial Fission through miR-9.
We previously reported that miR-9 regulates macrophage function and protects against inflammatory responses through various mechanisms [39]. Subsequent studies further described the strong effects miR-9 exerts on mitochondrial function [40]. We therefore examined whether mitochondrial fission is regulated by miR-9 in ox-LDL-treated macrophages. Indeed, ox-LDL treatment significantly reduced miR-9 levels in macrophages (Figure 6(a)). To determine whether decreased miR-9 is involved in ox-LDL-mediated mitochondrial fission and macrophage dysfunction, cell viability and mitochondrial fission were examined in macrophages cocultured with a miR-9 mimic before ox-LDL treatment. As shown in Figures 6(b)–6(d), compared to the control group, numbers of fragmented mitochondria increased in response to ox-LDL treatment, and the miR-9 mimic inhibited this effect. We also found that transcription of Drp1, but not Fis1, was repressed by miR-9 mimic exposure prior to ox-LDL treatment, suggesting that miR-9 may modulate Drp1 expression at the posttranscriptional level (Figures 6(e) and 6(f)). In addition, a CCK-8 assay demonstrated that the miR-9 mimic maintained macrophage viability after ox-LDL treatment (Figure 6(g)). Similarly, miR-9 mimic restored antioxidative factors to normal levels (Figures 6(h) and 6(i)) and inhibited the transcription of proinflammatory factors (Figures 6(j) and 6(k)) in macrophages. Together, these results highlight the important role of miR-9 in regulating mitochondrial fission, oxidative stress, and inflammatory response in ox-LDL-treated macrophages.

3. Discussion

In this study, we found that ox-LDL treatment activated mitochondrial fission in macrophages. Furthermore, inhibition of mitochondrial fission significantly reduced ox-LDL-mediated macrophage damage. Mechanistically, inhibition of mitochondrial fission increased macrophage viability,
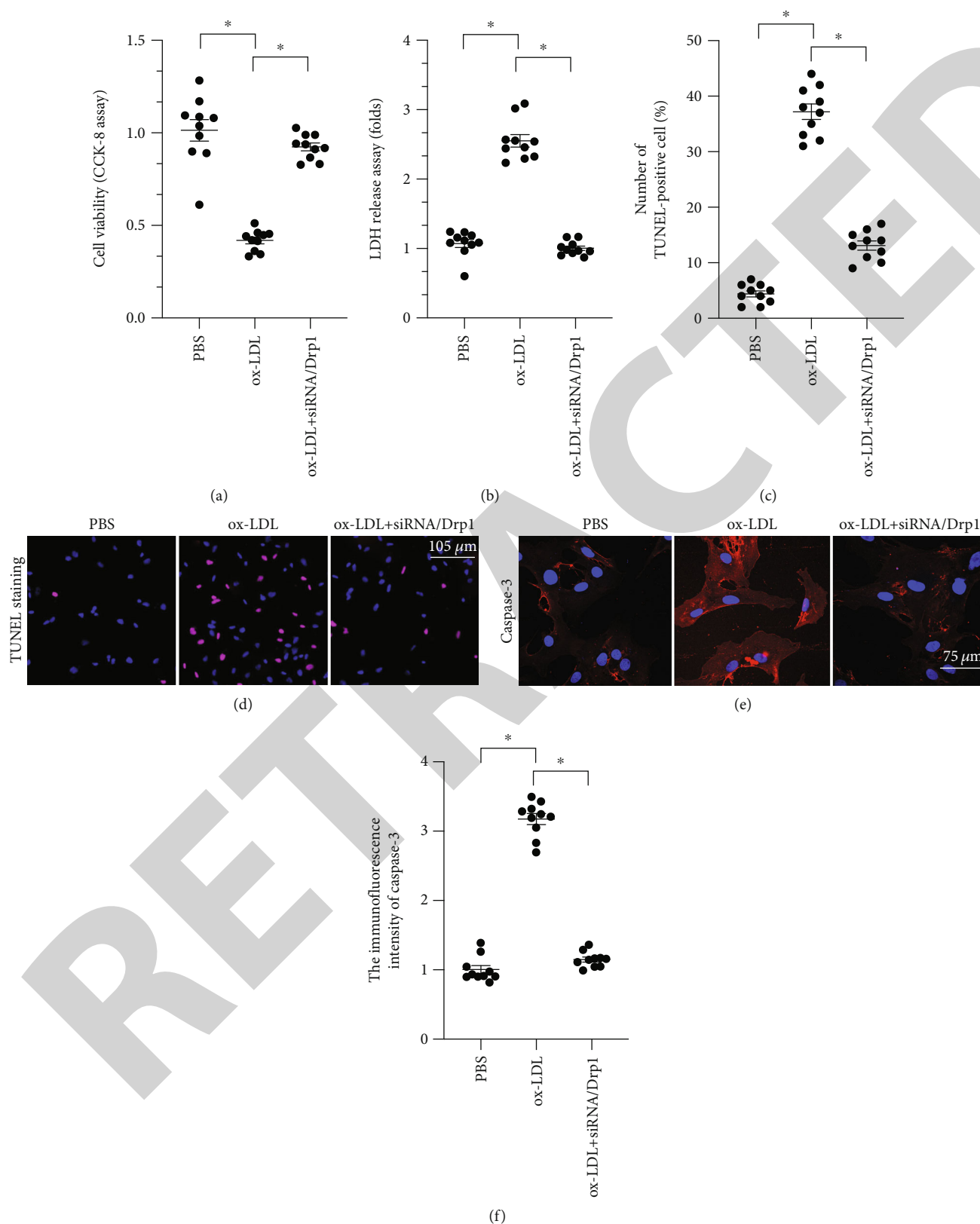
(a)

(b)

(c)

(d)

(e)

(f)

Figure 2: Inhibition of Drp1-related mitochondrial fission attenuates macrophage death induced by ox-LDL. (a) Cell viability was measured through the CCK-8 assay after ox-LDL and siRNA/Drp1 treatments. (b) LDH release assay was used to detect the concentration of LDH in the medium after ox-LDL and siRNA/Drp1 treatments. (c, d) TUNEL staining was used to analyze apoptosis rates in macrophages in response to LDH and siRNA/Drp1 treatments. (e, f) Caspase-3 expression was detected through immunofluorescence after ox-LDL and siRNA/Drp1 treatment. $^*p < 0.05$.
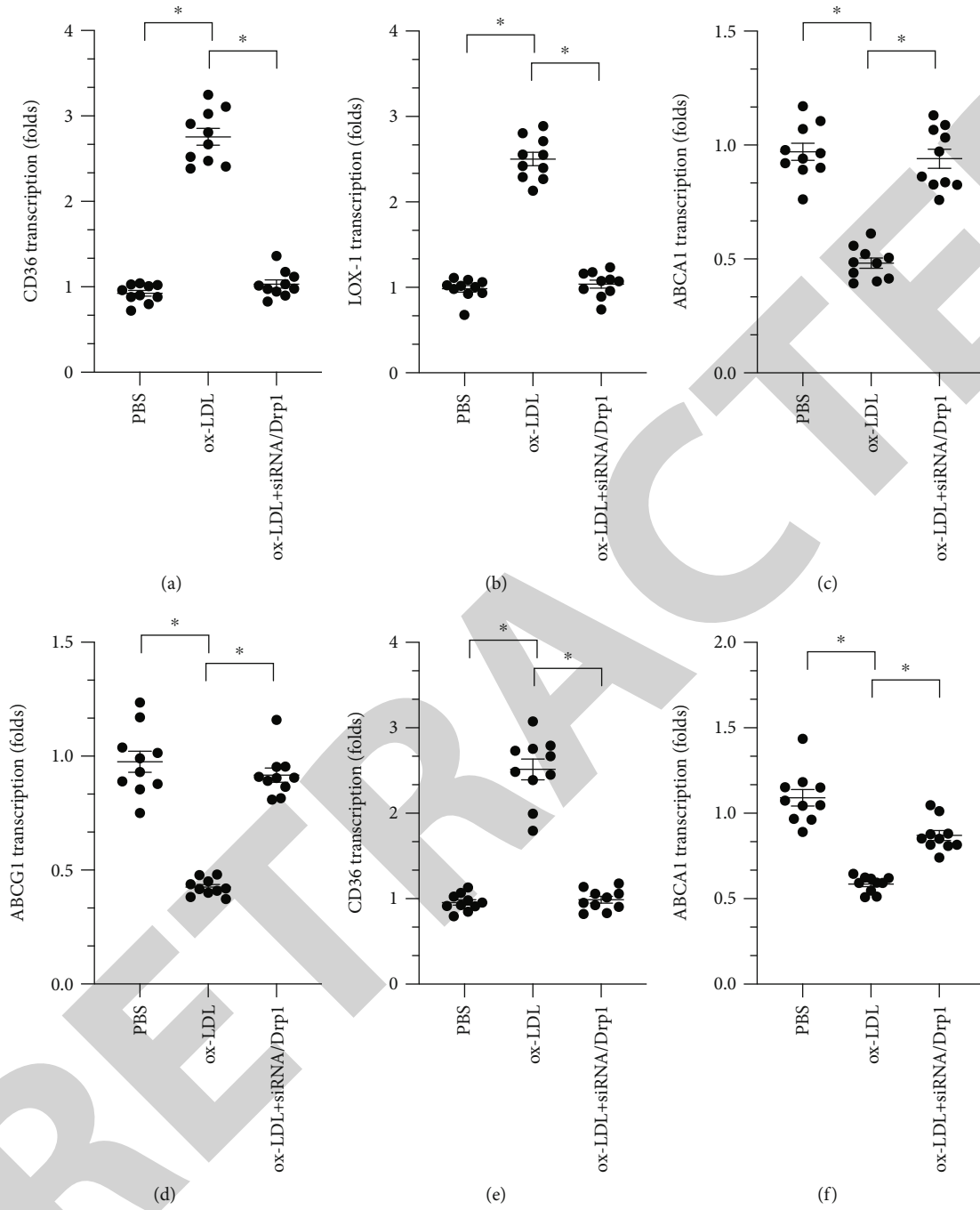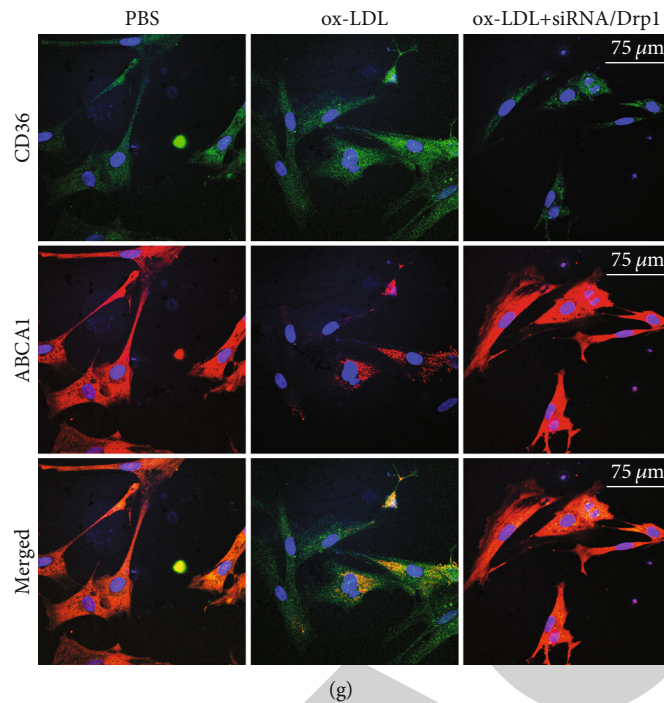
(a)

(b)

(c)

(d)

(e)

(f)

Figure 3: Continued.

(g)

Figure 3: Inhibition of Drp1-related mitochondrial fission improves cholesterol metabolism in macrophages. (a, b) A qPCR assay was used to measure levels of CD36 and LOX-1 after ox-LDL and siRNA/Drp1 treatments. (c, d) ABCA1 and ABCG1 transcription was measured through qPCR after ox-LDL and siRNA/Drp1 treatments. (e–g) Macrophage LOX-1 and ABCA1 levels were measured through immunofluorescence after ox-LDL and siRNA/Drp1 treatments. $^*p < 0.05$.

repressed oxidative stress, attenuated inflammatory response, and improved cholesterol metabolism. We also found that ox-LDL-induced mitochondrial fission was regulated by miR-9 in macrophages. Reduced miR-9 levels resulted in increased transcription of Drp1, which in turn activated mitochondrial fission. These results define a novel miR-9/Drp1/mitochondrial fission signaling pathway that affects macrophage function and cholesterol metabolism. Treatment strategies targeting miR-9 and mitochondrial fission might therefore benefit patients suffering from AS.

During hyperlipidemia, macrophages play a crucial role in maintaining balanced cholesterol levels by regulating scavenger receptors, cholesterol metabolism enzymes, and cholesterol transporters [22]. After scavenger receptors initially interact with free cholesterol, cholesterol transporters facilitate uptake of free cholesterol by macrophages; mitochondria then use cholesterol to generate ATP through cholesterol metabolism enzymes [41]. Importantly, cholesterol transporters can also facilitate excretion of excess cholesterol from cells [42]. The balance between cholesterol uptake and release therefore affects macrophage function. In this study, we found that genes related to cholesterol uptake were significantly upregulated while the genes related to cholesterol efflux were significantly downregulated in response to ox-LDL, suggesting that hyperlipidemia increases intake and inhibits release of cholesterol in macrophages. Excessive cholesterol accumulation in macrophages promotes foam cell formation during atherogenesis [43]. As far as we know, ours is the first investigation to demonstrate that mitochondrial fission improves cholesterol metabolism in macrophages.

However, some topics require further investigation. First, additional studies are required to identify the molecular mechanism underlying mitochondrial fission-mediated normalization of cholesterol receptor levels. In addition, whether decreased mitochondrial fission inhibits mitochondrial cholesterol metabolism in macrophages remains unknown and should be examined.

miRNAs decrease gene expression by binding to the $3'$-untranslated region (UTR) of target RNAs, resulting in their degradation [44]. miRNA expression profiles have diagnostic and prognostic value for cancer, and miRNAs may serve as potential targets for antitumor immunotherapies [45]. Several miRNAs that are associated with cholesterol metabolism in macrophages have been identified. For example, miR-144-5p regulates inflammatory response in macrophages by mediating the expression of TLR2 and OLR1 [46]. ox-LDL-induced cholesterol accumulation in macrophages seems to be modulated by miR-33a through the ERK/AMPK/SREBP1 signaling pathway [47]. ox-LDL-induced macrophage apoptosis and oxidative stress are also linked to miR-140-5p [48]. In addition, miR-202-3p upregulation promotes foam cell formation [49]. In this study, we found that miR-9 regulates macrophage cholesterol metabolism. miR-9 exerts important effects on diabetic peripheral neuropathy progression by regulating the OSL1-mediated sonic hedgehog signaling pathway [50]. Macrophage M1 polarization [40], macrophage foam cell formation [51], and macrophage inflammatory response [52] are also regulated by miR-9. More importantly, recent studies have also demonstrated that miR-9 regulates the stabilization of
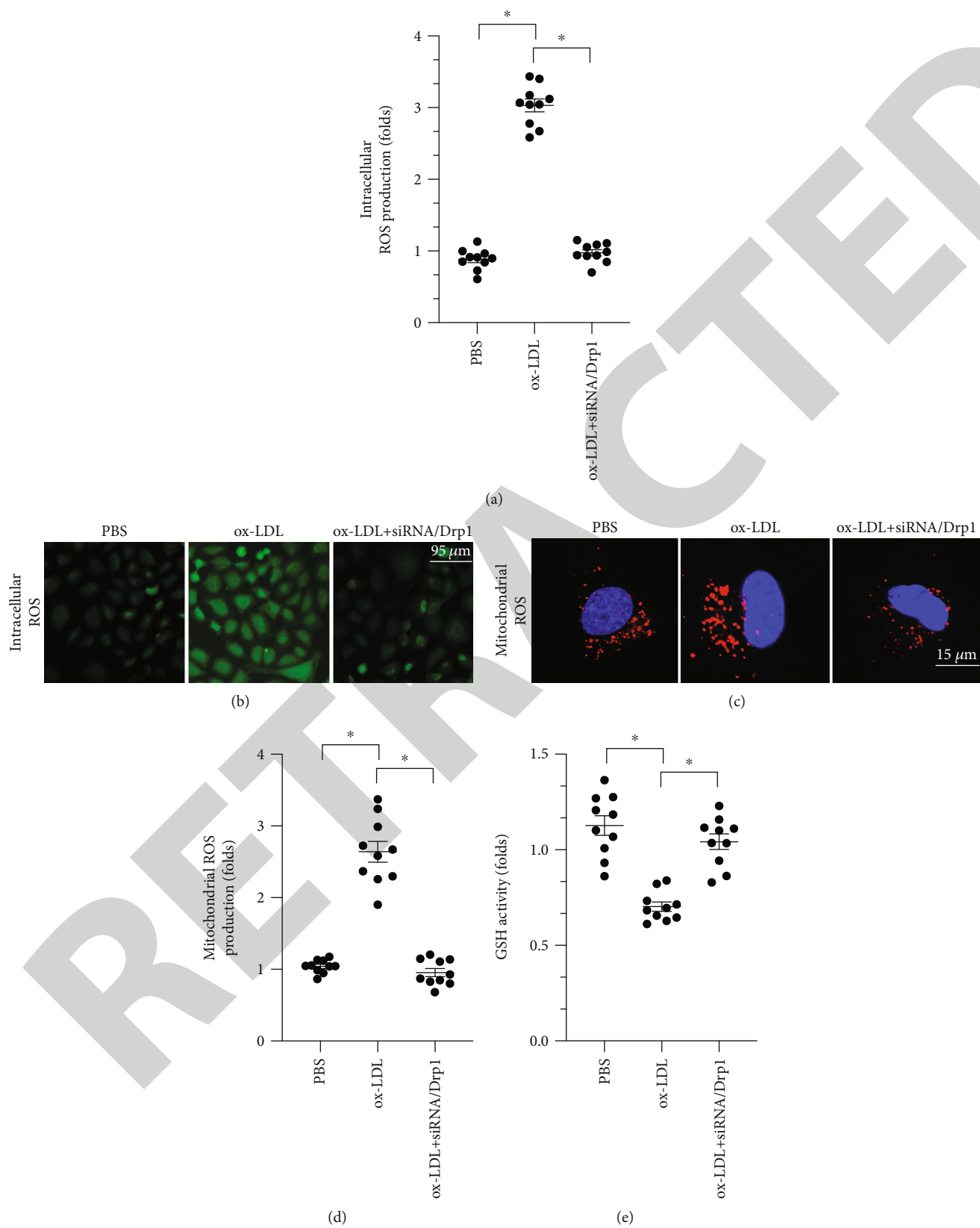
(a)

(b)

(c)

(d)

(e)

Figure 4: Continued.
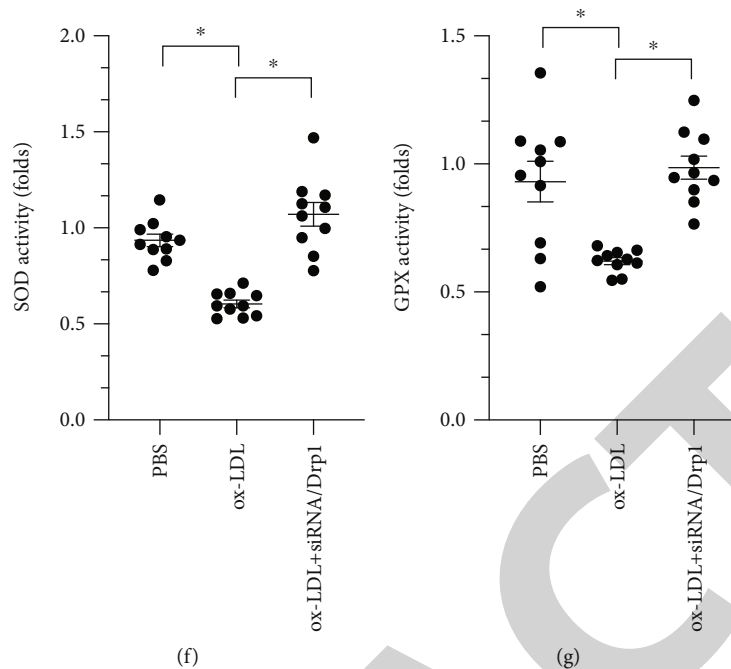
(f)   (g)

Figure 4: ox-LDL triggers oxidative stress in macrophages through Drp1-related mitochondrial fission. (a, b) Cellular ROS were measured in an immunofluorescence assay using a DCFHDA probe after ox-LDL and siRNA/Drp1 treatments. (c, d) Mitochondrial ROS were measured in an immunofluorescence assay using a MitoSOX probe after ox-LDL and siRNA/Drp1 treatments. (e–g) Activity of the antioxidative factors GSH, GPX, and SOD was measured through ELISA after ox-LDL and siRNA/Drp1 treatments. $^*p < 0.05$.

mitochondria-related proteins [31] and mitochondrial tRNA-modifying enzymes [53]. In this study, we identified the regulatory mechanisms underlying miR-9-modified mitochondrial fission in macrophages. However, additional animal studies are needed to confirm our findings.

In summary, we found that macrophage viability and cholesterol metabolism are regulated by a miR-9/Drp1/mitochondrial fission signaling pathway. miR-9 levels were reduced by ox-LDL treatment, which contributed to upregulation of Drp1 transcription and led to macrophage mitochondrial fission. Excessive mitochondrial fission induced oxidative stress, inflammatory response, and cholesterol metabolism dysregulation in macrophages. These findings suggest that modulating macrophage function via the miR-9/Drp1/mitochondrial fission signaling pathway may be a novel treatment for AS.

4. Methods

4.1. Cell Culture. Macrophage induction and differentiation from monocytes were performed as previously described [39]. Macrophages were cultured in RPMI 1640 medium (Gibco, NY, USA) supplemented with 10% fetal bovine serum (FBS), penicillin, and streptomycin. ox-LDL at a concentration of $50\,\mu$g/mL was also added to the macrophage medium for 24 hours. Additionally, an miR-9 precursor (pre-miR-9) was constructed and transfected into macrophages as previously described [39].

4.2. Cell Viability Assay. Macrophage viability was evaluated using a CCK-8 kit (Dojindo, Japan) [54]. Cells were seeded

onto 96-well plates at a density of 2.5×10^4 cells/well. Cells were washed twice with PBS and incubated with $100\,\mu$L of culture medium containing 10% CCK-8 solution every 12 h after plating at 37°C. Absorbance at 450 nm was quantified using a DTX-880 multimode microplate reader (Beckman, US) [55].

4.3. siRNA Transfection. Macrophages were plated at subconfluence (10^5 cells in each well of a 6-well plate) without antibiotics, which can interfere with siRNA transfection efficiency. The next day, cells were transfected with Lipofectamine® RNAiMAX transfection reagent (Invitrogen, 13778-150) according to the manufacturer's protocol [56]. Macrophages were transfected with Drp1 siRNA or control siRNA, which were purchased from GenePharma (Shanghai, China), for 24 h. After siRNA transfection, macrophages were serum starved in RPMI 1640 medium for 24 hours prior to the start of the indicated experimental protocols [57]. Assays were performed 48 hours after siRNA transfection.

4.4. ELISA Quantification Assay. GSH, SOD, GPX, and proinflammatory factor activity was quantified using Quantikine ELISA Immunoassay kits (R&D Systems). In brief, after macrophages underwent siRNA transfection, 1 mL of fresh cell culture medium was added to each well of a 6-well plate, and conditioned medium was collected 6 hours after elastase exposure [58]. Conditioned media were centrifuged at $3,000 \times g$ for 15 minutes to remove cell debris. Undiluted conditioned media were used to quantify target protein
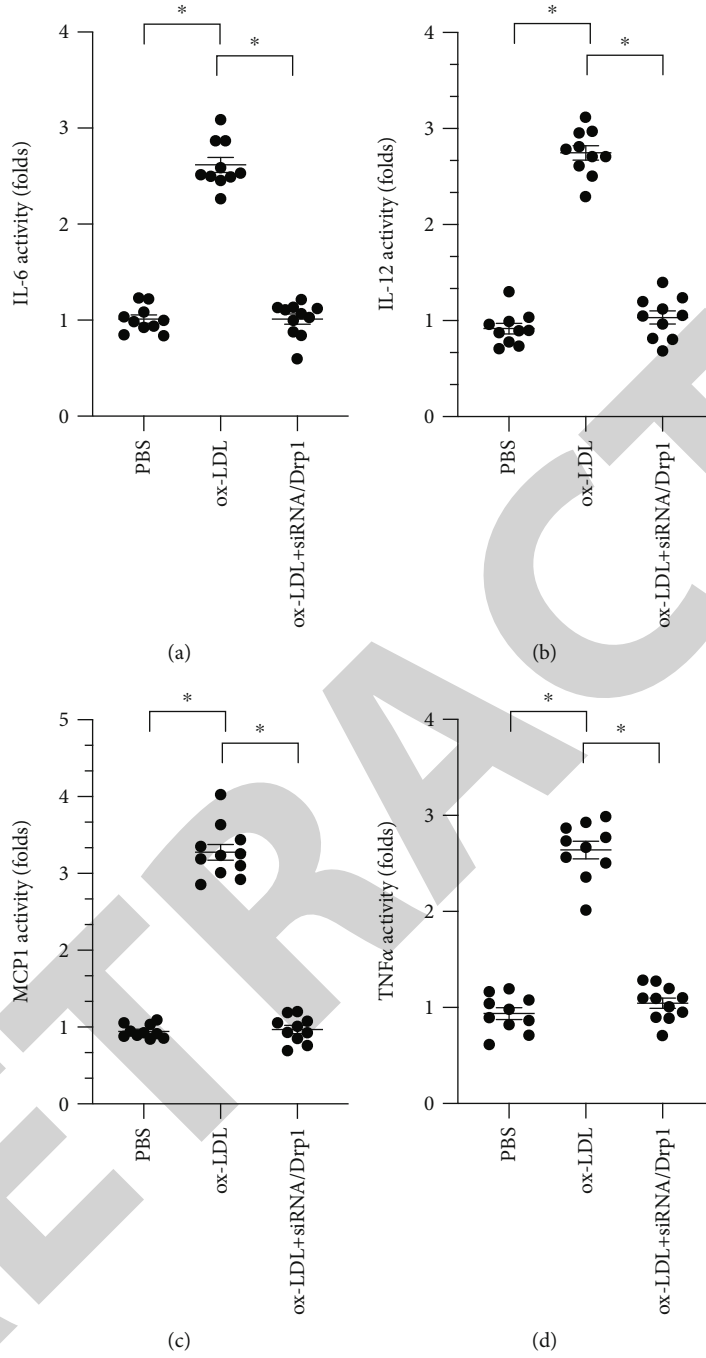
(a)

(b)
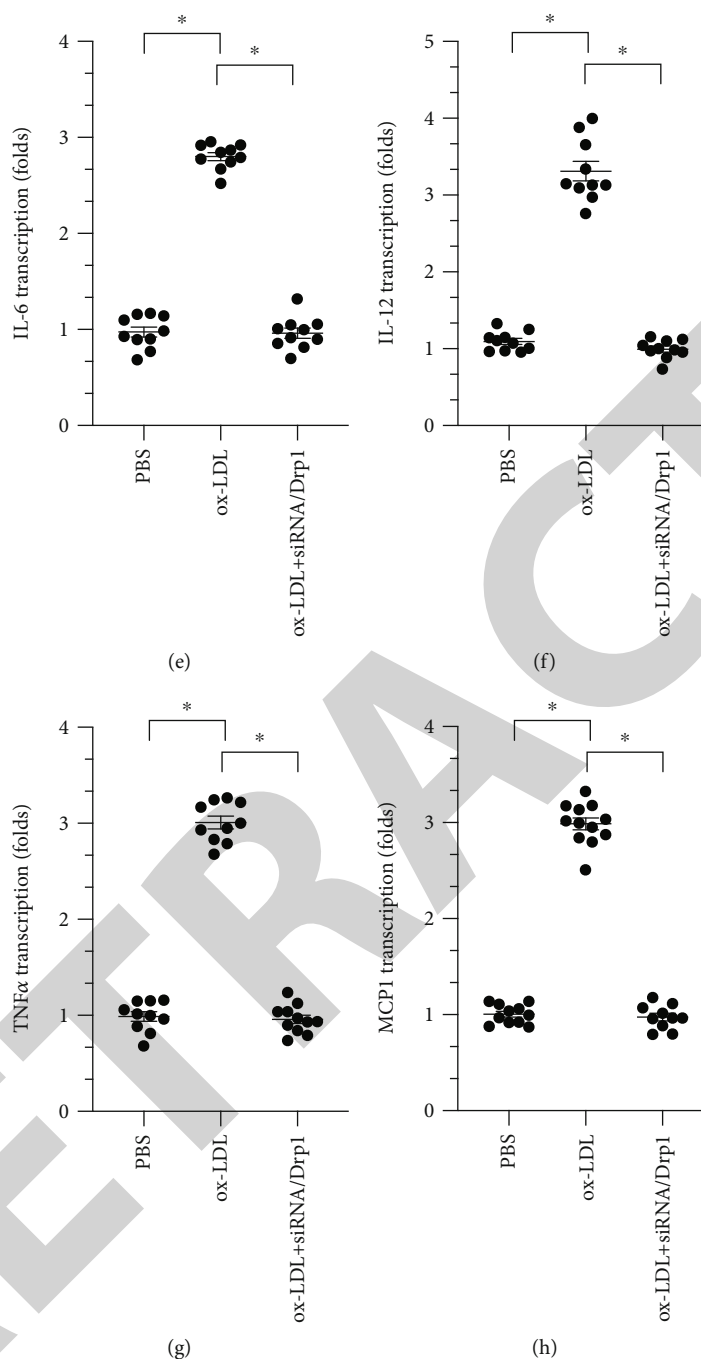

(c)

(d)

Figure 5: Continued.

(e)

(f)

(g)

(h)

FIGURE 5: ox-LDL induces inflammatory response dependent on Drp1-related mitochondrial fission in macrophages. (a–d) A qPCR assay was used to measure IL-6, IL-12, MCP1, and TNFα levels in RNA isolated from macrophages after ox-LDL and siRNA/Drp1 treatments. (e–h) ELISA was used to detect IL-6, IL-12, MCP1, and TNFα activity in macrophages after ox-LDL and siRNA/Drp1 treatments. $^{*}p < 0.05$.

levels according to the manufacturer's instructions [59]. All samples were run in triplicate.

4.5. Immunofluorescence. Samples were drop fixed in 10% buffered formalin overnight and cryopreserved in 30% sucrose in PBS overnight [60, 61]. Samples were then blocked with 2% Donkey serum in 0.1% Tween™ 20 in PBS (antibody diluent) for 30 minutes at room temperature. Antibodies

were diluted as follows: TOM20 (Abcam, ab186735, 1 : 100), CD36 (Abcam, ab133625, 1 : 200), caspase-3 (Abcam, ab13847, 1 : 250), ABCA1 (Abcam, ab18180, 1 : 200), and incubated at 4°C overnight. Samples were washed three times in PBS and incubated with the proper fluorescent secondary antibody (Alexa Fluor 488/555/647, Invitrogen) diluted 1 : 800 for two hours at room temperature. Samples were washed three times with PBS and incubated with DAPI
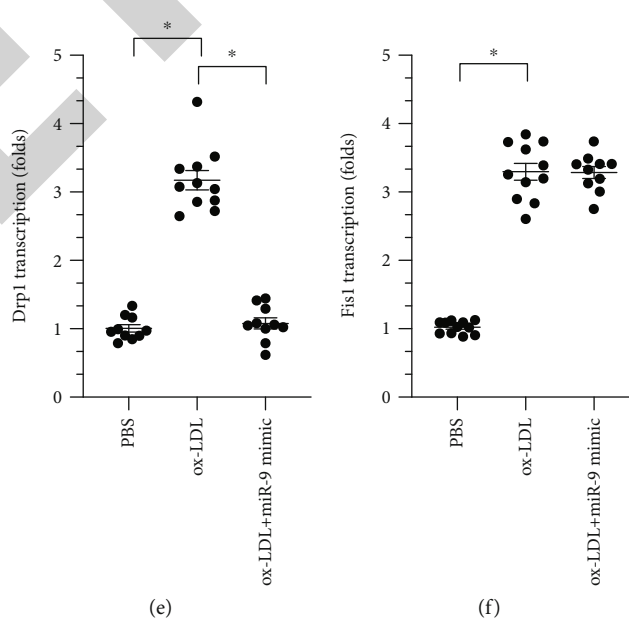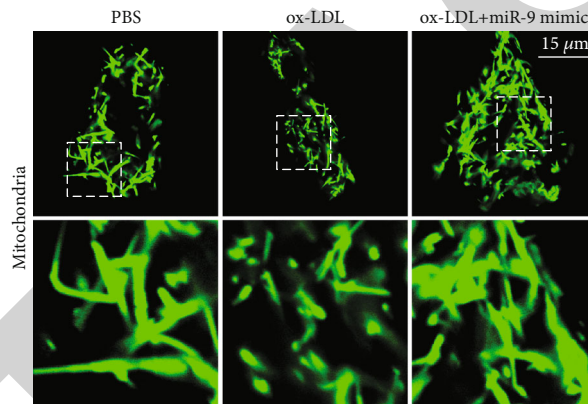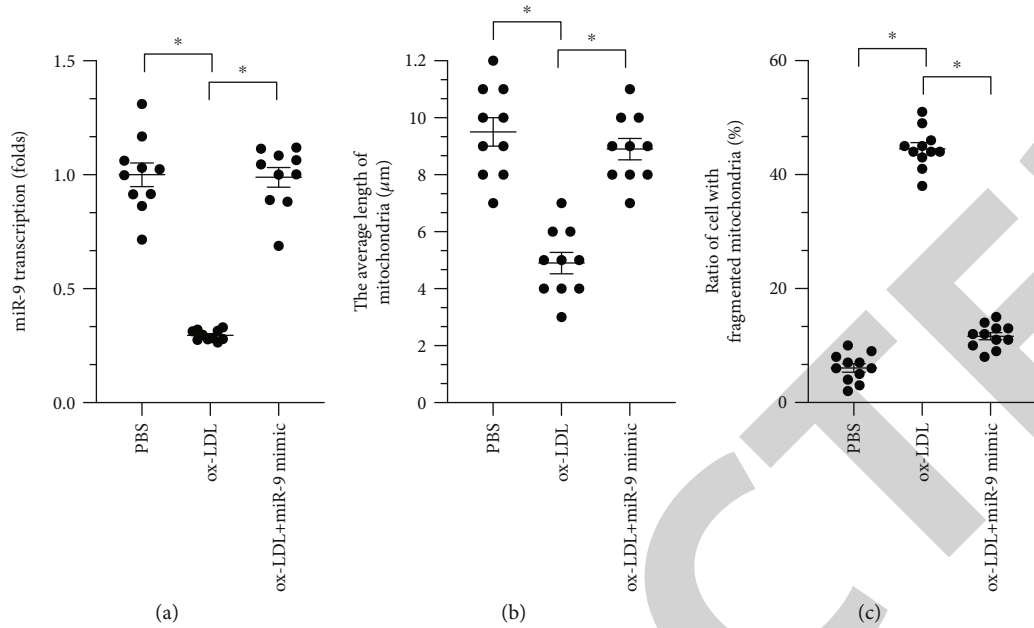
(a)

(b)

(c)
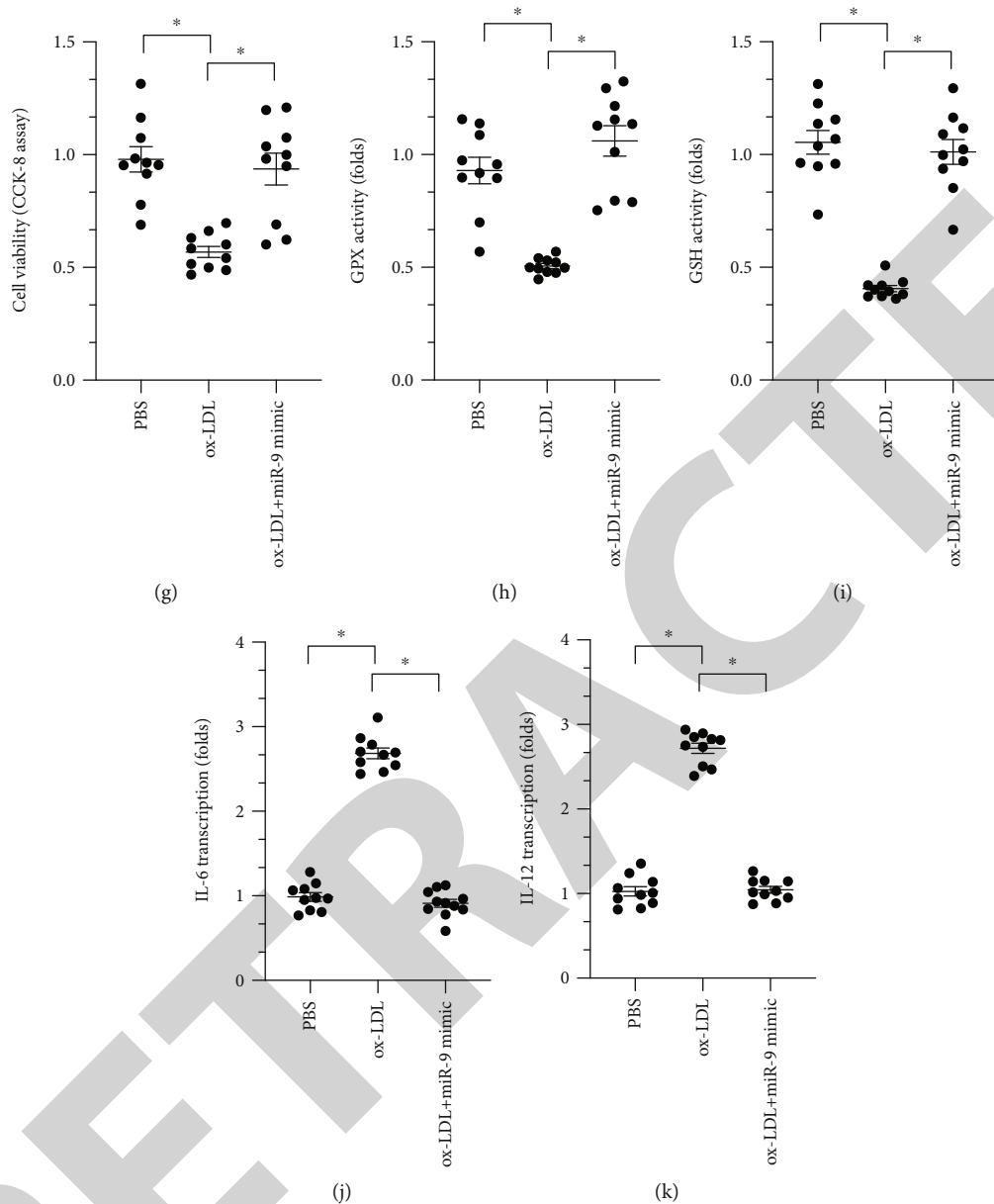
(d)

(e)

(f)

Figure 6: Continued.

FIGURE 6: ox-LDL regulates Drp1-related mitochondrial fission through miR-9. (a) Transcription of miR-9 in response to ox-LDL treatment. (b–d) Mitochondrial morphology was observed using immunofluorescence. (e, f) A qPCR assay was used to measure transcription of Fis1 and Drp1 in macrophages after ox-LDL treatment. (g) Cell viability was measured in a CCK-8 assay after ox-LDL and miR-9 mimic treatments. (h, i) ELISA was used to measure GSH and SOD activity. (j, k) A qPCR assay was used to measure IL-6 and MCP1 levels in macrophages. $^*p < 0.05$.

(Sigma, B2883) for 1 minute. Samples were then washed three times with PBS and mounted with fluoromount (SouthernBiotech) or ProLong™ Gold antifade reagent (Invitrogen, P10144) [62]. Images were taken on a Nikon Eclipse Ti epifluorescence microscope or a Zeiss LSM700 confocal microscope.

4.6. Reverse Transcription Real-Time Quantitative PCR. RNA was extracted from cultured cells using the RNeasy mini kit (Qiagen, Germany). cDNA was synthesized using the iScript cDNA Synthesis Kit (Bio-Rad) [63]. Real-time PCR was performed with SYBR Green Master Mix (TOYOBO, Japan) and

an ABI 7500 Fast Real-Time PCR System (Applied Biosystems, US). Relative gene expression was determined by normalizing to GAPDH [64].

4.7. ROS Staining. After treatment, cells were washed with cold PBS and then stained with two types of ROS probes [65, 66]. DCFHDA (Molecular Probes, USA) was used to stain intracellular ROS while MitoSOX red mitochondrial superoxide indicator (Molecular Probes, USA) was used to stain mitochondrial ROS [67]. In brief, 5μg/L DCFHDA and 2μg/L MitoSOX were added to the medium and incubated for about 30 min in the dark. Cells were then washed

three times with PBS and stained with DAPI, and images were taken on a Nikon Eclipse Ti epifluorescence microscope or a Zeiss LSM700 confocal microscope.

4.8. Statistics. Results are expressed as mean ± SEM. The Kruskal-Wallis one-way analysis of variance was used to compare each measure when there were three or more independent groups. Comparisons between groups were performed using Dunn's multiple comparisons test when statistically significant differences were identified in ANOVAs. A p value < 0.05 was considered significant. The Mann–Whitney test was used to compare two groups. All data were analyzed using Prism 5.0 (GraphPad Software Inc.).

Data Availability

All data are contained within the manuscript and additional files.

Conflicts of Interest

The authors declare that they have no conflicts of interest.

References

[1] M. G. Tinajero and A. I. Gotlieb, "Recent developments in vascular adventitial pathobiology: the dynamic adventitia as a complex regulator of vascular disease," *The American Journal of Pathology*, vol. 190, no. 3, pp. 520–534, 2020.

[2] C. B. Afonso and C. M. Spickett, "Lipoproteins as targets and markers of lipoxidation," *Redox Biology*, vol. 23, article 101066, 2019.

[3] V. Guerrini and M. L. Gennaro, "Foam cells: one size doesn't fit all," *Trends in Immunology*, vol. 40, no. 12, pp. 1163–1179, 2019.

[4] S. Yang, H. Q. Yuan, Y. M. Hao et al., "Macrophage polarization in atherosclerosis," *Clinica Chimica Acta*, vol. 501, pp. 142–146, 2020.

[5] D. A. Chistiakov, D. A. Kashirskikh, V. A. Khotina, A. V. Grechko, and A. N. Orekhov, "Immune-inflammatory responses in atherosclerosis: the role of myeloid cells," *Journal of Clinical Medicine*, vol. 8, no. 11, p. 1798, 2019.

[6] S. Guo, J. Lu, Y. Zhuo et al., "Endogenous cholesterol ester hydroperoxides modulate cholesterol levels and inhibit cholesterol uptake in hepatocytes and macrophages," *Redox Biology*, vol. 21, article 101069, 2019.

[7] F. C. Wu and J. G. Jiang, "Effects of diosgenin and its derivatives on atherosclerosis," *Food & Function*, vol. 10, no. 11, pp. 7022–7036, 2019.

[8] J. D. Matthews, A. R. Reedy, H. Wu et al., "Proteomic analysis of microbial induced redox-dependent intestinal signaling," *Redox Biology*, vol. 20, pp. 526–532, 2019.

[9] H. Zhou, P. Zhu, J. Wang, H. Zhu, J. Ren, and Y. Chen, "Pathogenesis of cardiac ischemia reperfusion injury is associated with CK2α-disturbed mitochondrial homeostasis via suppression of FUNDC1-related mitophagy," *Cell Death and Differentiation*, vol. 25, no. 6, pp. 1080–1093, 2018.

[10] R. B. Li, S. Toan, and H. Zhou, "Role of mitochondrial quality control in the pathogenesis of nonalcoholic fatty liver disease," *Aging*, vol. 12, no. 7, pp. 6467–6485, 2020.

[11] H. Zhou, S. Toan, P. Zhu, J. Wang, J. Ren, and Y. Zhang, "DNA-PKcs promotes cardiac ischemia reperfusion injury through mitigating BI-1-governed mitochondrial homeostasis," *Basic Research in Cardiology*, vol. 115, no. 2, p. 11, 2020.

[12] J. Wang, P. Zhu, R. Li, J. Ren, and H. Zhou, "Fundc1-dependent mitophagy is obligatory to ischemic preconditioning-conferred renoprotection in ischemic AKI via suppression of Drp1-mediated mitochondrial fission," *Redox Biology*, vol. 30, article 101415, 2020.

[13] W. Peng, G. Cai, Y. Xia et al., "Mitochondrial dysfunction in atherosclerosis," *DNA and Cell Biology*, vol. 38, no. 7, pp. 597–606, 2019.

[14] M. S. Gibson, N. Domingues, and O. V. Vieira, "Lipid and non-lipid factors affecting macrophage dysfunction and inflammation in atherosclerosis," *Frontiers in Physiology*, vol. 9, p. 654, 2018.

[15] Z. Hoseini, F. Sepahvand, B. Rashidi, A. Sahebkar, A. Masoudifar, and H. Mirzaei, "NLRP3 inflammasome: its regulation and involvement in atherosclerosis," *Journal of Cellular Physiology*, vol. 233, no. 3, pp. 2116–2132, 2018.

[16] J. D. Short, K. Downs, S. Tavakoli, and R. Asmis, "Protein thiol redox signaling in monocytes and macrophages," *Antioxidants & Redox Signaling*, vol. 25, no. 15, pp. 816–835, 2016.

[17] J. Wang, S. Toan, and H. Zhou, "New insights into the role of mitochondria in cardiac microvascular ischemia/reperfusion injury," *Angiogenesis*, vol. 23, no. 3, pp. 299–314, 2020.

[18] J. Wang, S. Toan, and H. Zhou, "Mitochondrial quality control in cardiac microvascular ischemia-reperfusion injury: new insights into the mechanisms and therapeutic potentials," *Pharmacological Research*, vol. 156, article 104771, 2020.

[19] H. Zhou, J. Wang, P. Zhu et al., "NR4A1 aggravates the cardiac microvascular ischemia reperfusion injury through suppressing FUNDC1-mediated mitophagy and promoting Mff-required mitochondrial fission by CK2α," *Basic Research in Cardiology*, vol. 113, no. 4, p. 23, 2018.

[20] J. Wang, P. Zhu, R. Li, J. Ren, Y. Zhang, and H. Zhou, "Bax inhibitor 1 preserves mitochondrial homeostasis in acute kidney injury through promoting mitochondrial retention of PHB2," *Theranostics*, vol. 10, no. 1, pp. 384–397, 2020.

[21] S. T. Feng, Z. Z. Wang, Y. H. Yuan et al., "Dynamin-related protein 1: a protein critical for mitochondrial fission, mitophagy, and neuronal death in Parkinson's disease," *Pharmacological Research*, vol. 151, article 104553, 2020.

[22] A. Graham, "Mitochondrial regulation of macrophage cholesterol homeostasis," *Free Radical Biology & Medicine*, vol. 89, pp. 982–992, 2015.

[23] E. R. Stead, J. I. Castillo-Quan, V. E. M. Miguel et al., "Age-phagy - adapting autophagy for health during aging," *Frontiers in Cell and Development Biology*, vol. 7, p. 308, 2019.

[24] H. Zhou, P. Zhu, J. Wang, S. Toan, and J. Ren, "DNA-PKcs promotes alcohol-related liver disease by activating Drp1-related mitochondrial fission and repressing FUNDC1-required mitophagy," *Signal Transduction and Targeted Therapy*, vol. 4, no. 1, p. 56, 2019.

[25] S. Shoeibi, "Diagnostic and theranostic microRNAs in the pathogenesis of atherosclerosis," *Acta Physiologica*, vol. 228, article e13353, 2020.

[26] C. J. Donaldson, K. H. Lao, and L. Zeng, "The salient role of microRNAs in atherogenesis," *Journal of Molecular and Cellular Cardiology*, vol. 122, pp. 98–113, 2018.

[27] A. Shapouri-Moghaddam, S. Mohammadian, H. Vazini et al., "Macrophage plasticity, polarization, and function in health and disease," *Journal of Cellular Physiology*, vol. 233, no. 9, pp. 6425–6440, 2018.

[28] D. A. Chistiakov, A. A. Melnichenko, V. A. Myasoedova, A. V. Grechko, and A. N. Orekhov, "Mechanisms of foam cell formation in atherosclerosis," *Journal of Molecular Medicine (Berlin, Germany)*, vol. 95, no. 11, pp. 1153–1165, 2017.

[29] D. Dlouha and J. A. Hubacek, "Regulatory RNAs and cardiovascular disease - with a special focus on circulating microRNAs," *Physiological Research*, vol. 66, Supplement 1, pp. S21–S38, 2017.

[30] E. L. Solly, C. G. Dimasi, C. A. Bursill, P. J. Psaltis, and J. T. M. Tan, "MicroRNAs as therapeutic targets and clinical biomarkers in atherosclerosis," *Journal of Clinical Medicine*, vol. 8, no. 12, p. 2199, 2019.

[31] K. Tan, Y. Ge, J. Tian, S. Li, and Z. Lian, "miRNA-9 inhibits apoptosis and promotes proliferation in angiotensin II-induced human umbilical vein endothelial cells by targeting MDGA2," *Reviews in Cardiovascular Medicine*, vol. 20, no. 2, pp. 101–108, 2019.

[32] H. E. Bøtker, D. Hausenloy, I. Andreadou et al., "Practical guidelines for rigor and reproducibility in preclinical and clinical studies on cardioprotection," *Basic Research in Cardiology*, vol. 113, no. 5, p. 39, 2018.

[33] S. M. Davidson, S. Arjun, M. V. Basalay et al., "The 10th Biennial Hatter Cardiovascular Institute workshop: cellular protection-evaluating new directions in the setting of myocardial infarction, ischaemic stroke, and cardio-oncology," *Basic Research in Cardiology*, vol. 113, no. 6, p. 43, 2018.

[34] B. K. Ooi, B. H. Goh, and W. H. Yap, "Oxidative stress in cardiovascular diseases: involvement of Nrf2 antioxidant redox signaling in macrophage foam cells formation," *International Journal of Molecular Sciences*, vol. 18, no. 11, p. 2336, 2017.

[35] D. A. Chistiakov, Y. V. Bobryshev, and A. N. Orekhov, "Macrophage-mediated cholesterol handling in atherosclerosis," *Journal of Cellular and Molecular Medicine*, vol. 20, no. 1, pp. 17–28, 2016.

[36] E. Taghizadeh, F. Taheri, P. G. Renani, Z. Reiner, J. G. Navashenaq, and A. Sahebkar, "Macrophage: a key therapeutic target in atherosclerosis?," *Current Pharmaceutical Design*, vol. 25, no. 29, pp. 3165–3174, 2019.

[37] B. W. L. Lee, P. Ghode, and D. S. T. Ong, "Redox regulation of cell state and fate," *Redox Biology*, vol. 25, article 101056, 2019.

[38] A. J. Kowaltowski, "Strategies to detect mitochondrial oxidants," *Redox Biology*, vol. 21, article 101065, 2019.

[39] Y. Wang, Z. Han, Y. Fan et al., "MicroRNA-9 inhibits NLRP3 inflammasome activation in human atherosclerosis inflammation cell models through the JAK1/STAT signaling pathway," *Cellular Physiology and Biochemistry*, vol. 41, no. 4, pp. 1555–1571, 2017.

[40] F. Tong, X. Mao, S. Zhang et al., "HPV + HNSCC-derived exosomal miR-9 induces macrophage M1 polarization and increases tumor radiosensitivity," *Cancer Letters*, vol. 478, pp. 34–44, 2020.

[41] D. Castaño, C. Rattanasopa, V. F. Monteiro-Cardoso et al., "Lipid efflux mechanisms, relation to disease and potential therapeutic aspects," *Advanced Drug Delivery Reviews*, 2020.

[42] R. Peng, H. Ji, L. Jin et al., "Macrophage-based therapies for atherosclerosis management," *Journal of Immunology Research*, vol. 2020, Article ID 8131754, 11 pages, 2020.

[43] P. Ahmad, S. S. Alvi, D. Iqbal, and M. S. Khan, "Insights into pharmacological mechanisms of polydatin in targeting risk factors-mediated atherosclerosis," *Life Sciences*, vol. 254, article 117756, 2020.

[44] N. Hadebe, M. Cour, and S. Lecour, "The SAFE pathway for cardioprotection: is this a promising target?," *Basic Research in Cardiology*, vol. 113, no. 2, p. 9, 2018.

[45] G. Heusch, "25 years of remote ischemic conditioning: from laboratory curiosity to clinical outcome," *Basic Research in Cardiology*, vol. 113, no. 3, p. 15, 2018.

[46] X. Shi, W. Ma, Y. Li et al., "MiR-144-5p limits experimental abdominal aortic aneurysm formation by mitigating M1 macrophage-associated inflammation: suppression of TLR2 and OLR1," *Journal of Molecular and Cellular Cardiology*, vol. 143, pp. 1–14, 2020.

[47] Q. A. Han, D. Su, C. Shi et al., "Urolithin A attenuated ox-LDL-induced cholesterol accumulation in macrophages partly through regulating miR-33a and ERK/AMPK/SREBP1 signaling pathways," *Food & Function*, vol. 11, no. 4, pp. 3432–3440, 2020.

[48] H. Liu, Z. Mao, J. Zhu, M. Shen, and F. Chen, "MiR-140-5p inhibits oxidized low-density lipoprotein-induced oxidative stress and cell apoptosis via targeting toll-like receptor 4," *Gene Therapy*, 2020.

[49] L. Li, F. Wu, Y. Xie et al., "MiR-202-3p inhibits foam cell formation and is associated with coronary heart disease risk in a Chinese population," *International Heart Journal*, vol. 61, no. 1, pp. 153–159, 2020.

[50] Q. Sun, J. Zeng, Y. Liu et al., "MicroRNA-9 and -29a regulate the progression of diabetic peripheral neuropathy via ISL1-mediated sonic hedgehog signaling pathway," *Aging*, vol. 12, no. 12, pp. 11446–11465, 2020.

[51] D. Shao, Y. Di, J. Lian et al., "Grape seed proanthocyanidins suppressed macrophage foam cell formation by miRNA-9 via targeting ACAT1 in THP-1 cells," *Food & Function*, vol. 11, no. 2, pp. 1258–1269, 2020.

[52] J. Zhen, W. Chen, L. Zhao, X. Zang, and Y. Liu, "A negative Smad2/miR-9/ANO1 regulatory loop is responsible for LPS-induced sepsis," *Biomedicine & Pharmacotherapy*, vol. 116, article 109016, 2019.

[53] S. Meseguer, A. Martinez-Zamora, E. Garcia-Arumi, A. L. Andreu, and M. E. Armengod, "The ROS-sensitive microRNA-9/9∗ controls the expression of mitochondrial tRNA-modifying enzymes and is involved in the molecular mechanism of MELAS syndrome," *Human Molecular Genetics*, vol. 24, no. 1, pp. 167–184, 2015.

[54] A. L. Aalto, A. K. Mohan, L. Schwintzer et al., "M1-linked ubiquitination by LUBEL is required for inflammatory responses to oral infection in Drosophila," *Cell Death and Differentiation*, vol. 26, no. 5, pp. 860–876, 2019.

[55] F. Tang, M. E. LeBlanc, W. Wang et al., "Anti-secretogranin III therapy of oxygen-induced retinopathy with optimal safety," *Angiogenesis*, vol. 22, no. 3, pp. 369–382, 2019.

[56] H. E. Baker, A. M. Kiel, S. T. Luebbe et al., "Inhibition of sodium-glucose cotransporter-2 preserves cardiac function during regional myocardial ischemia independent of alterations in myocardial substrate utilization," *Basic Research in Cardiology*, vol. 114, no. 3, p. 25, 2019.

[57] T. Cao, S. Fan, D. Zheng et al., "Increased calpain-1 in mitochondria induces dilated heart failure in mice: role of mitochondrial superoxide anion," *Basic Research in Cardiology*, vol. 114, no. 3, p. 17, 2019.